Physics of Ionized Gases

Boris M. Smirnov

With the editorial collaboration of Howard R. Reiss

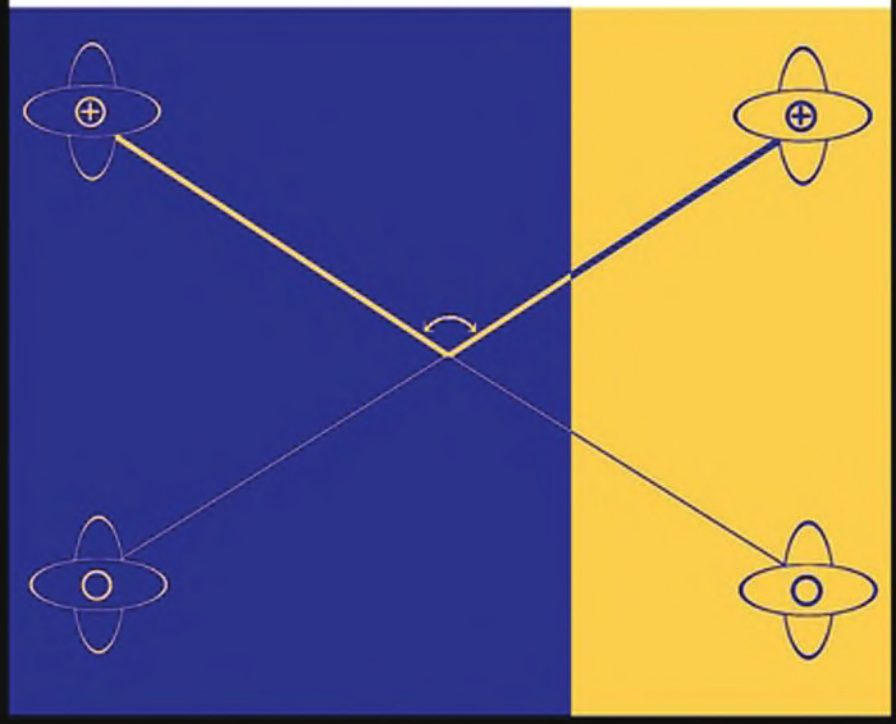

PHYSICS OF IONIZED GASES

PHYSICS OF IONIZED GASES

BORIS M. SMIRNOV
Russian Academy of Sciences

With the editorial collaboration of Howard R. Reiss

A Wiley-Interscience Publication
JOHN WILEY & SONS, INC.
New York / Chichester / Weinham / Brisbane / Singapore / Toronto

This book is printed on acid-free paper. ♾

Published simultaneously in Canada.

For ordering and customer service, call 1-800-CALL-WILEY

Library of Congress Cataloging in Publication Data:

Smirnov, B. M. (Boris Mikhailovich), 1938-
Physics of ionized gases / Boris M. Smirnov
p. cm
Includes bibliographical references and index
ISBN 0-471-17594-3 (cloth : alk. paper)
1. Plasma (Ionized gases) I. Title.

QC718.S5635 2001
530 21.--dc'4 00-047761

Printed in the United Kingdom

10 9 8 7 6 5 4 3 2 1

CONTENTS

PREFACE

This book is based on lecture courses on plasma physics given by the author in various educational institutions in Russia and other countries during the last thirty years. The courses were intended for both beginning and advanced graduate students in the physics and engineering professions. The notes for these lectures are the basis for eight previous books on the physics of ionized gases. The present book uses some of the material of the earlier ones, but many new developments in the physics of ionized gases and plasmas are included here.

The main goal of the book is to acquaint the reader with the fundamental concepts of plasma physics. It can be useful both for students and for mature scientists who work in diverse aspects of this area of investigation. The book is designed to preserve the level of sophistication of contemporary theoretical plasma physics, while at the same time using simple, physically motivated descriptions of the problems. These requirements may seem to be contradictory. Nevertheless, the author tried to achieve these goals by using limiting cases of problems to reduce the obscuring complexity of fully general treatments, and to employ simple models that have proven their value. It has been found possible to expound the contemporary state of the physics of ionized gases in a relatively accessible form.

A small part of the book where an introduction to some problems is given (as in Chapter 1) contains an entirely qualitative description. In the main part of the book, guided by the insight of specialists, the author avoids an overly descriptive approach to the problems treated. In this way, attention can be focused on the fundamental physics of the problems treated to allow the reader to develop his independent insight into the details, while preserving the modern level of understanding of these problems.

Since this book presupposes the active participation of the reader, it contains up-to-date information in the text ot its tables and in the appendices. The bibliography is selected to allow one to study in detail specialized subjects in this area of investigation. Because some chapters of the book relate to distinct applications of plasma physics, portions of these chapters may be studied independently of other chapters.

The author thanks Professor Howard R. Reiss, who prepared the excellent English version of this book.

BORIS M. SMIRNOV

PHYSICS OF IONIZED GASES

CHAPTER 1

PLASMA IN NATURE AND IN LABORATORY SYSTEMS

1.1 PLASMA AS A STATE OF MATTER

The name "plasma" was introduced into physics in the 1920s to describe a conducting gas. Charged particles in a conducting gas result from detachment of electrons from atoms or molecules. In order to understand the conditions for the existence of such a system, we compare it with an ordinary chemical system. Let us consider, for example, atmospheric air, consisting mainly of nitrogen and oxygen molecules. At high temperatures, along with the nitrogen and oxygen, nitrogen oxides can be formed. The following chemical equilibrium is maintained in air:

$$N_2 + O_2 \leftrightarrow 2NO - 41.5 \text{ kcal/mol}. \tag{1.1}$$

Here and below, the sign $\leftrightarrow$ means that the process can proceed either in the forward or in the reverse direction. According to the *Le Chatelier principle*, an increase in the temperature of the air leads to an increase in the concentration of the NO molecules.

A similar situation takes place in the case of formation of charged particles in a gas, but this process requires a higher temperature. For example, the ionization equilibrium for nitrogen molecules has the form

$$N_2 \leftrightarrow N_2^+ + e - 360 \text{ kcal/mol}. \tag{1.2}$$

Thus, the chemical and ionization equilibria are analogous, but ionization of atoms or molecules proceeds at higher temperatures than chemical transformations. To illustrate this, Table 1.1 contains examples of chemical and

TABLE 1.1. Temperatures Corresponding to Dissociation of 0.1% of Molecules or Ionization of 0.1% of Atoms at a Pressure of 1 atm

Chemical Equilibrium	T, K	Ionization Equilibrium	T, K
$2CO_2 \leftrightarrow 2CO + O_2$	1550	$H \leftrightarrow H^+ + e$	7500
$H_2 \leftrightarrow 2H$	1900	$He \leftrightarrow He^+ + e$	12000
$O_2 \leftrightarrow 2O$	2050	$Cs \leftrightarrow Cs^+ + e$	2500
$N_2 \leftrightarrow 2N$	4500		
$2H_2O \leftrightarrow 2H_2 + O_2$	1800		

ionization equilibria. This table gives the temperatures at which 0.1% of molecules are dissociated in the case of chemical equilibrium or 0.1% of atoms are ionized for ionization equilibrium. The pressure of the gas is 1 atm. Thus, a weakly ionized gas, which we shall call a *plasma*, has an analogy with a chemically active gas. Therefore, though a plasma has characteristic properties which we shall describe, it is not really a new form or state of matter as is often asserted.

In most actual cases a plasma is a weakly ionized gas with a small degree of ionization. Table 1.2 gives some examples of real plasmas and their parameters—the number densities of electrons (N_e) and of atoms (N_a), the temperature (or the average energy) of electrons (T_e), and the gas temperature (T). In addition, some types of plasma systems are given in Figs. 1.1 and 1.2.

It is seen that generation of an equilibrium plasma requires strong heating of a gas. One can create a conducting gas by heating the charged particles only. This takes place in gaseous discharges when an ionized gas is placed in an external electric field. Moving in this field, electrons acquire energy from the field and transfer it to the gas. As a result, the mean electron energy may exceed the thermal energy of neutral particles of the gas, and the electrons can produce the ionization which is necessary for maintaining an electric current in the system. Thus, a gaseous discharge is an example of a plasma which is maintained by an external electric field. If the temperatures of electrons and neutral particles are identical, the plasma is called an *equilibrium* plasma; in the opposite case we have a *nonequilibrium* plasma. Figure 1.3 gives some examples of equilibrium and nonequilibrium plasmas.

TABLE 1.2. Parameters of Some Plasmas[a]

Type of Plasma	N_e, cm^{-3}	N, cm^{-3}	T_e, K	T, K
Sun's photosphere	10^{13}	10^{17}	6000	6000
E-layer of ionosphere	10^5	10^{13}	250	250
He–Ne laser	3×10^{11}	2×10^{16}	3×10^4	400
Argon laser	10^{13}	10^{14}	10^5	10^3

[a] N_e, N are the number densities of electrons and neutral atomic particles respectively, and T_e, T are their temperatures.

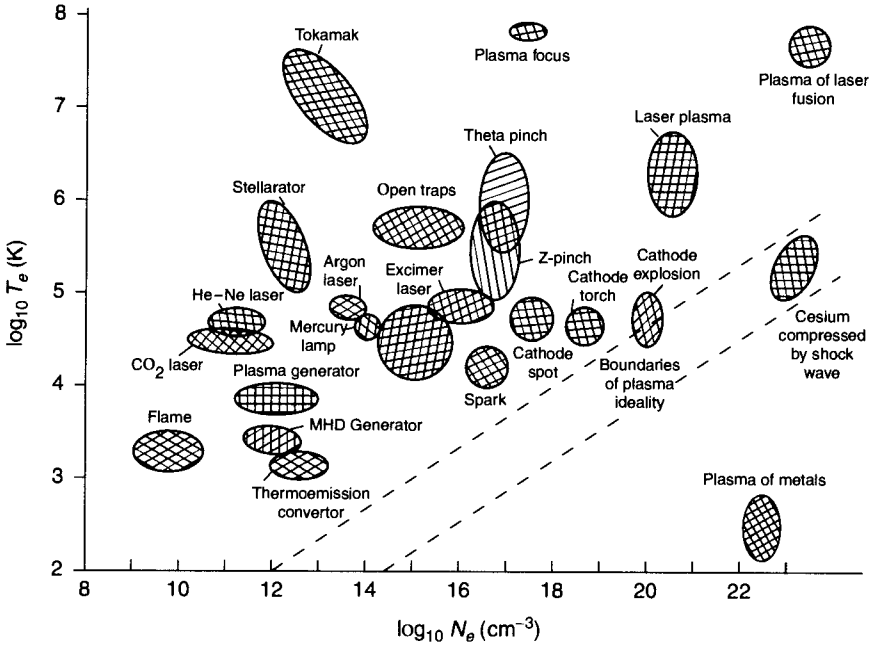

Figure 1.1 Parameters of laboratory plasmas.

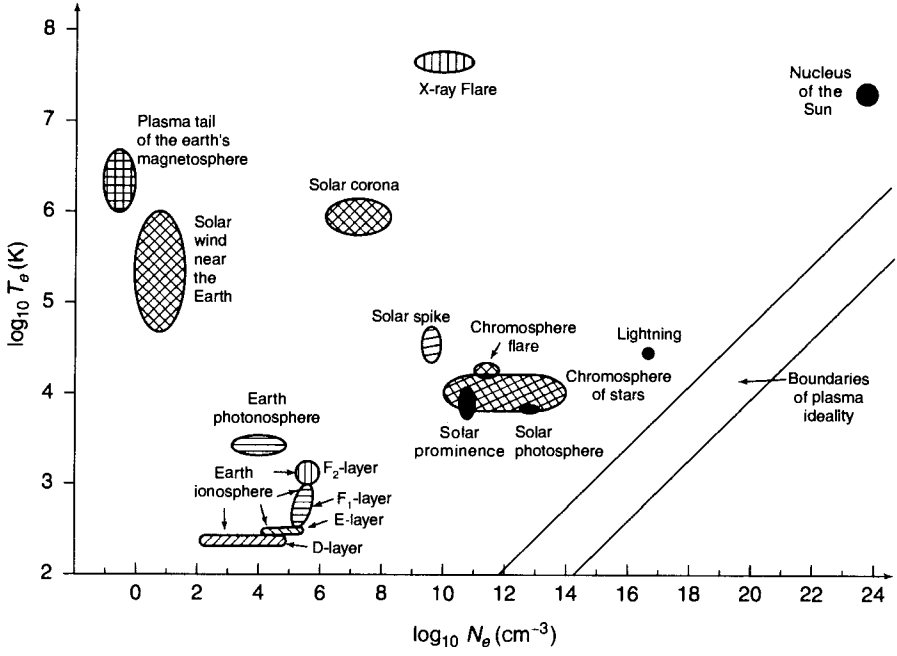

Figure 1.2 Parameters of plasmas found in nature.

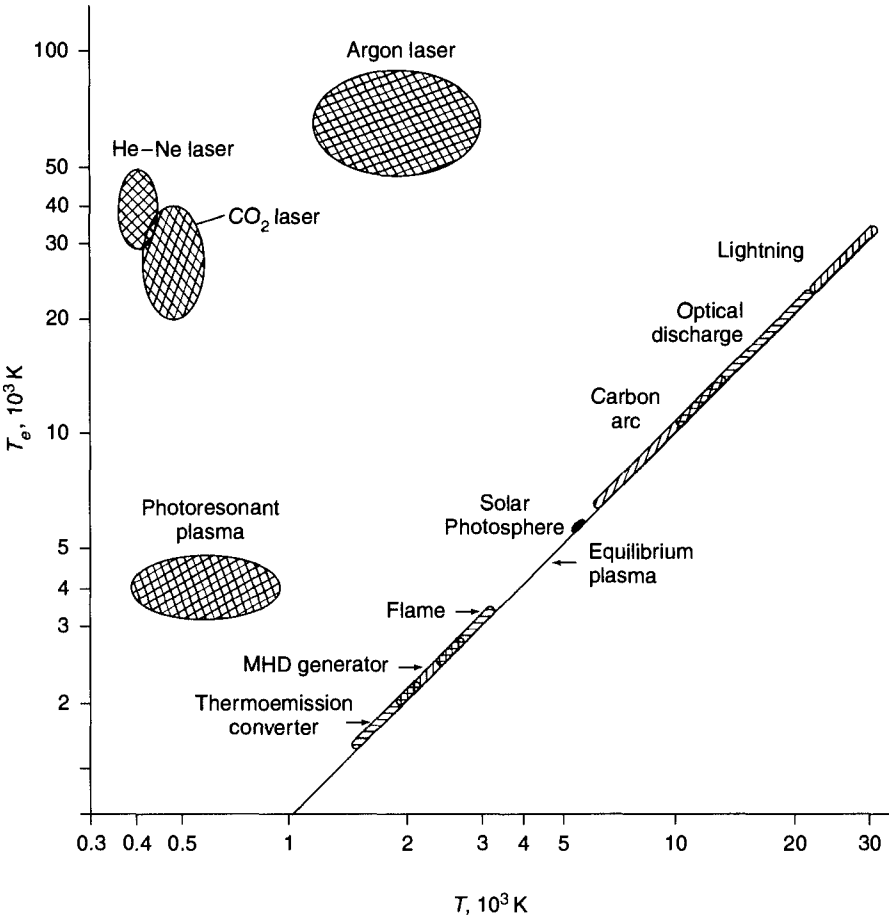

Figure 1.3 Electron and gas temperatures of laboratory plasmas. The straight line corresponds to the equilibrium plasma whose electron and gas temperatures are the same.

Thus, plasma as a physical object has definite properties that characterize it. The presence of charged particles makes possible various types of interaction with external fields that lead to a special behavior of this object, which is absent in ordinary gaseous systems. Furthermore, it creates a variety of means for generation and application of plasmas, which will be considered below.

1.2 METHODS OF PLASMA GENERATION

Let us review methods of plasma generation. The simplest method uses the action of an external electric field on a gas to produce electrical breakdown of the gas. Gaseous discharge and gas discharge plasma have a long history.

We can date the start of its study from 1705, when the English scientist Francis Hauksbee made an electrostatic generator whose power allowed him to study luminous electric discharges in gases. In 1734, Charles Francois de Cisternay Dufay (France) discovered that air is conducting in the vicinity of hot bodies. In 1745, E. J. von Kleist (Germany) and P. V. Musschenbroek (Netherlands) constructed independently a type of electric capacitor named the Leyden jar. It made possible the study of electrical breakdown in air. In 1752, the American scientist and statesman Benjamin Franklin created a theory of lightning on the basis of experiments. He considered the phenomenon to be a flow of electricity in accordance with its contemporary understanding. Thus, the above investigations gave the first understanding of the processes of passage of electric charges through gases, and were connected more or less with gaseous discharges.

A gas-discharge plasma is a common form of plasma which can have a variety of parameters. It can be either stationary or pulsed, depending on the character of the external fields. An external electric field may cause electrical breakdown of gas, which then generates different forms of plasma depending on the conditions of the process. In the first stage of breakdown, a uniform current of electrons and ions may arise. If the electric field is not uniform, an ionization wave can propagate in the form of an electron avalanche streamer. In the next stage of the breakdown process, the electric current establishes a distribution of charged particles in space. This is a gaseous discharge, which can exist in a variety of forms.

After the external electric field is switched off, the plasma decays as a result of recombination of electrons with ions, and spatial diffusion of the plasma occurs. Plasma in these conditions is called an *afterglow* plasma, and is used for study of recombination and diffusion processes involving charged and excited atoms.

A convenient way to generate plasma uses resonant radiation, that is, radiation whose wavelength corresponds to the energy of atomic transitions in the atoms constituting the excited gas. As a result of the excitation of the gas, a high density of excited atoms is formed, and collision of these atoms leads to formation of free electrons. Thus the atomic excitation in the gas leads to its ionization and to plasma generation. This plasma is called a *photoresonant* plasma. The possibility of generating such a plasma has improved with the development of laser techniques. In contrast to a gas discharge plasma, a photoresonant plasma is formed as a result of excitations of atoms and therefore has special properties. In particular, the temperature of the excited atoms can be somewhat in excess of the electron temperature. This plasma has various applications: it is used for generation of multicharged ions, as a source of acoustic waves, and so on.

A laser plasma is created by laser irradiation of a surface and is characterized by parameters such as the laser power and the time duration of the process. In particular, if a short (nanosecond) laser pulse is focused onto a surface, material evaporates from the surface in the form of a plasma. If the number density of its electrons exceeds the critical density (in the case of a

neodymium laser, where the radiation wavelength is 1.06 μm, this value is 10^{21} cm^{-3}), the evolving plasma screens the radiation, and subsequent laser radiation goes to heating the plasma. As a result, the temperature of the plasma reaches tens of electron volts, and this plasma can be used as a source of X-ray radiation or as the source of an X-ray laser. Laser pulses can be compressed and shortened to $\approx 2 \times 10^{-14}$ s. This makes possible the generation of a plasma during very short times, and it permits the study of fast plasma processes.

If the laser power is relatively low, the evaporating material is a weakly ionized vapor. Then, if the duration of the laser pulse is not too short (more than 10^{-6} s), there is a critical laser power (10^7–10^8 W/cm^2) beyond which laser radiation is absorbed by the plasma electrons, and *laser breakdown* of the plasma takes place. For values of the laser power smaller than the critical value, laser irradiation of a surface is a method for generating beams of weakly ionized vapor. This vapor can be used for formation and deposition of atomic clusters.

A widely used method of plasma generation is based on the passage of electron beams through a gas. Secondary electrons can then be used for certain processes. For example, in *excimer lasers*, secondary electrons are accelerated by an external electric field for generation of excited molecules with short lifetimes. The electron beam as a source of ionization is convenient for excimer and chemical lasers because the ionization process lasts such a short time.

A chemical method of plasma generation is the use of flames. The chemical energy of reagents is spent on formation of radicals or excited particles, and chemoionization processes with participation of active particles generate charged particles. The transformation of chemical energy into the energy of ionized particles is not efficient, so the degree of ionization in flames is small.

Electrons in a hot gas or vapor can be generated by small particles. Such a process takes place in products of combustion of solid fuels.

Introduction of small particles and clusters into a weakly ionized gas can change its electrical properties because these particles can absorb charged particles, that is, electrons and ions, or negative and positive ions can recombine on these particles by attachment to them. This process occurs in an *aerosol plasma*, that is, an atmospheric plasma that contains aerosols. On the contrary, in hot gases small particles or clusters can generate electrons.

Plasma can be created under the action of fluxes of ions or neutrons when they pass through a gas. Ionization near the Earth's surface results from the decay of radioactive elements which are found in the Earth's crust. Ionization processes and the formation of an ionized gas in the upper atmosphere of the Earth are caused by energetic radiation from the Sun. Thus, methods of plasma generation are many and varied, and lead to the formation of different types of plasmas.

1.3 PLASMAS IN LABORATORY DEVICES

Various laboratory devices and systems contain a plasma. This plasma is called a low-temperature plasma or a hot plasma, depending on the temperature of the charged particles. In a hot plasma the thermal energy of the atomic particles exceeds a characteristic atomic value (which may be the ionization potential of the plasma atoms), and in a low-temperature plasma, it is much less. Correspondingly, plasma devices containing hot plasmas or low-temperature plasmas are different in principle. An example of a hot plasma is a thermonuclear fusion plasma, that is, a plasma for a controlled thermonuclear reaction. This reaction proceeds with participation of nuclei of deuterium or of tritium—isotopes of hydrogen. In order to achieve this reaction, it is necessary that during the time of plasma confinement, that is, during the time when ions of deuterium or tritium are present in the reaction zone, these ions have a chance to participate in a thermonuclear reaction. Both a high ion temperature (about 10 keV) and a high number density of ions must be present if the thermonuclear reaction is to proceed. The threshold number density of ions (N_i) for the thermonuclear reaction depends on the plasma lifetime τ in such a way that the product of these values, $N_i\tau$, must exceed a certain value. This condition is called the *Lawson criterion*. At temperatures of several keV, the Lawson criterion corresponds to an onset value of $N_i\tau = 10^{16}$ cm^{-3} s for a deuterium plasma, and 10^{14} cm^{-3} s for a deuterium-tritium plasma. These values are reached in contemporary plasma fusion devices.

The other method to solve the problem of thermonuclear fusion uses pulsed systems. In this case a deuterium pellet is irradiated on its entire surface by a laser pulse or a fast ion beam. When the pulse impinges on the pellet, the pellet is heated and compressed by a factor 10^2–10^3. The heating and compression is intended to promote a thermonuclear fusion reaction. Note that the dense hot plasma that is formed during compression of the pellet is a special state of matter that does not have an analog in an ordinary laboratory setting.

A hot plasma is used in plasma engines. There, a flux of plasma causes the motion of a system in the opposite direction according to Newton's third law. The plasma flow velocities may attain 10^8 cm/s, and exceed by one or two orders of magnitude the corresponding value for conventional chemical-fuel engines. Therefore, despite producing power small compared to that of chemical engines, plasma engines are used in space engineering where the problem of the weight of fuel is critical.

The low-temperature plasma differs from a hot one in both its parameters and its applications. Since the most widespread methods of plasma generation under laboratory conditions are based on gas discharges, most gas lasers and light sources use such discharges. Let us first consider installations using a low-temperature plasma for generation of electrical energy. The magnetohydrodynamic (MHD) generator uses a stream of hot, weakly ionized gas

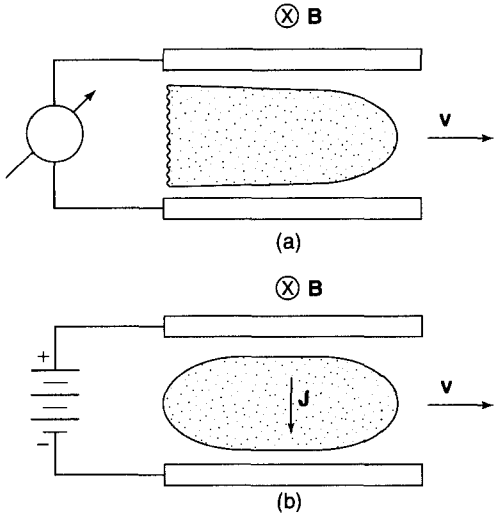

Figure 1.4 A schematic diagram of an (a) MHD generator and (b) an ion engine. In the first case the electric field is generated by the motion of a plasma in a magnetic field. In the second case electrons and ions are accelerated as they pass through crossed electric and magnetic fields.

flowing in a transverse magnetic field. This induces electric current in a direction perpendicular to the directions of the stream and magnetic field, to permit the system to transform the energy of flow into electrical energy (see Fig. 1.4a). The efficiency of this transformation is quite high because the flowing gas is hot. The principles of action of MHD generators and plasma engines bear a resemblance to each other (see Fig. 1.4), and an MHD-generator may be adapted as a plasma engine (Fig. 1.4).

There are stationary MHD generators which may be used as components of electric power stations, and there are pulsed MHD generators. The pulsed MHD generator can be regarded as a gun where a weakly ionized plasma is used instead of a shell. The plasma is formed as a result of combustion of gunpowder or some equivalent source of propellant gas. When this plasma passes through a region with an external magnetic field, electric power is created. In order to estimate the possibilities of this system, let us make a simple calculation. Assume the plasma velocity equals the velocity a bullet acquires in a gun. Take the efficiency of energy transformation to be of the order of 50%, and the length of the region with a magnetic field to be 1 m. Then the specific power of this generator is of the order of 10^8 W/g, and the pulse duration is $\approx 7 \times 10^{-4}$ s. Thus the power of a pulsed MHD generator, for this brief instant, corresponds to the total power of all the electric power plants of the world if the mass of the powder used is of the order of 10 g. The pulsed MHD generator transforms the chemical energy of the powder into

electrical energy. Due to the simplicity and yield parameters of these systems, they are convenient for special applications as autonomous pulsed sources of electric energy.

The other system where a plasma is used for generation of electric energy is the *thermoemission converter*. It contains two parallel metal plates with different work functions (the *work function* is the binding energy of an electron at a surface). One of these plates is heated and emits electrons which reach the other plate. An electric current is created. Connection of the plates through a load leads to the release of electrical energy in the load. It is evident that a plasma is not the underlying basis for this device. Nevertheless, the use of a plasma in the gap between the plates makes it possible to overcome an important difficulty attendant on this system. If there is no plasma in the gap, electron charge is accumulated in this region and creates an electric potential between the plates that increases with electron number density in the gap, and is opposite in direction to the potential that initiated the phenomenon. Beyond a certain level the counterpotential will stop the generation of electric energy. For typical energy fluxes in these systems (~ 1 W/cm^2) the distance between plates must be less than 10 μm. It is difficult to combine this condition with a high temperature of the heated plate (≈ 2000 K). Introduction of a plasma in the gap between plates provides a means of overcoming this difficulty.

In various applications of a plasma with an intense input of energy, the plasma is generated in a moving medium. The source of this plasma is called a *plasmatron* or plasma generator. It is usually an arc discharge established in a flowing gas or vapor. Such plasma generators produce plasma torches, which have wide application to various technological problems, including incineration of waste and special medical uses. Many plasma applications are based on the possibility of introducing a high level of electrical energy into the plasma. It leads to the creation and maintenance of an ionized gas containing active atomic particles: electrons, ions, excited atoms, radicals. These particles can be analyzed by a variety of techniques, and therefore a plasma can used not only in energetic systems, but also in measuring instruments. In particular, plasma-based methods of spectral analysis are widely practiced in metallurgy. In these methods a small amount of metal in the form of a solution or powder is introduced in a flowing discharge plasma, and spectral analysis of the plasma makes it possible to determine the metal composition. The accuracy of spectral determination of admixture concentration with respect to a primary component is of the order of 0.01–0.001%.

It is interesting that the principles of operation of MHD generators, thermoemission converters, and plasmatrons were suggested as early as the end of the nineteenth century. Now, with the advantage of contemporary materials and technology, these devices have acquired a new life.

The *optogalvanic* technique in plasma diagnostics uses another principle. The weakly ionized gas in a gas discharge (usually it is a glow gas discharge) is irradiated by a tuned laser, and the discharge electric current is measured

as a function of the radiation wavelength. If the laser radiation is resonant with atomic transitions of atoms in the discharge plasma, this radiation causes photoionization at a rate strongly dependent on the identity of the atoms being irradiated. The measured effect is a change in the discharge current. Thus, measured current jumps can be associated with the presence of particular atoms in the discharge plasma. The degree of certainty in the identification of the atom is greatly increased if many resonances can be identified. The optogalvanic method makes it possible to identify admixtures in a plasma with concentration of the order of 10^{-10}–10^{-12} with respect to the principal component of the plasma. An appreciation of the precision of this method can be gained by noting that its accuracy is comparable to having knowledge of the total population of the Earth to within an accuracy of one individual. Thus, a plasma is a uniquely useful tool for a variety of applications.

1.4 PLASMA IN CONTEMPORARY TECHNOLOGY

Plasmas are currently widely employed in industry, and their range of application broadens continuously. The usefulness of plasmas in technology can be ascribed to two qualities: Plasmas make available much higher temperatures than can be achieved with chemical fuel torches; and a large variety of ions, radicals, and other chemically active particles are generated therein. Therefore, either directly within a plasma or with its help, one can conduct technological or chemical processes of practical importance. Another advantage of a plasma follows from the possibility of introducing large specific energies in a simple fashion.

The oldest applications of a plasma as a heat-transfer agent are in the welding and cutting of metals. Since the maximum temperature in chemical torches is about 3000 K, they cannot be used for some materials. The arc discharge (electric arc) makes it possible to increase this temperature by a factor of three, so that melting or evaporation of any material is possible. Therefore the electric discharge has been used since the beginning of this century for welding and cutting of metals. Presently, plasma torches with power up to 10 MW are used for melting iron in cupolas, for melting scrap, for production of steel alloys, and for recovering steel in tundishes.

Plasma processing is used for extraction of metals from ores. In some cases plasma methods compete with traditional ones which are based on chemical heating. Comparing the plasma with chemical methods in cases when either can be used, the conclusion is that plasma methods provide a higher specific output, a higher quality of product, and a smaller amount of waste, but require a larger energy expenditure and more expensive equipment.

Another application of a plasma as a heat-transfer agent relates to fuel energetics. The introduction of a plasma in the burning zone of low-grade

coals leads to improvements in the efficiency of the burning with an accompanying reduction in particle emissions, in spite of a relatively small energy input from the plasma. Plasmas are used also for pyrolysis and other methods of processing and cleaning of fuel.

Plasmas have been employed extensively for the processing and treatment of surfaces. The good heat-transfer capabilities of a plasma are useful for treatment of surfaces. During plasma processing of surfaces the chemical composition of the surface does not change, but its physical parameters may be improved. Another aspect of the processing of a surface by a plasma refers to the case when active particles of the plasma react chemically with the surface. The upper layer of the surface can acquire a chemical composition different from that of the substrate. For example, plasma hardening of a metallic surface occurs when metal nitrides or carbides are formed in the surface layer. These compounds are generated when ions or active atoms in the plasma penetrate into the surface layer.

A third mechanism for the plasma action on a surface is realized when the surface material does not itself participate in the chemical process, but material from the plasma is deposited on the surface in the form of a thin film. This film can have special mechanical, thermal, electric, optical, and chemical properties that are useful for specific problems and requirements. It is convenient to use for this purpose plasma beams that flow from jets. Such beams can give rise to clusters as a result of expansion of the beam. The *ion-cluster beam* method is used for deposition of thin films. Because of the smaller heat release during the deposition of clusters than during the deposition of atoms, the ion-cluster beam method provides improved quality of films formed thereby, even though ion-cluster beams have a lower intensity than beams of atoms or atomic ions. Beam methods for deposition of micrometer-thickness films are widespread in the manufacture of microelectronics, mirrors, and special surfaces.

In addition to the deposition processes resulting from plasma flows containing atoms or clusters, a plasma spraying process is used for deposition of molten powder particles on a sample. The powder particles are introduced into a plasma jet resulting from the passage of a gas through an arc discharge. These particles are heated and accelerated in the plasma jet, which is directed onto a target. Molten particles impinge with high velocities on the surface, adhere, and form a covering layer.

An important area of plasma applications—*plasma chemistry*—relates to production of chemical compounds. The first industrial plasmachemical process was employed for ammonia production at the beginning of the twentieth century. It was later replaced by a cheaper method that produced ammonia from nitrogen and hydrogen in a high-temperature, high-pressure reactor with a platinum catalyst. Another plasmachemical process is to produce ozone in a barrier discharge. This method has been used for several decades. Large-scale development of plasma chemistry was long retarded by the required high power intensity. When other criteria became the limiting factors, new plasmachemical processes were mastered. At present, the array

of chemical compounds produced industrially by plasmachemical methods includes C_2H_2, HCN, TiO_2, Al_2O_3, SiC, XeF_6, KrF_2, O_2F_2 and many others. Though the number of such compounds constitutes a rather small fraction of the products of the chemical industry, this fraction is steadily increasing. The products of a plasmachemical process may exist either in the form of a gas or in the form of condensed particles. Plasmachemical industrial production of ceramic-compound powders such as SiC and Si_3N_4, or powders of metals and metal oxides, leads to an end product of high quality.

Plasmachemical processes with participation of organic compounds are used as well as those with inorganic materials. Organic-compound applications include the production of polymers and polymeric membranes, fine organic synthesis in a cold plasma, and so on. In a qualitative assessment of the technological applications of plasmas, we conclude that plasma technologies have a sound basis and present prospects for important further improvements.

Plasma processing for environmental applications is developing in two directions. The first is decomposition of toxic substances, explosive materials, and other hazardous wastes, which can be decomposed in a plasma into their simple chemical constituents. The second is improvement of air quality. A corona discharge of low power is used for this purpose. The discharge generates active atomic particles such as oxygen atoms. These atoms have an affinity for active chemical compounds in air, and react with them. Such discharges also destroy microbes, but present no hazards to humans because of the low concentrations of these particles.

1.5 TERRESTRIAL ATMOSPHERIC PLASMA

It is convenient to categorize plasmas occurring in nature as terrestrial plasma (in the Earth's atmosphere or in near-Earth space), solar plasma, and cosmic plasma. Properties of the plasma of the Earth's atmosphere depend on the altitude of the atmospheric layer in which it occurs. At low altitudes the plasma is maintained by ionization of air under the action of cosmic rays and of atmospheric electric fields. Near the Earth's surface, a portion of the ionization of air arises from the decay of radioactive elements of the Earth's crust. Plasma in lower layers of the atmosphere is characterized by a low density of charged particles. The presence of plasma is limited by the tendency of electrons to attach quickly to oxygen molecules, forming negative ions. Therefore, plasmas in the lower atmosphere contain negative charge in the form of negative ions. If aerosol particles are present in air, ions may attach to them. Therefore charged aerosol particles play a role in this plasma.

Atmospheric plasma underlies the electrical phenomena of the atmosphere. One of them is lightning—electrical breakdown under the action of electric fields in the atmosphere. Lightning is one of the processes in the atmosphere which originate in the formation of clouds, and arises from the charging of aerosols and clouds. As a result, electric fields occur in the

atmosphere and cause the generation of electric currents and, in particular, lightning. Another electrical phenomenon of the atmosphere is corona discharge: the appearance of electric currents near conductors in a quiet atmosphere. Under the influence of intense electric fields in wet atmospheric air, these currents can cause the formation of *Saint Elmo's lights*—a glow in the vicinity of protruding objects. Electrical discharges in atmospheric air are often associated with energetic natural phenomena of a nonelectrical nature, such as volcanic eruptions, earthquakes, sandstorms, and waterspouts.

The majority of charged particles of the upper atmosphere are formed as a result of photoionization of atomic oxygen or molecular nitrogen under the action of the hard ultraviolet (UV) radiation from the Sun. This region of the atmosphere is called the *ionosphere*. The existence of the ionosphere plays an important role in terrestrial radio communications. It is responsible for the reflection of radio signals from the atmosphere that makes possible propagation of radio waves to large distances.

The ionosphere is divided into a number of layers. The lowest of them is called the D-layer, and occurs at altitudes in the range of 50–90 km. It contains a rarefied plasma with the number density of charged particles on the order of 10^2–10^4 cm^{-3}. The negative charge of the D-layer arises from negative ions. Charged particles penetrate the D-layer from the higher E and F layers of the ionosphere, where they are generated by the action of UV radiation from the Sun. The E-layer of the ionosphere exists at altitudes of 90–140 km. The F-layer of the ionosphere is usually divided into the F_1-layer (140–200 km) and the F_2-layer (200–400 km). The number density of charged particles in these layers is of the order of 10^5–10^6 cm^{-3} in the daytime, and the negative charge is in the form of electrons. These layers of the ionosphere reflect radio signals and are the radio mirror of the Earth's atmosphere.

In these layers the beautiful phenomenon of the aurora is observed. This phenomenon originates from charged-particle ejection from solar plasma. The charged particles proceed to the Earth, where they come under the influence of the Earth's magnetic field. They move along the magnetic field lines, and the more energetic particles can proceed to the vicinity of the Earth's magnetic poles, where the magnetic lines of force are directed perpendicular to the Earth surface. Where the magnetic field lines enter the upper atmosphere, the electron component of the solar particles is stopped by the convergence of the magnetic field lines as the magnetic pole is approached, whereas the more massive solar protons penetrate into the upper atmosphere along the magnetic lines of force. As they are braked as a result of collisions with atmospheric atoms or molecules, these protons ionize and excite atoms of the upper atmosphere. Radiation of metastable oxygen and nitrogen atoms formed by these collisions creates the observed glow of the aurora. Because the magnetic poles of the Earth are at high latitudes, the aurora is observed in the region near the geographical poles.

Above the ionosphere the Earth is surrounded by a relatively cold plasma named the *plasmasphere* and located at altitudes of 1000–20,000 km. This

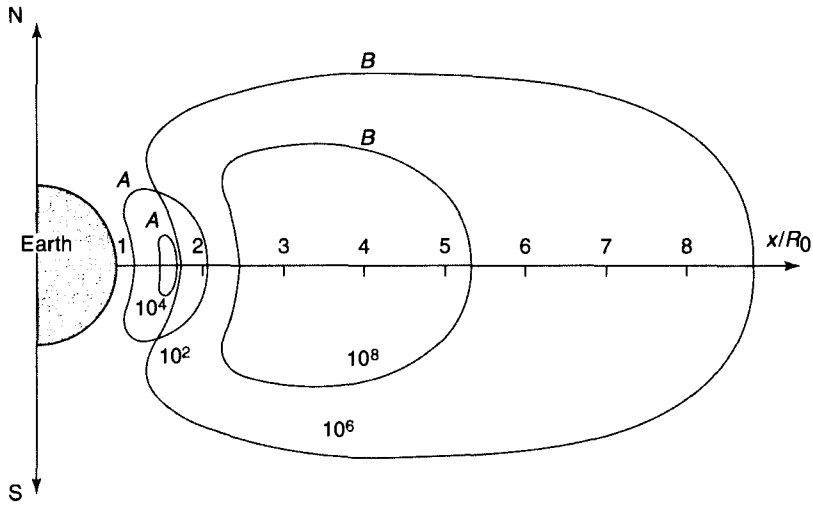

Figure 1.5 Radiation belts near the Earth. Curves A define regions where fast protons with energies of more than 30 MeV are captured. Curves B correspond to regions in which slow electrons with an energy of 0.1–5 MeV are captured. Numbers on the curves refer to particle fluxes expressed in $cm^{-2} s^{-1}$, R_0 is the Earth's radius, and x is the distance from the Earth.

plasma consists mainly of protons and electrons with a number density in the range of 10^3–10^5 cm^{-3}. The plasma density decreases slowly with increasing altitude, and then falls sharply by two orders of magnitude at the outer boundary of the plasmasphere. This boundary is called the *plasmapause*.

The so-called *radiation belts* are located at a distance of several Earth radii (see Fig. 1.5). Protons and electrons are captured by the magnetic field of the Earth, and populate these belts.

Thus, the upper atmosphere of the Earth contains different types of plasmas whose properties are determined by interaction of solar radiation and particle flows with the Earth's fields and flows.

1.6 SOLAR PLASMA

The properties of solar plasma depend on where in the Sun it is located. The Sun's core contains a plasma with a temperature of about 17 MK and a number density of the order of 10^{24} cm^{-3}. As one moves from the center of the Sun, the number density of particles in the plasma and its temperature both decrease. The Sun's *photosphere* is of principal importance both for Earth processes and for the solar energy balance. The photosphere is a thin layer of the Sun whose thickness (about 1000 km) is small compared to the

Sun's radius, but that emits most of the energy radiated from the Sun. Hence the temperature of this layer (about 6000 K) determines the yellow color of the Sun and the temperature of the solar radiation that reaches the Earth.

The next layer of the solar atmosphere is the *chromosphere*, whose name is owed to the red color observed on the disk of the Moon during a total eclipse of the Sun. The temperature of the chromosphere decreases at first and then increases with increasing distance from the Sun's center. The density of the solar atmosphere decreases with increasing distance from the Sun's center. The chromosphere is transparent because it is rarefied.

The next higher, more rarefied region of the Sun's atmosphere is called the solar *corona*. This beautiful name is suggested by the glow in this region that is observed during a total eclipse of the Sun. The peculiarity of the solar corona is its high temperature ($\sim 10^6$ K). Therefore, the solar corona emits hard UV radiation.

Because of its high temperature and small temperature gradient, the solar corona is not stable. Expansion of the solar corona into space creates a plasma flow directed outward from the Sun. This flow is called the *solar wind*. The solar wind creates the interplanetary plasma and leads to various phenomena in the upper terrestrial atmosphere. In particular, it is the origin of the terrestrial aurora. At the location of the Earth, the solar wind moves with a velocity of 200–900 km/s and is characterized by a proton flux of 10^8–10^{10} cm^{-2} s^{-1} and a proton number density of 4–100 cm^{-3}. The mean proton temperature in the solar wind is 5 eV, and the mean electron temperature is about 20 eV . Interaction of the solar wind with the Earth's magnetic field gives rise to the magnetosphere of the Earth (see Fig. 1.6). Its boundary is located at a distance of 8–12 Earth radii on the side facing the Sun, and has a long tail extending from the other side. The solar wind flows around the Earth along this boundary. The magnetic lines of force of the

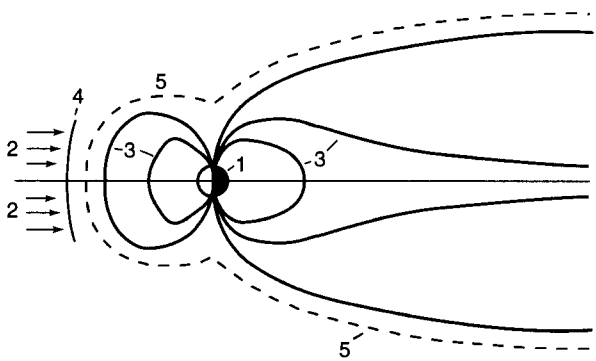

Figure 1.6 The magnetosphere of the Earth. 1, Earth; 2, solar wind; 3, magnetic lines of force; 4, shock wave; 5, magnetosphere boundary where the solar-wind pressure is balanced by the pressure of the Earth's magnetic field.

terrestrial magnetic field rise almost vertically near the Earth's poles. This makes possible the penetration of plasma fluxes into the Earth's atmosphere in these locations. Therefore, magnetic storms in the upper atmosphere of the Earth, and the aurora, are observed in this region.

There are in the Sun a number of phenomena that result from interaction of the solar plasma with its magnetic fields. *Spicules*—separated columns of moving plasma—are formed in the chromosphere and create chromospheric bushes. With typical solar conditions, approximately 10^6 spicules are observed simultaneously. Spicules result from reconnection of magnetic lines of force. An increase in the magnetic field strength in some zones of the solar atmosphere leads to scattering of gas on these zones, and causes the formation of cylindrical structures in the plasma motion. This mechanism is the basis for the generation of spicules.

Another structure of the solar plasma observed in the solar corona is the *prominence*. Prominences are clots of dense plasma of different forms with temperatures of the order of 10^4 K. They are generated as a result of interaction of plasma streams with magnetic fields and propagate in a corona from the chromosphere.

Solar flares are observed in an upper chromosphere or in corona. They are a result of development of plasma instabilities, in particular, reconnection of magnetic lines of force (see Chapter 13). Solar flares last several minutes. A sharp increase of the plasma temperature in flares causes an increase in emission of short-wave radiation. Solar flares generate short intense fluxes of solar plasma and can strongly enhance the solar wind. Such signals reach the Earth in 1.5–2 days, and cause magnetic storms and auroras in the terrestrial atmosphere.

In summary, there are several varieties of solar plasma, and interaction of the plasma with solar magnetic fields leads to the generation of a number of phenomena and plasma structures. The astrophysical plasma to be found in interstellar space and in stars is even more variegated, and may cause new specific effects.

1.7 PLASMA WITH A CONDENSED PHASE

Various types of plasmas or ionized gases that contain clusters or small particles have the properties of the encompassing medium altered by the inclusions. Examples are a plasma with a dispersed condensed phase, and a colloidal plasma. (*Colloids* are microspheres.) There are three types of plasma with a condensed phase that are commonly encountered in nature and in the laboratory. A plasma of the Earth's atmosphere containing small particles is called an aerosol plasma, and the particles themselves are known as aerosols. Properties of the aerosol plasma and the influence of small particles on its parameters depend on the altitude and on environmental factors. In particular, dust and mist are dispersed bases of an aerosol plasma

near the Earth's surface. At low altitudes, surface ions and small particles of aerosol plasmas include molecules of water, sulfur dioxide, nitrogen oxides, ammonia, salts of sulfur, and nitrogenic acids. At low altitudes, small dust particles or small liquid drops may carry positive and negative charges, with the number density of charged particles of the order of 10^3 cm^{-3}. Aerosols collect atomic and molecular atmospheric ions. The presence of aerosols in the atmosphere influences the properties of the plasma. The charged aerosols fall due to gravity. This creates an electric current in the atmosphere, and this electric current charges clouds. Therefore, the transport of charged aerosols in the atmosphere is the basis of atmospheric electrical phenomena.

Two other types of plasma with small particles—a dusty plasma and a cluster plasma—differ each from other by the stability of the inclusions. Small particles of a *dusty* plasma are stable and are not destroyed by plasma processes. For example, soot particles resulting from combustion of solid fuels may be ionized due to high temperatures or may get a negative charge due to attachment of electrons or negative ions. The electrical charge of the soot particles can be used for their separation from the flow of gaseous combustion products. Dusty plasmas also exist in astrophysical systems, including interstellar clouds, where small dust particles account for about 1% of the mass. Dust particles are of importance for the formation of stars and planets. They also influence the interaction of comets with the solar wind, where the particle charge is of importance.

Evolution of a *cluster* plasma is accompanied by cluster evaporation and by growth resulting either from attachment of atoms or molecules to the clusters or from their coagulation—the joining of two colliding particles. Usually, the size of clusters or particles in a cluster plasma is less than that in a dusty plasma because of the instability of clusters. Nucleation and evaporation lead to the instability of uniform and nonuniform cluster plasmas, and the size distribution function of clusters in a cluster plasma varies with time (see Chapter 12). As an example of a cluster plasma, we can consider the plasma in the positive column of an arc containing a buffer gas at high pressure with a small component of the vapor of a refractory metal. Then, metallic clusters are formed in the discharge region at moderate temperatures, where the pressure of the metallic vapor is higher than the saturation vapor pressure temperature. As clusters grow, their transport in a hot region where they evaporate ceases, and all the vapor is transformed into clusters. Since clusters grow in time, the cluster plasma is not stationary.

CHAPTER 2

STATISTICS OF A WEAKLY IONIZED GAS

2.1 DISTRIBUTION FUNCTIONS

Determination of the statistics of a gas amounts to the analysis of the distribution functions of the constituent particles of the gas. A plasma consists of atoms or molecules with an admixture of charged particles, so in this case our goal is to analyze the distributions of both neutral and charged particles simultaneously. Since free electrons belong to the continuum in atomic or molecular spectra, it is necessary to analyze equilibria in continuum–continuum, discrete–discrete, and discrete–continuum transitions in both directions. We start from a general energy distribution for weakly interacting particles in a closed system. In an ensemble of a large number of particles, each of the particles is in one of a set of states described by the quantum numbers i. The goal is to find the average number of particles that are found in one of these states. For example, if we have a gas of molecules, the problem is to find the molecular distribution in its vibrational and rotational states. We shall treat problems of this type below.

Consider a closed system of N particles, so that this number does not change with time. Denote the number of particles in the ith state by n_i. Then the condition of conservation of the total number of particles has the form

$$N = \sum_i n_i, \tag{2.1}$$

Since the system of particles is closed, that is, it does not exchange energy with other systems, we require conservation of the total energy E of the

particles, where

$$E = \sum_i \varepsilon_i n_i, \tag{2.2}$$

and ε_i is the energy of a particle in the ith state. In the course of the evolution of the system, an individual particle can change its state, but the average number of particles in each state stays essentially the same. Such a state of a closed system is called a state of *thermodynamic equilibrium.*

Transitions of individual particles between states result from collisions with other particles. The probability that a particle is found in a given state (as well as the average number of particles in this state) is determined by several variables. Denote by $W(n_1, n_2, \ldots, n_i, \ldots)$ the probability that n_1 particles are found in the first state, n_2 particles are found in the second state, ..., n_i particles are found in the ith state, ... We wish to calculate the number of possible realizations of this distribution. First take the n_1 particles for the first state from the total number of particles N. There are

$$C_N^{n_1} = \frac{N!}{(N - n_1)!\, n_1!}$$

ways to do this. Next, select n_2 particles corresponding to the second state from the remaining $N - n_1$ particles. This can be done in $C_{N-n_1}^{n_2}$ ways. Continuing this operation, we find the probability distribution to be

$$W(n_1, n_2, \ldots, n_i, \ldots) = \text{Const} \times \frac{N!}{\prod_i n_i!}, \tag{2.3}$$

where Const is a normalization constant.

2.2 THE BOLTZMANN DISTRIBUTION

Let us determine the most probable number $\bar{n}_i$ of particles that are to be found in a state i. We use the large-number hypothesis $\bar{n}_i \gg 1$, and we require that the probability W as well as its logarithm have maxima at $n_i = \bar{n}_i$. We then introduce $dn_i = n_i - \bar{n}_i$, assume that $\bar{n}_i \gg dn_i \gg 1$, and expand $\ln W$ over the interval dn_i near its maximum. Using the relation

$$\ln n! = \ln\left(\prod_{m=1}^{n} m\right) \approx \int_1^n dx \ln x,$$

we have $(d/dn)(\ln n!) \approx \ln n$.

On the basis of this relation, we obtain from formula (2.3)

$$\ln W(n_1, n_2, \ldots, n_i, \ldots) = \ln W(\bar{n}_1, \bar{n}_2, \ldots, \bar{n}_i, \ldots) - \sum_i \ln \bar{n}_i \, dn_i - \sum_i \frac{dn_i^2}{2\bar{n}_i}. \tag{2.4}$$

The condition for this quantity to be maximal is

$$\sum_i \ln \bar{n}_i \, dn_i = 0. \tag{2.5}$$

In addition to this equation, we take into account the relations following from equations (2.1) and (2.2) that

$$\sum_i dn_i = 0, \tag{2.6}$$

$$\sum_i \varepsilon_i \, dn_i = 0. \tag{2.7}$$

Equations (2.5), (2.6), and (2.7) allow us to determine the average number of particles in a given state. Multiplying equation (2.6) by $-\ln C$ and equation (2.7) by $1/T$, where C and T are characteristic parameters of this system, and adding the resulting equations, we have

$$\sum_i \left(\ln \bar{n}_i - \ln C + \frac{\varepsilon_i}{T} \right) dn_i = 0.$$

Because this equation is fulfilled for any dn_i, one can require that the expression in the parentheses equals zero. This leads to the following expression for the most probable number of particles in a given state:

$$\bar{n}_i = C \exp(-\varepsilon_i / T). \tag{2.8}$$

This formula is called the Boltzmann distribution.

We now want to determine the physical nature of the parameters C and T in equation (2.8) that follows from the additional equations (2.1) and (2.2). From equation (2.1) we have $C\Sigma_i \exp(-\varepsilon_i/T) = N$. This means that C is the normalization constant. The energy parameter T is called the system temperature and characterizes the average energy of a particle. Below we express this parameter in energy units, and hence we will not use the dimensioned proportionality factor—the Boltzmann constant $k = 1.38 \times 10^{-16}$ erg/K—as is often done. Thus the kelvin is the energy unit, equal to 1.38×10^{-16} erg (see Appendix 2).

We can prove that at large $\bar{n}_i$ the probability of observing a significant deviation from $\bar{n}_i$ is small. According to equations (2.4) and (2.5) the

requisite probability is

$$W(n_1, n_2, \ldots, n_i, \ldots) = W(\bar{n}_1, \bar{n}_2, \ldots, \bar{n}_i, \ldots)\exp\left(-\sum_i \frac{(n_i - \bar{n}_i)^2}{2\bar{n}_i}\right).$$

From this it follows that a significant shift of n_i from its average value $\bar{n}_i$ is $|n_i - \bar{n}_i| \sim \bar{n}_i^{\frac{1}{2}}$. Since $\bar{n}_i \gg 1$, the relative shift of the number of particles in one state is small: $|n_i - \bar{n}_i|/\bar{n}_i \sim 1/\bar{n}_i^{\frac{1}{2}}$. Thus the observed number of particles in a given state differs little from its average value.

2.3 STATISTICAL WEIGHT OF A STATE AND DISTRIBUTIONS OF PARTICLES IN GASES

In the above work, a subscript i related to one state of a particle. Below we consider a general case where i characterizes a set of degenerate states. We introduce the statistical weight g_i of a state that is one of a number of degenerate states i. For example, a diatomic molecule in a rotational state with the rotational quantum number J has the statistical weight $g_i = 2J + 1$, equal to the number of momentum projections on the molecular axis. Including the accounting for the statistical weight, equation (2.8) takes the form

$$\bar{n}_j = Cg_j\exp(-\varepsilon_j/T),$$

where C is the normalization factor and the subscript j refers to a group of states. In particular, this formula gives the relation between the number densities N_0 and N_j of particles in the ground and excited states, respectively:

$$N_j = N_0(g_j/g_0)\exp(-\varepsilon_j/T), \tag{2.9}$$

where ε_j is the excitation energy, and g_0 and g_j are the statistical weights of the ground and excited states.

We now determine the statistical weights of states in a continuous spectrum. The wave function of a free particle with a momentum p_x moving along the x-axis is given by $\exp(ip_x x/\hbar)$ (to within an arbitrary factor) if the particle is moving in the positive direction, and by $\exp(-ip_x x/\hbar)$ if the particle is moving in the negative direction. (The quantity $\hbar = 1.054 \times 10^{-27}$ erg s is the Planck constant h divided by 2π.) Suppose the particle is in a potential well with infinitely high walls. The particle can move freely in the region $0 < x < L$, and the wave function on the walls goes to zero. To construct a wave function that corresponds to free motion inside the well and goes to zero at the walls, we superpose the basic free-particle solutions, so

that $\psi = C_1 \exp(ip_x x/\hbar) + C_2 \exp(-ip_x x/\hbar)$. From the boundary condition $\psi(0) = 0$ it follows that $\psi = C \sin(p_x x/\hbar)$, and from the second boundary condition $\psi(L) = 0$ we obtain $p_x L/\hbar = \pi n$, where n is an integer. This procedure thus yields the allowed quantum energies for a particle moving in a rectangular well with infinitely high walls.

From this it follows that the number of states for a particle with a momentum in the range from p_x to $p_x + dp_x$ is given by $dn = L\,dp_x/(2\pi\hbar)$, where we take into account the two directions of the particle momentum. For a space interval dx, the number of particle states is

$$dn = \frac{dp_x\,dx}{2\pi\hbar}. \tag{2.10a}$$

Generalizing to the three-dimensional case, we obtain

$$dn = \frac{dp_x\,dx}{2\pi\hbar}\frac{dp_y\,dy}{2\pi\hbar}\frac{dp_z\,dz}{2\pi\hbar} = \frac{d\mathbf{p}\,d\mathbf{r}}{(2\pi\hbar)^3}. \tag{2.10b}$$

Here and below we use the notation $d\mathbf{p} = dp_x\,dp_y\,dp_z$, $d\mathbf{r} = dx\,dy\,dz$. The quantity $d\mathbf{p}\,d\mathbf{r}$ is called a differential element of the *phase space*, and the number of states in Eqs. (2.10) is the statistical weight of the continuous spectrum states, because it is the number of states for an element of the phase space.

Let us consider now some cases of the Boltzmann distribution of particles. First we analyze the distribution of diatomic molecules in vibrational and rotational states. The excitation energy for the vth vibrational level from the ground state of the molecule is given by $\hbar\omega v$ if the molecule is modeled by a harmonic oscillator. Here $\hbar\omega$ is the energy difference between neighboring vibrational levels. On the basis of Eq. (2.9) we have

$$N_v = N_0 \exp(-\hbar\omega v/T), \tag{2.11}$$

where N_0 is the number density of molecules in the ground vibrational state. Because the total number density of molecules is

$$N = \sum_{v=0}^{\infty} N_v = N_0 \sum_{v=0}^{\infty} \exp\left(-\frac{\hbar\omega v}{T}\right) = \frac{N_0}{1 - \exp(-\hbar\omega/T)},$$

the number density of excited molecules is then

$$N_v = N\frac{\exp(-\hbar\omega v/T)}{1 - \exp(-\hbar\omega/T)}. \tag{2.12}$$

The excitation energy of the rotational state with angular momentum J is given by $BJ(J+1)$, where B is the rotational constant of the molecule. The

statistical weight of this state is $2J + 1$. Using the normalization condition $\Sigma_J N_{vJ} = N_v$ and assuming $B \ll T$ (as is usually the case), the number density of molecules in a given vibrational–rotational state is

$$N_{vJ} = N_v\left(\frac{B}{T}\right)(2J + 1)\exp\left(-\frac{BJ(J + 1)}{T}\right). \tag{2.13}$$

As an example of the particle distribution in an external field, let us consider the distribution of particles in the Earth's gravitational field. In this case Eq. (2.9) gives $N(x) \sim \exp(-U/T)$, where U is the potential energy of the particle in the external field. For the gravitational field we have $U = mgh$, where m is the mass of the molecule, g is the free-fall acceleration, and h is the altitude above the Earth's surface. Equation (2.9) then has the form

$$N(h) = N(0)\exp(-mgh/T), \tag{2.14}$$

where $N(z)$ is the number density of molecules at an altitude z. This is called the *barometric distribution*. For atmospheric air at room temperature, we have $mg = 0.11\ \text{km}^{-1}$. That is, atmospheric pressure falls noticeably at altitudes of a few kilometers.

2.4 THE MAXWELL DISTRIBUTION

We now consider the velocity distribution of free particles. This distribution is the end result of energy-changing collisions of the particles. The Boltzmann formula (2.9) provides the necessary information. In the one-dimensional case, the particle energy is mv_x^2, and the statistical weight of this state is proportional to dv_x, that is, to the number $n(v_x)$ of particles whose velocity is in the interval from v_x to $v_x + dv_x$. Equation (2.9) then yields

$$n(v_x)dv_x = C\exp\left(-\frac{mv_x^2}{2T}\right)dv_x,$$

where C is the normalization factor. Correspondingly, in the three-dimensional case we have

$$n(v)d\mathbf{v} = C\exp\left(-\frac{mv^2}{2T}\right)d\mathbf{v},$$

where the vector $\mathbf{v}$ has components v_x, v_y, v_z; $d\mathbf{v} = dv_x\,dv_y\,dv_z$; and the kinetic energy of the particle $mv^2/2$ is the sum of the kinetic energies for all the directions of motion. In particular, for the number density of particles $N(\mathbf{v})$ we have, after using the normalization condition,

$$N(\mathbf{v}) = N\left(\frac{m}{2\pi T}\right)^{3/2}\exp\left(-\frac{mv^2}{2T}\right), \tag{2.15}$$

where N is the total number density of particles. When we introduce the function $\varphi(v_x) \sim n(v_x)$, normalized so that

$$\int_{-\infty}^{\infty} \varphi(v_x)\, dv_x = 1, \qquad \varphi(v_x) = \left(\frac{m}{2\pi T}\right)^{1/2} \exp\left(-\frac{mv_x^2}{2T}\right), \tag{2.16}$$

then

$$N(\mathbf{v}) = N\varphi(v_x)\varphi(v_y)\varphi(v_z) = N\left(\frac{m}{2\pi T}\right)^{3/2} \exp\left(-\frac{mv^2}{2T}\right).$$

These particle velocity distributions are called Maxwell distributions. The average kinetic energy of particles following from Eq. (2.15) is

$$\tfrac{1}{2}m\overline{v^2} = \tfrac{1}{2}m\overline{v_x^2} + \tfrac{1}{2}m\overline{v_y^2} + \tfrac{1}{2}m\overline{v_z^2} = \tfrac{3}{2}m\overline{v_x^2}.$$

This is to be combined with the result

$$\begin{aligned}\frac{1}{2}m\overline{v_x^2} &= \frac{\int_{-\infty}^{\infty} (mv_x^2/2)\exp\left[-mv_x^2/(2T)\right] dv_x}{\int_{-\infty}^{\infty} \exp\left[-mv_x^2/(2T)\right] dv_x} \\ &= -\frac{d}{d(1/T)} \ln \int_{-\infty}^{\infty} \exp\left(-\frac{mv_x^2}{2T}\right) dv_x \\ &= -\frac{d}{d(1/T)} \ln\left(aT^{1/2}\right) = \frac{T}{2},\end{aligned}$$

where the constant a does not depend on the temperature. Thus, the particle kinetic energy per degree of freedom is $T/2$, and correspondingly the average particle kinetic energy in the three-dimensional space is $m\overline{v^2}/2 = 3T/2$. These relations can be used as the definition of the temperature.

2.5 THE SAHA DISTRIBUTION

We considered above the distributions of gas particles in bound or free states. Now we analyze the specific distribution for plasma systems that contain both bound and free electron states. We must examine the equilibrium between continuous and discrete electron states. This equilibrium is maintained by the processes

$$\mathrm{A}^+ + e \leftrightarrow \mathrm{A},$$

where e is the electron, A^+ is the ion, and A is the atom. We consider a quasineutral plasma in which the electron and ion number densities are the same.

Consider an ionized gas in a volume Ω, and denote the average number of electrons, ions and atoms in this volume by n_e, n_i, and n_a respectively (and note that $n_e = n_i$ here). Equation (2.9) gives the ratio between free and bound states of electrons as

$$\frac{n_i}{n_a} = \frac{g_e g_i}{g_a} \frac{1}{(2\pi\hbar)^3} \int \exp\left(-\frac{J + p^2/2m_e}{T}\right) d\mathbf{p}\, d\mathbf{r}.$$

Here $g_e = 2$, g_i, and g_a are the statistical weights of electrons, ions, and atoms corresponding to their electronic states, J is the atomic ionization potential, and p is the free-electron momentum, so that $J + p^2/(2m_e)$ is the energy of transition from the ground state of the atom to a given state of a free electron. It is assumed that atoms are to be found only in the ground state.

Integration of this expression over electron momenta yields

$$\frac{n_i}{n_a} = \frac{g_e g_i}{g_a} \left(\frac{m_e T}{2\pi\hbar^2}\right)^{3/2} \exp\left(-\frac{J}{T}\right) \int d\mathbf{r}.$$

Integrating over the volume, we take into account that transposition of the states of any pair of electrons does not change the state of the electron system. Therefore $\int d\mathbf{r} = \Omega/n_e$. Introducing the number densities of electrons ($N_e = n_e/\Omega$), ions ($N_i = n_i/\Omega$), and atoms ($N_a = n_a/\Omega$), we deduce for ionization equilibrium that

$$\frac{N_e N_i}{N_a} = \frac{g_e g_i}{g_a} \left(\frac{m_e T}{2\pi\hbar^2}\right)^{3/2} \exp\left(-\frac{J}{T}\right). \tag{2.17}$$

This result is called the *Saha distribution.*

We can write the Saha distribution in the form of the Boltzmann distribution (2.9) as

$$\frac{N_i}{N_a} = \frac{g_c}{g_a} \exp\left(-\frac{J}{T}\right), \tag{2.18}$$

where

$$g_c = \frac{g_e g_i}{N_e} \left(\frac{m_e T}{2\pi\hbar^2}\right)^{3/2}$$

is the effective statistical weight of the continuous spectrum. For an ideal plasma, this statistical weight is rather large because the electron number density N_e is small compared to a typical atomic number density. This leads to the following conclusions: Even at relatively small temperatures, $T \ll J$, some atomic ionization occurs. However, the probability of atomic excitation is very small at these temperatures; that is, the number density of excited atoms is small. Hence, at these temperatures, atoms are either in the ground state or are ionized.

2.6 DISSOCIATIVE EQUILIBRIUM IN MOLECULAR GASES

Equilibrium between atoms and molecules in a molecular gas is maintained by the processes

$$X + Y \leftrightarrow XY.$$

This equilibrium bears an analogy to the equilibrium between discrete and continuous spectral states corresponding to bound and free states of atoms. We can find the relation between the equilibrium number densities of atoms and molecules in this case by analogy with the Saha distribution. On the basis of Eq. (2.17), we can express the relationship between the number densities of atoms and molecules in the ground state as

$$\frac{N_X N_Y}{N_{XY}(v = 0, J = 0)} = \frac{g_X g_Y}{g_{XY}} \left(\frac{\mu T}{2\pi\hbar^2} \right)^{3/2} \exp\left(-\frac{D}{T} \right), \qquad (2.19)$$

where g_X, g_Y, and g_{XY} are the statistical weights of atoms and molecules with respect to their electron states, μ is the reduced mass of atoms X and Y, and D is the dissociation energy of the molecule.

In contrast to the ionization equilibrium of atoms, in this case most molecules are found in excited states. Using Eqs. (2.12) and (2.13), which connect the number density of molecules in the ground state to their total number density, we can transform Eq. (2.19) for dissociative equilibrium to the form

$$\frac{N_X N_Y}{N_{XY}} = \frac{g_X g_Y}{g_{XY}} \left(\frac{\mu T}{2\pi\hbar^2} \right)^{3/2} \left(\frac{B}{T} \right) \left[1 - \exp\left(-\frac{\hbar\omega}{T} \right) \right] \exp\left(-\frac{D}{T} \right), \qquad (2.20)$$

where N_{XY} is the total molecular number density.

2.7 LAWS OF BLACKBODY RADIATION

An ionized gas contains excited atoms or molecules that emit radiation, so it is necessary to examine how the gas interacts with radiation. If the interaction of radiation with a gas is strong, the distance that an individual photon travels before being absorbed is small. Then we deal with so-called *equilibrium radiation*. Radiation in a vessel whose walls are at a temperature T will be absorbed and emitted by the walls, and these processes establish the equilibrium between the radiation and the walls of the vessel. This radiation is called *blackbody* radiation.

To calculate the average number of photons in a particular state, we use the fact that photons obey Bose–Einstein statistics. Therefore the presence of a photon in a given state does not depend on whether other photons of this energy are also in this state. Then according to the Boltzmann formula

(2.9), the relative probability that n photons of an energy $\hbar\omega$ are found in a given state is equal to $\exp(-\hbar\omega n/T)$. Thus the mean number of photons in this state is

$$\overline{n_\omega} = \frac{\Sigma_n n \exp(-\hbar\omega n/T)}{\Sigma_n \exp(-\hbar\omega n/T)} = \frac{1}{\exp(\hbar\omega/T) - 1}. \tag{2.21}$$

This formula is called the *Planck distribution.*

We introduce the spectral radiation density U_ω as the radiation energy per unit time and volume in a unit frequency range. We shall show below how this quantity can be determined. The radiation energy in the frequency interval from ω to $\omega + d\omega$ is $\Omega U_\omega \, d\omega$. Alternatively, this quantity can be expressed as $2\hbar\omega n_\omega \Omega \, d\mathbf{k}/(2\pi)^3$, where the factor 2 takes account of the two polarizations of an electromagnetic wave, $\mathbf{k}$ is the photon wave vector, n_ω is the number of photons in a single state, and $\Omega \, d\mathbf{k}/(2\pi)^3$ is the number of states in an element of the phase space. Using the dispersion relation $\omega = ck$ between the frequency ω and wave number k of the photon (c is the light velocity), the equivalence of these two aspects of the same quantity yields the result

$$U_\omega = \frac{\hbar\omega^3}{\pi^2 c^3} n_\omega. \tag{2.22}$$

When the Planck distribution (2.21) is inserted into Eq. (2.22), we obtain the Planck radiation formula

$$U_\omega = \frac{\hbar\omega^3}{\pi^2 c^3 [\exp(\hbar\omega/T) - 1]}. \tag{2.23}$$

In the limiting case $\hbar\omega \ll T$, this result transforms to the *Rayleigh–Jeans formula*

$$U_\omega = \frac{\omega^2 T}{\pi^2 c^3}, \qquad \hbar\omega \ll T. \tag{2.24}$$

This expression corresponds to the classical limit, and hence does not contain the Planck constant. The opposite limit yields the *Wien formula*

$$U_\omega = \frac{\hbar\omega^3}{\pi^2 c^3} \exp\left(-\frac{\hbar\omega}{T}\right), \qquad \hbar\omega \gg T. \tag{2.25}$$

We shall now apply Eq. (2.23) to find the radiative flux emitted by a blackbody surface. It may be defined as the flux of radiation coming from a hole in a cavity with perfectly absorbing walls when this cavity contains the

blackbody radiation. The blackbody surface emits an isotropic flux $c\int_0^\infty U_\omega\, d\omega$, so that the energy flux

$$\frac{d\Theta}{4\pi} c \int_0^\infty U_\omega\, d\omega$$

is radiated into the element of solid angle $d\Theta = d\varphi\, d\cos\theta$. Taking the projection of the radiation flux onto the direction perpendicular to the emitting surface, we find that the radiative flux leaving the emitting surface is

$$J = \int_0^{\pi/2} \int_0^\infty \frac{c}{4\pi} U_\omega\, d\omega\, 2\pi \cos\theta\, d\cos\theta = \frac{c}{4}\int_0^\infty U_\omega\, d\omega = \sigma T^4, \quad (2.26)$$

where θ is the angle between the normal to the surface and the direction of motion of an emitted photon. The constant σ is called the *Stefan–Boltzmann constant*. It is given by

$$\sigma = \frac{1}{4\pi^2 c^2 \hbar^3} \int_0^\infty \frac{1}{e^x - 1} x^3\, dx = \frac{\pi^2}{60 c^2 \hbar^3} = 5.67 \times 10^{-12} \frac{\text{W}}{\text{cm}^2\ \text{K}^4}.$$

Equation (2.26) is called the *Stefan–Boltzmann law*.

One can evaluate the functional dependence of the radiation flux (2.26) in a simple way on the basis of dimensionality considerations. The result must depend on the following parameters: T (the radiation temperature), $\hbar$ (the Planck constant), and c (the light velocity). From these parameters one can compose only one combination that has the dimension of a flux. It is $J \sim T^4 \hbar^{-3} c^{-2}$, consistent with Eq. (2.26).

2.8 IONIZATION EQUILIBRIUM IN AN AEROSOL PLASMA

Plasma properties can be influenced by the presence in the plasma of small particles on a variety of size scales, including atomic and molecular clusters. We shall refer to all such small bulk particles as aerosols, and to the plasma containing them as an aerosol plasma, although the size of the particles can have an influence on the plasma properties. One such plasma property is the ionization equilibrium. The presence of small particles in a hot gas may alter the ionization equilibrium because the electron binding energy with a surface is smaller than the ionization potential of atoms constituting this surface. For example, the ionization potential of copper is 7.73 eV, while its work function —the electron binding energy with a copper surface—is 4.40 eV. The corresponding values are 7.58 and 4.3 eV for silver, and 3.89 and 1.81 eV for cesium. Thus the presence of such particles in a hot vapor alters the equilibrium density of charged particles. We assume in the following that electrons in a hot gas or vapor result from small particles only. Our goal is to

determine the equilibrium charge of these particles and the number density of electrons in a plasma.

For simplicity we assume all particles to be spherical and to have the same radius r_0. This radius is taken to be sufficiently large that

$$r_0 \gg e^2/T. \tag{2.27}$$

This criterion allows us to consider a particle as bulk matter, rather than needing to describe its microscopic properties. The addition of a single electron to the aerosol particle makes only a slight difference in the electric potential of the particle. We use this fact to write the relationship between the number densities of particles n_Z and n_{Z+1} that possess charges Z and $Z + 1$ respectively. By analogy with the Saha distribution (2.17), we have

$$\frac{n_Z N_e}{n_{Z+1}} = 2\left(\frac{m_e T}{2\pi\hbar^2}\right)^{3/2} \exp\left(-\frac{W_Z}{T}\right), \tag{2.28}$$

where W_Z is the electron binding energy for the particle with the charge Z, N_e is the electron number density, and the factor 2 takes account of the electron statistical weight (two spin projections). The electron binding energy W_Z for a charged particle is the sum of the electron binding energy W_0 for the neutral particle of a given material and the potential energy of the charged particle. Using the electric potential for a particle of charge $Z + \frac{1}{2}$ (the average between Z and $Z + 1$), we have

$$W_Z = W_0 + \left(Z + \tfrac{1}{2}\right)e^2/r_0.$$

Substituting this into Eq. (2.28) transforms it to the form

$$\frac{n_Z N_e}{n_{Z+1}} = 2\left(\frac{m_e T}{2\pi\hbar^2}\right)^{3/2} \exp\left(-\frac{W_0}{T} - \frac{\left(Z + \frac{1}{2}\right)e^2}{r_0 T}\right). \tag{2.29}$$

This relation gives the charge distribution of the charged particles. If the average charge is large, this distribution is sharp. Specifically, introducing n_0 —the number density of neutral particles—into Eq. (2.29) leads to

$$n_Z = n_{Z-1} A \exp\left(-\frac{Ze^2}{r_0 T}\right) = n_0 A^Z \exp\left(-\frac{Z^2 e^2}{2r_0 T}\right),$$

where $A = (2/N_e)[m_e T/(2\pi\hbar^2)]^{3/2} \exp(-W_0/T)$. For charges that are close to the average, this relationship is conveniently written in the form

$$n_Z = n_{\bar{Z}} \exp\left(-\frac{(Z - \bar{Z})^2}{2\Delta Z^2}\right),$$

where $\Delta Z^2 = r_0 T/e^2 \gg 1$ because of (2.27). The average charge of the particles follows from the relation $\bar{Z}e^2/(r_0 T) = \ln A$, which gives

$$\bar{Z} = \frac{r_0 T}{e^2} \ln \left[\frac{2}{N_e} \left(\frac{m_e T}{2\pi\hbar^2} \right)^{3/2} \exp\left(-\frac{W}{T} \right) \right]. \tag{2.30a}$$

This result must be combined with the condition for plasma quasineutrality if electrons result from ionization of small particles:

$$N_e = \bar{Z} n, \tag{2.30b}$$

where n is the total number density of particles. Combining these equations to remove the electron number density, we find the average charge of the particles to be

$$\bar{Z} = \frac{r_0 T}{e^2} \left\{ \ln \left[\frac{2}{\bar{Z} n} \left(\frac{m_e T}{2\pi\hbar^2} \right)^{3/2} \right] - \frac{W}{T} \right\}. \tag{2.31}$$

2.9 THERMOEMISSION OF ELECTRONS

For high temperature or large particle size, the parameter $Ze^2/(r_0 T)$ becomes small. For example, at $r_0 = 10$ μm and $T = 2000$ K, the very large particle charge $Z = 1200$ would be required to make this parameter unity. If the parameter is small, then it follows from Eq. (2.30a) that

$$N_e = \left(\frac{m_e T}{2\pi\hbar^2} \right)^{3/2} \exp\left(-\frac{W}{T} \right). \tag{2.32}$$

(Here and below we omit the subscript 0 on the work function W.) This is the *Richardson–Dushman formula*, describing the equilibrium density of electrons above a flat surface. In this case the electric potential of the particle is small compared to a typical thermal energy. Therefore the conditions near the particle and far from it are identical. Then the average particle charge is determined by Eq. (2.30b), where number densities of electrons and of particles are both known.

Equation (2.32) allows us to obtain a simple expression for the electron current from the surface of a hot cathode. In the case of equilibrium between electrons and a hot surface, the electron current from the surface is equal to the current toward it. Assuming the probability of electron attachment to the surface to become unity upon contact, we obtain for the electron current

TABLE 2.1. Parameters for Electron Thermoemission from Metals[a]

Material	A_R, A/(cm^2 K^2)	W, eV	T_b, K	i_b, A/cm^2
Ba	60	2711	1910	600
C	30	4.34	4070	2100
Cs	160	1.81	958	0.045
Cu	60	4.57	2868	4.6
Hf	14	3.53	5470	2.4×10^5
Mo	51	4.2	5070	8.8×10^4
Nb	57	3.96	5170	2.1×10^5
Pd	60	4.99	3830	240
Re	720	4.7	5870	2.3×10^6
Ta	55	4.2	5670	3.3×10^5
Th	70	3.38	4470	2.2×10^5
Ti	60	3.86	3280	750
W	75	4.5	5740	2.8×10^5
Y	100	3.27	3478	3.5×10^3
Zr	330	4.12	4650	2.4×10^5

[a]The boiling point of elemental materials is T_b, and i_b is the electron thermoemission current at the boiling point (Neuman 1987).

density towards the surface (equal to the electron current density from the surface)

$$i = e\left(\frac{T}{2\pi m_e}\right)^{1/2} N_e = \frac{em_e T^2}{4\pi^2\hbar^3}\exp\left(-\frac{W}{T}\right). \tag{2.33}$$

This result is also known as the Richardson–Dushman formula, and this type of emission is called *thermoemission* of electrons. For the analysis of gaseous discharge problems, it is convenient to rewrite the Richardson–Dushman formula (2.33) for the thermoemission current density in the form

$$i = A_R T^2 \exp(-W/T), \tag{2.34}$$

wherein the Richardson parameter A_R, according to Eq. (2.33), has the value 120 A/(cm^2 K^2). Table 2.1 contains the values of this parameter for real metals. In this table W is the metal's work function, T_b is its boiling point, and i_b is the current density at the boiling point.

2.10 THE TREANOR EFFECT

A weakly ionized gas can be regarded as a system of weakly interacting atomic particles. This system can be divided into subsystems, and in the first approximation each subsystem can be considered as an independent closed

system. The next approximation, taking account of a weak interaction between subsystems, makes it possible to establish connections among subsystem parameters. There are a variety of ways in which this connection can be done, with the selection depending on the nature of the problem. Often it is convenient to divide an ionized gas into atomic and electronic subsystems. Energy exchange in electron–atom collisions is slight due to the large difference in their masses, so equilibrium within the atomic and electronic subsystems is established separately. If a weakly ionized gas is in an external electric or electromagnetic field, the result is different electronic and atomic temperatures. It means that both atoms and electrons can be characterized by Maxwell distributions for their translational energies, but with different mean energies.

Another example of weakly interacting subsystems, which we shall consider below, relates to a molecular gas in which exchange of vibrational energy between colliding molecules has a resonant character. This is a more effective process than collisions of molecules with transitions wherein vibrational energy is transferred to excitations in rotational and translational degrees of freedom. If vibrational and translational degrees of freedom are excited or are cooled in different ways, then different vibrational and translational temperatures will exist in such a molecular gas. This situation occurs in gas-discharge molecular lasers, where vibrational degrees of freedom are excited selectively; and in gasdynamical lasers, where rapid cooling of translational degrees of freedom occurs as a result of expansion of a gas. The same effect occurs in shock waves and as a result of the expansion of jets. There is a thus a wide variety of situations where a molecular gas is characterized by different vibrational and translational temperatures. However, the resonant character of exchange of vibrational excitation takes place only for weakly excited molecules. At moderate excitations, the resonant character is lost because of molecular anharmonicity. This leads to a particular type of distribution of molecular states, which we shall now analyze.

We consider a nonequilibrium gas consisting of diatomic molecules where the translational temperature T differs from the vibrational temperature T_v. The equilibrium between vibrational states is maintained by resonant exchange of vibrational excitations in collisions of molecules, as expressed by

$$M(\upsilon_1) + M(\upsilon_2) \leftrightarrow M(\upsilon_1') + M(\upsilon_2'), \tag{2.35}$$

where the quantities in the parentheses are vibrational quantum numbers. Assuming molecules to be harmonic oscillators, we obtain from this the condition

$$\upsilon_1 + \upsilon_2 = \upsilon_1' + \upsilon_2'.$$

The excitation energy of a vibrational level is

$$E_\upsilon = \hbar\omega\left(\upsilon + \tfrac{1}{2}\right) - \hbar\omega x_e\left(\upsilon + \tfrac{1}{2}\right)^2,$$

where ω is the harmonic oscillator frequency, and x_e is the anharmonicity parameter. The second term of this expression is related to the establishment

of equilibrium in the case being considered, where translational and vibrational temperatures are different. Specifically, the equilibrium condition (2.35) leads to the relation

$$N(\upsilon_1)N(\upsilon_2)k(\upsilon_1,\upsilon_2 \to \upsilon_1',\upsilon_2') = N(\upsilon_1')N(\upsilon_2')k(\upsilon_1',\upsilon_2' \to \upsilon_1,\upsilon_2),$$

where $N(\upsilon)$ is the number density of molecules in a given vibrational state, and $k(\upsilon_1,\upsilon_2 \to \upsilon_1',\upsilon_2')$ is the rate constant of a given transition. Because these transitions are governed by the translational temperature, the equilibrium condition gives

$$k(\upsilon_1,\upsilon_2 \to \upsilon_1',\upsilon_2') = k(\upsilon_1',\upsilon_2' \to \upsilon_1,\upsilon_2)\exp(\Delta E/T),$$

where $\Delta E = \Delta E(\upsilon_1) + \Delta E(\upsilon_2) - \Delta E(\upsilon_1') - \Delta E(\upsilon_2')$ is the difference of the energies for a given transition, and $\Delta E(\upsilon) = -\hbar\omega x_e(\upsilon + \frac{1}{2})^2$. From this, one finds the number density of excited molecules to be

$$N(\upsilon) = N_0\exp\left(-\frac{\hbar\omega\upsilon}{T_\upsilon} + \frac{\hbar\omega x_e\upsilon(\upsilon+1)}{T}\right), \tag{2.36}$$

where N_0 is the number density of molecules in the ground vibrational state. This formula is often called the *Treanor distribution.*

Equation (2.36) gives a nonmonotonic population of vibrational levels as a function of the vibrational quantum number. Assuming the minimum of this function to correspond to large vibrational numbers, we have for the position of the minimum

$$\upsilon_{\min} = \frac{1}{2x_e}\frac{T}{T_\upsilon} \gg 1, \tag{2.37}$$

and the minimum number density of excited molecules is given by

$$N(\upsilon_{\min}) = N_0\exp\left(-\frac{\hbar\omega\upsilon_{\min}}{2T_\upsilon}\right).$$

Below we give the values of the first factor in Eq. (2.37) for some molecules:

Molecule	H_2	OH	CO	N_2	NO	O_2
$1/(2x_e)$	18	22	82	84	68	66

The effect considered is remarkable at $\upsilon \sim 10$ in terms of the distinction between vibrational and translational temperatures.

Thus, the special feature of the Treanor effect is that at high vibrational excitations, collisions of molecules with transfer of vibrational excitation energy to translational energy become effective. This causes a mixing of

vibrational and translational subsystems, and invalidates the Boltzmann distribution for excited states as a function of vibrational temperature. Note that the model employed is not valid for very large excitations because of the vibrational relaxation processes.

2.11 NORMAL DISTRIBUTION

A commonly encountered case in plasma physics as well as in other types of physics is one in which a variable changes by small increments, each of which occurs randomly, and the distribution of the variable after many steps is studied. Examples of this are the diffusive motion of a particle and the energy distribution of electrons in a gas. This energy distribution as it occurs in a plasma results from collisions of electrons with atoms, with each collision between an electron and an atom leading to an energy exchange between them that is small because of the large difference in their masses. Thus, in a general statement of this problem, we seek the probability that some variable z has a given value after $n \gg 1$ steps, if the distribution for each step is random and its parameters are given.

Let the function $f(z, n)$ be the probability that the variable has a given value after n steps, with $\varphi(z_k)\,dz_k$ the probability that after the kth step the change of the variable lies in the interval between z_k and $z_k + dz_k$. Since the functions $f(z)$ and $\varphi(z)$ are probabilities, they are normalized by the condition

$$\int_{-\infty}^{\infty} f(z, n)\,dz = \int_{-\infty}^{\infty} \varphi(z)\,dz = 1.$$

By definition of the above functions we have

$$f(z, n) = \int_{-\infty}^{\infty} dz_1 \cdots \int_{-\infty}^{\infty} dz_n \prod_{k=1}^{n} \varphi(z_k),$$

and

$$z = \sum_{k=1}^{n} z_k. \tag{2.38}$$

We introduce the Fourier transforms

$$G(p) = \int_{-\infty}^{\infty} f(z)\exp(-ipz)\,dz,$$

$$g(p) = \int_{-\infty}^{\infty} \varphi(z)\exp(-ipz)\,dz, \tag{2.39}$$

which can be inverted to give

$$f(z) = \frac{1}{2\pi}\int_{-\infty}^{\infty} G(p)\exp(ipz)\,dp,$$

$$\varphi(z) = \frac{1}{2\pi}\int_{-\infty}^{\infty} g(p)\exp(ipz)\,dp.$$

Equation (2.39) yields

$$g(0) = \int_{-\infty}^{\infty} \varphi(z)\, dz = 1,$$

$$g'(0) = -i\int_{-\infty}^{\infty} z\varphi(z)\, dz = -i\overline{z_k}, \tag{2.40}$$

$$g''(0) = -\overline{z_k^2},$$

where $\overline{z_k}$, $\overline{z_k^2}$ are the mean shift and the mean squared shift of the variable after one step. From Eqs. (2.38) and (2.40) it follows that

$$G(p) = \int_{-\infty}^{\infty} \exp\left(-ip\sum_{k=1}^{n} z_k\right) \prod_{k=1}^{n} \varphi(z_k)\, dz_k = g^n(p),$$

and hence

$$f(z) = \frac{1}{2\pi}\int_{-\infty}^{\infty} g^n(p)\exp(ipz)\, dp = \frac{1}{2\pi}\int_{-\infty}^{\infty} \exp(n\ln g + ipz)\, dp.$$

Since $n \gg 1$, the integral converges at small p. Expanding $\ln g$ in a power series in p, we have

$$\ln g = \ln\left(1 - i\overline{z_k}p - \frac{\overline{z_k^2}p^2}{2}\right) = -i\overline{z_k}p - \frac{\overline{z_k^2}p^2}{2} + \frac{(\overline{z_k})^2 p^2}{2},$$

which gives the result

$$f(z) = \frac{1}{2\pi}\int_{-\infty}^{\infty} \exp\left(ip(n\overline{z_k} - z) - \frac{n\overline{z_k^2}p^2}{2}\right) dp$$

$$= \frac{1}{\sqrt{2\pi\Delta^2}} \exp\left(-\frac{(z-\bar{z})^2}{2\Delta^2}\right). \tag{2.41}$$

In this expression, $\bar{z} = n\overline{z_k}$ is the mean shift of the variable for n steps, $\overline{z^2} = n\overline{z_k^2}$, and $\Delta^2 = \overline{z^2} - (\bar{z})^2$ is the root-mean-square deviation of this value. Formula (2.41) is called the normal distribution, or the *Gaussian distribution.* It is valid if the principal contribution to the integral (2.40) comes from small values of p, that is, if $\overline{z_k}p \ll 1$ and $\overline{z_k^2}p^2 \ll 1$. Because this integral is determined by $n\overline{z_k^2}p^2 \sim 1$, the Gaussian distribution is valid for a large number of steps $n \gg 1$.

CHAPTER 3

THE IDEAL PLASMA

3.1 CONDITIONS FOR AN IDEAL PLASMA

We shall consider primarily a plasma whose properties are similar to those of a gas. As in a gas, each particle of the plasma will follow a straight trajectory as a free particle most of the time. These free-particle intervals will occasionally be punctuated by strong interactions with surrounding particles that will cause a change in energy and direction of motion. This situation obtains if the mean interaction potential of the particle with its neighbors is small compared to the mean kinetic energy of the particle. This is the customary description of the gaseous state of a system, and a plasma that also satisfies this description is called an ideal plasma.

We now wish to formulate a quantitative criterion for a plasma to be ideal. The Coulomb interaction potential between two charged particles has the absolute value $|U(R)| = e^2/R$, where e is the charge of an electron or singly charged ion, and R is the distance between interacting particles. Thus the interaction potential at the mean distance between particles ($R_0 \sim N_e^{-1/3}$) is equal to $|U| \sim e^2 N_e^{1/3}$, and because the mean thermal energy of the particles is of the order of T (the plasma temperature expressed in energy units), the condition for a plasma to be ideal is

$$\gamma = N_e e^6/T^3 \ll 1, \tag{3.1}$$

where γ is called the plasma parameter. In the following, we shall deal primarily with a plasma whose parameters satisfy the relation (3.1).

3.2 CHARGED PARTICLES IN A GAS

We define a weakly ionized gas as a gas with a small concentration of charged particles. Nevertheless, some properties of the weakly ionized gas are governed by the charged particles. For example, the degree of ionization of power discharge molecular lasers is 10^{-7}–10^{-5}. In these lasers, the energy is first transferred from an external source of energy to electrons, and then it is transformed to the energy of laser radiation. As we shall see, a relatively small concentration of electrons determines the operation of this system.

Some properties of a weakly ionized gas are determined by the interaction between charged and neutral particles, while other properties are due to charged particles only. Though the concentration of charged particles in a plasma is small, the long-range Coulomb interaction between them may be more important than a short-range interaction between neutral particles. We consider below the plasma properties that are associated with the presence of charged particles. The short-range interaction of neutral particles is not important for these properties.

3.3 PENETRATION OF ELECTRIC FIELDS INTO PLASMAS

We wish to study the penetration of an externally produced electric field into a plasma. Since this field leads to a redistribution of the charged particles of a plasma, it creates an internal electric field that opposes the external field. This has the effect of screening the plasma from the external field. To analyze this effect, we begin with the fact that an electric field in a plasma is determined by the Poisson equation

$$\nabla \cdot \mathbf{E} = -\Delta\varphi = 4\pi e(N_i - N_e). \tag{3.2}$$

Here $\mathbf{E} = -\nabla\varphi$ is the electric field strength, φ is the potential of the electric field, N_e and N_i are the number densities of electrons and ions respectively, ions are assumed to be singly charged, and Δ is the Laplacian operator. The effect of an electric field is to cause a redistribution of charged particles. According to the Boltzmann formula (2.9), the ion and electron number densities are given by

$$N_i = N_0 \exp(-e\varphi/T), \qquad N_e = N_0 \exp(e\varphi/T), \tag{3.3}$$

where N_0 is the average number density of charged particles in a plasma, and T is the plasma temperature. Substitution of Eqs. (3.3) into the Poisson equation (3.2) gives

$$\Delta\varphi = 8\pi N_0 e \sinh(e\varphi/T).$$

Assuming that $e\varphi \ll T$, we can transform this equation to

$$\Delta\varphi = \varphi / r_D^2, \tag{3.4}$$

where

$$r_D = \left(\frac{T}{8\pi N_e e^2} \right)^{1/2} \tag{3.5}$$

is the so-called *Debye–Hückel radius.*

The solution of Eq. (3.4) describes an exponential decrease with distance from the plasma boundary. For example, if an external electric field penetrates through a flat boundary of a uniform plasma, the solution of equation (3.5) has the form $\mathbf{E} = \mathbf{E}_0 \exp(-x/r_D)$, where x is the distance from the plasma boundary in the normal direction.

When the electron and ion temperatures are different, then Eq. (3.3) has the form

$$N_i = N_0 \exp(-e\varphi/T_i), \qquad N_e = N_0 \exp(e\varphi/T_e),$$

and we will obtain the same results as above, except that the Debye–Hückel radius takes the more general form

$$r_D = \left[4\pi N_0 e^2 (1/T_e + 1/T_i) \right]^{-1/2}. \tag{3.6}$$

Now let us calculate the field from a test charge placed in a plasma. In this case the equation for the potential due to the charge has the form

$$\Delta\varphi \equiv \frac{1}{r} \frac{d^2}{dr^2}(r\varphi) = \frac{\varphi}{r_D^2},$$

where r is the distance from the charge considered. If this charge is located in a vacuum, the right-hand side of this equation is zero, and the solution has the form $\varphi = q/r$, where q is the value of the charge. Requiring the solution of the above equation to be coincident with this one at $r \to 0$, we obtain for the potential of a test charged particle in a plasma

$$\varphi = \frac{q}{r} \exp\left(-\frac{r}{r_D} \right). \tag{3.7}$$

Thus, the Debye–Hückel radius is a typical distance at which fields in a plasma are shielded by its charged particles. The field of a charged particle is eliminated on this scale by fields of surrounding particles.

Now we shall check the validity of the condition $e\varphi \ll T$, which allowed us to simplify the equation for the electric field strength. Because this

condition must work at distances of the order of r_D, it has the form

$$\frac{e^2}{r_D T} \sim \left(\frac{e^6 N_0}{T^3}\right)^{1/2} \ll 1.$$

This condition coincides with the condition (3.1) for an ideal plasma.

We can determine the number of charged particles that participate in shielding the field of a test particle. This value is of the order of magnitude of the number of charged particles located in a sphere of radius r_D. The number of charged particles is, to within a numerical factor,

$$r_D^3 N_0 \sim \sqrt{e^6 N_0 / T^3} \ll 1.$$

Thus this value is large for an ideal plasma.

We have shown that the Debye–Hückel radius is the fundamental parameter of an ideal quasineutral plasma. It is the distance over which a collection of charged particles of the plasma shields external electric fields or fields of individual plasma particles.

3.4 DEFINITION OF A PLASMA

Consider a gas-filled gap subjected to an external electric field. If the gas does not contain charged particles, the field is uniform in the gap. In the presence of charged particles in the gas, an external electric field is shielded near edges of the gap (see Fig. 3.1) over distances of the order of the Debye–Hückel radius. Thus the character of the distribution of the electric field inside the gas is different in these two cases. Note that here we assume the plasma to be quasineutral up to its boundaries, an assumption that can be violated in real cases. Based on the above considerations, one can define a plasma as a weakly ionized gas whose Debye–Hückel radius is small compared with its size L, that is,

$$L \gg r_D. \tag{3.8}$$

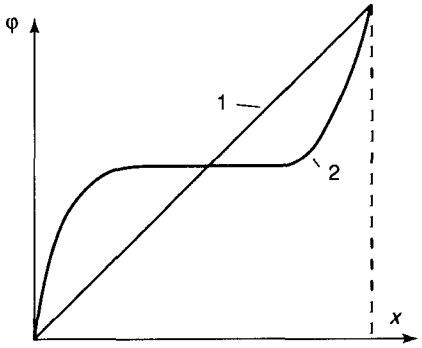

Figure 3.1 The electric potential distribution in a gap containing an ionized gas; for a Debye–Hückel radius large (curve 1) or small (curve 2) compared to the gap size.

TABLE 3.1. Parameters of Some Plasmas

Type of Plasma	N_e, cm^{-3}	T_e, K	r_D, cm	L, cm
E-layer of ionosphere	10^5	300	0.3	10^6
He–Ne laser	10^{11}	3×10^4	3×10^{-3}	1
Mercury lamp	10^{14}	5×10^4	3×10^{-5}	0.1
Sun's chromosphere	5×10^8–5×10^9	3×10^4–3×10^5	0.01–0.1	10^9
Lightning	10^{17}	3×10^4	3×10^{-6}	100

As an example, we can calculate the minimum density of charged particles in a plasma for a gap size of the order of 10 cm and for an electron temperature of $T_e \sim 1$ eV. We have an electron density $N_e \gg 10^4$ cm^{-3} for this case. This is a very small value (see Figs. 1.1 and 1.2). For example, the electron number density of a glow discharge lies in the range 10^7–10^{12} cm^{-3}. Table 3.1 contains parameters of some plasma types in terms of a typical number density N_e and temperature T_e of electrons, and also the Debye–Hückel radius r_D of the plasma and its size L. These examples are a representative sampling of real plasmas.

3.5 OSCILLATIONS OF PLASMA ELECTRONS

The Debye–Hückel radius is the parameter that characterizes an ideal quasineutral plasma. We can estimate a typical time for the response of a plasma to an external field. For this purpose we study the behavior of a uniform infinite plasma if all the plasma electrons are shifted at the initial time by a distance x_0 to the right, starting from a plane $x = 0$. This creates an electric field whose strength corresponds to the Poisson equation (3.2):

$$dE/dx = 4\pi e(N_i - N_e).$$

Assuming the electric field strength at $x < 0$ to be zero, the Poisson equation gives an electric field strength for $x > x_0$ of $E = 4\pi e N_0 x_0$, where N_0 is the average number density of charged particles in the plasma. The movement of all the electrons under the influence of the electric field leads to a change in the position of the boundary. The equation of motion for each of the electrons can be written as

$$m_e \frac{d^2(x + x_0)}{dt^2} = -eE,$$

where m_e is the electron mass, and x is the distance of an electron from the boundary. Because x is a random value, not dependent on the phenomenon

being considered, one can assume this value to be independent of time. Thus the equation of motion of an electron gives

$$d^2x_0/dt^2 = -\omega_p^2 x_0,$$

where the quantity

$$\omega_p = (4\pi N_0 e^2/m_e)^{1/2} \tag{3.9}$$

is called the *Langmuir*, or *plasma, frequency.*

The solution of the equation obtained predicts an oscillatory character for the electron motion. Accordingly, $1/\omega_p$ is a typical time for a plasma response to an external signal. Note that $r_D\omega_p = \sqrt{2T/m_e}$ is the thermal electron velocity. From this it follows that a typical plasma response time for an external signal is a time during which the electrons experience a displacement of the order of the Debye–Hückel radius. Thus we have two fundamental parameters of an ideal quasineutral plasma: the Debye–Hückel radius r_D, which is a shielding distance for fields in a plasma; and the plasma frequency ω_p, so that the value ω_p^{-1} is a typical time for the plasma to respond to external signals.

3.6 INTERACTIONS IN IDEAL PLASMAS

We now calculate the average interaction energy in an ideal plasma and the distribution function for the interaction energies of charged particles. Based on the interaction potential (3.7) for two charged particles, we have for its average value

$$\bar{U} = \int_0^\infty e\varphi\left[N_0 \exp\left(-\frac{e\varphi}{T}\right) - N_0 \exp\left(\frac{e\varphi}{T}\right)\right] d\mathbf{r}.$$

Equation (3.7) gives the electric potential φ from an individual plasma particle as

$$\varphi = (e/r)\exp(-r/r_D).$$

The above result for the mean interaction potential in an ideal plasma accounts for pairwise interactions of all the charged particles in a volume that have a Boltzmann distribution. In the case of an ideal plasma the principal contribution to the integral occurs at small interactions $e\varphi \ll T$, so that

$$\bar{U} = -\frac{2N_0}{T}\int_0^\infty (e\varphi)^2 4\pi r^2\, dr = -\frac{4\pi N_0 e^4 r_D}{T} = -\frac{e^2}{2r_D T}, \tag{3.10}$$

where we have used the expression (3.5) for the Debye–Hückel radius. Thus the average energy of a charged particle in an equilibrium plasma is

$$\bar{\varepsilon} = \frac{3T}{2} - \frac{e^2}{2r_D}. \tag{3.11}$$

To estimate fluctuations ΔU of the interaction potential for a charged particle in a plasma, we assume this value to be determined by positions of other charged particles in a sphere of the Debye–Hückel radius centered on the test particle. The mean number of charged particles in this region is $n \sim N_0 r_D^3 \gg 1$, with fluctuations of the order of $\sqrt{n}$. Hence the fluctuation of the interaction potential of the test charged particle in a plasma is

$$\Delta U \sim \sqrt{n}\, e^2/r_D \sim e^2 N_0^{1/2} r_D^{1/2}. \tag{3.12}$$

Since $\Delta U \gg U$, the distribution function for the interaction potentials yields $\overline{U} = 0$ and, according to Eq. (2.41), has the form

$$f(U) = (2\pi\, \Delta U^2)^{-1/2} \exp\left(-\frac{U^2}{2\Delta U^2}\right), \tag{3.13}$$

where $f(U)\, dU$ is the probability that the interaction potential lies in the interval from U to $U + dU$. The squared deviation of the distribution (3.13) is

$$\Delta U^2 = \overline{U^2} = 2\int_0^\infty (e\varphi)^2 N_0 4\pi r^2\, dr = 4\pi N_0 e^4 r_D = \overline{U}T \gg \overline{U}^2, \tag{3.14}$$

where the factor 2 takes into account the presence of charged particles of the opposite sign, and N_0 is the mean number density of charged particles of one sign. We see that an ideal plasma has

$$\overline{U} \ll \Delta U \ll T.$$

3.7 BEAM PLASMA

We return now to the example shown in Fig. 3.1, which we used for explaining the character of the distribution of an external electric field in an ideal quasineutral plasma. In this example, a plasma is assumed to have overall quasineutrality. In reality, plasma boundaries (called plasma sheaths) contain a nonneutral plasma. Plasma properties in this region depend on processes that occur there. If charged particles are generated by a metallic surface or charged particles recombine on walls, an intermediate layer of nonneutral plasma arises between the plasma and the surface. It is called a

double layer. A nonneutral plasma occurs also if charged particles are collected in certain regions, or traps, or if they are transported through space due to the action of external fields in the form of beams. The primary peculiarity of nonneutral plasma arises from the strong fields created by the particle charge, and that restrict the plasma density. As an illustration, we shall consider a classic example of nonneutral plasma formed near a hot cathode.

One can generate an electron beam in a simple way by heating a metallic surface in a vacuum, so that the surface emits an electron flux as a result of thermoemission (see Chapter 2). Using electric fields allows us to accelerate electrons and remove them from the surface in the form of a beam. But the parameters of this beam can be limited by internal electric fields that arise due to electron charges. We can find the properties of such a beam, created between two flat plates a distance L apart, with an electric potential U_0 between them.

The electron current density j is constant in the gap, because electrons neither are produced nor recombine in the gap. This gives

$$j = eN_e(x)v_e(x) = \text{const},$$

where x is the distance from the cathode, N_e is the electron number density, $v_e = \sqrt{2eU(x)/m_e}$ is the electron velocity, and the electric potential is zero at the cathode surface, that is, $U(0) = 0$. An electron charge creates an electric field that slows the electrons. We can analyze this connection. The electric field strength $E = -dU/dx$ satisfies the Poisson equation

$$\frac{dE}{dx} = -4\pi eN_e(x) = -4\pi j\sqrt{\frac{m_e}{2eU}}\,. \tag{3.15}$$

Multiplication of this equation by $E = -dU/dx$ provides an integrating factor that makes a simple integration possible. We obtain

$$E^2 = E_0^2 + 16\pi j\sqrt{\frac{m_e U}{2e}}\,, \tag{3.16}$$

where $E_0 = E(0)$.

We need to establish the boundary condition on the cathode. We consider the regime where the current density of the beam is small compared to the electron current density of thermoemission. This means that most of the emitted electrons return to the metallic surface, and the external electric field does not significantly alter the equilibrium between the emitted electrons and the surface. Then the boundary condition on the cathode is the same as in the absence of the external electric field, so that $E(0) = 0$. Equation (3.16) leads to the distribution of the electric potential in the gap,

given by

$$U = \left(9\pi j\sqrt{\frac{m_e}{2e}}\right)^{2/3} x^{4/3}.$$

This can be inverted to obtain the connection between the electron current density and the parameters of the gap:

$$j = \frac{2}{9\pi}\sqrt{\frac{e}{2m_e}}\,\frac{U_0^{3/2}}{L^2}. \tag{3.17}$$

This dependence is known as the *three-halves power law*. It shows how the behavior of an electron plasma in a space between plates is determined by an electric charge of this beam plasma.

CHAPTER 4

ELEMENTARY PLASMA PROCESSES

4.1 PARTICLE COLLISIONS IN PLASMAS

We begin by seeking to identify a parameter to characterize the elementary act of collision of two particles in a gas or plasma. Consider the collision of a test particle designated A with some other particle in the gas that is labeled B. The collision of these two particles can lead to a change in the internal state of particle A. The initial state of particle A will be designated by the subscript i, and the final state by f. We assume that each collision can result in transitions only between these states. Then the probability $P(t)$ that particle A remains in the initial state up to time t is given by

$$\frac{dP}{dt} = -\nu_{if} P, \tag{4.1}$$

where ν_{if} is the probability per unit time of a collisional transition.

A coordinate frame is employed in which the test particle A is motionless. The transition probability per unit time, ν_{if}, is proportional to the incident flux j of particles B. Hence, the ratio of these values, ν_{if}/j—the cross section for the process—is characteristic of the elementary act of particle collisions and does not depend on the number density of the particles B. If all the particles B move with the identical velocity $\mathbf{v}_B$, their flux is given by $|\mathbf{v}_A - \mathbf{v}_B|[B]$, where [B] is the number density of particles B, and $\mathbf{v}_A$ is the velocity of a particle A. Thus the transition frequency ν_{if} is connected with the transition cross section σ_{if} by the expression

$$\nu_{if} = [B]|\mathbf{v}_A - \mathbf{v}_B|\sigma_{if}, \tag{4.2}$$

where the cross section σ_{if} can depend on the relative velocity of the particles.

If particles A and B have definite velocity distributions, the transition probability per unit time has the form

$$\nu_{if} = [\mathrm{B}]\langle|\mathbf{v}_\mathrm{A} - \mathbf{v}_B|\sigma_{if}\rangle = [\mathrm{B}]\langle k_{if}\rangle, \tag{4.3}$$

where the angle brackets signify an average over relative velocities of the particles, and the quantity

$$k_{if} = \langle|\mathbf{v}_\mathrm{A} - \mathbf{v}_\mathrm{B}|\sigma_{if}\rangle$$

is called the *rate constant* of the process. This parameter also characterizes the elementary act of collision. The rate constant of the process is useful when we are interested in the frequency of transition averaged over the velocities of the particles.

We can write balance equations for the number density of particles A found in a given state i by taking into account transitions of the A-particle to other states. These equations have the form

$$\frac{dN_i}{dt} = [\mathrm{B}]\sum_f k_{fi}N_f - [\mathrm{B}]N_i\sum_f k_{if}, \tag{4.4}$$

where k_{if} is the rate constant for transitions between states i and f of the particle A resulting from collision with the particle B. The balance equations (4.4) can be extended to include other processes.

4.2 ELASTIC COLLISIONS

When two particles collide elastically, the internal states of the colliding particles remain unchanged. The particle motion is described by Newton's equations

$$M_1\frac{d^2\mathbf{R}_1}{dt^2} = -\frac{\partial U}{\partial \mathbf{R}_1}, \qquad M_2\frac{d^2\mathbf{R}_2}{dt^2} = -\frac{\partial U}{\mathbf{R}_2}.$$

Here $\mathbf{R}_1$ and $\mathbf{R}_2$ are the position vectors of the particles, M_1 and M_2 are their masses; and U is the interaction potential of the force between the particles, assumed to depend only on the relative position vector between them. That is, the potential has the form $U = U(\mathbf{R}_1 - \mathbf{R}_2)$. Then $-\partial U/\partial \mathbf{R}_j$ is the force acting on the particle j due to the other particle, and $\partial U/\partial \mathbf{R}_1 = -\partial U/\partial \mathbf{R}_2$.

We now introduce as new vector variables the location of the center of mass, $\mathbf{R}_c = (M_1\mathbf{R}_1 + M_2\mathbf{R}_2)/(M_1 + M_2)$, and the relative position vector, $\mathbf{R} = \mathbf{R}_1 - \mathbf{R}_2$. Newton's equations in terms of these variables are

$$(M_1 + M_2)\frac{d^2\mathbf{R}_c}{dt^2} = 0, \qquad \mu\frac{d^2\mathbf{R}}{dt^2} = -\frac{\partial U}{\partial \mathbf{R}},$$

where $\mu = M_1M_2/(M_1 + M_2)$ is the reduced mass of the particles. It can be seen that the center of mass travels with a constant velocity, and the scattering is determined by the character of the relative motion of the particles in the center-of-mass frame. Though the above analysis was made within the framework of classical mechanics, the situation in quantum mechanics is the same. That is, in quantum mechanics, free motion of the center of mass obtains in the absence of external fields, and collision is characterized by the relative coordinates. Thus, the problem of collisions of two particles reduces to the problem of the motion of one particle with a reduced mass in coordinates fixed to the center-of-mass frame of axes.

Figure 4.1 shows the trajectory of particles in the center-of-mass system when the central interaction potential depends only on the scalar distance between the particles, $|\mathbf{R}_1 - \mathbf{R}_2|$. The parameters of the collision are given in Fig. 4.1. We can determine the connection between the impact parameter ρ and the distance of closest approach r_0. Using conservation of momentum, the momentum $\mu\rho v$ at large distances between the particles is the same as the momentum $\mu v_\tau r_0$ at the distance of closest approach. Here $v = |\mathbf{v}_1 - \mathbf{v}_2|$ is the relative velocity of the particles, and v_τ is the tangential component of the velocity at the distance of closest approach, where the normal component of the velocity is zero. Energy conservation gives the relation $\mu v_\tau^2/2 = \mu v^2/2 - U(r_0)$. This leads to the expression

$$1 - \frac{\rho^2}{r_0^2} = \frac{U(r_0)}{\varepsilon}, \tag{4.5}$$

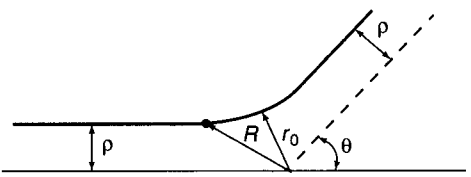

Figure 4.1 The trajectory of a particle in a central field in the center-of-mass frame of reference. $\mathbf{R}$ is the radius vector of the particle with the reduced mass μ, ρ is the impact parameter, θ is the scattering angle in the center-of-mass frame of reference, and r_0 is the distance of closest approach; that is, it is the minimum distance between particles for a given impact parameter.

where $\varepsilon = \mu v^2/2$ is the kinetic energy in the center-of-mass frame of reference.

The two-particle scattering process, when treated in the center-of-mass frame, can be considered as the motion of a single particle of the reduced mass μ in the field $U(R)$. The differential scattering cross section is the number of scattering events per unit time and unit solid angle divided by the flux of incident particles. In the case of a central force field the elementary solid angle is $d\Theta = 2\pi d(\cos\vartheta)$, and particles are scattered into this element of solid angle from the range of impact parameters between ρ and $\rho + d\rho$. The particle flux is Nv, where N is the number density of particles B and v is the relative velocity of collision; and the number of particles scattered per unit time into a given solid angle is $2\pi\rho\, d\rho\, Nv$, so the differential cross section is

$$d\sigma = 2\pi\rho\, d\rho. \tag{4.6}$$

Elastic scattering determines many gas and plasma parameters. For bulk parameters of an ionized gas, an averaged cross section is usually the quantity of most importance if these parameters are determined by large-angle scattering. We can estimate a typical scattering cross section for large angles. Then the interaction potential at the distance of closest approach is comparable to the kinetic energy of the colliding particles, and this cross section is given by the relation

$$\sigma = \pi\rho_0^2, \qquad \text{where} \quad U(\rho_0) \sim \varepsilon. \tag{4.7}$$

The averaged elastic scattering cross section most often used is the so-called diffusion, or transport, cross section, defined as

$$\sigma^* = \int (1 - \cos\vartheta)\, d\sigma, \tag{4.8}$$

where ϑ is the scattering angle. Small scattering angles are not significant for the diffusion cross section, since they appear in the integrand with a weight factor $\vartheta^2/2$. All the bulk parameters that are determined by electron–atom scattering are expressed through the diffusion cross section. Some transport parameters of a gas, such as the thermal conductivity and viscosity coefficients, are expressed through another averaged cross section, $\sigma^{(2)} = \int(1 - \cos^2\theta)\, d\sigma$, which is the other form of a scattering cross section at large angles. Often the name *gas-kinetic* cross section is used for the scattering cross section at large angles. At room temperatures it is of the order of 10^{-15} cm^2 (see Appendix 4). Since $\nu \sim Nv\sigma$ is the frequency of collision, its reciprocal $\tau \sim 1/\nu$ is the time between successive collisions, and $\lambda = v\tau \sim 1/(N\sigma)$ is the *mean free path*, that is, the distance traveled by an atom between two successive collisions.

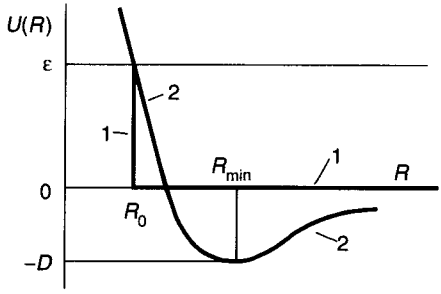

Figure 4.2 The interaction potential of two atoms (curve 2) and the model potential (curve 1) corresponding to the hard-sphere model.

Note that the case of the Coulomb interaction of particles is an exception to the conclusion that the main contribution to the diffusion scattering cross section of (4.8) is at large scattering angles, because in this case the cross section has a logarithmic divergence at small angles. If the collision proceeds in a plasma, minimum scattering angles are determined both by Debye–Hückel shielding of charges and by many-body scattering.

4.3 HARD-SPHERE MODEL

The interaction potential of two atoms as a function of the relative distance between them is given in Fig. 4.2. In order to understand the character of the scattering of atoms at large collision energies as a function of the depth D of the interaction well, a simple model for the interaction potential given in Fig. 4.2 is useful. This potential has the form

$$U(R) = \begin{cases} 0, & r > R, \\ \infty, & r < R, \end{cases} \tag{4.9}$$

where R_0 is the interaction radius of the atoms. This scattering model is called the *hard-sphere* model, and is used widely in the kinetics of neutral gases.

To determine the scattering cross section within the framework of the hard-sphere model, we can consult Fig. 4.3, which shows the dependence of the distance of closest approach on the impact parameter of the collision. In this case the scattering is like scattering from a hard spherical surface. From Fig. 4.4, the scattering angle is $\vartheta = \pi - 2\alpha$, where $\sin\alpha = \rho/R_0$, so that $\rho = R_0\cos(\vartheta/2)$. Equation (4.6) gives the differential cross section

$$d\sigma = 2\pi\rho\, d\rho = \left(\pi R_0^2/2\right) d(\cos\vartheta), \tag{4.10}$$

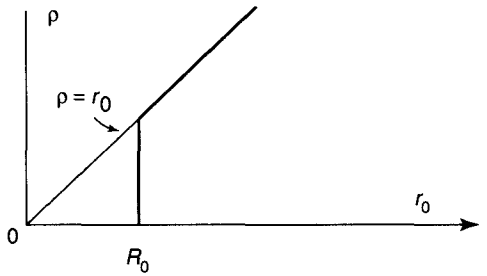

Figure 4.3 The dependence of the impact parameter on the distance of closest approach for the hard-sphere model.

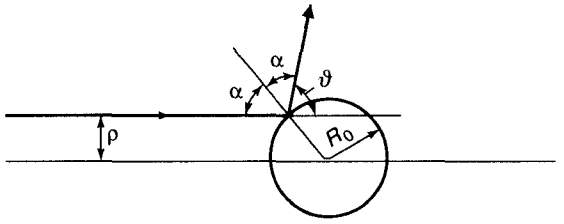

Figure 4.4 Scattering for the hard-sphere model: R_0 is the sphere radius, ϑ is the scattering angle, and the thick line is the particle trajectory.

which leads to the diffusion scattering cross section

$$\sigma^* = \pi R_0^2. \tag{4.11}$$

Equation (4.11) is in agreement with the estimate given in Eq. (4.7) for the scattering cross section.

4.4 CAPTURE CROSS SECTION

We now turn our attention to the other limiting case of atomic scattering: when the collision energy is small compared to the well depth D. The dependence on the distance of closest approach, calculated on the basis of Eq. (4.5), is given in Fig. 4.5. This curve is divided into two regions, whose boundary is marked with an arrow. Region 2 is not related to collisions of particles, and hence will not be considered. Effectively, the region of impact parameters is divided into two parts, and their boundary corresponds to the impact parameter ρ_c. At $\rho > \rho_c$, values of the impact parameter and the corresponding distance of closest approach are comparable. If the impact

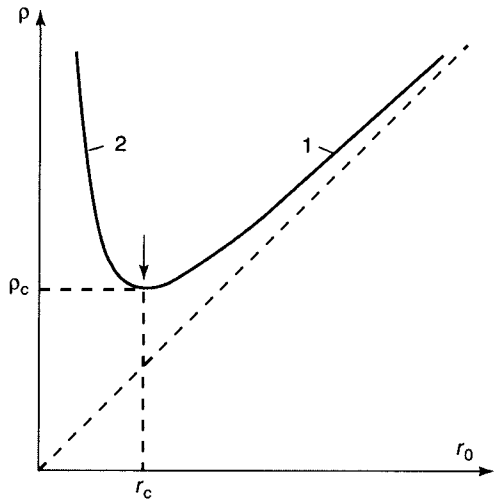

Figure 4.5 The dependence of the impact parameter on the distance of closest approach for an attractive interaction potential according to Eq. (4.5).

parameter is smaller than ρ_c, the distance of closest approach r_0 is close to r_{min}, defined by $U(r_{min}) = 0$. Then collision capture occurs, and the bound system reduces its size until finally a short-range repulsion halts the contraction.

Since the capture is governed by the long-range part of the interaction potential, we can approximate the interaction potential by the dependence $U(R) = -C/R^n$. The impact parameter for capture, ρ_c, is determined as the minimum of the dependence $\rho(r_0)$, and, according to Eq. (4.5), the capture cross section is

$$\sigma_c = \pi\rho_c^2 = \frac{\pi n}{n-2}\left(\frac{C(n-2)}{2\varepsilon}\right)^{2/n}. \tag{4.12}$$

The dependence of the cross section on parameters is like Eq. (4.7). In particular, in the case of polarization interaction of an ion and atom, $U(R) = -\beta e^2/(2R^4)$ (β is the atomic polarizability), the polarization capture cross section of an atom by an ion is

$$\sigma_c = 2\pi\left(\frac{\beta e^2}{\mu v^2}\right)^{1/2}. \tag{4.13}$$

The final result shows that particle capture is determined by a long-range part of the interaction potential. Specifically, Eq. (4.5) gives, for $r_0 = r_c$, $-U(r_c)/\varepsilon = 2/(n-2)$, and because $\varepsilon \ll D$, we have $|U(r_c)| \ll D$. That is,

the capture is determined by the long-range part of the interaction. Since usually we have $n \gg 1$, in the region $r_0 > r_c$ the interaction potential is small compared to the kinetic energy of the particles. This means that the main contribution to the capture cross section is for impact parameters $\rho < \rho_c$ that correspond to particle capture.

Capture of particles is associated with a strong interaction. In fact, since

$$r_c \sim r_{min}(D/\varepsilon)^{1/n} \gg r_{min},$$

then small distances between particles are reached in the capture process. At these distances an attractive interaction potential greatly exceeds the kinetic energy of the particles. A strong interaction of particles in this region is also associated with a strong scattering of particles. Therefore, one can assume that the capture of particles leads to their isotropic scattering, and the diffusion scattering cross section of Eq. (4.7) almost coincides with the capture cross section of (4.12). For instance, in the case of polarization interaction of particles, the diffusion cross section of particle scattering exceeds the capture cross section by about 10%.

4.5 TOTAL SCATTERING CROSS SECTION

The total cross section for elastic scattering is found by integrating the differential cross section over all solid angles: $\sigma_t = \int d\sigma$. In classical terms the total cross section must be infinite. Classical particles interact and are scattered at any distance between them, and scattering takes place at any impact parameter. Therefore, the classical total cross section will tend to infinity if Planck's constant $\hbar \to 0$.

We can evaluate the total collision cross section by assuming that the colliding particles are moving along classical trajectories. The variation of the particle's momentum is given by the expression

$$\Delta \mathbf{p} = \int_{-\infty}^{\infty} \mathbf{F}\, dt, \tag{4.14}$$

where $\mathbf{F} = -\partial U/\partial \mathbf{R}$ is the force with which one particle acts upon the other, and U is the interaction potential between the particles. From Eq. (4.14) it follows that $\Delta p \sim U(\rho)/v$, where ρ is the impact parameter. According to the Heisenberg uncertainty principle, the value of Δp can be determined up to an accuracy $\hbar/\rho$. Therefore, the principal contribution to the total scattering cross section is given by values of the impact parameter that satisfy the relation $\Delta p(\rho) \sim \hbar/\rho$. This leads to the estimate

$$\sigma_t \sim \rho_t^2, \qquad \text{where} \quad \frac{\rho_t U(\rho_t)}{\hbar v} \sim 1, \tag{4.15}$$

for the total scattering cross section. In particular, if $U(R) = C/R^n$, the total cross section is

$$\sigma_t \sim \left(\frac{C}{\hbar v}\right)^{2/(n-1)}. \tag{4.16}$$

Since the scattering cross section is determined by quantum effects, it approaches infinity in the classical limit. This is demonstrated by Eq. (4.16), which indeed approaches infinity in the limit $\hbar \to 0$.

Particle motion will obey classical laws if the kinetic energy ε satisfies the condition

$$\varepsilon \gg \hbar/\tau, \tag{4.17}$$

where τ is a typical collision time. Since $\tau \sim \rho/v$ and $\varepsilon = \mu v^2/2$, it follows that $l = \mu\rho v/\hbar \gg 1$, where l is the collisional angular momentum of the particles. If this criterion is fulfilled, the motion of the particles can be expected to follow classical trajectories. Furthermore, in this case the total cross section (4.15) is greatly in excess of the cross section σ for large-angle scattering given by Eq. (4.7). In particular, for a monotonic interaction potential $U(R)$ Eqs. (4.7) and (4.15) give $U(\rho_0)/U(\rho_t) \sim \mu\rho_t v/\hbar \gg 1$. It follows from the monotonicity of $U(R)$ that $\rho_t \gg \rho_0$, so that

$$\sigma_t \gg \sigma. \tag{4.18}$$

Note that if the condition (4.17) is not satisfied and the scattering has a quantum nature, then the large-angle scattering cross section and the total scattering cross section have the same order of magnitude. In particular, this is the situation for elastic scattering of electrons by atoms and molecules.

4.6 GASEOUS-STATE CRITERION

The condition that defines the gaseous state of a system of particles can be formulated in terms of the collision cross section. A gas is a system of particles with weak interactions among them. This means that each particle follows a straight trajectory most of the time. Only occasionally does a particle interact strongly enough with another particle to lead to large-angle scattering. This situation can be expressed by stating that the mean free path of a particle, $\lambda = 1/(N\sigma)$, is large compared to the interaction radius $\sqrt{\sigma}$. Thus, the condition to be satisfied for a system to be in a gaseous state is

$$N\sigma^{3/2} \ll 1. \tag{4.19}$$

We can analyze this problem from another standpoint. We can express the gaseous-state condition as

$$U(N^{-1/3}) \ll \mu v^2.$$

This criterion signifies a weakly interacting system, since the interaction potential of a test particle with its neighbors is small compared to its mean kinetic energy. The notation $U(N^{-1/3})$ signifies that the potential is evaluated at the mean distance between particles, $N^{-1/3}$. On the basis of this expression and Eq. (4.7), we have $U(N^{-1/3}) \ll U(\rho_0)$. For a monotonic interaction potential this is equivalent to $N^{-1/3} \gg \rho_0$, and that inequality returns us to the condition stated in Eq. (4.19).

The next step is to apply this criterion to a system of charged particles, that is, to a plasma. Because of the Coulomb interaction $|U(R)| = e^2/R$ between charged particles, Eq. (4.7) gives

$$\sigma \sim e^4/T^2 \tag{4.20}$$

for a typical large-angle scattering cross section, where T is the average energy of the particles. Specifically, T is their temperature expressed in energy units. The condition (4.19) for a collection of particles to be a true gas is transformed in the case of a plasma to

$$Ne^6/T^3 \ll 1,$$

where N is the number density of charged particles, and T is their temperature. This is the same as Eq. (3.1), the condition for a plasma to be ideal.

4.7 SLOW INELASTIC COLLISIONS

Collisions of atomic particles—ions, atoms, and molecules—are called *slow* collisions if the velocity of their relative motion is small compared to a typical internal atomic velocity v_e. (For the hydrogen atom, $v_e = e^2/\hbar$.) In this case the electron distribution in each of the colliding atomic particles responds primarily to the internal fields of the particles, and differs little from their distributions when the particles are at rest. Then one can analyze particle collisions within a framework of electron terms found by supposing that the nuclei of the particles are at rest. The electrons respond only as a function of the distances between them, as if the electrons were bound to fixed nuclei.

Transition between two electron terms is characterized by the ratio of the difference of their energies, $\Delta\varepsilon$, to the quantum indefiniteness in energy, $\hbar v/a$, where v is the collision velocity, and a is a typical distance between nuclei associated with a significant change of the corresponding terms. The

above criterion is expressed in terms of the Massey parameter

$$\xi = \frac{\Delta\varepsilon\, a}{\hbar v}. \tag{4.21}$$

If the Massey parameter is large, the probability of the corresponding transition is adiabatically small, that is, it behaves as $\exp(-c\xi)$, where $c \sim 1$ is a numerical coefficient. Therefore, transitions between electronic states in slow atomic collisions can be a result of intersections or pseudointersections of corresponding electron terms.

Consider as an example the charge exchange process

$$A^+ + B^- \rightarrow A^* + B. \tag{4.22}$$

In this case the Coulomb interaction takes place in the initial channel of the process, with only a weak interaction of neutral particles in the final channel. The intersection of electron terms takes place at the distance between nuclei given by

$$R_c = \frac{e^2}{J - EA}, \tag{4.23}$$

where EA is the electron binding energy in the negative ion B (the electron affinity of an atom B), and J is the ionization potential of the atom A. The transition transferring the electron from the field of one atomic particle to the other takes place near the intersection distance R_c.

Resonant collision processes are characterized by $\Delta\varepsilon = 0$ at infinite distances between colliding particles, and a small Massey parameter corresponds to these processes at finite distances between particles. Hence, resonant processes proceed effectively. One can consider a resonant process as an interference of the states between which the transition proceeds. Then the transition probability is ~ 1 if the phase shift $\int \Delta\varepsilon(R)\, dt/\hbar \sim 1$. Thus the cross section of a resonant process is of the order of R_0^2, where R_0 is the collision impact parameter for which the phase shift is of the order of unity, that is,

$$\sigma \sim \pi R_0^2, \qquad \text{where} \quad \int \Delta\varepsilon(R)\, dt/\hbar \sim 1. \tag{4.24}$$

Let us consider as an example the excitation transfer process

$$A^* + A \rightarrow A + A^*.$$

This process can cause broadening of spectral lines. The interaction potential of the atoms in the ground and excited states is $U \sim D^2/R^3$, where D is the matrix element of the dipole moment operator between these states, and R is

the distance between the atoms. From Eq. (4.24), the cross section of this process [$\sigma \sim R_0^2$, where $(D^2/R_0^3)(R_0/v) \sim \hbar$] is

$$\sigma = \frac{CD^2}{\hbar v}, \tag{4.25}$$

where $C \sim 1$. Because $D \sim ea_0$, where $a_0 = \hbar^2/(me^2)$ is the Bohr radius, and $v \ll e^2/\hbar$, it follows that $\sigma \gg a_0^2$. That is, the cross section is much larger than a typical atomic cross section.

4.8 AUTOIONIZING AND AUTODETACHING STATES IN COLLISION PROCESSES

Autoionizing and autodetaching states are of importance as intermediate states in collision processes. An autoionizing state is a bound state of an atom or positive ion whose energy is above the boundary of the continuous spectrum. Hence an electron can be released in the decay of such a state. For example, the autoionizing state $He(2s^2, {}^1S)$ is the state of the helium atom where both electrons are located in the excited $2s$ state. This autoionizing state can decay. As a result of such a decay one electron makes a transition to the ground state, and the other electron ionizes. The scheme of this process is

$$He(2s^2, {}^1S) \rightarrow He^+(1s, {}^2S) + e + 57.9\,eV. \tag{4.26}$$

An autodetaching state is identical to an autoionizing state, but occurs in a negative ion. The decay of such a state proceeds with the formation of a free electron and an atom or molecule. An example of an autodetaching transition is

$$H^-(2s^2, {}^1S) \rightarrow H(1s, {}^2S) + e + 9.56\,eV. \tag{4.27}$$

Formation of autoionizing and autodetaching states determines the character of some collision processes involving electrons. These states give resonances in cross sections as a function of the electron energy in both elastic and inelastic scattering of electrons by atoms and molecules. They can be present as intermediate states in such processes. For instance, the cross section for vibrational excitation of molecules by electron impact increases by two to three orders of magnitude if this process proceeds through excitation of autodetaching states instead of by direct excitation. There are some

processes that can proceed only through excitation of autoionizing or autodetaching states, such as dissociative attachment of electrons to molecules and dissociative recombination of electrons with positive molecular ions. Then the cross section of the process as a function of the electron energy exhibits resonances corresponding to autoionizing or autodetaching states. As a demonstration of this, Fig. 4.6 gives a schematic display of terms that can determine the process of dissociative attachment of an electron to a molecule. Figure 4.7 shows the energy dependence of the cross section for dissociative attachment of an electron to a CO_2 molecule.

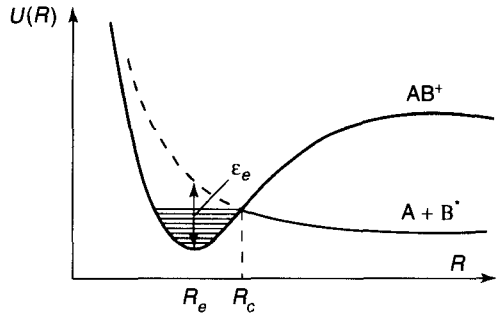

Figure 4.6 Electron terms of a molecule (solid line) and negative ions (dashed line) that determine the dissociative attachment process; ε_e is the energy of the captured electron when the distance between nuclei is R_e.

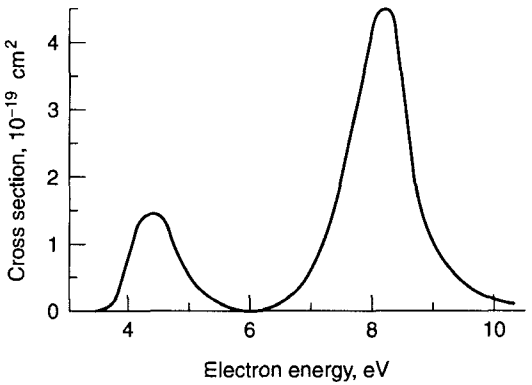

Figure 4.7 The cross section for dissociative attachment of an electron to a carbon dioxide molecule ($e + CO_2 \rightarrow O^- + CO$) as a function of the electron energy. The maxima of the cross section at the electron energies 4.4 and 8.2 eV correspond to positions of the autodetachment levels of the negative ion CO_2^-.

Some collision processes of slow atomic particles are determined by transitions of the quasimolecule consisting of colliding atomic particles in autoionizing or autodetaching states. In this case an electron term intersects the boundary of continuous spectra at some distance between the colliding particles. In the region of smaller distances this term is the autoionizing or autodetaching term, and the system of colliding particles can decay with the release of an electron. The process is

$$A^- + B \rightarrow (AB^-)^{**} \rightarrow AB + e, \tag{4.28}$$

where two asterisks denote an autodetaching state. Electronic terms for this process are given in Fig. 4.8. In this case the term of an autodetaching state of a negative ion has a form other than in Fig. 4.6, and the final state of the process relates to the electron release. At distances between nuclei $R < R_c$ the relevant state of AB^- is an autodetaching state, and the decay of this state leads to the above channel of the process. The other process of this group is the associative ionization

$$A^* + B \rightarrow (AB)^{**} \rightarrow AB^+ + e. \tag{4.29}$$

The character of the process and the behavior of the corresponding terms (see Fig. 4.9) are similar to the previous case.

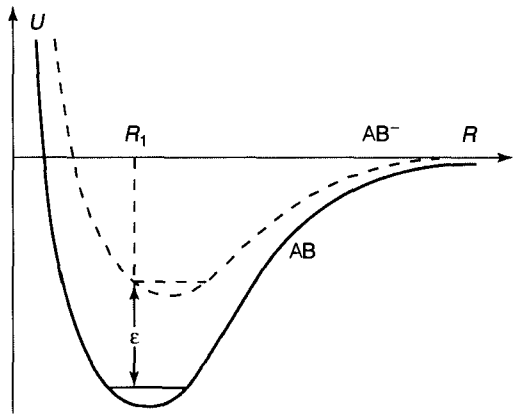

Figure 4.8 Potential energy diagrams illustrating molecular electron terms that cause the electron-impact excitation of vibrational levels through an autodetachment state.

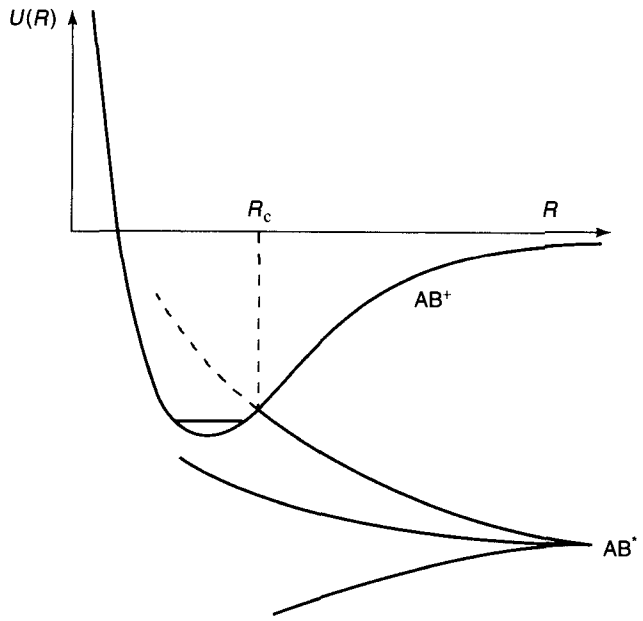

Figure 4.9 Potential energy diagrams illustrating molecular electron terms that cause dissociative recombination and associative ionization.

4.9 TYPES OF ELEMENTARY PROCESSES

A summary of the elementary processes occurring in weakly ionized gases is given in Tables 4.1–4.3. The following comments contain details and special features of these processes:

1. Typically, the cross section is of the order of the gas-kinetic cross section.
2. See Chapter 8.
3. See Chapter 5.
4. J and J' are angular momenta of the molecule. The cross section is, typically, less by one or two orders of magnitude than the cross section for elastic collision of a slow electron and the molecule. A selection rule determines the difference $J - J'$ depending on the molecular species and on the collision energy.
5. Processes proceed via formation of an autodetaching state AB^-. The probability of the process depends on the relative position of the electron energy and the autodetaching state energy. The cross section

TABLE 4.1. Collision Processes of Electrons with Atoms and Molecules

Process	Scheme	Comment Number
Elastic collision of electrons with atoms and molecules	$e + A \rightarrow e + A$	1
Inelastic collision of electrons with atoms and molecules	$e + A \leftrightarrow e + A^*$	2
Ionization of atoms or molecules by electron impact	$e + A \rightarrow 2e + A^+$	3
Transitions between rotational levels of molecules	$e + AB(J) \rightarrow e + AB(J')$	4
Transitions between vibrational levels of molecules	$e + AB(v) \rightarrow e + AB(v')$	5
Dissociative attachment of an electron to a molecule	$e + AB \rightarrow A + B^-$	5
Dissociative recombination	$e + AB^+ \rightarrow A + B^*$	3,5
Dissociation of a molecule by electron impact	$e + AB \rightarrow e + A + B$	6
Electron attachment to an atom in three-body collisions	$e + A + B \rightarrow A + B^-$	3
Electron–ion recombination in three-body collisions	$2e + A^+ \rightarrow e + A$, $e + A^+ + B \rightarrow A^* + B$	3

for the process has a resonant energy dependence, and the maximum cross section is less than or of the order of the atomic cross section.

6. The process proceeds via excitation of a molecule into a repulsive electron term. The dependence of the cross section on the electron energy is the same as for excitation of vibrational levels of the molecule by electron impact.
7. For thermal energies of collision, the cross section has the gas-kinetic magnitude ($\sim 10^{-15}$ cm^2).
8. See Chapter 4.
9. Under adiabatic conditions, these processes have a small transition probability for collision energies of a few electron volts, and the relative cross sections are smaller than typical atomic cross sections by several orders of magnitude.
10. For thermal collision energies, the cross section for the transition is smaller than the gas-kinetic cross section by several orders of magnitude.
11. For thermal collision energies, the cross section for the transition is of the order of a typical atomic cross section.

TABLE 4.2. Collision Processes of Atoms and Molecules

Process	Scheme	Comment Number
Elastic collision of atoms and molecules	$A + B \rightarrow A + B$	7, 8
Excitation of electron levels in collisions with atoms	$A + B \rightarrow A^* + B$	8, 9
Ionization in collisions of atoms	$A + B \rightarrow A^+ + e + B$	
Transitions between vibrational levels of molecules	$A + BC(v) \rightarrow A + BC(v')$	10
Transitions between rotational levels of molecules	$A + BC(J) \rightarrow A + BC(J')$	11
Quenching of excited electronic states in atomic collisions	$A^* + B(BC) \rightarrow A + B(BC)$	8, 9, 20
Associative ionization	$A^* + B \rightarrow AB^+ + e$	2
Penning process	$A^* + B \rightarrow A + B^+ + e$	2
Transfer of excitation	$A^* + B \rightarrow A + B^*$	8
Spin exchange and transitions between hyperfine structure states	$A + B(\downarrow) \rightarrow A + B(\uparrow)$	8, 12
Transitions between fine-structure states	$A + B(j) \rightarrow A + B(j')$	8, 13
Atom depolarization in collisions	$A + B(\downarrow) \rightarrow A + B(\uparrow)$	8, 14
Formation of molecules in three-body collisions	$A + B + C \rightarrow AB + C$	3, 15, 20
Chemical reactions	$A + BC \rightarrow AB + C$	16, 20

TABLE 4.3. Collision Processes Involving Ions

Process	Scheme	Comment Number
Resonant charge exchange	$A^+ + A \rightarrow A + A^+$	3, 17
Nonresonant charge exchange	$A^+ + B \rightarrow A + B^+$	18
Mutual neutralization of ions	$A^+ + B^- \rightarrow A + B$	3
Decay of negative ions in atomic collisions	$A + B^- \rightarrow AB + e$ $A + B^- \rightarrow A + B + e$	8
Ion–molecular reactions	$A^+ + BC \rightarrow AB^+ + C(AB + C^+)$	19, 20
Conversion of atomic ions to molecular ions in three-body collisions	$A^+ + B + C \rightarrow AB^+ + C$	3, 21
Ion–ion recombination in three-body collisions	$A^+ + B^- + C \rightarrow A + B + C$	3, 22

12. Arrows indicate spin orientation of valence electrons. This is a resonant process. Consider, as an example, collision of two alkali-metal atoms in the ground electron state. Then spin exchange corresponds to exchange of valence electrons, so that the spin transition causes the transition between hyperfine structure levels of each atom.
13. If the energy difference for fine-structure levels is sufficiently small and the Massey parameter (4.21) is small for the transition, this process is resonant and is characterized by large cross sections.
14. Arrows mean directions of atomic angular momenta. This is a resonant process.
15. For thermal energies, the rate constant of the process is of the order of 10^{-33}–10^{-32} cm^6/s.
16. Participation of various electron terms in the process and transitions between them can make important changes in the process.
17. The cross section of the process is larger than the gas-kinetic process (see Appendices 6, 9).
18. The cross section depends on the value of the Massey parameter.
19. These reactions are akin to chemical reactions.
20. See Chapter 19.
21. For thermal collision energies, the rate constant of this process is of the order of 10^{-31} cm^6/s. Formation of an autodetaching state $(AB^+)^{**}$ in the course of the collision can exceed this value by several orders of magnitude.
22. See Chapter 11.

CHAPTER 5

PROCESSES INVOLVING CHARGED PARTICLES

5.1 ATOMIC IONIZATION BY ELECTRON IMPACT

Processes in which ions and free electrons are either introduced into a plasma or removed from it are fundamental to the establishment of plasma properties. Below we analyze basic processes of this type. We consider first the ionization of an atom by electron impact:

$$e + \mathrm{A} \rightarrow 2e + \mathrm{A}^{+}.$$

In this process the incident electron interacts with a valence electron, transfers to it a part of its kinetic energy, and causes the detachment of the valence electron from the initially neutral atom. We can analyze this process in terms of a simple model developed by J. J. Thomson, in which it is assumed that electron collisions can be described on the basis of classical laws, and that the electrons do not interact with the atomic core in the course of the collision. Despite the fact that the atom is a quantum system, this model gives a correct qualitative description of the process because the cross sections for elastic collisions governed by the Coulomb interaction are identical in the classical and quantum cases. Within the framework of this model, ionization occurs if the energy transferred to the valence electron exceeds the ionization potential J of the atom. Hence, we have to find the cross section for collisions in which the energy exchange between electrons $\Delta\varepsilon$ exceeds the atom ionization potential. When $\Delta\varepsilon$ is small compared to the kinetic energy of the incident electron, $\varepsilon = m_e v^2/2$, the incident electron can be taken to move along a straight trajectory, the valence electron may be assumed to be at rest during the collision, and the change of the electron

momentum is perpendicular to the path of the incident electron in the plane of motion.

The variation of the electron momentum is given by Eq. (4.14). For Coulomb interaction of electrons, the force between the electrons is $\mathbf{F} = e^2\mathbf{R}/R^3$, where R is the distance between the electrons. From the symmetry of the problem, the change in momentum is in a direction perpendicular to the trajectory of the incident electron. The magnitude of the momentum change is

$$\Delta p = \int_{-\infty}^{\infty} \frac{e^2\rho}{R^3}\,dt = \frac{2e^2}{\rho v}. \tag{5.1}$$

For the free motion of the incident electron, we take $R^2 = \rho^2 + v^2t^2$, where ρ is the impact parameter of the collision, v is the velocity of the incident electron, and t is time. From this we find the energy lost by the incident electron to be

$$\Delta\varepsilon = \frac{\Delta p^2}{2m_e} = \frac{2e^4}{\rho^2 m_e v^2} = \frac{e^4}{\rho^2\varepsilon},$$

where ε is the energy of the incident electron. The cross section for collisions accompanied by the exchange of energy $\Delta\varepsilon$ is

$$d\sigma = 2\pi\rho\,d\rho = \frac{\pi e^4\,d\Delta\varepsilon}{\varepsilon(\Delta\varepsilon)^2}. \tag{5.2}$$

Though this formula was deduced for the case $\varepsilon \gg \Delta\varepsilon$, it is valid for any relative magnitudes of these parameters. When we use this expression to determine the ionization cross section within the Thomson model, we take into account that the ionization occurs with $\varepsilon > \Delta\varepsilon > J$. This gives the ionization cross section

$$\sigma_{\text{ion}} = \Delta\varepsilon\int_J^{\varepsilon} d\sigma = \frac{\pi e^4}{\varepsilon}\left(\frac{1}{J} - \frac{1}{\varepsilon}\right). \tag{5.3}$$

This expression for the ionization cross section is called the Thomson formula. Although this result is for an atom with one valence electron, it can be generalized for atoms with several valence electrons.

Since the process was treated classically, the ionization cross section depends on classical parameters of the problem: m_e (the electron mass), e^2 (the interaction parameter), ε (the electron energy), and J (the ionization potential). The most general form of the cross section expressed through these parameters is

$$\sigma_{\text{ion}} = \frac{\pi e^4}{J^2} f\left(\frac{\varepsilon}{J}\right), \tag{5.4}$$

where $f(x)$ is, within the framework of the approach we employ, a universal function identical for a valence electron in all atoms. In particular, for the Thomson model this function is

$$f(x) = 1/x - 1/x^2.$$

The Thomson formula gives the correct qualitative behavior of the ionization cross section. In the vicinity of the threshold, it gives $\sigma_{\text{ion}} \sim \varepsilon - J$, and the maximum of the cross section occurs at $\varepsilon = 2J$ with the value $\sigma_{\max} = \pi e^4/(4J^2)$. It is therefore of the order of magnitude of a typical atomic cross section. For high collision energies the Thomson formula gives the correct energy dependence—the ionization cross section decreases as the reciprocal of the energy. A more correct accounting for the behavior of valence electrons inside atoms does not change the qualitative character of the cross section.

The Thomson formula can be used for estimates of ionization rates in a plasma. Based on the Thomson formula and averaged over the Maxwell distribution function for electron velocities, the rate constant of atomic ionization by electron impact is

$$k_{\text{ion}} = \langle v_e \sigma_{\text{ion}} \rangle = k_0 \frac{\sqrt{z}}{1+z} \exp(-z), \quad z = \frac{J}{T_e}, \quad k_0 = \frac{\pi e^4}{J^2} \sqrt{\frac{2J}{m_e}}.$$

Here the angle brackets mean the average over the Maxwell distribution function of electrons, v_e is the electron velocity, m_e is the electron mass, and T_e is the temperature. The rate constant has a maximum $k_{\text{ion}} = 0.3\, k_0$ at $z = 0.3$, and at low electron temperatures it gives

$$k_{\text{ion}} = \frac{\pi e^4}{m_e} \sqrt{\frac{2T_e}{m_e}} \exp\left(-\frac{J}{T_e}\right), \quad T_e \ll J.$$

5.2 COLLISION OF TWO CHARGED PARTICLES IN A PLASMA

Below we calculate the diffusion cross section of two charged particles in a plasma. This cross section is a measure of the exchange of energy and momentum between charged particles in a plasma and is widely useful in expressing plasma properties. Small scattering angles ϑ give the principal contribution to this cross section, which can thus be written as

$$\sigma^* = \int (1 - \cos\vartheta) 2\pi\rho \, d\rho \approx \int \vartheta^2 \pi\rho \, d\rho,$$

where ρ is the impact parameter for the collision. The scattering angle is $\vartheta = \Delta p/p$, where $p = \mu g$ is the momentum of the colliding particles in the

center-of-mass frame, meaning that μ is the reduced mass of the particles, g is the relative velocity of the particles, and, according to Eq. (5.1), the change in momentum of the particles is $\Delta p = 2e^2/(\rho g)$, where e is the particle charge. Hence $\vartheta = e^2/(\varepsilon\rho)$, where $\varepsilon = \mu g^2/2$ is the particle energy in the center-of-mass frame. Substituting this into the expression for the diffusion cross section of charged particle scattering gives

$$\sigma^* \approx \int \vartheta^2 \pi\rho \, d\rho = \frac{\pi e^4}{\varepsilon^2} \int \frac{d\rho}{\rho}.$$

This integral diverges in both the small- and large-impact-parameter limits. It is possible to adjust these limits to finite values by examining the nature of the divergences. The divergence at small impact parameters is due to violation of the assumption of small scattering angles. This limit should really correspond to $\vartheta \sim 1$, or $\rho_{\min} \sim e^2/\varepsilon$. The divergence at large impact parameters is caused by the infinite range of the unscreened Coulomb interaction potential of charged particles in a vacuum, e^2/r. It is more correct to use the Debye–Hückel interaction potential (3.7) of charged particles in a plasma, $e^2\exp(-r/r_D)/r$, where r is the distance between particles, and r_D is the Debye–Hückel radius. Hence $\rho_{max} = r_D$, and the diffusion cross section for the scattering of two charged particles is

$$\sigma^* = \frac{\pi e^4}{\varepsilon^2} \ln \Lambda, \qquad \Lambda = r_D e^2/\varepsilon. \tag{5.5}$$

The quantity $\ln \Lambda$ is called the *Coulomb logarithm*. According to its definition, $\Lambda \gg 1$, and the value of Λ is known up to a factor of the order of one. Thus, the accuracy of Eq. (5.5) improves with an increase in the Coulomb logarithm.

5.3 MUTUAL RECOMBINATION OF POSITIVE AND NEGATIVE IONS

Pairwise recombination of positive and negative ions is described by the scheme

$$A^+ + B^- \rightarrow A^* + B. \tag{5.6}$$

The mutual recombination consists of the valence electron transferring from the field of the atom B to the field of the ion A^+. The process proceeds effectively if the distance between nuclei permits a tunneling transition of the electron. Based on this mechanism, we use a simple model for which the transition probability is unity if the distance of closest approach of the colliding particles, r_0, is less than or equal to R_0, and the transition probability is zero at larger values of r_0. Equation (4.7) then gives the cross

section for the ion–ion pair recombination as

$$\sigma_{\text{rec}} = \pi\rho_0^2 = \pi R_0^2\left(1 + \frac{e^2}{R_0\varepsilon}\right), \tag{5.7}$$

where ρ_0 is the impact parameter at which the closest approach of the colliding particles is R_0, and ε is the kinetic energy of the ions in the center-of-mass system.

In particular, for low collision energy $\varepsilon \ll e^2/R_0$, this relation gives

$$\sigma_{\text{rec}} = \pi R_0 e^2/\varepsilon. \tag{5.8}$$

Equation (5.8) gives the recombination rate constant $\alpha = v\sigma_{\text{rec}}$, so that $\alpha = 2\pi e^2 R_0/(2\varepsilon\mu)^{1/2}$, where μ is the reduced mass of the colliding ions. Averaging this value over the Maxwell energy distribution for the ions yields

$$\alpha = \langle v\sigma_{\text{rec}} \rangle = 2\sqrt{\frac{2\pi}{\mu T}}\, R_0 e^2, \tag{5.9}$$

where the angle brackets denote averaging over the relative velocities of the ions. We introduce in this model a parameter R_0 that describes the tunneling transition of the valence electron. Though this parameter depends on the structure of the negative ion and on the collision velocity, the range of its values is not wide. One can estimate the value $R_0 = 10\, a_0$ for thermal collisions.

5.4 THREE-BODY COLLISION PROCESSES

Collisions represented by the scheme

$$\text{A} + \text{B} + \text{C} \rightarrow \text{AB} + \text{C} \tag{5.10}$$

are referred to as three-body processes. In such collisions, particles A and B combine to form a bound system, and the particle C carries away the energy released thereby. The balance equation for the number densities of particles in the interaction (5.10) has the form

$$d[\text{AB}]/dt = K[\text{A}][\text{B}][\text{C}], \tag{5.11}$$

where [X] is the number density of particles X, and K is the rate constant of the three-body process, with dimensionality cm^6/s. Equation (5.11) can be viewed as the definition of the three-body rate constant.

The Thomson theory can be used again to evaluate the three-body rate constant. Though Thomson developed his theory for simple charged-particle interactions, it can be extended readily to the treatment of three-body

processes in general. The assumptions are made that the binding energy of the end-product molecule AB is much larger than thermal energies, and the motion of the particles is governed by classical laws. The formation of a bound state of particles A and B occurs in the following way. As particles A and B approach each other, their energy increases as the potential energy of interaction is converted into kinetic energy. If a third particle C interacts strongly with A or B when these particles are close to each other, then the third particle may take from A or B an energy in excess of the initial kinetic energy of these particles. The bound state of particles A and B is thus formed as a result of a collision with the third particle.

This physical picture can be used as a basis for estimation of the rate constant of a three-body process. Typical kinetic energies of the particles are of the order of the thermal energy T. Assume the mass of the third particle C to be comparable to the mass of either particle A or B. Since the energy exchange must exceed the initial kinetic energy of A and B, the interaction potential between these particles during collision with C must also be of the order of T. Thus, let us define a critical radius b by the relation

$$U(b) \sim T, \tag{5.12}$$

where $U(R)$ is the interaction potential for the particles A and B.

Now we can estimate the rate constant of the three-body process. The frequency of conversion of particle B into particle AB is of the order of magnitude of the product of two factors. One measures the probability for B to be located in the critical region near A, and is given by $[A]b^3$. The other factor is the frequency $[C]v\sigma$ of collisions with particle C. Here v is a typical relative collision velocity, and σ is the cross section for the collision between C and either A or B, resulting in an energy exchange of the order of T. If the masses of the colliding particles are similar, this cross section is comparable to the cross section for elastic collision. The estimate for the rate of formation of particle AB is thus

$$d[AB]/dt \sim [A][B]b^3[C]v\sigma.$$

Comparison of this expression with the definition (5.11) of the constant of the three-body process gives the estimate for the rate constant

$$K \sim vb^3\sigma. \tag{5.13}$$

The transition expressed in (5.10) is a three-body process if the number density for C is small, and therefore the probability of collision of A and B with C is small when A and B are located the critical distance b apart. This condition is valid if the critical radius is small compared to the mean free path of particles A and B in a gas of particles C, or

$$[C]\sigma b \ll 1. \tag{5.14}$$

5.5 THREE-BODY RECOMBINATION OF ELECTRONS AND IONS

Three-body recombination of electrons and ions proceeds according to the scheme

$$2e + A^+ \rightarrow e + A^*, \tag{5.15}$$

and is of importance for a dense plasma. According to the Thomson theory, the three-body process produces initially an excited atom whose ionization potential is of the order of the thermal energy T ($T \ll J$, where J is the atomic ionization potential), and this atom later makes a transition to the ground state as a result of subsequent collisions. The Thomson theory is applicable to this process because classical laws are valid for a highly excited atom.

An estimate for the rate constant of the process (5.15) can be made on the basis of Eq. (5.13). Because the cross section of elastic scattering of electrons is $\sigma \sim e^4/T^2$ according to Eq. (4.14), and the critical radius is $b \sim e^2/T$ according to Eq. (5.12), then the rate constant of the process (5.15) is

$$K = \frac{\alpha}{N_e} = C\frac{e^{10}}{m_e^{1/2}T^{9/2}}. \tag{5.16}$$

In this expression, α is the recombination coefficient, defined as the rate constant for the decay of charged particles in the pair process, and $C \sim 1$ is a numerical coefficient. The validity criterion for Eq. (5.16) requires fulfillment of condition (5.14), which in this case has the form $N_e e^6/T^3 \ll 1$ and coincides with the condition for an ideal plasma given in Eq. (3.1).

Equation (5.16) gives a correct relationship between the recombination coefficient and the parameters of the problem. This relationship can be obtained in a simpler way on the basis of dimensional analysis. For the suggested mechanism of the process (5.15), the rate constant must depend only on the interaction parameter e^2, the electron mass m_e, and the thermal energy T (the electron temperature). There is only one combination of these parameters that has the dimension cm^6/s of the rate constant for the three-body process, and it can be seen that this combination coincides with Eq. (5.16).

The value of the numerical coefficient C in Eq. (5.16) is of interest. According to the nature of the process, this value does not depend on the type of atom, because the nature of the process is such that this coefficient is determined by properties of highly excited states where the Coulomb interaction takes place between the atomic core and electron. Additional analysis gives $C = 4 \pm 1$ for this value.

A similar procedure can be used to determine the rate constant for the three-body process of conversion of atomic ions into molecular ions, as

expressed by

$$A^+ + 2A \rightarrow A_2^+ + A. \tag{5.17}$$

This process occurs because of the polarization interaction between the ion and atom, so the interaction potential has the form $U(R) = -\beta e^2/(2R^4)$, where β is the polarizability of the atom. The rate constant of this process can be constructed by dimensional analysis on the basis of the following parameters: βe^2 (the interaction parameter), M (the mass of the atom), and T (the temperature or a typical thermal energy of the particles). The only combination with the dimensionality of the rate constant of the three-body process that can be constructed from these parameters is

$$K \sim \frac{(\beta e^2)^{5/4}}{M^{1/2} T^{3/4}}. \tag{5.18}$$

The same expression for the rate constant of this process can be obtained on the basis of the Thomson theory (5.13).

5.6 THREE-BODY RECOMBINATION OF POSITIVE AND NEGATIVE IONS

Three-body recombination of positive and negative ions follows the scheme

$$A^+ + B^- + C \rightarrow A^* + B + C. \tag{5.19}$$

The process gives rise initially to a bound state of the positive and negative ions A^+ and B^-, then a valence electron transfers from the field of atom B to the field of ion A^+, and the bound state decays into two atoms A* and B. The second stage of the process occurs spontaneously during the approach of the negative and positive ions, so that the three-body recombination is determined by formation of the bound state of these ions.

We can estimate the rate constant of the process (5.19) using the Coulomb interaction between the ions and a polarization interaction between each ion and atom. Assuming the atomic mass to be comparable to the mass of one of the ions, we use Eq. (4.12) for the cross section of the atom–ion collision and the Thomson formula (5.13) for the rate constant of the three-body recombination process. As a result, we have

$$K = \frac{\alpha}{N_i} \sim \frac{e^6}{T^3}\left(\frac{\beta e^2}{M}\right)^{1/2}. \tag{5.20}$$

The criterion (5.14) for the validity of Eq. (5.20) gives, in this case,

$$\frac{[C]e^2(\beta e^2)^{1/2}}{T^{3/2}} \ll 1. \tag{5.21}$$

Inserting the polarizability of the atom, which is several atomic units, into Eq. (5.21), we find that at room temperature the number density [C] must be much less than 10^{20} cm^{-3}. Hence, the criterion for the three-body character of the recombination of positive and negative ions cannot be satisfied if the gas pressure is of the order of one atmosphere.

5.7 STEPWISE IONIZATION OF ATOMS

The mean electron energy in a gas-discharge plasma is usually considerably lower than atomic ionization potentials. Therefore single ionization of atoms can occur only in collisions with high-energy electrons from the tail of the distribution function. Ionization can also occur as a result of the collision of an electron with an excited atom. For ionization by electrons that are not energetic enough to produce ionization directly, the atom must pass through a number of excited states, with transitions to these states caused by collisions with electrons. This mechanism for ionization of an atom is called *stepwise ionization.* We shall estimate the rate constant of stepwise ionization assuming that the electron energy distribution is Maxwellian, and taking the electron temperature to be considerably lower than the atom ionization potential, so that

$$T_e \ll J. \tag{5.22}$$

Stepwise ionization of atoms by electron impact can take place only with a high number density of electrons, so that there are no competing channels for transitions between excited states. Then the stepwise ionization process is the detailed-balance inverse process to the three-body recombination of electrons and ions. In inverse processes, atoms undergo the same transformations but in opposite directions.

Assume the electrons of the system to be in thermodynamic equilibrium with the atoms. Then the generation of charged particles is due to stepwise ionization, and their decay is due to the three-body recombination process, with the equilibrium expressed by a zero value in the rate equation. That is, we have the equation

$$dN_e/dt = 0 = N_e N_a k_{st} - \alpha N_e N_i.$$

Here N_e, N_i, and N_a are the number densities of electrons, ions, and atoms respectively, and k_{st} is the rate constant for stepwise ionization.

Since electrons, ions, and atoms are in thermodynamic equilibrium, their number densities are connected by the Saha distribution (2.17). This gives the relationship between the rate constants of the inverse processes as

$$k_{st} = \frac{\alpha}{N_c} \frac{g_e g_i}{g_a} \left[\frac{m_e T_e}{2\pi\hbar^2} \right]^{3/2} \exp\left(-\frac{J}{T_e} \right), \tag{5.23}$$

where g_e, g_i, and g_a are the statistical weights of electrons, ions, and atoms respectively, and T_e is the electron temperature. Because the rate constants k_{st} and α/N_e do not depend on the number densities, Eq. (5.23) is valid even if the Saha distribution does not hold. Thermodynamic equilibrium in the system is used here as a method that allows us to establish a relationship between the rate constants of direct and inverse processes.

Equation (5.23) together with Eq. (5.16) for the rate constant of the three-body process gives

$$k_{st} = A \frac{g_i}{g_a} \frac{m_e e^{10}}{\hbar^3 T_e^3} \exp\left(-\frac{J}{T_e}\right), \tag{5.24}$$

where $A \approx 8$ is a numerical factor, which is the same for all atoms.

We can compare the rate constant of stepwise ionization (5.24) with the rate constant of ionization in a single collision, which is given for the present case by

$$k_{ion} = \int_J^\infty \frac{2\varepsilon^{1/2}}{\pi^{1/2} T_e^{3/2}} \exp\left(-\frac{\varepsilon}{T_e}\right)\left(\frac{2\varepsilon}{m_e}\right)^{1/2} \sigma_{ion}\, d\varepsilon,$$

where ε is the energy of the incident electron. If the condition (5.22) is satisfied, this integral converges in the vicinity of the process threshold, where the cross section for direct ionization has the form $\sigma_{ion} = \sigma_0[(\varepsilon/J) - 1]$, and the parameter σ_0 is of the order of the atomic cross section. In particular, the Thomson model gives $\sigma_0 = \pi e^4/J^2$ in accordance with Eq. (5.4). Using this expression, the rate constant for direct ionization is

$$k_{ion} = \left(\frac{8T_e}{\pi m_e}\right)^{1/2} \sigma_0 \exp\left(-\frac{J}{T_e}\right). \tag{5.25}$$

Comparing Eqs. (5.24) and (5.25), and taking into account that the atomic ionization potential is of the order of an atomic unit of energy, $J \sim m_e e^4/\hbar^2$, we obtain

$$\frac{k_{ion}}{k_{st}} \sim \left[\frac{\hbar^2 T_e}{m_e e^4}\right]^{7/2} \sim \left(\frac{T_e}{J}\right)^{7/2} \ll 1. \tag{5.26}$$

This ratio is much less than unity owing to the condition (5.22) and to the fact that the ionization potential of the atom, J, is of the order of $m_e e^4/\hbar^2$. Hence, if conditions are suitable for stepwise ionization, this process proves to be more effective at low electron temperatures than ionization by single collisions.

5.8 DISSOCIATIVE RECOMBINATION

Dissociative recombination is a process in which a positive molecular ion is neutralized by recombination with a free electron, as a consequence of which the molecule dissociates into two parts. The scheme is

$$e + AB^+ \rightarrow A^* + B. \tag{5.27}$$

As an effective pair process, dissociative recombination is of importance for plasma properties. Figure 4.9 demonstrates the mechanism of dissociative recombination that proceeds via autoionizing states of the molecule AB. The excited state of the molecule AB is an autoionizing state if the distance between the atoms is smaller than the distance R_c to the intersection of this term with the boundary of the continuous spectrum. In the course of dissociative recombination, the electron colliding with the molecular ion is captured into a repulsive autoionizing term. The atoms move apart, and if the autoionizing state has not led to decay when the atoms reach the intersection distance R_c, then the dissociative recombination process occurs.

Dissociative recombination is a fairly complicated process. First, there are many autoionizing states that can participate in this process. Second, vibrational excitation of the ions has a strong influence on the value of the recombination coefficient. Therefore, we will not calculate expressions for the recombination coefficient. We note only that at thermal energies its value is of the order of, or exceeds, typical atomic values (see Table 13.1). If in this process complex or cluster ions participate, there is a strong interaction between the electron and the molecular ion. Then one can use a simple model for the analysis of this process. Introduce the ion radius R_0 such that at smaller distances between the electron and ion, an inelastic transition takes place because of the strong interaction between the electron and ion at these distances. This means that if the electron is found in a region of such size, it is captured by the ion and dissociative recombination occurs. Using Eq. (5.9) for the rate constant of the process and assuming the electron behavior to be governed by classical laws, we have for the dissociative recombination coefficient in this case

$$\alpha = 5R_0 e^2/\sqrt{m_e T_e}. \tag{5.28}$$

The parameter R_0 is several atomic units in size for complex ions and is equal to the ion radius for cluster ions. Therefore at room temperature the coefficient of dissociative recombination of an electron and a complex ion predicted by Eq. (5.28) is of the order of 10^{-6} cm^3/s. It is sufficiently large to be significant. Note that the above model, which describes a case of a strong interaction of the colliding electron and ion, gives an upper limit for the value of the dissociative recombination coefficient.

5.9 DIELECTRONIC RECOMBINATION

Dielectronic recombination of an electron and an ion takes place by capture of the electron into an autoionizing state of the atom and subsequent decay of the autoionizing state by radiative transition to a stable state. This process is of importance for recombination of electrons and multicharged ions because the radiative lifetime of the multicharged ion decreases strongly ($\sim Z^{-4}$) with increase of its charge Z. The scheme of the process under consideration is

$$e + A^{+Z} \rightarrow [A^{+(Z-1)}]^{**}, \tag{5.29a}$$

$$[A^{+(Z-1)}]^{**} \rightarrow A^{+Z} + e, \tag{5.29b}$$

$$[A^{+(Z-1)}]^{**} \rightarrow A^{+(Z-1)} + \hbar\omega. \tag{5.29c}$$

We denote the rate constant of the first process as k, the radiative lifetime of the autoionizing state as τ, the width of the autoionizing level as Γ, and the energy of excitation of the autoionizing state $[A^{+(Z-1)}]^{**}$ above the ground state as E_a. We shall obtain the expression for the recombination coefficient of an electron and multicharged ion for the process described in Eq. (5.29).

The rate equation for the number density N_{ai} of ions in a given autoionizing state is

$$\frac{dN_{ai}}{dt} = N_e N_Z k - N_{ai}\frac{\Gamma}{\hbar} - N_{ai}\frac{1}{\tau},$$

where N_e is the electron number density, and N_Z is the number density of ions of charge Z. From this we find the number density of ions in the autoionizing state N_{ai} and the rate of recombination $J = N_{ai}/\tau$ to be

$$N_{ai} = \frac{N_e N_Z k}{\Gamma/\hbar + 1/\tau}, \qquad J = \frac{N_{ai}}{\tau} = \frac{N_e N_Z k}{\Gamma\tau/\hbar + 1}. \tag{5.30}$$

The end result is the recombination coefficient α, given by

$$\alpha = \frac{J}{N_e N_Z} = \frac{k}{\Gamma\tau/\hbar + 1}. \tag{5.31}$$

In order to obtain the expression for the rate constant k for electron capture in the autoionizing state, we assume there is thermodynamic equilibrium between the autoionizing state and other ion states. The Saha formula, Eq. (2.17), for this autoionizing state is

$$\frac{N_Z N_e}{N_{ai}} = \frac{g_e g_Z}{g_{ai}}\left(\frac{m_e T_e}{2\pi\hbar^2}\right)^{3/2} \exp\left(\frac{E_a}{T_e}\right), \tag{5.32}$$

where g_e, g_Z, and g_{ai} are statistical weights for the participating atomic states, and T_e is the electron temperature. Because thermodynamic equilibrium corresponds to $\tau \rightarrow \infty$, comparison of the first expression in (5.30) with

Eq. (5.32) gives for the rate constant of electron capture in the autoionizing state of the ion

$$k = \frac{g_{ai}}{g_e g_Z}\left(\frac{2\pi\hbar^2}{m_e T_e}\right)^{3/2}\frac{\Gamma}{\hbar}\exp\left(-\frac{E_a}{T_e}\right). \tag{5.33}$$

Equations (5.31) and (5.33) yield the recombination coefficient of electrons and ions,

$$\alpha = \frac{g_{ai}}{g_e g_Z}\left(\frac{2\pi\hbar^2}{m_e T_e}\right)^{3/2}\frac{\Gamma/\hbar}{\Gamma\tau/\hbar + 1}\exp\left(-\frac{E_a}{T_e}\right). \tag{5.34}$$

We can summarize the qualitative features of electron capture in an autoionizing state. The process corresponds to excitation of valence or internal electrons of the ion, accompanied by the capture of an incident electron in a bound state. The energy of the incident electron matches the excitation energy E_a of the autoionizing state. Equation (5.33) is obtained from imposition of the condition of thermodynamic equilibrium among the atomic particles participating in the process. This requires the Maxwell distribution function for kinetic energies of the electrons. Hence, we have the criterion for the validity of Eq. (5.34):

$$N_Z k \ll N_e k_{ee}, \tag{5.35}$$

where k_{ee} is the rate constant for the elastic electron–electron collisions that establish the Maxwell distribution function. If we have some other energy distribution function $f(\varepsilon)$ for electrons of energy ε, normalized by the relation $\int f(\varepsilon)\,d\mathbf{v} = 1$, Eq. (5.41) takes the form

$$\alpha = \frac{g_{ai}}{g_e g_Z}\left(\frac{2\pi\hbar}{m_e}\right)^3 f(E_a)\frac{\Gamma/\hbar}{\Gamma\tau/\hbar + 1}. \tag{5.36}$$

This expression also requires that the criterion (5.35) be satisfied. This means that the electron energy distribution function is Maxwellian in its dominant portion. This makes it possible to introduce the electron temperature; but the tail of the distribution function, responsible for excitation of the autoionizing state, may be distorted.

5.10 CHARGE-EXCHANGE PROCESSES

Various resonant processes are accompanied by the transfer of an electron from one atomic particle to another. Among these processes are resonant charge exchange, mutual neutralization of negative and positive ions, spin exchange, and some types of excitation transfer. The electron exchange in these processes determines their character. We consider the example of resonant charge exchange and analyze the behavior of its cross section.

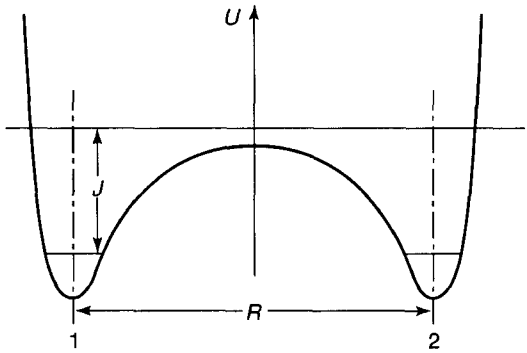

Figure 5.1 Planar section of the potential energy diagram of an electron in the field of two identical atomic cores. 1 and 2 are positions of the nuclei of the cores, R is the distance between them, and J is the atomic ionization potential, that is, the electron binding energy for one atom.

Figure 5.1 shows the nature of the potential well in which a valence electron is located. If positions of the nuclei are fixed, the electron will shuttle between one atom and the other. The frequency ω of this tunneling transition depends as a negative exponential on the distance between the nuclei. The exponent is proportional to the barrier width, so that ω behaves as $\exp(-\gamma R)$, where $\gamma = (2mJ/\hbar^2)^{1/2}$, and J is the atomic ionization potential. This is the essential character of the dependence on R at large distances between the nuclei.

We can evaluate the dependence of the cross section for this process on the collision velocity, assuming that the main contribution to the cross section comes from collisions with large impact parameters. Based on the character of the transition, it is plausible that the probability of the transition is $\frac{1}{2}$, if a typical collision time a/v is of the order of the transition frequency ω. Here a is a distance that characterizes the interaction potential between the atom and ion. From this it follows that the cross section of the resonant charge exchange process is

$$\sigma = \pi R_0^2/2, \qquad \text{where} \quad \omega(R_0) \sim a/v.$$

Using the exponential dependence of ω on R, we get a result in the form

$$\sigma_{\text{res}} = \sigma_0 \ln^2(v_0/v), \tag{5.37}$$

where v_0 is a velocity parameter, and $\sigma_0 = \pi/(2\gamma^2)$.

Appendix 9 contains values of resonant charge-exchange cross sections at low energies. Cross sections are seen to depend weakly on collision energy, and are notably larger than gas-kinetic cross sections. Hence, the resonant charge-exchange process is far more important than elastic ion–atom collisions in determining the kinetic parameters of ions in a gas of neutral atoms of the same type (see Chapter 11).

CHAPTER 6

RAREFIED AND DENSE PLASMAS

6.1 CRITERIA FOR AN IDEAL PLASMA

Many varieties of plasmas are known, most of them composed of weakly interacting particles (see Figs. 1.1–1.3). These plasma systems are analogs of gaseous systems of neutral particles. When they experience weak interactions, the system of charged particles is an ideal plasma, with the criterion for plasma ideality expressed by the relations (3.1) and (4.19) between plasma parameters. The small parameter of the theory has the form

$$\gamma = N_c e^6 / T_c^3, \tag{6.1}$$

and the condition to have an ideal plasma is $\gamma \ll 1$. Specific values for γ can be estimated on the basis of fundamental physical considerations.

The first criterion for an ideal plasma refers to the condition that the mean interaction energy of a plasma particle with its neighbors must be small compared to its kinetic energy $3T/2$. (We assume in the following that electrons and other plasma particles have the same temperature.) The electric potential arising from a charged plasma particle is given by Eq. (3.7), and is

$$\varphi = q/r - q/r_D, \qquad r \ll r_D,$$

where q is the particle charge, r is the distance from this particle, and r_D is the Debye–Hückel radius. The first term of this expression is the particle potential in vacuum, and the second term is the electric potential that is created by the neighboring plasma particles. This means that the average

interaction energy of a particle of charge e with other plasma particles is equal to e^2/r_D [compare with Eq. (3.11)], and the criterion for an ideal plasma ($e^2/r_D \ll 3T/2$) leads to the value

$$\gamma \ll 9/(32\pi) = 0.09. \tag{6.2}$$

A second criterion follows from the condition that many charged particles are located in the sphere of the radius r_D, that is, that $4\pi r_D^3 N_e/3 \gg 1$. This gives the value

$$\gamma \ll 1/(96\pi) = 0.003. \tag{6.3}$$

The two criteria (6.2) and (6.3) contain identical combinations of parameters, but yield different numerical values. The criterion (6.2) is to be preferred, because it encompasses a larger region in which the ratio of the potential energy of a particle to its kinetic energy can be small, and it is thus useful for expansion of plasma parameters. Nevertheless, Figs. 1.1 and 1.2 display both the criteria (6.2) and (6.3) as boundaries between an ideal plasma and a dense plasma.

The quantity selected to characterize a plasma may not be γ, but may instead be some function of γ. Often one uses the coupling constant Γ of the plasma, introduced as the ratio of the Coulomb interaction potential of a charged particle with its nearest neighbors to the thermal energy,

$$\Gamma = \frac{e^2}{r_W T} = \left(\frac{4\pi\gamma}{3}\right)^{1/3}, \tag{6.4}$$

where $r_W = (4\pi N_e/3)^{-1/3}$ is the *Wigner–Seitz radius*. A dense plasma is one with $\Gamma \gg 1$, and is called a *strongly coupled plasma*. The condition for the plasma to be ideal is $\Gamma \ll 1$, which implies that

$$\gamma \ll \frac{3}{4\pi} = 0.2. \tag{6.5}$$

We can express plasma properties as a function of the plasma coupling constant Γ. The ratio of the average interaction energy of a charged plasma particle with other particles to its mean kinetic energy has the form

$$\frac{e^2}{r_D}\frac{2}{3T} = \frac{4}{3}\sqrt{2\pi\gamma} = \frac{(2\Gamma)^{3/2}}{3^{1/2}}.$$

The number of electrons in a sphere of radius r_D is

$$N_D = \frac{4\pi r_D^3 N_e}{3} = \frac{1}{6\sqrt{8\pi\gamma}} = \frac{1}{(6\Gamma)^{3/2}} = \frac{0.07}{\Gamma^{3/2}}.$$

In the above discussion, we considered a plasma to be a two-component system containing charged particles, with each charge having the magnitude of the electron charge. If a plasma contains multicharged ions, the above criteria must refer to the ion charge Ze. An example would be a dusty plasma, which is a gas-discharge plasma with dielectric particles of micron sizes. These particles are negatively charged because the electron mobility is far greater than for ions. Traps introduced into a gas discharge can capture these particles to form a structure called a plasma crystal. Structures that can serve as traps include nonuniformities of a gas-discharge plasma, striations, regions near electrodes, and so on. Typical distances between charged particles are of the order of 1 μm, and the particle charge can reach to $Z \sim 10^3$–10^4, depending on their size and on the conditions of the gas discharge.

6.2 CONDITIONS FOR IDEAL EQUILIBRIUM PLASMAS

We expect a plasma to fail to be ideal as the plasma density increases. The nature of this failure will now be examined. Consider a weakly ionized gas at a low temperature, and ascertain the dependence of the parameter γ on the plasma density when there is equilibrium between charged and neutral plasma particles. From the Saha distribution (2.17) for the electron (N_e) and atom (N_a) number densities in a quasineutral plasma, we obtain the relation

$$\frac{N_e^2}{N_a} = g\left(\frac{m_e T}{2\pi\hbar^2}\right)^{3/2} \exp\left(-\frac{J}{T}\right), \tag{6.6}$$

where $g = g_e g_i / g_a$; g_e, g_i, and g_a are the statistical weights of electrons, ions and atoms, respectively; and J is the atomic ionization potential. Take the total number density of nuclei, $N = N_e + N_a$ ($N_e = N_i$), as a parameter, and determine the dependence $\gamma(N)$.

We write the Saha distribution in the form

$$\gamma^2 = \left(N - \frac{\gamma T^3}{e^6}\right)\frac{C}{T^{9/2}} \exp\left(-\frac{J}{T}\right),$$

where $C = g m_e^{3/2} e^{12} / [\hbar^3 (2\pi)^{3/2}]$. Concentrating our attention on plasmas with the maximum departure from ideal plasma conditions, we choose the plasma temperature at a given N such that the parameter γ is maximal. The condition $d\gamma/dT = 0$ leads to the expressions

$$N = g\frac{3T(J - 3T/2)}{(J - 9T/2)^2}\left(\frac{m_e T}{2\pi\hbar^2}\right)^{3/2} \exp\left(-\frac{J}{T}\right), \tag{6.7}$$

$$N_e = N\left(\frac{J - 9T/2}{J - 3T/2}\right). \tag{6.8}$$

The maximum values of γ are located at $T \leq 2J/9$, and, in the limit of large N, the temperature approaches $2J/9$. In this limit the degree of plasma ionization goes to zero as N grows, and the plasma parameter γ increases with the growth of N. On the basis of the above equations, we analyze the limiting case where there is a fundamental violation of the conditions for an ideal plasma. We take into account that Eqs. (6.7) and (6.8) are valid for an ideal plasma. The maximum values of γ at a given large N lead to the expressions for the temperature T and the degree of ionization N_e/N:

$$\frac{(T - T_0)^2}{T^2} = \frac{4g}{9N}\left(\frac{m_e T_0}{2\pi\hbar^2}\right)^{3/2} e^{-9/2}, \tag{6.9}$$

$$\frac{N_e}{N} = \frac{3}{2}\frac{(T - T_0)}{T_0}. \tag{6.10}$$

The parameter T_0 is defined as $T_0 = 2J/9$. It is evident that the plasma parameter behaves as $\gamma \sim (Na_0^3)^{1/2}$ in the limit of large N, and the coupling constant of the plasma is estimated to be $\Gamma \sim (Na_0^3)^{1/6}$, where a_0 is the Bohr radius. In particular, in the limit of large N, these expressions for a hydrogen plasma become

$$\frac{N_e}{N} = \frac{5.1 \times 10^{-3}}{(Na_0^3)^{1/2}}, \qquad \gamma = 3.7(Na_0^3)^{1/2}, \qquad \Gamma = 2.5(Na_0^3)^{1/6}, \tag{6.11}$$

with validity constrained by $Na_0^3 \ll 1$. From this, it follows for the hydrogen plasma that $\Gamma = 1$ at $Na_0^3 = 0.004$.

One can conclude from these results that the degree of plasma ionization decreases with an increase of the plasma density. This means that departure from the ideal nature of the plasma is accompanied by an increase in the number density of neutral particles. Thus, interaction involving neutral atomic particles is of importance for the properties of a strongly coupled plasma.

6.3 INSTABILITY OF TWO-COMPONENT STRONGLY COUPLED PLASMAS

From the above analysis it follows that a plasma consisting only of electrons and ions cannot experience major departures from ideal plasma conditions. However, a dense plasma without neutral particles can be created only for brief intervals under nonequilibrium conditions. We now estimate the lifetime of such a plasma and compare it with actual times for plasma generation.

The situation examined is that of a dense plasma consisting of electrons and ions, and the decay of this plasma resulting from ionization and recombination. The balance equation for the electron number density of this plasma has the form

$$dN_e/dt = -KN_eN_iN_a + k_{ion}N_eN_a, \tag{6.12}$$

where N_i and N_a are the ion and atom number densities, K is the rate constant for three-body recombination of electrons and ions as given by Eq. (5.16), and k_{ion} is the rate constant for stepwise ionization of atoms by electron impact [Eq. (5.30)]. Equation (6.12) takes into account the processes

$$2e + A^+ \leftrightarrow e + A^* \leftrightarrow e + A. \tag{6.13}$$

We are interested in the nonequilibrium case when the number density of atoms is small compared to a plasma in equilibrium. This corresponds to the assumption $N_a \approx 0$, which allows us to neglect the second term in Eq. (6.12). The lifetime of the nonequilibrium plasma is thus expressed through the rate constant of the three-body recombination of electrons and ions. The energy resulting from the recombination process goes into heating of the plasma.

Along with the balance of the electron number density, we take into account the heat balance of the plasma, described by the equation

$$\frac{d(3N_eT)}{dt} = -\frac{J\,dN_e}{dt}. \tag{6.14}$$

We assume in this equation that the electron and ion temperatures are the same, so that the plasma energy per unit volume is $3N_eT$. In addition, we take the thermal energy of the charged particles to be small compared to the atomic ionization potential ($T \ll J$). That is, we assume that the recombination of one electron with an atom leads to the release of energy J. Then equation (6.14) takes the form

$$\frac{dT}{dt} = -\frac{J}{3}\frac{d\ln N_e}{dt}. \tag{6.15}$$

The equation for the plasma parameter γ following from Eqs. (6.12) and (6.15) is

$$d\gamma/dt = -\gamma^2/\tau, \tag{6.16}$$

where $\tau = m_e^{1/2}e^2/(CJT^{1/2})$, and we use Eq. (5.16) for the rate constant of the three-body recombination of electrons and ions. In particular, at the temperature $T = 2000$ K, the parameter τ in Eq. (6.16) is $\tau = 5 \times 10^{-16}$ s for a cesium plasma and $\tau = 10^{-16}$ s for an argon plasma.

One can compare these times with typical times for plasma generation. The minimum time for plasma generation corresponds to the use of short-pulse lasers, and minimum times for laser pulses are of the order of 10^{-14} s.

Hence, the relaxation time τ/γ of the plasma being examined exceeds by orders of magnitude a typical time for plasma generation. This means that it is impossible to create a strongly coupled plasma of a low temperature without neutral particles. Therefore, the neutral component of a plasma is essential to the properties of this plasma. From this it follows that the determination of plasma properties requires that a neutral component be included. We contrast this with an ideal plasma, many of whose properties (such as plasma oscillations, interaction with electromagnetic waves, etc.) are independent of its neutral components. Thus, the word "plasma" in its general sense of a system of charged particles is not appropriate for dense plasma of low temperature, whereas it is a suitable description for ideal plasmas that are weakly ionized gases at low temperature.

6.4 SPECIAL FEATURES OF STRONGLY COUPLED PLASMAS

The above analysis of a strongly coupled plasma makes it possible to identify the distinguishing features of such an object. We first present a contrast to a weakly coupled plasma.

When we apply the term "plasma" to a weakly ionized gas, we concentrate on properties that are determined by charged particles. These properties of an ideal plasma do not depend on the presence of neutral particles, even though the density of neutral particles is greatly in excess of the density of charged particles. For example, the presence of neutral atoms in the Earth's ionosphere has no effect on the character of the propagation of electromagnetic waves through it. This explicitly plasma property is qualitatively distinct from such ionosphere properties as thermal capacity and thermal conductivity that are determined by the neutral component only. We can thus use the term "plasma" as a universal description of a wide variety of systems of weakly ionized gases whose electrical or electromagnetic properties are determined by charged particles only. It allows us to analyze in a general way the properties of systems that may be very diverse in terms of the properties arising from their neutral components.

The explanation for this situation is to be found in the character of the interactions in a weakly ionized gas. There is a short-range interaction between neutral particles—atoms or molecules—and the long-range Coulomb interaction between charged particles. These interactions produce effects that can be treated independently in a gaseous system. Therefore, if a particular property of this system is determined by a long-range interaction between charged particles, one can neglect the short-range interactions in this system. That is, the presence of neutral particles does not affect these properties of the system. It follows from the nature of this deduction that such a conclusion can be valid only for systems with weak interactions among its constituents; that is, it can apply only to gaseous systems. On the other hand, a strongly coupled plasma is a system with strong interactions among the particles, and these strong interactions make it impossible to divide

interactions into independent short-range and long-range types. Therefore the term "strongly coupled plasma" cannot be employed as a generic description for a wide variety of systems as can be done in the case of an ideal plasma.

We can illustrate this conclusion with some examples of strongly coupled plasmas. Consider a metallic plasma. Taking a metal of a singly valent element, we assume that all the valence electrons contribute to the conductivity, and that the metallic ions form the metal lattice. Then the electron number density is $N_e = \rho/m$, where ρ is the density of the metal and m is the atomic mass. For example, in the case of copper, we have $N_e = 8.4 \times 10^{22}$ cm^{-3} at room temperature, along with the parameters $\gamma = 1.5 \times 10^7$ and $\Gamma = 400$. Assuming this plasma to be classical, we find that it is a strongly coupled plasma. Another example of a nonideal plasma is an electrolyte, which is a solution with positive and negative ions. The high density of molecules in the solution makes it a strongly coupled plasma.

These examples refer to stationary strongly coupled plasmas. The strong action of an intense, short pulse of energy on matter can generate a nonstationary strongly coupled plasma. Plasmas of this type can result from a strong explosion that compresses the matter. Another example of this type is the plasma associated with laser fusion, where the target is irradiated by short laser pulses directed onto the target simultaneously from different directions. The energy transferred to the target causes extreme heating and compression, with a dense plasma created as a result.

These examples illustrate the above conclusion for a strongly coupled plasma: namely, that its properties are determined by interactions involving both neutral and charged particles. Different physical objects of this type do not have general properties determined only by the charged particles. Therefore when one describes a system as a "strongly coupled plasma", the immediate implication is that it is not one of a general class with identical properties as in the case of an ideal plasma.

6.5 QUANTUM PLASMAS

We can treat a dense, low-temperature plasma of metals as a degenerate Fermi gas. Because of the low temperature and large density, the system has quantum properties. Let us consider the limit when $T = 0$, and take into consideration the Pauli principle according to which two electrons cannot be in the same state. With the positive charge distributed uniformly over the plasma volume, this plasma is a degenerate electron gas. At zero temperature the plasma electrons have distinct momenta p in the interval $0 \leq p \leq p_F$. The Fermi momentum p_F is found from the relation

$$n = 2\int \frac{d\mathbf{p}\, d\mathbf{r}}{(2\pi\hbar)^3},$$

where n is the total number of plasma electrons, the factor 2 takes account of the two possible directions of the electron spin, and $d\mathbf{p}$ and $d\mathbf{r}$ are elements of the electron momentum and the plasma volume. Introducing the electron number density $N_e = n/\int d\mathbf{r}$, we have $p_F = (3\pi^2\hbar^3 N_e)^{1/3}$ for the Fermi momentum, and the *Fermi energy* is

$$\varepsilon_F = \frac{p_F^2}{2m_e} = \frac{(3\pi^2 N_e)^{2/3}\hbar^2}{2m_e}. \tag{6.17}$$

The parameters of a classical plasma satisfy the relation $\varepsilon_F \ll T$ or $r_D^2 N_e^{1/3} \gg a_0$. We define a quantum plasma to be a charged-particle system characterized by the small parameter

$$\eta = T/\varepsilon_F, \tag{6.18}$$

exactly opposite to the condition for a classical plasma.

The Fermi energy is a fundamental parameter of a degenerate electron gas, and it is this parameter that is used for the analysis of a quantum plasma. We introduce the parameter characterizing the ideal nature of a quantum plasma by analogy with Eq. (6.2) as the ratio of the Coulomb interaction energy of electrons to the Fermi energy, or

$$\xi = \frac{e^2/r_W}{\varepsilon_F} = \frac{2^{5/3}}{3\pi a_0 N_e^{1/3}} = \frac{0.337}{a_0 N_e^{1/3}}, \tag{6.19}$$

where r_W is the Wigner–Seitz radius, and a_0 is the Bohr radius. The ideal degenerate electron gas has a large density compared to a characteristic atomic density: $N_e a_0^3 \gg 1$. From Eq. (6.19), this is equivalent to $\xi \ll 1$. It means that the larger the electron number density, the more the properties of a degenerate electron gas determine the properties of a quantum plasma. To the contrary, the role of the Coulomb interaction between charged particles of the plasma decreases with increase of the electron number density.

We can apply the model of a degenerate electron gas to describe the behavior of electrons in metals. Table 6.1 lists parameters of real metallic plasmas at room temperature. It can be seen that the parameter η is small, meaning that the metallic plasma has the character of a quantum plasma. But the Coulomb interaction involving electrons and ions of metals is comparable to the exchange interaction potential of electrons, determined by the Pauli principle. Thus, a metallic plasma is a quantum plasma in which the potential of the Coulomb interaction of charged particles and the exchange interaction potential of the electrons have the same order of magnitude.

Positive ions of real metals form a crystalline lattice at low temperatures. An important role in these crystals is played by the non-Coulomb interaction

TABLE 6.1. Parameters of Metallic Plasmas at Room Temperature

Metal	N_e, 10^{22} cm^{-3}	η, 10^{-3}	ξ
Li	4.6	5.5	1.8
Na	2.5	8.2	2.2
Mg	8.6	3.6	1.4
Al	18	2.2	1.1
K	1.3	13	2.7
Cu	8.4	3.7	1.4
Ag	5.9	4.6	1.6
Cs	0.85	17	3.1
Au	5.9	4.6	1.6
Hg	8.5	3.6	1.4

of free electrons with ions and bound electrons. Consider a simplified problem where electrons and ions of the metal participate only in the Coulomb interactions between them. The energy per coupled pair of charged particles (one electron and one ion) is

$$\varepsilon = \frac{3p_F^2}{10m_e} - \kappa e^2 N_e^{1/3}, \tag{6.20}$$

where the first term is the mean electron kinetic energy, the second term is the mean energy of the Coulomb interaction between charged particles, and the parameter κ depends on the lattice type. Here we take into account the redistribution of charged particles resulting from their interaction that leads to the attractive character of the mean interaction energy.

Noting that $p_F \sim N_e^{1/3}$ and optimizing the expression (6.20) for the specific plasma energy, we find that the optimal parameters of the plasma are

$$\begin{aligned} a_0 N_e^{1/3} &= \frac{5\kappa}{3^{5/3}\pi^{4/3}} = 0.174\kappa, \\ \varepsilon_{\min} &= -2.5 \times 3^{-5/3}\pi^{-4/3}\kappa^2\left(m_e e^4/\hbar^2\right) = -\varepsilon_0 \kappa^2, \end{aligned} \tag{6.21}$$

where $\varepsilon_0 = 2.4$ eV. This manipulation shows that the system may have a stable configuration of bound ions and electrons (i.e., $\varepsilon_{\min} < 0$). The stable distribution of charged particles corresponds to the value of the parameter $\xi = 1.9/\kappa$. The system so described is called the *Wigner crystal*. It can be seen that the Wigner crystal, like real metals, is characterized by an electron number density of the order of the typical atomic number density a_0^{-3}.

6.6 IDEAL ELECTRON–GAS AND ION–GAS SYSTEMS

The gaseous-state condition for a weakly ionized gas relates not only to interactions among charged particles or among neutral particles as separate groups, but also to interactions between charged and neutral particles. The interaction between neutral atomic particles has a short-range character, while the interaction of a charged particle with neutrals may be long-range and is stronger than the interaction between neutral particles. Therefore, one can expect a violation of the condition for the gaseous state to occur in the interaction of one charged particle with surrounding particles in a dense gas. That is, in a system of atoms and a single charged particle, where the interaction of the atoms satisfies the gaseous criterion, the interaction of the charged particle with the atoms does not have a gaseous character, that is, the charged particle interacts with many atoms simultaneously. We now consider this phenomenon in detail.

We begin by examining the behavior of electrons in a dense gas. The gaseous character of the interaction between electrons and atoms implies the condition

$$\lambda = (N\sigma)^{-1} \gg \bar{r}, \tag{6.22}$$

where λ is the mean free path of an electron in the gas, σ is the cross section for electron–atom scattering, N is the number density of atoms, and $\bar{r}$ is the mean distance between particles. We take $\bar{r}$ to be the Wigner–Seitz radius, so that $\bar{r} = (4\pi N/3)^{-1/3}$. The electron–atom cross section is represented by $\sigma = 4\pi L^2$, where L is the scattering length for slow electrons scattered by atoms.

We can write the condition (6.22) as

$$N \ll N_{\text{cr}}^{e}, \tag{6.23}$$

where $N_{\text{cr}}^{e} = (4\pi L^3\sqrt{3})^{-1}$. Table 6.2 lists values of N_{cr}^{e} and the critical pressure $p_{\text{cr}} = N_{\text{cr}}^{e}T$ for electron interaction at $T = 300$ K. It is seen that the gas condition for interaction of electrons with atoms can be violated in a dense gas.

TABLE 6.2. Critical Parameters for Interaction of Electrons and Ions with a Gas

Gas, vapor	N_{cr}^{e}, 10^{21} cm^{-3}	p_{cr}^{e}, atm	N_{cr}^{i}, 10^{21} cm^{-3}
He	200	8000	6.3
Ar	90	3000	2.8
Kr	7	300	2.6
Xe	1	50	2.0
Cs	0.03	1	0.12

The other gaseous conditions for the electron–atom interaction in a dense gas require that positions of neighboring atoms should not influence electron–atom scattering . These relationships give

$$L \gg \bar{r}, \qquad p\bar{r}/\hbar \ll 1. \tag{6.24}$$

The first condition in Eq. (6.24) gives $N \ll 3\sqrt{3}N_{cr}$, so that it is less restrictive than the condition (6.23). The second condition in Eq. (6.24) has the form

$$N \ll N_1(T), \tag{6.25}$$

where

$$N_1(T) = \frac{3\hbar^3}{4\pi(2m_eT)^{3/2}}.$$

This is independent of the identity of the gas. At a temperature $T = 300$ K, we have $N_1 = 2 \times 10^{22}$ cm^{-3}, corresponding to the gas pressure 700 atm.

For a gas consisting of atoms plus ions arising from those atoms, we have the gaseous-state condition (6.22), where σ is the cross section of the resonant charge-exchange process, and $\bar{r}$ is the mean distance between particles. The charge-exchange cross section is large, and therefore the gaseous-state condition for ions is violated at small densities of the gas. Table 6.2 lists values of gas densities $N_{cr}^i = (\pi/2)^{1/2}\sigma^{-3/2}$ at which the criterion to have a gaseous state for interaction of ions and atoms is violated at a gas temperature of 1000 K.

We conclude that electron–atom or ion–atom interactions in a weakly ionized gas can be nonpairwise even when the interaction between neutral particles satisfies the gaseous-state condition. Then charged particles interact simultaneously with several neutrals, and the gaseous character of the interaction is lost.

6.7 DECREASE OF THE ATOMIC IONIZATION POTENTIAL IN PLASMAS

A dense plasma alters the states of its constituent atoms, and thereby can change the atomic spectrum. In particular, spectra of metallic plasmas differ significantly from spectra of isolated atoms of the metals. The greater the plasma density, the more drastic is the change in atomic parameters, including the ionization potential. Below we estimate the decrease of the atomic ionization potential as a function of the plasma density.

The decrease in the ionization potential is caused by two factors. First, the presence of free ions makes it possible for a bound electron to jump from

one ion to another, and if such jumps occur freely, this type of excitation relates to the entire system rather than to a single atom. Second, collisions between an electron and an excited atom result in transitions between neighboring levels. If the frequency of such transitions is higher than the difference between the frequencies of electron circulation in the orbits corresponding to these levels, one can no longer ascribe discrete energies to these levels.

According to the first criterion, an atom cannot be regarded as isolated if its size r_a is of the order of the mean distance $N_i^{-1/3}$ between neighboring ions. When we relate the atomic size to the ionization potential $J(r_a \sim e^2/J)$, the estimated decrease in the ionization potential is

$$\Delta J \sim e^2 N_i^{1/3}. \tag{6.26}$$

The decrease of the ionization potential arising from the second mechanism is determined by the relationship

$$\Delta J \sim \Delta E/\hbar \sim N_e v \sigma, \tag{6.27}$$

where v is a typical electron velocity, ΔJ is the electron energy at which the electron ceases to be bound, ΔE is the energy difference between neighboring levels of a given symmetry for a highly excited electron located in a Coulomb field, and σ is the transition cross section between neighboring levels of a highly excited atom due to electron impact. We can make a classical estimate for this cross section. The collision cross section for two free electrons resulting in an energy exchange in the range from ε to $\varepsilon + d\varepsilon$ is, according to Eq. (5.2),

$$d\sigma = \frac{2\pi e^4}{m_e v^2} \frac{d\varepsilon}{\varepsilon^2},$$

where m_e is the electron mass. Hence, the cross section for an electron collision with a highly excited atom resulting in transfer of energy larger than the energy difference ΔE between neighboring levels is

$$\sigma = \frac{2\pi e^4}{m_e v^2 \Delta E}.$$

The energy difference between neighboring levels of a highly excited atom with ionization potential J is

$$\Delta E \sim J^{3/2} \frac{\hbar^2}{m_e e^4}.$$

From this and Eq. (6.27), the ionization potential of highly excited levels that make a transition to the continuum is

$$J \sim e^2 N_e^{1/3} \left(\frac{e^2}{\hbar v} \right)^{1/2} .$$

States with ionization potentials of this order cease to be stationary. Since $v \sim \sqrt{T/m_e}$, the decrease of the ionization potential due to this mechanism is

$$\Delta J \sim e^2 N_e^{1/3} \left(\frac{m_e e^4}{\hbar^2 T} \right)^{1/4} . \tag{6.28}$$

Though formally the criterion (6.28) is stronger than (6.26), the actual difference between them is small. From these criteria it follows that the denser the plasma, the larger is the decrease of the atomic ionization potential. Note that the decrease of the ionization potential of atoms located in an ideal plasma is small compared to the thermal energy of the plasma particles.

6.8 INTERACTIONS AND STRUCTURES IN DUSTY PLASMAS

Strong coupling of a plasma consisting of electrons and singly charged positive ions takes place if the plasma parameter (6.1) or (6.4) is of the order of unity, corresponding to densities of charged particles that are comparable to densities of neutral particles in condensed matter. In the case when the ion charge Z is large, the plasma parameter (6.4) for ions has the form

$$\Gamma_i \sim \frac{Z^2 N_i^{1/3} e^2}{T_i}, \tag{6.29}$$

where T_i is the ion temperature and N_i is the ion number density. From this it follows that the plasma parameter increases dramatically for a plasma with multicharged ions, and strong coupling sets in at relatively small number densities of ions. This takes place in a gas-discharge plasma that incorporates micron-sized dust particles. The particle charge is typically $Z \sim 10^4$–10^5, so that a dusty plasma can be a strongly coupled plasma even for small densities of electrons and other plasma particles.

The field created by a charged dust particle in a gas-discharge plasma is similar to that of a singly charged particle as expressed in Eq. (3.6), if the parameter $Ze^2/(r_D T_e)$ is small. Here r_D is the Debye–Hückel radius (3.7), which is determined by the electrons only, because ions are absorbed by the dust particle. For the example of an argon plasma in a glow discharge with an

electron temperature $T_e = 4$ eV, the number density of electrons and ions is about $N_0 = 10^{10}$ cm^{-3} when the particles have a charge $Z = 2 \times 10^5$. Electrons will then screen the Coulomb field of a particle on a distance scale of $r_D = 100\mu$m, and for a radius $r = 1\mu$m we have $Ze^2/(r_D T_e) = 1$. That is, the ideality criterion fails in this case. If the number density of dust particles exceeds $\sim 10^5$ cm^{-3}, the Coulomb interaction between particles is important. For lower particle densities, only neighboring particles interact. We see that the conditions for an ideal plasma are violated for small number densities of dust particles.

When small particles in a gas discharge are captured in a trap, they are localized in the plasma of this trap. Interaction of these particles with ions and electrons of the plasma and with walls of the trap leads to formation of small-particle structures within the trap. Such a structure of captured particles is called a *plasma crystal.* This crystal is stable and can be considered to be a well-defined physical object. It has many of the usual properties of crystals, and like ordinary crystals, the plasma crystal can be melted or can be dissociated by an external field. However, these processes take place in a manner unique to plasma crystals.

We shall analyze small particle structures that form in an electric trap of a gas discharge in a cylindrical tube. Spatial positioning of the particles in layers depends on the nature of the interaction between particles. We first consider the case when there is a Coulomb repulsion between particles, and when all the particles have the same charge. From symmetry considerations, the particle layers are in planes directed perpendicular to the discharge axis. The electric field of a layer of charged particles in the plane of the layer plane is directed along the radius that connects a given point and the layer center. In the case of the Coulomb interaction, the particles are located on circles. and within the limits of one circle they form regular polygons. This occurs when there is a large number of layers.

If the Debye–Hückel radius of the gas-discharge plasma is smaller than the distance between nearest particles, and the interaction takes place between nearest-neighbor particles only, then a different type of structure is formed. If we take any particle of the layer, its nearest neighbors form a regular polygon, so that the total force acting on a particle by its neighbors is zero. The number of polygon vertices is $2k$, where k is an integer. Then the total force acting on each particle is zero. This corresponds to a structure consisting of regular polygons. Positions of peripheral particles are determined also by the interaction of particles with a field associated with the walls of the trap. Hence, the regular structure of particles is altered near walls of the trap, and the boundary conditions for particles near walls are of importance for the symmetry of their structure. That is, the particle structure depends on the spatial form of the electric discharge trap in which charged particles are captured.

CHAPTER 7

RADIATIVE PROCESSES IN WEAKLY IONIZED GASES

7.1 INTERACTION OF RADIATION WITH ATOMIC SYSTEMS

Interaction of a plasma with radiation affects plasma properties, and in systems such as gas lasers or the plasma generated by laser radiation, these processes determine the plasma parameters. Electromagnetic fields cause transitions in atomic systems, and Table 7.1 gives a list of single-photon processes that are of interest for plasmas. The interaction is weak, and is characterized by the fine-structure constant $\alpha = e^2/(\hbar c) \approx \frac{1}{137}$. The ratio of a typical velocity internal to an atom to the velocity of light is approximately equal to the fine structure constant, and so it is a measure of the nonrelativistic character of the motion of valence electrons in atoms. Another small parameter that characterizes radiative processes in plasmas is the ratio of the electric field of an electromagnetic wave to a typical field internal to an atom. This ratio is small except for extremely intense fields, and so radiative processes in atomic systems involving absorption or emission of photons usually proceed slowly on the scale of atomic times.

In external fields, emission of a photon leads to atom transitions to a lower excited state or to the ground state. The lifetime τ of an excited atom with respect to this process is considerably longer than a typical atomic time. The reciprocal quantity $1/\tau$ (the frequency of spontaneous radiation) with respect to a characteristic atomic frequency is measured by the cube of the fine structure constant, $[e^2/(\hbar c)]^3$, and hence is lower by at least six orders of magnitude than the frequency of the emitted photons. In particular, the radiative lifetime of the first excited state of the hydrogen atom, H($2p$), is 2.4×10^{-9} s, while the characteristic atomic time is $\hbar^3/(me^4) = 2.4 \times$

TABLE 7.1. Elementary Interactions between Atoms and Radiation

Process	Scheme of the Process
Excitation as a result of photon absorption	$\hbar\omega + A \rightarrow A^*$
Spontaneous radiation of an excited atom	$A^* \rightarrow \hbar\omega + A$
Stimulated photon emission	$\hbar\omega + A^* \rightarrow 2\hbar\omega + A$
Atomic photoionization	$\hbar\omega + A \rightarrow A^+ + e$
Photodetachment of a negative ion	$\hbar\omega + A^- \rightarrow A + e$
Photodissociation of a molecule	$\hbar\omega + AB \rightarrow A + B$
Photorecombination of an electron and an ion	$e + A^+ \rightarrow A + \hbar\omega$
Radiative attachment of an electron to an atom	$e + A \rightarrow A^- + \hbar\omega$
Atomic photorecombination	$A + B \rightarrow AB + \hbar\omega$
Bremsstrahlung in electron-atom or electron-ion collisions	$e + A \rightarrow e + A + \hbar\omega$

10^{-17} s. The weakness of typical electromagnetic fields in plasmas allows us to neglect multiphoton processes. In particular, we can ignore two-photon processes compared to single-photon processes. The lowest excited state of the atom from which it is possible to have a single-photon transition to the ground state is called a *resonantly excited state*. Radiative transitions involving resonantly excited states of atoms are the main subject of this chapter.

7.1 SPONTANEOUS AND STIMULATED EMISSION

Radiative transitions between discrete states of an atom or molecule are summarized in a simple fashion in Fig. 7.1. We designate by n_ω the number of photons in a given state. This value is increased by one as a result of a transition to the ground (lower) state and is decreased by one after absorption of a photon. Because the absorption rate is proportional to the number of photons present, we write the probability of photon absorption by one atom per unit time in the form

$$W(i, n_\omega \rightarrow f, n_{\omega-1}) = An_\omega, \tag{7.1}$$

where, in accord with Fig. 7.1, we denote the lower state by subscript i and the upper state by subscript f. Equation (7.1) accounts for the fact that no

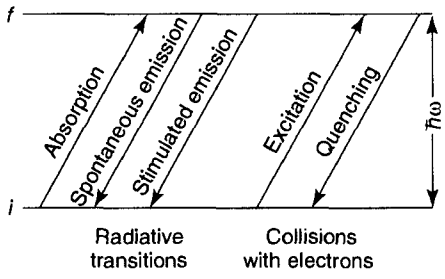

Figure 7.1 Collisional and radiative transitions between two states.

transitions occur in the absence of photons ($n_\omega = 0$) and only single-photon transitions take place. The quantity A does not depend on the electromagnetic field strength and is determined only by properties of the atom.

The probability per unit time for an atomic transition with emission of a photon can be represented in the form

$$W(f, n_\omega \to i, n_{\omega-1} + 1) = 1/\tau + Bn_\omega. \tag{7.2}$$

Here $1/\tau$ is the reciprocal lifetime of the upper state with respect to spontaneous radiative transitions (those that proceed in the absence of the electromagnetic field) to the lower state, and the quantity B refers to the radiation stimulated by the external electromagnetic field. Both values depend only on atomic properties. The quantities A and B in Eqs. (7.1) and (7.2) are known as the *Einstein coefficients*.

Relationships among the parameters $1/\tau$, A, and B can be obtained by an analysis of the thermodynamic equilibrium existing with the atoms and photons. The relation between the number densities of atoms, N_i and N_f, in the ground and excited states, respectively, are given by the Boltzmann law (2.9):

$$N_f = \frac{g_f}{g_i} N_i \exp\left(-\frac{\hbar\omega}{T}\right),$$

where g_i and g_f are the statistical weights of the ground and excited states, and the photon energy $\hbar\omega$ coincides with the energy difference between the two states. The mean number of photons in a given state is determined by the Planck distribution (2.21):

$$\bar{n}_\omega = \left[\exp\left(\frac{\hbar\omega}{T}\right) - 1\right]^{-1}.$$

In thermodynamic equilibrium, the number of emissions per unit time must be equal to the number of absorptions per unit time. Applying this condition to a unit volume, we have

$$N_i W(i, \bar{n}_\omega \to f, \bar{n}_\omega - 1) = N_f W(f, \bar{n}_\omega - 1 \to i, \bar{n}_\omega).$$

From Eqs. (7.1) and (7.2), this relation takes the form

$$N_i A\bar{n}_\omega = N_f (1/\tau + B\bar{n}_\omega). \tag{7.3}$$

Using the above expressions for the connection between the equilibrium number densities of atoms and the equilibrium average number of photons in a given state, we obtain for the Einstein coefficients that $A = g_f/(g_i\tau)$ and

$B = 1/\tau$. We then find the rates of the single-photon processes to be

$$W(i, n_\omega \to f, n_\omega - 1) = \frac{g_f}{g_i \tau} n_\omega,$$
$$W(f, n_\omega \to i, n_\omega - 1) = \frac{1}{\tau} + \frac{n_\omega}{\tau}. \tag{7.4}$$

Note that thermodynamic equilibrium requires the presence of stimulated radiation, which is described by the last term and is of fundamental importance.

7.3 BROADENING OF SPECTRAL LINES

The simplest view of the emission of a photon in an atomic transition is that the photon energy is exactly equal to the difference between the quantum energies of the initial and final atomic states. A more detailed analysis identifies a number of mechanisms that cause a departure from this simple resonance rule, and result in the broadening of both emission and absorption lines in the spectrum. The width of spectral lines is small compared to the excitation energy, but it is nevertheless an essential element in the interaction of radiation with atomic gases and plasmas. Therefore, we now turn our attention to an analysis of the broadening of spectral lines.

We introduce the frequency distribution function a_ω that describes relative amplitudes within the range of frequencies that occurs in both the absorption and the emission of photons. Then $a_\omega d\omega$ is the probability that the radiation frequency lies in the interval from ω to $\omega + d\omega$. All the photon frequencies are in the vicinity of the central frequency ω_0 that is determined by the relation $\varepsilon_f - \varepsilon_i = \hbar\omega_0$, where ε_i and ε_f are the energies of the ground and excited states of the atom. The width of the spectral line can be defined as an average deviation $|\omega - \omega_0|$ that is small compared to ω_0. We now examine the mechanisms and the magnitudes of line-broadening influences.

The simplest broadening mechanism arises from the motion of the emitting atoms. An electromagnetic wave of frequency ω_0, emitted by a moving atom with a velocity v_x in the direction of propagation of the photon, is perceived by a stationary detector as having the frequency ω given by the Doppler law

$$\omega = \omega_0(1 - v_x/c).$$

Assuming radiating atoms to have the Maxwell distribution of velocities (2.15), we find that the frequency distribution of photons measured by a fixed detector outside the gas is

$$a_\omega = \frac{1}{\omega_0}\left(\frac{Mc^2}{\pi T}\right)^{1/2} \exp\left(-\frac{Mc^2}{T}\frac{(\omega - \omega_0)^2}{\omega_0}\right), \tag{7.5}$$

where M is the mass of the atom. To obtain this relation, we assumed that the emitted frequency is determined solely by the atomic velocity. In addition, we employed the connection $a_\omega\, d\omega = \varphi(v_x)\, dv_x$, between the frequency distribution function and the Maxwell distribution function $\varphi(v_x)$ given in Eq. (2.15). The broadening (7.5) due to motion of the emitting system is known as *Doppler broadening*. From Eq. (7.5) one can estimate a Doppler width of a spectral line as $\Delta\omega \sim \omega_0 v_T/c$, where $v_T \sim (T/M)^{1/2}$ is a typical thermal velocity of an atom. The Doppler width of a spectral line in gases is ordinarily less than the photon frequency by about six orders of magnitude.

The other simple broadening mechanism for spectral lines stems from the fact that the states between which the transition occurs have finite lifetimes. In order to construct the photon frequency distribution function a_ω, we employ the following chain of reasoning. The time dependence of the ground state wave function has the form $\psi_i \sim \exp(-i\varepsilon_i t/\hbar)$, the wave function of the excited state is $\psi_f \sim \exp(-i\varepsilon_f t/\hbar)$, and the amplitude of the radiative transition is proportional to the product $\psi_i^*\psi_f \sim \exp(-i\omega_0 t)$. The photon frequency distribution function is proportional to $|f_\omega|^2$ where f_ω is the Fourier component of the product $\psi_i^*\psi_f$. Supposing the states to be stationary, we obtain $a_\omega = \delta(\omega - \omega_0)$, that is, when both states in the transition are assumed to be stationary, the photon energy coincides exactly with the difference of the energies of the initial and final states in the transition.

Now we take into consideration the finite lifetime of the states. The probability P_k for the atom to remain in its initial state k is determined by the equation $dP_k/dt = -P_k/\tau_k$, where τ_k is the lifetime of this state. The solution is $P_k = \exp(-t/\tau_k)$, and the time-dependent wave function must be multiplied by $\exp[-t/(2\tau_k)]$. The time-dependent amplitude of the transition is then given by

$$f(t) = \psi_i^*\psi_f \sim \exp(i\omega_0 t - \nu t),$$

where

$$2\nu = 1/\tau_i + 1/\tau_f,$$

and τ_i, τ_f are the lifetimes of the ground and excited states. From this we have

$$f_\omega = \frac{1}{2\pi}\int_{-\infty}^{\infty} f(t)\exp(-i\omega t)\, dt \sim \frac{1}{\nu + i(\omega - \omega_0)}.$$

Accounting for $a_\omega \sim |f_\omega|^2$, and normalizing the photon frequency distribution function to $\int_{-\infty}^{\infty} a_\omega\, d\omega = 1$, we obtain

$$a_\omega = \frac{\nu}{\pi}\frac{1}{\nu^2 + (\omega - \omega_0)^2}. \tag{7.6}$$

The width of the spectral line is of the order of ν in this case. The photon frequency distribution function (7.6) is known as the *Lorentz profile* of spectral lines.

If there are two mechanisms for broadening of spectral lines with the distribution functions $a_\omega^{(1)}$ and $a_\omega^{(2)}$, the resultant distribution function has the form of the convolution

$$a_\omega = \int_{-\infty}^{\infty} a_\omega^{(1)} a_{\omega-\omega'}^{(2)}\, d\omega'. \tag{7.7}$$

We can also treat the case when the broadening is created by both Doppler and Lorentz mechanisms, and the Doppler width of the spectral line is larger than the Lorentz width. Then from Eq. (7.7) and also Eqs. (7.5) and (7.6) for the distribution functions $a_\omega^{(1)}$ and $a_\omega^{(2)}$, it follows that the central part of the spectral line is described by the Doppler formula (7.6), while the wing of the spectral line has the Lorentz shape

$$a_\omega = \frac{\nu}{\pi(\omega - \omega_0)^2}. \tag{7.8}$$

7.4 IMPACT BROADENING OF SPECTRAL LINES

Other mechanisms that broaden spectral lines result from the interaction of the radiating atom with surrounding atoms. The character of this broadening depends on the density of the surrounding gas. If this density is small, the broadening results from individual collisions of the excited atom with others in the gas. Each collision is an independent event, and these events are relatively infrequent. Most of the time there is no interaction at all of the excited atom with others, until such time as a strong interaction with a neighboring atom abruptly occurs. The line broadening caused in this fashion is called *impact broadening*. A contrasting type of line broadening takes place in a dense gas. There the radiating atom interacts simultaneously with many other atoms in the gas, and the displacement of multiple atoms amounts to a relatively weak averaged interaction. This mechanism is known as *quasistatic* or *statistical broadening* of spectral lines.

We shall first analyze the impact broadening of spectral lines. As remarked above, the effect is a result of separate, independent collisions with atoms in the gas. For most of its time of existence, the excited atom does not interact with other atoms, and the amplitude of the radiative transition depends on time as $f(t) \sim \psi_i^* \psi_f \sim \exp(-i\omega_0 t)$. During a collision the energies of the excited and ground states of the emitting atom are shifted, and as a result of the collision the phase of the transition amplitude is also shifted. The altered time dependence of the transition amplitude can be written in the form

$$f(t) \sim \psi_i^* \psi_f \sim \exp\left(-i\omega_0 t + \sum_k \chi_k \eta(t - t_k)\right).$$

Here $\eta(x)$ is the unit step function, that is, $\eta(x) = 0$ for $x < 0$, and $\eta(x) = 1$ for $x > 0$; t_k is the time of the kth collision; and χ_k is a phase shift resulting from this collision. A result in this form means that we assume the collision time to be small compared to the time between two successive collisions. Note that if the time between successive collisions is such that $\chi_k \sim 1$, this is equivalent to a random value for the phase shift.

Taking the Fourier component of the transition amplitude, the frequency distribution function of the emitted photons is

$$a_\omega \sim |f_\omega|^2, \qquad f_\omega \sim \sum_k \frac{1 - \exp(-i\omega_0\tau_k)}{\omega - \omega_0} \exp\left(i \sum_{j<k} \chi_j + i\frac{\pi}{2}\right),$$

where τ_k is the time interval between the kth and $(k + 1)$th collisions. We can average this expression using the assumption that τ_k and χ_k have random values. Then we have $\langle \exp[i(\chi_j - \chi_k)] \rangle = \delta_{jk}$, where the angle brackets mean averaging over random phases, and the Kronecker symbol δ_{jk} is defined to be 1 if $j = k$, and 0 if j and k are different. Averaging over the time between successive collisions gives

$$a_\omega = C \frac{\langle 1 - \cos[(\omega - \omega_0)t] \rangle}{(\omega - \omega_0)^2},$$

where C is a normalization coefficient and the angle brackets denote averaging over the time interval t between collisions. The time distribution between collisions is given by $P(t) = \exp(-t/\tau)$, where τ is the average time between collisions. Averaging on the basis of this distribution function and normalizing the frequency distribution function a_ω for emitted photons, we obtain

$$a_\omega = \frac{\tau}{\pi} \frac{1}{(\omega - \omega_0)^2 \tau^2 + 1}. \tag{7.9}$$

Impact broadening has a Lorentz profile, as does the broadening due to the finite lifetime (7.6). The parameter τ can be estimated to be

$$1/\tau \sim N v \sigma, \tag{7.10}$$

where N is the number density of gas atoms, v is a typical collision velocity, and σ is the cross section for this collision.

In order to understand the nature of the collisions that lead to the broadening, we assume that particle collisions are classical and that the ground state of the emitting atom does not participate in the broadening. Then the broadening is determined by the interaction potential $U(R)$ between the emitting atom and its neighbors in the gas, where R is the distance

between them. The main contribution to the cross section is at impact parameters $\rho \sim \rho_0$ for which the phase shift χ is of the order of unity. Because the phase shift has the dependence $\chi \sim \int U(R)\,dt/\hbar$, this cross section can be estimated to be

$$\sigma \sim \rho_0^2, \qquad \text{where} \quad \frac{\rho_0 U(\rho_0)}{\hbar v} \sim 1. \tag{7.11}$$

We can see that this estimate for the broadening cross section coincides with the total cross section (4.15) for particle collision.

Impact broadening of spectral lines requires that a typical collision time ρ_0/v be small compared to the time $(Nv\sigma)^{-1}$ between successive collisions. This gives

$$N\sigma^{3/2} \ll 1. \tag{7.12}$$

This criterion is fulfilled at small number densities of the atoms constituting the gas, and has an analogy with the criterion (4.19) for the gaseous state, even though different collision cross sections are used in Eqs. (4.19) and (7.12). Note that this criterion refers to the total range of emitted frequencies. The function $U(R)$ decreases monotonically with increasing R. Then since the relation (7.12) gives $\rho_0 \ll N^{-1/3}$, it follows from (7.11) that

$$\frac{N^{-1/3} U(N^{-1/3})}{\hbar v} \ll 1, \tag{7.13}$$

under conditions in which the impact mechanism for the broadening of spectral lines holds true.

7.5 STATISTICAL BROADENING OF SPECTRAL LINES

Another mechanism for broadening of spectral lines occurs in a gas with a high particle number density. Then one can neglect atomic motions in the gas, and the shift of the spectral line for given positions of atoms in the gas in relation to the object atom has the form

$$\omega - \omega_0 = \frac{1}{\hbar} \sum_j V(\mathbf{R}_j), \tag{7.14}$$

where $\mathbf{R}_j$ is the position of the jth gas particle and $V(\mathbf{R})$ is the difference of the interaction potentials of the emitting and gas atoms for the excited and ground states of the radiating atom for the separation $\mathbf{R}$ between them. It is evident that we are assuming the interaction of the emitting and gas atoms to be independent of the positions of other atoms in the gas. This assumption is justified if the interparticle interactions are weak.

We take $|V(R)|$ to decrease monotonically with an increase in R. Then Eq. (7.14) shows that the line shifts from each atom in the gas are additive, so that the mean width $\Delta\omega$ of the spectral line is of the same order of magnitude as the mean shift. Since the mean distance between neighboring atoms is of the order of $N^{-1/3}$ (where N is the number density of atoms in the gas), the mean width $\Delta\omega$ as well as the mean shift of the spectral line is estimated to be

$$\Delta\omega \sim \frac{1}{\hbar} V(N^{-1/3}). \tag{7.15}$$

Now we turn our attention to the photon frequency distribution function in the wings of the line profile. The shift in the wings of the line profile is larger than the mean shift, and is created by gas particles located close to the emitting atom, namely at distances $R \ll N^{-1/3}$. The probability for an atom in the gas to be located in this region is $N d\Omega$, where $d\Omega$ is the volume element, so that the frequency distribution function at the wing of the spectral line has the form

$$a_\omega \, d\omega = N 4\pi R^2 \, dR, \qquad \text{where} \quad \omega - \omega_0 = \frac{1}{\hbar} V(R). \tag{7.16}$$

In particular, if $V(R) = CR^{-n}$, this equation yields the photon frequency distribution in the wing of the line given by

$$a_\omega \, d\omega = \frac{4\pi N C^{3/n}}{n} \frac{d\omega}{(\omega - \omega_0)^{1+3/n}}. \tag{7.17}$$

We now examine the validity of statistical theory for the broadening of spectral lines. It was assumed that atoms in the gas do not change their positions during interactions. This assumption will be valid if the distance that atoms move during the interaction, of the order of $v/\Delta\omega$, is small compared to the mean distance $N^{-1/3}$ between atoms in the gas. We must thus require

$$vN^{1/3} \ll \Delta\omega \sim \frac{1}{\hbar} V(N^{-1/3}), \tag{7.18}$$

where v is a typical collision velocity. Assume that the broadening is caused only by interactions of the excited state of the emitting particle. Then, rather than use $V(R)$ in Eq. (7.18), we use instead the interaction potential of the excited state $U(R)$. The condition (7.18) now takes the form

$$\frac{N^{-1/3} U(N^{-1/3})}{\hbar v} \gg 1. \tag{7.19}$$

Equation (7.19) states a condition opposite to the criterion (7.13) for the validity of the impact mechanism for the broadening of spectral lines. Thus the impact broadening theory and the statistical broadening theory relate to opposite limiting cases of the interaction between an emitting atom and the surrounding atoms in a gas.

The validity of the statistical theory of broadening for the central part of the spectral line can be written as

$$N\sigma^{3/2} \gg 1. \tag{7.20}$$

This is exactly the opposite of the impact-theory criterion in Eq. (7.12). It is based on the requirement that a typical time $1/\Delta\omega$ during which the broadening is created be large compared to a typical time R/v through which the interaction of particles varies. For any part of the spectral line this criterion has the form

$$|\omega - \omega_0| \gg v/R, \tag{7.21}$$

where $\omega - \omega_0$ is given by Eq. (7.14). It follows from this that the condition for the validity of the statistical theory of broadening is better fulfilled for the wing of the spectral line than for its central part.

There is an intermediate case where the impact theory of broadening is valid for the central part of a spectral line, whereas the wing of the spectral line is described by the statistical theory of broadening. Then, as follows from the impact theory, a transition region between these limiting cases corresponds to the estimate $|\omega - \omega_0| \sim v/R \sim U(R)/\hbar$, where R is a typical distance between interacting atoms that determines a given shift of the spectral line. Note that the last relation $[v/R \sim U(R)/\hbar]$ gives $R \sim \sqrt{\sigma}$, where σ is the total scattering cross section. From this, we conclude that the photon frequency distribution function in the transition region on the basis of the statistical theory of broadening has the form

$$a_\omega = 4\pi R^2 N\hbar \left|\frac{dU}{dR}\right|^{-1} \sim \frac{\hbar N R^3}{|U(R)|} \sim \frac{N\sigma^{3/2}}{|\omega - \omega_0|} \sim \frac{N\sigma^2}{v}.$$

According to the impact theory of broadening, the behavior is

$$a_\omega \sim \frac{\nu}{|\omega - \omega_0|^2} \sim \frac{Nv\sigma}{v^2\sigma} \sim \frac{N\sigma^2}{v}.$$

We see that both theories predict the same behavior in the transition region. This confirms once more the connection between the impact and statistical theories of spectral line broadening as opposite limiting cases of the interaction between the emitting and the surrounding atoms.

7.6 CROSS SECTIONS FOR PHOTON EMISSION AND ABSORPTION

The shape and width of the spectral line determine the cross sections for absorption and stimulated radiation. We shall now determine this connection. By definition, the cross section of a process is the ratio of the transition probability per unit time to the flux of particles causing the transition. In this case the photon flux is $c\,dN_\omega$, where c is the velocity of light, and the number density of photons is $dN_\omega = 2n_\omega\,d\mathbf{k}/(2\pi)^3$. The number of photons in a given state is n_ω, the factor 2 accounts for the two independent polarization states, and $d\mathbf{k}/(2\pi)^3$ is the number of states in the differential element $d\mathbf{k}$ of the wave vector. Using the dispersion relation $\omega = kc$ for photons, we obtain $\omega^2\,d\omega/(\pi^2c^2)$ for the photon flux. The absorption probability per unit time in an interval $d\omega$ of photon energies is given by $An_\omega a_\omega\,d\omega$, according to Eq. (7.1). Taking the ratio of the reduced transition probability to the photon flux, we find that the absorption cross section is

$$\sigma_{\text{abs}} = \frac{\pi^2c^2}{\omega^2}Aa_\omega = \frac{\pi^2c^2}{\omega^2}\frac{g_f}{g_i}\frac{a_\omega}{\tau}. \tag{7.22}$$

The same operation yields the stimulated photon emission cross section

$$\sigma_{\text{em}} = \frac{\pi^2c^2}{\omega^2}Ba_\omega = \frac{\pi^2c^2}{\omega^2}\frac{a_\omega}{\tau}. \tag{7.23}$$

We can find the maximum absorption cross section corresponding to the center of the spectral line. For a given transition, the maximum cross section corresponds to minimal broadening of the spectral line, so that it is determined by the radiative lifetime. Then we have $a_\omega = 2\tau/\pi$, and the maximum cross section is

$$\sigma_{\text{abs}} = 2\pi\frac{g_f}{g_i}\frac{c^2}{\omega^2} = \frac{g_f}{g_i}\frac{\lambda^2}{2\pi}, \tag{7.24}$$

where $\lambda = 2\pi c/\omega$ is the photon wavelength. Thus, the maximum absorption cross section is of the order of the square of the photon wavelength. In particular, for photons in the optical region of the spectrum, this value is of the order of 10^{-10}–10^{-9} cm^2, and so exceeds typical atomic and gas-kinetic cross sections by several orders of magnitude.

We can write integral relations for the radiative cross sections. Using the normalization condition $\int a_\omega\,d\omega = 1$, and recognizing that the integral con-

verges in a narrow region of photon frequencies, we obtain

$$\int \sigma_{\text{abs}}(\omega)\, d\omega = \frac{\pi^2 c^2}{\omega^2} \frac{g_f}{g_i} \frac{1}{\tau},$$
$$\int \sigma_{\text{em}}(\omega)\, d\omega = \frac{\pi^2 c^2}{\omega^2} \frac{1}{\tau}. \tag{7.25}$$

These relations are useful for estimations of the cross sections.

7.7 THE ABSORPTION COEFFICIENT

The absorption coefficient k_ω in a gas is defined by the expression

$$dI_\omega/dx = -k_\omega I_\omega, \tag{7.26}$$

where I_ω is the intensity of radiation of frequency ω that passes through a gas, and x is the direction of propagation of this radiation in the gas. Taking into account both absorption and stimulated emission, we can express the absorption coefficient as

$$k_\omega = N_i \sigma_{\text{abs}} - N_f \sigma_{\text{em}} = N_i \sigma_{\text{abs}} \left(1 - \frac{N_f}{N_i} \frac{g_i}{g_f}\right), \tag{7.27}$$

where the cross sections for absorption (σ_{abs}) and for stimulated emission (σ_{em}) are given by Eqs. (7.22), and (7.23). The number densities N_i and N_f refer to populations in the ground and excited states, and g_i and g_f are the statistical weights of these states.

From Eq. (7.27) it follows that if the condition

$$\frac{N_i}{N_f} < \frac{g_i}{g_f} \tag{7.28}$$

is fulfilled, the absorption coefficient is negative, so that the photon flux passing through the gas is amplified. A situation where this occurs is known as an *inversion*, or as an *inverted population of levels*, and a medium for which the condition (7.28) is valid is called an *active medium*. Active media are used in lasers, which are generators of monochromatic radiation. In the case of thermodynamic equilibrium between the ground and resonantly excited states, Eq. (7.27) has the form

$$k_\omega = N_i \sigma_{\text{abs}} - N_f \sigma_{\text{em}} = N_i \sigma_{\text{abs}} \left[1 - \exp\left(-\frac{\hbar\omega}{T}\right)\right]. \tag{7.29}$$

7.8 PROPAGATION OF RESONANT RADIATION THROUGH A GAS

Radiation that causes transitions between the ground and resonantly excited states of gaseous atoms is called *resonant radiation*, and the corresponding photon is called a *resonant photon*. We want to examine how resonant photons propagate through a gas. The mean free path of resonant photons is small because, for one thing, photons are absorbed by atoms in the ground state, which normally have a relatively large number density. Additionally, the absorption cross section near the center of the spectral-line center is large, and is greater by several orders of magnitude than gas-kinetic cross sections. Hence, reemission of photons is of importance for propagation of resonant radiation through a gas.

When the mean free path of resonant photons is small compared to the dimensions of a gaseous system, the propagation of photons is not diffusive in nature. The reason is that a photon emitted far from the center of a spectral line is more likely to propagate large distances than is a photon emitted near the center, where repeated emissions and absorptions will occur with high probability. Hence the principal contribution to long-distance propagation of resonant photons comes from the wings of the spectral line, where the mean free path of these photons is of the order of the dimensions of the gaseous system through which the photons propagate.

We now want to examine the flow of photons outside a gaseous system, assuming that the photon transport process does not affect the density of excited atoms. We can take the mean free path of photons corresponding to the center of the spectral line to be small compared to a size L of the system, so that

$$k_0 L \gg 1,$$

where $k_0 = N_i \sigma_{\text{abs}}(\omega_0) - N_f \sigma_{\text{em}}(\omega_0)$ is the absorption coefficient for line-center photons, and ω_0 is the central photon frequency. Under these conditions, thermodynamic equilibrium is established between the atoms and the line-center photons whose free path length is small compared to the system size. Let i_ω be the flux of photons of frequency ω inside the gas. Then the number of photons absorbed per unit volume per unit time in a frequency range from ω to $\omega + d\omega$ is given by $i_\omega k_\omega \, d\omega$, where k_ω is the absorption coefficient determined by Eq. (7.26). The reduced number of absorbing photons is equal to the corresponding number of emitting photons, which is given by $N_* a_\omega \, d\omega/\tau$. Then, on the basis of Eqs. (7.22), (7.23), and (7.27), we have

$$i_\omega = \frac{a_\omega N_*}{k_\omega \tau} = \frac{\omega^2}{\pi^2 c^2} \left(\frac{N_i}{N_f} \frac{g_f}{g_i} - 1 \right)^{-1}. \tag{7.30}$$

This photon flux is isotropic and can be detected at any point of the medium that is separated from the system boundary by at least a photon

mean free path. The photon flux outside a system with a flat surface is

$$j_\omega = \int_0^{\pi/2} i_\omega \cos\theta \, d(\cos\theta) \left(\int_{-\pi/2}^{\pi/2} d(\cos\theta) \right)^{-1} = \frac{i_\omega}{4}. \tag{7.31}$$

Here θ is the angle between the normal to the gas surface and the direction of photon propagation, and we have taken into account that the total photon flux outside the system is normal to the system surface. The flux of photons of frequency ω outside the gaseous system is

$$i_\omega = \frac{\omega^2}{4\pi^2 c^2} \left(\frac{N_i}{N_f} \frac{g_f}{g_0} - 1 \right)^{-1}, \qquad k_\omega L \gg 1. \tag{7.32}$$

If the plasma temperature is constant, this expression leads to

$$j_\omega = \frac{\omega^2}{4\pi^2 c^2} (e^{\hbar\omega/T} - 1)^{-1}, \qquad k_\omega L \gg 1. \tag{7.33}$$

Equation (7.33) is identical to Eq. (2.23) for blackbody radiation.

The expression for the radiation flux from a flat layer of plasma has the form

$$j_\omega = \frac{1}{2} \int_0^1 d(\cos\theta) \int_0^L dx \frac{N_f}{\tau} a_\omega \exp\left(- \int_0^x \frac{k_\omega \, dx}{\cos\theta} \right), \tag{7.34}$$

where the factor $\frac{1}{2}$ takes account of the departure of photons from only one side of the layer, $N_f a_\omega / \tau$ is the number of emitting photons per unit time and volume for unit frequency range, x is the distance from the surface, θ is the angle between the photon direction and the normal to the surface, and L is the layer thickness. We assume all the plasma parameters to be dependent only on x. The quantity

$$u_\omega = \int_0^L k_\omega \, dx \tag{7.35}$$

is called the *optical thickness* of the layer. Using Eq. (7.6) for the absorption coefficient, one can rewrite Eq. (7.34) in the form

$$j_\omega = \frac{\omega^2}{2\pi^2 c^2} \int_0^1 d(\cos\theta) \int_0^{u_\omega} du \exp\left(- \frac{u}{\cos\theta} \right) \left(\frac{N_i}{N_f} \frac{g_f}{g_i} - 1 \right)^{-1}. \tag{7.36}$$

In particular, Eq. (7.36) follows from Eq. (7.32) if the optical thickness of the layer is large and the ratio of the number densities of atoms in the excited and ground states is constant in a range $u \sim 1$.

It is possible to estimate the width of the spectral line for photons that leave the plasma. The boundaries of the spectral line can be estimated from the relation

$$u_\omega = \int_0^L k_\omega \, dx \sim k_\omega L \sim 1. \tag{7.37}$$

In the case of Lorentz broadening of the spectral line we use Eq. (7.8) $[k_\omega = k_0 \nu^2/(\omega - \omega_0)^2]$ for the line wing. The width of the spectral line for the total radiation flux is then

$$\Delta\omega \sim \nu\sqrt{k_0 L}, \qquad k_0 L \gg 1. \tag{7.38}$$

In the same way, when the spectral line has the Doppler shape (7.5), the width of the spectral line is

$$\Delta\omega \sim \Delta\omega_D \sqrt{\ln(k_0 L)}, \qquad k_0 L \gg 1, \tag{7.39}$$

where $\Delta\omega_D$ is the width of the Doppler-broadened spectral line in the case of small optical thickness of the plasma system. Thus resonant radiation exiting from a gas is characterized by broader spectral lines than is radiation from individual atoms, because the principal contribution to the emergent radiation arises largely from the wings of the spectra of individual atoms.

7.9 SELF-REVERSAL OF SPECTRAL LINES

We considered in the foregoing the propagation of resonant radiation in a uniform plasma. In reality, the temperature on plasma boundaries is smaller than it is in the bulk of the plasma. The radiation emanating from a plasma for frequencies near the center of a spectral line originates in a plasma region near its boundaries. Hence, the radiative flux (7.33) for the central part of the spectral line is associated with a lower temperature than is that part of the radiation arising from spectral regions removed from the center of the line, which is created within deeper layers of the plasma. Therefore, the radiated flux as a function of frequency has the form shown in Fig. 7.2. There is a local minimum at the line center. This phenomenon is known as *self-reversal* of spectral lines.

It is possible to establish the condition under which the radiated flux has a dip at the line center. According to Eq. (7.36), this occurs if there is significant variation in the integrand at distances of the order of the photon mean free path at the center of the spectral line, given by $1/k_0$. Equation (7.36) gives the criterion to have a local minimum of j_ω as

$$\frac{1}{k_0} \frac{\hbar\omega}{T} \frac{dT}{dx} \gg 1 \tag{7.40}$$

when $\hbar\omega > T$.

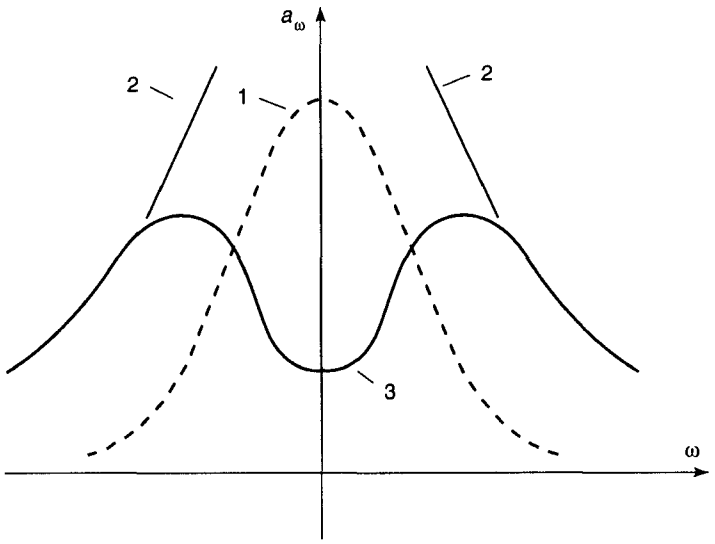

Figure 7.2 Self-reversal of a spectral line. The spectral line of an individual atom is given by curve 1; in a gas with a constant temperature this line is broadened due to reemission (curve 2). The line profile at low temperature near the gas boundary is shown by curve 3.

7.10 PHOTORESONANT PLASMA

An examination of the propagation of resonant radiation in an excited gas shows a strong absorption near the center of the spectral line. This means that resonant radiation can be transformed into excitation of the gas. It is a property used as a diagnostic technique for the analysis of gases and flames. The *optogalvanic method* is based on measurement of a current through an excited or ionized gas as a function of the radiation wavelength. Absorption of radiation by certain atoms leads to formation of electrons and ions that can be detected by changes in the electric current. Calibration of this method makes it possible to measure the content of some admixtures at very low concentrations.

A more widespread application based on absorption of resonant radiation concerns the generation of a photoresonant plasma. To accomplish this, the energy of the resonant radiation absorbed by a gas or vapor is transformed into the energy required to ionize the gas. There is a sequence of processes that determine the generation of a plasma by this means. Resonantly excited atoms are formed as a result of the absorption of resonant radiation. Collision of these excited atoms with each other leads to the formation of more highly excited atoms and subsequently to their ionization. Electrons released in the ionization process establish an equilibrium with the excited atoms. As a result, a plasma is formed wherein the electron temperature and the temperature of the excited atoms are nearly the same.

Along with the processes that create an equilibrium plasma, plasma decay processes also proceed. The main decay process is the expansion of the developing plasma, which determines a lifetime τ that behaves as

$$\tau \sim \frac{r}{c_s}, \tag{7.41}$$

where r is a plasma dimension, and c_s is the sound velocity, typically of the order of the thermal velocity of the atoms. Equation (7.41) yields $\tau \sim 10^{-4}$–10^{-5} s for $r \sim 1$ cm. During this time the photoresonant plasma can be used for measurements and applications. Another cause of energy loss comes from radiation of excited atoms, whose effective lifetime τ_{ef} is, according to Eq. (7.38) for the Lorentz profile of the spectral line, $\tau_{ef} \sim \tau_r(k_0 r)^{1/2}$. In this expression, τ_r is the radiative lifetime of an individual atom, and k_0 is the absorption coefficient at the line center.

From this it follows that the generation of a photoresonant plasma has a threshold character. It is necessary to support the equilibrium in the plasma during its lifetime. This requires that the number density of excited atoms and electrons be sufficiently large. In turn, an adequate amount of energy must be absorbed by the plasma. Using the example of an alkali metal plasma, we give in Table 7.2 parameters of resonantly excited atoms of alkali metals and of alkaline-earth metals. Under the conditions we are considering, the spectral line width $\Delta\omega$ for resonant photons in a metallic vapor is

TABLE 7.2. Parameters of Resonantly Excited Atoms[a]

Atom (state)	λ, nm	τ_r, ns	k_0, cm^{-1}
Li(^2P)	670.8	27.3	3.6
Na($3\,^2P_{1/2}$)	589.6	16.4	1.2
Na($3\,^2P_{3/2}$)	589.0	16.3	1.5
Mg($3\,^1P_1$)	285.2	2.1	5.3
K($4\,^2P_{1/2}$)	769.9	27	0.9
K($4\,^2P_{3/2}$)	766.5	27	1.1
Ca($4\,^1P_1$)	422.7	4.6	2.9
Zn($4\,^1P_1$)	213.9	1.4	6.0
Rb($5\,^2P_{1/2}$)	798.4	28.5	0.8
Rb($5\,^2P_{3/2}$)	780.0	26.5	1.1
Sr($5\,^1P_1$)	460.7	6.2	2.3
Cd($5\,^1P_1$)	228.8	1.7	5.3
Cs($6\,^2P_{1/2}$)	894.4	31	0.8
Cs($6\,^2P_{3/2}$)	852.1	31	0.9
Ba($6\,^1P_1$)	553.6	8.5	2.2
Hg($6\,^1P_1$)	185.0	1.3	5.6

[a]λ is the wavelength of a resonant photon, τ_r is the radiative lifetime of the resonantly excited atom, and k_0 is the absorption coefficient at the line center.

determined by impact broadening. Then $\Delta\omega \sim N$, where N is the number density of atoms, and the absorption coefficient at the line center is $k_0 \sim N\lambda^2/(\Delta\omega\tau_r)$ according to Equations (7.22) and (7.29). Hence, k_0 does not depend on the number density of the atoms, and when $\hbar\omega \gg T$ it does not depend on the temperature. Table 7.2 shows the absorption coefficient at the line center under these conditions.

Assume the effective time of radiation for excited atoms to be small compared to the plasma expansion time (7.41). Then an equilibrium is established between absorption and radiation of resonant photons. The numbers of photons produced per unit time and per unit volume are equal according to Eq. (7.38), so that $N_f/\tau_{ef} \sim N_f/\tau_r\sqrt{k_0 r}$, where N_f is the number density of excited atoms, and k_0 is the absorption coefficient at the center of the spectral line. From this it follows that the equilibrium number density of excited atoms is

$$N_f = CP/r^{5/2}, \tag{7.42}$$

where P is the power of absorbed resonance radiation, and where a spherical configuration of radius r is assumed for the photoresonant plasma. The coefficient C for alkali metals is estimated to be $C = 10^{13}$ W^{-1} cm$^{-1/2}$.

The generation of excited atoms leads to a chain of successive processes such as

$$A^* + A^* \rightarrow A^{**} + A, \quad A^{**} + A \rightarrow A_2^+ + e, \quad e + A^* \rightarrow e + A. \tag{7.43}$$

We can make a rough estimate of the parameters necessary for the equilibrium of a photoresonant plasma. The criterion $N_f k_{ion}\tau \gg 1$ required for equilibrium between excited atoms and ions must be fulfilled, where k_{ion} is the rate constant for transformation of excitation into ionization. Taking $k_{ion} \sim 10^{-9}$ cm^3/s, we obtain $N_f \gg 10^{13}$ cm^{-3}, so that a high level of excitation must exist in a photoresonant plasma. The power of absorbed radiation following from Eqs. (7.41) and (7.42) is estimated to be $P \gg a/r^{3/2}$, where $a \sim 1$–10 W/cm$^{3/2}$, and the total energy of absorbed resonant radiation is $\varepsilon = P\tau \gg \text{const}/r^{5/2}$, where const $\sim 10^{-4}$ J/cm$^{5/2}$. From this it follows that a photoresonant plasma can be created by a low-power source of resonant radiation.

The number density of electrons providing equilibrium between excited and unexcited atoms must satisfy the inequality $N_e \gg 1/(k_q\tau)$, where $k_q \sim 10^{-7}$ cm^3/s is the rate constant for quenching of resonantly excited atoms. This condition gives $N_e \gg 10^{12}$ cm^{-3}. Usually the number density of electrons in a photoresonant plasma is in the range $N_e \sim 10^{13}$–10^{15} cm^{-3}, the temperature of electrons and excited atoms is $T_e \sim 1$ eV, and the gas temperature is $T \sim 1000$ K. Thus, pulsed plasmas are sufficiently dense to be photoresonant.

There are other special features of a photoresonant plasma. Because of high absorption by resonant lines, a photoresonant plasma can be produced

by radiation tuned to transitions between excited levels of atoms or to transitions to ionized states. In such cases an additional source of radiation is required for the initial excitation of the gas. A simple example of this process uses a stepwise excitation in which a low-power source of radiation excites atoms from the ground state, and a high-power source of radiation is tuned to transitions between excited levels of atoms or to continuum levels.

Another special feature of a photoresonant plasma relates to the heating of atoms and ions resulting from elastic collisions of electrons with atoms or ions. In addition, the associative ionization process may give a contribution to gas heating. Typical times for gas heating are large compared to the lifetime of a photoresonant plasma. Hence, the temperature of the atoms and ions is small compared to the electron temperature, though their temperature is significantly greater than the initial gas temperature.

There are many applications for photoresonant plasmas. In particular, because a part of the absorbed energy is transformed to energy of the plasma expansion at the end of the process, a photoresonant plasma is a convenient way to generate acoustic signals with adjustable parameters. Another type of application makes use of the high specific absorbed energy. Then a photoresonant plasma can be a source of multicharged ions. Other applications of photoresonant plasmas make use of both of these special properties of the plasma, as well as the possibility of transforming atoms into ions for ease in their detection.

7.11 RADIATION FROM THE SOLAR PHOTOSPHERE

We concentrated in the foregoing on resonant radiation because of its strong interaction with excited gases. At large plasma densities and sizes, other interaction processes between radiation and plasma particles become essential that are weak in a laboratory plasma. As one such example we shall examine the radiation of the Sun's photosphere, which is created and governed by the processes

$$e + \mathrm{H} \leftrightarrow \mathrm{H}^- + \hbar\omega. \tag{7.44}$$

We assume that local thermodynamic equilibrium obtains in the photosphere, which is supported by the processes

$$e + \mathrm{H} \leftrightarrow 2e + \mathrm{H}^+, \qquad e + \mathrm{H}^- \leftrightarrow 2e + \mathrm{H}. \tag{7.45}$$

This equilibrium leads to Saha relations between the number densities of the corresponding particles, which have the form

$$\begin{aligned} N_e &= \left(\frac{m_e T}{2\pi\hbar^2}\right)^{3/4} N_{\mathrm{H}}^{1/2} \exp\left(-\frac{J}{T}\right), \\ N_- &= \frac{1}{4}\left(\frac{m_e T}{2\pi\hbar^2}\right)^{-3/4} N_{\mathrm{H}}^{3/2} \exp\left(-\frac{\varepsilon_0}{T}\right). \end{aligned} \tag{7.46}$$

Here T is the temperature; N_H, N_e, and N_- are the number densities of hydrogen atoms, electrons, and negative ions, respectively; $J = 13.605$ eV is the ionization potential of the hydrogen atom; and $\varepsilon_0 = J/2 - \mathrm{EA} = 6.048$ eV, where EA = 0.754 eV is the electron affinity of the hydrogen atom. We use the condition of plasma quasineutrality $N_e = N_p$, where N_p is the number density of protons. The second expression in Eq. (7.46) is the Saha distribution for the equilibrium between negative ions, hydrogen atoms, and electrons. In Eq. (7.46) for the number density of negative ions, the electron number density is taken from the Saha distribution corresponding to the equilibrium (7.45) between protons, electrons and hydrogen atoms. In the problem being examined, $N_H \gg N_e \gg N_-$.

To calculate the radiation flux emitted by the solar photosphere and observed on the Earth, we conceive of a Sun-centered sphere of radius r—the distance between Earth and Sun. Because of the uniformity of the radiation flux on this sphere, we find that the solar radiation flux j_ω^E at the position of the Earth is

$$j_\omega^E = j_\omega(R^2/r^2),$$

where R is the solar radius, and j_ω is the radiation flux at the Sun's surface. Thus the spectral distribution for radiation near the Sun and the Earth is the same.

We employ Eq. (7.36) in the form

$$j_\omega = \frac{\omega^2}{2\pi^2 c^2}\int_0^1 d(\cos\theta)\int_0^\infty du_\omega \exp\left(-\frac{u_\omega}{\cos\theta}\right)F(u_\omega),$$

where $F(u_\omega) = [\exp(\hbar\omega/T) - 1]^{-1}$. Assume the dependence $F(u_\omega)$ to be weak. Expanding this function in a series

$$F(u_\omega) = F(u_0) + (u_\omega - u_0)F'(u_0) + \tfrac{1}{2}(u_\omega - u_0)^2 F''(u_0),$$

we choose the parameter u_0 such that the second term is zero after integration. This yields $u_0 = \frac{2}{3}$, and the radiation flux is

$$j_\omega = j_\omega^{(0)}\left[\frac{1 - 5F''(u_0)}{18F(u_0)}\right], \tag{7.47}$$

where $j_\omega^{(0)} = \omega^2(4\pi^2c^2)^{-1}[\exp(\hbar\omega/T) - 1]^{-1}$ is the radiation flux of a blackbody at a temperature that corresponds to the point where the optical thickness is $u_\omega = \frac{2}{3}$. The second term in the brackets of Eq. (7.47) makes it possible to estimate the accuracy of the operation employed.

We now apply Eq. (7.47) to the solar atmosphere. Approximating the height dependence for the number density of negative ions by $N_-(z) =$

$N_-(0)\exp(-z/l)$, we obtain from the relation $u_0 = \frac{2}{3}$ the expression

$$N_- = (2l\sigma_\omega/3)^{-1} \tag{7.48}$$

for the number density of negative ions, where σ_ω is the cross section for H^- photodetachment. The effective radiative temperature for a given frequency is taken to be the temperature of the solar atmosphere at the height implied by Eq. (7.48).

The photodetachment cross section of the negative hydrogen ion has a threshold at the photon energy $\hbar\omega = \mathrm{EA}$, and has a maximum, $\sigma_{\max} = 4 \times 10^{-17}$ cm^2, at $\hbar\omega_{\max} = 2\mathrm{EA} = 1.51$ eV corresponding to the photon wavelength $\lambda = 0.8$ μm. Using parameters for the average quiet solar photosphere, we find from Eq. (7.48) that the effective temperature for this wavelength is $T_{ef} = 6100$ K. The layer of the average solar atmosphere with this temperature contains plasma constituents with number densities $N_H = 1 \times 10^{17}$ cm^{-3}, $N_e = 4 \times 10^{13}$ cm^{-3}, and $N_- = 4 \times 10^9$ cm^{-3}. The variation of the number density of negative ions is determined principally by the temperature dependence in Eq. (7.46): $N_- \sim \exp(-\varepsilon_0/T)$. This gives the effective thickness of a radiating layer

$$l = \left(\frac{\varepsilon_0}{T}\frac{d\ln T}{dz}\right)^{-1} = 40 \text{ km}.$$

The effective radiation temperature T_ω depends on the photodetachment cross section σ_ω at this frequency according to Eq. (7.48). Taking it in the form $T_\omega = \Delta T + T_{ef}$, we obtain

$$\Delta T = l\frac{dT}{dz}\ln\left(\frac{\sigma_{\max}}{\sigma_\omega}\right).$$

For example, take $\hbar\omega = 2\hbar\omega_{\max}$ ($\lambda = 0.4$ μm). Then $\sigma_\omega = 0.65\sigma_{\max}$, and we have $\Delta T = 200$ K. This corresponds to an increase in the radiation flux by 20% over that at the radiation temperature T_{ef}.

To check the validity of the expansion used for the function $F(u_\omega)$, we take $F(u_\omega) = \exp(-\hbar\omega/T)$, which is valid when $\hbar\omega \gg T$. In this case the second term in the brackets of Eq. (7.47) is

$$\frac{5}{18}\frac{F''(u_0)}{F(u_0)} = \frac{5}{18}\left(\frac{\hbar\omega}{T}\frac{d\ln T}{du}\right)^2 = \frac{5}{18}\left(\frac{\hbar\omega}{T}\frac{1}{u_0}\frac{d\ln T}{dz}\right)^2 = \frac{5}{18}\left(\frac{\hbar\omega}{\varepsilon_0}\right)^2,$$

where we use Eq. (7.49) and $u_0 = \frac{2}{3}$. At the photon energy $\hbar\omega_{\max}$ the second term in the brackets of Eq. (7.47) gives a correction of 7%.

In summary, when we assumed the temperature of the solar atmosphere to be a smooth function of the height, we reduced the problem of the

radiation from a plasma of variable temperature to the problem with constant temperature. To solve this problem, it was necessary to use two parameters of the solar atmosphere: $N_H(T_0)$ and dT/dz, where the temperature T_0 is close to the effective temperature of the radiation. Hence, two parameters of the solar atmosphere must be introduced into the problem for the determination of radiation fluxes from the photosphere. Note that the spectrum of its radiation is close to the blackbody spectrum. Thus, the above method makes it possible to reduce the problem of radiation by a plasma with a distribution of temperatures to that of a gas with a constant temperature. This arises from the character of the radiation process, in that the main contribution to radiation of a certain frequency comes from layers of the solar atmosphere whose optical thickness for this frequency is of order unity.

CHAPTER 8

EXCITED ATOMS IN GASES AND PLASMAS

8.1 EXCITATION AND QUENCHING OF EXCITED STATES BY ELECTRON IMPACT

Excited atoms play a fundamental role in the properties of weakly ionized gases and, in particular, of gas discharges. Excited atoms can be responsible for the generation of the electron component of a plasma, and are basic to an understanding of the radiation from these systems. Usually, the primary mechanism for creation of excited atoms in a plasma results from collisions of atoms with electrons. Below we consider the processes of excitation and quenching of atomic excited states by electron impact. These processes are represented by the simple scheme

$$e + \mathrm{A} \leftrightarrow e + \mathrm{A}^*. \tag{8.1}$$

First we find the connection between the rate constants for the direct and inverse processes (8.1). The initial and final states of the process (8.1) are denoted as i and f. We consider one electron and one atom in a volume Ω, and regard all collisions with the walls as elastic. If the interaction between an electron and an atom is described by the interaction operator V, the probability of excitation per unit time is

$$w_{if} = \frac{2\pi}{\hbar}|V_{if}|^2 \frac{dg_f}{d\varepsilon} = \frac{v_i \sigma_{\mathrm{ex}}}{\Omega}, \tag{8.2a}$$

where V_{if} is the matrix element between the states in the transition, $dg_f/d\varepsilon$ is the statistical weight of the final state per unit of energy, and v_i is the

relative velocity of collision in the initial channel (which is essentially the electron velocity since the electron mass is so small compared to that of the atom). The last expression of Eq. (8.2a) gives the definition of the excitation cross section σ_{ex}. In like fashion, one can introduce the transition probability per unit time for the inverse process (8.1) as

$$w_{if} = \frac{2\pi}{\hbar}|V_{fi}|^2 \frac{dg_i}{d\varepsilon} = \frac{v_f \sigma_q}{\Omega}, \tag{8.2b}$$

where v_f is the electron velocity in the final channel, and σ_q is the quenching cross section.

The principle of detailed balance connects the rate constants for a process and its inverse. We shall employ this principle to connect the cross sections for excitation of atoms by electron impact, and for the quenching of that excitation by electron impact. The principle of detailed balance uses the invariance of the Hamiltonian with respect to time reversal, so that the matrix elements satisfy the relation $V_{if} = V_{fi}^*$. This connects the impact cross sections for atomic excitation and quenching by the relation

$$v_i \frac{dg_i}{d\varepsilon}\sigma_{ex} = v_f \frac{dg_f}{d\varepsilon}\sigma_q. \tag{8.3}$$

This detailed balance relationship for transitions between two discrete states is quite general.

The statistical weight of the ground state in an excitation is

$$dg_i = g_i \frac{\Omega\, d\mathbf{p}_i}{(2\pi\hbar)^3}, \tag{8.4}$$

where g_i is the statistical weight of the atomic ground state. We use the same expression for the final state of the transition and apply the energy conservation law $E = \varepsilon + \Delta\varepsilon$, where E is the electron kinetic energy in the initial channel, ε is the electron energy for the final channel, and $\Delta\varepsilon$ is the excitation energy. From Eq. (8.3) we obtain the result

$$g_i E \sigma_{ex}(E) = g_f \varepsilon \sigma_q(\varepsilon), \tag{8.5}$$

where g_f is the statistical weight of the excited atom.

In the frequently encountered case of a weakly ionized gas, with the mean electron energy small compared to the excitation energy, the threshold dependence for the excitation cross section has the form $\sigma_{ex} \sim \sqrt{E - \Delta\varepsilon} \sim \sqrt{\varepsilon}$. Therefore, near threshold, the rate constant for quenching, $k_q = \sqrt{2\varepsilon/m_e}\,\sigma_q$, does not depend on the electron energy when $\varepsilon \ll \Delta\varepsilon$. Thus the quenching rate constant in a plasma with slow electrons is independent of both the mean electron energy and the shape of the electron energy distribution.

The quenching rate constant is larger for resonantly excited states than for metastable states because of a larger interaction probability for an incident electron with the respective excited states. For example, the quenching rate constant by impact of a slow electron for the resonantly excited alkali metal states $K(4^2P_{1/2,3/2})$, $Rb(5^2P_{1/2,3/2})$, and $Cs(6^2P_{1/2,3/2})$ are in the range $(3\text{–}4) \times 10^{-7}$ cm^3/s, while the rate constant for quenching of the helium metastable state $He(2^3S)$ is 3×10^{-9} cm^3/s.

8.2 EQUILIBRIUM OF RESONANTLY EXCITED ATOMS IN A PLASMA

Inelastic collisions of electrons with atoms establish thermodynamic equilibrium between atoms in the ground and excited states, and as a result of these collisions the number density N_f of atoms in an excited state f is given by the Boltzmann formula (2.9):

$$N_f^{\mathrm{B}} = \left(\frac{g_f}{g_0}\right) N_0 \exp\left(-\frac{\Delta\varepsilon}{T_e}\right), \tag{8.6}$$

where T_e is the electron temperature, N_0 is the number density of atoms in the lower or ground state, g_0 and g_f are statistical weights of the corresponding states, and $\Delta\varepsilon$ is the excitation energy. If the excited state is resonantly excited, radiative transitions to the ground state may be of importance. This process may change the character of the equilibrium. Consider the equilibrium of resonantly excited atoms in a plasma whose properties are based on the transitions shown in Fig. 7.1. Then the rate equation (4.4) for excited atoms has the form

$$\frac{dN_f}{dt} = N_e N_0 k_{\mathrm{ex}} - N_e N_f k_{\mathrm{q}} - \frac{N_f}{\tau}, \tag{8.7}$$

where k_{ex},k_{q} are the rate constants for excitation and quenching of an atom by electron impact, and τ is the radiative lifetime corresponding to transport of resonant photons outside the plasma. In the stationary case $dN_f/dt = 0$, the number density of excited atoms is

$$N_f = \frac{N_0 N_e k_{\mathrm{ex}}}{N_e k_{\mathrm{q}} + 1/\tau}. \tag{8.8}$$

In the limit of large radiative time $\tau \to \infty$, the solution of the equilibrium equation (8.7) is the Boltzmann distribution (8.6). Then Eq. (8.8) can be expressed in the form

$$N_f = \frac{N_f^{\mathrm{B}}}{1 + 1/(N_e k_{\mathrm{q}} \tau)}, \tag{8.9}$$

where N_f^B is the number density of excited atoms in accordance with the Boltzmann law (8.6); that is, it corresponds to thermodynamic equilibrium between excited and unexcited atomic states. This equation has broader applicability than just the application to resonantly excited states. It is necessary to take as τ the lifetime of an excited state with respect to its decay by any channel other than electron collisions—in particular, as a result of collisions with atoms or by transport to walls.

Equation (8.9) reflects the character of the equilibrium for resonantly excited atoms. Note that thermodynamic equilibrium is ascertained by comparison of the lifetime of excitations τ in a gas with the typical time $(N_e k_q)^{-1}$ of atomic quenching (not excitation!). That is, the presence of thermodynamic equilibrium is established by the criterion

$$N_e k_q \tau \gg 1. \tag{8.10}$$

This is also the condition for validity of Eq. (5.24) for the rate constant of stepwise ionization of atoms. Indeed, considering this process as a result of transitions between different excited atomic states, we assume that the lifetime of an excited atom is determined only by electron collisions. Then the criterion (8.10) must be fulfilled for excited atomic states that participate in this process. The lifetime τ in this formula takes into account atomic radiation and its transport to walls.

8.3 LIFETIMES OF RESONANTLY EXCITED ATOMS IN A PLASMA

Because of reemission in a plasma, the lifetime of a resonantly excited state exceeds that of an individual atom if resonant radiation is retained within the plasma, that is, if $k_0 L \gg 1$, where k_0 is the absorption coefficient for the center of the spectral line, and L is a length characterizing the extent of the plasma. The connection between the effective lifetime of an excited state (τ_{ef}) which must be included in Eqs. (8.9) and (8.10), and that of an individual atom (τ) depends on the character of the broadening of the spectral line. We shall now examine this connection.

The effective lifetime τ_{ef} of excited atoms in a plasma can be defined by

$$\tau_{ef}/\tau = P/P_0, \tag{8.11}$$

where $P = S\int j_\omega \, d\omega$ is the radiated power from the total plasma volume for the radiative transition being examined, and $P_0 = N_i \Omega/\tau$ is this quantity for a plasma of small optical thickness when all the emitted photons leave the plasma volume. Here Ω is the plasma volume, S is the area of its surface, and j_ω is the equilibrium radiation flux. We assume the plasma to be uniform, and make an estimate for τ_{ef} on the basis of Eq. (8.11). Equation

(7.36) gives $P_0 \sim Sj_\omega \nu u$, where ν is the width of the spectral line of an individual atom, and the optical thickness of the plasma is $u \sim k_0 L$, where L is the size of the plasma and k_0 is the absorption coefficient in the line center. This is to be compared with the estimate $P \sim Sj_\omega \Delta\omega$, where $\Delta\omega$ is the spectral line width for radiation that leaves the plasma. Thus we have for the effective lifetime of an excited atom in a plasma

$$\tau_{ef} \sim \tau k_0 L \nu / \Delta\omega. \tag{8.12}$$

In particular, using the expressions (7.38) and (7.39) for the width of the spectral line $\Delta\omega$, we find that the effective lifetime of an excited atom in the case of Lorentz broadening of the spectral line is

$$\tau_{ef} \sim \tau\sqrt{k_0 L}, \quad k_0 L \gg 1, \tag{8.13}$$

and in the case of Doppler broadening of the spectral line it is

$$\tau_{ef} \sim \frac{\tau k_0 L}{\sqrt{\ln k_0 L}}, \qquad k_0 L \gg 1. \tag{8.14}$$

A typical size of a plasma system can be estimated as $L \sim \Omega/S$. Equation (8.13) for Lorenz broadening can be written in the form

$$\tau_{ef} \approx 1.8\tau\sqrt{k_0 \Omega / S}, \tag{8.15}$$

where the numerical coefficient is correct within an error of about 25%, depending on the shape of the plasma boundaries. In the same way, when the spectral line is Doppler-broadened, the spectral line has the effective lifetime

$$\tau_{ef} \approx \frac{\tau k_0 \Omega}{2S}\sqrt{\frac{\pi}{\ln(k_0 \Omega / S)}}. \tag{8.16}$$

8.4 STEPWISE IONIZATION THROUGH RESONANTLY EXCITED STATES

Stepwise ionization of atoms by electron impact refers to a chain of transitions between atomic states as a result of collisions with electrons. Within the framework of this process, the lifetime of these states is assumed to be large compared to a typical time for quenching of this state by electron impact. In practice, the lowest excited state of an atom is usually the resonantly excited one. That is true, for example, of atoms of alkali metals. This creates a special character of the excitations of these atoms. First, the resonantly

excited state has a small excitation energy, and therefore the stepwise ionization of an atom always passes through this state, while other excited states may participate in the stepwise ionization process only partially. Second, the radiative lifetime of the first resonantly excited state is smaller than for other excited states. Therefore the condition for stepwise ionization (lifetime much greater than typical quenching time) is violated for this state at a smaller number density of electrons than for other excited states.

Extracting the first resonantly excited state and considering it separately, one can extend the condition of stepwise ionization to a lower number density of electrons. Assuming that this process always passes through the first resonantly excited state, we can rewrite the expression for the rate constant k_{st} of stepwise ionization in the form

$$k_{st} = k_{st}^{f} N_f / N_0,$$

where k_{st}^{f} is the rate constant of stepwise ionization from the resonantly excited state, and N_0 and N_f are the number densities of atoms in the ground and resonantly excited states. Then, using Eqs. (8.9) and (5.28), we find the rate constant of stepwise ionization of an atom by electron impact to be

$$k_{st} = 2\frac{g_i}{g_a}\frac{m_e e^{10}}{\hbar^3 T_e^3}\frac{1}{1 + 1/(N_e k_q \tau)}\exp\left(-\frac{J}{T}\right), \tag{8.17}$$

where g_i and g_a are the statistical weights for the ion formed and for the atom in the ground state, J is the ionization potential of an atom in the ground state, and τ is the effective lifetime of the first resonantly excited state. The validity of this formula depends only on excited states other than the first.

8.5 ASSOCIATIVE IONIZATION AND THE PENNING PROCESS

Associative ionization proceeds according to the scheme

$$A^* + B \rightarrow AB^+ + e. \tag{8.18}$$

Its inverse is, in principle, dissociative recombination (see Fig. 4.9). But in reality these processes proceed through different vibrational states of a molecular ion AB^+ and different electron terms of the molecule AB^*. It is favorable for the energetics of the process that the electron energy of the final state should be lower than that of the initial state. For this reason the dissociative recombination process proceeds through repulsive terms of AB^*, while in the case of associative ionization it goes through attractive terms of AB^*. Hence, the cross section for associative ionization is of the order of gas-kinetic cross sections for those excited states for which this process is effective.

Another ionization process resulting from collisions of excited and unexcited atoms is the *Penning process*

$$A^* + B \rightarrow A + B^+ + e, \tag{8.19}$$

where A* is a metastable atom whose excitation energy exceeds the ionization potential of an atom B. The metastable atomic state is an excited state that, because of quantum selection rules, cannot decay in the presence of resonant radiation. Such metastable states exist, for instance, in atoms of inert gases or atoms of alkaline-earth metals, but not in atoms of alkali metals. Because of the large lifetime of metastable atoms, their concentration in an excited gas may be sufficiently large that it may sometimes be comparable to the concentration of charged particles. Hence, the Penning process is important for the generation of electrons and ions under certain conditions in an ionized gas whose atoms have metastable states.

By its nature, the Penning process occurs in the decay of an autoionization state A*B. At large distances between nuclei the lifetime of this system is large because of the weak interaction between atomic particles. Therefore this process occurs in close collisions, and its cross section is usually smaller than the gas-kinetic cross section.

8.6 PROCESSES INVOLVING FORMATION OF A LONG-LIVED COMPLEX

A long-lived complex is an intermediate state formed as a result of the collision of two atoms. Subsequent evolution of this complex can lead to formation of a bound state of these particles. For example, the formation of molecular ions in three-body collisions can occur through the processes

$$A^+ + B \xrightarrow{k_c} (A^+B)^{**}, \tag{8.20a}$$

$$(A^+B)^{**} \xrightarrow{\tau} A^+ + B, \tag{8.20b}$$

$$(A^+B)^{**} + C \xrightarrow{k_q} AB^+ + C, \tag{8.20c}$$

$$(A^+B)^{**} + C \xrightarrow{k_d} A^+ + B + C. \tag{8.20d}$$

Here $(A^+B)^{**}$ is an autodetachment state of the colliding particles, and the quantities written over the arrows are the rate constants k for the collision processes or the lifetime τ of the autodetachment state $(A^+B)^{**}$.

Equations (8.20) lead to the balance equations for the number densities of autodetachment states,

$$\frac{d}{dt}[(A^+B)^{**}] = 0$$

$$= [A][B]k_c - \frac{[(A^+B)^{**}]}{\tau} - [(A^+B)^{**}][C](k_q + k_d),$$

where [X] stands for the number density of particles X. The solution of this equation gives

$$[(A^+B)^{**}] = \frac{[A][B]k_c}{1/\tau + [C](k_q + k_d)}.$$

However, the balance equation for the process (8.20c) has the form

$$\frac{d[AB^+]}{dt} = k_q[(A^+B)^{**}][C] = [A][B][C]\frac{k_c k_q \tau}{1 + [C](k_q + k_d)\tau}.$$

A comparison of this balance equation and the definition of the rate constant for three-body processes shows that (8.20c) can be characterized as a three-body process only if

$$[C](k_q + k_d) \ll 1. \tag{8.21}$$

Then the three-body rate constant is

$$K = k_q k_d \tau. \tag{8.22}$$

For another limiting case

$$[C](k_q + k_d) \gg 1, \tag{8.23}$$

the number density of particles C is so high that the rate constant for formation of the bound state A^+B does not depend on this number density, and the formation of the bound state A^+B can be considered to be two-body in nature with the rate constant

$$k = K[C] = \frac{k_c k_q}{k_q + k_d}. \tag{8.24}$$

The particles C affect the factor $k_q/(k_q + k_d)$ in equation (8.24), which is the probability that collision of the autodetachment ion $(A^+B)^{**}$ and the particle C leads to formation of the bound state AB^+.

In reality, both regimes can be fulfilled for formation of bound states through formation of a long-lived complex. For example, the lifetime of the long-lived complex consisting of electrons and large molecules is of the order of 10^{-6}–10^{-4} s, so that the criterion (8.23) is satisfied for number densities $[C] \gg 10^{15}$–10^{17} cm^{-3}. At small number densities for particles C the process of formation of the bound state is three-body. Note that the Thomson formula for the three-body process follows from Eq. (8.22) if the collision time of the particles is used as the lifetime of a long-lived complex.

8.7 EXCIMER MOLECULES

An excimer molecule is an excited molecule A*B such that the corresponding molecule AB in the ground state of the atom A has no stable bound state. It is usually an inert-gas atom that plays this role in an excimer molecule. Excimer molecules are used in excimer lasers that operate on bound–free molecular transitions.

Atoms of inert gases Ne, Ar, Kr, Xe in the ground state have a filled electron shell p^6, so that they do not form any chemical bonds. The lowest excited states of these atoms have the electron shell configuration p^5s, so that their valence electron is found in an s-state, as are valence electrons of alkali metal atoms. Therefore, an alkali metal atom is a suitable model for an excited inert-gas atom.

Excited states of inert gas atoms have ionization potentials that are close to those of alkali metal atoms in the ground state. For example, the lowest resonantly excited states of the inert gas atoms $Ar(^3P_1)$ and $Kr(^3P_1)$ have ionization potentials 4.14 and 3.97 eV, while the corresponding alkali metal atoms in the ground states $K(4\,^2S)$ and $Rb(5\,^2S)$ have ionization potentials 4.34 and 4.18 eV. The analogy between excited atoms of inert gases and atoms of alkali metals in their ground states means that excited inert-gas atoms form strong chemical bonds with halogen atoms. For example, the dissociation energy of the lowest state of the excimer molecule $KrF(^2B_{1/2})$ is 5.3 eV.

The radiative lifetime of excimer molecules is of the order of that for excited atoms of inert gases, specifically, in the range 10^{-7}–10^{-8} s. Therefore, generation of excimer molecules requires short pulses of energy. Electron beams or ultrahigh-frequency gas discharges are commonly used for this purpose. In these cases a pulse of electrical energy is transformed into the UV-radiation energy emitted by excimer molecules. The efficiency of this transformation reaches ten percent.

The transformation of the initial electron energy to energy of radiation starts from the formation of excited atoms as a result of excitation by electron impact. In the following stage of the process, these excited atoms react with molecules containing a halogen or oxygen. This chemical reaction proceeds according to the so-called *harpoon*, or *avoided crossing*, mechanism (see Fig. 8.1). This refers to a mechanism in which an atom loses an electron during a collision, with that electron becoming attached to the other participant in the collision—a molecule that contains a halogen atom. The Coulomb attraction of the resulting oppositely charged ions causes a closer approach in the collision than would otherwise occur. As a result, the cross section for this type of collision is much larger than the gas-kinetic cross section.

We can demonstrate this process by the example

$$Ar(^3P_1) + Cl_2 \rightarrow Ar^*Cl + Cl. \qquad (8.25)$$

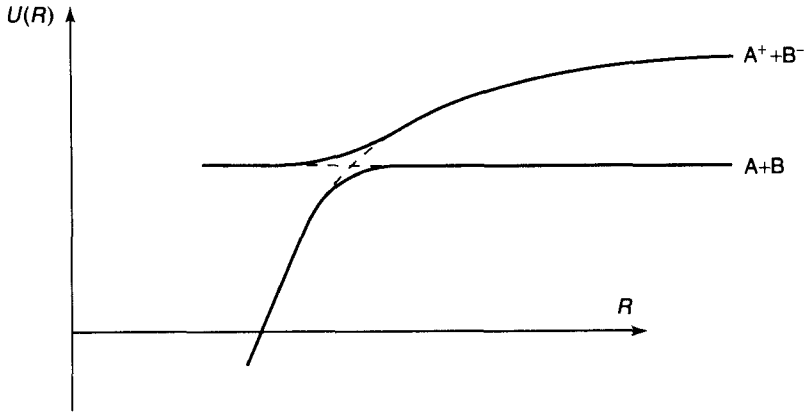

Figure 8.1 The schematic character of molecular terms that exhibit the harpoon, or avoided-crossing, reaction.

We first compare the two electron terms Ar* + Cl_2 and $Ar^+ + Cl_2^-$ at large distances between the colliding particles. The first term is of lower energy than the second at large distances by the amount $J - EA = 1.7$ eV, where $J = 4.14$ eV is the ionization potential of $Ar(^3P_1)$ and EA = 2.44 eV is the electron affinity of Cl_2. At large distances, a Coulomb interaction exists for the second term, and at the distance $R_c = e^2/(J - EA) = 16\,a_0$ (where a_0 is the Bohr radius) these terms intersect. In reality, a pseudointersection of the terms takes place, so that the terms are separated by a gap at the distance R_c (see Fig. 8.1). At smaller distances between the particles the total system is found in the lowest term, and a Coulomb interaction occurs between the colliding particles. This decreases the distance of approach. If we assume that the rearrangement of chemical bonds occurs at a distance $R_0 < R_c$ between the colliding systems, then the process (8.25) takes place. Equation (5.9) gives the rate constant for this process. Thus, the rate constant for formation of excimer molecules is far greater than the corresponding gas-kinetic value. This rate constant is 7×10^{-10} cm^3/s for the process (8.25) at room temperature, and the rate constant for formation of other excimer molecules lies in an interval 10^{-10}–10^{-9} cm^3/s at thermal energies.

Excimer molecules emit radiation in the ultraviolet range of the spectrum and are characterized by small lifetimes. To give examples illustrating these statements, we note that an average wavelength $\lambda = 193$ nm and lifetime $\tau = 4$ ns is exhibited by the excimer molecule $ArF(^2B_{1/2})$; $\lambda = 175$ nm and $\tau = 9$ ns by $ArCl(^2B_{1/2})$; $\lambda = 248$ nm and $\tau = 8$ ns by $KrF(^2B_{1/2})$; and $\lambda = 222$ nm and $\tau = 19$ ns by $KrC(^2B_{1/2})$. Excimer molecules can be formed with such atoms as Hg, Mg, and Ca instead of inert-gas atoms, and oxygen atoms can replace the halogens.

CHAPTER 9

PHYSICAL KINETICS OF GASES AND PLASMAS

9.1 THE BOLTZMANN KINETIC EQUATION

Our goal is to give a mathematical description of the behavior of gaseous systems of particles including plasmas, and to analyze processes and phenomena that occur in these systems. We employ the physically motivated hypothesis that most of the time a test particle within a gas does not interact with surrounding particles, and for only a small part of the time, of the order of $N\sigma^{3/2}$, does it interact strongly with other particles. (Here, N is the particle number density, σ is the two-body collision cross section, and for a gas $N\sigma^{3/2} \ll 1$; see Chapter 4.) Fulfillment of the criterion for a gaseous state corresponds to a small probability for three-body collisions, which behaves as $N\sigma^{3/2}$ as compared to the probability of pairwise collisions. Thus, for description of a gas in first approximation, it is sufficient to take account of two-body collisions only.

We shall now introduce a particle distribution function $f(\mathbf{v}, J, \mathbf{r}, t)$, defined such that $f(\mathbf{v}, J, \mathbf{r}, t)\, d\mathbf{v}$ is the number of particles in a unit volume located at the point $\mathbf{r}$ at moment t with velocity in the range from $\mathbf{v}$ to $\mathbf{v} + d\mathbf{v}$. The parameter J represents all internal quantum numbers. Hence, the number density of particles at point $\mathbf{r}$ at moment t is

$$N(\mathbf{r}, t) = \sum_J \int f(\mathbf{v}, J, \mathbf{r}, t)\, d\mathbf{v}. \tag{9.1}$$

The distribution function allows one to analyze the evolution of the system. The equation that describes the variation of the distribution function in time

is called the *kinetic equation.* This equation has the form

$$\frac{df}{dt} = I_{\text{col}}(f), \tag{9.2}$$

where $I_{\text{col}}(f)$ is the so-called *collision integral* that takes into account the variation of the number of particles in a given state as a result of pairwise collisions.

The left-hand side of the kinetic equation that describes the motion of particles in external fields is

$$\frac{df}{dt} = \frac{f(\mathbf{v} + d\mathbf{v}, J, \mathbf{r} + d\mathbf{r}, t + dt) - f(\mathbf{v}, J, \mathbf{r}, t)}{dt}.$$

In the absence of collisions $d\mathbf{v}/dt = -\mathbf{F}/m$, where $\mathbf{F}$ is the external force that acts on a single particle, m is the particle mass, and $d\mathbf{r}/dt = \mathbf{v}$. Thus we have

$$\frac{df}{dt} = \frac{\partial f}{\partial t} + \mathbf{v} \cdot \frac{\partial f}{\partial \mathbf{r}} + \frac{\mathbf{F}}{m} \cdot \frac{\partial f}{\partial \mathbf{r}},$$

and the kinetic equation (9.2) takes the form

$$\frac{\partial f}{\partial t} + \mathbf{v} \cdot \frac{\partial f}{\partial \mathbf{r}} + \frac{\mathbf{F}}{m} \cdot \frac{\partial f}{\partial \mathbf{r}} = I_{\text{col}}(f). \tag{9.3}$$

Equation (9.3) is called the *Boltzmann kinetic equation.*

The collision integral contained in the kinetic equation characterizes the evolution of the system as a result of pairwise collisions of particles. A typical relaxation time of the distribution function in a gas can be estimated as $\tau \sim (N\sigma v)^{-1}$, where v is a typical collision velocity. This value suggests the simple approximation

$$I_{\text{col}}(f) = -\frac{f - f_0}{\tau} \tag{9.4}$$

for the collision integral, where f_0 is the equilibrium distribution function. This approximation is called the *tau approximation.* The nature of this approximation can be illustrated by a simple example. If we disturb an equilibrium state of the system described by the distribution function f_0 so that the distribution function at the initial time is $f(0)$, then the subsequent evolution of the system is described by the equation

$$\frac{df}{dt} = -\frac{f - f_0}{\tau},$$

and its solution has the form

$$f = f_0 + [f(0) - f_0]\exp(-t/\tau).$$

Thus, the relaxation time τ of the system is of the order of the time between consecutive collisions of a test particle with others. It can be dependent on the collision velocity.

9.2 MACROSCOPIC GAS EQUATIONS

The distribution function contains detailed information about a gaseous system. A variety of macroscopic parameters of the system can be obtained by averaging of the distribution function over particle velocities and internal quantum numbers. Correspondingly, the evolution of these parameters can be analyzed by averaging of the kinetic equation. This procedure is followed below in order to obtain equations describing the mean parameters of a system.

We begin by integrating the kinetic equation (9.3) over particle velocities. The right-hand side of the equation is the total variation of the density of particles per unit time due to collisions. Assuming there is no formation or decomposition of particles inside the system volume, the right-hand side of the resulting equation is zero, and the kinetic equation becomes

$$\int \frac{\partial f}{\partial t}\, d\mathbf{v} + \int \mathbf{v} \cdot \frac{\partial f}{\partial \mathbf{r}}\, d\mathbf{v} + \frac{\mathbf{F}}{m} \cdot \int \frac{\partial f}{\partial \mathbf{v}}\, d\mathbf{v} = 0.$$

We reverse the order of differentiation and integration in the first two terms, and introduce the definitions $\int f d\mathbf{v} = N$ and $\int \mathbf{v} f d\mathbf{v} = N\mathbf{w}$, where N is the particle number density and $\mathbf{w}$ is the mean velocity of the particles, referred to as the drift velocity. The third term is zero because the distribution function for infinite velocity is zero. Thus we obtain

$$\frac{\partial N}{\partial t} + \operatorname{div}(N\mathbf{w}) = 0. \tag{9.5}$$

This is a standard form for a continuity equation.

This equation corresponds to an one-component system where internal states of the particles are not distinguished. In fact, by definition, $\int I_{\text{col}}(f)\, d\mathbf{v}$ is the variation of the particle number density due to collision processes, so that it is zero for the total number density summed over internal quantum numbers. If we discriminate internal states, the right-hand side of the continuity equation is akin to Eq. (4.4), so that the continuity equation has

the form of the balance equations

$$\frac{\partial N_i}{\partial t} + \operatorname{div}(N_i \mathbf{w}) = \sum_f k_{fi} N_j - \sum_f k_{if} N_j \tag{9.6}$$

where indices i and f refer to internal states of particles, and k_{if} is the rate constant for transition between states i and f.

We can obtain another type of information if we multiply the kinetic equation by mv_α and integrate over particle velocities, using the notation that v_α is a component of the particle velocity, where $\alpha = x, y$, or z. The right-hand side of the resulting equation is the variation of the total momentum of the particles due the rate at which collisions occur. For a system of identical particles, collisions do not change the total momentum of the particles, so that the right-hand side of the equation is zero and the macroscopic equation has the form

$$\int m v_\alpha \frac{\partial f}{\partial t}\, d\mathbf{v} + \int m v_\alpha v_\beta \frac{\partial f}{\partial x_\beta}\, d\mathbf{v} + F_\beta \int v_\alpha \frac{\partial f}{\partial v_\beta}\, d\mathbf{v} = 0.$$

Here the indices α and β both denote vector components ($\alpha, \beta = x, y, z$) with a summation over β, and x_β is a coordinate. If we change the order of the integration and summation in the first two terms and integrate the third term by parts, we obtain

$$\int v_\alpha \frac{\partial f}{\partial v_\beta}\, dv_\beta = v_\alpha f \Big|_{-\infty}^{+\infty} - \int \delta_{\alpha\beta}\, dv_\beta = -N\delta_{\alpha\beta},$$

where $\delta_{\alpha\beta}$ is the Kronecker symbol: $\delta_{\alpha\beta} = 1$ if $\alpha = \beta$, and $\delta_{\alpha\beta} = 0$ if $\alpha \neq \beta$. Finally, we obtain

$$\frac{\partial}{\partial t}(mNv_\alpha) + \frac{\partial}{\partial x_\beta}\left(N\langle m v_\alpha v_\beta\rangle\right) - NF_\alpha = 0,$$

where angle brackets denote averaging over the particle distribution function.

We define the pressure tensor as

$$P_{\alpha\beta} = \langle m(v_\alpha - w_\alpha)(v_\beta - w_\beta)\rangle. \tag{9.7}$$

Inserting this tensor into the above equation, we have

$$\frac{\partial}{\partial t}(mNv_\alpha) + \frac{\partial P_{\alpha\beta}}{\partial x_\beta} + \frac{\partial}{\partial x_\beta}(mNw_\alpha w_\beta) - NF_\alpha = 0.$$

Subtracting from this the continuity equation in the form

$$mw_\alpha\left(\frac{\partial N}{\partial t}+\frac{\partial}{\partial x_\beta}(Nw_\alpha)\right)=0,$$

we obtain finally for the momentum equation

$$m\frac{\partial w_\alpha}{\partial t}+\frac{1}{N}\frac{\partial P_{\alpha\beta}}{\partial x_\beta}+mw_\beta\frac{\partial w_\alpha}{\partial x_\beta}-F_\alpha=0. \tag{9.8}$$

The form of this equation for the mean particle momentum depends on the representation of the momentum tensor, which is determined by properties of the system. Below we discuss special forms of the representation of this tensor. The macroscopic equation for the mean energy has an even more complicated form.

The macroscopic Eqs. (9.5) and (9.8) have been derived for a one-component gas. We can generalize these equations to be applicable to multicomponent systems. The right-hand side of the continuity equation is the variation of the number density of particles of a given species per unit volume and per unit time due to production or consumption of this type of particle. In the absence of production of particles of one species as a result of decomposition of particles of other species, the continuity equation has the form (9.5) or (9.6) regardless of processes involving other particles.

The right-hand side of Eq. (9.8) for a multicomponent system contains the variation per unit time of the momentum of particles of a given species as a result of collisions with particles of other types. If the mean velocities of the two types of particles are different, a momentum transfer will occur between them. The momentum transfer between two species is proportional to the difference between their mean velocities. Therefore, one can rewrite Eq. (9.8) as

$$\frac{\partial w_\alpha^{(q)}}{\partial t}+\frac{1}{m^{(q)}N^{(q)}}\frac{\partial P_{\alpha\beta}^{(q)}}{\partial x_\beta}+w_\beta^{(q)}\frac{\partial w_\alpha^{(q)}}{\partial x_\beta}-\frac{F_\alpha}{m_q}=\sum_s\frac{w_\alpha^{(s)}-w_\alpha^{(q)}}{\tau_{qs}}. \tag{9.9}$$

The superscripts q and s denote here the particle species, and τ_{qs} is the characteristic time of the momentum transfer from the species q to the species s. Since the transfer does not change the total momentum of the system, the characteristic time of the momentum transfer satisfies the relation

$$m^{(q)}N^{(q)}/\tau_{qs}=m^{(s)}N^{(s)}/\tau_{sq}. \tag{9.10}$$

9.3 EQUATION OF STATE

The relation between the bulk parameters of a gas (pressure p, temperature T, and particle number density N) is given by the equation of state. Below we derive this equation for a homogeneous gas. For this purpose we employ a

frame of reference where the gas (or a given volume of the gas) is at rest. The pressure is the force in this frame of reference that acts on a unit area of an imaginary surface in the system. For evaluation of this force we observe that if an element of this surface is perpendicular to the x-axis, the flux through it of particles with velocities in an interval from v_x to $v_x + dv_x$ is given by $dj_x = v_x f dv_x$, where f is the distribution function. Elastic reflection of a particle from this surface leads to inversion of v_x, that is, $v_x \to -v_x$ as a result of the reflection. Therefore, a reflecting particle of mass m transfers to the area the momentum $2mv_x$. The force acting on this area is the momentum change per unit time. Hence, the gas pressure—the force acting per unit area—is

$$p = \int_{v_x>0} 2mv_x f dv_x = m\int v_x^2 f dv_x = mN\langle v_x^2\rangle.$$

We account for the fact that the pressure on both sides of the area is the same.

In the above expression v_x is the velocity component in the frame of axes where the gas as a whole is at rest. Transforming back to the original axes, we have

$$p = mN\langle (v_x - w_x)^2\rangle, \tag{9.11}$$

where w_x is the x-component of the mean gas velocity. Because the distribution function is isotropic in the reference frame where the gas as a whole is at rest, the gas pressure is the same in all directions, and we have

$$p = mN\left\langle (v_x - w_x)^2\right\rangle = mN\langle (v_y - w_y)^2\rangle = mN\langle (v_z - w_z)^2\rangle. \tag{9.12}$$

This gives a simple expression for the pressure tensor (9.7),

$$P_{\alpha\beta} = p\delta_{\alpha\beta}, \tag{9.13}$$

where $\delta_{\alpha\beta}$ is the Kronecker symbol. Since this relationship is valid also for an isotropic liquid, the equations describe not only a gas but also a liquid.

The definition of the gas temperature (2.16) relates the temperature to the mean particle velocity in the frame of reference where the mean velocity is zero, so we obtain

$$\frac{3T}{2} = \frac{m}{2}\langle (\mathbf{v} - \mathbf{w})^2\rangle.$$

Using this in Eq. (9.12), the relationship between pressure and temperature is

$$p = NT. \tag{9.14}$$

Equation (9.14) is the equation of state for a perfect gas.

Equation (9.8) for the mean particle momentum can be rewritten for the case when the pressure tensor has the form (9.13). Insertion of Eq. (9.13) into Eq. (9.8) yields

$$\frac{\partial \mathbf{w}}{\partial t} + (\mathbf{w} \cdot \nabla)\mathbf{w} + \frac{\nabla p}{\rho} - \frac{\mathbf{F}}{m} = 0. \tag{9.15}$$

Here $\mathbf{w}$ is the mean velocity of the gas, $\rho = mN$ is the mass density, and $\mathbf{F}$ is the force on a single particle from external fields. In the absence of external fields ($\mathbf{F} = 0$), this equation is called the *Euler equation.* Equation (9.9) for a multicomponent system, with (9.10) taken into account, is transformed in this case to

$$\frac{\partial \mathbf{w}_q}{\partial t} + (\mathbf{w}_q \cdot \nabla)\mathbf{w}_q + \frac{\nabla p}{\rho_q} - \frac{\mathbf{F}_q}{m_q} = \sum_s \frac{\mathbf{w}_s - \mathbf{w}_q}{\tau_{qs}}. \tag{9.16}$$

9.4 COLLISION INTEGRAL

The collision integral represents changes in the distribution function as a result of pairwise collisions of particles. We analyze first the collision integral in the case of an atomic gas, where it is expressed in terms of the elastic scattering cross section of atoms. The transition probability per unit time per unit volume is denoted by $W(\mathbf{v}_1, \mathbf{v}_2 \to \mathbf{v}_1', \mathbf{v}_2')$, so that $W d\mathbf{v}_1' d\mathbf{v}_2'$ is the probability per unit time and per unit volume for collision of two atoms with velocities $\mathbf{v}_1$ and $\mathbf{v}_2$, if their final velocities are in an interval from $\mathbf{v}_1'$ to $\mathbf{v}_1' + d\mathbf{v}_1'$ and from $\mathbf{v}_2'$ to $\mathbf{v}_2' + d\mathbf{v}_2'$, respectively. By definition, the collision integral is

$$I_{\text{col}}(f) = \int (f_1' f_2' W' - f_1 f_2 W)\, d\mathbf{v}_1'\, d\mathbf{v}_2'\, d\mathbf{v}_2, \tag{9.17}$$

where we use the notation that $f_1 = f(\mathbf{v}_1)$, $W = W(\mathbf{v}_1, \mathbf{v}_2 \to \mathbf{v}_1', \mathbf{v}_2')$, and other quantities take subscripts according to the same rule.

The principle of detailed balance, which yields the reversed evolution of a system as would occur in the case of a physical time reversal $t \to -t$, yields $W = W'$. [Compare with Eqs. (8.2) and (8.3).] The elastic scattering cross section follows from its definition as the ratio of the number of scattering events per unit time to the flux of incident particles. The differential cross section for elastic scattering is

$$d\sigma = \frac{f_1 f_2 W\, d\mathbf{v}_1\, d\mathbf{v}_2\, \mathbf{v}_1' \mathbf{v}_2'}{f_1\, d\mathbf{v}_1 f_2\, d\mathbf{v}_2} = \frac{W d\mathbf{v}_1'\, d\mathbf{v}_2'}{|\mathbf{v}_1 - \mathbf{v}_2|}.$$

Substitution of this expression into Eq. (9.17) gives the collision integral

$$I_{\text{col}}(f) = \int (f_1' f_2' - f_1 f_2) |\mathbf{v}_1 - \mathbf{v}_2|\, d\sigma\, d\mathbf{v}_1'\, d\mathbf{v}_2'\, d\mathbf{v}_2. \tag{9.18}$$

The nine integrations implied in Eq. (9.1) are replaced by five integrations in Eq. (9.18). This is a consequence of taking into account the conservation of momentum for the colliding particles (three integrations) and the conservation of their total energy (one more integration).

The equilibrium of a gas of atoms when the kinetic Eq. (9.3) has the form $I_{\text{col}}(f) = 0$, combined with Eq. (9.18) for the collision integral, requires that $f_1 f_2 = f_1' f_2'$ for any pair of colliding atoms. Rewriting this relation in the form

$$\ln f(\mathbf{v}_1) + \ln f(\mathbf{v}_2) = \ln f(\mathbf{v}_1') + \ln f(\mathbf{v}_2')$$

shows that $\ln f(\mathbf{v})$ is an additive function of the integrals of motion. Taking into account the conservation of total momentum and total energy of the atoms, we obtain the general form of the distribution function as

$$\ln f(\mathbf{v}) = C_1 + \mathbf{C}_2 \cdot \mathbf{p} + C_3 \varepsilon,$$

where $\mathbf{p}$ and ε are the momentum and kinetic energy of an atom. This leads to the distribution function in the form

$$f(\mathbf{v}) = A \exp\left[-\alpha(\mathbf{v} - \mathbf{w})^2\right].$$

This expression is exactly Eq. (2.15) for the Maxwell distribution function if A is the normalization constant, $\mathbf{w}$ is the average velocity of the distribution, and $\alpha = m/(2T)$, where m is the mass of an atom and T is the temperature of the gas.

9.5 MACROSCOPIC EQUATION FOR ION MOTION IN A GAS

The expression (9.18) for the collision integral provides the basis for a derivation of the balance equation for ions in a gas subjected to an external electric field $\mathbf{E}$. If the number density of ions is small compared to the number density of atoms, elastic collisions with atoms govern the character of the ion motion in a gas. Using the tau approximation (9.4) for the collision integral, we obtain the balance equation

$$e\mathbf{E} = m\mathbf{w}_i/\tau \tag{9.19}$$

under the conditions considered, where $\mathbf{w}_i$ is the average ion velocity, and τ is the characteristic time between successive collisions of the ion with atoms. This time can be estimated as $\tau \sim (N_a v \sigma)^{-1}$, where N_a is the number density of atoms, v is a typical relative velocity of an ion–atom collision, and σ is a typical cross section for this collision. The left-hand side of this equation is the force on the ion from the electric field, and the right-hand side is the frictional force arising from collisions of the ion with the gas atoms. We shall determine the frictional force below without resort to the tau approximation.

When we multiply Eq. (9.18) by $m\mathbf{v}_1$ and integrate over $d\mathbf{v}_1$, we obtain

$$e\mathbf{E}N_i = \int m(\mathbf{v}_1' - \mathbf{v}_1) g \, d\sigma \, f_1 f_2 \, d\mathbf{v}_1 \, d\mathbf{v}_2. \tag{9.20}$$

The quantities $\mathbf{v}_1$ and $\mathbf{v}_2$ are the initial velocities of the ion and atom, respectively, of masses m and m_a and number densities N_i and N_a, and g is the relative velocity of the colliding particles, conserved in the collision. We have made use of the principle of detailed balance, which assures the invariance under time reversal of the evolution of the system, and yields in this case

$$\int \mathbf{v}_1 f_1' f_2' \, d\sigma \, d\mathbf{v}_1 \, d\mathbf{v}_2 = \int \mathbf{v}_1' f_1 f_2 \, d\sigma \, d\mathbf{v}_1 \, d\mathbf{v}_2.$$

The invariance under time reversal ($t \to -t$) of $d\sigma \, d\mathbf{v}_1 \, d\mathbf{v}_2$ must be examined. If we express the ion velocity $\mathbf{v}_1$ in Eq. (9.20) in terms of the relative ion–atom velocity $\mathbf{g}$, and express the center-of-mass velocity $\mathbf{V}$ by the relation $\mathbf{v}_1 = \mathbf{g} + m_a\mathbf{V}/(m + m_a)$, then we find that $m(\mathbf{v}_1 - \mathbf{v}_1') = \mu(\mathbf{g} - \mathbf{g}')$, where μ is the reduced mass of the ion and atom. The relative velocity after collision has the form $\mathbf{g}' = \mathbf{g}\cos\vartheta + \mathbf{k}g\sin\vartheta$, where ϑ is the scattering angle, and $\mathbf{k}$ is a unit vector directed perpendicular to $\mathbf{g}$. Because of the random distribution of $\mathbf{k}$, the integration over scattering angles gives $\int(\mathbf{g} - \mathbf{g}')\, d\sigma = \mathbf{g}\sigma^*(g)$, where $\sigma^*(g) = \int(1 - \cos\vartheta)\, d\sigma$ is the diffusion cross section (4.8) of ion–atom scattering. Thus Eq. (9.20) takes the form

$$e\mathbf{E}N_i = \int \mu \mathbf{g} g \sigma^*(g) f_1 f_2 \, d\mathbf{v}_1 \, d\mathbf{v}_2. \tag{9.21}$$

In the case of polarization interaction between the ion and the atom, the diffusion cross section is close to the cross section of polarization capture (4.13), and is inversely proportional to the relative velocity g of collision. Since

$$\int \mathbf{g} f_1 f_2 \, d\mathbf{v}_1 \, d\mathbf{v}_2 = (\mathbf{w}_i - \mathbf{w}_a) N_i N_a = \mathbf{w}_i N_i N_a,$$

where $\mathbf{w}_i$ is the average ion velocity, and $\mathbf{w}_a = 0$ is the average atom velocity, Eq. (9.21) leads to

$$\mathbf{w}_i = e\mathbf{E}/(\mu N_a k_c), \tag{9.22}$$

where $k_c = 2\pi\sqrt{\beta e^2/\mu}$ is the rate constant of the polarization capture process, and β is the polarizability of the atom. Note that this formula is valid at any electric field strength including very strong fields, when the ion distribution function is very different from the Maxwell distribution dependence on the ion velocities. The integral equation (9.21) can be a basis for the analysis of ion behavior in a gas in any external electric field.

9.6 COLLISION INTEGRAL FOR ELECTRONS IN A GAS

The specifics of electron–atom collisions in a gas follow from the small ratio of the electron mass m_e to the mass M of an atom. Even if the electron momentum experiences a large change as a result of collision with an atom, the electron energy varies little. Therefore the velocity distribution of electrons is nearly symmetrical with respect to directions of electron motion. If the electrons move in a gas in an external electric field, their distribution function can be represented in the form

$$f(\mathbf{v}) = f_0(v) + v_x f_1(v), \tag{9.23}$$

where the x-axis is in the direction of the electric field **E**.

Assuming the electron number density N_e to be small compared to the atom number density N_a, we find that the presence of electrons in a gas does not affect the Maxwell distribution function $\varphi(v_a)$ of the atoms, and the electron–atom collision integral has a linear dependence on the distribution function $f(\mathbf{v})$. Thus, the electron–atom collision integral I_{ea} has the form

$$I_{ea}(f) = I_{ea}(f_0) + I_{ea}(v_x f_1). \tag{9.24}$$

We obtain first the expression for the second term in Eq. (9.23). Using Eq. (9.17), and taking into account that the velocity $\mathbf{v}_a$ of an atom does not change as a result of collision with an electron, and that the magnitude of $\mathbf{v}_a$ is small compared to the velocity of the electron, we obtain

$$I_{ea}(v_x f_1) = \int (\mathbf{v}' - \mathbf{v})_x v d\sigma f_1(v) \varphi(v_a) \, d\mathbf{v}_a,$$

where $\mathbf{v}$ and $\mathbf{v}'$ are the electron velocities before and after collision. By analogy with the procedure followed above, we obtain $\int (\mathbf{v}' - \mathbf{v})_x \, d\sigma = -v_x \sigma^*(v)$, where $\sigma^*(v)$ is the diffusion cross section (4.8) of electron–atom scattering. Then, using the normalization condition $\int \varphi(v_a) \, d\mathbf{v}_a = N_a$, we obtain

$$I_{ea}(v_x f_1) = -\nu v_x f_1(v), \tag{9.25}$$

where $\nu = N_a v \sigma^*(v)$ is the frequency of electron–atom collisions.

For determination of $I_{ea}(f_0)$ we take into account that the change of the electron energy in any single collision is small compared to the total electron energy. In a group of such processes, where the variable z changes by a small increment in each individual event, the system is diffusive in the variable z. We define the probability $W(z_0, t_0; z, t)$ such that the value z occurs at time t if at moment t_0 it was equal to z_0. The normalization condition for this probability is

$$\int W(z_0, t_0; z, t) \, dz = 1. \tag{9.26}$$

Because of the continuous character of the evolution of the probability W, it satisfies the continuity equation

$$\frac{\partial W}{\partial t} + \frac{\partial j}{\partial z} = 0,$$

where the flux j can be represented in the form

$$j = AW - B\frac{\partial W}{\partial z}.$$

Here the first term is associated with the hydrodynamic flux, and the second with the diffusion flux. By definition, the coefficients of these processes are

$$A(z,t) = \lim_{\tau\to 0} \frac{1}{\tau}\int (x - z)W(x,t;z,t+\tau)\,dx,$$

$$B(z,t) = \lim_{\tau\to 0} \frac{1}{2\tau}\int (x - z)^2 W(x,t;z,t+\tau)\,dx.$$

The corresponding equation for the probability is called the *Fokker–Planck equation*, and has the form

$$\frac{\partial W}{\partial t} = -\frac{\partial (AW)}{\partial z} + \frac{\partial^2 (BW)}{\partial z^2}. \tag{9.27}$$

This equation can be generalized for the case when the normalization condition has the form

$$\int \rho(z)W(z_0,t_0;z,t)\,dz = 1$$

in place of Eq. (9.26). The quantity W in Eq. (9.27) must be replaced by ρW, and the Fokker–Planck equation then takes the form

$$\rho\frac{\partial W}{\partial t} = -\frac{\partial (\rho AW)}{\partial z} + \frac{\partial^2 (\rho BW)}{\partial z^2}. \tag{9.28}$$

The right-hand side of this equation can be used as the collision integral of the spherical part of the electron distribution function, because it describes the incremental changes of the electron energy. To accomplish this, we replace $W(z_0,t_0;z,t)$ in Eq. (9.26) with the distribution function f_0, and in place of z we substitute the electron energy ε. Then $\rho(\varepsilon)$ behaves as $\varepsilon^{1/2}$, and the collision integral takes the form

$$I_{ea}(f_0) = \frac{1}{\rho(\varepsilon)}\frac{\partial}{\partial \varepsilon}\left(-A\rho f_0 + \frac{\partial}{\partial \varepsilon}(B\rho f_0)\right).$$

The connection between A and B is found from the condition that if the distribution function coincides with the Maxwell distribution function, the collision integral will be zero. This condition yields

$$I_{ea}(f_0) = \frac{1}{\rho(\varepsilon)} \frac{\partial}{\partial \varepsilon} \left[\rho(\varepsilon) B(\varepsilon) \left(\frac{\partial f_0}{\partial \varepsilon} + \frac{f_0}{T} \right) \right], \tag{9.29}$$

where T is the gas temperature.

By definition, the quantity $B(\varepsilon)$ is

$$B(\varepsilon) = \frac{1}{2} \left\langle \int (\varepsilon - \varepsilon')^2 N_a v \, d\sigma(\varepsilon \to \varepsilon') \right\rangle,$$

where the angle brackets signify an average over atomic energies, and $d\sigma$ is the electron–atom cross section corresponding to a given variation of the electron energy. We can make use of the constancy of the relative electron-atom velocity in the collision process, or $|\mathbf{v} - \mathbf{v}_a| = |\mathbf{v}' - \mathbf{v}_a|$, where $\mathbf{v}$ and $\mathbf{v}'$ are the electron velocities before and after the collision, and $\mathbf{v}_a$ is the velocity of the atom, unvarying in a collision with an electron. From this it follows that $v^2 - (v')^2 = 2\mathbf{v}_a(\mathbf{v} - \mathbf{v}')$, which yields the result

$$B(\varepsilon) = \frac{m_e^2}{2} \left\langle \frac{v_a^2}{3} \right\rangle \int (\mathbf{v} - \mathbf{v}')^2 N_a v \, d\sigma = T \frac{m_e^2}{M} N_a v \sigma^*(v). \tag{9.30}$$

In Eq. (9.30), $\langle v_a^2/3 \rangle = T/M$, T is the gas temperature, m_e and M are the electron and atom masses, $|\mathbf{v} - \mathbf{v}'| = 2v \sin(\vartheta/2)$, ϑ is the scattering angle, and $\sigma^*(v) = \int (1 - \cos \vartheta) \, d\sigma$ is the diffusion cross section of electron–atom scattering. Thus the collision integral from the spherical part of the electron distribution function has the form

$$I_{ea}(f_0) = \frac{m_e}{M} T \frac{\partial}{v^2 \partial v} \left[v^3 \nu \left(\frac{\partial f_0}{m_e v \partial v} + \frac{f_0}{T} \right) \right], \tag{9.31}$$

where $\nu = N_a v \sigma^*(v)$ is the frequency of electron–atom collisions.

9.7 ELECTRONS IN A GAS IN AN EXTERNAL ELECTRIC FIELD

We now examine the behavior of electrons in an atomic gas subjected to an external electric field. The number density of electrons is relatively small, so that collisions between electrons are not essential in this process. The nature of the electron behavior is determined both by the character of electron–atom collisions and by the mechanism of the transfer, mediated by the electrons, of energy from an electric field to the gas. We shall treat this problem formally

by solving the kinetic equation for the electrons: $(e\mathbf{E}/m_e)\,\partial f/\partial \mathbf{v} = I_{ea}(f)$. Taking into account the expansion (9.23) for the distribution function and expressions (9.25) and (9.31) for the electron–atom collision integral, we obtain the kinetic equation in the form

$$\frac{eE}{m_e}\left(\frac{v_x}{v}\frac{df_0}{dv} + f_1 + v_x^2\frac{df_1}{dv}\right) = -\nu v_x f_1 + I_{ea}(f_0). \tag{9.32}$$

To solve this equation we first extract from it the spherical harmonics. To achieve this, we multiply the equation by $\cos\theta$ and integrate it over $d(\cos\theta)$, where θ is the angle between the vectors $\mathbf{v}$ and $\mathbf{E}$. Then we have the set of equations

$$\begin{aligned} a\frac{df_0}{dv} &= -\nu v f_1, \\ \frac{a}{3v^2}\frac{d(v^3 f_1)}{dv} &= I_{ea}(f_0), \end{aligned} \tag{9.33}$$

where $a = eE/m_e$. The solution of this set of equations yields

$$\begin{aligned} f_0(v) &= A\exp\left(-\int_0^v \frac{m_e v'\,dv'}{T + Mu^2/3}\right), \\ f_1(v) &= \frac{m_e u}{T + Mu^2/3} f_0(v), \end{aligned} \tag{9.34}$$

where $u = eE/(m_e\nu) = eE/[m_e N_a v\sigma^*(v)]$ and A is the normalization factor. From this it follows that the electron drift velocity in a gas is

$$w_e = \int v_x^2 f_1\,d\mathbf{v} = \frac{eE}{3m_e}\left\langle \frac{1}{v^2}\frac{d}{dv}\left(\frac{v^3}{\nu}\right)\right\rangle, \tag{9.35}$$

where the averaging is done over the spherical distribution function of the electrons. In particular, if $\nu = \text{const}$, the electron drift velocity w_e and the mean energy $\bar{\varepsilon}$ are given by

$$\begin{aligned} w_e &= \frac{eE}{m_e\nu}, \\ \bar{\varepsilon} &= \frac{3}{2}T + \frac{M}{2}w_e^2. \end{aligned} \tag{9.36}$$

If $\sigma^*(v) = \text{const}$, the distribution functions (9.34) yield in the limit $\bar{\varepsilon} \gg T$ [here $\lambda = 1/(N_a\sigma^*)$]

$$w_e = 0.897\left(\frac{m_e}{M}\right)^{1/4}\sqrt{\frac{eE\lambda}{m_e}}\,,$$
$$\bar{\varepsilon} = 0.427\sqrt{\frac{M}{m_e}}\,eE\lambda = 0.530Mw_e^2. \tag{9.37}$$

9.8 ELECTRON EQUILIBRIUM IN A GAS

When analyzing the behavior of electrons in a gas, we customarily neglect electron–electron collisions because of the small number density of electrons compared to that of atoms. However, this approximation can be violated even at low electron number densities, for two reasons. First, the change of electron energy in electron–atom collisions contains a small parameter m_e/M that leads to a small energy exchange between electron and atomic subsystems. Second, because of the Coulomb interaction between electrons, electron–electron collisions are more consequential than electron collisions with neutral particles. Therefore, it is important to examine more precisely the conditions under which we can neglect electron–electron collisions, and to analyze the limiting case when energy equilibrium is determined by the electron–electron collisions. This will now be done.

The electron–electron collision integral can be determined from the spherical part of the distribution function $I_{ee}(f_0)$. We take into account that the main contribution to the cross section comes from small scattering angles, so that the change of the electron velocity $\Delta\mathbf{v}$ is relatively small. We denote by $\mathbf{v}$ the velocity of a test electron before collision, and by $\mathbf{v}' = \mathbf{v} + \Delta\mathbf{v}$ the velocity after collision. Then the corresponding velocities of the second electron are $\mathbf{v}_2$ and $\mathbf{v}_2 - \Delta\mathbf{v}$. The relative collision velocity is $\mathbf{g} = \mathbf{v} - \mathbf{v}_2$ before collision, and $\mathbf{g}' = \mathbf{g} + \Delta\mathbf{g} = \mathbf{g} + 2\,\Delta\mathbf{v}$ after collision. Using Eq. (5.1), the electron momentum change in the laboratory frame of axes (where one electron is at rest) is $\Delta p = 2e^2/(\rho g)$, where ρ is the impact parameter of the collision. This gives $\Delta g = \Delta p/m_e$ and $\Delta\mathbf{v} = \Delta\mathbf{g}/2 = e^2/(\rho g m_e)$. (Note that the reduced mass of the colliding electrons is $m_e/2$.)

The expression (9.31) can be used for the electron–electron collision integral by assuming that the variation of the electron energy resulting from a single electron–electron collision is relatively small. It is necessary to replace the gas temperature T in Eq. (9.31) by the electron temperature T_e, and the value $B(\varepsilon)$ by its definition takes the form

$$B(\varepsilon) = \frac{1}{2}\int(\varepsilon - \varepsilon')^2 N_e g\,d\sigma = \frac{m_e^2 v^2 N_e g}{6}\int\Delta\mathbf{v}^2\,d\sigma\,,$$

where the variation of the electron energy in one collision is taken as $\varepsilon - \varepsilon' = m_e \mathbf{v} \cdot \Delta\mathbf{v}$, and N_e is the electron number density. Using the above expression for $\Delta\mathbf{v}$, we have

$$\int (\Delta v)^2 \, d\sigma = \frac{2\pi e^4}{g^2 m_e^2} \int_{\rho_{\min}}^{\rho_{\max}} \frac{d\rho}{\rho}.$$

This integral converges. As the lower limit of integration we take $\rho_{\min} \sim e^2/T$, which corresponds to large scattering angles, and the upper limit of integration is given by $\rho_{\max} \sim r_D$, where r_D is the Debye–Hückel radius. The Coulomb interaction of the electrons is taken to be screened by the plasma. Thus we have

$$B_{ee}(\varepsilon) = \frac{4\pi e^4 N_e v^2}{3} \left\langle \frac{1}{g} \right\rangle \ln \Lambda, \tag{9.38}$$

where $\ln \Lambda = \ln(r_D e^2/T)$ is the Coulomb logarithm (5.5), and the averaging is done over velocities of the second electron. For simplicity we take the case $v \gg v_2$ $(g = v)$ and will consider this condition as a model for a situation where one cannot make the usual assumption of neglecting the electron–electron interaction if this indeed results. Then the electron–electron collision integral is given by the following expression:

$$I_{ee}(f_0) = \frac{4\pi e^4 N_e \ln \Lambda}{3} \frac{\partial}{v^2 \, \partial v} \left[v^2 \left(\frac{\partial f_0}{m_e v \, \partial v} + \frac{f_0}{T_e} \right) \right]. \tag{9.39}$$

Comparing it with the electron–atom collision integral (9.31), one can see that the neglect of electron–electron collisions corresponds to the condition

$$\frac{4\pi}{3} \frac{e^4}{T^2} \sqrt{\frac{T}{m_e}} N_e \ln \Lambda \frac{\sqrt{T/m_e}}{v} \ll \frac{m_e}{M} \nu, \tag{9.40}$$

where $\nu = N_a \sigma^*(v)$ is the frequency of electron–atom collisions.

We now consider the limiting case inverted with respect to (9.40). Then the first approximation for the kinetic equation

$$\frac{e\mathbf{E}}{m_e} \frac{\partial f}{d\mathbf{v}} = I_{ea}(f) + I_{ee}(f_0) \tag{9.41}$$

has the form $I_{ee}(f_0) = 0$. This gives the Maxwell distribution function for electrons, where the electron temperature T_e is a parameter. The meaning of this is that the equilibrium of the energy distribution function is established by electron–electron collisions, while the drift velocity of the electrons is

maintained by electron–atom collisions. In order to determine the electron temperature, we multiply Eq. (9.41) by $m_e v^2/2$ and integrate over electron velocities. We have $\int (m_e v^2/2) I_{ee}(f_0)\, d\mathbf{v} = 0$, because collisions between electrons do not change the total energy of the electron subsystem. Then Eq. (9.31) leads to

$$eEw_e = \int \frac{m_e v^2}{2} I_{ea}(f_0)\, d\mathbf{v} = \frac{m_e^2}{M}\left(1 - \frac{T}{T_e}\right)\langle v^2 \nu \rangle. \tag{9.42}$$

In addition, the first equation in (9.33) gives the electron drift velocity

$$w_e = \frac{eE}{3T_e}\left\langle \frac{v^2}{\nu} \right\rangle, \tag{9.43}$$

where ν is the frequency of electron–atom collisions. Thus we have

$$T_e - T = \frac{Ma^2}{3} \frac{\langle v^2/\nu \rangle}{\langle v^2 \nu \rangle}, \tag{9.44}$$

where $a = eE/m_e$. In particular, if $\nu = \text{const}$, we have

$$w_e = \frac{eE}{m_e \nu}, \qquad T_e - T = \frac{M}{3} w_e^2. \tag{9.45}$$

If $\sigma^*(v) = \text{const}$, Eqs. (9.43) and (9.44) yield [with $\lambda = (N_a \sigma^*)^{-1}$]

$$w_e = \frac{4eE\lambda}{\sqrt{2\pi T_e m_e}}, \qquad T_e - T = \frac{3\pi}{32} M w_e^2. \tag{9.46}$$

In practice, the electron concentration $c_e = N_e/N_a$ of this regime is not high. For example, in argon plasma at the temperature $T_e = 1000$ K, the criterion for this regime is $c_e \gg 2 \times 10^{-7}$, and at $T_e = 10^4$ K it is $c_e \gg 5 \times 10^{-6}$.

9.9 THE LANDAU COLLISION INTEGRAL

Equations (9.38) and (9.39) give the collision integral for electron–electron collisions, obtained under the assumption of a small change of the electron energy in any single collision with another electron. This assumption is valid when the Coulomb logarithm is large, so that small-angle scattering gives the principal contribution to the electron–electron scattering cross section. This fact allows us to formulate the problem in another way. Because the electron momentum varies little in small-angle scattering, one can represent the

collision integral by the three-dimensional Fokker–Planck equation. This form of the collision integral is named the *Landau collision integral.* We develop it below.

We start from the general expression (9.17) for the collision integral. The principle of detailed balance for elastic collisions of identical particles has the form

$$W(\mathbf{v}_1, \mathbf{v}_2 \to \mathbf{v}_1', \mathbf{v}_2') = W(\mathbf{v}_1', \mathbf{v}_2' \to \mathbf{v}_1, \mathbf{v}_2),$$

and this, with Eq. (9.17), leads to

$$I_{ee}(f) = -\int [f(\mathbf{v}_1)f(\mathbf{v}_2) - f(\mathbf{v}_1')f(\mathbf{v}_2')]W(\mathbf{v}_1, \mathbf{v}_2 \to \mathbf{v}_1', \mathbf{v}_2')\, d\mathbf{v}_1'\, d\mathbf{v}_2'\, d\mathbf{v}_2.$$

Introducing $\Delta\mathbf{v} = \mathbf{v}_1' - \mathbf{v}_1$, conservation of total momentum in a collision gives $\mathbf{v}_2' = \mathbf{v}_2 - \Delta\mathbf{v}$. Then one can reduce the collision integral to

$$I_{ee}(f) = -\int [f(\mathbf{v}_1)f(\mathbf{v}_2) - f(\mathbf{v}_1 + \Delta\mathbf{v})f(\mathbf{v}_2 - \Delta\mathbf{v})] \times W(\mathbf{v}_1, \mathbf{v}_2 \to \mathbf{v}_1', \mathbf{v}_2')\, d\mathbf{v}_1'\, d\mathbf{v}_2'\, d\mathbf{v}_2, \quad (9.47)$$

and the transition probability $W(\mathbf{v}_1, \mathbf{v}_2 \to \mathbf{v}_1', \mathbf{v}_2')$ can be written as

$$W = W\left(\frac{\mathbf{v}_1 + \mathbf{v}_1'}{2}, \frac{\mathbf{v}_2 + \mathbf{v}_2'}{2}, \Delta\mathbf{v}\right) = W\left(\mathbf{v}_1 + \frac{\Delta}{2}, \mathbf{v}_2 - \frac{\Delta\mathbf{v}}{2}, \Delta\mathbf{v}\right).$$

From the principle of detailed balance it follows that the probability W is an even function of $\Delta\mathbf{v}$. That is, W has the property $W(\Delta\mathbf{v}) = W(-\Delta\mathbf{v})$. The leading term in the expansion of the collision integral in the small parameter $\Delta\mathbf{v}$ is

$$I_{ee}(f) = -\int \left(f(\mathbf{v}_2)\frac{\partial f(\mathbf{v}_1)}{\partial \mathbf{v}_1} - f(\mathbf{v}_1)\frac{\partial f(\mathbf{v}_2)}{\partial \mathbf{v}_2} \right) \Delta\mathbf{v} W\, d\Delta\mathbf{v}\, d\mathbf{v}_2.$$

Since $W(\mathbf{v}_1 + \Delta\mathbf{v}/2, \mathbf{v}_2 - \Delta\mathbf{v}/2, \Delta\mathbf{v})$ is an even function of $\Delta\mathbf{v}$, this approximation gives zero. In the second-order approximation in $\Delta\mathbf{v}$ we have

$$I_{ee}(f) = -\int d\Delta\mathbf{v}\, d\mathbf{v}_2\, W \left(\frac{1}{2}\Delta_\alpha \Delta_\beta \frac{\partial^2 f_1}{\partial v_{1\alpha}\, \partial v_{1\beta}} f_2 - \Delta_\alpha \Delta_\beta \frac{\partial f_1}{\partial v_{1\alpha}} \frac{\partial f_2}{\partial v_{2\beta}} + \frac{1}{2}\Delta_\alpha \Delta_\beta f_1 \frac{\partial^2 f_2}{\partial v_{2\alpha}\, \partial v_{2\beta}} \right)$$

$$- \int d\Delta\mathbf{v}\, d\mathbf{v}_2 \frac{1}{2}\Delta_\alpha \left(\frac{\partial W}{\partial v_{1\alpha}} - \frac{\partial W}{\partial v_{2\alpha}} \right) \Delta_\beta \left(\frac{\partial f_1}{\partial v_{1\beta}} f_2 - f_1 \frac{\partial f_2}{\partial v_{2\beta}} \right),$$

where $f_1 \equiv f(\mathbf{v}_1)$, $f_2 \equiv f(\mathbf{v}_2)$, $\Delta_\alpha \equiv \Delta v_\alpha$, and the summation convention is invoked, in which any index repeated in a term is to be summed over all values of that index. One can calculate some of the terms in the above expression by using the method of integration by parts. We have

$$\frac{1}{2}\int d\Delta\mathbf{v}\, d\mathbf{v}_2\, W\Delta_\alpha\Delta_\beta \frac{\partial f_1}{\partial v_{1\alpha}}\frac{\partial f_2}{\partial v_{2\beta}} + \frac{1}{2}\int d\Delta\mathbf{v}\, d\mathbf{v}_2\, \Delta_\alpha\Delta_\beta \frac{\partial W}{\partial v_{2\alpha}}\frac{\partial f_1}{\partial v_{1\beta}} f_2$$

$$= \frac{1}{2}\int d\Delta\mathbf{v}\, d\mathbf{v}_2\, \Delta_\alpha\Delta_\beta \frac{\partial f_1}{\partial v_{1\alpha}}\frac{\partial}{\partial v_{2\beta}}(Wf_2) = 0,$$

$$\frac{1}{2}\int d\Delta\mathbf{v}\, d\mathbf{v}_2\, W\Delta_\alpha\Delta_\beta f_1 \frac{\partial^2 f_2}{\partial v_{2\alpha}\,\partial v_{2\beta}} + \frac{1}{2}\int d\Delta\mathbf{v}\, d\mathbf{v}_2\, \Delta_\alpha\Delta_\beta \frac{\partial W}{\partial v_{2\alpha}} f_1 \frac{\partial f_2}{\partial v_{2\beta}}$$

$$= \frac{1}{2}\int d\Delta\mathbf{v}\, d\mathbf{v}_2\, \Delta_\alpha\Delta_\beta f_1 \frac{\partial}{\partial v_{2\alpha}}\left(W\frac{\partial f_2}{\partial v_{2\beta}}\right) = 0,$$

since the distribution function is zero at $v_{2\beta} \to \pm\infty$. After elimination of these terms we obtain

$$I_{ee}(f) = -\frac{1}{2}\int d\Delta\mathbf{v}\, d\mathbf{v}_2\, \Delta_\alpha\Delta_\beta\left(W\frac{\partial^2 f_1}{\partial v_{1\alpha}\,\partial v_{1\beta}} f_2 - W\frac{\partial f_1}{\partial v_{1\alpha}}\frac{\partial f_2}{\partial v_{2\beta}} + \frac{\partial W}{\partial v_{1\alpha}}\frac{\partial f_1}{\partial v_{1\beta}} f_2 - \frac{\partial W}{\partial v_{2\alpha}} f_1 \frac{\partial f_2}{\partial v_{2\beta}}\right)$$

$$= -\frac{\partial j_\beta}{\partial v_{1\beta}},$$

where the flux in electron-velocity space is

$$j_\beta = \int d\mathbf{v}_2\left(f_1\frac{\partial f_2}{\partial v_{2\beta}} - \frac{\partial f_1}{\partial v_{1\beta}} f_2\right) D_{\alpha\beta},$$

$$D_{\alpha\beta} = \frac{1}{2}\int \Delta_\alpha\Delta_\beta W\, d\Delta\mathbf{v}.$$

This symmetrical form of the electron–electron collision integral is called the Landau collision integral. It is analogous to the right-hand side of the Fokker–Planck equation in velocity space. For evaluation of the tensor $D_{\alpha\beta}$, Eq. (5.1) gives

$$\Delta_\alpha = \frac{2e^2\rho_\alpha}{\rho^2 g m_e},$$

where g is the relative velocity of the colliding electrons. This gives

$$D_{\alpha\beta} = \frac{1}{2}\int \Delta_\alpha \Delta_\beta W d\Delta\mathbf{v} = \frac{1}{2}\int \Delta_\alpha \Delta_\beta g\, d\sigma$$

$$= \frac{2e^4}{m_e g}\int \frac{\rho_\alpha \rho_\beta}{\rho^4}\, d\sigma.$$

To aid in the evaluation of this tensor, we first take the direction of the collision velocity $\mathbf{g}$ to be along the x-axis, and take the plane of motion to be the xy plane. Then only Δ_y is nonzero, so that only the tensor component D_{yy} is nonzero. For this component of the tensor we obtain

$$D_{yy} = \frac{2e^4}{m_e g}\int \frac{1}{\rho^2} 2\pi\rho\, d\rho = \frac{4\pi e^4}{m_e g}\ln\Lambda,$$

where the integral over impact parameters of the collision are evaluated in a straightforward way, and $\ln\Lambda$ is the Coulomb logarithm. Next, taking into account that the direction of the relative velocity of collision is a random value, one can write the expression for the tensor $D_{\alpha\beta}$ in an arbitrary frame of reference. Because this tensor is symmetric with respect to its indices, it can be constructed on the basis of the symmetrical tensors $\delta_{\alpha\beta}$ and $g_\alpha g_\beta$. It is evident that it has the form

$$D_{\alpha\beta} = \frac{4\pi e^4}{m_e g^3} g_\alpha g_\beta \ln\Lambda.$$

The Landau collision integral that represents collisions between electrons is thus of the form

$$I_{ee}(f) = -\frac{\partial j_\beta}{\partial v_{1_\beta}},$$

$$j_\beta = \int d\mathbf{v}_2 \left(f_1 \frac{\partial f_2}{\partial v_{2\beta}} - \frac{\partial f_1}{\partial v_{1\beta}} f_2 \right) D_{\alpha\beta}, \tag{9.48}$$

$$D_{\alpha\beta} = \frac{4\pi e^4}{m_e g^3} g_\alpha g_\beta \ln\Lambda.$$

It is analogous to Eq. (9.39) for the electron energy space, and is a version of the Fokker–Planck equation.

9.10 EXCITATION OF ATOMS IN A PLASMA

Inelastic collisions of electrons and atoms in a gas can affect the electron distribution function, because such collisions remove fast electrons whose energy exceeds the atomic excitation energy. This part of the distribution function can be restored by elastic collisions of electrons. Competition of these processes establishes the distribution function and determines the rate of atomic excitation. We shall now analyze this problem and evaluate the rate of atomic excitation in a plasma. We consider the case of a high electron density where the electron distribution function in the principal range of electron velocities is Maxwellian. This corresponds to the condition $B_{ee} \gg B_{ea}$, where B_{ee} and B_{ea} are the coefficients in the Fokker–Planck equation (9.28) that are given by expressions (9.30) and (9.38). In the case being considered, these quantities are taken at the excitation energy $\Delta\varepsilon$ of the atom. Hence, the condition (9.40) has the form

$$\frac{N_e}{N_a} \gg \frac{m_e}{M} \frac{3T\Delta\varepsilon\,\sigma_{ea}^*(v_0)}{2\pi e^4 \ln\Lambda} \tag{9.49}$$

in this case, where $\sigma_{ea}^*(v_0)$ is the diffusion cross section for electron–atom elastic collisions at the velocity $v_0 = \sqrt{2\,\Delta\varepsilon/m}$, and $\ln\Lambda$ is the Coulomb logarithm.

In analyzing the character of atom excitations in a plasma, we assume for simplicity that excited states decay only by radiation. That is, we assume that quenching by electron impact does not occur. We shall consider two limiting cases of atomic excitation. In the first case, the Maxwell distribution function obtains at all velocities because electron–electron collisions restore it in the region of high electron energies. In the second case, processes restoring the distribution function are weak, and all the electrons at energies $\varepsilon \geq \Delta\varepsilon$ expend their energy in the excitation of atoms.

The excitation rate in the first case is

$$\frac{dN_*}{dt} = N_a \int 4\pi v^2\, dv\, \varphi(v)\, v k_{ex}(v),$$

where N_* is the number density of excited atoms, N_a is the number density of atoms in the ground state, $\varphi(v)$ is the Maxwell distribution function of the electrons, and k_{ex} is the rate constant for atomic excitation by electron impact. Using the principle of detailed balance (8.5) for excitation and quenching of atoms, we have near the excitation threshold

$$k_{ex} = \frac{g_* k_q}{g_0} \sqrt{\frac{\varepsilon - \Delta\varepsilon}{\Delta\varepsilon}},$$

where k_q is the rate constant for quenching of the excited atom by a slow electron, and g_0 and g_* are statistical weights for the ground and excited states of the atom. From this, it follows that the excitation rate is

$$\frac{dN_*}{dt} = \frac{N_a N_e k_q g_*}{g_0} \exp\left(-\frac{\Delta\varepsilon}{T_e}\right), \tag{9.50}$$

so that the effective rate constant of the atom excitation process is

$$\bar{k}_{ex} = \frac{g_* k_q}{g_0} \exp\left(-\frac{\Delta\varepsilon}{T_e}\right). \tag{9.51}$$

In the other limiting case, the excitation rate is determined by electron diffusion to the boundary of the region in energy space where excitation is possible. Hence, on the basis of the kinetic equation (9.3), we have

$$\frac{dN_*}{dt} = \int_{v_0}^{\infty} 4\pi v^2 \, dv \frac{\partial f}{\partial t} = -\int_{v_0}^{\infty} 4\pi v^2 dv I_{ee}(f_0)$$

$$= \frac{4\pi v_0}{m_e} B_{ee}(v_0)\left(\frac{f_0}{T_e} - \frac{df_0}{d\varepsilon}\right),$$

where the distribution function f_0 in the final expression is taken at the energy $\Delta\varepsilon$. The form of the distribution function follows from the equation $I_{ee}(f_0) = 0$ and the boundary condition $f_0(v_0) = 0$. The result is

$$f_0(v) = N_e\left(\frac{m_e}{2\pi T_e}\right)^{3/2}\left[\exp\left(-\frac{\varepsilon}{T_e}\right) - \exp\left(-\frac{\Delta\varepsilon}{T_e}\right)\right], \qquad \varepsilon \le \Delta\varepsilon. \tag{9.52}$$

Using this distribution function and the expression (9.38) for $B_{ee}(v)$, we obtain

$$\frac{dN_*}{dt} = \frac{8\sqrt{2}}{3} \frac{N_e^2 e^4 \Delta\varepsilon \ln\Lambda}{m_e^{1/2} T_e^{5/2}} \exp\left(-\frac{\Delta\varepsilon}{T_e}\right). \tag{9.53}$$

Equation (9.51) is valid at high electron number densities, in which domain establishment of equilibrium for the electron velocity distribution function takes place rapidly. The corresponding condition has the form

$$N_e/N_a \gg k_q/k_{Coul}, \tag{9.54}$$

where the effective rate constant k_{Coul} for the Coulomb interaction of electrons is

$$k_{Coul} = \frac{8\sqrt{2}}{3} \frac{g_0}{g_*} \frac{e^4}{T_e^2} \sqrt{\frac{T_e}{m_e}} \frac{\Delta\varepsilon}{T_e} \ln\Lambda. \tag{9.55}$$

Equation (9.53) is valid under the condition opposite to that of (9.54). It is evident that the criterion (9.54) is much stronger than (9.49) because $m_e \ll M$. Thus both regimes being considered for atomic excitation in a plasma are possible. At relatively small electron number densities, the distribution function is given by Eq. (9.52), while the Maxwell distribution function for the electrons is valid at high degrees of ionization. Correspondingly, the expression for the atomic excitation rate varies from (9.53) up to (9.50) as the electron number density increases.

For comparison, we consider the case of a small number density of electrons and find the electron distribution function in the energy region $\varepsilon \geq \Delta\varepsilon$. Then it is necessary to include in the kinetic equation for electrons the contribution of inelastic electron–atom collisions. We assume that quenching of the excited atom proceeds by a mechanism other than electron impact because of the small number density of electrons. Then the kinetic equation (9.33) takes the form

$$-\frac{a}{3v^2}\frac{d}{dv}(v^3 f_1) = I_{ea}(f_0) - \nu_{ex} f_0,$$

where $\nu_{ex} = N_a k_{ex}$, N_a is the number density of atoms, and k_{ex} is the rate constant for excitation of the atom by electron impact. The collision integral I_{ea} takes into account elastic electron–atom collisions. Using the connection (9.33) between f_0 and f_1, we obtain

$$\frac{a}{3v^2}\frac{d}{dv}\left(\frac{v^2}{\nu}\frac{df_0}{dv}\right) + I_{ea}(f_0) - \nu_{ex} f_0 = 0$$

as the equation for f_0. When we use the expression for the electron–atom collision integral in Eq. (9.31), and neglect the atomic kinetic energy ($\sim T$) compared to the electron energy, we have

$$\frac{a}{3v^2}\frac{d}{dv}\left(\frac{v^2}{\nu}\frac{df_0}{dv}\right) + \frac{m_e}{M}\frac{1}{v^2}\frac{d}{dv}(v^3 \nu f_0) - \nu_{ex} f_0 = 0. \qquad (9.56)$$

We assume that the average electron energy $\bar{\varepsilon}$ is much smaller than the atom's excitation energy $\Delta\varepsilon$. It then follows from Eq. (9.36) that $\bar{\varepsilon} \sim Ma^2/\nu^2$. Furthermore, we assume that atomic excitations influence the electron distribution function, so that

$$\nu \gg \nu_{ex} \gg \frac{m_e}{M}\nu\frac{\Delta\varepsilon}{\bar{\varepsilon}}. \qquad (9.57)$$

This allows us to neglect the second term of the kinetic equation (9.56). We can solve the resulting simplified kinetic equation for the tail of the distribution function by a quasiclassical method, accepting that $f_0 = A\exp(S)$, where

$S(v)$ is a smooth function. We mean by that statement that $(S')^2 \gg S''$. This gives $S' = \sqrt{3\nu_{ex}\nu}/a$, $a = eE/m_e$, and the distribution function for $\varepsilon \gg \bar{\varepsilon}$ has the form

$$f_0(v) = f_0(v_0) \exp\left(-\int_{v_0}^{v} dv \frac{\sqrt{3\nu_{ex}\nu}}{a}\right), \tag{9.58}$$

where $v_0 = \sqrt{2\Delta\varepsilon/m_e}$ and $f_0(v_0)$ is determined by elastic electron–atom collisions. Near the threshold for atomic excitation, this formula gives

$$S = \frac{2}{3}\frac{\sqrt{3\nu_{ex}\nu}}{a}\frac{(v - v_0)}{v_0}^{3/2}\frac{g_*}{g_0} = C(v - v_0)^{3/2}, \tag{9.59}$$

where $\nu_0 = \nu(v_0)$, $\nu_q = N_a k_q$, k_q is the rate constant for quenching of the excited atom by electron impact, g_0 and g_* are the statistical weights of the ground and excited atom states, and we use the principle of detailed balance to connect the rate constants of atomic excitation and quenching by electron impact. Note that in the case of large electron densities when the electron distribution function is Maxwellian, this quantity has the form

$$S = \frac{\varepsilon - \Delta\varepsilon}{T_e} = 3\nu_0^2\frac{\varepsilon - \Delta\varepsilon}{Ma^2}. \tag{9.60}$$

Here, for simplicity, we assume that $\nu(v) = \text{const}$. Because of the criterion (9.57), Eq. (9.60) gives less of a decrease of the distribution function with increase in the electron energy than follows from Eq. (9.59). On the basis of the distribution function (9.58), we obtain the atomic excitation rate

$$\frac{dN_*}{dt} = \int_{v_0}^{\infty} 4\pi v^2\, dv f_0(v) N_a k_{ex}(v) = \frac{v_0^2 f_0(v_0) a^{4/3}}{\nu_0^{2/3}\lambda^{1/3}}, \tag{9.61}$$

where

$$\lambda^{-1} = \frac{N_a k_{ex}}{v - v_0} = \frac{N_a k_q g_*}{g_0 v_0}.$$

We considered above the excitation of atoms in a plasma under conditions where the detachment of excited atoms is not due to electron impact but is determined by other processes. This corresponds to a condition opposite to that of Eq. (8.10). Now we consider the case when the criterion (8.10) is satisfied. Then, based on the condition (9.57), we have the situation where fast electrons are generated and destroyed as a result of inelastic collisions between electrons and atoms. Because of the equilibrium between the atomic

states involved, we find

$$\nu_{ex} f_0(v) v^2 \, dv = \nu_q f_0(v') v'^2 \, dv'.$$

Here, we have $v^2 = 2\Delta\varepsilon/m_e + v'^2$, v and v' are the velocities of fast and slow electrons, and $\nu_{ex} = N_a k_{ex}$, $\nu_q = N_i k_q$ are the frequencies of excitation and quenching of atomic states by electron impact. Then with N_a and N_* giving the number densities of atoms in the ground and excited states, respectively, and with the rate constants k_{ex} and k_q for the corresponding processes connected by the principle of detailed balance (8.5), we have

$$\frac{N_a}{g_0} f_0(v) = \frac{N_*}{g_*} f_0\left(\sqrt{v^2 - v^2}\right), \qquad v > \sqrt{\frac{2\Delta\varepsilon}{m}}.$$

This relation establishes the connection between the distribution functions of slow and fast electrons. The relation can be written in the form

$$f_0(v) = \frac{f_0(v_0) f_0\left(\sqrt{v^2 - v_0^2}\right)}{f_0(0)}. \tag{9.62}$$

In particular, for the Maxwell distribution of slow electrons [$f_0 \sim \exp(-\varepsilon/T_e)$] this expression gives

$$f_0(v) = f_0(v_0) \exp\left(\frac{\varepsilon - \Delta\varepsilon}{T_e}\right), \tag{9.63}$$

where T_e is the electron temperature, and $\varepsilon = m_e v^2/2$ is the electron energy. Thus, in this case, inelastic collisions restore the Maxwell distribution function above the threshold for atomic excitation.

The cases of atom excitation in a plasma treated above show that this process depends on the nature of the processes that establish the electron distribution function near the excitation threshold. The result depends both on the rate of restoration of the electron distribution function by electron–electron or electron–atom collisions, and on the character of the quenching of excited atoms. Competition of these processes yields a complicated form for the electron distribution function and for the excitation rate of atoms in a plasma.

CHAPTER 10

TRANSPORT PHENOMENA IN GASES

10.1 TRANSPORT OF PARTICLES IN GASES

Parameters of thermodynamic equilibrium such as the number density of atoms or molecules of each species, the temperature, and the mean velocity of atoms or molecules, are constants in a region. If some of these values should vary in this region, appropriate fluxes arise in order to equalize these parameters over the total volume of a gas or plasma. The fluxes are small if variations of the parameters are small over distances of the order of the mean free path for atoms or molecules. Then a stationary state of the system with fluxes exists, and such states are conserved during times much longer than typical times between particle collisions. In other words, the inequality

$$\lambda \ll L, \tag{10.1}$$

is satisfied for the systems under discussion, where λ is the mean free path for particles in collision, and L is a typical size of the system or a distance over which a parameter varies noticeably. If this criterion is fulfilled, the system is in a stationary state to first approximation, and transport of particles, heat or momentum occurs in the second approximation in terms of an expansion over a small parameter defined in accordance with Eq. (10.1). Various types of such transport will be considered below.

The coefficients of proportionality between fluxes and corresponding gradients are called kinetic coefficients or transport coefficients. For instance, the diffusion coefficient D is introduced as the proportionality factor

between the particle flux $\mathbf{j}$ and the gradient of concentration c of a given species:

$$\mathbf{j} = -DN\nabla c. \tag{10.2}$$

Here N is the total particle number density. If the concentration of a given species is low ($c_k \ll 1$), that is, this species is an admixture to the gas, the flux of particles of this species can be written as

$$\mathbf{j} = -D_k \nabla N_k, \tag{10.3}$$

where N_k is the number density of particles of the given species k. The thermal conductivity coefficient κ is defined as the proportionality factor between the heat flux $\mathbf{q}$ and the temperature gradient,

$$\mathbf{q} = -\kappa \nabla T. \tag{10.4}$$

The viscosity coefficient η is the proportionality factor between the frictional force acting on a unit area of a moving gas, and the gradient of the mean gas velocity in the direction perpendicular to the surface of a gas element. If the mean gas velocity $\mathbf{w}$ is parallel to the x-axis and varies in the z-direction, the frictional force is proportional to $\partial w_x/\partial z$ and acts on an xy surface in the gas. Thus the force F per unit area is

$$F = -\eta \partial w_x/\partial z. \tag{10.5}$$

This definition, as well as the previous ones, refers to liquids as well as gases.

We can estimate the value of the diffusion coefficient. The diffusive flux is the difference of fluxes in opposite directions. Each of these, in order of magnitude, is $N_k v$, where N_k is the number density of particles of species k, and v is a typical velocity. Thus the particle flux behaves as $j \sim \Delta N_k\, v$, where ΔN_k is the difference of the number densities of oppositely directed particles participating in the transport. Particles that reach a given point without collisions have distances from it of the order of the mean free path $\lambda \sim (N\sigma)^{-1}$, where σ is a typical cross section for elastic collisions, and N is the total number density of gas particles. Hence $\Delta N_k \sim \lambda \nabla N_k$, and the diffusive flux behaves as $j \sim \lambda v \nabla N_k$. Comparing this with the definition of the diffusion coefficient (10.2), we obtain

$$D \sim v\lambda \sim \frac{\sqrt{T}}{N\sigma\sqrt{m}}. \tag{10.6}$$

Here T is the gas temperature, and m is the mass of particles of a given species, assumed to be of the same order of magnitude of the masses of other particles constituting the gas. In this analysis we do not need to consider the

sign of the flux, because it is simply opposite to the number density gradient, and tends to equalize the particle number densities at neighboring points. The same can be said about the signs of the fluxes and gradients for the other transport phenomena.

10.2 DIFFUSIVE PARTICLE MOTION

We now examine the properties of diffusion. The continuity equation has the form $\partial N_k/\partial t + \operatorname{div}\mathbf{j} = 0$ [compare with equation (9.5)]. The continuity equation is a statement of the fact that particles are neither lost nor generated in a region. For simplicity, we consider the case $N_k \ll N$ and omit below the subscript k. Diffusive motion can be referred to test particles in a single-component gas. Using the expression (10.3) for the flux in the continuity equation, the equation describing the diffusive motion of particles is

$$\frac{\partial N}{\partial t} = D\,\Delta N, \tag{10.7}$$

where Δ is the Laplacian operator. It follows from this that a characteristic time for particle transport over a distance of the order of L is $\tau_L \sim L^2/D$. Using the estimate (10.6) for the diffusion coefficient, we find that $\tau_L \sim \tau_0(L/\lambda)^2$, where $\tau_0 \sim \lambda/v$ is a typical time between successive collisions. The condition (10.1) leads to $\tau_L \gg \tau_0$, which is the identifying feature allowing us to consider this process as time-independent.

To further study the diffusion of test particles, we introduce the probability $W(\mathbf{r}, t)$ that a test particle is at point $\mathbf{r}$ at moment t. Assuming this particle to be located at the spatial origin at time zero, the probability will be spherically symmetrical. The normalization condition is

$$\int_0^\infty W(r,t)\,4\pi r^2\,dr = 1. \tag{10.8}$$

The probability W satisfies equation (10.7), which in the spherically symmetrical case takes the form

$$\frac{\partial W}{\partial t} = \frac{D}{r}\frac{\partial^2}{\partial r^2}(rW).$$

To find mean values for the diffusion parameters, we multiply this equation by $4\pi r^4\,dr$ and integrate the result over all r. The left-hand side of the equation yields

$$\int_0^\infty 4\pi r^4\,dr\frac{\partial W}{\partial t} = \frac{d}{dt}\int_0^\infty r^2 W\,4\pi r^2\,dr = \frac{d}{dt}\overline{r^2},$$

where $\overline{r^2}$ is the mean square of the distance from the origin. Integrating twice by parts and using the normalization condition (10.8), we transform the right-hand side of the equation into

$$D\int_0^\infty 4\pi r^4\, dr \frac{1}{r}\frac{\partial^2}{\partial r^2}(rW) = -3D\int_0^\infty 4\pi r^2\, dr \frac{\partial}{\partial r}(rW)$$

$$= 6D\int_0^\infty W 4\pi r^2\, dr = 6D.$$

The resulting equation is $d\overline{r^2} = 6D\,dt$. Since at zero time the particle is located at the origin, the solution of this equation has the form

$$\overline{r^2} = 6Dt. \tag{10.9}$$

Because the motion in different directions is independent and has a random character, it follows from this that

$$\overline{x^2} = \overline{y^2} = \overline{z^2} = 2Dt. \tag{10.10}$$

The solution of Eq. (10.7) can be obtained from the normal distribution (2.41), which is appropriate for this process. Diffusion consists of random displacements of a particle, and the result of many collisions of this particle with its neighbors fits the general concept of the normal distribution. In the spherically symmetric case we have

$$W(\mathbf{r}, t) = w(x, t)w(y, t)w(z, t),$$

and substituting $\Delta = \langle x^2 \rangle = 2Dt$ in Eq. (2.39), we obtain

$$w(x, t) = (4\pi Dt)^{-1/2} \exp\left(-\frac{x^2}{4Dt}\right).$$

for each w-function. This yields

$$W(r, t) = (4\pi Dt)^{-3/2} \exp\left(-\frac{r^2}{4Dt}\right). \tag{10.11}$$

10.3 DIFFUSION OF ELECTRONS IN GASES

We can establish the electron diffusion coefficient in a weakly ionized gas when it is determined by Eq. (10.3): $\mathbf{j}_e = -D_e \nabla N_e$. Then the Boltzmann kinetic equation has the form

$$v_x \nabla f = I_{ea}(f),$$

where the electron distribution function in accordance with the expansion (9.23) is $f = f_0(v) + v_x f_1(v)$, and the x-axis is in the direction of the gradient of the electron number density. Taking into account the property that $f \sim N_e$, we have $\nabla f = f \nabla N_e / N_e$. Then Eq. (9.25) yields

$$v_x f_0 \nabla N_e / N_e = -\nu v_x f_1,$$

or

$$f_1 = -f_0 \nabla N_e / (\nu N_e).$$

The electron flux is then given by

$$\mathbf{j}_e = \int \mathbf{v} f d\mathbf{v} = \int v_x^2 f_1 \, d\mathbf{v} = -\frac{\nabla N_e \int v_x^2 f_0 \, d\mathbf{v}}{\nu N_e}$$

$$= -\nabla N_e \langle v_x^2 / \nu \rangle,$$

where angle brackets mean averaging over the electron distribution function. Comparing this formula with Eq. (10.3), we find that the electron diffusion coefficient is

$$D_e = \left\langle \frac{v^2}{3\nu} \right\rangle. \tag{10.12}$$

Equation (10.12) is correct only for transverse diffusion, because only in this case can one separate corrections to the spherical electron distribution function due to the electric field and due to the gradient of the electron number density.

We now determine the coefficient for transverse diffusion of electrons in a strong magnetic field if the directions of the electric and magnetic fields coincide. This corresponds to the condition $\omega_H \gg \nu$, where $\omega_H = eH/(m_e c)$ is the *electron cyclotron frequency*. The projection of the electron trajectory on a plane perpendicular to the field consists of circles whose centers and radii vary after each collision. The diffusion coefficient, by its definition, is $D_\perp = \langle x^2 \rangle / t$, where $\langle x^2 \rangle$ is the mean square of the displacement for a time t in the direction x perpendicular to the field. We have $x - x_0 = r_H \cos \omega_H t$, where x_0 is the x-coordinate of the center of the electron's rotational motion, and $r_H = v_\rho / \omega_H$ is the Larmor radius, so that v_ρ is the electron velocity in the direction perpendicular to the field, and ω_H is the electron cyclotron frequency. From this it follows that

$$\langle x^2 \rangle = n \langle (x - x_0)^2 \rangle = n v_\rho^2 / (2\omega_H^2),$$

where n is the number of collisions. Since $t = n/\nu$, where ν is the frequency of electron-atom collisions, we obtain

$$D_\perp = \left\langle \frac{v_\rho^2 \nu}{2\omega_H^2} \right\rangle = \left\langle \frac{v^2 \nu}{3\omega_H^2} \right\rangle, \qquad \omega_H \gg \nu,$$

where angular brackets mean averaging over electron velocities. Combining this result with Eq. (10.12), we find that the transverse diffusion coefficient for electrons in a gas, moving perpendicular to electric and magnetic fields, is

$$D_\perp = \frac{1}{3}\left\langle \frac{v^2 \nu}{\omega_H^2 + \nu^2} \right\rangle. \tag{10.13}$$

10.4 THE EINSTEIN RELATION

If a particle is subjected to an external field while traveling in a vacuum, it is uniformly accelerated. If this particle travels in a gas, collision with gas particles creates a frictional force, and the mean velocity of the particle in the gas is established both by the external field and by the interactions with other particles. The proportionality coefficient between the particle mean velocity $\mathbf{w}$ and the force $\mathbf{F}$ acting on the particle from an external field is called the particle *mobility*. Thus the definition of the mobility b of a particle is

$$\mathbf{w} = b\mathbf{F}. \tag{10.14}$$

We now assume that the test particles in a gas are in thermodynamic equilibrium with the gas while subjected to the external field. According to the Boltzmann formula (2.9), the distribution for the number density of the test particles is $N = N_0 \exp(-U/T)$, where U is the potential due to the external field, and T is the temperature of the gas. The diffusive flux of the test particles according to Eq. (10.3) is $\mathbf{j} = -D\nabla N = D\mathbf{F}N/T$, where $\mathbf{F} = -\nabla U$ is the force acting on the test particle. Because thermodynamic equilibrium exists, the diffusion flux is compensated by the hydrodynamic particle flux, $\mathbf{j} = \mathbf{w}N = b\mathbf{F}N$. Equating these fluxes, we find that the kinetic coefficients are related as

$$b = D/T. \tag{10.15}$$

This expression is known as the *Einstein relation*. It is valid for small fields that do not disturb the thermodynamic equilibrium between the test and gas particles. From Eqs. (10.15) and (10.6), we can estimate the particle mobility to be

$$b \sim \frac{1}{N\sigma\sqrt{mT}}. \tag{10.16}$$

10.5 HEAT TRANSPORT

Heat transport can be treated in a manner analogous to that employed for particle transport. The heat flux is defined as

$$\mathbf{q} = \int \mathbf{v} \frac{mv^2}{2} f d\mathbf{v}, \tag{10.17}$$

where f is the velocity distribution function of the particles, and the relation between the heat flux and the temperature is given by Eq. (10.4). For estimation of the thermal conductivity coefficient, we use the same procedure as in the case of the diffusion coefficient. Take the heat flux through a given point as a difference of the fluxes in opposite directions, and express the difference of the heat fluxes in terms of the difference of temperatures. From Eq. (10.17), the heat flux can be estimated to be $q \sim Nv\Delta T$ because the energies of particles reaching this point from opposite sides are different. Because only particles located within a distance of about λ reach the given point without collisions, we have $\Delta T \sim \lambda \nabla T$. Substituting this in the equation for the heat flux and comparing the result with Eq. (10.4), we find that our estimate for the thermal conductivity coefficient is

$$\kappa \sim Nv\lambda \sim \frac{v}{\sigma} \sim \frac{\sqrt{T}}{\sigma\sqrt{m}}. \tag{10.18}$$

The thermal conductivity coefficient is independent of the particle number density. An increase in the particle number density leads to an increase in the number of particles that transfer heat, but this then causes a decrease in the distance of this transport. These two effects cancel.

Our next step is to derive the heat transport equation for a gas where thermal conductivity supplies the mechanism. Denote by $\bar{\varepsilon}$ the mean energy of a gas particle, and for simplicity consider a single-component gas. Assuming there are no sources and sinks for heat, we obtain a heat equation exactly analogous to the continuity equation (9.5) for the number density of particles, namely

$$\frac{\partial}{\partial t}(\bar{\varepsilon} N) + \operatorname{div} \mathbf{q} = 0.$$

We take the gas to be contained in a fixed volume. With $\partial\bar{\varepsilon}/\partial T = c_p$ as the heat capacity per gas particle at a constant pressure, the above equation takes the form

$$\frac{\partial T}{\partial t} + \mathbf{w} \cdot \nabla T = \frac{\kappa}{c_p N} \Delta T, \tag{10.19}$$

where $\mathbf{w}$ is the mean velocity of the particles, and where we use the continuity equation (9.5) for $\partial N/\partial t$ and the expression (10.4) for the heat flux. For a motionless gas this equation is analogous to the diffusion equation (10.7), and its solution can be obtained by analogy with Eq. (10.12).

10.6 THERMAL CONDUCTIVITY DUE TO INTERNAL DEGREES OF FREEDOM

An additional channel of heat transport arises from the energy transport associated with internal degrees of freedom. Excited atoms or molecules that move through a region with a relatively low temperature can transfer their excitation energy to the gas, and successive transfers of this nature amount to the transport of energy. The inverse process can also take place, in which ground-state atoms or molecules pass through a region with a relatively high temperature, are excited in this region, and then transport this excitation energy to other regions in the gas. This mechanism of heat transport is significant if a typical distance over which excited and nonexcited atoms reach equilibrium is small as compared to a length typifying the size of the system.

The heat flux can be represented as a sum of two terms

$$\mathbf{q} = -\kappa_t \nabla T - \kappa_i \nabla T,$$

where κ_t is the thermal conductivity coefficient due to the transport of translational energy, while the second term arises from transport of energy in the internal degrees of freedom. The thermal conductivity coefficient is then just the sum of these two terms, or

$$\kappa = \kappa_t + \kappa_i. \tag{10.20}$$

We shall now analyze the second term.

The internal state of the gas particle is denoted by the subscript i. Because of the presence of a temperature gradient, the number density of particles in this state is not constant in space, and the diffusion flux given by

$$\mathbf{j}_i = -D_i \nabla N_i = -D_i \frac{\partial N_i}{\partial T} \nabla T$$

occurs. This leads to the heat flux

$$\mathbf{q} = \sum_i \varepsilon_i \mathbf{j}_i = -\sum_i \varepsilon_i D_i \frac{\partial N_i}{\partial T} \nabla T,$$

where ε_i is the excitation energy of the ith state. Assuming the diffusion coefficient to be the same for excited and nonexcited particles, the thermal

conductivity coefficient due to internal degrees of freedom is

$$\kappa_i = \sum_i \varepsilon_i D_i \frac{\partial N_i}{\partial T} = D \frac{\partial}{\partial T} \sum_i \varepsilon_i N_i = D \frac{\partial}{\partial T}(\bar{\varepsilon} N) = D c_p, \quad (10.21)$$

where $\bar{\varepsilon} = \sum_i \varepsilon_i N_i / N$ is the mean excitation energy of the particles, $N = \sum_i N_i$ is the total number density, and $c_p = \partial \bar{\varepsilon} / \partial T$ is the heat capacity per particle. Using the estimates (10.6) and (10.18) for the diffusion coefficient and the thermal conductivity coefficient, one can conclude that $\kappa_i \sim \kappa_t$ if the excitation energy of internal states is of the order of the thermal energy of the particle.

Another example of this mechanism for thermal conductivity occurs when a dissociated gas undergoes recombination upon entering a cold region. We examine the example of a gas that consists of atoms coexisting in thermodynamic equilibrium with a small admixture of diatomic molecules representing the bound system of these atoms. The dissociation and recombination proceed in accordance with the simple scheme

$$A + A \leftrightarrow A_2.$$

The number densities of atoms (N_a) and molecules (N_m) are connected by the Saha formula (2.17), so that $N_a^2 / N_m = F(T) \exp(-D/T)$, where D is the dissociation energy and $F(T)$ has a temperature dependence that is weak compared to exponential dependence. Because $N_a \gg N_m$ and $D \gg T$, we have $\partial N_m / \partial T = (D/T^2) N_m$, and from Eq. (10.21) it follows that

$$\kappa_i = \left(\frac{D}{T} \right)^2 D_m N_m, \quad (10.22)$$

where D_m is the diffusion coefficient of molecules in an atomic gas. Comparing this expression with the thermal conductivity coefficient (10.18) due to translational heat transport, we have

$$\frac{\kappa_i}{\kappa_t} \sim \left(\frac{D}{T} \right)^2 \frac{N_m}{N_a}. \quad (10.23)$$

In the regime we have been treating, we have the inequality $N_a \gg N_m$, while $D \gg T$. Therefore the ratio (10.23) can be about unity for low concentrations of molecules in the gas. Note that these results are valid if the dissociation equilibrium in the gas is reestablished over distances sufficiently short that only small variations in the temperature take place.

10.7 THERMAL CAPACITY OF MOLECULES

Equation (10.19) for heat transfer allows us to obtain expressions for thermal capacities. This equation refers to a gas contained within a fixed volume. If the process proceeds in a small part of a large volume of gas, it is necessary

to replace the thermal capacity at constant volume, c_V, in Eq. (10.19) by the thermal capacity at constant pressure, c_p. It is convenient to rewrite equation (10.19) in the form

$$\frac{\partial T}{\partial t} + \mathbf{w} \cdot \nabla T = \chi \Delta T, \tag{10.24}$$

where $\chi = \kappa/(c_V N)$ is the thermal diffusivity coefficient.

To find the connection between the thermal capacities c_V and c_p, let the temperature of an element of gas containing n molecules vary by dT. Then the energy variation of this gas element is $dE = nc_p\, dT$. This energy change can also be stated as $dE = nc_V\, dT + p\, dV$, where p is the gas pressure and V is the volume. The equation of state (9.14), $p = Tn/V$, allows us to rewrite the second energy-change relation as $dE = nc_V\, dT + n\, dT$. Comparing the two expressions for dE yields the result

$$c_p = c_V + 1. \tag{10.25}$$

The thermal capacity c_V of a molecule can be written as the sum of terms due to different degrees of freedom, so that

$$c_V = c_{\text{tr}} + c_{\text{rot}} + c_{\text{vib}}, \tag{10.26}$$

where the thermal capacities c_{tr}, c_{rot}, and c_{vib} correspond to translational, rotational, and vibrational degrees of freedom. Because the mean kinetic energy of particles in thermal equilibrium is $3T/2$, we have $c_{\text{tr}} = \frac{3}{2}$. According to Eq. (2.13), the mean excitation energy of rotational states is T for a diatomic molecule. This yields $c_{\text{rot}} = 1$ for $B \gg T$ (B is the rotational constant) for a diatomic molecule. In the case of polyatomic molecules, there are three rotational degrees of freedom instead of two for a diatomic molecule. Hence, the rotational thermal capacity of polyatomic molecules is $\frac{3}{2}$ if the thermal energy is much greater than a rotational excitation energy. This condition is satisfied at room temperature for rotational degrees of freedom of most molecules, but can be violated for the vibrational degrees of freedom. Therefore, we determine the vibrational thermal capacity by any available relation between the excitation energy for the first vibrational level and a thermal energy of the molecule.

Using the expression

$$\varepsilon_{\text{vib}} = \frac{\hbar\omega}{2} + \frac{\hbar\omega}{\exp(\hbar\omega/T) - 1}$$

for the average excitation energy of the harmonic oscillator, where ω is the frequency of the oscillator, we find that the vibrational thermal capacity corresponding to a given vibration is

$$c_{\text{vib}} = \frac{\partial \varepsilon_{\text{vib}}}{\partial T} = \left(\frac{\hbar\omega}{T}\right)^2 \frac{\exp(-\hbar\omega/T)}{[1 - \exp(-\hbar\omega/T)]^2}. \tag{10.27}$$

This expression yields $c_{vib} = 1$ in the classical limit $\hbar\omega \ll T$. For the opposite limit $\hbar\omega \gg T$, the vibrational thermal capacity is exponentially small.

The above analysis yields

$$c_V = \tfrac{3}{2} + n_{rot}/2 + c_{vib} \tag{10.28}$$

for the thermal capacity of a molecule, where n_{rot} is the number of rotational degrees of freedom of the molecules, and the vibrational thermal capacity is a sum of individual vibrations for which Eq. (10.27) can be used. Note that the analysis uses the assumption of thermodynamic equilibrium among different degrees of freedom.

10.8 MOMENTUM TRANSPORT

Transport of momentum takes place in a moving gas such that the mean velocity of the gas particles varies in the direction perpendicular to the mean velocity. Particle transport then leads to an exchange of particle momenta between gas elements with different average velocities. This creates a frictional force that slows those gas elements with a higher velocity and accelerates those having smaller velocities. We can estimate the value of the viscosity coefficient by analogy with the procedures employed for diffusion and thermal conductivity coefficients. The force acting per unit area as a result of the momentum transport is $F \sim \upsilon m \Delta w_x$, where $N\upsilon$ is the particle flux, and $m \Delta w_x$ is the difference of the mean momentum carried by particles moving in opposite directions at a given point. Since particles reaching this point without collision are located at distances from it of the order of the mean free path λ, we have $m \Delta w \sim m\lambda \, \partial w_x/\partial z$. Hence the force acting per unit area is $F \sim N\upsilon m\lambda \, \partial w_x/\partial z$. Comparing this with Eq. (10.5), and using $(T/m)^{1/2}$ instead of υ and $(N\sigma)^{-1}$ instead of λ, we obtain the estimate

$$\eta \sim \frac{\sqrt{mT}}{\sigma} \tag{10.29}$$

for the viscosity coefficient η. The viscosity coefficient is found to be independent of the particle number density. As was true for the thermal conductivity coefficient, this independence comes from the compensation of opposite effects occurring with the momentum transport. The number of momentum carriers is proportional to the number density of atoms, while a typical transport distance is inversely proportional to it. The effects offset each other.

10.9 THE NAVIER–STOKES EQUATION

We now derive the equation for momentum transport in a viscous gas based on Eq. (9.8). The expression for the pressure tensor must take the gas viscosity into account. From Eq. (10.5), the term due to gas viscosity has the

form $P'_{xz} = -\eta\,\partial w_x/\partial z$. Using the conventions adopted above, the only nonzero component of the mean velocity is directed along the x-axis, and the mean velocity varies in the z-direction.

Because the pressure tensor is symmetrical, a general expression for it takes the form

$$P'_{\alpha\beta} = -\eta\left[\frac{\partial w_\alpha}{\partial x_\beta} + \frac{\partial w_\beta}{\partial x_\alpha} + a\delta_{\alpha\beta}\frac{\partial w_\alpha}{\partial x_\beta}\right]. \tag{10.30}$$

The summation convention is assumed here, in which a repeated subscript in any given term is to be summed over all values of that subscript. The factor a can be found as follows. The forces of viscous friction in a gas are due to the fact that neighboring gas layers move with different velocities. If the gas could be decelerated as a whole, this friction mechanism would have no effect and the force due to the gas viscosity would vanish. Hence, the trace of the pressure tensor is zero. This yields $a = -\frac{2}{3}$, and the viscosity term in the pressure tensor can be written in the form

$$P'_{\alpha\beta} = -\eta\left[\frac{\partial w_\alpha}{\partial x_\beta} + \frac{\partial w_\beta}{\partial x_\alpha} - \frac{2}{3}\delta_{\alpha\beta}\frac{\partial w_\alpha}{\partial x_\beta}\right]. \tag{10.31}$$

With the viscosity part of the pressure tensor taken into account, Eq. (9.8) takes the form

$$\frac{\partial \mathbf{w}}{\partial t} + (\mathbf{w}\cdot\nabla)\mathbf{w} = -\frac{\nabla p}{\rho} + \frac{\eta}{\rho}\Delta\mathbf{w} + \frac{\eta}{3\rho}\nabla\mathbf{w} + \frac{\mathbf{F}}{m}. \tag{10.32}$$

This equation describes momentum transport, and is called the *Navier–Stokes equation.*

To determine the force acting on a spherical particle of radius R moving in a gas with a velocity w, we assume that the particle radius is large compared to the mean free path, $R \gg \lambda$, and that the velocity w is not very high, so that the resistive force arises from viscosity effects. The total resistive force is proportional to the particle area, so Eq. (10.5) gives $F \sim \eta R w$. A more precise determination of the numerical coefficient gives the relation

$$F = 6\pi\eta R w \tag{10.33}$$

for the force. This expression is known as the *Stokes formula.*

10.10 THERMAL DIFFUSION OF ELECTRONS

We have examined the principal transport phenomena in gases and plasmas that are caused by gradients of concentration, temperature, and mean flow velocity and by an external electric field. In addition to the fluxes we have

already considered, these same gradients and fields can create cross-fluxes. Below we consider the simplest of these transport phenomena, namely, the electron flux due to a gradient of the electron temperature. This flux is

$$\mathbf{j} = -D_{\mathrm{T}} \nabla \ln T_e, \tag{10.34}$$

with this expression serving to define the *thermodiffusion coefficient* D_{T}. We shall calculate this coefficient with the condition that the electron number density should be sufficiently high [condition (9.40)] to allow us to introduce the electron temperature T_e.

The Boltzmann kinetic equation for electrons in this case has the form

$$\mathbf{v} \cdot \nabla f = I_{ea}(f). \tag{10.35}$$

The temperature gradient leads to a nonsymmetric part of the electron distribution function, which can be written in the form of Eq. (9.23), that is to say

$$f = f_0(v) + v_x f_1(v),$$

where $f_0(v)$ is the Maxwell distribution function for the electrons, and the x-axis is directed along the temperature gradient. Substituting this in Eq. (10.35), and using Eq. (9.25) for the collision integral for the nonsymmetric part of the distribution function, we obtain

$$v_x \frac{\partial f_0}{\partial x} = -\nu v_x f_1, \tag{10.36}$$

where ν is the frequency of electron–atom elastic collisions.

We now calculate the electron flux created by the nonsymmetric part of the distribution function. Using the fact that the flux is directed along the x-axis, we have

$$j_x = \int v_x f_x \, d\mathbf{v} = \int v_x^2 f_1 \, d\mathbf{v} = -\frac{1}{3} \int \frac{v^2}{\nu} \frac{\partial f_0}{\partial x} \, d\mathbf{v} = -\frac{d}{dx}\left(N_e \left\langle \frac{v^2}{3\nu} \right\rangle \right),$$

where the angle brackets mean averaging over electron velocities. Since the x-dependence is contained in the electron temperature, we obtain

$$j_x = -\nabla T_e \frac{d}{dT_e}\left(N_e \left\langle \frac{v^2}{3\nu} \right\rangle \right).$$

Comparing this with Eq. (10.35), we find the expression for the thermodiffusion coefficient to be

$$D_{\mathrm{T}} = T_e \frac{d}{dT_e}\left(N_e \left\langle \frac{v^2}{3\nu} \right\rangle \right) = T_e \frac{d}{dT_e}(N_e D), \tag{10.37}$$

where D is the electron diffusion coefficient given in Eq. (10.13).

Since the electron pressure $p_e = N_e T_e$ is constant, this expression can be written as

$$D_T = N_e T_e^2 \frac{d}{dT_e}\left(\frac{D}{T_e}\right). \tag{10.38}$$

In particular, if $\nu = \text{const}$, this equation gives $D_T = 0$. Using the dependence $\nu \sim v^n$, we obtain

$$D_T = -nN_e D. \tag{10.39}$$

This means that the direction of the electron flux with respect to the temperature gradient depends on the sign of n.

10.11 ELECTRON THERMAL CONDUCTIVITY

Because of the small mass of electrons, their transport can give an important contribution to the thermal conductivity of a weakly ionized gas. We shall calculate the thermal conductivity coefficient of the electrons. For this purpose we represent the electron distribution function as

$$f = f_0(v) + (\mathbf{v} \cdot \nabla \ln T_e) f_1(v), \tag{10.40}$$

and the kinetic equation (10.35) has the form

$$f_0\left(\frac{m_e v^2}{2T_e} - \frac{5}{2}\right)\mathbf{v} \cdot \nabla T_e = I_{ea}(f).$$

Here we take into account that the x-dependence of the electron distribution function is due to T_e, and that the electron pressure $p_e = N_e T_e$ is constant in space. From this, and from $I_{ea}(v_x f_1) = -\nu v_x f_1$ obtained from Eq. (9.35), we find

$$f_1 = -\frac{f_0}{\nu}\left(\frac{m_e v^2}{2T_e} - \frac{5}{2}\right)$$

for the nonsymmetric part of the distribution function.

The electron heat flux is

$$\mathbf{q}_e = \int \frac{m_e v^2}{2} v_x f d\mathbf{v} = \int \frac{m_e v^2}{2} v_x^2 \nabla \ln T_e f_1 \, d\mathbf{v}.$$

Introducing the thermal conductivity coefficient of electrons by the relation

$$\mathbf{q}_e = -\kappa_e \nabla T_e, \tag{10.41}$$

we obtain

$$\kappa_e = N_e \left\langle \frac{v^2}{3\nu} \frac{m_e v^2}{2T_e} \left(\frac{m_e v^2}{2T_e} - \frac{5}{2} \right) \right\rangle, \tag{10.42}$$

where the angle brackets mean averaging over the electron distribution function.

Assuming $\nu \sim v^n$, that is, taking $\nu(v) = \nu_0 z^{n/2}$, where $z = m_e v^2/(2T_e)$, Eq. (10.42) gives

$$\kappa_e = \frac{4}{3\sqrt{\pi}} \frac{T_e N_e}{\nu_0 m_e} \left(1 - \frac{n}{2}\right) \Gamma\left(\frac{7-n}{2}\right). \tag{10.43}$$

In particular, if $\nu = \text{const}$, the result is

$$\kappa_e = \frac{5T_e N_e}{2\nu_0 m_e}. \tag{10.43a}$$

If $n = 1$, that is, if $\nu = v/\lambda$ (where λ is the mean free path), we are led to

$$\kappa_e = \frac{2}{3\sqrt{\pi}} N_e \lambda \sqrt{\frac{2T_e}{m_e}}. \tag{10.43b}$$

To determine the contribution of the electron thermal conductivity to the total thermal conductivity coefficient, it is necessary to connect the gradients of the electron and atomic temperatures T_e and T. We can explore this problem in the case when the increase of the electron temperature is determined by an external electric field, and the connection between the electron and atomic temperatures is given by Eq. (9.44). If $\nu \sim v^n$, this formula gives

$$\nabla T_e = \frac{\nabla T}{1 + n - nT/T_e}. \tag{10.44}$$

When we have the strong inequality $T_e \gg T$, then the total thermal conductivity coefficient is

$$\kappa = \kappa_a + \kappa_e \frac{\nabla T_e}{\nabla T} = \kappa_a + \frac{\kappa_e}{1+n}, \tag{10.45}$$

where κ_a is the thermal conductivity coefficient of the atomic gas. Using the estimate (10.18) for the atom thermal conductivity coefficient, one can see that the electron thermal conductivity can give a significant contribution to the total value because of the small mass of the electron and the high

electron temperature. We assume that the condition opposite to that expressed in Eq. (9.40) allows us to introduce the electron temperature.

The peculiarity of the electron thermal conductivity is that cross fluxes can be essential in this case. We consider the electron thermal conductivity of a weakly ionized gas in an external electric field. Then the fluxes are

$$\begin{aligned} \mathbf{j} &= N_e K \mathbf{E} - D_T \nabla \ln T_e, \\ \mathbf{q} &= -\kappa_e \nabla T_e + \alpha e \mathbf{E}. \end{aligned} \tag{10.46}$$

We treat the case where displacement of the electrons as a whole does not violate plasma quasineutrality. This corresponds to plasma regions far from electrodes and walls. Then the mobility K in Eq. (10.46) is the electron mobility, and one can neglect ion mobility including the ambipolar diffusion. The expression for the electron thermodiffusion coefficient is given by Eq. (10.39), and Eq. (10.46) gives the thermal conductivity coefficient. Next we determine the coefficient α by the standard approach of expanding Eq. (9.23) for the electron distribution function.Then Eq. (9.23) yields $f_1 = eEf_0/(\nu T_e)$, and the coefficient α is

$$\alpha = \frac{m_e N_e}{6T_e} \left\langle \frac{v^4}{\nu} \right\rangle = \frac{4T_e N_e}{3\sqrt{\pi} m_e \nu_0} \Gamma\left(\frac{7}{2} - \frac{n}{2}\right),$$

where we take

$$\nu = \nu_0 \left(\frac{v}{\sqrt{2T_e/m_e}} \right)^n.$$

For $n = 0$ this gives

$$\alpha = \frac{5T_e N_e}{2m_e \nu}, \tag{10.47a}$$

and for $n = 1$, when $\nu = v/\lambda$, it gives

$$\alpha = \sqrt{\frac{2T_e}{m_e}} \frac{\lambda}{3\sqrt{\pi}} = \frac{2\lambda N_e}{3v_T}, \tag{10.47b}$$

where $v_T = \sqrt{8T_e/\pi m_e}$ is the mean electron velocity.

The relationships (10.46) together with the corresponding expressions for the kinetic coefficients allow us to determine the electron heat flux under different conditions in the plasma. We now evaluate the effective thermal conductivity coefficient in the direction perpendicular to an external electric field **E**. If the plasma is placed in a metallic enclosure, there is no transverse

electric field, so $E = 0$ and Eq. (10.41) follows from Eq. (10.44). If the walls are dielectric, we have $\mathbf{j} = 0$. This corresponds to the regime of ambipolar diffusion where the electrons travel together with the ions. On the scale considered, this gives $\mathbf{j} = 0$, meaning that an electric field of strength $\mathbf{E} = D_T \nabla \ln T_e/(N_e K)$ arises. We represent the heat flux in the form

$$\mathbf{q} = -C\kappa_e \nabla T_e, \tag{10.48}$$

where the coefficient is $C = 1 - \alpha D_T e/(\kappa_e T_e N_e K)$. Using Eq. (10.39) for the electron thermodiffusion coefficient and the Einstein relation (10.15), we obtain $C = 1 + \alpha n/\kappa_e$.

On the basis of Eqs. (10.43), (10.47), and (10.48), we have

$$C = \frac{1 + n/2}{1 - n/2}. \tag{10.49}$$

This shows that the effective thermal conductivity coefficient for electrons in the case of both metallic and dielectric walls depends on n. For $n = 0$ its value is the same in both cases. For $n = 1$ it is greater by a factor of 3 in the second case as compared to the first.

CHAPTER 11

CHARGED-PARTICLE TRANSPORT IN GASES

11.1 MOBILITY OF CHARGED PARTICLES

The mobility K of a charged particle is defined as the ratio of its drift velocity w to the electric field strength E, or

$$K = w/E. \tag{11.1}$$

This differs from the definition of the mobility b of a neutral particle [Eq. (10.14)], which is the ratio of the drift velocity to the force acting on the particle from an external field. For electrons and singly charged ions we have

$$b = K/e. \tag{11.2}$$

Correspondingly, the Einstein relation (10.15) has the form

$$K = eD/T \tag{11.3}$$

for charged particles, where D is the diffusion coefficient. Using the estimate (10.6) for the particle diffusion coefficient, we obtain the estimate

$$K \sim e(\mu T)^{-1/2}(N\sigma)^{-1} \tag{11.4}$$

for the mobility of charged particles, where μ is the reduced mass of the charged and gas particles, and σ is their elastic collision cross section.

11.2 MOBILITY OF IONS IN A FOREIGN GAS

Equation (11.4) leads to an estimate for the mobility of ions. If the ions and gas atoms are not of the same species, ion–atom scattering is determined principally by the polarization interaction between them, and their scattering cross section is close to that of polarization capture. From Eqs. (4.13), (9.22), and (11.1) we obtain

$$K = (2\pi N)^{-1}(\beta\mu)^{-1/2} \tag{11.5}$$

for the ion mobility, where β is the polarizability of the atom, and N is the number density of the gas atoms. Elastic scattering in ion–atom collisions exceeds the effective capture cross section by about 10%. Hence, the mobility in the polarization ion–atom interaction is about 10% less than is given in Eq. (11.5).

The ion drift velocity is proportional to the electric field strength E for small fields, as given in Eq. (11.1). If the ion and atom masses are similar in magnitude, the condition that the electric field strength is small has the form

$$eE\lambda \ll T, \tag{11.6}$$

where λ is the mean free path of ions. This condition implies that the energy that the ion takes from the electric field between subsequent collisions is small compared to its thermal energy. As a result, the ion drift velocity is small compared to a typical ion thermal velocity in this case.

If the condition (11.6) is satisfied, the ion distribution function is almost Maxwellian, and therefore can be written in the form

$$f(\mathbf{v}) = \varphi(v)[1 + v_x\psi(v)], \tag{11.7}$$

where $\varphi(v)$ is the Maxwell distribution function of the ion, the electric field is along the x-axis, and the function $\psi(v)$ can be determined by solving the ion's kinetic equation.

We use the approximation that ψ is independent of the ion velocity. Then the parameter ψ can be determined by the integral relation (9.21) for the ion distribution function, and furthermore Eq. (11.7) yields the ion drift velocity as $w = \psi\langle v^2\rangle/3 = \psi T/m$, where m is the ion mass. The above approximation is called the *first Chapman-Enskog approximation.* It yields

$$K_1 = \frac{3e\sqrt{\pi}}{8N\bar{\sigma}\sqrt{2T\mu}} \tag{11.8}$$

for the ion mobility, where μ is the reduced mass of the ion–atom system, and the mean cross section $\bar{\sigma}$ corresponds to an average of the diffusion cross section $\sigma^*(v)$ of the ion–atom scattering, with the averaging done over

the Maxwellian ion velocity distribution. This average has the form

$$\bar{\sigma}(T) = \frac{1}{2}\int_0^\infty \sigma^*(x) e^{-x} x^2\, dx, \qquad x = \frac{\mu g^2}{2T}, \tag{11.9}$$

where g is the relative velocity of the ion–atom collision.

The Chapman–Enskog approximation is a general method for calculating the kinetic coefficients. It is based on an expansion in powers of the reduced velocity for the correction to the Maxwell distribution function, if this correction is induced by small field gradients in an equilibrium gas. Even the first Chapman–Enskog approximation is cumbersome, so we did not use this method for the earlier analysis of transport phenomena; but in the present case of ion transport, this approximation simplifies due to the integral relation (9.21). By employing the Einstein relation (11.3), one can find from Eq. (11.8) the ion diffusion coefficient, and this can also be applied to atoms in the limiting case $e \to 0$. Thus, we have the expression

$$D_1 = \frac{3\sqrt{\pi T}}{8N\bar{\sigma}\sqrt{2\mu}} \tag{11.10}$$

for the diffusion coefficient for both neutral and charged atoms in the first Chapman–Enskog approximation, where the average cross section $\bar{\sigma}$ is given by Eq. (11.9).

11.3 MOBILITY OF IONS IN THE PARENT GAS

Resonant charge exchange is described by the scheme

$$A + A^+ \rightarrow A^+ + A. \tag{11.11}$$

This process is of importance for movement of ions within an atomic gas of the same species. At thermal energies, the cross section for the ion–atom resonant charge transfer is several times larger than a gas-kinetic cross section (see Appendices 6 and 9). The cross section for resonant charge exchange is insensitive to increase of the ion energy, while the cross section for elastic scattering declines strongly with an increase of the ion energy. Hence, for subthermal ion energies, one can ignore elastic ion–atom scattering compared to charge exchange. Figure 11.1 illustrates the exchange character of ion scattering in the parent gas. Ion motion of this type due to resonant change exchange is called the *Sena effect*. The scattering results in a transfer of charge from one atomic core to the other, and hence the charge exchange cross section characterizes the ion mobility. As seen in the center-of-mass frame, this process leads to effective ion scattering by the angle

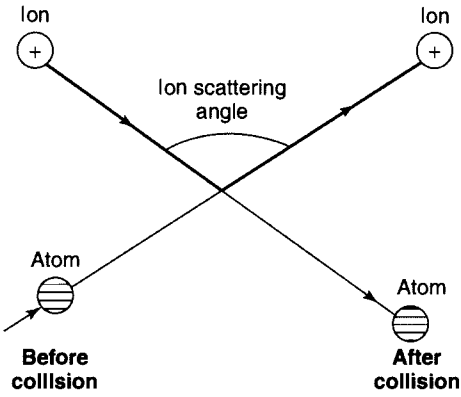

Figure 11.1 Illustration of the resonant charge exchange of an ion and atom without elastic scattering (Sena effect).

$\vartheta = \pi$. Correspondingly, the diffusion cross section is

$$\sigma^* = \int (1 - \cos\vartheta)\, d\sigma = 2\sigma_{\text{res}}, \tag{11.12}$$

where σ_{res} is the cross section of the resonant charge-exchange process. Then, assuming σ_{res} to be independent of the collision velocity, Eq. (11.8) gives

$$K_1 = \frac{3e\sqrt{\pi}}{16N\sigma_{\text{res}}\sqrt{Tm}}, \tag{11.13}$$

where m stands for the mass of either the ion or the atom.

With large electric fields, the condition (11.6) is reversed. In this case the ion drift velocity is much greater than its thermal velocity, and because of the absence of elastic scattering, ion velocities in the field direction are much larger than in other directions. The sequence of events in a strong electric field is that the ion accelerates under the action of the field, stops as a result of the charge exchange, and then repeats this process.

The probability $P(t)$ that the ion does not participate in charge exchange during time t after the last exchange event satisfies the equation

$$\frac{dP}{dt} = -\nu P. \tag{11.14}$$

where $\nu = Nv_x\sigma_{\text{res}}$. Its solution is $P(t) = \exp(-\int_0^t \nu dt')$. The equation of motion for the ion, $mdv_x/dt = eE$, relates the ion velocity to the time after the last collision by the expression $v_x = eEt/m$, so that $P(t)$ is the velocity distribution function for the ions. Assuming the cross section of the resonant charge transfer process σ_{res} to be independent of the collision velocity, the

distribution function is

$$f(v_x) = C \exp\left(-\frac{mv_x^2}{2eE\lambda}\right), \qquad v_x > 0, \tag{11.15}$$

where C is a normalization factor, and the mean free path is $\lambda = 1/(N\sigma_{\text{res}})$. The ion drift velocity and the mean ion energy are

$$w = \langle v_x \rangle = \sqrt{\frac{2eE\lambda}{\pi m}},$$
$$\bar{\varepsilon} = \left\langle \frac{mv_x^2}{2} \right\rangle = \frac{eE\lambda}{2}. \tag{11.16}$$

These results are valid under the condition that

$$eE\lambda \gg T, \tag{11.17}$$

which is opposite to that of Eq. (11.6). It can be seen that the ion drift velocity is much greater than its thermal velocity, and the average ion energy is large compared to the thermal energy T. Furthermore, if the ion mobility is defined by Eq. (11.1), it depends on the electric field strength as $E^{-1/2}$.

11.4 ENERGETIC TOWNSEND COEFFICIENT

When electrons travel in a gas in external fields, their velocity distribution function is nearly spherically symmetric because of the nature of scattering of a light particle by a heavy one. The electron distribution function for a constant electric field was found in Chapter 9, and according to Eqs. (9.23) and (9.33) it has the form

$$f(\mathbf{v}) = f_0(v) - \frac{eE}{m_e \nu} \frac{v_x}{v} \frac{df_0}{dv}.$$

This gives the electron drift velocity

$$w_e = \langle v_x \rangle = -\frac{eE}{m_e} \int_0^\infty \frac{v_x^2}{v\nu} \frac{df_0}{dv} 4\pi v^2 \, dv = \frac{eE}{3m_e} \left\langle \frac{1}{v^2} \frac{d}{dv}\left(\frac{v^3}{\nu}\right) \right\rangle. \tag{11.18}$$

Here the angle brackets mean averaging over the spherical electron velocity distribution function. In particular, if the collision frequency ν does not depend on the collision velocity, Eq. (11.18) gives

$$w_e = \frac{eE}{m_e \nu}. \tag{11.19}$$

In the course of electron motion in a gas, the electron energy can vary over a wide range after many collisions, during which an electron changes its

direction of motion many times. The electron motion at a given moment, when the electron velocity is v, is characterized by the diffusion coefficient $D = v^2/(3\nu)$ and the drift velocity

$$w_e = \frac{eE}{3m_e v^2} \frac{d}{dv}\left(\frac{v^3}{\nu}\right).$$

We introduce the energetic Townsend coefficient as

$$\eta = \frac{eED_\perp}{Tw} = \frac{eD_\perp}{TK}, \tag{11.20}$$

where $D_\perp$ is the transverse diffusion coefficient of electrons, and K is their mobility. For thermal electrons with a Maxwellian distribution, Eq. (11.20) gives $\eta = 1$ on the basis of the Einstein relation (10.14). If we introduce the electron temperature, so that we have the Maxwell energy distribution with the electron temperature T_e, it follows from Eq. (11.20) that

$$\eta = \frac{T_e}{T}.$$

Thus, the *energetic Townsend coefficient* that can be constructed from measuring electron parameters characterizes the average electron energy.

The general expression for the energetic Townsend coefficient (11.20), as it follows from Eqs. (10.13) and (11.18), has the form

$$\eta = \left\langle \frac{m_e v^2}{\nu} \right\rangle \left(T \left\langle \frac{1}{v^2} \frac{d}{dv} \frac{v^2}{\nu} \right\rangle \right)^{-1}. \tag{11.21}$$

If the electron–atom collision frequency ν is independent of the electron velocity, this equation gives

$$\eta = \left\langle \frac{m_e v^2}{3T} \right\rangle. \tag{11.22}$$

In this case the energetic Townsend coefficient is the ratio of the mean electron energy to the mean energy of the atom. Such a relation holds both for the case $\nu = \text{const}$ and for the Maxwell distribution function of electrons. If the electron distribution function is determined by electron–atom collisions and is given by Eq. (9.34), then Eq. (11.20) has the form

$$\eta = \frac{\langle v^2/\nu \rangle}{\langle v^2/\nu(1 + Mu^2/3T) \rangle},$$

where $u = eE/(m_e\nu)$. In particular, if the electric field is strong and the electron–atom cross section does not depend on the electron velocity ($\nu \sim v$), it follows from Eq. (11.22) that

$$\eta = 1.14\left\langle \frac{m_e v^2}{3T} \right\rangle.$$

This demonstrates the extent to which the energetic Townsend coefficient is the ratio between the average electron and atom energies. Thus, the energetic Townsend coefficient is a convenient parameter characterizing the mean electron energy with respect to that of the atom.

11.5 CONDUCTIVITY OF A WEAKLY IONIZED GAS

The gas conductivity Σ is defined as the proportionality factor between the electric current density and the electric field strength $\mathbf{E}$ in Ohm's law $\mathbf{j} = \Sigma\mathbf{E}$. The electric current is a sum of two components: the current due to the electrons, and that due to the ions. The total current is thus

$$\mathbf{j} = -eN_e\mathbf{w}_e + eN_i\mathbf{w}_i, \tag{11.23}$$

where N_e and N_i are the electron and ion number densities, and $\mathbf{w}_e$ and $\mathbf{w}_i$ are the electron and ion drift velocities. Expressing the drift velocity of a charged particle through its mobility by Eq. (11.1), the conductivity of a quasineutral ionized gas is

$$\Sigma = e(K_e + K_i), \tag{11.24}$$

where K_e and K_i are the electron and ion mobilities. Using the estimate (11.4) for the mobility of a charged particle, one can see that electrons give the primary contribution to the gas conductivity. Furthermore, Eqs. (11.4) and (11.24) yield the estimate

$$\Sigma \sim N_e e^2 (m_e T_e)^{-1/2} (N\sigma_{ea})^{-1}, \tag{11.25}$$

for the gas conductivity, where σ_{ea} is a typical electron–atom scattering cross section.

10.6 CONDUCTIVITY OF A STRONGLY IONIZED PLASMA

The conductivity of a weakly ionized gas is governed by electron–atom collisions, while in a strongly ionized plasma electron–ion collisions predominate over electron–atom collisions. Note that electron–electron collisions do not change the total electron momentum and have no influence on the

plasma conductivity. The electron–ion elastic scattering cross section is much larger than the electron–atom cross section, and so the term "strongly ionized plasma" can refer to a plasma with only slight ionization, but with a conductivity much larger than that of a weakly ionized plasma.

The drift velocity of the electrons is given by Eq. (11.18). Then Eq. (11.24) leads to the plasma conductivity

$$\Sigma = \frac{N_e e^2}{3m_e}\left\langle \frac{1}{v^2}\frac{d}{dv}\left(\frac{v^3}{\nu}\right)\right\rangle, \tag{11.26}$$

where $\nu = N_i v\sigma^*$, and the averaging is done over the electron distribution function. Because of the plasma's quasineutrality ($N_e = N_i$), its conductivity does not depend on the electron number density. The diffusion cross section for the Coulomb interaction between a colliding electron and ion is given by Eq. (5.5), which has the form $\sigma^* = (\pi e^4 \ln\Lambda)/\varepsilon^2$, where ε is the electron energy, the Coulomb logarithm is $\ln\Lambda = \ln[e^2/(r_D T)]$, and r_D is the Debye–Hückel radius. Using the Maxwell distribution function for the electrons, the expression we finally obtain for the plasma conductivity is

$$\Sigma = \frac{2^{5/2} T_e^{3/2}}{\pi^{3/2} m_e^{1/2} e^2 \ln\Lambda}. \tag{11.27}$$

This is known as the *Spitzer formula*.

11.7 AMBIPOLAR DIFFUSION

Violation of plasma quasineutrality creates strong electric fields within the plasma. The fields between electrons and ions are associated with attractive forces, tending to move them together. We consider a special regime of plasma expansion in a gas wherein the electrons, being much lighter than the ions, have a larger diffusion coefficient and move with higher velocity than the ions. But separation of electrons and ions in a gas creates an electric field that slows the electrons and accelerates the ions. This establishes a self-consistent regime of plasma motion called *ambipolar diffusion*. We shall examine this regime and establish the conditions necessary to achieve it.

To describe this regime of plasma evolution, we use expressions for the electron flux $\mathbf{j}_e$ and ion flux $\mathbf{j}_i$ flux given by

$$\begin{aligned} \mathbf{j}_e &= -D_e \nabla N_e - K_e E N_e, \\ \mathbf{j}_i &= -D_i \nabla N_i + K_i E N_i, \end{aligned} \tag{11.28}$$

where N_e and N_i are the number densities of electrons and ions respectively, D_e and D_i are their diffusion coefficients, and K_e and K_i are their mobilities. Because the electric field acts on electrons and ions in opposite directions, the field enters into the flux expressions with different signs. The

electric field strength $\mathbf{E}$ is determined by Poisson's equation

$$\operatorname{div}\mathbf{E} = 4\pi e(N_i - N_e). \tag{11.29}$$

Since a plasma converges to quasineutrality during evolution, the charge difference is small: $\Delta N = |N_i - N_e| \ll N_e$. This gives $N_e \approx N_i \approx N$. Because the plasma motion is self-consistent, we have $\mathbf{j}_e \approx \mathbf{j}_i$. Next, according to Eqs. (10.6) and (11.4) the kinetic coefficients of electrons are large compared to those of ions. In order to satisfy to all these conditions, it is necessary to require that the electron flux is zero ($j_e = 0$) on the scale of electron quantities. We recall the equality $j_e \approx j_i$, but $D_e\nabla N_e \gg j_i$ and $eEK_eN_e \gg j_i$, so in terms of the magnitudes of electron parameters, we conclude again that $\mathbf{j}_e = 0$. From this it follows that

$$\mathbf{E} = -\frac{D_e}{eK_e}\frac{\nabla N}{N}, \tag{11.30}$$

and we find the flux of charged particles to be

$$\mathbf{j} = \mathbf{j}_i = -\left(D_i + D_e\frac{K_i}{K_e}\right)\nabla N = -D_a\nabla N,$$

where D_a is the *coefficient of ambipolar diffusion*. Thus the plasma evolution has a diffusive character with a self-consistent diffusion coefficient. In particular, when electrons and ions exhibit the Maxwell velocity distribution, we obtain

$$D_a = D_i\left(1 + \frac{T_e}{T_i}\right) \tag{11.31}$$

with the help of the Einstein relation (11.3). In the regime we have been examining, we find that a plasma expands with the speed of the ions rather than that of the electrons.

We can state the condition necessary to be in this regime, taking into account the quasineutrality of an expanding plasma, that is, when $\Delta N = |N_i - N_e| \ll N$ holds true. From Eq. (11.29) we have $\Delta N \sim E/(4\pi eL)$, where L is a typical dimension of the plasma. Equation (11.30) together with the Einstein relation (11.3) give $E \sim T/(e^2L)$, where for simplicity we assume the electron and ion temperatures to be equal. Thus we have $\Delta N \sim Nr_D^2/L^2$. From this it follows that the criterion for the presence of the ambipolar diffusion regime is the same as the plasma definition (3.8): $L \gg r_D$.

11.8 ELECTROPHORESIS

A weakly ionized gas can be used to achieve the separation of isotopes and elements in a mixture of gases, by making use of the different currents for different types of charged atomic particles. As such an example, we consider electrophoresis in a gas-discharge plasma. This phenomenon corresponds to a partial separation of the components of the system. Suppose a gas in a cylindrical tube consists of two components: a buffer gas (for example, helium), and an admixture of easily ionized atoms (for example, mercury, cadmium, zinc). The admixture atoms will give rise to an ionic component because of the small ionization potentials. The number densities of the components satisfy the inequalities

$$N \gg N_a \gg N_i,$$

where N is the number density of the atoms of the buffer gas, N_a is the number density of admixture atoms, and N_i is the number density of ions.

Because the ion current arises from the admixture ions, we have the balance equation

$$-D\frac{dN_a}{dx} + wN_i = 0,$$

for the admixture, where D is the diffusion coefficient of the admixture atoms in the buffer gas, w is the ion drift velocity, and the x-axis is directed along the axis of the tube. Assuming the ion diffusion coefficient is such that $D_i \sim D$, and using the Einstein relation (10.15) for a typical size $L = (d \ln N_a/dx)^{-1}$ responsible for the gradient of the admixture number density, we find that

$$L \sim \frac{T}{eEc_i}.$$

In this expression, $c_i = N_i/N_a$ is the degree of ionization of the admixture, T is the temperature of atoms or ions, and E is the electric field strength.

This phenomenon causes a discharge plasma to be nonuniform, and the glowing of this plasma due to radiation from the excited atoms of the admixture is concentrated near the cathode. Electrophoresis is established for a time $\tau \sim L/(c_i w)$ after switching on the discharge. In fact, in a region near the anode, the number density of admixture atoms and ions decreases. An increase of the rate constant of ionization is required, so that the electric field strength in this region must be increased. Thus, electrophoresis can change the parameters of a gas discharge.

11.9 RECOMBINATION OF IONS IN DENSE GASES

The recombination of positive and negative ions in a dense gas is a three-body process that satisfies a condition opposite to that of Eq. (5.21). Specifically, we require

$$\lambda \ll b, \tag{11.32}$$

where $b = e^2/T$ is the critical radius and λ is the mean free path of ions in a gas. Under such circumstances, frequent collisions of the ions with gas particles prevent them from approaching each other, and thus the typical recombination time significantly exceeds the time required for the ions to approach each other. If the distance between ions is R, each ion is subjected to the field produced by the other ion, and the electric field strength is $E = e/R^2$. This field causes oppositely charged ions to move towards each other with the velocity $w = e(K_+ + K_-)/R^2$, where K_+ and K_- are the mobilities of the positive and negative ions in the gas. This expression is valid if $R \gg \lambda$.

To determine the frequency of decay of the positive ions due to recombination, imagine a sphere of radius R around the positive ion, and compute the number of negative ions entering this sphere per unit time. This is given by the product of the surface area of the sphere, $4\pi R^2$, and the negative ion flux

$$N_- w = N_- e(K_+ + K_-)/R^2.$$

Thus, the balance equation for the number density of positive ions is

$$\frac{dN_+}{dt} = -N_+ N_- 4\pi e(K_+ + K_-).$$

Comparing this with the definition of the recombination coefficient, we find this coefficient to be

$$\alpha = 4\pi e(K_+ + K_-). \tag{11.33}$$

This relation is known as the *Langevin formula*.

The sequence of events in this process is that the ions approach under the action of the Coulomb force, and collide with gas particles in the course of this approach. The criterion (11.32) leads to the condition $eE\lambda \ll T$, where E is the electric field strength acting on one ion due to the other, if the distance between them is of the order of the critical distance b. This means that at distances of ion approach that give the primary contribution to the recombination coefficient, the ions move in a weak electric field. That is, the ion mobilities K_+ and K_- in Eq. (11.33) correspond to small fields consistent with the condition (11.6). Because of Eq. (11.4), the recombination

coefficient of ions at large gas density is inversely proportional to the number density of gas atoms. In fact, an increase of the gas density leads to an increase in the frictional force for ions that slows the approach of the ions.

11.10 GAS-DENSITY DEPENDENCE OF THE IONIC RECOMBINATION COEFFICIENT

In Chapter 5 above and again here, we considered the recombination of positive and negative ions at various gas densities. We can summarize the results graphically. Figure 11.2 shows the qualitative dependence on the gas density of the recombination coefficient for positive and negative ions. For a low gas density (region 1), recombination is due to pairwise collisions of ions, and the recombination coefficient is given by Eq. (5.9). The order-of-magnitude estimate for the recombination coefficient is $\alpha_1 \geq \hbar^2/(m_e^2 \mu T)^{1/2}$, if we set $R_0 \gg a_0$ in Eq. (5.9). Here, m_e is the electron mass, μ is the reduced mass of the ions, and $a_0 = \hbar^2/(m_e e^2)$ is the Bohr radius. Since the recombination coefficient in region 2 is given by Eq. (5.20), we have $\alpha_2 \sim [\mathrm{C}](e^6/T^3)(\beta e^2/\mu)^{1/2}$, where β is the polarizability of the particle C, [C] is its particle number density, and μ is the reduced mass of the ion and the particle C. The gas number density corresponding to transition from region 1 to region 2 is of the order of

$$[\mathrm{C}]_1 \sim a_0 (T/e^2)^{5/2} \beta^{-1/2}.$$

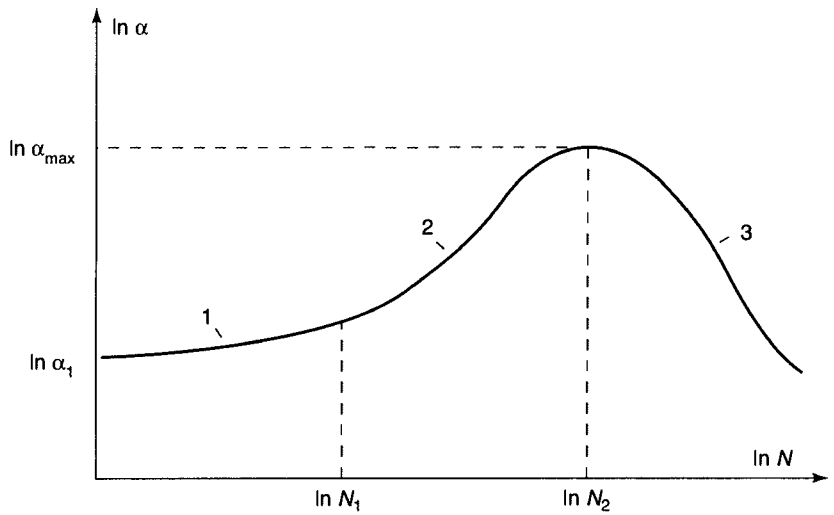

Figure 11.2 The recombination coefficient α of positive and negative ions as a function of gas density, denoted here as N.

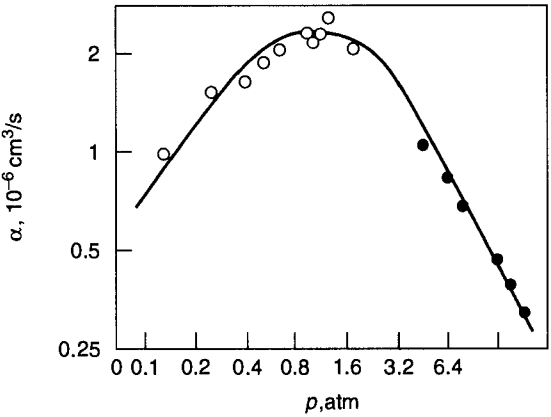

Figure 11.3 The recombination coefficient of positive and negative ions of air as a function of pressure. The curve is an approximation to experimental data that are shown by small circles.

Region 3 in Fig. 11.2 is described by the Langevin theory, and Eqs. (11.4) and (11.33) give the order-of-magnitude estimate $\alpha_3 \sim e/([C]\sqrt{\beta\mu})$ for the recombination coefficient in this region, if we assume that the polarization interaction potential acts between the colliding ion and atom. The transition between regions 2 and 3 is associated with the number density

$$[C]_2 \sim \frac{T^{3/2}}{e^3\sqrt{\beta}}.$$

This number density corresponds to the largest recombination coefficient, $\alpha_{max} \sim e^4\mu^{-1/2}T^{-3/2}$. The relevant physical process is pairwise ion–ion recombination if the cross section corresponds to elastic scattering of particles experiencing the Coulomb interaction. Thus, the maximum recombination coefficient has the same order of magnitude as the elastic rate constant of ions.

Typical values for the quantities indicated in Fig. 11.2 for ions produced in air at room temperature can be cited: $[C]_1 \sim 10^{17}$ cm^{-3}, $[C]_2 \sim 10^{20}$ cm^{-3}, $\alpha_1 \sim 10^{-9}$ cm^3/s, and $\alpha_{max} \sim 10^{-6}$ cm^3/s. Figure 11.3 shows measured rate constants for recombination of positive and negative ions in air as a function of pressure. The maximum of the recombination coefficient can be seen to occur at atmospheric pressure.

CHAPTER 12

SMALL PARTICLES IN PLASMAS

12.1 PLASMAS WITH DISPERSED INCLUSIONS

The presence of particles in a plasma can alter its basic properties. For example, in Chapter 2 we considered ionization equilibrium in a hot vapor, with small metallic particles providing a source of free electrons. Small particles in a plasma carry electric charge and thus influence the electric properties of the plasma. They may act as a collector for electrons and ions, so that the presence of small particles leads to decay of the plasma. In addition, particles emit radiation in a hot vapor and can play a determining role in the optical properties of a plasma. These problems will be considered below.

Different names are used for small particles depending on their size, their type, and the scientific area where they are studied. Small particles in the atmosphere are usually called *aerosols*, a plasma containing small particles is called a plasma with dispersed inclusions, sometimes small particles in a gas are referred to as dust, and so on. In physics, small particles consisting of from tens up to tens of thousands of atoms or molecules are called *clusters*. Clusters are an intermediate state of matter between individual atoms and atoms in bulk (or condensed matter), and their properties can differ from the properties of condensed matter. In particular, even large clusters are characterized by so-called *magic numbers* of atoms, which correspond to extremal values of some parameters as a function of the size of the cluster. In other words, some cluster parameters have local maxima or minima at particular numbers of atoms in the cluster. At these special numbers of atoms, the binding energy of a released atom, the cluster ionization potential, and the

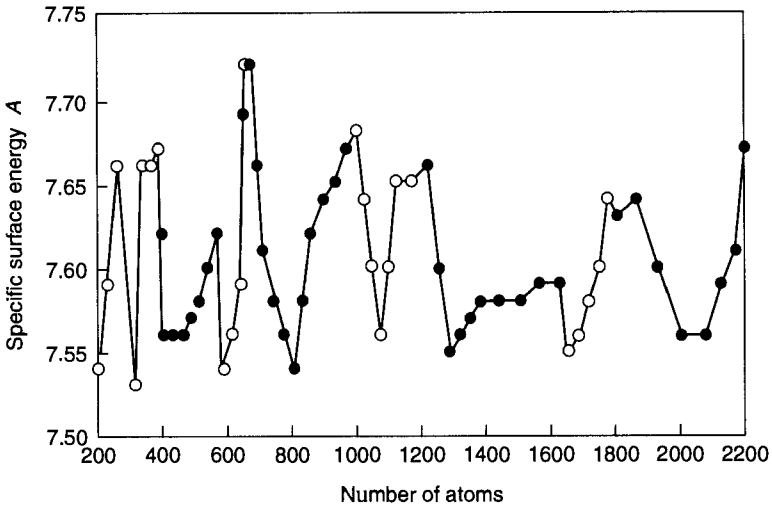

Figure 12.1 The specific surface energy of clusters with pairwise interaction of atoms. Clusters have the face-centered cubic structure, and only nearest-neighbor interactions occur. The specific surface energy is expressed in units of the dissociation energy of the diatomic molecule.

cluster electron affinity are more than for clusters containing one more or one less atom than the magic number.

The existence of magic numbers for clusters shows that clusters have stable structures that correspond to extrema of cluster parameters, and these parameters are nonmonotonic functions of the number of atoms in the cluster. Despite this fact, bulk models of clusters are helpful in understanding their properties. They allow one to describe the dependence of cluster parameters on cluster size in an average sense. For example, the total binding energy E of cluster atoms can be written as a function of the number of cluster atoms n as

$$E(n) = \varepsilon_0 n - A(n)n^{2/3}, \tag{12.1}$$

where ε_0 is the binding energy per atom of a bulk system, and the function $A(n)$ is the specific surface energy, which approaches a constant at large n. This is illustrated in Fig. 12.1, showing the behavior of $A(n)$ for clusters of face-centered cubic structure and with a short-range atomic interaction. The function $A(n)$ is nonmonotonic, and can deviate from its average value by several percent for large clusters. This is a measure of the accuracy of the expansion of the cluster energy (12.1) in a parameter that is small as a consequence of the large number of atoms in the cluster.

Along with clusters, small particles of sizes larger than clusters may be introduced into a plasma. Small particles in the atmosphere are usually called

aerosols. Bearing in mind the qualitative character of the analysis of the properties of clusters, aerosol particles, and small particles, we shall give them a unified treatment in the following. That is, we make no distinctions among these particles. For simplicity we assume each small particle to be spherical. This corresponds to the *liquid-drop model* for the particle. Within the framework of this model, we assume clusters or small particles to be like a liquid drop of the same material, and the drop density ρ is taken to be the same as the density of this liquid material in bulk. Then the number of atoms n in this particle is

$$n = \frac{4\pi r_0^3 \rho}{3m} = \left(\frac{r_0}{r_W}\right)^3, \tag{12.2}$$

where r_0 is the particle radius, m is the atomic mass, and $r_W = [3m/(4\pi\rho)]^{1/3}$ is the Wigner–Seitz radius. The liquid-drop model allows one to analyze electrical, electromagnetic, radiative, and other properties of these particles, and also to ascertain the influence of small particles on the properties of a plasma containing them. Such problems will be considered below.

12.2 POLARIZABILITY OF SMALL PARTICLES

We first determine the *polarizability* β of a spherical particle, defined as the coefficient of proportionality between the dipole moment $\mathbf{D}$ of the particle and the electric field $\mathbf{E}$ that induces it, as expressed by $\mathbf{D} = \beta\mathbf{E}$. The electric field potential of the particle, evaluated at a point outside the particle, is

$$\varphi = \varphi' - \mathbf{E} \cdot \mathbf{r},$$

where $\mathbf{r}$ is the distance from the particle center, and φ' is the potential from induced charges on the particle. Because there are no charges outside the particle, the electric potential of the induced charges satisfies the Laplace equation

$$\Delta\varphi' = 0.$$

Far from the particle the solution of this equation has the form $\varphi' = -\mathbf{D} \cdot \mathbf{r}/r^3$, so that outside the particle the electric potential is

$$\varphi = -\mathbf{E} \cdot \mathbf{r} - \frac{\mathbf{D} \cdot \mathbf{r}}{r^3}, \qquad r \geq r_0, \tag{12.3}$$

where r_0 is the particle radius.

The boundary condition on the particle surface has the form

$$\varepsilon \frac{\partial\varphi}{\partial r}\left(r \xrightarrow[r<r_0]{} r_0\right) = \frac{\partial\varphi}{\partial r}\left(r \xrightarrow[r>r_0]{} r_0\right), \tag{12.4}$$

where ε is the dielectric constant of the particle. This relation is the continuity condition for the electric field vector. The potential inside the particle is induced by an external electric field and therefore has a finite value. These conditions allow us to construct the scalar potential φ and the vectors $\mathbf{E}$ and $\mathbf{r}$ in the general form

$$\varphi = -C\mathbf{E} \cdot \mathbf{r}, \qquad r < r_0.$$

The coefficient C can be obtained from the continuity condition for the scalar potential at the particle surface and from the continuity condition (12.4) for the electric field vector. Using Eq. (12.3) for the potential outside the particle, we have

$$C = \frac{3\varepsilon}{\varepsilon + 2}, \qquad \beta = \frac{\varepsilon - 1}{\varepsilon + 2} r_0^3, \tag{12.5}$$

where the value of the polarizability follows from the expression connecting the induced dipole moment and the electric field strength. Equation (12.5) for a metallic particle ($\varepsilon \gg 1$) yields

$$\beta = r_0^3. \tag{12.6}$$

Equation (12.5) can be used for the particle polarizability in a variable field if the field frequency is not large, as expressed by

$$\omega \ll \Sigma, \tag{12.7}$$

where Σ is the conductivity of the particle material. In this case the field inside the particle is readily established, and the polarizability can be written as

$$\beta(\omega) = \frac{\varepsilon(\omega) - 1}{\varepsilon(\omega) + 2} r_0^3. \tag{12.8}$$

12.3 ABSORPTION CROSS SECTION FOR SMALL PARTICLES

The scattering and absorption of electromagnetic waves incident on a small particle of dimension r_0 is characterized by a parameter r_0/λ, where λ is the wavelength. This parameter is normally very small, and the corresponding cross sections are thus small compared to cross sections associated with particle interactions. The small size of this parameter allows us to limit our treatment to only the dipole interaction of an electromagnetic field with the particle. We demonstrate the procedure by treating the absorption of a monochromatic electromagnetic wave by a small particle. The interaction

energy between the induced dipole moment $\mathbf{D}$ and the field of an electromagnetic wave is $-\mathbf{E} \cdot \mathbf{D}$, where $\mathbf{E}$ is the electric field vector, and the power absorbed by the particle is

$$P = -\langle \mathbf{E} \cdot d\mathbf{D}/dt \rangle, \tag{12.9}$$

where the angle brackets denote averaging over a time large compared to the period of wave oscillations.

We take the electric field of the wave to be in the form

$$\mathbf{E} = \mathbf{E}_0 e^{i\omega t} + \mathbf{E}_0^* e^{-i\omega t},$$

where ω is the wave frequency. The specific flux of incident radiation averaged over a time large compared to the period of oscillations is given by the Poynting vector $c\langle |\mathbf{E} \times \mathbf{H}| \rangle = cE_0^2/(2\pi)$. The dipole moment induced by the electromagnetic field is

$$\mathbf{D} = \beta(\omega)\mathbf{E}_0 e^{i\omega t} + \beta^*(\omega)\,\mathbf{E}_0^* e^{-i\omega t},$$

where $\beta(\omega)$ is the particle polarizability (12.8). The result for the absorbed power (12.9) is

$$P = i\omega |E_0|^2 (\beta^* - \beta). \tag{12.10}$$

Dividing this value by the radiation flux $cE_0^2/(2\pi)$, we obtain the absorption cross section

$$\sigma_{\text{abs}} = 4\pi \frac{\omega}{c} \operatorname{Im} \beta(\omega). \tag{12.11}$$

Using Eq. (11.8) for the particle polarizability, we find

$$\sigma_{\text{abs}}(\omega) = \frac{12\pi\omega}{c} \frac{\varepsilon''}{(\varepsilon' + 2)^2 + (\varepsilon'')^2} r_0^3, \tag{12.12}$$

where the complex dielectric constant of the particle material is taken in the form $\varepsilon(\omega) = \varepsilon'(\omega) + i\varepsilon''(\omega)$ with ε' and ε'' real. We see the expected result that the absorption cross section $\sigma_{\text{abs}} \sim (r_0/\lambda) r_0^2$ is small compared to the particle cross section πr_0^2.

The absorption cross section is proportional to the cluster volume or to the number of cluster atoms n. From this it follows that the specific absorption cross section, that is, the cross section per atom, does not depend on the cluster size. As a demonstration of this result, Fig. 12.2 gives the measured absorption cross section of lithium clusters of different sizes. The proportionality of the absorption cross section of clusters to the number of

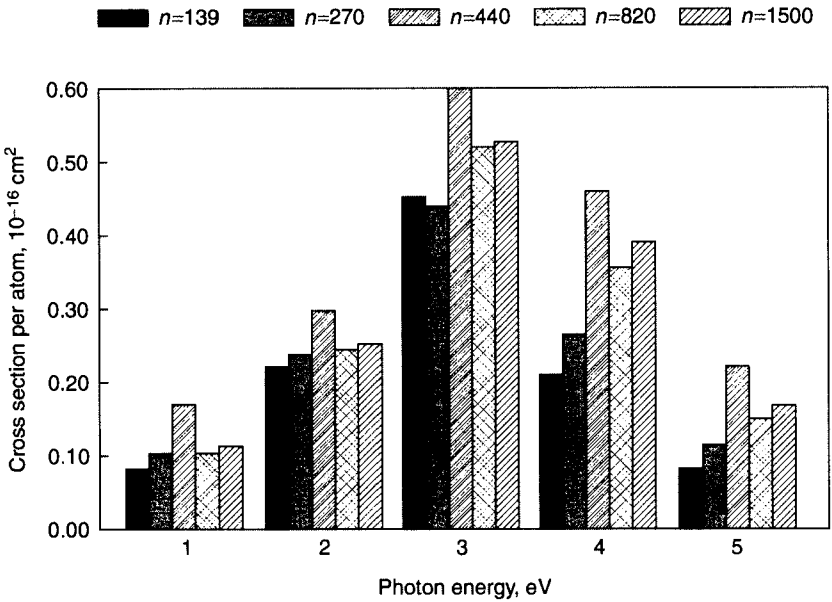

Figure 12.2 The specific absorption cross section of lithium clusters of different sizes. From left to right, the number of cluster atoms is 139, 270, 440, 820, and 1500.

cluster atoms holds true with an accuracy of 20%–30% which is within the accuracy of measurement of the absolute values of these cross sections.

The absorption cross section allows one to determine the radiated power $p(\omega)$ of a particle placed in a hot gas or vapor. The equilibrium of the particle with blackbody radiation gives

$$p(\omega) = \hbar\omega i(\omega)\sigma_{abs}(\omega) = \frac{\hbar\omega^3/\pi^2c^3}{\exp(\hbar\omega/T) - 1}\sigma_{abs}(\omega). \qquad (12.13)$$

Here $i(\omega)$, given by Eq. (7.30), is the random photon flux of blackbody radiation in the space where this radiation propagates, and T is the particle temperature.

The power radiated is proportional to the particle volume. Then if the radiation of the plasma is due to the particles within it, the total power of the radiation is proportional to the total number of atoms constituting these particles. Correspondingly, the radiated power does not depend on the size distribution of the particles. This result follows from the model of a bulk particle and Eq. (11.7). It simplifies the analysis of radiation by gases containing clusters or small particles.

12.4 MOBILITY OF LARGE CLUSTERS

Because clusters or small particles contain large numbers of atoms, their mobility in a gas is far less than that of individual atoms or molecules. We shall now examine the mobility and diffusion coefficient of clusters in a gas, within the framework of the liquid-drop model for the clusters. First we consider the case when the cluster radius r_0 is large compared to the mean free path λ of gas molecules: $r_0 \gg \lambda$. Assume the cluster to have a charge e and to be moving in the electric field $\mathbf{E}$. Then the electric force $e\mathbf{E}$ acting on the cluster is equal to the frictional force given by the Stokes formula, so that

$$e\mathbf{E} = 6\pi r_0 \eta \mathbf{v},$$

where η is the gas viscosity coefficient, and $\mathbf{v}$ is the average cluster velocity due to the electric field. This gives the expression

$$K = \frac{|\mathbf{v}|}{|\mathbf{E}|} = \frac{e}{6\pi r_0 \eta} \tag{12.14}$$

for the cluster mobility. Using the Einstein relation gives the diffusion coefficient

$$D = \frac{KT}{e} = \frac{T}{6\pi r_0 \eta} \tag{12.15}$$

for the cluster. Equation (12.15) shows that the cluster diffusion coefficient does not depend on the cluster material. The only cluster parameter in the above expression for the diffusion coefficient is the radius.

Now we consider the other limiting case: $\lambda \gg r_0$. Then the cluster diffusion coefficient is determined by successive collisions with gas molecules, and is given by Eq. (10.6). Because the collision cross section of a gas molecule and the cluster is πr_0^2, Eq. (10.6) gives

$$D \sim \frac{\sqrt{T/m}}{N r_0^2}, \qquad \lambda \gg r_0,$$

where m and N are the molecule mass and number density, respectively. Combining the above equations, we have

$$D = \frac{T}{6\pi r_0 \eta}(1 + a\,\mathrm{Kn}), \tag{12.16}$$

where $a = 3.1$ is a numerical coefficient, and $\mathrm{Kn} = \lambda/r_0$ is the *Knudsen number*. In particular, for air at atmospheric pressure and room temperature,

this expression can be rewritten in the form

$$D = \frac{D_0}{r_0}\left(1 + \frac{0.14}{r_0}\right),$$

where $D_0 = 1.3 \times 10^{-7}$ cm^2/s and r_0 is expressed in microns.

We can obtain a comparison of the cluster diffusion coefficient with that of atomic particles in a gas (D_p) for the case $r_0 \ll \lambda$. According to Eq. (10.6), the ratio of these values is

$$\frac{D}{D_p} = \sqrt{\frac{\mu}{m}}\left(\frac{\rho_0}{r_0}\right)^2,$$

where μ is the reduced mass of the given atomic particle and a gas molecule, and ρ_0 is the interaction radius of atomic particles, which can be estimated according to Eq. (4.7). This value depends weakly on the collision energy and on gas parameters. In particular, for atmospheric air at room temperature, the quantities appearing in the expression have the values $\rho_0 = 40$ nm, $D_p N = 4.8 \times 10^{18}$ cm^{-1} s^{-1}, and $DNr_0^2 = 4.6 \times 10^3$ cm/s, where N is the number density of air molecules.

12.5 RECOMBINATION COEFFICIENT OF SMALL CHARGED CLUSTERS

If electrons and ions in a plasma are attached to clusters, reduction of separated charges in the system occurs, as it does in the absence of clusters, by recombination of positive and negative ions. We assume that the cluster size is small ($r_0 \ll e^2/T$) and that clusters can have only a single charge. The recombination coefficient of two clusters with opposite charges is given by

$$\alpha = 4\pi e(K_+ + K_-) = 4\pi e^2(D_+ + D_-)/T, \qquad (12.17)$$

from the Langevin formula (11.33), where D_+ and D_- are the diffusion coefficients of positive and negative clusters in a gas. From Eq. (12.15), when $r_0 \ll \lambda$, it follows that $\alpha \sim r_0^{-2}$. In particular, for air at room temperature and atmospheric pressure, we have $\alpha r_0^2 = 2.6 \times 10^{-20}$ cm^5/s.

12.6 MULTICHARGED CLUSTERS IN HOT GASES AND PLASMAS

The work function of metals is usually small compared to the ionization potential of the constituent atoms. (See data in Appendices 10 and 12.) In like fashion, the ionization potential of clusters is smaller than that of atoms.

This leads to ionization of clusters in hot gases under conditions where the degree of atomic ionization is small. As a result, a plasma containing clusters is formed in hot gases, and the clusters are a source of electrons. We can evaluate the average charge of the clusters in a hot vapor. The number densities N_Z and N_{Z+1} of clusters consisting of n atoms and with charges Z and $Z + 1$ are related to the electron number density N_e by the equation

$$\frac{N_Z(n)N_e}{N_{Z+1}(n)} = 2\left(\frac{m_eT_e}{2\pi\hbar^2}\right)^{3/2}\exp\left(-\frac{I_Z(n)}{T_e}\right) \tag{12.18}$$

analogous to the Saha formula (2.17), where $I_Z(n)$ is the ionization potential of cluster ions of charge Z consisting of n atoms. For large metallic clusters we have

$$I_Z(n) = I_{Z-1}(n) + e^2/r_0,$$

where r_0 is the cluster radius and e^2/r_0 is the energy required for electron removal from the cluster surface to asymptotic distances. We can write the cluster ionization potential for $Z = 0$ in the form

$$I_0(n) = W_0 + an^{-1/3}, \tag{12.19}$$

where W_0 is the work function of the corresponding metallic surface, $a = I_0 - W_0$, and I_0 is the atomic ionization potential. Thus the ionization potential for the cluster of charge Z is

$$I_Z(n) = W_0 + \frac{a}{n^{1/3}} + \frac{Ze^2}{r_0} = W_0 + \frac{a}{n^{1/3}} + \frac{Zb}{n^{1/3}}, \tag{12.20}$$

where, in accord with Eq. (12.2), we have $b = e^2/r_W = e^2[\,4\pi\rho/(3m_e)]^{1/3}$.

Equations (12.18) and (12.20) determine the mean charge Z_n of a cluster ion, obtainable from the relation $N_Z(n) = N_{Z+1}(n)$, which has the form

$$Z_n = \frac{r_0T_e}{e^2}\left\{\ln\left[\frac{2}{N_e}\left(\frac{m_eT_e}{2\pi\hbar^2}\right)^{3/2}\right] - \frac{W_0}{T_e} - \frac{a}{b}\right\} + \frac{1}{2}.$$

If clusters are the only donors of electrons, plasma quasineutrality leads to $NZ_n = N_e$, where N is the number density of clusters and Z_n is their average charge. One can see that the average cluster charge increases weakly with increase of its radius.

12.7 CHARGING OF SMALL PARTICLES IN A PLASMA

At low temperatures, small particles in a plasma can absorb electrons and ions. This process leads to decay of the plasma and charging of the small particles. We consider this process in the context of a plasma containing positive and negative ions and with the liquid drop model for the cluster. We first assume the mean free path λ of the ions to be small compared to the particle radius r_0. Ion motion is then determined by its diffusion and drift under the influence of the electric field of the charged particle. The number density of ions on the particle surface is zero, and approaches an equilibrium value at large distances from the particle. We can determine the ion current on the particle surface from this information. The current of positive ions directed towards the particle of charge Z at a distance r from it is

$$I = 4\pi r^2(-D_+ \, dN/dr + K_+ EN)e.$$

The first term arises from diffusion effects, the second term corresponds to drift motion, D_+ and K_+ are the diffusion coefficient and the mobility of positive ions, e is an ion charge (usually just the electron charge), and $E = Ze/r^2$ is the electric field strength due to the particle. Using the Einstein relationship (11.3) between the diffusion coefficient and the mobility of ions, the positive-ion current at the particle surface is

$$I = -4\pi r^2 D_+ e\left(\frac{dN}{dr} - \frac{Ze^2}{Tr^2}N\right).$$

This expression can be considered to be the equation for the ion number density. We take into account that the ions do not decay in space and hence that the ion current does not depend on r. Solving this equation with the boundary condition $N(r_0) = 0$, we obtain

$$N(r) = \frac{I}{4\pi D_+ e}\int_{r_0}^{r}\frac{dr'}{r'^2}\exp\left(\frac{Ze^2}{Tr'} - \frac{Ze^2}{Tr}\right)$$

$$= \frac{IT}{4\pi D_+ qe^2}\left[\exp\left(\frac{Ze^2}{Tr_0} - \frac{Ze^2}{Tr}\right) - 1\right].$$

Since at large r the ion number density tends to the equilibrium value in a plasma N_+, we obtain the expression

$$I_+ = \frac{4\pi D_+ N_+ Ze^3}{T\left[\exp(Ze^2/Tr_0) - 1\right]} \tag{12.21}$$

for the ion current. This is the *Fuchs formula*. In the limit when the particle charge is zero, this expression transforms to the *Smoluchowski formula* for the diffusive flux of particles on the surface of an absorbing sphere,

$$I_+/e = 4\pi D_+ N_+ r_0. \tag{12.22}$$

Equation (12.21) describes the positive-ion current. In order to obtain the expression for the negative ion current, it is necessary to make the change $Z \to -Z$, and replace positive-ion parameters by those for negative ions. The negative-ion current to the particle is then

$$I_- = \frac{4\pi D_- N_- Ze^3}{T\left[1 - \exp\left(Ze^2/Tr_0\right)\right]}. \tag{12.23}$$

If the positive- and negative-ion parameters are identical, the negative-ion current is greater than the positive-ion current because the particle has a positive charge and attracts negative ions. In the limit $Ze^2/(r_0T) \gg 1$, Eq. (12.23) reduces to the Langevin formula (11.33).

We can determine the equilibrium charge of the particle in a quasineutral plasma, where $N_+ = N_-$. Then the positive- and negative-ion currents are the same, which gives the particle charge

$$Z = \frac{r_0 T}{e^2} \ln\left(\frac{D_+}{D_-}\right). \tag{12.24}$$

Thus the particle has a positive charge if $D_+ > D_-$, so that positive ions have a higher mobility than negative ions. Note that Eq. (12.24) is valid under the condition

$$r_0 \gg \frac{e^2}{T}. \tag{12.25}$$

In this case an individual ion captured by the particle does not significantly change the particle potential. The above expressions are valid if $r_0 \gg \lambda$. For atmospheric air at room temperature, the relation (12.25) is valid for $r_0 \gg 0.06\ \mu$m and $\lambda = 0.1\ \mu$m.

12.8 CHARGED PARTICLES IN AN AEROSOL PLASMA

Ions in a plasma tend to adhere to small particles, and so these particles influence the parameters of the plasma. This fact is of special importance for atmospheric plasmas. We shall consider a plasma regime wherein charged atomic particles are created in the plasma by an external source, and their

decay occurs through ion–ion recombination. The presence of small particles or clusters in such a plasma can change its properties. The balance equations for the number densities N_+ of positive ions and N_- of negative ions in the plasma have the form

$$\frac{dN_+}{dt} = G - \alpha N_+ N_- - \frac{I_+ N_p}{e},$$
$$\frac{dN_-}{dt} = G - \alpha N_+ N_- - \frac{I_- N_p}{e},$$

where G is the rate of ionization by an external source, α is the ion–ion recombination coefficient, N_p is the number density of particles, and I_+ and I_- are ion currents to a particle as given by Eqs. (12.21) and (12.23).

For simplicity we consider the case $Z < r_0 T/e^2$, when the ion current is described by the Smoluchowski formula (12.22). Then $N_+ = N_- = N_i$, and the balance equation in the stationary case has the form

$$G - \alpha N_i^2 - k N_i N_p = 0,$$

where $k = 4\pi D r_0$, and $D = (D_+ + D_-)/2$ is the average diffusion coefficient of ions in a gas. This equation shows that the recombination of ions through the participation of particles is stronger than in particle-free space when

$$N_p \gg \sqrt{G\alpha}\,/k. \tag{12.26}$$

Then the number density of ions is

$$N_i = G/(kN_p). \tag{12.27}$$

To make numerical estimates for an atmospheric plasma, we take $G \sim 10\ \mathrm{cm^{-3}\ s^{-1}}$ and $\alpha \sim 10^{-6}\ \mathrm{cm^3/s}$; and for ions with a mobility $K = 1\ \mathrm{cm^2/(V\ s)}$, we have $k/r_0 = 0.3\ \mathrm{cm^2/s}$. The condition (12.26) has the form $N_p r_0 \gg 0.01\ \mathrm{cm^{-2}}$. In particular, for particles of size $r \sim 10\ \mu\mathrm{m}$, this gives $N_i \gg 100\ \mathrm{cm^{-3}}$ (corresponding to densities $\rho \gg 4 \times 10^{-7}\ \mathrm{g/cm^3}$ for water vapor), so that Eq. (12.27) leads to the estimate $N_i N_p \sim 3 \times 10^4\ \mathrm{cm^{-6}}$.

Note that Eq. (12.24) for the particle mean charge relates to a criterion opposite to that expressed in (12.26), in that the number of small particles in a plasma is relatively small and they do not change the plasma properties. If the condition (12.26) is valid, the particle charge is small. In addition, according to the Smoluchowski formula, we have $N_+ D_+ = N_- D_-$, and the condition of the plasma quasineutrality $N_+ + Zn = N_-$ together with Eq. (12.27) gives

$$Z = \frac{N_- - N_+}{N_p} = \frac{G}{4\pi r_0 N_p^2}\left(\frac{1}{D_-} - \frac{1}{D_+}\right) \tag{12.28}$$

for the mean particle charge Z. Thus, at large number densities of particles N_p, their average charge decreases as N_p^{-2}.

Let us consider the case of particles sufficiently small that $r_0 \ll e^2/T$. Then particles are mostly neutral, and the number of particles with charge $2e$ or more is exponentially small because the Coulomb barrier of a charged particle is greatly in excess of the thermal ion energy. We introduce the rate constant $k_{m,m+1}$ for a particle of a charge m to increase its charge by one as a result of attachment of positive ions, and use the same notation as for other rate constants. According to the Smoluchowski formula (12.22), we have

$$k_{0,1} = 4\pi D_+ r_0, \qquad k_{0,-1} = 4\pi D_- r_0, \tag{12.29a}$$

and the Langevin formula for the other processes gives

$$\begin{aligned} k_{1,0} &= 4\pi e K_- = 4\pi D_- e^2/T, \\ k_{-1,0} &= 4\pi e K_+ = 4\pi D_+ e^2/T. \end{aligned} \tag{12.29b}$$

From this we can solve for the number densities N_0, N_1, and N_{-1} of neutral, positive, and negative small particles by using the charge balance equations (for example, $k_{0,1} N_0 N_+ = k_{1,0} N_1 N_-$) to obtain

$$N_1 = N_0 \frac{r_0 T}{e^2} \frac{N_+}{N_-}, \quad N_{-1} = N_0 \frac{r_0 T}{e^2} \frac{N_-}{N_+}; \qquad r_0 \ll e^2/T. \tag{12.30}$$

Note that the number density of double-charged particles is exponentially small ($\sim \exp[-e^2/(r_0 T)]$).

In the regime being examined, where $\lambda \ll r_0 \ll e^2/T$, small particles are mostly neutral, and neglecting the recombination of charged particles corresponds to the condition $k_{1,0} N_1 N_{-1} \gg \alpha N_1 N_{-1}$. In accordance with the above expression, this criterion can be rewritten in the form

$$N_0 \gg \frac{\sqrt{G/\alpha}\, e^2}{r_0 T}. \tag{12.31}$$

In particular, for water vapor at room temperature this amounts to $N_0 \gg 4 \times 10^5 \sqrt{G}$, where G is expressed in $\mathrm{cm}^{-3}\mathrm{s}^{-1}$, and N_0 is in cm^{-3}.

Thus, three parameters with the dimensions of size—r_0, e^2/T, and λ—determine the nature of the charging of a particle. If $r_0 \gg e^2/T$, the variation of the particle's electric potential resulting from an attachment of one ion is small compared to T/e; if $r_0 \ll e^2/T$, the particle can have only a single charge, and ion interactions with charged and neutral particles are significantly different. If $r_0 \gg \lambda$, the diffusive character of ion motion in a gas determines the attachment of an ion to the particle; if $r_0 \ll \lambda$, charging of the particle results from successive collisions with ions. Thus, the nature of the charging of a small particle depends on the relative magnitudes of the above size parameters.

12.9 ELECTRIC FIELDS IN AEROSOL PLASMAS

We now consider a mechanism that occurs in the Earth's atmosphere, in which a charge separation results from the action of gravity on charged aerosols in the atmosphere. This charge separation creates electric fields in the plasma. The electric current thus generated is counterbalanced by an ion current. Thus we have

$$Zenv = eE(K_+N_+ + K_-N_-), \tag{12.32}$$

where n is the number density of aerosol particles, Ze is their mean charge, v is the velocity with which they fall, E is the electric field strength, and K_+ and K_- are ion mobilities. The velocity with which a particle of radius $r_0 \gg \lambda$ falls follows from the condition that the particle weight is equalized by the Stokes force, which gives the expression

$$\tfrac{4}{3}\pi r_0^3 \rho_0 g = 6\pi r_0 \eta v,$$

where ρ_0 is the mass density of the particle and η is the gas viscosity coefficient. From this it follows that

$$v = \frac{2r_0^2 \rho_0 g}{9\eta}. \tag{12.33}$$

For simplicity we consider the case of nearly equal ion mobilities. We introduce the quantities $N = (N_+ + N_-)/2$, $K = (K_+ - K_-)/2$, and $\Delta K = K_+ - K_-$. Then equation (12.32) gives

$$E = \frac{Znv}{2KN}. \tag{12.34}$$

When the plasma contains aerosol particles of large sizes as well as ions, and the number density of particles is large, then Eq. (12.26) is relevant. Then, according to Eqs. (12.27) and (12.28), the electric field strength is

$$E = \frac{\Delta K}{K}\frac{v}{2K}. \tag{12.35}$$

12.10 ELECTRIC PROCESSES IN CLOUDS

The above results can be applied to analyze the processes that occur in clouds and cause charging of the Earth. These processes begin with the condensation of water vapor at altitudes of several kilometers, where the temperature is lower than near the surface of the Earth. This leads to the formation of clouds consisting of small water particles in the liquid and solid

(ice) states. In the course of condensation, the particles increase in size, and they fall under the action of gravity. Simultaneously, these particles acquire electric charge that is mainly negative, because the diffusion coefficient of negative ions in the atmosphere is higher than that of positive ions. The free fall of charged aerosol particles causes an electric current in a cloud and leads to separation of the charges in it. As a result, a storm cloud is formed with an electric potential of several million volts with respect to the Earth. Breakdown between a cloud and the Earth charges the Earth negatively. Thus the separation of charges in a cloud can have important effects on the operation of devices on Earth that depend on electrical processes.

We have seen that electrical processes in the Earth are connected with hydrological processes in the atmosphere. We can give some data that measure the magnitude of these phenomena. As a result of water evaporation, a total of 4×10^{14} metric tons of water per year, or 13 million tons per second, circulates through the atmosphere. This water leads to charging of the Earth with a mean current of about 1700 A. Thus, the specific transfer of electricity is 1.3×10^{-10} C/g. We can compare this value with the specific charge of a water drop. Because $D_+/D_- = 0.8$ on the average for atmospheric air, Eq. (12.24) gives the specific charge of 1.5×10^{-9} C/g for a water drop of radius 10 μm, and 1.5×10^{-11} C/g for a drop with a radius of 100 μm. This formula is valid for a small particle charge. If this constraint is violated, Eq. (12.24) overestimates the charge. From these data, it follows that the average size of water drops does not exceed several tens of microns for drops whose fall creates the electric potential of a cloud.

We shall make one more estimate on the basis of Eq. (12.24), according to which the charge on a particle is proportional to its radius while the velocity of fall is proportional to the square of its radius [see Eq. (12.33)]. Thus, the contribution to the current from a single particle is proportional to the cube of its radius, and the total current resulting from the free fall of charged particles is proportional to the total mass of water participating in the process. Assume that the current resulting from the free fall of charged particles in clouds is equal to the current to the Earth's surface, which is 1700 A. Then we find that it is necessary to have 4×10^{11} metric tons of water in the atmosphere in the form of drops or particles in order to produce the observed current. We use an understated estimate because Eq. (12.24) gives overstated values for the particle charge. In actuality, the Earth's atmosphere contains $(3\text{–}8) \times 10^{12}$ metric tons of water, which can clearly provide the charging rate of the Earth that is necessary for the observed currents.

Parameters typical of a storm cloud are that the average cloud thickness is $L \approx 4$ km, and a typical electric field strength is $E \approx 100$ V/cm, so that a typical cloud potential is of the order of 10^7 V. In addition, the number density of noncompensated charge is $\Delta N \sim E/(4\pi L) \sim 2 \times 10^{-17}$ C/cm^3, and that corresponds to a number density of electron charges of about 100 cm^{-3}. This is several times smaller than the number density of molecular ions in the atmosphere.

We can make one further estimate stemming from these data. Assuming in Eq. (12.34) that $\Delta K/K = 0.2$, $K = 1$ cm^2/(V cm), and $E = 100$ V/cm, we obtain from this equation that $r_0 = 300$ μm. This is greater than the above upper limit for the drop radius. This contradiction testifies to the complicated character of processes in a storm cloud compared to the simple nature of Eq. (12.34). Along with ions and small particles (of size ~ 10 μm), small particles of sizes smaller than 1 μm are present in a cloud. Small drops carry the main part of the plasma charge, and change the ratio between the number densities of positive and negative ions in a plasma. Indeed, according to Eq. (12.28), the particle charge in a two-component system falls with an increase of the particle number density if the criterion (12.26) is valid. Then the number density of ions of each charge is determined by the particle number density. This connection is broken in a many-component system, where the particle charge does not depend on its density, and electrical processes become more effective.

We can make estimates for a storm cloud assuming that small particles regulate the ion number density in a plasma, and that large particles with sizes of tens of microns cause the charge separation in the cloud. We use Eqs. (12.24) and (12.34) for a charged particle with typical parameters $\Delta K/K = 0.2$, $K = 1$ cm^2/(V cm), $E = 100$ V/cm, typical ion number densities $N \sim 10^2$–10^3 cm^{-3}; and a number density of water particles, n, that creates an electric current $nr_0^3 \sim 5 \times 10^{-7}$–$5 \times 10^{-6}$. This corresponds to the water content in cloud particles of 2–20 g per kilogram of air. In reality, a storm cloud is formed if the water content exceeds 7 g of water per kilogram of air. Thus, the physics of processes in real clouds is relatively straightforward. But even the above simplified scheme shows the complex character of the phenomenon.

12.11 SIZE DISTRIBUTION OF CLUSTERS IN GASES

For clusters situated in a plasma or hot gas, their size distribution function (we characterize the cluster size by the number of atoms n in a cluster) is determined by processes governing cluster growth and evaporation. Clusters will be in equilibrium with a gas or vapor consisting of the same atoms. The equilibrium is maintained by processes

$$A_n + A \leftrightarrow A_{n+1}. \tag{12.36}$$

We shall apply the liquid-drop model of the cluster to the analysis of this equilibrium. We assume the parameters of the cluster surface to be identical to those of the surface of the same matter in bulk. From this hypothesis we evaluate the flux of atoms attaching to the cluster surface and the flux of atoms evaporating from the cluster. First we consider these processes for a

bulk surface. The attachment flux of atoms in a gas to the bulk surface is

$$j_{\text{at}} = \sqrt{\frac{T}{2\pi m}}\, N\xi, \tag{12.37}$$

where the first factor is the average velocity component directed perpendicular to the surface, m is the mass of the atom, N is the number density of the atoms, and ξ is the probability of an atom adhering to the surface after contact. The flux of evaporating atoms is given by the expression

$$j_{\text{ev}} = C \exp(-\varepsilon_0/T), \tag{12.38}$$

where ε_0 is the cohesive energy of the bulk surface in accordance with Eq. (12.1), and the parameter C depends weakly on the temperature and is determined by properties of the surface. If the atom number density is the same as the number density of saturated vapor N_{sat} at this temperature, the attachment flux becomes equal to the evaporation flux:

$$j_{\text{ev}} = j_{\text{at}} = \sqrt{\frac{T}{2\pi m}}\, N_{\text{sat}}(T)\,\xi, \tag{12.39}$$

where $N_{\text{sat}}(T) = N_0 \exp(-\varepsilon_0/T)$. This determines the factor C in Eq. (12.38) as

$$C = \sqrt{\frac{T}{2\pi m}}\, N_0\,\xi.$$

Within the framework of the liquid-drop model of the cluster, we have the expression (12.37) for the flux of attaching atoms. If we associate properties of the bulk surface with the surface of a cluster of the same material, we can use the above expression for the evaporation flux by replacing the atomic binding energy ε_0 of the bulk surface by the cohesive energy ε_n of cluster atoms. Then Eq. (12.39) acquires the form

$$j_{\text{ev}} = \text{Const} \cdot \exp\left(-\frac{\varepsilon_n}{T}\right) = \sqrt{\frac{T}{2\pi m}}\, N_{\text{sat}}(T)\,\xi \exp\left(-\frac{\varepsilon_n - \varepsilon_0}{T}\right). \tag{12.40}$$

In thermodynamic equilibrium between clusters containing $n-1$ and n atoms, the rates of decay and formation of clusters must be the same, so that

$$N_n j_{\text{ev}} = N_{n-1} j_{\text{at}}, \tag{12.41}$$

where N_n is the number density of clusters containing n atoms. This leads to the relation

$$\frac{N_{n-1} N}{N_n} = N_{\text{sat}} \exp\left(-\frac{\varepsilon_n - \varepsilon_0}{T}\right) \tag{12.42}$$

between the equilibrium number densities of clusters of neighboring sizes. This equation has the form of the Saha distribution (2.17).

12.12 CRITICAL SIZE OF CLUSTERS

We can rewrite the relation (12.42) with the help of Eq. (12.1) for the cohesive energy of a large cluster. Within the context of the liquid-drop model, we assume that the specific surface energy of clusters does not depend on the cluster size, so that Eq. (12.1) gives $A = \frac{3}{2}\Delta\varepsilon = \text{const}$. With the relations $\varepsilon_n = dE_n/dn = \varepsilon_0 - \Delta\varepsilon/n^{1/3}$, this yields

$$\frac{N_n}{N_{n-1}} = S\exp\left(-\frac{\Delta\varepsilon}{n^{1/3}T}\right), \tag{12.43}$$

where $S = N/N_{\text{sat}}$ is the degree of supersaturation of the vapor. Condensation of atoms takes place at $S > 1$ if the vapor density exceeds its saturation value for a given temperature. Then from Eq. (12.43) it follows that the cluster number density as a function of cluster size has a minimum at the critical number of cluster atoms

$$n_{\text{cr}} = \left(\frac{\Delta\varepsilon}{T\ln S}\right)^3. \tag{12.44}$$

The concept of the critical size plays a primary role in the description of the nucleation of neutral vapors. In other words, for clusters whose size exceeds the critical size, the probability of their growth exceeds the probability of their evaporation, while the opposite relation holds for clusters with $n < n_{\text{cr}}$. Then the condensation rate is proportional to the equilibrium number density of clusters of the critical size. The greater is the degree of supersaturation, the smaller is the critical radius. For large charged clusters at high degrees of supersaturation, the critical-radius criterion is violated. This is because higher-order terms in the expansion in n of the binding energy in Eq. (12.1) change the behavior of the number density of clusters as a function of their size. For this reason, ions are nuclei of condensation in a plasma.

According to Eq. (12.43), the number density of clusters as a function of their size has a minimum at the cluster critical size. This leads to an important conclusion. Clusters are an intermediate phase of matter between gaseous and condensed phases. According to Eq. (12.43), most atoms of a supersaturated vapor ($S > 1$) of a gas-condensed system are found in the condensed phase under conditions of thermodynamic equilibrium. On the contrary, in a nonsaturated vapor ($S < 1$), most atoms are found in the gaseous phase. This means that clusters constitute a small part of the atoms in the system at thermodynamic equilibrium. But transition from the gaseous to the condensed phase takes place through the formation and growth of clusters. From this one can conclude that a large content of atoms in clusters corresponds to nonequilibrium conditions. Hence methods of generation of

clusters are based on fast nucleation of vapors or gases in a space in a condition of violation of their thermodynamic equilibrium with a condensed phase. This occurs in the mixing of a flow of evaporating atoms from a solid surface with a flow of a cold gas, or by a free jet expansion of a vapor either in a buffer gas or without it.

12.13 CLUSTERS IN HOT, WEAKLY IONIZED GAS

One can accumulate clusters in a spatial region by transporting them to this region from where they are generated. This is done, for example, in cluster light sources when cluster radiators are gathered in a high-temperature plasma. Due to the charge of the clusters, their interaction with electrons is essential to the heat balance of the clusters. As a result, the temperature of the cluster will exceed that of the gas. We shall consider thermal equilibrium between clusters and a plasma that is supported by collisions of the clusters with atoms in the gas and with plasma electrons. We denote the cluster temperature by T_{cl} and, as usual, take the gas temperature T to be smaller than the electron temperature T_e. Colliding with clusters, atoms and electrons exchange energy with them, so that the cluster temperature is determined by the temperature of the gas and of the electrons. We can use a simple model for this process in which the mean energy of the atoms varies from $3T/2$ up to $3T_{cl}/2$ after collision with the cluster, and the mean electron energy varies from $3T_e/2$ to $3T_{cl}/2$. This takes place when a strong interaction exists between colliding atoms and clusters, and in particular if these collisions proceed through capture of the atom by the cluster surface. We assume that the process occurs as a result of contact of an atom or an electron with the cluster. Hence, the cross section for such a collision of an atom with a cluster is πr_0^2, where r_0 is the cluster radius; and the rate constant of electron–cluster collision is given by Eq. (5.9), where the parameter R_0 is equal to the cluster radius. Using the liquid-drop model and introducing the cluster charge Z, we find the rate constants k for atom–cluster (k_a) and electron–cluster (k_e) collisions to be

$$k_a = \langle v_a \pi r_0^2 \rangle = \sqrt{\frac{8T}{\pi m}}\, \pi r_0^2,$$
$$k_e = \left\langle v_e \pi r_0^2 \left(1 + \frac{Ze^2}{\varepsilon_e r_0}\right) \right\rangle = \sqrt{\frac{8T_e}{\pi m_e}}\, \pi r_0^2 \left(1 + \frac{Ze^2}{r_0 T_e}\right). \tag{12.45}$$

Here v_a and v_e are the atom and electron velocities, ε_e is the electron energy, and the averaging is done over the velocity distribution of atoms or electrons. We assume the cluster radius to be sufficiently large that collisions are governed by classical laws, but still small in comparison with the mean free path of atoms and electrons. Hence, each cluster collision is with a single particle.

From the above analysis, the equation for the cluster temperature is

$$(T - T_{cl})k_a N_a + (T_e - T_{cl})k_e N_e = 0,$$

where N_a and N_e are the number densities of atoms and electrons respectively. This leads to

$$T_{cl} = \frac{T + \zeta T_e}{1 + \zeta}, \qquad \zeta = \sqrt{\frac{T_e m}{T m_e}} \left(1 + \frac{Ze^2}{r_0 T_e}\right) \frac{N_e}{N_a}. \tag{12.46}$$

These relations make it possible to determine the temperature of clusters in a plasma. From Eq. (12.46) it follows that the cluster temperature is between the gas and electron temperatures. Because of the small electron mass and high electron temperature, the difference between the cluster and gas temperatures can be very slight when there is a low concentration of electrons in a plasma.

12.14 KINETICS OF CLUSTER PROCESSES IN THE PARENT VAPOR

We wish to examine the evolution of clusters in a plasma. Introduced into a plasma, clusters create their own vapor as a result of their partial evaporation, and then they interact further with this vapor by means of the processes (12.36). Note that other processes involving clusters, as their transport in the plasma and their heat balance, proceed through collisions of gas atoms and electrons with clusters. Since clusters are charged, one can neglect cluster–cluster collisions in the kinetics of clusters, because clusters do not contact each other in these collisions. Thus the equilibrium between clusters of different sizes is accomplished only through the processes (12.36). This equilibrium leads to some particular size distribution function for the clusters, and maintains a certain number density of free atoms. We shall consider this equilibrium and the character of the evolution of cluster sizes in this case.

First we find the expression for the collision integral I_n as a function of n. This collision integral is responsible for the variation of the size distribution function of clusters due to the processes (12.36). Evidently, it has the form of the Fokker–Planck equation (9.27) for the large clusters under consideration. We can rewrite the above expressions for the fluxes of attaching and evaporating atoms in terms of the rate constants of these processes. For the liquid-drop model, we have

$$j_{at} \pi r_0^2 = k_n N,$$

where r_0 is the cluster radius [determined by Eq. (12.2)], and the attachment flux is given by Eq. (12.37). Hence, the rate constant k_n for attachment of atoms to a cluster consisting of $n \gg 1$ atoms is

$$k_n = k_0 \xi n^{2/3},$$

where

$$k_0 = \pi r_W^2 \sqrt{\frac{8T}{\pi m}} = \pi \left(\frac{3m}{4\pi\rho} \right)^{2/3} \sqrt{\frac{8T}{\pi m}} = 1.93 T^{1/2} m^{1/6} \rho^{-2/3}. \quad (12.47)$$

Here m is the mass of the atom and ρ is the bulk density. The principle of detailed balance, used for deduction of Eq. (12.40) for a macroscopic cluster, gives the rate ν_{n+1} of evaporation of an atom from a cluster consisting $n + 1$ atoms as

$$\nu_{n+1} = k_n(T_{cl}) N_{sat}(T_{cl}) \exp\left(\frac{\Delta\varepsilon}{T_{cl} n^{1/3}} \right). \quad (12.48)$$

Here, according to Eq. (12.1), the cluster cohesive energy is $\varepsilon_n = dE_n/dn = \varepsilon_0 - \Delta\varepsilon/n^{1/3}$ ($\Delta\varepsilon = 2A/3$), T_{cl} is the cluster temperature, and $N_{sat}(T_{cl})$ is the number density of atoms at the pressure of saturated vapor corresponding to the temperature T_{cl}. On the basis of these rate constants, the balance equation for the number density of clusters N_n consisting of n atoms is

$$\frac{\partial N_n}{\partial t} = I_n = N k_{n-1} N_{n-1} - N k_n N_n - \nu_n N_n + \nu_{n+1} N_{n+1}. \quad (12.49)$$

When $n \gg 1$, as in the case being considered, the relation $f_n = f_{n-1} + \partial f_n/\partial n$ holds true for any function f_n, so one can rewrite the kinetic equation for clusters using Eq. (12.49) to obtain

$$\frac{\partial N_n}{\partial t} = I_n = -\frac{\partial}{\partial n} \left\{ k_0(T) \xi n^{2/3} \left[N N_n - N_{sat}(T_{cl}) \sqrt{\frac{T_{cl}}{T}} \exp\left(\frac{\Delta\varepsilon}{T_{cl} n^{1/3}} \right) N_{n+1} \right] \right\}. \quad (12.50)$$

The right-hand part of this equation, the collision integral, is a fundamental result, and is responsible for transitions between clusters of different sizes. For large n, which is the case at hand, this equation has the form of the Fokker–Planck equation. Writing $N_{n+1} = N_n + \partial N_n/\partial n$, one can represent the collision integral as the sum of two fluxes. The first one, the hydrodynamic flux, is expressed through the first derivative with respect to n; and the

second flux, the diffusion flux, depends on the second derivative with respect to n. The diffusion flux is small compared to the hydrodynamic flux, but it is responsible for the width of the size distribution function of clusters. Neglecting it, we represent the collision integral in the form

$$I_n = -\frac{\partial}{\partial n}\left\{k_0(T)\xi n^{2/3}N_n\left[N - N_{\text{sat}}(T_{\text{cl}})\sqrt{\frac{T_{\text{cl}}}{T}}\exp\left(\frac{\Delta\varepsilon}{T_{\text{cl}}n^{1/3}}\right)\right]\right\}. \quad (12.51)$$

Taking into account only processes (12.36) for the growth and evaporation of clusters, the conservation of the total number density of clusters in a space is

$$N + N_{\text{tot}} = \text{const} \gg N_{\text{sat}}(T_{\text{cl}}), \quad (12.52)$$

where N is the number density of free atoms, $N_{\text{tot}} = \sum_n nN_n$ is the total number density of atoms in clusters, or atoms bound together, and the number density of free and bound atoms is large. From this and Eq. (12.50), the balance equation for the number density of free atoms has the form

$$\frac{dN}{dt} = -\frac{d}{dt}\sum_n nN_n = -\sum_n n\frac{\partial N_n}{\partial t}$$

$$= -\int dn\, k_0(T)\xi n^{2/3}N_n\left[N - N_{\text{sat}}(T_{\text{cl}})\sqrt{\frac{T_{\text{cl}}}{T}}\exp\left(\frac{\Delta\varepsilon}{T_{\text{cl}}n^{1/3}}\right)\right]. \quad (12.53)$$

The first term in the brackets of Eqs. (12.51) and (12.53) corresponds to attachment of atoms to clusters, and the second term to the evaporation of atoms from the cluster surface. According to the definition of the cluster critical size n_{cr}, for which the rates of these processes are equal, we have

$$N = N_{\text{sat}}(T_{\text{cl}})\sqrt{\frac{T_{\text{cl}}}{T}}\exp\left(\frac{\Delta\varepsilon}{T_{\text{cl}}n_{\text{cr}}^{1/3}}\right). \quad (12.54)$$

Note that the critical radius and the number density N of free atoms are determined by processes of cluster generation and cluster decay in a cluster plasma, where most of the atoms of a given sort are bound in clusters. We can determine the size distribution function in this case by introducing parameters of these processes: M_n, the generation rate of clusters; and τ, the cluster lifetime, assumed to be independent of the cluster size. We consider the limiting case when the cluster lifetime is sufficiently long that the average cluster size is large compared to the critical size. This corresponds to a criterion containing the ratio of the cluster life τ to the kinetic life $(k_0N)^{-1}$:

$$\beta = k_0N\tau\xi \gg 1. \quad (12.55)$$

The kinetic equation for the distribution function in this case has the form

$$\frac{\partial N_n}{\partial t} = 0 = I_n + M_n - \frac{I_n}{\tau}, \tag{12.56}$$

and in the limit of large cluster sizes, $n \gg n_c$, one can neglect cluster evaporation. That is, the second term in the expression of the collision integral (12.51) can be neglected, and the kinetic equation (12.56) for large n takes the form

$$\frac{d}{dn}\left(n^{2/3}N_n\right) + \frac{N_n}{\beta} = 0. \tag{12.57}$$

This corresponds to the condition $N \gg N_{sat}(T)$, or $\Delta\varepsilon \gg Tn_c^{1/3}$. Here we take into account the fact that clusters being generated concentrate in a size range of the order of the critical size, so that for large clusters $M_n = 0$. The solution of Eq. (12.57) is

$$N_n = \frac{C}{n^{2/3}} \exp\left(-\frac{3n^{1/3}}{\beta}\right), \qquad n \gg n_c. \tag{12.58}$$

From this we find the average cluster size supposing that it is determined by large clusters. From formula (12.58) we have

$$\bar{n} = \frac{\int n^2 N_n\, dn}{\int n N_n\, dn} = \frac{80}{81}\frac{C\beta^7}{N_{tot}}, \qquad n_c \ll \beta^3.$$

If we assume that large clusters give the main contribution to the normalization condition of the size distribution function, we get

$$N_{tot} = \frac{2}{9}C\beta^4, \qquad \bar{n} = \frac{40}{9}\beta^3, \qquad N_n = \frac{C}{n^{2/3}} \exp\left(-3\frac{n^{1/3}}{\beta}\right). \tag{12.59}$$

We can construct the size distribution function of clusters of all sizes for the regime under consideration. The equality of the total rates of atomic attachment and cluster evaporation leads to the relation

$$\int_0^\infty n^{2/3} N_n\, dn \exp\left(\frac{\Delta\varepsilon}{Tn^{1/3}}\right) = \frac{2}{9}C\beta^3 S. \tag{12.60}$$

Here $S = N/N_{sat}(T)$ is the degree of supersaturation, and in the regime we are examining, we have $S \gg 1$. We take into account that the rate of atom attachment is determined by large clusters, and insert the size distribution

function (12.58) in the right-hand side of the relation. Using this asymptotic expression, we can represent the size distribution function of clusters of all sizes in the form

$$N_n = \frac{C}{n^{2/3}} \exp\left(-\frac{a}{n} - \frac{3n^{1/3}}{\beta} \right). \tag{12.61}$$

The parameter a can be found from the relation (12.60), and if we suppose the integral (12.60) to be convergent in a narrow region of n, then the result is

$$a = (3\pi)^{1/7} (\beta^3 S)^{4/7} \left(\frac{\Delta\varepsilon}{3T} \right)^{9/7} = 0.34 (\beta^3 S)^{4/7} \left(\frac{\Delta\varepsilon}{T} \right)^{9/7}. \tag{12.62}$$

From this it follows that $a \gg 1$, and this parameter is connected with the cluster critical size. For this form of the distribution function, large cluster sizes give the principal contribution to the normalization condition, so that from Eq. (12.59) we have $N_{\text{tot}} = \frac{2}{9} C\beta^4$. This approximation gives the size distribution function of clusters for all n, and allows one to understand how it depends on the character of processes in a cluster plasma.

12.15 COAGULATION OF CLUSTERS IN EXPANDING GAS

A frequently employed method for the generation of clusters is to have a weakly ionized vapor expand as a free jet. This process generates a beam of clusters or cluster ions, and can be used for thin-film deposition on surfaces. If neutral clusters of large sizes are formed in a plasma, cluster growth proceeds by cluster coagulation as represented by the scheme

$$\mathrm{A}_l + \mathrm{A}_m \rightarrow \mathrm{A}_{l+m}. \tag{12.63}$$

That is, cluster growth results from the coalescence of colliding clusters. As a gas expands and the cluster density decreases, the process becomes slower. It terminates when a typical expansion time τ_{ex} is of the order of the characteristic time $(N_n k_n)^{-1}$ for cluster coagulation, where N_n is the number density for clusters consisting of n atoms, and k_n is the rate constant for their coalescence. Introducing the total number density of atoms inside clusters N_0, which must be conserved in the absence of expansion, we have $N_n \sim N_0/n$. This leads to the equation

$$n \sim N_0 k_n \tau_{\text{ex}} \tag{12.64}$$

for the average cluster size at the completion of the process.

Taking clusters to be both liquid and spherical, we assume that each contact between clusters leads to the joining of the clusters. Then the rate constant for the coagulation of two clusters of numbers of atoms n_1 and n_2 is

$$k(n_1, n_2) = \pi(r_1 + r_2)^2 \left(\frac{8T}{\pi\mu}\right)^{1/2} = k_0\left(n_1^{1/3} + n_2^{1/3}\right)^2 \sqrt{\frac{n_1 + n_2}{n_1 n_2}}. \quad (12.65)$$

Here k_0 is given by Eq. (12.47), and r_1 and r_2 are the radii of clusters with n_1 and n_2 atoms, respectively. This expression corresponds to the liquid-drop model of clusters. Then, using $k_n = k_0 n^{2/3}$ in Eq. (12.64), we find the average cluster size at the end of the process to be

$$\bar{n} = C(k_0 N_0 \tau_{ex})^{6/5}, \qquad \bar{n} \gg 1, \quad (12.66)$$

where $C \sim 1$ is a numerical coefficient. Its value can be obtained from the analysis of the kinetics of the cluster growth, which leads to $C = 3$. Equation (12.66) is the asymptotic expression for the average number of cluster atoms, valid when the inequality

$$N_0 k_0 \tau_{ex} \gg 1$$

holds true.

Equation (12.66) gives a faster cluster growth than in the case when growth is governed by processes (12.36), if the number of free atoms is small compared to the number of bound atoms. Thus, the growth of neutral clusters under conditions of high cluster density proceeds by the coagulation of clusters as in (12.63), if most of the atoms are bound in clusters.

12.16 METALLIC CLUSTERS IN ARC PLASMAS

As follows from Eq. (12.43), a uniform gas with an admixture of clusters is a nonstationary system that is inconsistent with thermodynamic equilibrium. The evaporation of a cluster or the attachment of parent atoms to a cluster is a transitional step in the evolution of a cluster into either an atomic vapor or a condensed system. An example of such an evolving system is a nonuniform cluster plasma such as occurs in the positive column of an arc in a high pressure buffer gas with a trace impurity of a heat-resistant metal. For simplicity, we assume the clusters to be charged, and because the charge on the clusters prevents them from contacting each other, the growth and decay of clusters follows the scheme

$$\mathrm{M}_n + \mathrm{M} \leftrightarrow \mathrm{M}_{n+1} \quad (12.67)$$

as shown in Eq. (12.36), where M is a metallic atom, and M_n is a cluster consisting of n atoms.

Due to the high pressure of the buffer gas, transport processes are slow, and local thermodynamic equilibrium obtains in the system. Clusters can then persist in low-temperature regions. In this scenario, attachment of metallic atoms or clusters to walls of the discharge tube corresponds to loss of the metal. To compensate for this, chemical regeneration is used, in which the metal is introduced in the form of gaseous molecules MX_k, where X is a halogen atom. This compound decomposes at high temperatures, so that equilibrium at a given point in the discharge is expressed by the reactions

$$MX_k \leftrightarrow M + kX. \tag{12.68}$$

Our goal is to find criteria for the existence of clusters in this system in an intermediate region of the discharge.

With the binding energy per halogen atom given by ε_X, the total binding energy of atoms in the compound MX_k is $k\varepsilon_X$. The binding energy per atom for a bulk metal is designated by ε_M. The inequality

$$\varepsilon_M < k\varepsilon_X$$

is a rough criterion for the existence of the chemical compound at low temperatures. From the chemical equilibrium of MX_k one can estimate a typical temperature T_1 where this compound decomposes into atoms, and from the chemical equilibrium of clusters one can find a typical temperature T_2 where clusters are transformed into atoms. These estimates are

$$T_1 = \frac{\varepsilon_X}{\ln(N_0/[X])}, \qquad T_2 = \frac{\varepsilon_M}{\ln(N_0/[M])}. \tag{12.69}$$

Here [X] denotes the total number density of free and bound atoms X, N_0 is a typical atomic number density, and [M] is the total number density of free and bound metallic atoms. Clearly, clusters exist in the temperature range

$$T_1 < T < T_2. \tag{12.70}$$

One can determine the temperature for decomposition of clusters more precisely from the expression

$$[M] \sim N_{sat}(T_3),$$

where $N_{sat}(T)$ is the saturated vapor density of atoms at the temperature T. The temperature designated as T_3 must be approximately the same as T_2, and the difference between these values is a measure of the accuracy of definition of these temperatures. If [X] ~ [M], the possibility of the existence of clusters stated in Eq. (12.70) corresponds to the condition $\varepsilon_X < \varepsilon_M$, which, together with the condition for the existence of MX_k, gives the constraint

$$\varepsilon_X < \varepsilon_M < k\varepsilon_X \tag{12.71}$$

for the presence of clusters in the system under consideration.

TABLE 12.1. Parameters of Some Compounds of Heat-Resistant Metals

Compound	ε_X, eV	ε_M, eV	T_1, 10^3 K	T_2, 10^3 K	T_3, 10^3 K	Cluster Existence
$HfCl_4$	4.2	6.0	2.4	3.0	3.2	+
HfF_4	6.3	6.0	3.5	3.0	3.2	–
$ThCl_4$	4.7	5.8	2.6	3.0	3.1	+
ThF_4	6.2	5.8	3.5	3.0	3.1	–
$TiBr_4$	3.0	4.4	1.7	2.2	2.3	+
$TiCl_4$	3.5	4.4	2.0	2.2	2.3	+
UCl_4	3.8	5.1	2.1	2.6	2.7	+
UF_4	5.7	5.1	3.2	2.6	2.7	–
VCl_4	3.0	4.7	1.7	2.4	2.4	+
VF_4	4.4	4.7	2.5	2.4	2.4	–
$ZrCl_4$	4.3	5.9	2.4	3.0	3.1	+
ZrF_4	6.5	5.9	3.6	3.0	3.1	–
$NbCl_5$	3.3	7.1	1.8	3.6	3.4	+
NbF_5	5.2	7.1	2.9	3.6	3.4	+
VF_5	4.1	4.7	2.3	2.4	2.4	–
IrF_6	2.2	6.4	1.2	3.2	3.2	+
MoF_6	3.9	6.3	2.2	3.2	3.2	+
UCl_6	3.0	5.1	1.7	2.6	2.7	+
UF_6	4.7	5.1	2.6	2.6	2.7	–
WCl_6	3.0	8.4	1.7	4.2	4.0	+
WF_6	4.5	8.4	2.5	4.2	4.0	+

Table 12.1 lists values of the parameters appearing in the above conditions for some compounds of heat-resistant metals. The binding energies ε_X and ε_M are obtained from Gibbs free energies or from enthalpies for these systems. From this, the accuracy of the temperatures T_1 and T_2 is estimated to be within about 100 K. The data relate to the number densities of metallic atoms $[M] = 10^{15}\ cm^{-3}$ and the number densities of halogen atoms $[X] = 10^{16}\ cm^{-3}$. Thus, insertion of some metallic compounds into the arc plasma may lead to the existence of metallic clusters in some regions in the arc, and these cases are marked in the table by +. A cluster plasma exists in these cases.

12.17 INSTABILITY IN A CLUSTER PLASMA

In a cluster plasma, the clusters exist in an intermediate region of the discharge-tube cross section where the condition (12.63) is satisfied. Then one can expect that a typical cluster size is determined by a balance between the times required for cluster growth and for transport away from the cluster region of the discharge. We shall analyze the size evolution for a large cluster located at the beginning in the cluster region. Neglecting the evaporation

process for this large cluster, we have the equation

$$\frac{dn}{dt} = Nk_0(T)\,\xi n^{2/3}, \tag{12.72}$$

where we use the rate (12.47) for the growth of the cluster. In this region of the discharge, the number density N of metallic atoms is assumed to be large compared to the number density of atoms in a saturated vapor at the same temperature. Using the diffusion mechanism for transport of clusters in a buffer gas, the distance x through which a cluster moves in the time t is $x^2 = 2D_n t$. The cluster diffusion coefficient D_n in a buffer gas as a function of its size is $D_n = D_0/n^{2/3}$, where D_0 is independent of n. Solving Eq. (12.72) with an initial cluster size n_0, we find the relation between the cluster displacement and its size to be

$$x = x_0\sqrt{1 - \left(\frac{n_0}{n}\right)^{1/3}}, \qquad x_0 = \sqrt{\frac{6D_0}{Nk_0\,\xi n_0^{1/3}}}.$$

It follows from this result that if the initial distance of a test cluster from the boundary of the cluster region exceeds x_0, the growing cluster remains in the cluster region.

The cluster we are examining is one in which an atomic vapor forms clusters located in the cluster region of an arc discharge. The development of the instability alters the size distribution of the clusters. As a result of cluster growth, the number density of free atoms decreases and clusters that are not large evaporate. Hence, the number of large clusters decreases with time and their size increases. This process stops when large clusters alter the gas discharge parameters and the temperature distribution across the cross section of the discharge tube is changed. Thus, this nonuniform cluster plasma is nonstationary.

CHAPTER 13

PLASMA IN EXTERNAL FIELDS

13.1 MOTION OF AN ELECTRON IN A GAS IN EXTERNAL FIELDS

Electric and magnetic properties of a weakly ionized gas are determined in large part by the behavior of electrons in the gas. Hence we begin by examining the motion of an electron in a gas subjected to an external field. The analysis can be accomplished with the kinetic equation if the collision integral is taken in the tau approximation. Then the kinetic equation for electrons has the form

$$\frac{\partial f}{\partial t} + \frac{\mathbf{F}}{m_e} \cdot \frac{\partial f}{\partial \mathbf{v}} = -\frac{f - f_0}{\tau}, \tag{13.1}$$

where $\mathbf{F}$ is the force acting on the electron from external fields, m_e is the electron mass, $1/\tau = N_a v \sigma_{ea}$ is the frequency of electron–atom collisions, N_a is the number density of atoms, and σ_{ea} is the cross section for electron–atom collisions. For simplicity, we assume τ to be independent of the collision velocity.

The most general form of the external force $\mathbf{F}$ that allows us to analyze a variety of aspects of the electron behavior is

$$\mathbf{F} = -e\mathbf{E}\exp(-i\omega t) - (e/c)(\mathbf{v} \times \mathbf{H}), \tag{13.2}$$

where $\mathbf{E}$ and $\mathbf{H}$ are the electric and magnetic fields, ω is the frequency of the electric field, and $\mathbf{v}$ is the electron velocity. We assume the magnetic field to be constant, and the electric field to be harmonic. We define a coordinate

system such that the vector **H** is directed along the z-axis and the vector **E** lies in the xz plane.

We multiply the kinetic equation (13.1) by $m_e\mathbf{v}$ and integrate over the electron velocity. Then we obtain the equation of motion for the electron in the form

$$m_e\frac{d\mathbf{w}_e}{dt} + m_e\frac{\mathbf{w}_e}{\tau} = -e\mathbf{E}\exp(-i\omega t) - \frac{e}{c}\mathbf{w}_e \times \mathbf{H}, \tag{13.3}$$

where $\mathbf{w}_e$ is the electron drift velocity. One can see from this equation that collisions of the electron with gas atoms gives rise to a frictional force $m_e\mathbf{w}_e/\tau$.

Equation (13.3) is equivalent to three scalar equations. Denoting by $\omega_H = eH/(m_e c)$ the so-called cyclotron frequency, and setting $a_x = -eE_x/m_e$ and $a_z = -eE_z/m_e$, we are led to the set of equations

$$\frac{dw_x}{dt} + \frac{w_x}{\tau} = a_x e^{i\omega t} + \omega_H w_y,$$

$$\frac{dw_y}{dt} + \frac{w_y}{\tau} = -\omega_H w_x,$$

$$\frac{dw_z}{dt} + \frac{w_z}{\tau} = a_z e^{i\omega t}.$$

The steady-state solution of this set of equations is independent of the initial conditions, and has the form

$$w_x = \frac{\tau(1 + i\omega\tau)a_x e^{i\omega t}}{1 + (\omega_H^2 - \omega^2)\tau^2 + 2i\omega\tau},$$

$$w_y = \frac{\omega_H \tau^2 a_x e^{i\omega t}}{1 + (\omega_H^2 - \omega^2)\tau^2 + 2i\omega\tau}, \tag{13.4}$$

$$w_z = \frac{\tau a_z e^{i\omega t}}{1 + i\omega\tau}.$$

13.2 CONDUCTIVITY OF A WEAKLY IONIZED GAS

The solutions in Eq. (13.4) can be used for the analysis of the behavior of a weakly ionized gas in external electric and magnetic fields. We begin with the case of the constant electric field ($\omega_H = \omega = 0$). Then the electron drift velocity **w** and consequent current **j** are

$$\mathbf{w} = -\frac{e\mathbf{E}\tau}{m_e}, \qquad \mathbf{j} = -eN_e\mathbf{w} = \Sigma_0\mathbf{E}, \qquad \Sigma_0 = \frac{N_e e^2 \tau}{m_e}, \tag{13.5}$$

where N_e is the electron number density, and Σ_0 is the plasma conductivity for a constant electric field.

We consider next a more general case on the basis of the relations (13.4). We can introduce the conductivity tensor $\Sigma_{\alpha\beta}$ in terms of a generalized Ohm's law

$$j_\alpha = \Sigma_{\alpha\beta} E_\beta, \tag{13.6}$$

which is valid at small values of the electric field strength or if the electron drift velocity is small compared to its thermal velocity. From Eqs. (13.5) and (13.6) one can obtain the general expression for the plasma conductivity tensor

$$(\Sigma_{ik}) = \Sigma_0 \begin{pmatrix} \dfrac{1 + i\omega\tau}{1 + (\omega_H^2 - \omega^2)\tau^2 + 2i\omega\tau} & \dfrac{\omega_H \tau}{1 + (\omega_H^2 - \omega^2)\tau^2 + 2i\omega\tau} & 0 \\ -\dfrac{\omega_H \tau}{1 + (\omega_H^2 - \omega^2)\tau^2 + 2i\omega\tau} & \dfrac{1 + i\omega\tau}{1 + (\omega_H^2 - \omega^2)\tau^2 + 2i\omega\tau} & 0 \\ 0 & 0 & \dfrac{1}{1 + i\omega\tau} \end{pmatrix}. \tag{13.7}$$

These results will be used for the analysis of the plasma interaction with external fields.

13.3 DIELECTRIC CONSTANT OF A WEAKLY IONIZED GAS

We can now find the connection between the dielectric tensor of a plasma and its conductivity tensor. The dielectric tensor $\varepsilon_{\alpha\beta}$ of a plasma is defined by the relation

$$D_\alpha = \varepsilon_{\alpha\beta} E_\beta, \qquad D_\alpha = E_\alpha + 4\pi P_\alpha, \tag{13.8}$$

where $\mathbf{D}$ is the electric displacement vector, and $\mathbf{P}$ is the polarization per unit volume of the plasma. That is, $\mathbf{P}$ is the dipole moment of a unit volume of the plasma produced under the action of the external electric field. In the case we are considering, the time dependence of the coordinate of an electron can be expressed as $\mathbf{r} = \mathbf{r}_0 + \mathbf{r}' \exp(i\omega t)$, where $\mathbf{r}_0$ is independent of the external field and $\mathbf{r}'$ is determined by the motion of the electron under the action of the field. Hence, the electron velocity induced by the external field is $\mathbf{w}_e = d\mathbf{r}/dt = i\omega\mathbf{r}' \exp(i\omega t)$. The plasma polarization is

$$\mathbf{P} = -e\sum_k \mathbf{r}'_k \exp(i\omega t) = -i\frac{N_e \mathbf{w}_e}{\omega},$$

where the index k labels the individual electrons, and the sum is taken over the electrons in a unit volume of the plasma. Introducing the electron current $\mathbf{j} = -eN_e\mathbf{w}_e$, Eq. (13.8) gives $\mathbf{D} = \mathbf{E} + 4\pi i\mathbf{j}/\omega$. Then from Eqs. (13.8) and (13.6) it follows that

$$\varepsilon_{\alpha\beta} = \delta_{\alpha\beta} + \frac{4\pi i}{\omega}\Sigma_{\alpha\beta}, \tag{13.9}$$

where $\delta_{\alpha\beta}$ is the Kronecker symbol, defined to be unity if both subscripts are the same, and zero if they are different. Thus the dielectric tensor of a system containing free electrons has the direct connection to the conductivity tensor expressed in Eq. (13.9).

13.4 PLASMA IN A TIME-DEPENDENT ELECTRIC FIELD

In the absence of a magnetic field, as well as in the direction of the magnetic field should it exist, the plasma conductivity is

$$\Sigma = \frac{\Sigma_0}{1 + i\omega\tau}. \tag{13.10}$$

In the limit $\omega\tau \gg 1$ the plasma conductivity does not depend on the frequency of electron–atom collisions, and the phase shift between the electric current and the electric field is $\pi/2$.

To consider this problem in more detail, we use the expansion of the electron distribution function (9.23) $f(\mathbf{v}, t) = f_0(v, t) + v_x f_1(v, t)$, and take the electric field in the form $E\cos\omega t$. This gives the set of equations

$$\begin{aligned} \frac{\partial f_0}{\partial t} + \frac{eE\cos\omega t}{3m_e}\frac{\partial(v^3 f_0)}{v^2\,\partial v} &= I(f_0), \\ \frac{\partial f_1}{\partial t} + \frac{eE\cos\omega t}{3m_e v}\frac{\partial f_0}{\partial v} &= -\nu f_1, \end{aligned} \tag{13.11}$$

analogous to (9.33), where $\nu = N_a v\sigma_{ea}^*$ is the frequency of electron–atom collisions. The solution of this set of equations depends on the connection between the field frequency ω and the frequency of the energy exchange between electrons and atoms $\nu_a \sim \nu m_e/M$. We shall consider the case where $\omega/\nu_a \sim (M/m_e)(\omega/\nu) \gg 1$. (The opposite case corresponds to a constant electric field.) Then the distribution function has the form

$$f(\mathbf{v}, t) = f_0(v) + v_x f_1(v)e^{i\omega t} + v_x f_{-1}(v)e^{-i\omega t}, \tag{13.12}$$

and the set of equations (13.11) becomes

$$\frac{a}{6v^2}\frac{d}{dv}\left[v^3(f_1 + f_{-1})\right] = I(f_0),$$

$$(i\omega + \nu) f_1 + \frac{a}{2v}\frac{df_0}{dv} = 0, \tag{13.13}$$

$$(-i\omega + \nu) f_{-1} + \frac{a}{2v}\frac{df_0}{dv} = 0,$$

where $a = eE/m_e$. This yields the electron drift velocity

$$w_x = \frac{a}{3}\left\langle \frac{1}{v^2}\frac{d}{dv}\left[\frac{\nu \cos \omega t + \omega \sin \omega t}{\omega^2 + \nu^2}\right]\right\rangle. \tag{13.14}$$

In the limit $\omega \ll \nu$, this equation transforms to (9.35) if one uses $E \cos \omega t$ instead of E.

If electron–electron collisions are neglected and Eq. (9.31) is used for the electron–atom collision integral, the solution of the set of equations (13.13) gives

$$f_0 = C \exp\left[-\int_0^v \left(T + \frac{Ma^2}{6(\omega^2 + v^2)}\right) m_e v\, dv\right]. \tag{13.15}$$

Other harmonics of the electron distribution function follow from the set of equations (13.13).

In the other limiting case, electron–electron collisions establish the Maxwell distribution function for electrons. Then Eq. (13.14) yields

$$w_x = \frac{eE}{3T_e}\left\langle v^2 \frac{\nu \cos \omega t + \omega \sin \omega t}{\omega^2 + \nu^2}\right\rangle. \tag{13.16}$$

for the electron drift velocity. The electron temperature can be found by analogy with the case of a constant electric field (Chapter 9) by means of an analysis of the balance equation for the electron energy that has the form

$$\overline{eEw \cos \omega t} = \int \frac{m_e v^2}{2} I_{ea}(f_0)\, d\mathbf{v},$$

where the bar above the symbols denotes averaging over time. Note that the expression for the electron–atom collision integral does not depend on external fields acting on a plasma. For the Maxwell distribution function, the integral of the right-hand part of the equation was calculated in Chapter 9 [see Eq. (9.42)]. This leads to the relation

$$\overline{eEw \cos \omega t} = \frac{eE}{6T_e}\left\langle \frac{v^2 \nu}{\omega^2 + \nu^2}\right\rangle.$$

Using the expression (13.16) for the electron drift velocity and taking into account the time averages $\overline{\cos^2 \omega t} = \frac{1}{2}$ and $\overline{\cos \omega t \sin \omega t} = 0$, we find the result

$$T_e - T = \frac{Ma^2}{6} \frac{\langle v^2 \nu / (\omega^2 + \nu^2) \rangle}{\langle v^2 \nu \rangle}. \tag{13.17}$$

Because the period of field oscillations is small compared to a typical time in which the electron energy changes as a result of collisions with atoms, one can consider the electron temperature to be constant. In the limit of small field frequency $\omega \ll \nu$, Eq. (13.17) agrees with Eq. (9.44) if in (9.44) the electric field strength E is replaced by the effective value $E/\sqrt{2}$.

13.5 THE HALL EFFECT

In the absence of a magnetic field, the plasma conductivity is a scalar quantity. When a magnetic field is applied to a weakly ionized gas, the conductivity acquires a tensor character. This means that an electric current can occur in directions in which the electric field component is zero. If we consider the case where a constant electric field is perpendicular to a magnetic field, then Eq. (13.7) yields ($\omega = 0$)

$$\begin{aligned} \Sigma_{xx} &= \Sigma_{yy} = \Sigma_0 \frac{1}{1 + \omega_H^2 \tau^2}, \\ \Sigma_{yx} &= -\Sigma_{xy} = \Sigma_0 \frac{\omega_H \tau}{1 + \omega_H^2 \tau^2}. \end{aligned} \tag{13.18}$$

In the limit case $\omega_H \tau \gg 1$, the total current is directed perpendicular to both the electric and magnetic fields. In this case the plasma conductivity and electric current do not depend on the collision time, because the change of the direction of electron motion is determined by the electron rotation in a magnetic field. Specifically, Eqs. (13.6) and (13.8) give

$$j_y = ecN_e E_x / H \tag{13.19}$$

in this case. We note that $\omega_H \tau \ll M/m_e$, where M is the atom mass. In the opposite case, ions would drift in the same direction as electrons, so that the total electric current would be small compared with that of Eq. (13.11). If the transverse electric current does not reach the plasma boundary, this results in a separation of charges that in turn creates an electric field that slows and eventually stops the electrons. This gives rise to an electric current in the direction perpendicular to the electric and magnetic fields. The phenomenon is known as the *Hall effect*.

We can analyze this process on the basis of the kinetic equation for electrons. Take the electric and magnetic fields to be constant and mutually perpendicular, with the electric field along the x-axis and the magnetic field along the z-axis. The electron distribution function has the form

$$f(\mathbf{v}) = f_0(v) + v_x f_1(v) + v_y f_2(v). \tag{13.20}$$

Using the same procedure as in the deduction of Eqs. (9.25) and (13.13), we obtain

$$\begin{aligned} vf_1 &= \frac{av}{\nu^2 + \omega_H^2}\frac{df_0}{dv}, \\ vf_2 &= \frac{a\omega_H}{\nu^2 + \omega_H^2}\frac{df_0}{dv}, \end{aligned} \tag{13.21}$$

where $a = eE/m_e$, and $\nu = N_a v \sigma_{ea}^*$ is the frequency of electron collisions with atoms. These equations lead to the expressions

$$\begin{aligned} w_x &= \frac{eE}{3m_e}\left\langle \frac{1}{v^2}\frac{d}{dv}\left(\frac{\nu v^2}{\nu^2 + \omega_H^2}\right)\right\rangle, \\ w_y &= \frac{eE}{3m_e}\left\langle \frac{1}{v^2}\frac{d}{dv}\left(\frac{\omega_H v^2}{\nu^2 + \omega_H^2}\right)\right\rangle. \end{aligned} \tag{13.22}$$

for the components of the electron drift velocity. In the limit $\omega_H \ll \nu$, the first of these equations transforms into Eq. (9.35).

For evaluation of the average electron energy, we use the procedure of Chapter 9 based on the balance equation for the electron energy that has the form

$$eEw_x = \int \frac{m_e v^2}{2} I_{ea}(f_0)\, d\mathbf{v}.$$

Using Eq. (13.22) for the electron drift velocity and Eq. (9.42) for the integral of the right-hand part of the equation, we obtain

$$T_e - T = \frac{Ma^2}{3}\frac{\langle v^2 \nu/(\nu^2 + \omega_H^2)\rangle}{\langle v^2 \nu\rangle}. \tag{13.23}$$

In particular, if $\nu = \text{const}$, this expression gives

$$T_e - T = \frac{Ma^2}{3(\nu^2 + \omega_H^2)}. \tag{13.24}$$

In the limit $\omega_H \gg \nu$, Eq. (13.23) yields

$$T_e - T = \frac{Ma^2}{3\omega_H^2} = \frac{Mc^2E^2}{3H^2}. \tag{13.25}$$

We now examine the case where a weakly ionized gas moves with an average velocity u in a transverse magnetic field of strength H. Then an electric field of strength $E' = Hu/c$ exists in the fixed frame of axes, where c is the light velocity. This field creates an electric current that is used for the production of electrical energy in magnetohydrodynamic (MHD) generators. The energy released in a plasma under the action of this electric current corresponds to a transformation of the flow energy of a gas into electric and heat energies. In consequence, this process leads to a deceleration of the gas flow and a decrease of its average velocity. In addition, the generation of an electric field causes an increase in the electron temperature as given by Eq. (13.25). The maximum increase of the electron temperature corresponds to the limit $\omega_H \gg \nu$. In this limit, Eq. (13.25) becomes

$$T_e - T = \frac{Ma^2}{3\omega_H^2} = \frac{1}{3}Mu^2. \tag{13.26}$$

13.6 CYCLOTRON RESONANCE

If $\omega\tau \gg 1$ and $\omega_H\tau \gg 1$, the conductivities $\Sigma_\parallel$ and $\Sigma_\perp$ in the directions parallel and perpendicular to the magnetic field are

$$\begin{aligned} \Sigma_\parallel &= \Sigma_0 \frac{1 + i\omega\tau}{1 + (\omega_H^2 - \omega^2)\tau^2 + 2i\omega\tau}, \\ \Sigma_\perp &= \Sigma_0 \frac{\omega_H\tau}{1 + (\omega_H^2 - \omega^2)\tau^2 + 2i\omega\tau}. \end{aligned} \tag{13.27}$$

The conductivity is seen to have a resonance at $\omega = \omega_H$, where its components are related by $\Sigma_\parallel = i\Sigma_\perp = \Sigma_0/2$. The resonance width is $\Delta\omega \sim 1/\tau$. This conductivity resonance is called the *cyclotron resonance*.

The cyclotron resonance has a simple physical explanation. In a magnetic field, there is a frame of reference where an electron travels in a circular orbit with the cyclotron frequency ω_H. If an electric field is applied in the plane of the circular orbit, and if this field varies so that its direction remains parallel to the electron velocity, the electron continuously receives energy from the field. As with electron motion in a constant electric field, the electron is accelerated until it collides with atoms. Hence, in both cases the conductivities are of the same order of magnitude and are expressed in terms

of the frequency $1/\tau$ of collisions between the electron and atoms. If the field frequency ω differs from the cyclotron frequency ω_H, the conductivity is considerably lower, since the conditions of interaction between the electron and field are not optimal.

We can analyze the cyclotron resonance from the standpoint of energy absorption. The power per unit volume absorbed by a plasma is $p = \mathbf{j} \cdot \mathbf{E}$. If we take the x-axis to be in the direction of the electric field, then the specific power absorbed by the plasma is

$$p = (\Sigma_{xx} + \Sigma_{xx}^*)E^2/2$$
$$= \frac{p_0}{2}\left(\frac{1 - i\omega\tau}{1 + (\omega_H^2 - \omega^2)\tau^2 - 2i\omega\tau} + \frac{1 + i\omega\tau}{1 + (\omega_H^2 - \omega^2)\tau^2 + 2i\omega\tau}\right), \tag{13.28}$$

where $p_0 = \Sigma_0 E^2$ is the specific absorbed power for the constant electric field. Absorption of energy by a plasma is connected with electron–atom collisions that lead to transfer to the atoms of energy obtained by the electrons from the field.

In the region of the cyclotron resonance, with $\omega\tau \gg 1$, $\omega_H\tau \gg 1$, and $|(\omega - \omega_H)\tau| \sim 1$, Eq. (13.28) yields

$$p = \frac{p_0}{2}\frac{1}{1 + (\omega_H - \omega)^2\tau^2}. \tag{13.29}$$

One can see that the resonant absorbed power is less than half of what is absorbed in a constant electric field. That the same order of magnitude is obtained for these values is explained by the related character of the electron motion in these cases.

13.7 MOTION OF CHARGED PARTICLES IN A NONUNIFORM MAGNETIC FIELD

We shall now explore the behavior of a charged particle in a nonuniform magnetic field as illustrated in Fig. 13.1. The particle trajectory is a helix wound around a magnetic line of force. Assume the magnetic lines of force to be close to straight lines, which is equivalent to the static case that a distance L over which the magnetic field exhibits a significant variation is large compared to the Larmor radius r_L of the particle. Within this approximation we shall analyze the motion of a charged particle in a magnetic field as in Fig. 13.1. The presence of charged particles does not influence the character of the magnetic field because of their small density, and the spatial variation of the magnetic field obeys the Maxwell equation $\operatorname{div} \mathbf{H} = 0$.

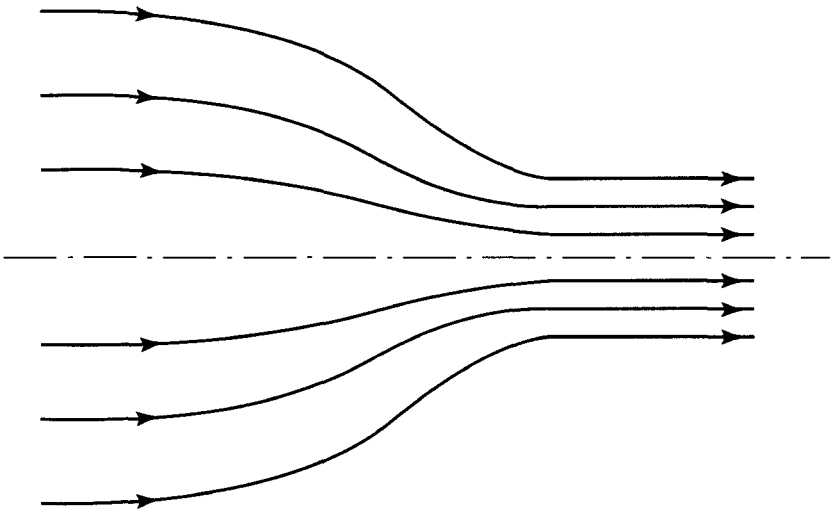

Figure 13.1 Magnetic lines of force in a magnetic trap with axial symmetry.

In the presence of cylindrical symmetry, div $\mathbf{H} = 0$ can be written as

$$\frac{1}{\rho}\frac{\partial}{\partial\rho}(\rho H_\rho) + \frac{\partial H_z}{\partial z} = 0. \tag{13.30}$$

At the axis, H_ρ is zero because of the axial symmetry of the problem. Near the axis, according to Eq. (13.30), one has

$$H_\rho = -\frac{\rho}{2}\left(\frac{\partial H_z}{\partial z}\right)_{\rho=0}.$$

The force acting on a charged particle because of the magnetic field along the axis is

$$F_z = -\frac{e}{c}v_\tau H_\rho = \frac{v_\tau \rho}{2c}\frac{\partial H_z}{\partial z}.$$

We can introduce the magnetic moment μ of the particle in the usual way as $\mu = JS/c$, where J is the particle current, S is the area enclosed by its trajectory, and c is the velocity of light . Since in this case $J = e\omega_H/(2\pi)$, and $S = \pi r_L^2$ (r_L is the Larmor radius of the particle), we have [$r_L = v_\tau/\omega_H$, $\omega_H = eH/(mc)$]

$$\mu = mv_\tau^2/(2H).$$

The force acting on the particle in the magnetic field direction can also be written

$$F_z = -\mu \frac{\partial H_z}{\partial z}.$$

The minus sign means that the force is in the direction of decreasing magnetic field.

One can prove that the magnetic moment of the particle is an integral of the motion; that is, it is a conserved quantity. We can analyze the particle motion along a magnetic line of force when averaged over gyrations. The equation of motion along the magnetic field gives $m\,dv_z/dt = F_z = -\mu\,dH_z/dz$, and since $v_z = dz/dt$, it follows from this that $d(mv_z^2/2) = -\mu\,dH_z$. From the energy conservation condition for the particle we have

$$\frac{d}{dt}\left(\frac{mv_\tau^2}{2} + \frac{mv_x^2}{2}\right) = \frac{d}{dt}\left(\mu H_z + \frac{mv_z^2}{2}\right)$$

$$= \frac{d}{dt}(\mu H_z) - \mu\frac{dH_z}{dt} = H_z\frac{d\mu}{dt} = 0.$$

This yields the equation for the magnetic moment of the particle motion

$$\frac{d\mu}{dt} = 0, \tag{13.31}$$

so that the magnetic moment is conserved during the motion of the particle.

We can now analyze the motion of a charged particle in a magnetic mirror field such as that shown in Fig. 13.1. As the magnetic field increases, part of the particle kinetic energy $mv_\tau^2/2$ increases proportionally. If this value becomes as large as the total initial kinetic energy, motion of the particle along the z-axis stops, and the particle starts to move in the opposite direction. This is the principle of a magnetic mirror, in which a particle moves along a magnetic line of force between a region with a weak magnetic field and a region with a strong magnetic field. Take $H_{\min}$ to be the minimum magnetic field and $H_{\max}$ to be the maximum magnetic field along this magnetic line of force; θ is the angle between the particle velocity and magnetic field line at the field minimum. Then if this angle exceeds θ_m, given by the relation

$$\sin^2 \theta_m = H_{\min}/H_{\max}, \tag{13.32}$$

the particle reflects from the region of the strong magnetic field and is trapped in a bounded space.

The above principle is the basis of various magnetic traps. It acts for both positively and negatively charged particles, so that this arrangement works for

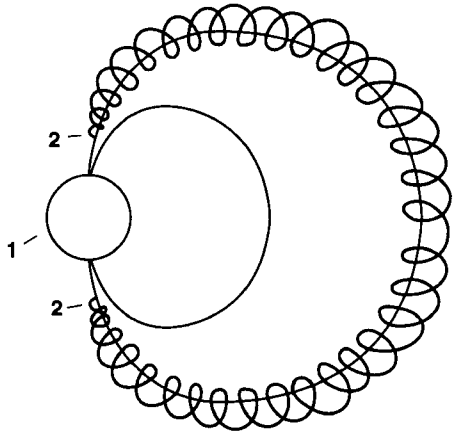

Figure 13.2 Trajectory of a charged particle captured by the magnetic field of the Earth as the particle moves along a magnetic line of force: 1, the Earth; 2, points of reflection of the particle.

both electrons and protons. Radiation belts of the Earth (see Figs. 1.5 and 13.2) act according to this principle. Fast electrons and protons captured in the region of a weak magnetic field of the Earth move along magnetic lines of force and are reflected near the Earth's poles where the magnetic field is relatively strong. Collisions of these particles with others lead to escape from the magnetic trap. Because of their larger mass, protons have a longer lifetime in the Earth's magnetic trap than do electrons, and hence the number of captured protons is greater than for electrons. In addition, due to the influence of the solar wind, this magnetic trap acts more effectively on the side of the Earth opposite to the Sun.

13.8 EXCITATION OF A WEAKLY IONIZED GAS BY EXTERNAL FIELDS

A plasma is a convenient means to accomplish energy transfer from an external electric field to a gas. It is used in plasma generators, gas lasers, and other devices for transformation of electrical energy to other forms. This method allows one to transfer a high specific energy and to create a nonequilibrium population of atomic levels and systems.

We can find the specific power transformed by a gas-discharge plasma in the small-electric-current regime where interaction of charged particles is nonessential and electric currents in the gas do not change its properties significantly. One electron moving in a gas in an external electric field E transfers to atoms of the gas the power eEw, where w is the electron drift velocity. Therefore the power transformed per unit volume of a plasma is

$$P = N_e eEw_e = N_e N_a w_e (eE/N_a), \tag{13.33}$$

TABLE 13.1. Parameters for the Excitation of a Weakly Ionized Gas in an External Electric Field[a]

Gas	ε eV	E/N Td	w_e 10^6 cm/s	η_{elas} %	η_{vib} %	η_{rot} %	η_{el} %	P/N_eN 10^{-29} W/cm^3	$(1/N_e)\,dT/dt$ 10^{-7} K cm^3/s
He	1	1.2	0.53	100	—	—	—	0.1	0.3
	3	3.6	0.94	100	—	—	—	0.54	1.6
Ar	1	0.2	0.2	100	—	—	—	0.006	0.02
	3	1.4	0.35	100	—	—	—	0.08	0.23
H_2	1	15	2.4	16	79	5	—	5.8	12
	3	60	7	6	93	1	—	67	140
N_2	1	4	0.93	8	83	9	—	0	1.2
	3	105	11	0.2	53	0.5	46	180	380
CO	1	17	3.1	0.7	98	1	—	8.4	17
	3	130	13	0.1	54	0.1	46	270	560
CO_2	1	2.4	7	0.1	85	15	—	2.7	4.3
	3	60	13	0.1	97	0.1	3	120	200

[a]Here N is the number density of gas atoms or molecules; 1 townsend (Td) is 1×10^{-17} Vcm^2; η is the energy fraction that goes into elastic (elas), vibrational (vib), rotational (rot), and electronic (elec) degrees of freedom; P/N_eN is the specific released energy; and $(1/N_e)\,dT/dt$ is the specific temperature variation.

where N_e is the electron number density, and N_a is the number density of atoms or molecules of the gas. Note that the electron drift velocity w_e depends on the ratio eE/N_a.

For an understanding of the practical physical quantities associated with the energy transformation process, Table 13.1 gives the parameters of Eq. (13.33) for mean electron energies of 1 and 3 eV. In addition, the table contains the rate of the temperature change,

$$\frac{dT}{dt} = N_e \frac{eE}{N_a} \frac{w_e}{c_p}, \tag{13.34}$$

in the first stage of heating of the gas.

The quantity c_p is the heat capacity at constant pressure per molecule. Table 13.1 contains also the pathways of energy consumption: η is the percentage of the energy transformed to the corresponding degree of freedom. In molecular gases in the first stage of the process, energy is transformed primarily to vibrational excitation. This is a property employed in gas-discharge molecular lasers that generate radiation by vibrational–rotational transitions of molecules.

To show the high efficiency for this method of energy input, we compare it with heating of a gas through the walls of an enclosure containing the gas.

Assuming that heat transfer occurs by thermal conductivity, we have the estimate

$$q \sim \kappa \Delta T / l$$

for the heat flux, where κ is the thermal conductivity coefficient, ΔT is the difference of temperatures for the walls of the enclosure, and l is a dimension of the enclosure. From this it follows that the specific power introduced by heating the enclosure walls is

$$P \sim \kappa \Delta T / l^2.$$

For a numerical estimate we take $\Delta T \sim 1000$ K, $\kappa \sim 10^{-3}$ W/(cm K) (a value corresponding to the thermal conductivity coefficient of air at $T \sim 1000$ K), and $l \sim 1$ cm. The result is $P \sim 1$ W/cm^3. Such a specific power is reached at atmospheric pressure and a number density of electrons of $N_e \sim 10^9$ cm^{-3}. Because the electron number density in a weakly ionized gas can be higher by several orders of magnitude, the electrical method for energy input into a gas by means of electrons is far more effective than gas heating.

13.9 MAGNETOHYDRODYNAMIC EQUATIONS

At high plasma densities it is necessary to take into account the fields produced by plasma motion. These fields, which are due to distribution and motion of a plasma, affect the motion of a plasma; that is, the plasma parameters and fields produced by plasma are interrelated. The motion of a plasma and variation of its parameters can be described by the continuity equation for the number density of electrons and ions (9.5), the equation for the average momentum of electrons and ions (9.8), Poisson's equation, and Maxwell's equations. The resulting set of equations is called the set of *equations of magnetohydrodynamics* and has the form

$$\begin{aligned}
\frac{\partial N}{\partial t} + \operatorname{div}(N\mathbf{w}) &= 0, \\
\frac{\partial \mathbf{w}}{\partial t} + (\mathbf{w} \cdot \nabla)\mathbf{w} + \frac{\nabla p}{mN} - \frac{\mathbf{F}}{N} &= 0, \\
\operatorname{div} \mathbf{E} &= 4\pi(N_i - N_e), \\
\operatorname{curl} \mathbf{H} &= \frac{4\pi}{c}\mathbf{j} - \frac{1}{c}\frac{\partial \mathbf{E}}{\partial t}, \\
\operatorname{curl} \mathbf{E} &= -\frac{1}{c}\frac{\partial \mathbf{H}}{\partial t}, \\
\operatorname{div} \mathbf{H} &= 0.
\end{aligned} \tag{13.35}$$

The first two equations can be written both for electrons and ions. Here $\mathbf{w}$ and N are the drift velocity and the number density of electrons or ions, respectively. To (13.35) we must add an equation of state of the type (9.11) and the thermodynamic equation for the process (for instance, the adiabatic equation of the process must be added if the variation of its parameters has an adiabatic character). These equations interrelate the number density, the temperature, and the pressure of plasma particles. We must add to these equations also Ohm's law relating the plasma current and the electric field strength. The set of hydrodynamic equations with the addition of the above-mentioned equations and the initial conditions will give a complete description of plasma evolution.

13.10 HIGH-CONDUCTIVITY PLASMA IN A MAGNETIC FIELD

A plasma with high conductivity will have electrons with velocities considerably greater than the velocities of the ions. Then the electric current is due to electrons and is given by

$$\mathbf{j} = -eN_e\mathbf{w}_e,$$

where $\mathbf{w}_e$ is the drift velocity of the electrons, and N_e is their number density. If the motion occurs in a magnetic field, an additional electric field is produced in the laboratory frame of axes, whose strength is

$$\mathbf{E}' = \frac{1}{c}(\mathbf{w}_e \times \mathbf{H}) = -\frac{1}{ecN_e}(\mathbf{j} \times \mathbf{H}). \tag{13.36}$$

This field acts on the electrons, giving rise to an additional force acting on the entire plasma. The force per unit volume of the plasma is

$$e\mathbf{E}'N_e = -\frac{1}{c}(\mathbf{j} \times \mathbf{H}). \tag{13.37}$$

If the plasma conductivity is sufficiently high, its response to the electric field (13.36) will result in the movement of electrons. This movement will continue until separation of the electrons and ions gives rise to an internal electric field in the plasma,

$$\mathbf{E} = -\frac{1}{c}(\mathbf{w}_e \times \mathbf{H}), \tag{13.38}$$

which will compensate the field (13.36). We insert equation (13.38) into the Maxwell equation $-\partial\mathbf{H}/\partial t = c$ curl $\mathbf{E}$, which yields

$$\frac{\partial \mathbf{H}}{\partial t} = \text{curl}(\mathbf{w}_e \times \mathbf{H}). \tag{13.39}$$

We shall analyze the variation of the magnetic field and the plasma motion when the electric current is due to electrons and the plasma conductivity is high. We transform equation (13.39) by writing $\text{curl}(\mathbf{w}_e \times \mathbf{H}) = \mathbf{w}_e \text{ div } \mathbf{H} + (\mathbf{H} \cdot \nabla)\mathbf{w}_e - (\mathbf{w}_e \cdot \nabla)\mathbf{H} - \mathbf{H} \text{ div } \mathbf{w}_e$. Using the Maxwell equation $\text{div } \mathbf{H} = 0$, and taking the expression for $\text{div } \mathbf{w}_e$ from the continuity equation for electrons, we obtain

$$\frac{\partial \mathbf{H}}{\partial t} - \frac{\mathbf{H}}{N_e}\frac{\partial N_e}{dt} + (\mathbf{w}_e \cdot \nabla)\mathbf{H} - \frac{\mathbf{H}}{N_e}(\mathbf{w}_e \cdot \nabla)N_e = (\mathbf{H} \cdot \nabla)\mathbf{w}_e. \quad (13.40)$$

We divide this equation by N_e and find that

$$\frac{d}{dt}\left(\frac{\mathbf{H}}{N_e}\right) = \left(\frac{\mathbf{H}}{N_e} \cdot \nabla\right)\mathbf{w}_e, \quad (13.41)$$

where

$$\frac{d}{dt}\left(\frac{\mathbf{H}}{N_e}\right) = \frac{\partial}{\partial t}\left(\frac{\mathbf{H}}{N_e}\right) + (\mathbf{w}_e \cdot \nabla)\frac{\mathbf{H}}{N_e}$$

is the derivative at a point that moves with the plasma.

To analyze the motion of an element of plasma volume with length $d\mathbf{l}$ and cross section $d\mathbf{s}$ containing $N_e\, d\mathbf{s}\, d\mathbf{l}$ electrons, we assume at first that the vector $d\mathbf{l}$ is parallel to the magnetic field $\mathbf{H}$ so that the magnetic flux through this elementary plasma volume is $H ds$. If the plasma velocity at one end of the segment $d\mathbf{l}$ is $\mathbf{w}_e$, then at its other end the velocity is $\mathbf{w}_e + (d\mathbf{l} \cdot \nabla)\mathbf{w}_e$, so that the variation of the segment length during a small time interval δt is $\delta t\,(d\mathbf{l} \cdot \nabla)\mathbf{w}_e$. Hence, the length of the segment satisfies the equation

$$\frac{d}{dt}(d\mathbf{l}) = (d\mathbf{l} \cdot \nabla)\mathbf{w}_e,$$

which is identical to equation (13.41). From this it follows: first, that in the course of plasma evolution the segment $d\mathbf{l}$ has the same direction as the magnetic field; and, second, that the length of the plasma element remains proportional to the quantity H/N_e, that is, the magnetic flux through this plasma element does not vary with time during the plasma motion. Thus, the magnetic lines of force are frozen into the plasma, that is, their direction is such that the plasma electrons travel along these lines. Remember that this is the case when the plasma conductivity is high.

To find the steady-state motion of a high-conductivity plasma, we start with equation (13.38), which gives the force on each plasma electron as

$$\mathbf{F} = -e\mathbf{E} = \frac{e}{c}(\mathbf{w}_e \times \mathbf{H}) = -\frac{1}{cN_e}(\mathbf{j} \times \mathbf{H}).$$

Inserting into the expression for the force the current density $\mathbf{j} = (c/4\pi)\text{curl}\,\mathbf{H}$, we obtain

$$\mathbf{F} = -\frac{1}{cN_e}(\mathbf{j} \times \mathbf{H}) = \frac{1}{4\pi N_e}(\mathbf{H} \times \text{curl}\,\mathbf{H}) = \frac{1}{4\pi N_e}\left(\frac{1}{2}\nabla H^2 - (\mathbf{H} \cdot \nabla)\mathbf{H}\right). \tag{13.42}$$

We now substitute equation (13.42) into the second equation of the set (13.35), and we assume that the drift velocity of the electrons is considerably smaller than their thermal velocity. Hence, we can neglect the term $(\mathbf{w}_e \cdot \nabla)\mathbf{w}_e$ compared to the term $\nabla p/(mN_e)$, and obtain

$$\nabla\left(p + \frac{H^2}{8\pi}\right) - \frac{(\mathbf{H} \cdot \nabla)\mathbf{H}}{4\pi} = 0. \tag{13.43}$$

The quantity $H^2/(8\pi)$ is called the *magnetic field pressure* or *magnetic pressure*; it is the pressure that the magnetic field exerts on the plasma.

13.11 PINCH EFFECT

We next analyze the properties of a cylindrical plasma column maintained by a direct current. Here the magnetic lines of force are cylinders, and because of the axial symmetry, equation (13.43) for the direction perpendicular to the field and current has the form

$$\nabla\left(p + \frac{H^2}{8\pi}\right) = 0.$$

The solution of this equation shows that the total pressure $p + H^2/(8\pi)$, which is the sum of the gas kinetic pressure and the magnetic field pressure, is independent of the transverse coordinate. Let the radius of the plasma column be a and the current in it be I, so that the magnetic field at the surface of the column is $H = 2I/(ca)$. The total pressure outside the column near its surface is equal to the magnetic field pressure $I^2/(2\pi c^2 a^2)$, and the total pressure inside the plasma column is equal to the gas kinetic pressure p. Equating these two pressures, we find the radius of the plasma column to be

$$a = \frac{I}{c\sqrt{2\pi p}}. \tag{13.44}$$

An increase in the current of the plasma column is accompanied by a corresponding increase in the magnetic field, which gives rise to a contraction of the plasma column. This phenomenon is called the *pinch effect*, and the state of the plasma column itself is known as *z-pinch*.

13.12 SKIN EFFECT

To consider the penetration of slowly varying fields into a plasma, we take the characteristic frequency of these fields to be small compared to the plasma frequency ω_p. Ohm's law for the plasma has the simple form

$$\mathbf{j} = \Sigma \mathbf{E},$$

where $\mathbf{j}$ is the current density in the plasma, $\mathbf{E}$ is the electric field strength, and Σ is the plasma conductivity. For the description of the field variation in the plasma, it is necessary to add the Maxwell equations

$$\operatorname{curl} \mathbf{H} = \frac{4\pi}{c}\mathbf{j} - \frac{1}{c}\frac{\partial \mathbf{E}}{\partial t}, \qquad \operatorname{curl} \mathbf{E} = -\frac{1}{c}\frac{\partial \mathbf{H}}{\partial t}, \qquad \operatorname{div} \mathbf{H} = 0$$

to Ohm's law, where $\mathbf{H}$ is the magnetic field strength.

Assume the typical frequency ω of variation of the external fields to be small compared to the plasma conductivity Σ, so that the first Maxwell equation has the form $\operatorname{curl} \mathbf{H} = 4\pi\Sigma\mathbf{E}/c$. Using this in the second Maxwell equation and taking the third one into account, we obtain

$$\frac{\partial \mathbf{H}}{\partial t} = \frac{c^2}{4\pi\Sigma}\Delta\mathbf{H}. \tag{13.45}$$

The equation for the electric field has a similar form. From this equation, one can find that a typical size corresponding to the field distribution under the conditions considered is

$$l \sim \sqrt{\frac{c^2}{4\pi\omega\Sigma}}. \tag{13.46}$$

If this size is small compared to a plasma size, external fields are concentrated near the plasma surface in a layer of a depth $\sim l$ and do not penetrate inside the plasma. This phenomenon is called the *skin effect*, and the layer into which external fields penetrate is called the *skin layer*. According to Eq. (13.46), the thickness of the skin layer decreases with increasing plasma conductivity and increasing frequency of variation of the fields.

A numerical example of the skin effect can be given for the plasma of the Earth's ionosphere at an altitude of about 100 km. The plasma conductivity is $\Sigma \sim 10^9$ Hz and the plasma frequency is $\omega_p \sim 3 \times 10^7$ Hz. For frequencies of the order of the plasma frequency, the penetration depth is of the order of 1 m. Electromagnetic waves with frequencies smaller than the plasma frequency cannot pass through the Earth's ionosphere.

13.13 RECONNECTION OF MAGNETIC LINES OF FORCE

In a cold plasma of high conductivity, magnetic lines of force are frozen in the plasma. This means that internal magnetic fields support electric currents inside the plasma. But plasma motion and the interaction of currents may cause a short circuit of some currents. This leads to an instability referred to as the reconnection of magnetic lines of force. As a result of this process, the energy of the magnetic fields is transformed into plasma energy in an explosive process that generates plasma fluxes. This phenomenon is observed in solar plasmas. Various solar plasma structures, such as spicules and prominences, result from this phenomenon.

We consider first a simple example, where there are two antiparallel currents of amplitude I located a distance $2a$ apart, and with length $l \gg a$. We assume these currents have transverse dimensions small compared to a. Taking the z-axis along the direction of the currents, taking the plane of the currents to be xz, and placing the origin of the coordinates midway between the currents, we find the magnetic field strength at distances $r \ll l$ from the origin to be

$$H_x = H_0 y\left(\frac{1}{(x-a)^2+y^2} + \frac{1}{(x+a)^2+y^2}\right),$$

$$H_y = -H_0\left(\frac{x-a}{(x-a)^2+y^2} + \frac{x+a}{(x+a)^2+y^2}\right),$$

where $H_0 = 2I/(ca)$. From this it follows that the energy released from reconnection of these currents can be estimated to be

$$\varepsilon = \int \frac{H^2}{8\pi}\, d\mathbf{r} \sim \frac{I^2 l}{c^2}.$$

This means that the released energy per unit length of the conductors is constant near them.

This estimate can be used for understanding the general properties of a turbulent plasma of high conductivity in a magnetic field. The plasma is characterized by a typical drift velocity v of the electrons and a typical length Δr over which this velocity varies. The energy of this plasma is contained both in the plasma motion and in its magnetic fields, which are of the order of $H \sim eN_e v/(c\,\Delta r)$, where N_e is the number density of electrons. As a result of reconnection of magnetic lines of force and reclosing of currents, transformation of the plasma magnetic energy into energy of its motion takes place, followed by a reverse transformation. In the end, these forms of energy will be transformed into heat. A typical time of reconnection is $\tau \sim \Delta\, r/v$. This

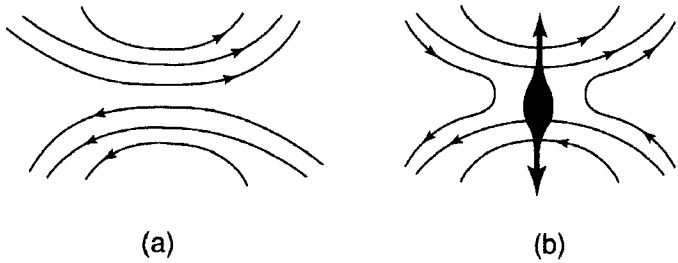

Figure 13.3 Reconnection of magnetic lines of force: (a) before reconnection; (b) after reconnection. A dark plasma that occurs as a pulse as a result of the reconnection moves in two opposite directions perpendicular to the lines of force.

plasma can be supported by external fields. Figure 13.3 gives an example of reconnection of magnetic lines of force. Released energy is transferred to a plasma and generates intense plasma flows. This phenomenon is of importance for the Sun's plasma. Then the resulting plasma flow inside the Sun creates a shock wave that is responsible for generation of X-rays. The plasma flows outside the Sun generate a hot plasma in the Sun's corona.

CHAPTER 14

INSTABILITIES OF EXCITED GASES

14.1 CONVECTIVE INSTABILITY OF GASES

Currents in a plasma lead to its heating, and thus cause new forms of gas motion that support the heat transport. Such heat transport provided by gas flows is called *convection.* It consists of the movement of streams of hot gas to a cooler region and streams of cold gas to a warmer region. Conditions for the development of this heat transport mechanism will be considered below.

To find the stability conditions for a gas with a temperature gradient dT/dz oriented in the same direction as an external force field, we assume the gas to be in equilibrium with this external force. If the external force is directed along the negative z-axis, the number density of gas molecules decreases with increase of z. We consider two elements of gas of the same volume located a distance dz from each other, and calculate the energy required for an exchange of their positions. The mass of the element with the smaller z-coordinate is larger by ΔM than that with the larger coordinate, so the work required for the exchange is $\Delta M g dz$, where g is the force per unit mass exerted by an external field. We neglect heat conductivity in this analysis. The gas element initially at larger z has its temperature increased by ΔT as a result of the exchange, and the element initially at smaller z is cooled by the same amount. Hence the heat energy taken from the gas as a result of the transposition of the two elements is $C_p \Delta M dT = c_p \Delta M dT/m$, where C_p is the heat capacity of the gas per unit mass and c_p is the heat capacity per molecule, so that m is the molecular mass. An instability criterion requires that the above exchange of gas elements be energetically

advantageous, and has the form

$$\frac{dT}{dz} > \frac{mg}{c_p}. \tag{14.1}$$

In particular, for atmospheric air subjected to the action of the Earth's gravitational field, this relation gives ($g = 10^3$ cm/s^2, $c_p = \frac{7}{2}$)

$$\frac{dT}{dz} > 10 \text{ K/km}. \tag{14.2}$$

The criterion (14.1) is a necessary condition for the development of convection, but its being satisfied does not mean that convection will necessarily occur. Indeed, if we transfer an element of gas from one point to another, it is necessary to overcome a resistive force that is proportional to the displacement velocity. The displacement work is proportional to the velocity of motion of the gas element. If this velocity is small, the gas element exchanges energy with the surrounding gas in the course of motion by means of the thermal conductivity of the gas, and this exchange is larger the more slowly the displacement proceeds. From these arguments it follows that the gas viscosity and thermal conductivity determine the nature of the development of convection. We shall develop a formal criterion for this process.

14.2 THE RAYLEIGH PROBLEM

If a motionless gas is to be unstable, small perturbations are able to cause a slow movement of the gas that corresponds to convection. Our goal is to find the threshold for this process and to analyze its character. We begin with the simplest problem of this type, known as the *Rayleigh problem.* The configuration of this problem is that a gas, located in a gap of length L between two infinite plates, is subjected to an external field. The temperature of the lower plate is T_1, the temperature of the upper plate is T_2, and the indices are assigned so that $T_1 > T_2$.

We can write the gas parameters as the sum of two terms, so that the first term refers to the gas at rest and the second term corresponds to a small perturbation due to the convective gas motion. Hence the number density of gas molecules is $N + N'$, the gas pressure is $p_0 + p'$, the gas temperature is $T + T'$, and the gas velocity $\mathbf{w}$ is zero in the absence of convection. When we insert the parameters in this form into the stationary equations for continuity (9.5), momentum transport (9.8), and heat transport (10.19), the zero-order approximation yields

$$\nabla p_0 = -\mathbf{F}N, \qquad \Delta T = 0, \qquad \mathbf{w} = 0,$$

where $\mathbf{F}$ is the force acting on a single gas molecule, and Δ is the Laplacian. The first-order approximation for these equations gives

$$\frac{\nabla(p_0 + p')}{N + N'} + \frac{\eta \Delta \mathbf{w}}{N + N'} + \mathbf{F} = 0,$$
$$w_z \frac{T_2 - T_1}{L} = \frac{\kappa}{c_V N} \Delta T'. \tag{14.3}$$

The parameters of the present problem are used in the last equation. The z-axis is taken to be perpendicular to the plates.

We transform the first term in the first equation of (14.3) with first-order accuracy, and obtain

$$\frac{\nabla(p_0 + p')}{N + N'} = \frac{\nabla p_0}{N} + \frac{\nabla p'}{N} - \frac{\nabla p_0}{N} \frac{N}{N'}$$
$$= \mathbf{F}\left(1 - \frac{N'}{N}\right) + \frac{\nabla p'}{N}.$$

According to the equation of state (9.14) for a gas, $N = p/T$, we have $N' = (\partial N/\partial T)_p T' = -NT'/T$. Inserting this relation into the second equation of (14.3), we can write this set of equations in the form

$$\operatorname{div} \mathbf{w} = 0,$$
$$-\frac{\nabla p'}{N} - \mathbf{F}\frac{T'}{T} - \frac{\eta \Delta \mathbf{w}}{N} = 0, \tag{14.4}$$
$$w_z = \frac{\kappa L}{c_V N (T_2 - T_1)} \Delta T'.$$

We can reduce the system (14.4) to an equation of one variable. For this goal we first apply the div operator to the second equation of (14.3) and take into account the first equation of (14.3). Then we have

$$\frac{\Delta p'}{N} - \frac{F \partial T'}{T \partial z} = 0. \tag{14.5}$$

Here we assume that $T_1 - T_2 \ll T_1$. Therefore, the unperturbed gas parameters do not vary very much within the gas volume. We can neglect their variation and assume the unperturbed gas parameters to be spatially constant.

Take w_z from the third equation of (14.4) and insert it into the z-component of the second equation. Applying the operator Δ to the result, we obtain

$$\frac{1}{N} \frac{\partial}{\partial z} \Delta p' - \frac{F \Delta T'}{T} + \frac{\eta \kappa L}{c_V N^2 (T_2 - T_1)} \Delta^2 T' = 0.$$

Using the relation (14.5) between $\Delta p'$ and T', we obtain finally

$$\Delta^3 T' = -\frac{R}{L^4}\left(\Delta - \frac{\partial^2}{\partial z^2}\right)T', \tag{14.6}$$

where the dimensionless combination of parameters

$$R = \frac{(T_1 - T_2)\, c_V\, FN^2 L^3}{\eta \kappa T} \tag{14.7}$$

is called the *Rayleigh number.*

The Rayleigh number is fundamental for the problem we are considering. We can rewrite it in a form that conveys clearly its physical meaning. Introducing the kinematic viscosity $\nu = \eta/\rho = \eta/(Nm)$, where ρ is the gas density, the thermal diffusivity coefficient is $\chi = \kappa/(Nc_V)$, and the force per unit mass is $g = F/m$, the Rayleigh number then takes the form

$$R = \frac{T_1 - T_2}{T}\frac{gL^3}{\nu\chi}. \tag{14.8}$$

This expression is couched in terms of the primary physical parameters that determine the development of convection: the relative difference of temperatures $(T_1 - T_2)/T_1$, the specific force g of the field, a typical system size L, and also the transport coefficients, taking into account the types of interaction of gas flows in the course of convection. Note that we use the specific heat capacity at constant volume (c_V) because that is the condition that obtains in our investigation. If equilibrium is maintained instead at a fixed external pressure, it is necessary to use the specific heat capacity at constant pressure in the above equations.

Equation (14.6) shows that the Rayleigh number determines the possibility of the development of convection. For instance, in the Rayleigh problem the boundary conditions at the plates are $T' = 0$ and $w_z = 0$. Also, the tangential forces $\eta\,\partial w_x/\partial z$ and $\eta\,\partial w_y/\partial z$ are zero at the plates. Differentiating the equation $\operatorname{div}\mathbf{w} = 0$ with respect to z and using the conditions for the tangential forces, we find that at the plates $\partial^2 w_z/\partial z^2 = 0$. Hence we have the boundary conditions

$$T' = 0, \qquad w_z = 0, \qquad \frac{\partial^2 w_z}{\partial z^2} = 0.$$

Denote the coordinate of the lower plate by $z = 0$ and the coordinate of the upper plate by $z = L$. A general solution of Eq. (14.6) with the stated boundary conditions at $z = 0$ can be expressed as

$$T' = C \exp\left[i(k_x x + k_y y)\right] \sin k_z z. \tag{14.9}$$

The boundary condition $T' = 0$ at $z = L$ gives $k_z L = \pi n$, where n is an integer. Inserting the solution (14.9) into Eq. (14.6), we obtain

$$R = \frac{(k^2L^2 + \pi^2 n^2)^3}{k^2 L^2}, \tag{14.10}$$

where $k^2 = k_x^2 + k_y^2$. The solution (14.9) satisfies all boundary conditions.

Equation (14.10) shows that convection can occur for values of the Rayleigh number not less than $R_{\min}$, where $R_{\min}$ refers to $n = 1$ and $k_{\min} = \pi/(L\sqrt{2})$. The numerical value of $R_{\min}$ is

$$R_{\min} = 27\pi^4/4 = 658.$$

The magnitude of $R_{\min}$ can vary widely depending on the geometry of the problem and the boundary conditions, but in all cases the Rayleigh number is a measure of the possibility of convection. Above we have considered the simplest example of generation of the convective motion that does not relate to real gases but exhibits the threshold character of the convective motion and allows us to examine the physical nature of this phenomenon.

14.3 CONVECTIVE MOVEMENT OF GASES

To gain some insight into the nature of convective motion, we consider the simple case of motion of a gas in the xy plane. Inserting the solution (14.9) into the equation $\operatorname{div} \mathbf{w} = \partial w_x/\partial x + \partial w_z/\partial z = 0$, the components of the gas velocity are

$$w_z = w_0 \cos kx \sin\frac{\pi nz}{L}, \qquad w_x = -\frac{\pi n}{kL} w_0 \sin kx \cos\frac{\pi nz}{L}, \tag{14.11}$$

where n is an integer, and the amplitude w_0 of the gas velocity is assumed to be small compared to the corresponding parameters of the gas at rest. In particular, w_0 is small compared to the thermal velocity of the gas molecules.

The equations of motion for an element of the gas are $dx/dt = w_x$ and $dz/dt = w_z$, where Eq. (14.11) gives the components of the gas velocity. We obtain $dx/dz = -[\pi n/(kL)]\tan(kx)\cot(\pi nz/L)$. This equation describes the path of the gas element. The solution of the equation is

$$\sin(kx)\sin(\pi nz/L) = C, \tag{14.12}$$

where C is a constant determined by the initial conditions. This constant is bounded by -1 and $+1$; its actual value depends on the initial position of the gas element. Of special significance are the lines at which $C = 0$. These lines are given by the equations

$$z = Lp_1/n, \qquad x = Lp_2/n, \tag{14.13}$$

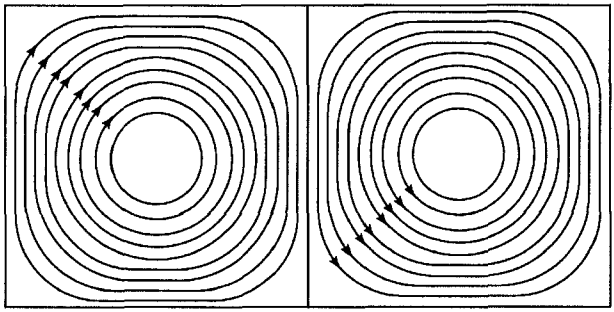

Figure 14.1 Paths of gas elements in the Rayleigh problem for $n = 1$, $k = \pi/L$.

where p_1 and p_2 are nonnegative integers. The straight lines determined by Eq. (14.13) divide the gas into cells. Molecules inside such a cell can travel only within it. Indeed, Eq. (14.13) shows that the component of the gas velocity directed perpendicular to a cell boundary is zero; that is, the gas cannot cross the boundaries between the cells. These cells are known as *Benard cells*.

Equation (14.13) shows that inside each cell the gas elements travel along closed paths around the cell center where the gas is at rest. Figure 14.1 shows the path of the elements of gas in the Rayleigh problem for $n = 1$ and $k = \pi/L$, corresponding to the Rayleigh number $R = 8\pi^4 = 779$. In the Rayleigh problem, the Benard cells are pyramids with regular polygons as bases; in the general case, these cells have a more complicated structure.

14.4 CONVECTIVE HEAT TRANSPORT

Convection is a more effective mechanism of heat transport than is thermal conduction. We can illustrate this by examining convective heat transport for the Rayleigh problem. There will be a boundary layer of thickness δ formed near the walls, within which a transition occurs from zero fluid velocity at the wall itself to the motion occurring in the bulk of the fluid. The thickness of the boundary layer is determined by the viscosity of the gas, and the heat transport in the boundary layer is accomplished by thermal conduction, so that the heat flux can be estimated to be $q = -\kappa \nabla T \sim \kappa(T_1 - T_2)/\delta$. Applying the Navier–Stokes equation (10.32) to the boundary region, one can estimate its thickness. This equation describes a continuous transition from the walls to the bulk of the gas flow. We now add the second term in the Navier–Stokes equation, $m(\mathbf{w} \cdot \nabla)\mathbf{w}$, which cannot be neglected here, to the expression in Eq. (14.3) . An order-of-magnitude comparison of separate terms in the z-component of the resulting equation yields $mw_z^2/\delta \sim$

$F(T_1 - T_2)/T \sim \eta w_z/N\delta^2$. Hence, we find that the boundary-layer thickness is

$$\delta \sim \left(\frac{\eta^2 T}{N^2 F m^3 (T_1 - T_2)} \right)^{1/3}. \tag{14.14}$$

In the context of the Rayleigh problem, we can compare the heat flux transported by a gas due to convection (q) and to thermal conduction (q_{cond}). The thermal heat flux is $q_{\text{cond}} = \kappa(T_1 - T_2)/L$, and the ratio of the fluxes is

$$\frac{q}{q_{\text{cond}}} \sim \frac{L}{\delta} \sim \left(\frac{N^2 F m L^3 (T_1 - T_2)}{\eta^2 T} \right)^{1/3} \sim G^{1/3}. \tag{14.15}$$

Here, G is the dimensionless combination of parameters

$$G = \frac{N^2 F m L^3 (T_1 - T_2)}{\eta^2 T} = \frac{\Delta T}{T} \frac{g L^3}{\nu^2}, \tag{14.16}$$

which is called the *Grashof number*. A comparison of the definitions of the Rayleigh number (14.7) and the Grashof number (14.16) gives their ratio as

$$\frac{R}{G} = \frac{c_V \eta}{m\kappa} = \frac{\nu}{\chi}.$$

The continuity equation (9.5), the equation of momentum transport (9.8), and the equation of heat transport (10.19) are valid not only for a gas but also for a liquid. Therefore, the results we obtain are applicable to liquids also. However, a gas does have some distinctive features. For example, Eqs. (10.18) and (10.29) show that for a gas the ratio $\eta/(m\kappa)$ is of order unity. Furthermore, the specific heat capacity c_V of a single molecule is also of order unity. Hence, the Rayleigh number has the same order of magnitude as the Grashof number for a gas. Since convection develops at high Rayleigh numbers, we find that for convection $G \gg 1$. Therefore, according to Eq. (14.15), we find that heat transport via convection is considerably more effective than heat transport in a motionless gas via thermal conduction.

The ratio (14.15) between the convective and conductive heat fluxes has been derived for an external force directed perpendicular to the boundary layer. We can derive the corresponding condition for an external force directed parallel to the boundary layer. We take the z-axis to be normal to the boundary layer and the external force to be directed along the x-axis. Then, to the second equation of the set of equations (14.3), we add the term $m(\mathbf{w} \cdot \nabla)\mathbf{w}$ and compare the x-components of the result. This comparison yields

$$\frac{m w_x^2}{L} \sim \frac{F(T_1 - T_2)}{T} \sim \frac{\eta}{N} \frac{w_x}{\delta^2}. \tag{14.17}$$

Equation (14.17) gives the estimate

$$\delta \sim \left(\frac{\eta^2 TL}{N^2 F m^3 (T_1 - T_2)} \right)^{1/4}$$

for the thickness of the boundary layer. Hence, the ratio of the heat flux q due to convection to the flux q_{cond} due to thermal conduction is

$$\frac{q}{q_{\text{cond}}} \sim \frac{L}{\delta} \sim G^{1/4}. \tag{14.18}$$

The ratio of the heat fluxes in this case is seen to be different from that when the external force is perpendicular to the boundary layer [see Eq. (14.15)]. However, the convective heat flux in this case is still considerably larger than the heat flux due to thermal conduction in a motionless gas.

14.5 INSTABILITY OF CONVECTIVE MOTION

New types of convective motion develop when the Rayleigh and Grashof numbers become sufficiently large. The orderly convective motion becomes disturbed, and this disturbance grows until the stability of the convective motion of a gas is entirely disrupted, giving rise to disordered and turbulent flow of the gas. This will happen even if the gas is contained in a stationary enclosure. To analyze the development of turbulent gas flow we consider once again the Rayleigh problem: a gas at rest between two parallel and infinite planes maintained at different constant temperatures is subjected to an external force. We shall analyze the convective motion of a gas described by Eqs. (14.11) and corresponding to sufficiently high Rayleigh numbers with $n \geq 2$. In this case there can develop simultaneously at least two different types of convection.

Figure 14.2 shows two types of convective motion for the Rayleigh number $R = 108\pi^4$, corresponding to the wave number $k_1 = 9.4/L$ for $n = 1$ and to $k_2 = 4.7/L$ for $n = 2$. To analyze this example using the above parameters, we combine the solutions so that the gas flows corresponding to $n = 1$ and to $n = 2$ travel in the same direction in some region of the gas volume. Then in other regions these flows must move in opposite directions. The existence of two solutions with opposite directions of gas flow does not mean that the ordered flow of gas is disturbed. A combination of two solutions is itself a solution. For opposite gas flows, a combination means that at some points the gas is motionless. Nevertheless, the fact that an increase of the Rayleigh number gives rise to new types of solutions means that the convective flow can become turbulent. Assume that there is an ordered convective flow in the system corresponding to one of the solutions. Then a small

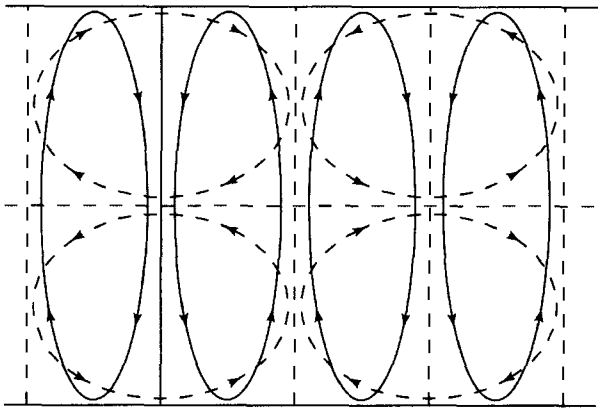

Figure 14.2 The types of convective motion in the Rayleigh problem for $R = 108\pi^4$. The mixing of the gas fluxes traveling in opposite directions finally results in a random gas motion, or turbulence. Regions of counter – currents are marked.

perturbation in one of the regions of the gas volume gives rise to a different type of flow. At the boundary of this region two opposite gas flows meet, so that the kinetic energy of motion of the gas is transformed into thermal energy of the gas. This results in disordered motion. The development of turbulence changes altogether the character of heat transport.

We can estimate the thermal conductivity coefficient in a plasma or hot gas with developed turbulence. For example, turbulent flow can occur in a column of hot gas resulting from the passage of an electric current through it, and the temperature evolution of this column is of interest. We add the force of an external field directed perpendicular to the temperature gradient (as in the case of lightning in air), so that the transport of heat occurs over small distances. We assume that a typical transverse size r of the column is large compared to a typical size l of small vortices, as determined by Eqs. (14.8) and (14.10), giving

$$R = \frac{\Delta T}{T}\frac{gl^3}{\nu\chi} = \frac{l}{r}\frac{gl^3}{\nu\chi} \sim 10^3.$$

In this case the thermal conductivity coefficient is given by Eq. (10.18), $\kappa \sim Nvl$, where l is the mean free path for vortices and v is a typical velocity in the fluxes. The value of v is obtained from the Navier–Stokes equation (10.32) as $v \sim (gl)^{1/2}$. The *Reynolds number* $\mathrm{Re} = vl/\nu$ for these motions can be estimated from the above expression for the Rayleigh number, yielding

$$R = \frac{l}{r}\frac{\nu}{\chi}\,\mathrm{Re}^2 \sim 10^3.$$

Since $l \ll r$ and $\nu \sim \chi$, it follows that $\mathrm{Re} \gg 1$. Thus, at large values of the Rayleigh number when several types of motion of gaseous flows are possible, the movement of the gas is characterized by large values of the Reynolds numbers. As these numbers increase, the gas motion tends toward disorder, and turbulent motion develops.

14.6 THERMAL EXPLOSION

We shall now consider the other type of instability of a motionless gas, which is called thermal instability or thermal explosion. It occurs in a gas experiencing heat transport by way of thermal conduction, where the heat release is determined by processes (chemical, for instance) whose rate depends strongly on the temperature. There is a limiting temperature beyond which heat release is so rapid that thermal conductivity processes cannot transport the heat released. Then an instability occurs that transforms internal energy of the system to heat and leads to a different regime of heat transport.

We shall analyze this instability within the framework of the geometry of the Rayleigh problem. Gas is located in a gap between two infinite plates with a distance L between them. The wall temperature is T_w. We take the z-axis perpendicular to the walls with $z = 0$ at the center of the gap, so that the coordinates of walls are $z = \pm L/2$. We introduce the specific power of heat release $f(T)$ as power per unit volume and use the Arrhenius law

$$f(T) = A \exp(-E_a/T), \tag{14.19}$$

for the temperature dependence of this value, where E_a is the activation energy of the heat release process. This dependence of the rate of heat release is identical to that of the chemical process and represents a strong temperature dependence because $E_a \gg T$.

To find the temperature distribution inside a gap in the absence of the thermal instability, we note that Eq. (10.19) for the transport of heat has the form

$$\kappa \frac{d^2T}{dz^2} + f(T) = 0.$$

We introduce a new variable $X = E_a(T - T_0)/T_0^2$, where T_0 is the gas temperature at the center of the gap, and obtain the equation

$$d^2X/dz^2 - Be^{-X} = 0,$$

where $B = E_a A \exp(-E_a/T_0)/(T_0^2\kappa)$. Solving this equation with the boundary conditions $X(0) = 0$, $dX(0)/dz = 0$ [the second condition follows from the symmetry $X(z) = X(-z)$ in this problem], we have

$$X = 2 \ln \cosh z.$$

The temperature difference between the center of the gap and the walls is

$$\Delta T \equiv T_0 - T_w = \frac{2T_0^2}{E_a} \ln\cosh\left[\frac{L}{2}\sqrt{\frac{AE_a}{2T_0^2\kappa}}\exp\left(-\frac{E_a}{2T_0}\right)\right]. \quad (14.20)$$

To analyze this expression we refer to Fig. 14.3, illustrating the dependence on T_0 for the left-hand and right-hand sides of this equation (curves 1 and 2, respectively) at a given T_w. The intersection of these curves yields the center temperature T_0. The right-hand side of the equation does not depend on the temperature of the walls and depends strongly on T_0. Therefore it is possible that curves 1 and 2 do not intersect. That would mean there is no stationary solution of the problem. The physical implication of this result is that thermal conduction cannot suffice to remove the heat release inside the gas. This leads to a continuing increase of the temperature, so that thermal instability occurs.

To find the threshold of the thermal instability corresponding to the curve 1′ of Fig. 14.3, we establish the common tangency point of the curves describing the left-hand and right-hand sides of Eq. (14.20). The derivatives of the two sides are equal when

$$\Delta T = \frac{2T_0^2}{E_a} \ln\cosh y, \qquad 1 = y \tanh y, \quad (14.21)$$

where

$$y = \frac{L}{2}\sqrt{\frac{AE_a}{2T_0^2\kappa}}\exp\left(-\frac{E_a}{2T_0}\right).$$

The solution of the second equation in (14.21) is $y = 1.2$, so that

$$\frac{AE_aL^2}{T_0^2\kappa}\exp\left(-\frac{E_a}{T_0}\right) = 11.5 \quad \text{and} \quad \Delta T = 1.19\frac{T_0^2}{E_a}. \quad (14.22)$$

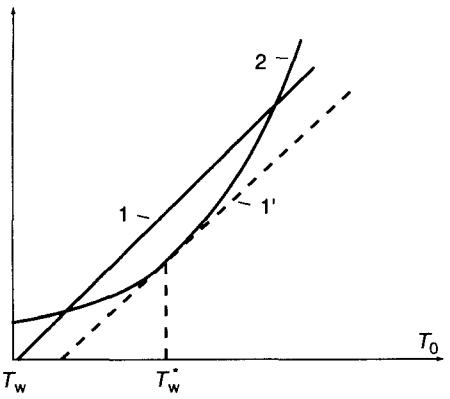

Figure 14.3 The dependence of the left-hand (curve 1) and right-hand (curve 2) sides of equation (14.20) on the temperature of the center. The wall temperature T_w^* corresponds to the threshold of the thermal instability.

From this, it follows that the connection between the specific powers of heat release is

$$f(T_w) = f(T_0)e^{-1.19} = 0.30f(T_0).$$

This makes it possible to state the condition for the threshold of thermal instability in terms of the parameters of heat release on walls as

$$\frac{L^2AE_a}{T_w^2\kappa}\exp\left(-\frac{E_a}{T_w}\right) = 3.5. \tag{14.23}$$

Though we referred to the Arrhenius law for the temperature dependence of the rate of heat release, in actuality we used only the implication that this dependence is strong. We can therefore rewrite the condition for the threshold of thermal instability in the form

$$\frac{L^2}{\kappa}\left|\frac{df(T_w)}{dT_w}\right| = 3.5. \tag{14.24}$$

The criterion for a sharp peak in the power involved in the heat release is

$$T_w\left|\frac{df(T_w)}{dT_w}\right| \gg 1. \tag{14.25}$$

The relation (14.24) has a simple physical meaning. It relates the rate of the heat release process to the rate of heat transport. If their ratio exceeds a particular value of the order of unity, then thermal instability develops.

14.7 THERMAL WAVES

The development of thermal instability can lead to the formation of a *thermal wave*. This takes place if the energy in some internal degree of freedom is significantly in excess of its equilibrium value. For example, it can occur in a chemically active gas or in a nonequilibrium molecular gas with a high vibrational temperature. In these cases the development of thermal instability is accompanied by the propagation of a thermal wave, leading to a rapid chemical reaction or to a vibrational relaxation.

Figure 14.4 shows the temperature distribution in a gas upon propagation of a thermal wave. Region 1 has the initial gas temperature. The wave has not yet reached this region at the time represented in the figure. The temperature rise observed in region 2 is due to heat transport from hotter regions. The temperature in region 3 is close to the maximum. Processes that release heat occur in this region. We use the strong temperature dependence

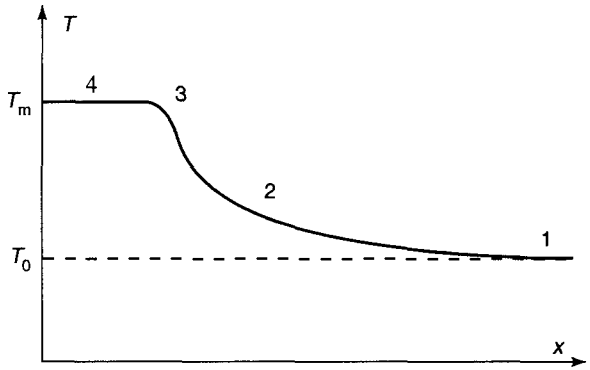

Figure 14.4 The temperature distribution in a gas in which a thermal wave propagates.

to establish the specific power of heat release, which according to (14.19) has the form

$$f(T) = f(T_m)\exp[-\alpha(T_m - T)], \qquad \alpha = E_a/T_m^2. \tag{14.26}$$

Here T_m is the final gas temperature, determined by the internal energy of the gas. Region 4 of Fig. 14.4 is located after the passage of the thermal wave. Thermodynamic equilibrium among the relevant degrees of freedom has been established in this region.

To calculate parameters of the thermal wave, we assume the usual connection between spatial coordinates and time dependence of propagating waves. That is, the temperature is taken to have the functional dependence $T = T(x - ut)$, where x is the direction of wave propagation and u is the velocity of the thermal wave. With this functional form, the heat balance equation (10.19) becomes

$$u\frac{dT}{dx} + \chi\frac{d^2T}{dx^2} + \frac{f(T)}{c_p N} = 0. \tag{14.27}$$

Our goal is to determine the eigenvalue u of this equation. To accomplish this, we employ the Zeldovich approximation method, which uses a sharply peaked temperature dependence for the rate of heat release. We introduce the function $Z(T) = -dT/dx$, so that for $T_0 < T < T_m$ we have $Z(T) \geq 0$. Since we have the connections

$$\frac{d^2T}{dx^2} = \frac{d}{dx}\left(\frac{dT}{dx}\right) = \frac{Z\,dZ}{dT},$$

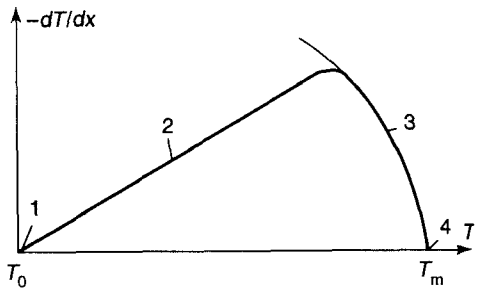

Figure 14.5 The solution of equation (14.28) for various regions of the thermal wave of Fig. 14.4.

Eq. (14.27) takes the form

$$-uZ + \chi \frac{Z\,dZ}{dT} + \frac{f(T)}{c_p N} = 0. \tag{14.28}$$

The solution of this equation for the regions defined in Fig. 14.4 is illustrated in Fig. 14.5. Before the thermal wave (region 1) and after it (region 4), we have $Z = 0$. In region 2 there is no heat release, and one can neglect the last term of Eq. (14.28). This yields

$$Z = u(T - T_0)/\chi. \tag{14.29a}$$

Neglecting the first term of Eq. (14.28), we obtain

$$Z = \sqrt{\frac{2}{c_p N \chi} \int_T^{T_m} f(T)\,dT} \tag{14.29b}$$

for region 3. Equations (14.29a) and (14.29b) are not strictly joined at the interface between regions 2 and 3, because there is no interval where one can neglect both terms of Eq. (14.28). But due to the very strong dependence of $f(T)$ on T, there is only a narrow temperature region where it is impossible to neglect one of these terms. This fact allows us to connect solution (14.29a) with (14.29b) and find the velocity of the thermal wave.

Introducing the temperature T_* that corresponds to the maximum of $Z(T)$, Eq. (14.28) gives

$$Z_{max} = Z(T_*) = \frac{f(T_*)}{uc_p N}.$$

Equation (14.28) for temperatures near T_* then takes the form

$$\frac{dZ}{dT} = \frac{u}{\chi}\left(1 - \frac{f(T)}{f(T_*)}\right).$$

Solving this equation and taking into account Eq. (14.26), we have

$$Z = \frac{u}{\chi}(T - T_0) - \frac{u}{\chi\alpha}\exp[\alpha(T - T_*)]. \tag{14.29c}$$

The boundary condition for this equation is that it should coincide with (14.29a) far from the maximum Z. In this region one can neglect the third term of Eq. (14.28), which is the approximation that leads to Eq. (14.29a). This is valid under the condition

$$\alpha(T_* - T_0) \gg 1. \tag{14.30}$$

Now we seek the solution of Eq. (14.28) at $T > T_*$. Near the maximum of $Z(T)$, Z is given by Eq. (14.29c), so (14.28) has the form

$$\frac{dZ}{dT} = \frac{Z_{\max}}{T_* - T_0}\{1 - \exp[\alpha(T - T_*)]\}.$$

This equation is valid in the region where the second term of Eq. (14.29c) is significantly smaller than the first one. According to Eq. (14.30), this condition is fulfilled at temperatures where $\exp[\alpha(T - T_*)] \gg 1$. Therefore, due to the exponential dependence of the second term of Eq. (14.28), there is a temperature region where that term gives scant contribution to Z, but nevertheless determines its derivative. This property will be used below. On the basis of the above information and the dependence given in Eq. (14.26), we find that the solutions of (14.28) at $T > T_*$ are

$$Z = \sqrt{\frac{2f(T_m)}{c_p N\chi\alpha}}\sqrt{1 - \exp[\alpha(T - T_m)]},$$

$$\frac{dZ}{dT} = \sqrt{\frac{2f(T_m)}{c_p N\chi\alpha}}\frac{\exp[\alpha(T - T_m)]}{\sqrt{1 - \exp[\alpha(T - T_m)]}}.$$

Comparing the expressions for dZ/dT near the maximum, one can see that these expressions can be connected if the condition stated in Eq. (14.30) is satisfied. Then the solution (14.29b) is valid in the temperature region $T_* < T \leq T_m$ up to temperatures near the maximum of Z. Connecting values of dZ/dT in regions where $\alpha(T - T_*) \gg 1$ and where $\alpha(T_m - T) \gg 1$, we obtain

$$Z_{\max} = \sqrt{\frac{2f(T_m)}{c_p N\chi\alpha}}(T_* - T_m)\exp[\alpha(T_* - T_m)].$$

Next, from (14.29c) it follows that $Z_{max} = Z(T_*) = f(T_*)/(uc_pN)$. Comparing these expressions, one can find the temperature T_* corresponding to the maximum of $Z(T)$ and hence to the velocity of the thermal wave. We obtain

$$\alpha(T_* - T_0)/2 = \exp[\alpha(T_m - T_*)], \tag{14.31}$$

$$u = \frac{T_m}{T_m - T_0}\sqrt{\frac{2\chi f(T_m)}{c_pNE_a}}. \tag{14.32}$$

We have used Eq. (14.26) for the parameter α. The relation (14.31) together with the condition (14.30) gives $T_m - T_* \ll T_* - T_0$. This was taken into account in Eq. (14.32).

Equation (14.32) corresponds to the dependence (14.26) for the rate of heat release near the maximum. In a typical case at $T = T_m$ all the "fuel" is used, and $f(T_m) = 0$. Then all the above arguments are valid, because the primary portion of the heat release takes place at temperatures T where $\alpha(T_m - T) \sim 1$, that is, where $\alpha(T - T_*) \gg 1$. Then, using the new form of the function $f(T)$ near the maximum of $Z(T)$, we transform Eq. (14.32) to the form

$$u = \frac{1}{T_m - T_0}\sqrt{\frac{2\chi}{c_pN}\int_T^{T_m} f(T)\,dT}. \tag{14.33}$$

This formula is called the *Zeldovich formula*.

We can analyze the problem from another standpoint. Take an expression for $Z(T)$ such that, in the appropriate limits, it would agree with Eqs. (14.29a) and (14.29b). The simplest expression of this type has the form

$$Z = \frac{u}{\chi}(T - T_0)\{1 - \exp[-\alpha(T_m - T)]\}.$$

Inserting this into Eq. (14.28), $f(T)$ is given by the expression

$$\begin{aligned}\frac{f(T)}{c_pN} &= uZ - \frac{\chi}{2}\frac{d}{dT}Z^2 \\ &= \frac{u^2}{\chi}(T - T_0)\sqrt{1 - e^{-\alpha(T_m - T)}}\left(1 - \sqrt{1 - e^{-\alpha(T_m - T)}}\right) \\ &\quad + \frac{\alpha u^2}{2\chi}(T - T_0)^2 e^{-\alpha(T_m - T)}.\end{aligned}$$

In the region $\alpha(T - T_0) \gg 1$, the first term is small compared to the second one and one can neglect it. Then the comparison of this expression with that

of Eq. (14.26) in the temperature region $\alpha(T_m - T) \sim 1$ and $T_m - T \ll T_m - T_0$ gives the velocity of the thermal wave as (where $\alpha = E_a/T_m^2$)

$$u = \frac{T_m}{T_m - T_0}\sqrt{\frac{2\chi}{E_a}\frac{f(T_m)}{c_p N}}\,.$$

This equation agrees exactly with Eq. (14.32) because of the identical assumptions used for construction of the solution in both cases.

One can use this method for the alternative case when the function $f(T)$ has an exponential dependence far from T_m and goes to zero at $T = T_m$. For example, take the approximate dependence

$$f(T) = A(T_m - T)\exp[-\alpha(T_m - T)]\,.$$

An approximate solution of Eq. (14.28) constructed on the basis of Eqs. (14.29a) and (14.29b) has the form

$$Z = \frac{u}{\chi}(T - T_0)\sqrt{1 - e^{-\alpha(T_m - T)}[\alpha(T_m - T) + 1]}\,.$$

Substituting this in Eq. (14.28), we have

$$\begin{aligned}\frac{f(T)}{c_p N} &= uZ - \frac{\chi}{2}\frac{d}{dT}Z^2 \\ &= \frac{u^2}{\chi}(T - T_0)\left\{1 - \sqrt{1 - e^{-\alpha(T_m - T)}[\alpha(T_m - T) + 1]}\right\} \\ &\quad \times\sqrt{1 - e^{-\alpha(T_m - T)}[\alpha(T_m - T) + 1]} \\ &\quad + \frac{\alpha^2 u^2}{2\chi}(T - T_0)^2(T_m - T)e^{-\alpha(T_m - T)}.\end{aligned}$$

In the region $\alpha(T - T_0) \gg 1$, where the heat release is essential, the first term is small compared to the second one. Then comparing this expression with the approximate dependence assumed above for $f(T)$, we find the velocity of the thermal wave ($\alpha = E_a/T_m^2$) to be

$$u = \frac{T_m^2}{E_a(T_m - T_0)}\sqrt{\frac{2\chi A}{c_p N}}\,.$$

This result is in agreement with the Zeldovich formula (14.33) for the dependence employed for $f(T)$. The above analysis shows that the Zeldovich formula for the velocity of a thermal wave is valid under the condition $\alpha(T_m - T_0) \gg 1$.

14.8 VIBRATIONAL-RELAXATION THERMAL WAVES

We shall apply the above results to the analysis of illustrative physical processes. First we consider a thermal wave of vibrational relaxation that can propagate in an excited molecular gas that is not in equilibrium. In particular, this process can occur in molecular lasers, where it can result in the quenching of laser generation. We consider the case where the number density of excited molecules is considerably greater than the equilibrium density. Vibrational relaxation of excited molecules causes the gas temperature to increase, and the relaxation process accelerates. There will be a level of excitation and a temperature at which thermal instability develops, leading to the establishment of a new thermodynamic equilibrium between excited and nonexcited molecules.

The balance equation for the number density N_* of excited molecules has the form

$$\frac{\partial N_*}{\partial t} = D\Delta N_* - NN_* k(T),$$

where N is the total number density of molecules, and where we assume $N \gg N_*$. The quantity D is the diffusion coefficient for excited molecules in a gas, and $k(T)$ is the rate constant of vibrational relaxation. Taking into account the usual dependence of traveling-wave parameters $N_*(x, t) = N_*(x - ut)$, where u is the velocity of the thermal wave, we transform the above equation to the form

$$u\frac{dN_*}{dx} + D\frac{d^2N_*}{dx^2} - N_* Nk(T) = 0. \tag{14.34}$$

In front of the thermal wave we have $N_* = N_{\max}$, and after the wave we have $N_* = 0$. That is, we are assuming the equilibrium number density of excited molecules to be small compared to the initial density. Introduce the mean energy $\Delta\varepsilon$ released in a single vibrational-relaxation event. Then the difference of the gas temperatures after (T_m) and before (T_0) the thermal relaxation wave is

$$T_m - T_0 = \frac{N_0 \Delta\varepsilon}{Nc_p},$$

where N_0 is the initial number density of excited molecules.

The heat balance equation (14.27) now has the form

$$u\frac{dT}{dx} + \chi\frac{d^2T}{dx^2} - \frac{\Delta\varepsilon N_* k(T)}{c_p} = 0. \tag{14.35}$$

The wave velocity can be obtained from the simultaneous analysis of Eqs. (14.34) and (14.35). The simplest case occurs when $D = \chi$. Then both balance equations are identical, and the relation between the gas temperature and the number density of excited molecules is

$$T_m - T = N_* \Delta\varepsilon/(Nc_p). \tag{14.36}$$

We have only one balance equation in this case. Comparing it with Eq. (14.27), we have $f(T)/(c_pN) = (T_m - T)Nk(T)$. On the basis of the Zeldovich formula we find the wave velocity to be

$$u = \frac{T_m^2}{E_a(T_m - T_0)}\sqrt{\frac{2\chi}{\tau(T_m)}}, \tag{14.37}$$

where $\tau(T_m) = 1/[Nk(T_m)]$ is a typical time for vibrational relaxation at the temperature T_m. Because of the assumption $\alpha(T_m - T_0) \gg 1$ and the dependence (14.26) for the rate constant of vibrational relaxation, the relation (14.37) with the assumptions employed gives

$$u \ll \sqrt{\frac{\chi}{\tau(T_m)}}.$$

We shall now examine the propagation of a vibrational-relaxation thermal wave for limiting relations between the parameters D and χ. We analyze first the case $D \gg \chi$. Figure 14.6a shows the distribution of the number density of excited molecules (N_*) and of the gas temperature T along the wave. We note that the centers of these two distributions coincide. This reflects the fact that quenching of excited molecules introduces heat into the gas.

We can analyze the balance equation (14.34) for the number density of excited molecules in a simple fashion by neglecting thermal conduction. We obtain the temperature distribution in the form of a step as shown in (Fig. 14.6a). At $x > 0$ the vibrational relaxation is weak, and the solution of Eq. (14.34) in this region has the form $N_* = N_{max} - (N_{max} - N_0)\exp(-ux/D)$ if $x > 0$, where N_0 is the number density of the excited molecules at $x = 0$ and N_0 is the integration constant. In the region $x < 0$ vibrational relaxation is of importance, but the gas temperature is constant. This leads to

$$N_* = N_0 \exp(\alpha x), \qquad x < 0, \quad \alpha = \sqrt{\left(\frac{u}{2D}\right)^2 + \frac{1}{D\tau}} - \frac{u}{2D},$$

where $\tau = 1/[Nk(T_m)]$. The transition region, where the gas temperature is not at its maximum but the vibrational relaxation is essential, is narrow under the conditions considered. Hence at $x = 0$ the above expressions must give

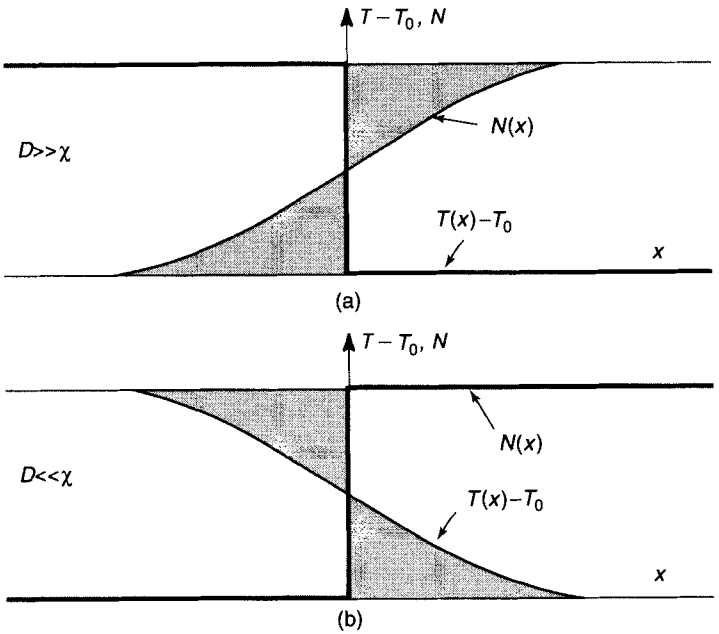

Figure 14.6 The distribution of gas temperature and number density of excited molecules in a vibrational-relaxation thermal wave for different limiting ratios between the diffusion coefficient D of excited molecules and the thermal diffusivity coefficient χ of the gas.

the same results both for the number density of excited molecules and for their derivatives. We obtain

$$\alpha = \frac{u}{D}, \qquad u = \sqrt{\frac{2D}{\tau(T)}} = \sqrt{2DNk(T_m)}, \quad D \gg \chi. \tag{14.38}$$

In this case the propagation of the thermal wave of vibrational relaxation is governed by the diffusion of excited molecules in a hot region where vibrational relaxation takes place. Hence, the wave velocity is of the order of $u \sim \sqrt{D/\tau}$ in accordance with Eq. (14.38). The width of the front of the thermal wave is estimated as $\Delta x \sim \sqrt{D\tau}$.

The opposite limiting case $\chi \gg D$ is shown in Fig. 14.6b, illustrating the distribution of the gas temperature and number density of excited molecules along the thermal wave for this case. Because at $x > 0$ the rate of vibrational relaxation is small, and at $x < 0$ excited molecules are absent, one can neglect the last term of Eq. (14.35). Assuming the transition region to be small, Eq. (14.35) leads to the result

$$T(x) = \begin{cases} T_0 + (T_m - T_0)\exp[-u(x + x_0)/\chi], & x > x_0, \\ T_m, & x < x_0, \end{cases}$$

where $-x_0$ is the back boundary of the thermal wave. This value can be determined from the condition that the positions of the centers for the gas temperature distributions and the number density of molecules are coincident; that is, the areas of the shaded regions of Fig. 14.6b must be the same. This yields $x_0 = \chi/u$ and

$$T(0) = T_r = T_m(1 - 1/e) + T_0/e, \tag{14.39}$$

where e is the base of Naperian logarithms. The wave velocity is determined by the Zeldovich formula (14.33), where $f(T) = \Delta\varepsilon_* Nk(T)$ and N_* is the step function. This allows one to take T_r as the upper limit of integration in Eq. (14.33), leading to the result

$$u = \frac{1}{T_r - T_0}\sqrt{\frac{2\chi f(T_r)}{c_p N\alpha}}.$$

This formula, with Eqs. (14.36) and (14.39), yields

$$u = \sqrt{\frac{2e}{e-1}}\,\frac{T_r}{\sqrt{E_a(T_m - T_0)}}\sqrt{\frac{\chi}{\tau(T)}}, \tag{14.40}$$

where $\tau(T_r) = [Nk(T_r)]^{-1}$ and $\alpha = E_a/T_r^2$. Since $\alpha(T_r - T_0) \gg 1$, we conclude that

$$u \ll \sqrt{\chi/k(T)}.$$

In this case the wave velocity is small compared to that for the case $D = \chi$, because the vibrational-relaxation process proceeds at lower temperatures and lasts longer than in the case $D = \chi$. Summing up the above results, we point out that the vibrational-relaxation thermal wave is created by the processes of diffusion of excited molecules in a gas, by thermal conductivity of the gas, and by vibrational relaxation of excited molecules. Hence, the wave velocity depends on the parameters D, χ, and a typical time τ of vibrational relaxation.

14.9 OZONE-DECOMPOSITION THERMAL WAVES

Since the propagation of thermal waves is so complicated, including diverse processes of transport and quenching of excited particles, we present here an explicit example where ozone decomposition in air or other gases proceeds in the form of a thermal wave. The propagation of the thermal wave results

from chemical processes whose main stages are

$$\begin{aligned} O_3 + M &\xrightarrow{k_{dis}} O_2 + O + M, \\ O + O_2 + M &\xrightarrow{K} O_3 + M, \\ O + O_3 &\xrightarrow{k_1} 2O_2, \end{aligned} \tag{14.41}$$

where M is the gas molecule, and the relevant rate constants of the processes are given above the arrows. If these processes proceed in air, the temperature T_m after the thermal wave is connected with the initial gas temperature T_0 by the relation

$$T_m = T_0 + 48c, \tag{14.42}$$

where the temperatures are expressed in kelvins, and c is the ozone concentration in air expressed as a percentage.

On the basis of the scheme (14.41) we obtain the set of balance equations

$$\begin{aligned} \frac{d[O_3]}{dt} &= -k_{dis}[M][O_3] + K[O][O_2][M] - k_1[O][O_3], \\ \frac{d[O]}{dt} &= k_{dis}[M][O_3] - K[O][O_2][M] - k_1[O][O_3], \end{aligned} \tag{14.43}$$

where [X] is the number density of particles X. Estimates show that at a gas pressure $p \leq 1$ atm and $T_m > 500$ K we have $K[O_2][M] \ll k_1[O_3]$, that is, the second term of the right-hand side of each equation in (14.43) is smaller than the third one. In addition, we know that $[O] \ll [O_3]$, so that $d[O]/dt \ll d[O_3]/dt$. This gives $d[O]/dt = 0$ and $[O] = k_{dis}[M]/k_1$. Using this result in the first equation of (14.43), we obtain

$$d[O_3]/dt = -2k_{dis}[M][O_3].$$

Then, with Eqs. (14.34) and (14.35), we obtain for the thermal wave

$$\begin{aligned} u\frac{d[O_3]}{dx} + D\frac{d^2[O_3]}{dx^2} - 2k_{dis}[M][O_3] &= 0, \\ u\frac{dT}{dx} + \chi\frac{d^2T}{dx^2} + \frac{2}{c_p}\Delta\varepsilon\, k_{dis}[O_3] &= 0, \end{aligned} \tag{14.44}$$

where $\Delta\varepsilon = 1.5$ eV is the energy released from the decomposition of one ozone molecule.

We can now substitute numerical parameters for the above processes for a thermal wave in air at atmospheric pressure, namely $D = 0.16$ cm^2/s and

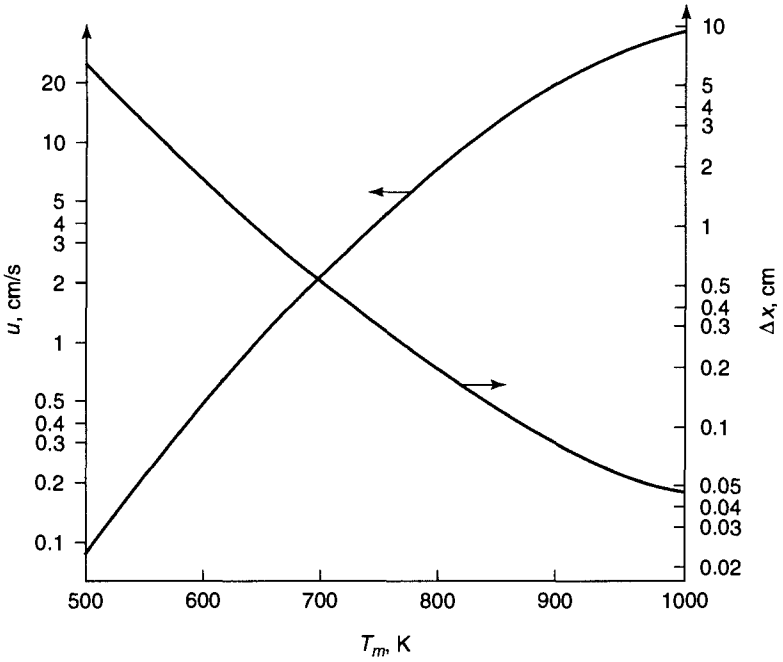

Figure 14.7 The velocity u of the thermal wave of ozone decomposition and the width of the wave front (Δx) as a function of the final temperature.

$\chi = 0.22$ cm^2/s. These quantities are almost equal numerically and have similar temperature dependence, so we take them to be equal and given by

$$D = \chi = \frac{0.19}{p}\left(\frac{T}{300}\right)^{1.78}.$$

Here D and χ are in cm^2/s, the air pressure p is in atmospheres, and the temperature is in kelvins. Next, we employ the expression $k_{\text{dis}} = (1.0 \times 10^{-9}$ cm^3/s) exp($-11{,}600/T$) for the dissociation rate constant. We can observe how equating the values of D and χ simplifies the problem. Then Eq. (14.37) gives the thermal wave velocity

$$u = \frac{1.3T_{\text{m}}^{2.39}}{T_{\text{m}} - T_0}\exp\left(-\frac{5800}{T_{\text{m}}}\right),$$

where the initial (T_0) and final (T_{m}) air temperatures are in kelvins, and the thermal wave velocity is in centimeters per second. Figure 14.7 illustrates the temperature dependence for the wave velocity with $T_0 = 300$ K. Note that it does not depend on the air pressure.

The width of the wave front can be characterized by the value $\Delta x = (T_m - T_0)/(dT/dx)_{max}$, where the maximum temperature gradient is $(dT/dx)_{max} = u(T_* - T_0)/\chi$ and the temperature T_* is determined by Eq. (14.31). Figure 14.7 gives this value as a function of the temperature. From the data of Fig. 14.7 one can see that the thermal wave velocity is small compared with the sound velocity. This means that the propagation of a thermal wave is a quiet process, in contrast to a shock wave.

CHAPTER 15

WAVES IN PLASMAS

15.1 ACOUSTIC OSCILLATIONS

Oscillations and noise in a plasma play a much greater role than in an ordinary gas because of the long-range nature of charged-particle interactions. If a plasma is not uniform and is subjected to external fields, a wide variety of oscillations can occur. Under some conditions these oscillations can become greatly amplified. Then the plasma oscillations affect basic plasma parameters and properties. Below we analyze the simplest types of oscillations in a gas and in a plasma.

The natural vibrations of a gas are acoustic vibrations, that is, propagating waves of alternating compressions and rarefactions. We shall analyze these waves with the goal of finding the relationship between the frequency ω of the oscillation and the wavelength λ, which is connected with the wave vector $\mathbf{k}$ by the expression $|\mathbf{k}| = 2\pi/\lambda$. It is customary to refer to the amplitude $k = |\mathbf{k}|$ as the wave number.

In our analysis, we assume the oscillation amplitudes to be small. Thus any macroscopic parameter of the system can be expressed as

$$A = A_0 + \sum_{\omega} A'_{\omega} \exp[i(kx - \omega t)], \tag{15.1}$$

where A_0 is an unperturbed parameter (in the absence of oscillations), A'_{ω} is the amplitude of the oscillations, ω is the oscillation frequency, and k is the appropriate wave number. The wave propagates along the x-axis. Since the oscillation amplitude is small, an oscillation at a given frequency does not depend on oscillations at other frequencies. In other words, there is no

coupling between waves of different frequencies when amplitudes are small. Therefore, one need retain only the leading term in the sum (15.1) and express the macroscopic parameter A in the form

$$A = A_0 + A' \exp[i(kx - \omega t)]. \tag{15.2}$$

To analyze acoustic oscillations in a gas, we can apply the relation (15.2) to the number density N of gas atoms (or molecules), the gas pressure p, and the mean gas velocity w, and take the unperturbed gas to be at rest ($w_0 = 0$). Using the continuity equation (9.5) and neglecting terms with squared oscillation amplitudes, we obtain

$$\omega N' = kN_0 w'. \tag{15.3a}$$

The gas velocity $\mathbf{w}$ is directed along the wave vector $\mathbf{k}$ for an acoustic wave (a longitudinal oscillation). Similarly, the Euler equation (9.15) in the linear approximation leads to the expression

$$\omega w' = \frac{k}{mN_0} p', \tag{15.3b}$$

where m is the mass of the particles of the gas.

Equations (15.3) connect the oscillation frequency ω and the wave number by the relation

$$\omega = c_s k, \tag{15.4}$$

where the speed of sound c_s is

$$c_s = \sqrt{\frac{p'}{mN'}} = \sqrt{\frac{1}{m}\frac{\partial p}{\partial N}}. \tag{15.5}$$

An equation of the type (15.4) that connects the frequency ω of the wave with its wave number k is called a *dispersion relation*. We see that here the group velocity of sound propagation, $\partial\omega/\partial k$, is the same as the phase velocity ω/k and does not depend on the sound frequency.

In order to find the sound velocity, it is necessary to know the connection between variations of the gas pressure and density in the acoustic wave. For long waves, the regions of compression and rarefaction do not exchange energy during wave propagation. Hence this process is adiabatic, and the parameters of the acoustic wave satisfy the adiabatic equation

$$pN^{-\gamma} = \text{const}, \tag{15.6}$$

where $\gamma = c_p/c_V$ is the adiabatic exponent; where c_p is the specific heat capacity at constant pressure, and c_V is the specific heat capacity at constant volume. From the expansion (15.2) the wave parameters are related by the expression

$$p'/p_0 = \gamma N'/N_0.$$

Because of the state equation (9.16) $p_0 = N_0 T$, where T is the gas temperature, we obtain $p'/N' = \partial p/\partial N = \gamma T$. Thus Eq. (15.4) yields

$$\omega = \sqrt{\frac{\gamma T}{m}}\, k. \tag{15.7}$$

The sound velocity is seen to be of the order of the thermal velocity of gas particles.

The dispersion relation (15.7) is valid under adiabatic conditions in the wave if a typical time τ of heat transport in the wave is large compared to the period of oscillations $1/\omega$. Assuming the heat transport in the wave to be due to thermal conductivity, we have $\tau \sim r^2/\chi \sim (\chi k^2)^{-1}$, where a distance r is of the order of the mean free path and χ is the thermal diffusion coefficient. From this we obtain the adiabatic criterion

$$\omega \ll c_s^2/\chi, \tag{15.8}$$

for the wave, where c_s is the wave velocity. For example, in the case of air under standard conditions ($p = 1$ atm), the condition (15.8) has the form $\omega \ll 5 \times 10^9\ \mathrm{s}^{-1}$. Because $\chi = \kappa/(c_p N) \sim v_T/\lambda$, and $c_s \sim v_T$, where λ is the free path length of gas molecules and v_T is a typical thermal velocity of the molecules, the condition (15.8) may be rewritten in the form

$$\lambda k \ll 1.$$

That is, the wavelength of the oscillations is large compared to the mean free path of the molecules of the gas.

15.2 PLASMA OSCILLATIONS

We want to analyze plasma oscillations that are due to the motion of charged particles. In the simplest case of a homogeneous plasma with no external fields, there are two types of natural plasma oscillations, since a plasma has two species of charged particles. These oscillation types are quite different, since the electrons and ions that are responsible for them differ greatly in mass. We first consider the high-frequency oscillations of the uniform plasma that are due to electron motion. They are called *plasma waves*, and the

limiting case of these oscillations corresponding to an infinite wavelength was analyzed in Chapter 3. As in that analysis, we assume the ions to be at rest and their charges to be uniformly distributed over the plasma volume. As with acoustic oscillations in a gas, we shall derive the dispersion relation for the plasma waves from the continuity equation (9.5), the Euler equation (9.15), and the adiabatic condition (15.6) for the wave. Moreover, we take into account that the motion of electrons produces an electric field owing to the disturbance of the plasma quasineutrality. The electric field term is introduced into the Euler equation (9.15), and the electric field strength is determined by Poisson's equation (3.2).

As with the deduction of the dispersion relation for acoustic oscillations, we assume that parameters of the oscillating plasma can be written in the form (15.2), and in the absence of oscillations both the mean electron velocity w and the electric field strength E are zero. Hence, we obtain

$$\begin{aligned} -i\omega N_e' + ikN_0 w' &= 0, \\ -i\omega w' + i\frac{kp'}{m_e N_0} + \frac{eE'}{m_e} &= 0, \\ \frac{p'}{p_0} = \gamma\frac{N_e'}{N_0}, \qquad ikE' &= -4\pi eN. \end{aligned} \tag{15.9}$$

Here k and ω are the wave number and the frequency of the plasma oscillations, N_0 is the mean number density of charged particles, $p_0 = N_0 m_e \langle v_x^2 \rangle$ is the electron gas pressure in the absence of oscillations, m_e is the electron mass, v_x is the electron velocity component in the direction of oscillations, and the angle brackets denote averaging over electron velocities. The quantities N_e', w', p', and E' in Eq. (15.9) are the oscillation amplitudes for the electron number density, mean velocity, pressure, and electric field strength, respectively.

Eliminating the oscillation amplitudes from the system of equations (15.9), we obtain the dispersion relation for plasma oscillations

$$\omega^2 = \omega_p^2 + \gamma \langle v_x^2 \rangle k^2, \tag{15.10}$$

where $\omega_p = \sqrt{4\pi N_0 e^2/m_e}$ is the plasma frequency [Eq. (3.9)]. Plasma oscillations are longitudinal, in contrast to electromagnetic oscillations. Hence, the electric field due to plasma waves is directed along the wave vector. This fact was used in deducing the set of equations (15.9).

The dispersion relation (15.10) is valid for adiabatic propagation of plasma oscillations. If heat transport is due to electron thermal conductivity, the adiabatic condition takes the form $\omega\tau \sim \omega/(\chi k^2) \gg 1$ [compare with Eq. (15.8)], where ω is the frequency of oscillations, $\tau \sim (\chi k^2)^{-1}$ is a typical

time for heat transport in the wave, χ is the electron thermal diffusion coefficient, and k is the wave number of the wave. Since $\chi \sim v_e \lambda$, then $\omega \sim \omega_p \sim v_e / r_D$, where v_e is the mean electron velocity, λ is the electron mean free path, and r_D is the Debye–Hückel radius. The adiabatic condition yields

$$\lambda r_D k^2 \ll 1. \tag{15.11}$$

If this inequality is reversed, then isothermal conditions in the wave are fulfilled. In this case the adiabatic parameter γ in the dispersion relation (15.10) must be replaced by the coefficient $\frac{3}{2}$.

Note that because the frequency of plasma oscillations is much greater than the reciprocal of a typical time interval between electron-atom collisions, we have $\omega_p \gg N_a v_e \sigma_{ea} \sim v_e / \lambda$. From this it follows that $\lambda \gg r_D$.

15.3 ION SOUND

We consider now the plasma oscillations that are due to the motion of ions in a homogeneous plasma. The special character of these oscillations is due to the large mass of ions. This stands in contrast to the small mass of electrons, which enables them to follow the plasma field, so that the plasma remains quasineutral on the average:

$$N_e = N_i.$$

Moreover, the electrons have time to redistribute themselves in response to the electric field in the plasma. Then the Boltzmann equilibrium is established, and the electron number density is given by the Boltzmann formula (2.8):

$$N_e = N_0 \exp\left(\frac{e\varphi}{T_e}\right) \approx N_0\left(1 + \frac{e\varphi}{T_e}\right),$$

where φ is the electric potential due to the oscillations, and T_e is the electron temperature. These properties of the electron oscillations allows us to express the amplitude of oscillations of the ion number density as

$$N_i' = N_0 \frac{e\varphi}{T_e}. \tag{15.12a}$$

We can now introduce the equation of motion for ions. The continuity equation (9.5), $\partial N_i / \partial t + \partial (N_i w_i) / \partial x = 0$, gives

$$\omega N_i' = k N_0 w_i, \tag{15.12b}$$

where ω is the frequency, k is the wave number, and w_i is the mean ion velocity due to the oscillations. Here we assume the usual harmonic dependence (15.2) for oscillation parameters. The equation of motion for ions due to the electric field of the wave has the form $M_i(d\mathbf{w}_i/dt) = e\mathbf{E} = -e\nabla\varphi$, where M is the ion mass. Taking into account the harmonic dependence (15.2) on the spatial coordinates and time, we have

$$M_i \omega w_i = ek\varphi. \tag{15.12c}$$

Eliminating the oscillation amplitudes of N_i, φ, and w_i in the set of equations (15.12), we obtain the dispersion relation

$$\omega = k\sqrt{\frac{T_e}{M_i}} \tag{15.13}$$

connecting the frequency and wave number. These oscillations caused by ion motion are known as *ion sound*. As with plasma oscillations, ion sound is a longitudinal wave; that is, the wave vector $\mathbf{k}$ is parallel to the oscillating electric field vector $\mathbf{E}$. The dispersion relation for ion sound is similar to that for acoustic waves. This is due to the fact that both types of oscillations are characterized by a short-range interaction. In the case of ion sound, the interaction is short-ranged because the electric field of the propagating wave is shielded by the plasma. This shielding is effective if the wave length of the ion sound is considerably larger than the Debye–Hückel radius for the plasma where the sound propagation occurs: $kr_D \ll 1$. The dispersion relation (15.13) is valid if this condition is fulfilled.

To find the dispersion relation for ion sound in a general case, we start with the Poisson equation for the plasma field in the form

$$\frac{d^2\varphi}{dx^2} = 4\pi e(N_e - N_i).$$

In the case of long-wave oscillations treated above, we took the left-hand side of this equation to be zero. Now, using the harmonic dependence of wave parameters on the coordinates and time, we obtain $-k^2\varphi$ for the left-hand side of this equation. Taking $N_e' = N_0(1 + e\varphi/T_e)$ in the right-hand side of this Poisson equation, we obtain

$$N_i' = N_0 \frac{e\varphi}{T_e}\left(1 + \frac{k^2 T_e}{4\pi N_0 e^2}\right).$$

In the treatment of long-wave oscillations, we neglected the second term in the parentheses. Hence, the dispersion relation (15.13) is now replaced by

$$\omega = k\sqrt{\frac{T_e}{M_i}}\sqrt{1 + \frac{k^2 T_e}{4\pi N_0 e^2}}\,. \tag{15.14}$$

This dispersion relation transforms into Eq. (15.13) in the limit $kr_D \ll 1$ when the oscillations are determined by short-range interactions in the plasma. In the opposite limit $kr_D \gg 1$ we get

$$\omega = \sqrt{\frac{4\pi N_0 e^2}{M_i}} . \tag{15.15}$$

In this case a long-range interaction in the plasma is of importance, and from the form of the dispersion relation, we see that ion oscillations are similar to plasma oscillations.

15.4 MAGNETOHYDRODYNAMIC WAVES

New types of oscillations arise in a plasma subjected to a magnetic field. We consider the simplest oscillations of this type in a high-conductivity plasma. In this case the magnetic lines of force are frozen in the plasma, and a change in the plasma current causes a change in the magnetic lines of force, which acts in opposition to this current. The oscillations thus generated are called *magnetohydrodynamic waves.*

For magnetohydrodynamic waves with wavelengths smaller than the radius of curvature of the magnetic lines of force, we have

$$\frac{1}{k} \ll \left| \frac{H}{\nabla H} \right|, \tag{15.16}$$

where H is the magnetic field strength. Then one can consider the magnetic lines of force to be straight lines. We construct a simple model of oscillations of a high-conductivity plasma, where the magnetic lines of force are frozen in the plasma. The displacement of the lines causes a plasma displacement, and due to the plasma elasticity, these motions are oscillations. The velocity of propagation of this oscillation is, according to Eq. (15.5), given by $c = \sqrt{\partial p / \partial \rho}$, where p is the pressure and $\rho = MN$ is the plasma density, so that M is the ion mass. Because the pressure of a cold plasma is equal to the magnetic pressure $p = H^2/(8\pi)$, we have

$$c = \sqrt{\frac{H \, \partial H / \partial N}{4\pi M}}$$

for the velocity of wave propagation. Since the magnetic lines of force are frozen in the plasma, $\partial H / \partial N = H/N$. This gives

$$c = c_A = \frac{H}{\sqrt{4\pi MN}} \tag{15.17}$$

for the velocity of these waves. The quantity c_A is called the *Alfvén speed.*

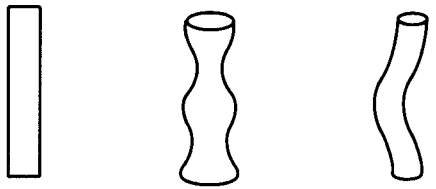

Figure 15.1 (a) A pipe of magnetic lines of force in equilibrium, and its distortion during (b) magnetic sound oscillations, and (c) magnetohydrodynamic oscillations.

The oscillations being examined may be of two types, depending on the direction of wave propagation (see Fig.15.1). If the wave propagates along the magnetic lines of force, it is called an *Alfvén wave* or magnetohydrodynamic wave. This wave is analogous to a wave propagating along an elastic string. The other wave type propagates perpendicular to the magnetic lines of force. Then the vibration of one magnetic line of force causes the vibration of a neighboring line. Such waves are called *magnetic sound.* The dispersion relation for both types of oscillations has the form

$$\omega = c_A k. \tag{15.18}$$

15.5 PROPAGATION OF ELECTROMAGNETIC WAVES IN PLASMAS

We shall now derive the dispersion relation for an electromagnetic wave propagating in a plasma. Plasma motion due to an electromagnetic field influences the wave parameters, and therefore the plasma behavior determines the dispersion relation for the electromagnetic wave. We employ Maxwell's equations

$$\operatorname{curl} \mathbf{E} = -\frac{1}{c}\frac{\partial \mathbf{H}}{\partial t}, \qquad \operatorname{curl} \mathbf{H} = \frac{4\pi}{c}\mathbf{j} + \frac{1}{c}\frac{\partial \mathbf{E}}{\partial t} \tag{15.19}$$

for the electromagnetic wave. Here $\mathbf{E}$ and $\mathbf{H}$ are the electric and magnetic fields in the electromagnetic wave, $\mathbf{j}$ is the density of the electron current produced by the action of the electromagnetic wave, and c is the light velocity. Applying the curl operator to the first equation of (15.19) and the operator $-(1/c)(\partial/\partial t)$ to the second equation, and then eliminating the magnetic field from the resulting equations, we obtain

$$\nabla \operatorname{div} \mathbf{E} - \Delta \mathbf{E} + \frac{4\pi}{c^2}\frac{\partial \mathbf{j}}{\partial t} + \frac{1}{c^2}\frac{\partial^2 \mathbf{E}}{\partial t^2} = 0, \tag{15.20}$$

where Δ is the Laplacian.

We assume the plasma to be quasineutral, so that according to Maxwell's equations $\operatorname{div}\mathbf{E} = 0$. The electric current is due to motion of the electrons, so that $\mathbf{j} = -eN_0\mathbf{w}$, where N_0 is the average number density of electrons, and $\mathbf{w}$ is the electron velocity due to the action of the electromagnetic field. The equation of motion for the electrons is $m_e\, d\mathbf{w}/dt = -e\mathbf{E}$, which leads to the relation

$$\frac{\partial \mathbf{j}}{\partial t} = -eN_0\frac{d\mathbf{w}}{dt} = \frac{e^2N_0}{m_e}\mathbf{E}.$$

Hence, we obtain

$$\Delta\mathbf{E} - \frac{\omega_p^2}{c^2}\mathbf{E} - \frac{1}{c^2}\frac{\partial^2\mathbf{E}}{\partial t^2} = 0,$$

for the electric field of the electromagnetic wave, where ω_p is the plasma frequency. Writing the electric field strength in the form (15.2) and substituting it in the above equation, we obtain the dispersion relation

$$\omega^2 = \omega_p^2 + c^2k^2. \tag{15.21}$$

for the electromagnetic wave. If the plasma density is low ($N_e \to 0$, $\omega_p \to 0$), the dispersion relation agrees with that for an electromagnetic wave propagating in a vacuum, $\omega = kc$. Equation (15.21) shows that electromagnetic waves do not propagate in a plasma if their frequencies are lower than the plasma frequency ω_p. A characteristic damping distance for such waves is of the order of $c/\sqrt{\omega_p^2 - \omega^2}$ according to Eq. (15.21).

15.6 THE FARADAY EFFECT FOR PLASMAS

The Faraday effect manifests itself as a rotation of the polarization vector of an electromagnetic wave propagating in a medium in an external magnetic field. This effect is due to electric currents in a medium subjected to a magnetic field, and leads to different refractive behavior for waves with left-handed and with right-handed circular polarization. Hence, electromagnetic waves with different circular polarizations propagate with different velocities, and propagation of electromagnetic waves with plane polarization is accompanied by rotation of the polarization vector of the electromagnetic wave.

We consider an electromagnetic wave in a plasma propagating along the z-axis while being subjected to an external magnetic field. The wave and the constant magnetic field $\mathbf{H}$ are in the same direction. We treat a frequency regime such that we can neglect ion currents compared to electron currents. Hence, one can neglect motion of the ions. The electron velocity under the

action of the field is given by Eqs. (13.4). The electric field strengths of the electromagnetic wave corresponding to right-handed (subscript $+$) and left-handed (subscript $-$) circular polarization are given by

$$E_+ = (E_x + iE_y)e^{-i\omega t},$$

$$E_- = (E_x - iE_y)e^{-i\omega t}.$$

For a plasma without collisions ($\omega\tau \ll 1$), Eqs. (13.4) lead to

$$j_+ = -eN_e(w_x + iw_y) = \frac{iN_e e^2 E_+}{m_e(\omega + \omega_H)} = \frac{i\omega_p^2 E_+}{4\pi(\omega + \omega_H)},$$

$$j_- = -eN_e(w_x - iw_y) = \frac{i\omega_p^2 E_-}{4\pi(\omega - \omega_H)}.$$

When we employ in equation (15.20) the harmonic dependence (15.2) on time and space coordinates of wave parameters, we have

$$k^2\mathbf{E} - 4\pi i\omega\mathbf{j}/c^2 - \omega^2\mathbf{E}/c^2 = 0. \tag{15.22}$$

In the physical problem being examined the electromagnetic wave propagates along the direction of the magnetic field. Using the above expressions for the density of the electron currents, we obtain the dispersion relations for the electromagnetic waves with different circular polarizations in the form

$$k_+^2 + \omega_+ \frac{\omega_p^2}{\omega_+ + \omega_H} - \frac{\omega_+^2}{c^2} = 0, \qquad k_-^2 + \omega_- \frac{\omega_p^2}{\omega_- - \omega_H} - \frac{\omega_-^2}{c^2} = 0, \tag{15.23}$$

where subscripts $+$ and $-$ refer to right-handed and to left-handed circular polarizations, respectively. Based on these dispersion relations, we can analyze the propagation of an electromagnetic wave of frequency ω in a plasma in an external magnetic field. At $z = 0$ we take the wave to be polarized along the x-axis, so that $\mathbf{E} = \mathbf{i}E\exp(-i\omega t)$, where we introduce the unit vectors $\mathbf{i}$ and $\mathbf{j}$ along the x and y axes, respectively. The electric field of this electromagnetic wave in the plasma is

$$\mathbf{E} = \mathbf{i}E_x + \mathbf{j}E_y = \frac{\mathbf{i}}{2}(E_+ + E_-) + \frac{\mathbf{j}}{2i}(E_+ - E_-).$$

We use the boundary condition

$$E_+ = E_0 e^{i(k_+ z - i\omega t)},$$

$$E_- = E_0 e^{i(k_- z - i\omega t)}.$$

Introducing $k = (k_+ + k_-)/2$ and $\Delta k = k_+ - k_-$, we obtain the result

$$\mathbf{E} = E_0 e^{i(kz-\omega t)}\left(\mathbf{i}\cos\frac{\Delta k z}{2} + \mathbf{j}\sin\frac{\Delta k z}{2}\right). \tag{15.24}$$

From the dispersion relations (15.23) it follows that

$$k_+^2 = \frac{\omega^2}{c^2}\left[1 - \frac{\omega_p^2}{\omega(\omega + \omega_H)}\right], \qquad k_-^2 = \frac{\omega^2}{c^2}\left[1 - \frac{\omega_p^2}{\omega(\omega - \omega_H)}\right]. \tag{15.25}$$

Assuming the inequalities $\Delta k \ll k$ and $\omega_H \ll \omega$, Eqs. (15.25) yield

$$\Delta k = \frac{\omega_H}{c}\frac{\omega_p^2}{\omega^2}. \tag{15.26}$$

This result establishes the rotation of the polarization vector during propagation of the electromagnetic wave in a plasma. The angle φ of the rotation in the polarization is proportional to the distance z of propagation. This is a general property of the Faraday effect. In the limiting case $\omega \gg \omega_p$, $\omega \gg \omega_H$ we have

$$\frac{\partial\varphi}{\partial z} = \frac{\Delta k}{2} = \frac{\omega_H}{c}\frac{\omega_p^2}{2\omega^2}.$$

For a numerical example we note that for maximum laboratory magnetic fields $H \sim 10^4$ G the first factor ω_H/c is about 10 cm^{-1}, so that for these plasma conditions the Faraday effect is detectable for propagation distances of the order of 1 cm.

From the above results it follows that the Faraday effect is strong in the region of the cyclotron resonance $\omega \approx \omega_H$. Then a strong interaction takes place between the plasma and the electromagnetic wave with left-handed polarization. In particular, it is possible to have the electromagnetic wave with left-handed polarization absorbed, while the wave with right-handed circular polarization passes through the plasma freely. Then the Faraday effect can be detected at small distances.

15.7 WHISTLERS

Insertion of a magnetic field into a plasma leads to a large variety of new types of oscillations in it. We considered above magnetohydrodynamic waves and magnetic sound, both of which are governed by elastic magnetic properties of a cold plasma. In addition to these phenomena, a magnetic field can produce electron and ion cyclotron waves that correspond to rotation of

electrons and ions in the magnetic field. Mixing of these phenomena of plasma oscillations, ion sound, and electromagnetic waves creates many types of hybrid waves in a plasma. As an example of this, we now consider waves that are a mixture of electron cyclotron and electromagnetic waves. These waves are called *whistlers* and are observed as atmospheric electromagnetic waves of low frequency (in the frequency interval 300–30,000 Hz). These waves are a consequence of lightning in the upper atmosphere and propagate along magnetic lines of force. They can approach the magnetosphere boundary and then reflect from it. Therefore, whistlers are used for exploration of the Earth's magnetosphere up to distances of 5–10 Earth radii. The whistler frequency is low compared to the electron cyclotron frequency $\omega_H = eH/(m_e c) \sim 10^7$ Hz, and it is high compared to the ion cyclotron frequency $\omega_{iH} = eH/(Mc) \sim 10^2$–$10^3$ Hz (M is the ion mass). Below we consider whistlers as electromagnetic waves of frequency $\omega \ll \omega_H$ that propagate in a plasma in the presence of a constant magnetic field.

We employ the relation (15.2) to give the oscillatory parameters of a monochromatic electromagnetic wave. Then equation (15.20) gives

$$k^2\mathbf{E} - \mathbf{k}(\mathbf{k}\cdot\mathbf{E}) - i4\pi\omega\mathbf{j}/c^2 = 0 \tag{15.27}$$

when $\omega \ll kc$. We express the current density of electrons in the form $\mathbf{j} = -eN_e\mathbf{w}$, where N_e is the electron number density. The electron drift velocity follows from the electron equation of motion (13.13), which, when $\nu \ll \omega \ll \omega_H$, has the form $e\mathbf{E}/m_e = -\omega_H(\mathbf{w}\times\mathbf{h})$, where $\mathbf{h}$ is the unit vector directed along the magnetic field. Substituting this in equation (15.27), we obtain the dispersion relation

$$k^2(\mathbf{j}\times\mathbf{h}) - \mathbf{k}[\mathbf{k}\cdot(\mathbf{j}\times\mathbf{h})] - i\mathbf{j}\omega\omega_p^2/(\omega_H c^2) = 0, \tag{15.28}$$

where $\omega_p = \sqrt{4\pi N_0 e^2/m_e}$ is the plasma frequency. We introduce a coordinate system such that the z-axis is parallel to the external magnetic field (along the unit vector $\mathbf{h}$) and the xz plane contains the wave vector. The x and y components of this equation are

$$-\frac{i\omega\omega_p^2}{\omega_H c^2}j_x + (k^2 - k_x^2)j_y = 0, \qquad -k^2 j_x - \frac{i\omega\omega_p^2}{\omega_H c^2}j_y = 0. \tag{15.29}$$

The determinant of this system of equations must be zero, which leads to the dispersion relation

$$\omega = \frac{\omega_H c^2 k k_z}{\omega_p^2} = \frac{\omega_H c^2 k^2 \cos\vartheta}{\omega_p^2}. \tag{15.30}$$

Here ϑ is the angle between the direction of wave propagation and the external magnetic field.

One can see that the whistler frequency is considerably higher than the frequency of Alfvén waves and magnetic sound. In particular, if the whistler propagates along the magnetic field, Eq. (15.30) gives $\omega = \omega_A^2/\omega_{iH}$, where ω_A is the frequency of the Alfvén wave, and ω_{iH} is the ion cyclotron frequency. Since we assume $\omega \gg \omega_{iH}$, this implies that

$$\omega \gg \omega_A \gg \omega_{iH}. \tag{15.31}$$

In addition, because $\omega \ll \omega_H$, the condition $\omega \ll kc$ leads to the inequalities

$$\omega \ll kc \ll \omega_p. \tag{15.32}$$

Whistlers are determined entirely by the motion of electrons. To examine the nature of these waves, we note first that the electron motion and the resultant current in the magnetized plasma give rise to an electric field according to equation (13.13). This electric field, in turn, leads to an electron current according to equation (15.27). In the end, the whistler oscillations are generated. Note that because the dispersion relation has the dependence $\omega \sim k^2$, the group velocity of these oscillations, $v_g = \partial\omega/\partial k \sim \sqrt{\omega}$, grows with the wave frequency. This leads to an identifying characteristic of the received signal if it is a short-time signal with a wide band of frequencies. The decrease of the tone of such a signal with time is the reason for the name "whistler".

The polarization of a whistler propagated along the magnetic field can be found from Eq. (15.29) together with the dispersion relation (15.30). The result is

$$j_y = ij_x, \qquad j_x = -ij_y. \tag{15.33}$$

From this it follows that the wave has circular polarization. This wave propagated along the magnetic field therefore has a helical structure. The direction of rotation of wave polarization is the same as the direction of electron rotation. The development of such a wave can be described as follows. Suppose electrons in a certain region possess a velocity perpendicular to the magnetic field. This electron motion gives rise to an electric field and compels electrons to circulate in the plane perpendicular to the magnetic field. This perturbation is transferred to the neighboring regions with a phase delay. Such a wave is known as a *helicon wave*.

CHAPTER 16

PLASMA INSTABILITIES

16.1 DAMPING OF PLASMA OSCILLATIONS IN IONIZED GASES

Interaction of electrons and atoms leads to damping of plasma oscillations because electron–atom collisions shift the phase of the electron vibration and change the character of collective interaction of electrons in plasma oscillations. We shall take this fact into account below, and include it in the dispersion relation for the plasma oscillations. To obtain this relation we use Eq. (9.16) instead of Eq. (9.15) as the equation for the mean electron momentum. Then the second equation in the system (15.9) is transformed into

$$-i\omega w' + i\frac{kp'}{m_e N_0} + \frac{eE'}{m_e} = \frac{w'}{\tau}, \tag{16.1}$$

and the remaining equations of this system are unchanged. Here τ is the characteristic time for electron–atom elastic collisions.

Replacing the first equation of the system (15.9) by Eq. (16.1), we obtain the dispersion relation

$$\omega = \sqrt{\omega_p^2 + \gamma\langle v_x^2\rangle k^2} - \frac{i}{\tau} \tag{16.2}$$

instead of (15.10). This dispersion relation requires the condition

$$\omega\tau \gg 1. \tag{16.3}$$

Substituting Eq. (16.2) into Eq. (15.2), we find that the wave amplitude decreases with time as $\exp(-t/\tau)$; this decrease is due to the scattering of electrons by atoms of the gas. The condition for existence of plasma oscillations is such that the characteristic time of the wave damping must be considerably higher than the oscillation period; namely, the inequality (16.3) must hold. The frequency of collisions between electrons and atoms is $1/\tau \sim N\sigma v$, where N is the atom number density, v is a typical velocity of the electrons, and σ is the cross section for electron–atom collisions. Assuming this cross section to be of the order of a gas-kinetic cross section, the mean electron energy to be ~ 1 eV, and the frequency of plasma oscillations to be given by Eq. (3.9), we find that the condition (16.3) is equivalent to the estimate

$$N_e^{1/2}/N \gg 10^{-12}\ \text{cm}^{3/2}.$$

This shows that in some gas-discharge plasmas the conditions for the existence of plasma oscillations are not fulfilled.

16.2 INTERACTION BETWEEN PLASMA OSCILLATIONS AND ELECTRONS

The above damping mechanism for plasma oscillations is due to electron–atom collisions. Collisions of an electron with atoms cause a phase shift of the oscillations of the colliding electron, leading to the damping of these oscillations. Now we consider another mechanism for interaction of electron with waves. Electrons can be captured by waves (see Fig. 16.1), and then a strong interaction between these electrons and the wave takes place. To analyze this process in detail, we note that in the frame of reference where the wave is at rest, a captured electron travels between the potential

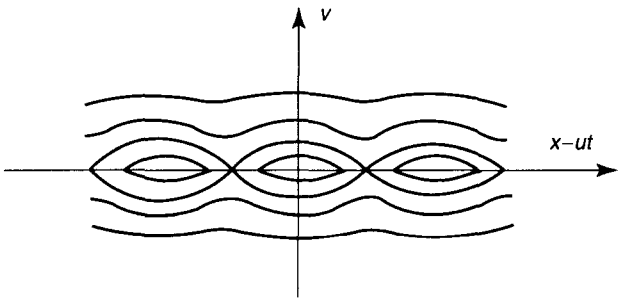

Figure 16.1 The phase space diagram for electrons in interaction with plasma oscillations. Plasma electrons captured by plasma oscillations have a closed trajectory in the phase space, where u is the phase velocity of the wave.

"walls" of the wave. Reflecting from one wall, an electron exchanges energy with the wave. If the electron velocity in this frame of reference is u, this energy is

$$\Delta\varepsilon = \tfrac{1}{2}m_e(v_p + u)^2 - \tfrac{1}{2}m_e(v_p - u)^2 = 2m_e v_p,$$

where $v_p = \omega/k$ is the phase velocity of the wave. A characteristic velocity of captured electrons in the frame of reference being considered is $u \sim (e\varphi/m_e)^{1/2}$, where φ is the amplitude of the scalar potential of the wave. We assume that collisions of a captured electron with other plasma electrons occur enough often that the captured electron can reflect only once from the potential wall of the wave. The subject electron obtains energy from the plasma electrons and escapes from the potential well. This means that the frequency of collisions with plasma electrons is greater than the frequency of oscillations of the captured electron in the potential well of the wave. The collision frequency according to Eq. (5.5) is $N_e e^4 T_e^{3/2} m_e^{-1/2} \ln\Lambda$, and the frequency of oscillations of the captured electron is of the order of $(e\varphi k/m_e)^{1/2} \sim \sqrt{eE'k/m_e} \sim \sqrt{e^2N'/m_e}$, where k is the wave number of the oscillation, and φ, E', and N' are the corresponding parameters of the oscillation. This gives the condition

$$N'/N_e \ll N_e e^6/T_e^3 \tag{16.4}$$

for the interaction between a captured electron and the wave.

Assuming this criterion to be satisfied, we now seek to establish the direction of the energy exchange between the wave and plasma electrons. The electron distribution function is not altered by the interaction with the wave, and it is necessary to compare the number of electrons with velocity $v_p + u$ that transfer energy to the wave and the number of electrons with velocity $v_p - u$ that take energy from the wave, where u is a positive quantity. The number of captured electrons is proportional to the electron distribution function $f(v)$. Hence, the wave gives its energy to electrons and is damped if $f(v_p + u)$ is larger than $f(v_p - u)$. This means that the wave is damped when

$$\left[\frac{\partial f}{\partial v_x}\right]_{v_x = v_p} < 0. \tag{16.5}$$

Here v_x is the component of the electron velocity in the direction of the wave propagation, and the derivative is taken for an electron velocity equal to the phase velocity v_p of the wave. When the condition (16.5) is not satisfied, the wave takes energy from the electrons and its amplitude increases.

In deriving the condition (16.5) for wave damping, we stated that the condition (16.4) is satisfied when the field of the wave does not affect the

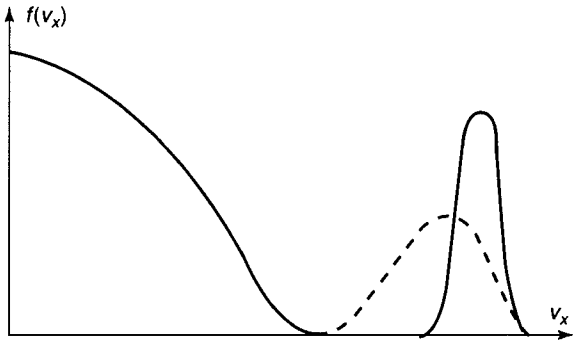

Figure 16.2 The electron distribution function for an electron beam injected into a plasma. The solid line corresponds to the initial distribution, and the dashed line to a later distribution.

electron distribution function. However, (16.5) holds also when the condition (16.4) is not satisfied and the electron distribution function is altered due to the interaction with the wave. Interaction with the wave tends to equalize the number densities of electrons with velocities $v_p + u$ and $v_p - u$, and hence to decrease the derivative $\partial f/\partial v_x$ at $v_x = v_p$, albeit without a change in its sign. That is, Eq. (16.5) remains valid even when the interaction with the wave alters the electron distribution function.

The condition (16.5) is satisfied if the electron distribution function is of Maxwellian form or if it is simply a monotonically decreasing function, and oscillations in such a plasma decrease with time owing to the interaction with electrons. However, when an electron beam is injected into the plasma producing the electron distribution function of Fig. 16.2, plasma oscillations in this system will be amplified, getting the necessary energy from the electrons. The interaction between plasma oscillations and electrons will reduce the velocity of the electrons until the electron distribution function again becomes monotonically decreasing.

Amplification of the oscillations can cause the amplitude to increase rapidly with time. If the oscillation amplitude is small and the oscillations do not alter the electron distribution function, that is, if the condition (16.4) is satisfied, then the oscillation amplitude will increase exponentially. When particles of the plasma transfer their energy to the plasma wave, thus amplifying it, such a state is termed an *unstable plasma state*.

16.3 ATTENUATION FACTOR FOR WAVES IN PLASMAS

We introduce into Eq. (15.2) the attenuation factor γ for the waves, so that the oscillation amplitude varies as $\exp(-\gamma t)$. We can estimate the attenuation factor when the wave does not affect the electron distribution in the

plasma, so that the condition (16.4) remains satisfied. Variation with time of the energy density W of the plasma oscillations can be estimated to be

$$\frac{dW}{dt} \sim \nu \int_{-u_0}^{u_0} f(v)\, \Delta\varepsilon\, du. \tag{16.6}$$

Here $\nu \sim u_0 k$ is the oscillation frequency for an electron captured in the potential well of the wave, $u_0 = (2e\varphi/m_e)^{1/2}$, φ is the amplitude of the potential oscillations, and $\Delta\varepsilon = 2m_e v_p u_0$ is the maximum change in the electron energy when the direction of the electron motion is reversed. (We take into account only the interaction between the wave and captured electrons.) The right-hand side of the Eq. (16.6) may be estimated as

$$\nu \frac{\partial f}{\partial v_x} u_0\, \Delta\varepsilon\, u_0 \sim u_0 k \frac{\partial f}{\partial v_x} u_0 m_e v_p u_0 \cdot u_0 \sim \frac{\partial f}{\partial v_x} \frac{e^2\omega}{m_e k_2} W,$$

where we use the relations $v_p = \omega/k$ and $W \sim (E')^2 \sim \varphi^2/k^2$ (E' is the amplitude of the electric field of the wave). From the definition of the attenuation factor γ of the plasma wave, we have $dW/dt = -\gamma W$, so we obtain the estimate

$$\gamma \sim \frac{e^2\omega}{m_e k^2} \frac{\partial f}{\partial v_x}. \tag{16.7}$$

Attenuation occurs when the condition (16.5) is satisfied. The attenuation factor (16.7), which is due to the interaction between the charged particles and the wave, is known as the *Landau damping factor*.

The condition for the existence of oscillations is

$$\gamma \ll \omega. \tag{16.8}$$

We can examine the implications of the condition (16.8) for plasma oscillations, and we can also investigate ion sound, assuming the Maxwell distribution function for the particles. Taking $\omega \sim \omega_p$, we obtain

$$kr_D \ll 1, \tag{16.9}$$

for plasma oscillations, where r_D is the Debye–Hückel radius (3.6). When this condition is fulfilled, the phase velocity of the wave is considerably higher than the thermal velocity, so that the electrons captured by the wave are at the tail of the distribution function.

When ion sound propagates in a plasma in which the temperatures of electrons and ions are the same, the phase velocity of the sound is of the order of the thermal velocity of the ions, and the attenuation factor is of the

order of the wave frequency. Therefore, ion sound can propagate only in plasmas in which the electron temperature T_e is considerably higher than the ion temperature T_i:

$$T_e \gg T_i. \tag{16.10}$$

16.4 BEAM–PLASMA INSTABILITY

Assume that an electron beam penetrates into a plasma, where the velocity of the electrons in the beam is much higher than a thermal velocity of the plasma electrons, while the number density N_b of the electrons in the beam is considerably lower than the number density N_0 of plasma electrons. Deceleration of the electron beam can occur owing to the scattering of electrons of the beam on electrons and ions of the plasma. There is, however, another mechanism for deceleration of the electron beam, known as beam instability. In the early days of plasma physics this phenomenon was known as the *Langmuir paradox*. Langmuir discovered that the temperature of the electrons in a beam ejected from a cathode surface becomes equal to the temperature of the electrons of the gas-discharge plasma into which it penetrates, at distances from the cathode that are small compared to the mean free path of the electrons. Because it was assumed in that era that energy exchange between beam and plasma electrons results only from collisions, the Langmuir effect was considered to be a paradox. In actuality, interaction of the beam electrons with plasma electrons proceeds more effectively through collective degrees of freedom of the beam–plasma system than through collisions. This interaction can be succinctly described as follows. Suppose plasma oscillations are generated in a plasma. Interacting with electrons of the beam and taking energy from them, these oscillations are amplified. Thus, some of the energy of the electron beam is transformed into the energy of plasma oscillations and remains in the plasma. This energy may subsequently be transferred to other degrees of freedom of the plasma.

We can estimate the amplification of the plasma oscillations in the above scenario assuming the oscillation amplitude to be small, and taking the temperatures of the electrons in the plasma and in the beam to be zero. Hence, the pressure of the electrons in the plasma and beam is zero. Applying the continuity equation (9.6) and the Euler equation (9.15) to the plasma electrons, we derive equations for the amplitudes of the plasma parameters that follow from the first two equations of (15.9) with $p' = 0$. Elimination of the electron velocity w' in the wave in these equations yields

$$N_e' = -i\frac{keE'}{m_e\omega^2}N_0. \tag{16.11a}$$

One can obtain the expression for the amplitude N_b' of oscillations of the electron number density in the beam in a similar way by writing the electron

number density N_b' in the beam as $N_b + N_b' \exp[i(kx - \omega t)]$ and the velocity of the electrons in the beam as $u + w_b \exp[i(kx - \omega t)]$, where the x-axis is parallel to the velocity of the beam, and N_b and u are, respectively, the electron number density and velocity in the unperturbed beam. Then we have

$$N_b' = -\frac{ikeE'N_b}{m_e(\omega - ku)^2}. \tag{16.11b}$$

As was done in arriving at the last equation of the system (15.9), Poisson's equation (3.2) yields the equation

$$ikE' = -4\pi e(N_e' + N_b') \tag{16.11c}$$

for the amplitude of the system's parameters. Eliminating the amplitudes N', N_b', and E' from the set of Eqs. (16.11), we obtain the dispersion relation

$$\frac{\omega_p^2}{\omega^2} + \frac{\omega_p^2}{(\omega - ku)^2}\frac{N_b}{N_0} = 1. \tag{16.12}$$

Here $\omega_p = (4\pi N_0 e^2/m_e)^{1/2}$ is the frequency of plasma oscillations. When the number density of the beam electrons is zero ($N_b = 0$), Eq. (16.12) reduces to the form taken by Eq. (15.10) when the electron temperature is taken to be zero. The strongest interaction between the beam and plasma occurs when the phase velocity of the plasma waves, ω/k, is equal to the velocity of the electron beam. Let us analyze this case. Since the number density N_b of the beam electrons is small compared to the number density N_0 of the plasma electrons, the frequency of the plasma oscillations is close to the plasma frequency ω_p. Hence, we shall consider waves with the wave number $k = \omega_p/u$, which have the most effective interaction with the electron beam. We write the frequency of these oscillations as $\omega = \omega_p + \delta$ and insert it into Eq. (16.12). Expanding the result in a series in the small parameter δ/ω_p, we obtain

$$\delta = \omega_p\left(\frac{N_b}{2N_0}\right)^{1/3}\exp\left(\frac{2\pi in}{3}\right),$$

where n is an integer. One can see that $\delta/\omega_p \sim (N_b/N_0)^{1/3} \ll 1$. That is, the expansion in δ/ω_p is valid.

If the imaginary component of the frequency (which is equal to the imaginary component of δ) is negative, the wave is attenuated; if it is positive, the wave is amplified. The maximum value of the amplification factor is given by ($n = 1$)

$$-\gamma = \frac{\sqrt{3}}{2}\left(\frac{N_b}{N_0}\right)^{1/3}\omega_p = 0.69\omega_p\left(\frac{N_b}{N_0}\right)^{1/3}. \tag{16.13}$$

The amplitude N_b' varies with time as $\exp(\gamma t)$; this result is valid if the plasma oscillations do not affect the properties of the plasma. This type of instability is known as the *beam–plasma instability*. As a result of this instability, the distribution function of the beam electrons expands (see Fig. 16.2), and the energy surplus is transferred to plasma oscillations.

16.5 THE BUNEMAN INSTABILITY

We now consider instability of another type that develops if the mean velocity of the electrons differs from the mean velocity of the ions. We formulate the problem by taking all the plasma ions to be at rest and all the electrons to travel with a velocity u with respect to the ions. The plasma is quasineutral: that is, the number densities of the electrons and ions are equal. Our goal is to determine the maximum amplification factor of the plasma oscillations. The electron beam is decelerated owing to the transfer of energy from the beam to the plasma oscillations.

With this formulation, the problem is equivalent to the previous case of interaction of an electron beam and a plasma. In both problems there is an electron beam penetrating the plasma, so that the dispersion relation can be derived in a similar way. Denoting the ion mass as M and taking into account the equality of ion and electron number densities, we obtain the dispersion relation

$$\frac{m_e}{M}\frac{\omega_p^2}{\omega^2} + \frac{\omega_p^2}{(\omega - ku)^2} = 1 \tag{16.14}$$

instead of the relation (16.12). If we let the ratio m_e/M go to zero, we obtain the dispersion relation $\omega = \omega_p + ku$. Hence, one can write the frequency of the plasma oscillations as

$$\omega = \omega_p + ku + \delta.$$

Substituting this frequency into Eq. (16.14) and expanding the result in a power series in the small parameter δ/ω_p, we obtain

$$\frac{2\delta}{\omega_p} = \frac{m_e}{M}\frac{\omega_p^2}{(\omega_p + ku + \delta)^2}.$$

The electron beam has the strongest interaction with the wave whose wave number is $k = -\omega_p/u$. For this wave we have

$$\delta = \left(\frac{m_e}{M}\right)^{1/3}\omega_p \exp\left(\frac{2\pi i n}{3}\right),$$

where n is an integer. The highest amplification factor corresponds to $n = 1$ and is given by

$$-\gamma = \operatorname{Im}\delta = \frac{\sqrt{3}}{2}\left(\frac{m_e}{2M}\right)^{1/3}\omega_p = 0.69\omega_p\left(\frac{m_e}{M}\right)^{1/3}. \qquad (16.15)$$

Note that the frequency of oscillations is of the order of the amplification factor. This type of instability of the electron beam due to interaction with plasma ions is known as the *Buneman instability*. The above analysis of the Buneman instability has a qualitative character because the wave frequency and the attenuation factor are of the same order of magnitude. Nevertheless, this analysis allows us to estimate the rate of destroy of the plasma motion.

16.6 HYDRODYNAMIC INSTABILITIES

The instabilities discussed above are so-called *kinetic* instabilities, for which the amplification of oscillations is due to the differences in the character of the motion of various groups of particles. The development of oscillations ultimately results in a change of the velocity distribution function for the charged particles of the plasma. Another class of instabilities is known as *hydrodynamic* instabilities. The development of hydrodynamic instabilities involves a displacement of the plasma regions and results, finally, in variation of the spatial configuration of the plasma. We shall analyze the simplest type of hydrodynamic instability: the *pinch* instability.

We examine the stability of the pinch configuration with respect to development of the so-called *sausage* instability. This instability changes the radius of the pinch but conserves its axial symmetry. We have to find under what conditions an accidental distortion of the pinch will not develop further. Let us assume that the distortion of the pinch results only in a slight curving of the magnetic lines of force; that is, the radius of curvature of the magnetic lines of force is considerably larger than the radius of the pinch. According to Eq. (13.43), the relation

$$p + \frac{H^2}{8\pi} = \text{const.}$$

is satisfied in the plasma region.

We must analyze the variation of the parameters of the pinch due to variation of its radius. The total current and magnetic flux through the cross section of the pinch will be conserved. The electric current is $I_z = caH_\varphi/2$, where a is the pinch radius and H_φ is the axial magnetic field strength. The condition $\delta I_z = 0$ yields $\delta a/a + \delta H_\varphi/H_\varphi = 0$, where δa is the variation of the pinch radius and δH_φ is the variation of the axial magnetic field at the pinch surface outside the plasma. The longitudinal magnetic field is frozen into the plasma, so that a displacement of plasma elements does not change

the magnetic flux through them. The condition for conservation of the magnetic flux, $\Phi_z = \pi a^2 H_z$, yields $2\,\delta a/a + \delta H_z/H_z = 0$ (where H_z is the longitudinal external magnetic field inside the plasma). Hence, $\delta H_z/H_z = 2(\delta H_\varphi/H_\varphi)$. The variation of the magnetic field pressure inside the plasma is $\delta[H_z^2/(8\pi)\,] = H_z\,\delta H_z/(4\pi)$, and the variation of the magnetic pressure outside the plasma is $H_\varphi\,\delta H_\varphi/(4\pi) = H_\varphi^2\,\delta H_z/(8\pi H_z)$. It can be seen that if

$$H_z^2 \geq H_\varphi^2/2 \tag{16.16}$$

holds true, the additional internal magnetic field pressure produced by the distortion of the pinch is smaller than the additional outside magnetic field pressure. When the condition (16.16) is satisfied, the pinch is stable with respect to displacements of the sausage type.

CHAPTER 17

NONLINEAR PHENOMENA IN PLASMAS

17.1 THE LIGHTHILL CRITERION

Plasma instabilities cause the development of certain types of oscillations. The subsequent evolution of these oscillations is determined by interactions between the oscillations and the plasma itself. The strength of these interactions depends on the wave amplitude. Hence, we deal with nonlinear plasma phenomena. But the role of nonlinear plasma processes is not restricted to the development of instabilities. Nonlinear processes affect the nature of wave propagation in a plasma. In fact, interaction between elementary waves is effected through the interaction of these waves with the plasma. Therefore, nonlinear phenomena determine both the profile and the character of the propagation of all waves in a plasma except those of small intensity.

To study the development of perturbations in a plasma, we examine a perturbation in the form of a one-dimensional wave packet consisting of waves encompassing a narrow range of wave numbers ($\Delta k \ll k$). The perturbation amplitude at a point x is

$$a(x,t) = \sum_k a(k) \exp(ikx - i\omega t), \tag{17.1}$$

where $a(k)$ is the amplitude of the wave with a wave number k. We take into account the wave dispersion, expressible as

$$\begin{aligned}\omega(k) &= \omega(k_0) + \frac{\partial\omega(k_0)}{\partial k}(k - k_0) + \frac{\partial^2\omega(k_0)}{\partial k^2}(k - k_0)^2 \\ &= \omega_0 + v_g(k - k_0) + \frac{1}{2}\frac{\partial v_g(k_0)}{\partial k}(k - k_0)^2.\end{aligned} \tag{17.2}$$

Here k_0 is the mean wave number of the wave packet, and v_g is the group velocity of the wave. Since wave number values are restricted to an interval of width Δk near k_0, then according to Eq. (17.1) the perturbation is initially concentrated in a spatial region of extent $\Delta x \sim 1/\Delta k$. As the wave packet evolves, it diverges due to the different group velocities of individual waves. The initial wave packet, which has a size of the order of $1/\Delta k$, diverges on a time scale given by $\tau \sim (\Delta k^2)^{-1}(\partial v_g/\partial k)^{-1}$. That is, wave dispersion usually leads to increasing spatial extension of the wave as a function of time.

The interaction of waves of different k-values influences the behavior of this process. In particular, it can even lead to compression of the waves. In order to assess this possibility, we take into account the dependence

$$\omega = \omega_0 - \alpha E^2 \tag{17.3}$$

of the wave frequency on its amplitude, where E is a (small) field amplitude, and ω_0 is the frequency of this wave. Inserting expansions (17.2) and (17.3) into Eq. (17.1), we obtain

$$a(x,t) = \sum_k a(k)\exp\Big(i(k-k_0)(x-x_0) - ik_0x_0 - i(k-k_0)^2\frac{v_g}{\partial k}t - i\alpha E^2(x)t\Big) \tag{17.4}$$

for the wave-packet amplitude. From Eq. (17.4) it follows that nonlinear wave interactions can lead to modulation of the wave packet. With certain types of modulation the wave packet may decay into separate bunches, or it may be compressed into a solitary wave—a soliton. This phenomenon is known as *modulation instability*.

Equation (17.4) shows that the compression of a wave packet or its transformation into separate bunches can take place only if the last two terms in the exponent in this equation have opposite signs. Only in this case can a nonlinear interaction compensate for the usual divergence of the wave packet. Therefore, modulation instability can only occur subject to the condition

$$\alpha\frac{\partial v_g}{\partial k} < 0. \tag{17.5}$$

This condition is called the *Lighthill criterion*.

17.2 THE KORTEWEG–de VRIES EQUATION

The above analysis shows that wave dispersion leads to divergence of the wave packet. If this divergence is weak, a weak nonlinearity is able to change its character. We now consider an example of such behavior when a wave is

characterized by small dispersion and nonlinearity. Consider the propagation of long-wavelength waves in a medium in which the dispersion relation has the form

$$\omega = v_g k(1 - r_0^2 k^2), \qquad r_0 k \ll 1. \tag{17.6}$$

This form describes a variety of oscillations, with sound and ion sound as examples. We shall obtain below a nonlinear equation that describes such waves.

Take as a starting point the Euler equation (9.8) for the velocity of particles in a longitudinal wave, which has the form

$$\frac{\partial v}{\partial t} + v\frac{\partial v}{\partial x} - \frac{F}{m} = 0. \tag{17.7}$$

Here $v(x, t)$ is the particle (gas atom or gas molecule) velocity in a longitudinal wave which propagates along the x-axis, F is the force per particle, and m is the particle mass. Within the framework of a linear approximation one can write the particle velocity in the form $v = v_g + v'$, where v_g is the group velocity, and v' is the particle velocity in the frame of reference where the wave is at rest. Because $v' \ll v_g$, we have

$$\frac{\partial v'}{\partial t} + v_g\frac{\partial v'}{\partial x} - \frac{F}{m} = 0$$

in the linear approximation. The last term is a linear operator with respect to v'. In the harmonic approximation we have $v' \sim \exp(ikx - i\omega t)$. We seek the form of the operator F/m that leads to the dispersion relation (17.6) in this approach. This gives the equation

$$\frac{\partial v'}{\partial t} + v_g\left(\frac{\partial v'}{\partial x} + r_0^2\frac{\partial^3 v'}{\partial x^3}\right) = 0.$$

The last term takes into consideration a weak dispersion of long-wave oscillations. In order to account for a nonlinearity of these waves, we analyze the second term of this equation. In the linear approach we replaced the particle velocity v by the group velocity v_g. Returning this term to its initial form, that is, taking into account weak nonlinear effects, we obtain

$$\frac{\partial v}{\partial t} + v\frac{\partial v}{\partial x} + v_g r_0^2\frac{\partial^3 v}{\partial x^3} = 0. \tag{17.8}$$

This equation is called the *Korteweg–de Vries equation* and was originally obtained in the analysis of wave propagation in shallow water.

The Korteweg–de Vries equation accounts for nonlinearity and weak dispersion simultaneously, and therefore serves as a convenient model equation for the analysis of nonlinear dissipative processes. As applied to plasmas, it describes propagation of long waves in a plasma for which the dispersion relation is given by Eq. (17.6).

17.3 SOLITONS

The Korteweg–de Vries equation has solutions that describe a class of solitary waves. These waves are called *solitons* and conserve their form in time. It follows from the dispersion relation (17.6) that short waves propagate more slowly than long waves, but nonlinear effects compensate for the spreading of the wave. We now show that this property holds true for waves that are described by the Korteweg–de Vries equation. We consider a wave of velocity u. The space and time dependence for the particle velocity has the form $v = f(x - ut)$. This gives $\partial v/\partial t = -u\,\partial v/\partial x$, and the Korteweg–de Vries equation is transformed to the form

$$(v - u)\frac{dv}{dx} + v_g r_0^2 \frac{d^3 v}{dx^3} = 0. \tag{17.9}$$

Assuming the perturbation to be zero at large distances from the wave, (that is, $v \to 0$, $d^2v/dx^2 \to 0$ as $x \to \infty$), this equation reduces to

$$v_g r_0^2 \frac{d^2 v}{dx^2} = uv - \frac{v^2}{2},$$

with the solution

$$v = 3u \cosh^{-2}\left(\frac{x}{2r_0}\sqrt{\frac{u}{v_g}}\right). \tag{17.10}$$

The wave described by Eq. (17.10) is concentrated in a limited spatial region and does not diverge in time. The wave becomes narrower with increase of its amplitude, with its extension inversely proportional to the square root of the wave amplitude.

In other words, the Korteweg–de Vries equation has stationary solutions describing a nonspreading solitary wave, or *soliton*. The amplitude a and extension $1/\alpha$ of solitons are such that the value a/α^2 does not depend on the wave amplitude. If the initial perturbation is sufficiently small, evolution of the wave packet leads to formation of one solitary wave. If it is large, the perturbation in the course of evolution of the system will split into several solitons. Thus, solitons not only are stable steady-state perturbations in the system, but also can play a role in the evolution of some perturbations in a nonlinear dispersive medium.

17.4 LANGMUIR SOLITON

The occurrence and propagation of solitons is associated with an electric field that exists in a plasma as the result of a wave process, and this field confines the perturbation to a restricted region. This can be demonstrated using the example of plasma oscillations. Denoting by $E(x,t)$ the electric field strength of the plasma oscillations, we have

$$W(x) = \frac{\overline{E^2}}{8\pi}$$

for their energy density, where the bar means a time average. Assuming the equality of electron and ion temperatures ($T_e = T_i = T$), the pressure of a quasineutral plasma is $p = 2N_eT$. The plasma pressure is established with a sound velocity that is larger than the velocity of propagation of long-wave oscillations. Then, because of the uniformity of plasma pressure at all points of the plasma, we have

$$2N(x)T + W(x) = 2N_0T, \tag{17.11}$$

where N_0 is the number density of charged particles at distances large enough that plasma oscillations are absent. (The plasma temperature is assumed to be constant in space.)

The dispersion relation (15.10) for plasma oscillations has the form

$$\omega^2 = \omega_p^2\left(1 - \frac{\overline{E^2}}{16\pi N_0T}\right) + \gamma\langle v_x^2\rangle k^2 \tag{17.12}$$

when Eq. (17.11) is taken into account, where ω_p is the plasma frequency in the absence of fields. We use in Eq. (17.12) the expression (3.9) for the plasma frequency.

We can write Eq. (17.12) in a more convenient form. Take the electric field strength of the wave in the form $E = E_0\cos\omega t$, so that $\overline{E^2} = E_0^2/2$. Using $\overline{v_x^2} = T/m_e$ for electrons and introducing the Debye–Hückel radius r_D according to Eq. (3.5), Eq. (17.12) gives

$$\omega^2 = \omega_p^2\left(1 - \frac{E_0^2}{32\pi N_0T} + 2\gamma r_D^2k^2\right). \tag{17.13}$$

The first term on the right-hand side of this expression is considerably larger than the other two.

One can see that the dispersion relation (17.13) satisfies the Lighthill criterion (17.5), because we have in this case

$$\alpha\frac{\partial v_g}{\partial k} = -\frac{\gamma\omega_p}{32\pi m_eN_0} < 0.$$

Thus, nonlinear Langmuir oscillations can form a soliton. The dispersion relation (17.13) shows that if the energy density of plasma oscillations is high enough [so that the second term of Eq. (17.13) is larger than the third one], the oscillations cannot exist far from the soliton. The oscillations create a potential well in the plasma and are enclosed in this well. They can propagate in the plasma together with the well and occupy a restricted spatial region. The size of the potential well (or the soliton size) decreases with increase of the energy density of the plasma oscillations. Because $r_D k \ll 1$, the solitons are formed when the energy density of the oscillations is small compared to the specific thermal energy of charged particles of the plasma. Thus, this analysis demonstrates the tendency to form solitons from long-wave plasma oscillations. However, the analysis used does not allow one to study the evolution of oscillations of large amplitudes.

17.5 NONLINEAR ION SOUND

We next analyze nonlinear ion sound when the nonlinearity is large. For this purpose we use the Euler equation (9.8), the continuity equation (9.5), and the Poisson equation (3.2), which, in the linear approach, leads to the dispersion relation (15.13) for ion sound. When we use these equations without any linear approximation, they can be written as

$$\frac{\partial v_i}{\partial t} + v_i \frac{\partial v_i}{\partial x} + \frac{e}{M}\frac{\partial \varphi}{\partial x} = 0,$$

$$\frac{\partial N_i}{\partial t} + \frac{\partial}{\partial x}(N_i v_i) = 0, \tag{17.14}$$

$$\frac{\partial^2 \varphi}{\partial x^2} = 4\pi e(N_e - N_i).$$

Here v_i is the velocity of ions in the wave, φ is the electric potential of the wave, N_e and N_i are the number densities of electrons and ions respectively, and M is the ion mass. As was discussed above, electrons are in equilibrium with the field owing to their high mobility. Therefore, the Boltzmann distribution applies to the electrons, so $N_e = N_0 \exp(e\varphi/T_e)$, where N_0 is the mean number density of charged particles, and T_e is the electron temperature.

We now analyze the motion of ions in the field of a steady-state wave when the plasma parameters v_i, N_i, and φ depend on time and the spatial coordinate as $f(x - ut)$, where u is the velocity of the wave. Then the set of

equations (17.14) can be rewritten as

$$\begin{aligned}(v_i - u)\frac{\partial v_i}{\partial x} + \frac{e}{M}\frac{\partial \varphi}{\partial x} &= 0,\\ \frac{\partial}{\partial x}[N_i(v_i - u)] &= 0,\\ \frac{\partial^2 \varphi}{\partial x^2} &= 4\pi e\left[N_0 \exp\left(\frac{e\varphi}{T_e}\right) - N_i\right].\end{aligned} \tag{17.15}$$

The perturbation is assumed to be zero far from the wave, so that $N_i \to N_0$, $v_i \to 0$ and $\varphi \to 0$, as $x \to \infty$. The first two equations of the set (17.15) then give

$$\begin{aligned}v_i^2/2 - uv_i + e\varphi/M &= 0,\\ N_i &= N_0 \frac{u}{u - v_i}.\end{aligned}$$

The second equation implies that $v_i < u$ because $N_i > 0$. This means that $\varphi \geq 0$ in the first equation, that is, the electric potential of this ion-acoustic wave is always positive. The first equation leads to $v_i = u - (u^2 - 2e\varphi/M)^{1/2}$, and the second equation gives $N_i = N_0 u(u^2 - 2e\varphi/M)^{-1/2}$. Substituting in the last equation of the system (17.15), we obtain the equation

$$\frac{d^2\varphi}{dx^2} = 4\pi e N_0\left[\exp\left(\frac{e\varphi}{T_e}\right) - \frac{u}{\sqrt{u^2 - 2e\varphi/M}}\right] \tag{17.16}$$

for the ion sound. This equation describes the potential of the electric field for the nonlinear ion-acoustic wave. It is in the form of an equation of motion for a particle if φ is regarded as the coordinate and x as time. A general property of this type of equation is that multiplication by the integration factor $d\varphi/dx$ makes it possible to perform one integration immediately. Equation (17.16) then becomes

$$\frac{1}{2}\left(\frac{d\varphi}{dx}\right)^2 - 4\pi N_0 T_e \exp\left(\frac{e\varphi}{T_e}\right) - 4\pi N_0 M u\sqrt{u^2 - \frac{2e\varphi}{M}} = \text{const}.$$

Assuming that at large distances from the wave the potential φ and the electric field strength of the wave $-d\varphi/dx$ are zero, we can evaluate the constant of integration and obtain

$$\frac{1}{2}\left(\frac{d\varphi}{dx}\right)^2 + 4\pi N_0 T_e\left[1 - \exp\left(\frac{e\varphi}{T_e}\right)\right] + 4\pi N_0 M u\left(u - \sqrt{u^2 - \frac{2e\varphi}{M}}\right) = 0. \tag{17.17}$$

This solution describes a solitary wave because, according to the boundary conditions, the perturbation goes to zero at large distances. The solution allows one to determine the shape of the soliton and the relation between its parameters for various amplitudes of the wave. We first determine from equation (17.17) the relation between the maximum potential φ_{max} of the wave and its velocity u. We can do this by putting $d\varphi/dx = 0$ and $\varphi = \varphi_{max}$ into Eq. (17.17). Introducing the reduced variables $\zeta = e\varphi_{max}/T_e$ and $\eta = Mu^2/(2T_e)$, one can rewrite Eq. (17.17) as

$$1 - \exp\zeta + 2\eta\left(1 - \sqrt{1 - \frac{\zeta}{\eta}}\right) = 0. \tag{17.18}$$

The limiting cases of this equation are instructive. For small amplitude of the ion-acoustic wave ($\zeta \to 0$), Eq. (17.18) gives $\eta = \frac{1}{2}$. This yields the phase velocity $u = (T_e/M)^{1/2}$ for this wave, corresponding to the dispersion relation (15.13) for ion sound of small amplitude. For large-amplitude waves, Eq. (17.18) implies $\zeta = \eta$, so that the equation for ζ takes the form

$$1 - \exp\zeta + 2\zeta = 0. \tag{17.19}$$

This equation yields $\zeta = 1.256$, so that $e\varphi_{max} = 1.256T_e$ and $u = 1.585(T_e/M)^{1/2}$. For larger wave amplitudes the electric potential at the wave center becomes too large to admit solutions of Eq. (17.18), and ions are reflected from the crest of the wave. As a result, part of the wave reverses and the wave becomes segmented. Thus, a solitary ion-acoustic wave exists only in a restricted range of wave amplitudes and velocities. Exceeding the limiting amplitude leads to a wave decaying into separate waves.

17.6 PARAMETRIC INSTABILITY

Nonlinear phenomena are responsible for interaction between different modes of oscillation. A possible consequence of this interaction is the decay of a wave into two waves. Since the wave amplitude depends on time and spatial coordinates by the harmonic dependence $\exp(i\mathbf{k}\cdot\mathbf{r} - i\omega t)$, such a decay corresponds to fulfilling the relations

$$\omega_0 = \omega_1 + \omega_2, \qquad \mathbf{k}_0 = \mathbf{k}_1 + \mathbf{k}_2, \tag{17.20}$$

where subscript 0 relates to the parameters of the initial wave, and subscripts 1 and 2 refer to the decay waves. This instability is called *parametric* instability. We consider below an example of this instability in which a plasma oscillation decays into a plasma oscillation of a lower frequency and an ion-acoustic wave (ion sound).

The electric field of the initial plasma oscillation is

$$\mathbf{E} = \mathbf{E}_0 \cos(k_0 x - \omega_0 t),$$

where x is the direction of propagation. In zero approximation we assume the electric field amplitude E_0 and other wave parameters to be real. The equation of motion for electrons, $m_e\, dv_0/dt = -eE$, yields the electron velocity $v_0 = u_0 \cos(k_0 x - \omega_0 t)$, where $u_0 = eE_0/(m_e \omega_0)$.

Let another plasma wave and the ion sound wave be excited in the system simultaneously with the initial plasma oscillation, and let their amplitudes be small compared to the amplitude of the initial oscillation. Consider the time development of these waves, taking into account their interaction with each other and with the initial oscillation. Since ion velocities are much lower than electron velocities, one can analyze these waves separately. The equation of motion and continuity equation for ions are

$$M\frac{dv_i}{dt} = eE,$$

$$\frac{\partial N_i'}{\partial t} + N_0 \frac{\partial v_i}{\partial} x = 0.$$

Here M is the ion mass, v_i is the ion velocity, N_0 is the equilibrium number density of ions, N_i' is the perturbation of the ion number density due to the oscillation, and E is the electric field due to the oscillations. Elimination of the ion velocity from these equations yields

$$\frac{\partial^2 N_i'}{\partial t^2} + \frac{eN_0}{M}\frac{\partial E}{\partial x} = 0. \tag{17.21}$$

We can find the electric field strength from the equation of motion for the electrons by averaging over fast oscillations. The one-dimensional Euler equation (9.8) can be rewritten for electrons as

$$\frac{\partial v_e}{\partial t} + v_e \frac{\partial v_e}{\partial x} + \frac{1}{m_e N}\frac{\partial p_e}{\partial x} + \frac{eE}{m_e} = 0, \tag{17.22}$$

where the electron gas pressure is $p_e = NT_e$, T_e is the electron temperature, and N is the electron number density. After averaging over fast oscillations, the first term in this equation is zero. We write the electron velocity as $v_e = v_0 + v_e'$, where v_e' is the electron velocity due to the small-amplitude plasma wave. Then we have

$$\overline{v_e \frac{\partial v_e}{\partial x}} = \frac{1}{2}\frac{\partial \overline{v_e^2}}{\partial x} = \frac{1}{2}\frac{\partial}{\partial x}\overline{(v_0 + v_e')^2} = \frac{\partial}{\partial x}\overline{v_0 v_e'},$$

where the bar denotes averaging over fast oscillations. We assume that $T_e = \text{const}$, corresponding to a high rate of energy exchange in the ion–acoustic wave. During the ion motion, the electron number density has a relaxation time for maintaining the quasineutrality of the plasma. Therefore, after averaging, the deviation of the electron number density from equilibrium is the same as that for ions, and the third term in the Euler equation (17.22) becomes

$$\frac{1}{m_e N}\frac{\partial p_e}{\partial x} = \frac{T_e}{m_e N_0}\frac{\partial N_i'}{\partial x} \qquad (N \approx N_0).$$

The Euler equation after averaging is transformed into

$$\frac{\partial}{\partial x}\overline{v_0 v_e'} + \frac{T_e}{m_e N_0}\frac{\partial N_i'}{\partial x} + \frac{eE}{m_e} = 0.$$

Substituting the electric field derived from this equation into equation (17.21), we obtain

$$\frac{\partial^2 N_i'}{\partial t^2} - \frac{T_e}{M}\frac{\partial^2 N_i'}{\partial x^2} - \frac{m_e N_0}{M}\frac{\partial^2}{\partial x^2}\overline{v_0 v_e'} = 0. \tag{17.23}$$

If we ignore the last term in equation (17.23) and assume harmonic dependence of the ion density on time and spatial coordinates, we obtain the dispersion relation (15.13) for ion sound: $\omega = c_s k$, $c_s = \sqrt{T_e/M}$. To take into account interaction between ion sound and plasma oscillations, we have to trace the motion of electrons in the field of the small-amplitude plasma wave. To do this, we shall use the Maxwell equation for the electric field of the small amplitude wave, assuming the magnetic field to be zero. This gives $\partial E'/\partial t + 4\pi j' = 0$. Here E' is the electric field of the wave, and j' is the electric current density generated by it.

For simplicity, we shall ignore thermal motion of the electrons, since it has only a small effect on the oscillation frequency. Therefore, when writing the expression for the current density, we can ignore the variation of the electron number density due to the electron pressure of the plasma wave. Assume the electron number density to have the form $N_e + N_i'$, where N_e includes the equilibrium electron number density and its variation under the action of the initial plasma wave, and N_i' is the variation of the ion number density owing to the motion of ions. Accordingly, the electron velocity is $v_0 + v_e'$, where v_0 is the electron velocity due to the initial plasma wave, and v_e' is the electron velocity due to the small-amplitude plasma wave. The current density due to the small-amplitude plasma wave is then

$$j' = -e(N_e + N_i')(v_0 + v_e') + eN_e v_0 = -eN_e v_e' - eN_i' v_0,$$

where we neglect second-order terms. The Maxwell equation $\partial E'/\partial t + 4\pi j' = 0$ can now be rewritten as

$$\frac{\partial E'}{\partial t} - 4\pi e N_i' v_0 - 4\pi e N_e v_e' = 0.$$

The electron equation of motion is

$$m_e \frac{dv_e'}{dt} = -eE'.$$

Eliminating E' from these equations, we obtain

$$\frac{\partial^2 v_e'}{\partial t^2} + \omega_p^2 v_e' + \frac{N_i'}{N_e}\omega_p^2 v_0 = 0 \tag{17.24}$$

as the equation for the electron velocity due to the small-amplitude plasma wave. Here $\omega_p = \sqrt{4\pi N_e e^2/m_e}$ is the frequency of plasma oscillations ignoring the thermal motion of electrons. One can see that if we do not take into account the interaction between the small-amplitude plasma wave with the initial plasma oscillation and the ion–acoustic wave [that is, if we ignore the last term in equation (17.24)], then the assumptions used here give the small-amplitude plasma wave frequency as being equal to the plasma frequency.

We must solve the set of equations (17.23) and (17.24). We take the parameters to have the forms

$$v_0 = u_0 \cos(k_0 x - \omega_0 t),$$
$$v_e = a \cos(k_e x - \omega_e t),$$
$$N_i' = bN_0 \cos(k_i x - \omega_i t),$$

where a and b are slowly varying oscillation amplitudes, ω_e and k_e are the frequency and the wave number of the small-amplitude plasma wave, ω_i and k_i are the frequency and the wave number of the ion sound, and N_0 is the equilibrium number density of the charged particles. [We assume that $N_e = N_0$ in equation (17.24).] Since the oscillation amplitudes vary slowly, the time and space dependences are identical, so we find from equations (17.23) and (17.24) that

$$\omega_0 = \omega_e + \omega_i, \qquad k_0 = k_e + k_i, \tag{17.25}$$

as in Eq. (17.20). This condition is similar to that for parametric resonance of coupled oscillators, and therefore the instability that we analyze is termed a parametric instability.

Taking into account a slow variation of the oscillation amplitudes and the condition (17.25), we find from equations (17.23) and (17.24) the equations

$$\frac{\partial a}{\partial t} = \omega_e u_0 b/4,$$

$$\frac{\partial b}{\partial t} = -m_e k_i u_0 a/(4M\omega_i)$$

for the oscillation amplitudes. Solution of these equations shows that the oscillations grow with the dependence $a,b \sim \exp(\gamma t)$ with

$$\gamma = \frac{1}{4}\sqrt{\frac{m_e \omega_e}{M\omega_i}}\, u_0 k_i = \frac{1}{4}\sqrt{\frac{m_e \omega_e}{M\omega_i}}\, \frac{eE_0}{m_e \omega_0} k_i. \tag{17.26}$$

Thus, the initial plasma wave is unstable. It can decay into a plasma wave of a lower frequency and ion sound. This instability is known also as the *decay instability*. The exponential growth parameter for the new wave is proportional to the amplitude of the decaying wave.

CHAPTER 18

IONIZATION INSTABILITIES AND PLASMA STRUCTURES

18.1 DRIFT WAVES

A laboratory ionized gas is usually maintained by an external electric field that generates an electric current and causes ionization in the gas. Electrons are the principal plasma component in the sense that electrons contribute most of the total electric current, and formation of new charged particles is due to collisions of electrons with gas atoms or molecules. Perturbations of the electron number density are thus of central importance to the oscillation properties of the plasma.

To examine the simplest form of perturbations in the plasma, we begin with the continuity equation (9.5),

$$\frac{\partial N_e}{\partial t} + \operatorname{div}\mathbf{j} = 0,$$

for electrons, and we assume that the electron flux $\mathbf{j}$ is determined solely by the electron drift in an external electric field. The current is then $\mathbf{j} = \mathbf{w}N_e$, where $\mathbf{w}$ is the electron drift velocity. Using Eq. (15.2) for a perturbation to the electron number density, we obtain the dispersion relation

$$\omega = kw. \tag{18.1}$$

That is, there is a wave associated with the perturbation that propagates together with the electric current. In other words, the perturbation moves together with the electric current. Such perturbative waves are called *drift waves*.

Damping or amplification of these waves can occur by several mechanisms. One such mechanism is the diffusive motion of the electrons. The electron flux is then $\mathbf{j} = \mathbf{w}N_e - D\nabla N_e$ (where D is the diffusion coefficient for electrons in the plasma), and the dispersion relation that follows from the continuity equation for electrons has the form

$$\omega = kw - iDk^2. \tag{18.2}$$

The diffusion of the electrons is seen to lead to damping of the drift wave because the dependence of electron parameters on time has the form $\exp(-i\omega t)$. As a result of electron diffusion, the perturbation region enlarges and the perturbation dissipates.

Drift-wave behavior depends on the type of ionization processes in the gas. Under certain conditions, the interaction of drift waves with ionization leads to amplification of the drift waves. This phenomenon is called *ionization instability*. Various types of ionization instability can occur, depending on the properties of the plasma and the processes within it. The development of ionization instability leads to formation of structures in the plasma that will be considered below.

18.2 IONIZATION INSTABILITY FROM THERMAL EFFECTS

A common causal mechanism for ionization instability is to be found in the positive column of an arc, where the instability arises from thermal processes. The equilibrium electron number density depends strongly on the plasma temperature, while the temperature dependence of the heat transport coefficient is weak. At high intensities, a thermal instability occurs because heat transport mechanisms are unable to cope with the amount of heat released. This instability may lead to contraction of the plasma, or it can cause the formation of new types of structures in the plasma. A simple example of this phenomenon arises when the heat transport in a cylindrical discharge tube depends upon the thermal conductivity. The heat balance equation in this case has the form

$$\frac{1}{\rho}\frac{d}{d\rho}\left(\rho\kappa(\rho)\frac{dT}{d\rho}\right) + p(\rho) = 0, \tag{18.3}$$

where ρ is the distance from the tube axis, κ is the thermal conductivity coefficient, $p(\rho) = iE$ is the specific power of heat release (where i is the current density), and E is the electric field strength. We assume that the rate at which heat energy is released is strongly dependent on the local plasma temperature, and is a function only of this temperature.

This model is descriptive of arc discharges at high currents and high pressures. If the discharge plasma is in equilibrium, the electron and gas

temperatures are nearly the same, and the electron number density can be estimated from the Saha formula to behave as $N_e \sim \exp[-J/(2T)]$, where J is the ionization potential of the gas atoms, and it is usually true that $T \ll J$. The specific power of heat release is $p = iE$, where the electric field strength E does not vary over the discharge cross section, and the current density i varies as N_e. The specific power of heat release in an arc discharge is not only determined entirely by the temperature, but it has a strong dependence on the temperature. In this case the equilibrium between ionization and recombination is maintained at each point in the plasma. This is called *local ionization equilibrium.*

We introduce the new variables $z = \rho^2/r_0^2$ and $\theta = (T - T_w)/T_w$ into Eq. (18.3), where r_0 is the tube radius, and T_w is the wall temperature. Then Eq. (18.3) can be written in the form

$$\frac{d}{dz}\left(z\frac{d\theta}{dz}\right) + A\exp(b\theta) = 0, \tag{18.4}$$

where $A = r_0^2 p(T_w)/[4T_w \kappa(T_w)]$, $b = T_w\, d\ln p(T_w)/dT_w$, and in this case $b \gg 1$. Because of the strong dependence of p on T, we can assume that the thermal conductivity coefficient κ is independent of the temperature. The solution of Eq. (18.4) is given by the Fock formula

$$\theta = \frac{1}{b}\ln\frac{2\gamma}{Ab(1+\gamma z)^2}, \tag{18.5}$$

where γ is a parameter to be determined by boundary conditions. One of the boundary conditions of Eq. (18.4) is $\theta(0) = 0$, following from the definition of this function. This gives the relation for γ that

$$2\gamma = Ab(1+\gamma)^2. \tag{18.6}$$

Since the parameter γ is real, we have $Ab \leq \frac{1}{2}$. If this condition is not satisfied, then Eq. (18.4) has no real solution. This means that thermal instability arises because heat extraction is not compensated by heat release. The instability then leads to a different discharge regime where the current occurs in a narrow region near the tube center.

The threshold for this instability corresponds to $\gamma = 1$ and $Ab = \frac{1}{2}$, that is, it has its onset when $p(T_0) = 4p(T_w)$, where T_0 is the temperature on the axis. The instability threshold at $Ab = \frac{1}{2}$ corresponds to

$$\left.\frac{dp(T)}{dT}\right|_{T_w} = \frac{2\kappa(T_w)}{r_0^2}. \tag{18.7}$$

If this instability leads to contraction of the plasma, these relations make it possible to estimate a radius ρ_0 for the new contracted regime of the plasma. Equation (18.7) then gives

$$\rho_0^2 \sim \kappa(T_0)\left[\frac{dp(T)}{dT}\right]^{-1}_{T=T_0}, \tag{18.8}$$

where T_0 is the temperature on the axis.

18.3 IONIZATION INSTABILITY OF A PLASMA IN A MAGNETIC FIELD

We wish to examine the above case in detail at small currents. In this problem, local ionization equilibrium exists everywhere within the plasma, so that the Saha relation for the electron number density is valid, but heat transport processes are not essential. We can examine the time evolution of a perturbation of the electron number density. The electron energy per unit volume is $W = 3N_eT_e/2$, and the balance equation for this quantity has, according to Eq. (9.41), the form

$$\frac{dW_e}{dt} = -eEw_eN_e - 3\frac{m_e}{M}(T_e - T)\nu N_e. \tag{18.9}$$

Here we take account of the negative direction of the electric field, m_e and M are the electron and atom masses, T_e and T are the electron and atom temperatures, and for simplicity we assume that the electron–atom collision frequency $\nu = N_a v\sigma_{ea}^*$ is independent of the electron velocity. The quantity N_a is the atom number density, σ_{ea}^* is the diffusion cross section of electron–atom collisions, and v is the electron velocity.

Because of the local ionization equilibrium, we have $N_e \sim \exp(-J/2T_e)$, where J is the atomic ionization potential. This gives the relation

$$\frac{N_e'}{N_e} = \frac{T_e'}{T_e}\frac{J}{2T_e}$$

between perturbation values of the electron number density N_e' and temperature T_e', so we can conclude that

$$\frac{T_e'}{T_e} \ll \frac{N_e'}{N_e}.$$

Based on this inequality, the term $T_e^{-1}\,dT_e/dt$ can be neglected compared to the term $N_e^{-1}\,dN_e/dt$ on the left-hand side of Eq. (18.9). This yields the result

$$\frac{dN_e}{dt} = -\gamma N_e', \qquad \text{where} \quad \gamma = \frac{4T_e}{J}\frac{m_e}{M}\nu. \tag{18.10}$$

Thus, the ionization perturbation being analyzed has a time scale for damping that is much greater than a typical time for electron–atom collisions.

We now develop the constant-magnetic-field case. We employ the geometry of Chapter 13, where the electric field is directed along the x-axis and the magnetic field along the z-axis. Then we obtain from Eqs. (13.22) the electron drift velocity $\mathbf{w}$ in the case where $\nu = \text{const}$, if we represent this relation in the vector form

$$\mathbf{w} = -\frac{e\mathbf{E}\nu}{m_e(\omega_H^2 + \nu^2)} + \frac{e\mathbf{E} \times \boldsymbol{\omega}_H}{m_e(\omega_H^2 + \nu^2)}, \tag{18.11}$$

where the vector $\boldsymbol{\omega}_H = e\mathbf{H}/(m_e c)$ is parallel to the magnetic field.

The physical framework for this problem is such that electrodes collect the electron current in the x-direction. Hence, there is no electric current along the y-axis. The electron drift velocity along the x-axis creates the electric field along the y-axis, and the strength of this electric field is

$$\mathbf{E} = -\frac{m_e\nu}{e}\mathbf{w} - \frac{m_e}{e}\boldsymbol{\omega}_H \times \mathbf{w}, \tag{18.12}$$

as follows from Eq. (18.11)

A perturbation in the electron number density causes a perturbation of the electric field strength and the electron drift velocity. We can determine these perturbations from Eq. (18.9), which is now

$$\frac{dW_e}{dt} = -eEwN_e' - eE'wN_e + \left(\frac{dW_e}{dt}\right)_T, \tag{18.13}$$

where the quantity $(dW_e/dt)_T = -3N_eT_e(m_e/M)$ is established by energy changes in electron–atom collisions, and was evaluated above.

The relationship between the perturbations w' and N_e' can be derived from the continuity equation (9.5) for electrons. This can be used in the steady-state form $\text{div}(N_e\mathbf{w}) = 0$, since the instability develops slowly. Writing the dependence on $\mathbf{r}$ in the form $\exp(i\mathbf{k} \cdot \mathbf{r})$, where $\mathbf{k}$ is the wave vector, we obtain

$$N_e(\mathbf{w}' \cdot \mathbf{k}) + N_e'(\mathbf{w} \cdot \mathbf{k}) = 0. \tag{18.14}$$

We can now apply Eq. (18.11) to eliminate the perturbed drift velocity of the electrons from this expression. First, we find the direction of $\mathbf{w}'$. Since the perturbation develops slowly, we can write $\mathbf{E}' = -\nabla\varphi'$, where φ' is the perturbation of the electric potential. As before, we assume $\varphi' \sim \exp(i\mathbf{k} \cdot \mathbf{r})$ and obtain $\mathbf{E}' = -i\mathbf{k}\varphi'$, that is, the vectors $\mathbf{E}'$ and $\mathbf{k}$ are either parallel or antiparallel. Then, using the relationship (18.11) between the vectors $\mathbf{w}'$ and $\mathbf{E}'$, we obtain

$$\mathbf{w}' = \text{const} \cdot \left(\mathbf{k} - \frac{\mathbf{k} \times \boldsymbol{\omega}_H}{\nu}\right).$$

Multiplying the vector $\mathbf{w}'$ by itself, we evaluate the constant in the above expression to obtain

$$\mathbf{w}' = \pm w' \frac{\nu \mathbf{k} - \mathbf{k} \times \boldsymbol{\omega}_H}{k\sqrt{\omega_H^2 + \nu^2}}.$$

Substituting this expression into the relationship derived from the continuity equation yields

$$\frac{w'}{w} = \pm \frac{N_e'}{N_e} \sqrt{\omega_H^2 + \nu^2} \cos\left(\frac{\alpha}{\nu}\right), \tag{18.15}$$

where $\cos\alpha = k_x/k$, with α the angle between vectors $\mathbf{w}$ and $\mathbf{k}$. Substitution of this into Eq. (18.13) gives, with the help of Eq. (18.10),

$$\frac{dW'}{dt} = \frac{d}{dt}\left(\frac{3N_eT_e}{2}\right) = N_e' m_e w^2 \nu \left(\frac{\omega_H \sin 2\alpha}{\nu} - \cos^2\alpha - \frac{T_e}{2J}\right). \tag{18.16}$$

If the right-hand side of this equation is positive, any random deviation of the electron number density from its equilibrium value continues to grow; that is, instability develops. This expression has a maximum when $\tan 2\alpha = -\omega_H/\nu$. For this direction of the vector $\mathbf{k}$, Eq. (18.16) has the form

$$\frac{dW'}{dt} = N_e' m_e w^2 \nu \left(\frac{\sqrt{\omega_H^2 + \nu^2}}{\nu} - 1 - \frac{T_e}{2J}\right). \tag{18.17}$$

From this it follows that this instability has a threshold, given by $\omega_H/\nu \geq (T_e/J)^{1/2}$. When the ratio ω_H/ν is large, the ionization instability develops for perturbations propagating at the angle $\alpha = 45^o$ to the direction of the current. If this ratio is small, the most unstable perturbations propagate in a direction almost perpendicular to the current.

18.4 ATTACHMENT INSTABILITY OF A MOLECULAR GAS

Several different instabilities are possible during the formation of negative ions by attachment of electrons to molecules. This process is related to the formation of positive ions by loss of electrons, and to recombination events. All of these processes can create ionization structures and waves in a plasma. As an example, we shall consider attachment as it occurs in the plasma of an excimer laser.

In an excited molecular gas (for example, HCl) the attachment rate constant increases with increase of the vibrational temperature. The positions of electron terms, as illustrated in Fig. 18.1, determine the properties of this

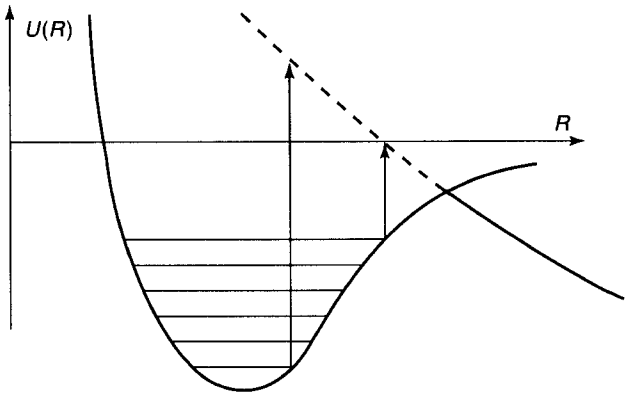

Figure 18.1 Electron terms that participate in the electron – attachment process determine the properties of the transition.

process. It proceeds according to the scheme

$$\begin{aligned} AB + e &\rightarrow (AB^-)^{**}, \\ (AB^-)^{**} &\rightarrow A + B^-, \\ (AB^-)^{**} &\rightarrow AB^* + e. \end{aligned} \tag{18.18}$$

Here $(AB^-)^{**}$ denotes an autodetaching state of the negative ion, and AB^* denotes a vibrational excited state of the molecule. The probability of attachment after formation of the autodetaching state $(AB^-)^{**}$ is proportional to the factor

$$\exp\left(-\frac{\int_{R_c}^{R}\Gamma(R)\,dR}{\hbar v}\right), \tag{18.19}$$

where $\Gamma(R)$ is the width of the autodetaching level, v is the relative velocity of the nuclei, R is the location of the electron captured into the autodetaching level, and R_c is the distance at which the terms intersect. The exponential factor is the survival probability of the autodetaching state, and it is usually quite small. Hence the greater the distance at which the electron is captured, the higher is the probability for formation of the negative ion. Because the capture distance grows with increase of the molecular vibrational temperature, so does the attachment rate constant .

We can apply these features to the analysis of the balance equations for the electron number density and vibrational temperature T_v, which have

the form

$$\frac{\partial N_e}{\partial t} = -\nu_{at} N_e + \nu_{ion} N_e,$$

$$\frac{\partial T_v}{\partial t} = N_e k_{ex} \hbar\omega - M_{rel}.$$

Here $\nu_{at} = Nk_{at}$ is the electron attachment frequency (k_{at} is the rate constant for this process, and N is the number density of molecules), ν_{ion} is the ionization frequency, k_{ex} is the rate constant for the vibrational excitation of molecules by electron impact, $\hbar\omega$ is the vibrational energy of the molecule, and M_{rel} is the vibrational relaxation rate. Linearizing these equations, assuming that perturbations of N_e and T_v vary with time as $\exp(-i\omega t)$, and taking $\nu_{at} = \nu_{ion}$ for an unperturbed state, we find that the process being studied is oscillatory in nature if $d\nu_{at}/dT_v > 0$. The frequency is

$$\omega_E^2 = k_{ex} N_e \hbar\omega \frac{d\nu_{at}}{dT_v}, \tag{18.20}$$

and the oscillations are known as Eletskii oscillations.

One can combine these oscillations and drift waves by inserting the electron drift into the balance equation for the electron number density. Then instead of Eqs. (18.1) and (18.20), we obtain the dispersion relation

$$\omega = kw/2 + \sqrt{k^2 w^2/4 + \omega_E^2}, \tag{18.21}$$

which transforms to Eq. (18.1) or (18.20) in the appropriate limits.

18.5 ELECTRIC DOMAIN

One of a variety of steady-state structures that can be formed by nonlinear processes in a plasma is called the *electric domain*—a perturbation of the electron number density and the electric field in a gas-discharge plasma that propagates with the electron current. The physical picture of this phenomenon is as follows. The external segment of an electric circuit that passes through a gas discharge has a large resistance that maintains a constant electric current density in the discharge. This constant current is

$$i_e = -ewN_e = \text{const}, \tag{18.22}$$

where w is the electron drift velocity, and N_e is the electron number density. The dependence of the electron drift velocity on the electric field strength has the behavior shown in Fig. 18.2, where two different electric current

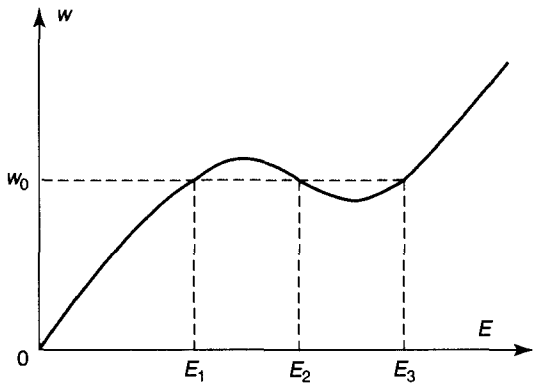

Figure 18.2 Dependence of the electron drift velocity on the electric field strength that can lead to the occurrence of an electric domain.

regimes are possible at some values of the electric field strength. This behavior can preserve a perturbation that propagates together with the current, meaning that it is a drift wave. Such a perturbation identifies what is called the electric domain.

To describe the electric domain, we use the continuity equation (9.5) and the Poisson equation (3.2), which here take the forms

$$\frac{\partial N_e}{\partial t} + \frac{\partial j_e}{\partial x} = 0, \qquad \frac{\partial E}{\partial x} = 4\pi e(N_0 - N_e), \tag{18.23}$$

where j_e is the electron flux, E is the electric field strength, and N_0 is the equilibrium number density of electrons. We first treat these equations in a linear approximation so as to analyze the electric domain at small intensity. The electron flux can be written

$$j_e = -N_e w - D\frac{\partial N_e}{\partial x}, \tag{18.24}$$

where D is the diffusion coefficient of electrons in a plasma, and the minus sign in the first term accounts for the direction of the electron current. Taking E and N_e to exhibit harmonic behavior as expressed by Eq. (15.2), we can write

$$E = E_0 + E'e^{i(kx-\omega t)}, \qquad N_e = N_0 + N'e^{i(kx-\omega t)}.$$

We then obtain the dispersion relation

$$\omega = -kw - iDk^2 - i4\pi N_0 e\frac{dw}{dE} \tag{18.25}$$

with the help of Eqs. (18.23) and (18.24). We have employed here the connection $\partial w/\partial x = (dw/dE)(dE/dx)$. The dispersion relation (18.25) describes drift waves (18.2) that move together with the electron current. The diffusion process removes electrons from the perturbation zone, thus causing damping of these waves. But if $dw/dE < 0$, long drift waves with $Dk^2 < -4\pi N_0 e\, dw/dE$ can develop.

We now study a nonlinear electric domain. In a nonsteady interval of the electric field strengths of Fig. 14.6, Eq. (18.24) has the form

$$j_0 = -N_0 w(E_2) = -N_e w(E) - D\frac{\partial N_e}{\partial x}.$$

We should add to this equation the Poisson equation (18.23). Eliminating the electron number density between these equations, we obtain

$$D\frac{d^2E}{dx^2} = w(E)\frac{dE}{dx} - 4\pi e N_0\left[w(E) - w(E_2)\right]. \tag{18.26}$$

Equation (18.26) describes the behavior of the electric field strength in the electric domain.

If we assume that diffusion plays a secondary role, and neglect diffusion in the first stage of the analysis, then Eq. (18.26) takes the form

$$\frac{dE}{dx} = 4\pi e N_0\left(\frac{w(E_2)}{w(E)} - 1\right). \tag{18.27}$$

We solve this equation with the boundary condition $E = E_2$ at $x = 0$. The solution is shown in Fig. 18.3a. As can be seen from Eq. (18.27), $E(x)$ increases with x until $E_2 < E < E_3$, where $w(E_3) = w(E_2)$. At $E = E_3$ we have $dE/dx = 0$, so that for subsequent values of x we obtain $E = E_3$. Thus this solution describes the conversion of the system from the unstable state E_2 to the stable state with $E = E_3$.

This transition means that the change of the discharge regime as a result of the perturbation of the electric field strength increases up to E_3. For this to take place throughout the plasma would require a variation of the discharge voltage that is impossible, because the discharge voltage is maintained by the external voltage. Therefore, the variation of the electric field strength from E_2 to E_3 is a perturbation that takes place in a limited region of the plasma. A return to the initial value of the field occurs as a result of diffusion, leading to decay of the perturbation. Hence, a typical size of the back boundary zone of the electric domain is of the order of D/w. The size of the forward boundary zone can be estimated from Eq. (18.27), and is $\Delta x = \Delta E/(4\pi e N_0\, \Delta w)$, where $\Delta E = E_3 - E_2$, and $\Delta w = w(E_2) - w_{\min}$ (see Fig. 18.2). A concomitant of the distribution of the electric field strength in the electric domain is the distribution of the electron number density shown in Fig. 18.3, arising from Poisson's equation (18.23).

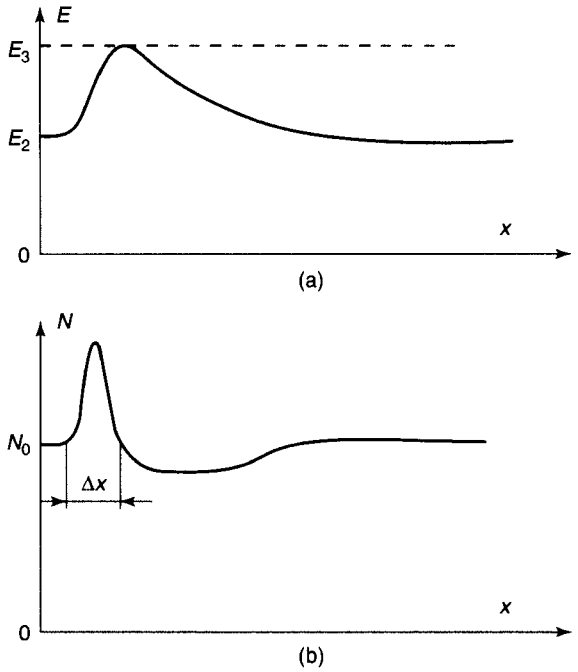

Figure 18.3 The distribution of (a) the electric field and the (b) electron number density in the electric domain.

18.6 STRIATIONS

Striations, or strates, are plasma structures that are observed in a positive column of a gas discharge of low or moderate pressure. The column is striped in an alternation of luminous and dark regions. Striations can move to electrodes or can be at rest. They exist only in certain ranges of currents and pressures. They have different properties for atomic and for molecular gases.

Striations are ionization instabilities whose nature is determined by the connection between the ionization rate and the electron number density. An increase in the electron number density leads to an increase in the ionization rate and in the average electron energy. This, in turn, affects the electron number density. If this connection leads to an instability, striations can be formed. From the standpoint of gas discharges, striations as oscillating structures can provide a lower voltage for discharge if an ionization instability can develop. Hence, the parameters describing striations and the range of their existence are determined by processes that lead to instabilities.

The study of the mechanisms that give rise to striations is complicated by the fact that striations exist in an intermediate range of plasma parameters where the ionization rate constant depends on the electron number density. We shall examine the case when this phenomenon arises from stepwise

ionization of atoms. This mechanism corresponds to low-pressure glow discharges in inert gases where metastable atoms are of importance for ionization processes.

The balance equation for the electron number density is

$$\frac{\partial N_e}{\partial t} + D_a \frac{\partial^2 N_e}{\partial x^2} = Z N_e, \tag{18.28}$$

where D_a is the ambipolar diffusion coefficient, the x-axis is along the axis of the discharge tube, and Z is the sum of the frequencies of generation and loss of electrons. Assuming that the ionization wave has a small amplitude, we have the usual harmonic dependence $N_e = N_0 + N' \exp(ikx - i\omega t)$, where $N' \ll N_0$. When we introduce the effective electron temperature $T_e = T_0 + T' \exp(ikx - i\omega t)$ and insert these relations into Eq. (18.26), we obtain the dispersion relation

$$\omega = -iD_a k^2 + iZ_T N_e \frac{\partial T_e}{\partial N_e} + iZ_N N_e \tag{18.29}$$

for the ionization wave, where we have used the notation $Z_N = \partial Z / \partial N_e$ and $Z_T = \partial Z / \partial T_e$, and have taken into account that $Z = 0$ at equilibrium.

This dispersion relation has been obtained by a formal procedure. It is of importance that the ionization rate Z depends both on the number density and the temperature of the electrons, and variation of one of these quantities alters the other. Depending on the connection between these quantities, waves can be either developed or damped. We give some illustrative examples.

Assume that the resistance of the external circuit is large enough to conserve the electron current density $\mathbf{j}$. (Note that we use here the notation $\mathbf{j}$ for the electric current density, not for the electron flux as is more usual.) Then we have

$$\mathbf{j} = \Sigma \mathbf{E} + eD_a \nabla N_e = \text{const.}$$

This gives the electric field

$$\mathbf{E} = \mathbf{j}/\Sigma - eD_a \nabla N_e / \Sigma, \tag{18.30}$$

where Σ is the plasma conductivity, and D_a is the coefficient of ambipolar diffusion that characterizes the diffusion of electrons in a plasma.

When we use the balance equation for the mean energy of electrons, and take into account elastic collisions of electrons and gas atoms, then the heat balance equation for electrons has the form

$$\operatorname{div} \mathbf{q} = \mathbf{j} \cdot \mathbf{E} - N_e \nu \, \delta\varepsilon = 0, \tag{18.31}$$

where $\mathbf{q}$ is the heat flux. The first term on the right-hand side of this equation represents heating of electrons under the action of the electric current. The second term takes into account elastic electron–atom collisions, so that ν is the collision frequency and $\delta\varepsilon$ is the mean energy transferred to atoms in a single collision. Further, we assume that $\delta\varepsilon$ is proportional to the mean electron energy and that the collision frequency is independent of the electron energy.

Assume that the heat flux q is determined by the electron thermal conductivity ($\mathbf{q} = -\kappa\nabla T_e$, where κ is the thermal conductivity coefficient of electrons) and $\Sigma \sim N_e$. Taking Σ and D_a to be dependent on T_e, Eqs. (18.30) and (18.31) give the dispersion relation

$$k^2\kappa T' = -\frac{j^2}{\Sigma}\frac{N'}{N_0} - \frac{ikEjD_a}{\Sigma}N' - \frac{j^2}{\Sigma}\left(\frac{N'}{N_0} + \frac{T'}{T_0}\right).$$

From this it follows that

$$\frac{\partial T_e}{\partial N_e} = \frac{T'}{N'} = \frac{T_0}{N_0}\frac{-2 - ik/k_0}{1 + k^2/k_1^2}, \tag{18.32}$$

where $k_0 = j/(eD_aN_0)$ and $k_1 = j\sqrt{\Sigma T_0\kappa}$. From Eqs. (10.43) we have $\kappa \sim N_0 v_e\lambda$, and from Eq. (13.5) we have $\Sigma \sim N_0e^2\lambda/(m_ev_e)$, where N_0 is the equilibrium electron number density, and $v_e \sim \sqrt{T_e/m_e}$ is a typical thermal electron velocity. From this we conclude that k_0 and k_1 have the same order of magnitude.

We now want to identify those conditions that will give rise to an ionization instability leading to the formation of striations. For this purpose we substitute Eq. (18.32) into (18.29) and analyze the resulting expression. Since the electron effective temperature T_e is small compared to the atomic ionization potential J ($T_e \ll J$), Eqs. (5.31) and (5.32) give $Z_T \sim (J/T_e^2)\nu_{\text{ion}}$, where ν_{ion} is the frequency for ionization of atoms by electron impact. Because of the dependence of Z on the electron number density, we have $Z_N \sim \nu_{\text{ion}}/N_0$. This gives $Z_NN_0 \ll Z_TT_e$, and for long-wave oscillations ($k \ll k_0$), Eqs. (18.29) and (18.32) give $\operatorname{Im}\omega < 0$, so that long-wave oscillations are damped. Therefore striations—nonlinear ionization waves—can only be short-wave oscillations. Then the criterion for the existence of striations (the *Rosen condition*) has the form

$$Z_N > 0. \tag{18.33}$$

There is a range of wave lengths satisfying the condition $k > k_0$ where $\operatorname{Re}\omega > \operatorname{Im}\omega$, so that ionization waves—striations—can exist. These waves are developed by nonlinear interaction.

Consider the example of ionization instability, governed by the stepwise nonlinear ionization of atoms by electron impact. We shall assume that there

is only one excited atomic state that contributes to the ionization. We denote this state by the subscript or superscript $*$. We thus have

$$Z = N_a k_{ion} + N_* k^*_{ion} - 1/\tau_D, \tag{18.34}$$

where N_a and N_* are the atom number densities in the ground and excited states, k_{ion} and k^*_{ion} are the rate constants for ionization of atoms in the ground and excited states by electron impact, and τ_D is the time for diffusion of electrons to the walls of the discharge tube. At equilibrium we have $Z = 0$. The dependence of Z on the electron number density due to ionization of excited atoms is

$$Z_N = k^*_{ion} \frac{\partial N_*}{\partial N_e}. \tag{18.35}$$

Using Eq. (8.9) for the number density of excited atoms, we obtain

$$N_* = N^B_* \left(1 + \frac{1}{N_e k_q \tau_D}\right)^{-1},$$

where N^B_* is given by the Boltzmann formula and corresponds to equilibrium between the ground and excited states. Substituting this into Eqs. (18.32) and (18.33), and using the relation $n_* = 1/(k_q \tau_D)$, we have

$$Z_N = \frac{k^*_{ion} n_* N^B_*}{(N_e + n_*)^2}, \qquad Z_T = \frac{J}{T_e^2}\left(k_{ion} N_a + \frac{k_{ion} N^B_* N_e}{N_e + n_*}\right).$$

Inserting these expressions into Eq. (18.27) yields

$$\begin{aligned} \mathrm{Re}\,\omega &= -\mathrm{Im}\left(Z_T N_e \frac{\partial T_e}{\partial N_e}\right) \\ &= \frac{J}{T_e^2}\left(k_{ion} N_a + \frac{k_{ion} N^B_* N_e}{N_e + n_*}\right)\frac{k/k_0}{1 + k^2/k_1^2}, \\ \mathrm{Im}\,\omega &= \frac{k^*_{ion} n_* N^B_* N_e}{(N_e + n_*)^2} - D_a k^2 - \frac{2J}{T_e^2}\left(k_{ion} N_a + \frac{k_{ion} N^B_* N_e}{N_e + n_*}\right)\frac{1}{1 + k^2/k_1^2} \end{aligned} \tag{18.36}$$

for the frequency and damping (or amplification) of the ionization wave.

Equations (18.36) identify that range of parameters where amplification of the ionization wave (Im $\omega > 0$) can occur. According to Eq. (5.32), we find that

$$\frac{k_{ion} N_a}{k^*_{ion} N^B_*} \sim \left(\frac{J_*}{J}\right)^2 < 1,$$

where J and J_* are the ionization potentials of the atom in the ground and excited states. Hence, when $N_e \sim N_*$ and $k > k_1(J/T_e)$, the last term in Eq. (18.36) for the growth of the ionization wave is not compensated by the first term. Then the ionization wave can develop until it will no longer decay as a result of electron diffusion. Thus the ionization wave can amplify in the range of wave vectors

$$k_1\sqrt{J/T_e} < k < \sqrt{k_{\text{ion}} N_*^{\text{B}}/D_{\text{a}}}\,. \tag{18.37}$$

If this condition is satisfied, ionization waves can develop, and striations arise. The plasma then exhibits a striped structure with a specific periodicity.

18.7 CHARACTERISTICS OF STRIATION FORMATION

We demonstrated above that striations, as ionization waves, can exist within an explicit range of parameters describing nonlinear processes involving electrons and transport phenomena. Now we consider a simple model for striations that allows us to analyze this phenomenon from another standpoint.

We assume ionization of an atom by electron impact to be a stepwise process, where the first step is excitation of the atom to a state with the excitation energy ε_{ex}. The subsequent ionization of such an excited atom arises from collisions with other atoms or slow electrons. We take the probability of ionization of an excited atom to be ξ and the probability of its quenching to be $1 - \xi$, so that $0 < \xi < 1$. We consider a one-dimensional positive gas discharge column, and introduce the lifetime τ (electrons and ions) with respect to losses by their attaching to walls. In the absence of ionization, the balance equation for the electron number density N_e is

$$w_e \frac{dN_e}{dx} - \frac{N_e}{\tau} = 0,$$

where the x-axis is directed along the axis of the gas discharge column, and w_e is the electron drift velocity in an electric field.

Now we consider the simplified *Tsendin model* of striations. This model assumes that all the electrons have zero energy at the origin $x = 0$. These electrons obtain energy from the electric field, when an electron has acquired the energy ε_{ex} it excites an atom, and this atom is then ionized by subsequent collisions . As a result, we obtain at this point $1 + \xi$ slow electrons instead of one fast electron.

The solution of the above balance equation is

$$N_e(x) = N_0 \exp\left(-\int_0^x \frac{dy}{w_e \tau}\right).$$

Let the first ionization process take place at $x = l$. Assuming $N_e(x)$ to be a periodic function of x, we obtain

$$\int_0^l \frac{dx}{w_e \tau} = \ln(1 + \xi). \tag{18.38}$$

This equation is the balance equation for electrons formed as a result of atomic ionization and lost by attachment of electrons to walls. The other relation between plasma parameters has the form

$$\int_0^l eE(x)\, dx = \varepsilon_{ex}. \tag{18.39}$$

Equation (18.39) holds in the absence of energy exchange between electrons and atoms as a result of elastic collisions, and in the absence of electron–electron collisions. The electric field strength $E(x)$ satisfies the Poisson equation

$$\frac{dE}{dx} = 4\pi e(N_i - N_e),$$

where N_i is the ion number density. Since a plasma is quasineutral on the average, we have

$$\int N_i\, dx = \int N_e\, dx.$$

Then the Poisson equation leads to $E(0) = E(l)$, where $E(x)$ is periodic with period l. Figure 18.4 shows the electron number density distribution and the electric field strength along the x-axis that follow from the above relations.

The condition of plasma quasineutrality on the average means equality of the lifetimes of electrons and ions. If the number of ionization events per period of the striation is ν, the total number of electrons and ions in one striation band is $\nu\tau$. However, ions are concentrated in an ionization zone near the point where they formed, whereas electrons formed in this ionization zone are distributed over a region of several striations.

We wish now to verify the validity of this model for real atomic gases. We take the energy exchange in electron–atom collisions to be small as a result of the small parameter m_e/M, where m_e is the electron mass and M is the mass of the atom. Hence, the energy that an electron obtains from the electric field is expended mostly on excitation of atoms. We next ascertain the stability of the electron distribution we are examining. We assume that ionization proceeds when electrons reach the energy ε_{ex}. Then the ionization process that leads to a jump in the electron number density and electric field strength occurs over the distance $l = \varepsilon_{ex}/(e\bar{E})$ from the origin, where $\bar{E}$ is

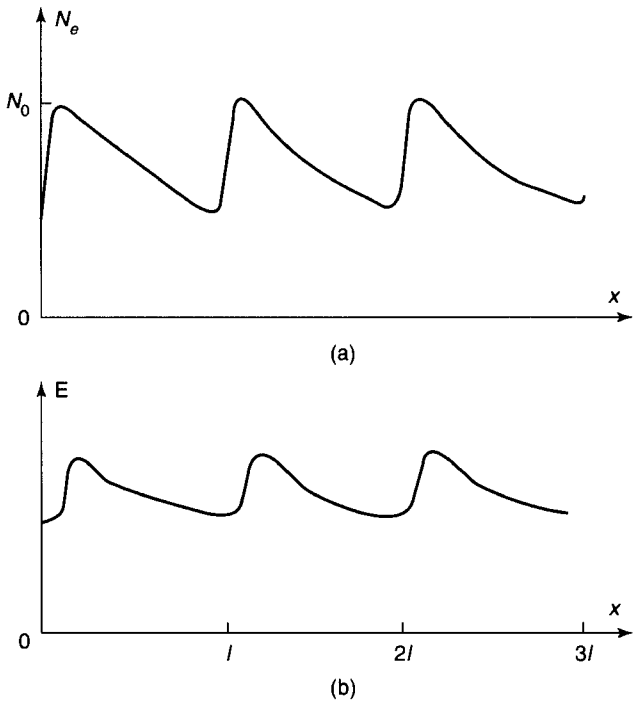

Figure 18.4 The distribution of (a) the number density of electrons and (b) the electric field strength (b) in the positive column of a glow gas discharge with striations.

the average electric field strength. Concurrently, a strong glow occurs near this point due to excitation of atoms by electron impact. In reality, the excitation cross section is zero at threshold, so that excitation proceeds in some region in space where the electron energy leads to effective atomic excitation. If the width of the excitation region increases with its population of electrons, the periodic structure of the plasma is destroyed. Let us examine this for the regime under consideration.

We follow the sequence of events where an electron that has zero energy at the origin excites an atom within a distance $l + \delta l_1$ from the origin, where it has the energy $\varepsilon_{ex} + e\bar{E}\,\delta l_1$. After excitation of k atoms this electron has traveled a distance $kl + \Sigma_{i=1}^{k} \delta l_i$, where δl_i is the distance required for the ith excitation beyond l, and ε_k is the electron energy after the kth excitation. Taking this energy to be zero, we obtain the relation

$$\sum_{i=1}^{k} \delta l_i = 0. \tag{18.40}$$

From this it follows that the distance required for k excitations by any electron approaches kl, which implies the bunching of electrons. This effect

suggests a periodic distribution structure for the electron and ion number densities and also for the electric field strength.

Evidently, accounting for the real behavior of this plasma leads to the broadening of ionization zones. In particular, within the framework of the simplified Tsendin model being used, we assume the spatial oscillation period l to be large compared to the tube radius. Because the lifetime τ of electrons and ions is the time required for ion drift over a distance of the order of the tube radius, the width of the ionization zone exceeds this value. This means that the bunching effect refers to long discharge tubes of small radius. Since each electron excites many atoms during its lifetime, that provides a basis for the bunching of electrons.

Despite the simplicity of this model, it helps us to understand the nature of striations. There are several mechanisms for broadening of ionization zones. For the stepwise ionization of atoms by electron impact that we are considering, ionization of excited atoms can result from collisions with slow electrons. This leads to broadening of the ionization zones. But if the ionization potential of excited atoms is small compared to that of atoms in the ground state, as is true for inert gases, the broadening of the ionization zones is relatively small.

We have now seen the conditions for the existence of striations by this ionization mechanism. Collisions of electrons lead to exchange of energy between them and destroy the effect, because when electron–electron collisions occur, ionization zones spread over all space. Hence, striations under consideration exist at small gas-discharge currents when the electron number density is small and collisions between electrons are infrequent.

This model shows that two regimes of the plasma can exist. In the first, the plasma is homogeneous, and ionization of atoms by electron impact occurs throughout the plasma. In the other regime, ionization occurs in narrow ionization zones distributed periodically over the length of the discharge tube. That is, striations exist in this regime. The regime in which the discharge plasma finds itself is determined by the energy available to the system, so that the characteristics of the external source of electricity are of great importance for the plasma behavior.

18.8 CURRENT-CONVECTIVE INSTABILITY

Just as there are a variety of mechanisms that can alter the manner in which unbound electrons can be introduced into and removed from a plasma, so also there are different ways in which ionization instabilities can develop. In addition to the above-described mechanisms for destabilizing a plasma, we now analyze one more case that involves a plasma in a strong magnetic field. The configuration we explore is one in which electric current flows in a cylindrical tube so that the electric and magnetic fields are directed along the axis of this plasma column. The magnetic field is so strong that electron and

ion motions in the plasma are dominated by the magnetic field. This means that the Larmor radii of electrons and ions are small compared to the mean free paths for these particles. Since charged particles recombine on the walls of the tube, the plasma is uniform across the diameter of the tube. These are the conditions in which an ionization instability called the *current-convective* instability may occur.

In the environment described, electrons will rotate with respect to ions in any cross section of the plasma column. This gives rise to an azimuthal electric field that enhances this motion. The development of the instability is slow if plasma quasineutrality is conserved. If a small inhomogeneity of the plasma is present in the direction of the current, then the plasma density is different in neighboring cross sections of the column. Since the current in the plasma is conserved, a decrease in the plasma density in any cross section of the column must be compensated by an additional electric field.

Now let us assume an "oblique" perturbation of the plasma density that is compensated by an electric field directed at an angle to the column axis. Then the azimuthal component of the electric field will produce rotation of the electrons and ions. This will enhance a suitably directed perturbation, leading to an instability.

We can derive a dispersion relation for such perturbations. The plasma is quasineutral and magnetized, so that the velocity of electrons and ions is

$$\mathbf{w} = c(\mathbf{E} \times \mathbf{H}_0)/H_0^2, \tag{18.41}$$

where $\mathbf{H}_0$ is the magnetic field, and $\mathbf{E}$ is the electric field of the wave. The magnetic field of the wave can be ignored, since the perturbation is slow. For the same reason, the electric field can be described by the potential φ, that is, $\mathbf{E} = -\nabla\varphi$.

The current density is $j_z = \Sigma E_z$, where the z-axis is along the axis of the column, and Σ is the plasma conductivity. The electric field is the sum of the external (E_0) and wave fields. Since the wave parameters are proportional to $\exp(i\mathbf{k} \cdot \mathbf{r} - i\omega t)$, we have $E_z = E_0 - ik_z\varphi$. The plasma conductivity is proportional to the electron number density, so that $\Sigma = \Sigma_0 + \Sigma' = \Sigma_0(1 + N_e'/N_0)$, where Σ_0 is the plasma conductivity, N_0 is the electron number density in the absence of perturbations, and Σ' and N_e' are the corresponding perturbed parameters. From the above expressions, the condition for conservation of the current density in the field direction is

$$-\Sigma_0 ik_z\varphi + \Sigma' E_0 = 0, \quad \text{or} \quad -ik_z\partial + \frac{N_e'}{N_0}E_0 = 0. \tag{18.42}$$

The continuity equation (9.5) for electrons is

$$\frac{\partial N_e}{\partial t} + \operatorname{div}(N_e\mathbf{w}) - D_a\frac{\partial^2 N_e}{\partial z^2} = 0,$$

where D_a is the ambipolar diffusion coefficient for the plasma. We have ignored the diffusive flux of electrons perpendicular to the magnetic field, assuming this flux to be small. Assuming harmonic dependence of the perturbed parameters on time and coordinates, we can rewrite this equation to first order as

$$\left(-i\omega + k_z^2 D_a\right) N_e' + w_x \frac{\partial N_0}{\partial x} = 0, \tag{18.43}$$

where the x-axis is in the direction of the maximum gradient of the equilibrium number density.

Equations (18.41) and (18.42) give

$$w_x = \frac{cE_y}{H_0} = -\frac{cik_y\varphi}{H_0} = \frac{k_y}{k_z}\frac{cE_0}{H_0}\frac{N_e'}{N_0}.$$

Substituting this in the dispersion relation (18.43), we obtain

$$i\omega = k_z^2 D_A + \frac{k_y}{k_z}\frac{cE_0}{H_0 L}, \tag{18.44}$$

where $1/L = -d(\ln N_0)/dx$. One can see that instability ($Im\ \omega < 0$) will develop if the ratio k_y/k_z has an appropriate sign and value. The instability has a threshold with respect to the electric field. The magnetic field must be high enough to meet the conditions described above.

Equation (18.44) shows that the optimum condition for this instability is such that the cyclotron frequency for ions is of the order of the collision frequency of ions with gas particles. The threshold for this instability is connected with the diffusion of charged particles. If the diffusion rate is sufficiently high, perturbations of the plasma are damped by the diffusion.

CHAPTER 19

ATMOSPHERIC PLASMAS

19.1 SPECIAL FEATURES OF ATMOSPHERIC PLASMAS

In the foregoing, we examined general principles and concepts relating to plasmas. We shall now apply these principles explicitly to two types of plasmas: atmospheric plasmas and gas-discharge plasmas. Each of these examples can display a broad variety of properties and parameters. An atmospheric plasma is realized in air, and a gas-discharge plasma is initiated upon ionization of gas atoms by the impact of electrons accelerated by an external electric field. Properties of atmospheric plasmas depend strongly on the altitude where they occur. Plasmas in the upper atmosphere are generated by the absorption of solar radiation that ionizes oxygen atoms and nitrogen molecules. Plasmas in the lower layers of the atmosphere have properties dependent on transport processes of charged and excited atoms, and also by the heat balance of these low-lying atmospheric layers.

Atmospheric plasmas can be used to illustrate the elementary collision processes that can occur in a weakly ionized plasma. Table 19.1 contains a list of basic atmospheric plasma processes, and will be referred to in the analysis of atmospheric phenomena. These processes are an explicit illustration of the data in Tables 4.1–4.3 and 7.1. We can use photoprocesses as the first example. Processes 1–3 in Table 19.1 are responsible for formation of charged particles in the upper atmosphere, and process 4 is associated with the production of atomic oxygen. The process inverse to 5 gives the main contribution to glow in the night sky, and processes 7–10 determine auroral radiation.

TABLE 19.1. Elementary Collision Processes in the Earth's Atmosphere[a]

Type	Number	Typical Process	Parameters[a]
Photoprocesses	1	$\hbar\omega + O \rightarrow O^+ + e$	$\nu = 3 \times 10^{-7}\ s^{-1}$ [b]
	2	$\hbar\omega + O_2 \rightarrow O_2^+ + e$	$\nu = 4 \times 10^{-7}\ s^{-1}$ [b]
	3	$\hbar\omega + N_2 \rightarrow N_2^+ + e$	$\nu = 3 \times 10^{-7}\ s^{-1}$ [b]
	4	$\hbar\omega + O_2 \rightarrow O(^1D) + O(^3P)$	$\sigma_{max} \sim 10^{-17}\ cm^2$
	5	$\hbar\omega + O^- \rightarrow O + e$	$\nu = 1.4\ s^{-1}$ [b]
	6	$\hbar\omega + O_2^- \rightarrow O_2 + e$	$\nu = 0.3\ s^{-1}$ [b]
	7	$O(^1S) \rightarrow O(^1D) + \hbar\omega$	$\tau = 0.8$ s, $\lambda = 558$ nm
	8	$O(^1D) \rightarrow O(^3P) + \hbar\omega$	$\tau = 140$ s, $\lambda = 630$ nm
	9	$N(^2D_{5/2}) \rightarrow N(^4S) + \hbar\omega$	$\tau = 1.4 \times 10^5$ s $\lambda = 520$ nm
	10	$N(^2D_{3/2}) \rightarrow N(^4S) + \hbar\omega$	$\tau = 6 \times 10^4$ s, $\lambda = 520$ nm
Ionization	11	$e + O_2 \rightarrow O_2^+ + e$	$k_{max} \sim 10^{-8}\ cm^3/s$
	12	$e + N_2 \rightarrow N_2^+ + e$	$k_{max} \sim 10^{-8}\ cm^3/s$
Recombination	13	$e + N_2^+ \rightarrow N + N$	$k = 2 \times 10^{-7}\ cm^3/s$
	14	$e + O_2^+ \rightarrow O + O$	$k = 2 \times 10^{-7}\ cm^3/s$
	15	$e + NO^+ \rightarrow N + O$	$k = 4 \times 10^{-7}\ cm^3/s$
	16	$e + N_4^+ \rightarrow N_2 + N_2$	$k = 2 \times 10^{-6}\ cm^3/s$
	17	$O^- + O_2^+ + N_2 \rightarrow O + O_2 + N_2$	$k_{ef} = 2 \times 10^{-6}\ cm^3/s$ [c]
	18	$O_2^- + O_2^+ + O_2 \rightarrow 3O_2$	$K = 1.6 \times 10^{-25}\ cm^6/s$
	19	$NO_2^- + NO^+ + N_2 \rightarrow NO + NO_2 + N_2$	$K = 1 \times 10^{-25}\ cm^6/s$
Electron attachment	20	$e + 2O_2 \rightarrow O_2^- + O_2$	$K = 3 \times 10^{-30}\ cm^6/s$
	21	$e + O_2 + N_2 \rightarrow O_2^- + N_2$	$K = 1 \times 10^{-31}\ cm^6/s$
	22	$e + O_2 \rightarrow O^- + O$	$k = 2 \times 10^{-10}\ cm^3/s$, $\varepsilon = 6.5$ eV
Negative ion detachment	23	$O^- + O_3 \rightarrow e + 2O_2 + 2.6$ eV	$k = 3 \times 10^{-10}\ cm^3/s$
	24	$O_2^- + O_2 \rightarrow e + O_3 + 0.62$ eV	$k = 3 \times 10^{-10}\ cm^3/s$
	25	$O^- + O_2 \rightarrow e + O_3 - 0.42$ eV	$k < 1 \times 10^{-12}\ cm^3/s$
Dissociation	26	$e + O_2 \rightarrow 2O + e$	$k = 2 \times 10^{-10}\ cm^3/s$, $\varepsilon > 6$ eV
Ion reactions	27	$O^+ + N_2 \rightarrow NO^+ + N + 1.1$ eV	$k = 6 \times 10^{-13}\ cm^3/s$
	28	$O^+ + O_2 \rightarrow O_2^+ + O + 1.5$ eV	$k = 2 \times 10^{-11}\ cm^3/s$
	29	$N^+ + O_2 \rightarrow O^+ + NO + 2.3$ eV	$k = 2 \times 10^{-11}\ cm^3/s$
	30	$N_2^+ + O \rightarrow NO^+ + N + 3.2$ eV	$k = 1 \times 10^{-10}\ cm^3/s$
Quenching	31	$2O_2(^1\Delta_g) \rightarrow O_2 + O_2(^1\Sigma_g^+)$	$k = 2 \times 10^{-17}\ cm^3/s$
	32	$O_2(^1\Delta_g) + O_2 \rightarrow 2O_2$	$k = 2 \times 10^{-18}\ cm^3/s$
	33	$O_2(^1\Sigma_g^+) + N_2 \rightarrow O_2 + N_2$	$k = 2 \times 10^{-17}\ cm^3/s$
	34	$N_2(A^3\Sigma_u^+) + O_2 \rightarrow N_2 + O_2$	$k = 4 \times 10^{-12}\ cm^3/s$
	35	$O(^1D) + O_2 \rightarrow O + O_2$	$k = 5 \times 10^{-11}\ cm^3/s$
	36	$O(^1D) + N_2 \rightarrow O + N_2$	$k = 6 \times 10^{-11}\ cm^3/s$
	37	$O(^1S) + O_2 \rightarrow O + O_2$	$k = 3 \times 10^{-13}\ cm^3/s$
	38	$O(^1S) + O \rightarrow O + O$	$k = 7 \times 10^{-12}\ cm^3/s$
Chemical reaction	39	$O + O_3 \rightarrow 2O_2$	$k = 7 \times 10^{-14}\ cm^3/s$
Three-body association	40	$O + 2O_2 \rightarrow O_3 + O_2$	$K = 7 \times 10^{-34}\ cm^6/s$
	41	$O + O_2 + N_2 \rightarrow O_3 + N_2$	$K = 6 \times 10^{-34}\ cm^6/s$

[a] Wavelength λ, lifetime τ, and room-temperature rate constants k for pair processes and K for three-body processes.
[b] Per atom, molecule, or ion for daytime atmosphere at zero zenith angle.
[c] At the pressure 1 atm.

TABLE 19.2. Heat Balance of the Earth[a]

Form of Energy	Process	Power, 10^{13} kW
Sun's radiation	Reaching Earth's atmosphere	17.3
	Reflected by the Earth	0.7
	Absorbed by the Earth	8.3
	Reflected by the atmosphere	5.4
	Absorbed by the atmosphere	2.9
Infrared radiation	Atmospheric emission to space	10.2
	Atmospheric emission to Earth	16.7
	Absorbed by the atmosphere	18.7
	Absorbed by the Earth	16.7
	Emitted by the Earth	19.7
	Transmitted through the atmosphere	1.0
Convection		1.3
Evaporation		4.0

[a]Convection of air and evaporation of water from the Earth's surface lead to transport of energy from the surface to the atmosphere.

As an introduction to the study of atmospheric plasmas, we consider general properties of the Earth's atmosphere. The heat balance of the Earth is represented in Table 19.2. The source of the Earth's heat balance is solar radiation. The Sun as a radiator can be considered to be a blackbody with a temperature of 5800 K, corresponding to a radiation flux of 6.4 kW/cm^2 from its surface, mostly in the visible region of the spectrum. This gives rise to a radiative flux of 0.14 W/cm^2 at the Earth's distance from the Sun, which translates to 1.74×10^{14} kW of solar power reaching the Earth's atmosphere. The same amount of power then emanates from the Earth in the form of emission from the Earth's surface and atmosphere as infrared radiation, and reflection by the Earth's surface and atmosphere. The surface of the Earth receives and returns 2.5×10^{14} kW of power, while the Earth including its atmosphere receives and returns 2.69×10^{14} kW of power. If the Earth is regarded as an ideal blackbody, the emitted infrared radiation corresponds to an effective surface temperature of 291 K.

The Earth's atmosphere at sea level consists mostly of molecular nitrogen (78%), molecular oxygen (21%), and argon (about 1%); the total number density of molecules and atoms is 2.7×10^{19} cm^{-3} (at a pressure of 1 atm). The number density of molecules decreases with increasing altitude h as given by the barometric distribution (2.14),

$$N(h) = N(0)\exp\left(-\int_0^h \frac{mg\,dz}{T}\right), \tag{19.1}$$

where m is the average molecular mass, g is the acceleration of free fall, and $T(z)$ is the temperature at an altitude z. To determine the change of

temperature with altitude, we can neglect heat transfer processes, and we can employ the adiabatic law $TN^{1-\gamma} = \text{const}$, where $\gamma = 1.4$ is the adiabatic exponent for air at the temperatures considered. This leads to $dT/T = (\gamma - 1)\,dN/N$, and from the barometric formula (19.1) we have $dN/N = -mg\,dz/T$. Hence $-dT/dz = mg(\gamma - 1) = 14$ K/km. The real value (10 K/km) is lower than this because of water vaporization in the atmosphere and other heat transport processes. Nevertheless, the adiabatic model used is suitable for estimations.

Heat transport in the atmosphere is primarily a result of convection. An estimate for the heat flux resulting from thermal conductivity gives $q = \kappa|dT/dz| = 3 \times 10^{-8}$ W/cm^2, while according to Table 13.1, convection is responsible for an average heat flux of 2×10^{-3} W/cm^2.

19.2 THE EARTH AS AN ELECTRICAL SYSTEM

In Chapter 12 we analyzed the processes in clouds that lead to formation and separation of charged particles in the atmosphere. Below we shall consider the electrical phenomena in the Earth's atmosphere from another standpoint. The Earth carries a negative charge. There must thus exist mechanisms in the Earth's atmosphere that lead to the acquisition of this charge. We begin with an overview of the processes that cause electrical phenomena in the atmosphere. Though it may seem strange at first glance, the charging of the Earth occurs as a result of lightning. Charge-transfer processes in clouds that are connected with charging and precipitation of drops (aerosols) lead to a redistribution of the charges therein. The lower part of a cloud is usually charged negatively, and the upper part positively. The electric potential of a cloud can reach hundreds of millions of volts, causing breakdown of the air. The discharge of a cloud to the Earth in the form of a lightning stroke is accompanied by the transfer of electrical charge to the Earth. About 10% of thunderstorms transfer a positive charge to the Earth, and 90% transfer negative charge. The net result is that the Earth acquires a negative charge.

The electrical parameters of the Earth can be stated simply. Its electric potential is about $U = 300$ kV, and the electric field strength near the Earth's surface is approximately 130 V/m. Since the electric field strength E and the surface charge σ of the Earth are connected by the relation $E = 4\pi\sigma$, the total charge of the Earth is $q = 4\pi R^2\sigma = R^2E = 5.8 \times 10^5$ C, where R is the Earth's radius. The Earth as an electrical system is like a spherical capacitor whose lower plate is charged negatively. In terms of this model, the distance l between the plates of this capacitor, assuming the electric field inside to be uniform, is $l = U/E = 2.3$ km. This estimate shows that the processes responsible for the Earth's charge occur in the lower layers of the Earth's atmosphere at altitudes of several kilometers.

Discharging of the Earth produces motion of ions. Measurements show that the average current density over land amounts to 2.4×10^{-12} A/m^2,

and over the ocean it is 3.7×10^{-12} A/m^2. This gives a total Earth current of approximately $I = 1700$ A. Taking the average mobility of atmospheric ions to be $K = 2.3$ cm^2/(V cm), we find the average ion number density to be $N_i = 300$ cm^{-3}.

We can estimate time scales for the electrical processes of the Earth. Positive and negative ions recombine under atmospheric conditions by three-body collisions, with an effective ion recombination coefficient of $\alpha = 2 \times 10^{-6}$ cm^3/s (see Table 9.1). This corresponds to a recombination time of about $\tau = (\alpha N_i)^{-1} = 0.5$ h. This contrasts with the much shorter characteristic time $q/I = 6$ min for discharging of the Earth, where q is the Earth's charge and I is the average atmospheric current. During their lifetime τ, ions travel a distance $s = KE\tau = 50$ m, where K is the ion mobility and E is the electric field strength near the Earth. Because this distance is small compared to the size of the Earth's layer where electrical phenomena develop, there must be a mechanism for the generation of these ions. The intensity of this process (i.e., the number of ions per unit time and per unit volume) is given by $\alpha N_i^2 = 0.1$ cm^{-3} s^{-1}. These ions are produced by cosmic rays, mostly generated by the Sun. Maximum ionization is observed at altitudes of 11 to 15 km, and is characterized by ionization rates of 30–40 cm^{-3} s^{-1}. This results in an ion number density of about 6×10^3 cm^{-3}. (The recombination coefficient is about 10^{-6} cm^3/s at this altitude.) To explain the observed currents of charged particles formed, it is necessary that the intensity of ionization in the lower atmospheric layers should be smaller than this maximum by a factor of 100.

Atmosphere charging is a process ancillary to the circulation of water in the atmosphere. Every year 4×10^{14} tonnes (metric tons) of evaporated water pass through the atmosphere, corresponding to 13 million tonnes of water per second. This requires a power of 4×10^{13} kW. The power associated with the passage of electric current through the atmosphere is $UI = 5 \times 10^5$ kW, where $U = 300$ kV is the Earth's potential and $I = 1700$ A is the atmospheric current. Considering a cloud potential during a thunderstorm exceeding the potential of the Earth by a factor of 10^3, then we find that the power expended in the charging of the Earth is three orders of magnitude greater than the power of the Earth discharging, but five orders of magnitude smaller than the power consumed in the evaporation of water. Therefore, the power expended on electrical processes during the circulation of water in the atmosphere is relatively small.

To create the observed charging current, it is necessary that the charge transfer should be 1.4×10^{-10} C per gram of water. Measurements show that a water drop of radius 2 μm suspended in a cloud carries an average charge of $20e$, corresponding to 10^{-7} C per gram of water. A drop of radius 6 μm suspended in a cloud acquires an average charge of $50e$, corresponding to 10^{-8} C per gram of water. Hence clouds of the terrestrial atmosphere ensure the operation of the electrical machine of the Earth by causing its charging.

We now have the following picture of the operation of the Earth as an electrical device. The electrical processes are a consequence of the circulation of water in the atmosphere. At an altitude of several kilometers water vapors are condensed into droplets—aerosols—that form clouds. Due to the different mobilities of positive and negative ions in the atmosphere, these aerosols are charged mostly negatively. In turn, positive and negative ions of the atmosphere are formed under the action of cosmic rays. Negatively charged drops fall under the action of gravity. The lower part of a cloud thus develops a high electric potential. Discharge from clouds to the Earth in the form of lightning strokes leads to negative charging of the Earth. The reverse (discharging) process is due to the mobility of atmospheric ions under the action of the Earth's field.

19.3 LIGHTNING

Lightning is a powerful electrical breakdown between a cloud and the Earth, between two clouds, or within one cloud. The length of the lightning channel is measured in kilometers. Lightning is the most widespread electrical phenomenon in the atmosphere. The action of lightning and the descent of charged raindrops to the Earth leads to charging of the Earth. The average charge carried by a single lightning stroke is about 25 C. If we assume that all charging of the Earth is accomplished by lightning, we conclude that it is necessary to have about 70 lightning strokes per second (i.e., about 6 million lightning strokes per day) for maintenance of the observed charging current. If we assume each lightning event is observable at a distance of up to 10 km, then one can observe an average of 3 or 4 lightning strokes every day. In actuality, the frequency depends on season and geographical location, but the above estimate shows that this phenomenon is widespread.

We shall examine the distinguishing features of lightning as an electrical discharge. The charge separation in a cloud results from the charging of drops (aerosols) that subsequently descend. This leads to separation of charge in a cloud, and creates an electric potential in the lower part of a cloud that amounts to hundreds of millions of volts. The subsequent discharging of the cloud in the form of a lightning stroke leads to the transfer of this charge to the Earth. The breakdown electric field strength of dry air is about 25 kV/cm, which exceeds by an order of magnitude the average electric field strength between the Earth and a cloud during a thunderstorm. Hence, lightning as a gas breakdown has a streamer nature. Random inhomogeneities of the atmosphere, dust, aerosols and various admixtures decrease the breakdown voltage.

The first stage of lightning is creation of the discharge channel. This stage is called the *stepwise leader*. The stepwise leader is a weakly luminous breakdown that propagates along a broken line with a segment length of tens of meters. A typical propagation velocity of the stepwise leader is of the

order of 10^7 cm/s, and that, in turn, is of the order of the electron drift velocity in the air in the fields under study.

After creation of the conductive channel, the electric current begins to flow through it, and its luminosity increases sharply. This stage is called the *recurrent stroke* and is characterized by a propagation velocity of up to 5×10^9 cm/s, corresponding to the velocity of propagation of the electric field front in conductors. The recurrent stroke is relatively short. Its first phase (the peak-current phase) lasts some microseconds, and the discharge is complete in less than 10^{-3} s. During this time the current channel does not expand, so that the released energy is spent on the heating of the channel and ionization of the air in it. To estimate the temperature of the channel, we take the charge passed to be $Q = 2$ C, with an electric field strength E in the channel of 1 kV/cm. The energy released per unit length of the channel is QE, and the typical increase of the air temperature in the channel is

$$\Delta T \sim QE/(c_p \rho S), \tag{19.2}$$

where $c_p \sim 1$ J/g is the heat capacity of air, $\rho \sim 10^{-3}$ g/cm^3 is its density, and $S \sim 100$ cm^2 is the channel cross section (of radius ~ 10 cm). From this it follows that $\Delta T \sim 2 \times 10^4$ K. This rough estimate makes clear that the air in the lightning channel is highly ionized. At such air temperatures, radiative processes restrict the subsequent increase of temperature. Usually, the temperature of the lightning channel is about 30,000 K.

The recurrent stroke creates a hot lightning channel. Its supersonic expansion creates an acoustic wave—the thunder. Equilibrium between the conductive channel and the surrounding air is established, and then the principal part of the atmospheric charge is carried through the channel. The lightning current in this stage of the process falls drastically in time, and the total duration of the recurrent stroke is about 10^{-3} s. Then the conducting channel disintegrates. If during its decay a redistribution of charges in the cloud has occurred, then the lightning flash can recur through this channel. This can take place if the time interval from the previous flash is no more than about 0.1 s. Then the new flash begins from the so-called *arrowlike leader*, which is similar to the stepwise leader, but is distinguished from it in that it travels the distance along the existing channel continuously, without delay on each step as in the case of the stepwise leader. After the passage of the arrowlike leader, a recurrent stroke occurs as in the first breakdown. After some delay, breakdown may again repeat by passage of an electric current through the existing channel. As a rule, one lightning stroke contains several charge pulses through the same channel.

Lightning is of interest as an intense source of radiation. To find the maximum efficiency of transformation of the electric energy into radiation, we assume that the conductive channel is a blackbody of temperature 30,000 K. Then the radiation flux of the conductive channel is $j = \sigma T^4 \sim 5 \times 10^5$ W/cm^2, and the radiation flux per unit length of the channel is $2\pi Rj \sim 10^7$ W/cm, where the channel radius is taken to be $R = 10$ cm. Since the above

temperature is maintained during $\tau \sim 10^{-4}$ s, we have an estimated upper limit for the specific radiation energy of $\varepsilon \sim 10^3$ J/cm. The electrical energy per unit length of the lightning channel is $QE = 2$ kJ/cm. This rough estimate leads to the conclusion that the electrical energy of lightning is transformed very efficiently into radiated energy.

Another distinguishing feature of radiation emitted by the lightning channel relates to the role of UV radiation. According to Wien's law, the maximum radiation energy for a blackbody with a temperature of 30,000 K occurs at wavelengths of about 100 nm. This estimate shows the possibility for lightning to emit copious UV radiation, though in reality, due to the limited transparency of an atmospheric plasma of the above temperature for ultraviolet and vacuum-ultraviolet radiation, visible radiation constitutes the principal portion of the radiation due to lightning.

19.4 PREBREAKDOWN PHENOMENA IN THE ATMOSPHERE

There is one more aspect of electrical phenomena in the atmosphere that we want to analyze. As was noted above, the electric field strength of a cloud during the occurrence of lightning is less by one or two orders of magnitude than the breakdown strength at atmospheric pressure [about $E = 25$ kV/cm ($E/N = 90$ Td) between plane electrodes], or the breakdown strength due to propagation of a positive streamer (about 5 kV/cm). We shall consider some reasons for this that extend our understanding of the nature of processes that accompany electrical phenomena in atmospheric air.

Consider a chain of processes that can lead to breakdown. We shall consider only one of several mechanisms in order to demonstrate the character of these processes. Assume that atmospheric air is subjected to an electric field of strength E, and elementary processes 11, 12, 17, 20, 23, 26, 40, and 41 of Table 19.1 are the determining factors. These processes lead to balance equations for the number densities of electrons (N_e), negative ions (N_-), and ozone ([O_3]) that can be stated as

$$\frac{dN_e}{dt} = (\nu_{\text{ion}} - \nu_{\text{at}})N_e + N_-[O_3]k_{23}, \tag{19.3}$$

$$\frac{dN_-}{dt} = \nu_{\text{at}}N_e - k_{17}N_-^2 - N_-[O_3]k_{23}, \tag{19.4}$$

$$\frac{d[O_3]}{dt} = M - \frac{[O_3]}{\tau} + 2\nu_{26}N_e. \tag{19.5}$$

We employ here the quantities $\nu_{\text{ion}} = k_{11}[O_2] + k_{12}[N_2]$, $\nu_{\text{at}} = k_{20}[O_2]$, and $\nu_{26} = k_{26}[O_2]$. We assume that process 17 of Table 19.1 gives the main contribution to recombination of positive and negative charges; we assume

further that the number density of ozone molecules is relatively small, so that the dissociation of an oxygen molecule leads automatically to formation of two ozone molecules as a result of processes 40 and 41. The rate of ozone formation is denoted by M, and τ is the lifetime of ozone molecules.

Solving the system of equations (19.3) and (19.4) under the assumption that $N_e \ll N_-$, the number densities of charged particles are given by

$$N_e = \frac{k_{23}^2}{k_{17}} \frac{\nu_{\text{ion}}}{(\nu_{\text{at}} - \nu_{\text{ion}})^2} [O_3]^2, \qquad N_- = \frac{k_{23}}{k_{17}} \frac{\nu_{\text{ion}}}{\nu_{\text{at}} - \nu_{\text{ion}}} [O_3]. \quad (19.6)$$

The subscripts in the rate constants correspond to the process numbers of Table 19.1. The expressions (19.6) show that a reverse connection between processes restores electrons. As a result, there are stable currents in atmospheric air subjected to an electric field. At $\nu_{\text{at}} = \nu_{\text{ion}}$, an instability develops that leads to breakdown in pure air. This will occur at $E = 25$ kV/cm, which is the breakdown strength of dry air in the case of uniform currents. However, the sequence of processes specified above leads to breakdown at smaller electric fields. An increase of the ozone number density leads to an increase of the electron number density, which in turn causes an increase of the ozone number density. Then at certain sets of parameter values an explosive instability can develop, meaning that breakdown has occurred. We now seek the threshold for this instability.

For this purpose, we analyze Eq. (19.5). Substituting in it Eq. (19.6) for the electron number density, we have

$$\frac{d[O_3]}{dt} = \frac{N_0}{\tau} - \frac{[O_3]}{\tau} + k_{\text{ef}}[O_3]^2, \quad (19.7)$$

where $N_0 = M\tau$ is the ozone number density in the absence of the electric field. The effective rate constant determined by the expression

$$k_{\text{ef}} = \frac{2k_{23}^2 \nu_{\text{ion}} \nu_{26}}{k_{17}(\nu_{\text{at}} - \nu_{\text{ion}})^2}$$

is the combination of the rate constants of the corresponding processes. Under typical atmospheric conditions we have $N_0 \sim 10^{12}$ cm^{-3}. The effective rate constant k_{ef} depends strongly on the electric field strength. It has the values 8×10^{-13} cm^3/s at $E/N = 30$ Td, 2×10^{-11} cm^3/s at 50 Td, and 6×10^{-10} cm^3/s at 80 Td.

In the stationary case, Eq. (19.7) has two solutions, of which one is stable. The instability corresponds to imaginary values for the solutions. Hence, the

instability that leads to breakdown corresponds to the condition

$$k_{ef} \geq (4N_0\tau)^{-1}. \tag{19.8}$$

The real lifetime of ozone molecules in the atmosphere is rather large ($\tau \sim 10^6$ s), because ozone is produced at high altitudes (40–80 km) and its loss results from chemical reactions (ozone cycles) or from transport to the Earth's surface. The parameter τ in Eq. (19.8) refers to a time during which an ozone molecule is located in a region with a large electric field. If we take such a region to be a cloud of size $L \sim 1$ km, and the velocity of transport from this region to be a wind velocity $v \sim 1$ m/s, then we have $\tau \sim 10^3$ s, and the condition (19.8) gives $k_{ef} \gg 2 \times 10^{-16}$ cm^3/s. The above values of k_{ef} show that the chain of processes we are considering leads to a severalfold reduction of the breakdown electric field strength.

We consider the ozone version of breakdown reduction to be merely illustrative. Further, we are guided by a notion of breakdown as being uniform, whereas breakdown in the atmosphere at large distances between electrodes develops in the form of a streamer—a nonuniform ionization wave—that requires lower threshold fields than uniform breakdown. Nevertheless, the above analysis exhibits important reasons for reduction of the electric field required to cause breakdown in natural air. Other reasons include heating of some regions of the atmosphere; presence of particles, drops, or chemical compounds in the atmosphere; inhomogeneities of the electric field; and so on. This listing exemplifies the wide variety of processes that can influence atmospheric electrical properties.

19.5 IONOSPHERE

The history of exploration of the Earth's ionosphere starts from Marconi's experiment in 1901 when he tried to establish radio contact between two continents. The transmitter had been set up in Europe on the Cornwall peninsula in England, and the receiver was located in Canada, on the Newfoundland peninsula. From the standpoint of wave propagation theory, this experiment seemed to be hopeless. According to the laws of geometrical optics, radio waves should propagate at such distances with rectilinear beams, and radio connection for these distances seemed to be precluded by the spherical form of the Earth's surface. The experiment led to a surprising result: the signal was detected by the receiver and its intensity exceeded estimates by many orders of magnitude.

The only explanation for this discrepancy was the existence of a radio mirror in the Earth's atmosphere that reflects radio waves. The radio-mirror

TABLE 19.3. Critical Number Densities of Plasma Electrons (N_{cr}) for Propagation of Radio Waves

Type of Radio Waves	Wavelength, m	N_{cr}, cm^{-3}
Long	10,000–1000	$10–10^3$
Medium	1000–100	$10^3–10^5$
Short	100–10	$10^5–10^7$

model assumes that waves follow rectilinear paths and repeatedly reflect between the surface of the Earth and this upper-atmosphere mirror. In 1902 O. Heaviside and A. Kennelly proposed that the role of this radio mirror is played by an ionized layer in the atmosphere. This fact was confirmed in 1925 by an experiment conducted by a group of English physicists from Cambridge University. Placing the receiver at a distance of 400 m from the transmitter, they determined by measurement of the delay time for the reflected signal to arrive that the reflector is at an altitude of 100–120 km. This reflecting layer, which was referred to earlier as the Heaviside layer, is now called the E-layer (based on the symbol for the electric field vector for radio waves). Subsequently, the existence of ionized gas was discovered at other altitudes. The part of the atmosphere that contains ionized gases is called the ionosphere.

The presence of electrons in the ionosphere prevents long electromagnetic waves from propagating therein if their frequencies are smaller than the frequency of plasma oscillations [see Eq. (15.21)]. Hence, radio waves reflect from the ionosphere and return to the Earth's surface. Table 19.3 summarizes limiting electron number densities at which the plasma frequency coincides with the frequency of plasma oscillations, so that longer radio waves cannot propagate. The maximum electron number density of the order of 10^6 cm^{-3} may be reached at an altitude of about 200 km. Therefore, the best reflection conditions are fulfilled for short waves within the range of 30 to 100 m. Because the electron number density at any particular altitude depends on season, time of day, and other factors, the quality of radio communications at a given wavelength varies continually. Long waves are reflected at low altitudes where the atmospheric density is relatively high, and reflection of the waves is accompanied by damping.

It has been established over time that the atmosphere possesses several ionized layers that differ in their properties. The lower D-layer occupies the altitude region of 50 to 90 km. A typical number density of charged particles therein is of the order of 10^3 cm^{-3}. The negative charge of the D-layer arises primarily from the presence of negative ions, and a great variety of both negative and positive ions reside there. In particular, the most widespread positive ion is the cluster ion $H_3O^+ \cdot H_2O$.

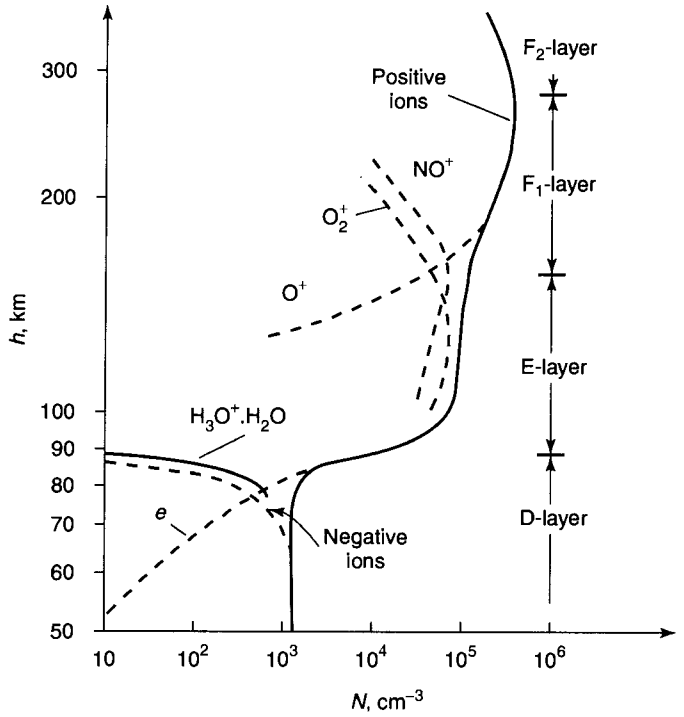

Figure 19.1 Charged atomic particles in the upper atmosphere.

The next higher layer of the ionosphere, the E-layer, is at an altitude of 90 to 140 km. Charged particles of the E-layer are formed by photoionization of air caused by solar UV radiation. These charged particles drift to lower layers of the atmosphere and are the source of plasma in the D-layer. The electron number density in the E-layer is of the order of 10^5 cm^{-3}. Negative ions are nearly nonexistent in this layer, and the basic types of positive ions are NO^+ and O_2^+ (see Fig. 19.1). The decay of charged particles in the E-layer is due to dissociative recombination of electrons and molecular ions, or to transport of charged particles to lower layers of the atmosphere.

A higher ionospheric layer, the F_1-layer, is located at an altitude of 140 to 200 km. Above it (up to an altitude of about 400 km) is the F_2-layer. The electron number density in these F-layers is 10^5 to 10^6 cm^{-3}. The basic type of positive ions is O^+. Charged particles of the F-layers of the ionosphere are formed by photoionization of atmospheric oxygen (the main component of the atmosphere at these altitudes) due to solar radiation. Loss of electrons from these layers is caused by photorecombination of electrons and oxygen ions, photoattachment of electrons to oxygen atoms, and transport of electrons to lower atmospheric layers.

The E and F layers of the ionosphere, having a high number density of electrons, are responsible for reflection of radio signals, constituting the radio mirror. But their role is broader than this function. These altitudes are the most convenient for operation of artificial satellites. Also, the interesting physical phenomenon of the aurora is developed just at these altitudes. Aurorae occur when a flow of solar protons penetrates into the atmosphere. Charge exchange of these protons and their deceleration take place in the E and F layers. The subsequent chain of elementary processes leads to formation of excited atoms, whose radiation is observed from the Earth as the aurora.

One of the peculiarities of aurorae is that their radiation is created by forbidden transitions of atoms and ions that cannot be detected in the laboratory. In particular, processes 7 to 10 of Table 19.1 usually give the principal contributions to the radiation of aurorae. Under laboratory conditions, these excited states of atoms and ions are quenched by collisions with air molecules. The probabilities for an excited atom to radiate and to be quenched are equal at the number density of quenching particles given by $(k\tau)^{-1}$, where τ is the radiative lifetime of the excited atom, and k is the rate constant for collisional quenching. The excited oxygen atom $O(^1S)$ is quenched in the upper atmosphere mainly by atomic oxygen (process 38 of Table 19.1), and the threshold number density of oxygen atoms is 2×10^{11} cm^{-3}. In the case of $O(^1D)$, the main quenching mechanism in the ionosphere is process 36 of Table 19.1. This gives the threshold number density of nitrogen molecules as 10^8 cm^{-3}. If the number density of quenching particles is lower than the above values, radiation of the corresponding excited atoms may be significant.

19.6 ATOMIC OXYGEN IN THE UPPER ATMOSPHERE

Atomic oxygen is one of the basic components of the upper atmosphere, so we shall examine those processes that determine its relative abundance in the atmosphere. Formation of atomic oxygen results from photodissociation of molecular oxygen (process 4 of Table 19.1) by solar radiation in the spectral range of 132 to 176 nm (corresponding to the photon energy range of 6 to 10.3 eV). This absorption range is called the *Schumann–Runge continuum* and is characterized by cross sections of 10^{-19} to 10^{-17} cm^2. The Schumann–Runge continuum is the determining factor in the generation of atomic oxygen at altitudes higher than 120 km. At lower altitudes, up to $h \approx 80$ km, the generation of atomic oxygen is accomplished mostly by dissociation of oxygen molecules due to the weak *Herzberg continuum* in the wavelengths range of 140 to 175 nm, where the absorption cross section is less than 2×10^{-24} cm^2.

The recombination rate for two oxygen atoms in three-body collisions decreases as the altitude increases, and hence the concentration of atomic

oxygen grows. The number density of atomic oxygen becomes equal to the number density of molecular oxygen at altitudes of 100 to 120 km, and atomic oxygen matches the number density of molecular nitrogen at altitudes of 150 to 200 km. For comparison, we note that the average total number densities of nitrogen and oxygen molecules vary from 7×10^{12} to 3×10^{9} cm^{-3}, and the number density of atomic oxygen is in the range of 6×10^{11} to 4×10^{9} cm^{-3} as the altitude varies from 100 up to 200 km. Thus, atomic oxygen is one of the basic components of the upper atmosphere at very high altitudes.

To analyze the absorption of short-wave solar radiation as a result of photodissociation of molecular oxygen, we write the balance equation for the intensity I_ω of solar radiation of a given frequency in the atmosphere in the form

$$dI_\omega/dz = -I_\omega \sigma_\omega [O_2], \tag{19.9}$$

where z is the altitude, $[O_2]$ is the number density of molecular oxygen, and σ_ω is the photodissociation cross section. We assume that solar radiation is incident perpendicularly on the Earth's surface, and that the number density of molecular oxygen varies according to the barometric formula (2.14): $[O_2] = N_0 \exp(-z/L)$, where $L = T/mg \approx 10$ km. Then the solution of equation (19.9) is

$$I_\omega(z) = I_\omega(\infty) \exp\left[-\exp\left(-\frac{z - z_0}{L}\right)\right], \tag{19.10}$$

where $I_\omega(\infty)$ is the intensity of solar radiation above the atmosphere, and the altitude z_0 is determined by the relation $\sigma_\omega L[O_2](z_0) = 1$. Equation (19.10) shows that the principal portion of the solar radiation of this part of the spectrum is absorbed near z_0. Because the photodissociation cross section is in the range of $\sigma_\omega \sim 10^{-19}$ to 10^{-17} cm^2, this absorption takes place at altitudes where $[O_2] \sim 10^{11}$ to 10^{13} cm^{-3}.

It is instructive to compare a decay time for the photodissociation of molecular oxygen and the characteristic time for transport of molecular oxygen to the altitudes at which absorption occurs. A typical dissociation time is

$$\tau_{dis} \sim \left[\frac{1}{4}\int \frac{dI_\omega\, \sigma_\omega}{\hbar\omega}\right]^{-1} \sim 2 \times 10^6 \text{ s},$$

where the factor $\frac{1}{4}$ results from averaging the radiation flux over the entire surface of the Earth, and $\hbar\omega = 6$–10 eV is the photon energy. The drift velocity of an atom or molecule as a result of its own weight is, according to the Einstein relation (10.14),

$$w = \frac{Dmg}{T} \sim g\left(N\sigma_g\sqrt{\frac{m}{T}}\right)^{-1} \sim \frac{3 \times 10^{13} \text{ cm}^{-2} \text{ s}^{-1}}{N}, \tag{19.11}$$

where we use the estimate (10.6) for the diffusion coefficient D of oxygen atoms and the quantity $\sigma_g = 3 \times 10^{-15}$ cm^2 is about the magnitude of a gas-kinetic cross section for atmospheric molecules and atoms. In this expression, N is the number density of atoms and molecules at some given altitude in the atmosphere. Assuming molecular nitrogen to be the primary component of the atmosphere at altitudes of maximum photodissociation, we have $[O_2] = N/4$. Because the concentration of molecular oxygen is about $[O_2] \sim 10^{11}$ cm^{-3}, a typical transport time is $\tau_{dr} \sim L/w \sim 10^4$ s. This gives the inequality $\tau_{dr} \ll \tau_{dis}$, so that the photodissociation process does not disrupt the barometric distribution of molecular oxygen at altitudes where photoabsorption of solar radiation takes place. The quantity τ_{dr} is a characteristic drift time.

To estimate the number density of atomic oxygen, we can compare the flux $w[O]$ of oxygen atoms and the rate of their formation, which is of the order of the flux of solar photons causing photodissociation. This flux I is $I \sim 3 \times 10^{12}$ cm^{-2} s^{-1} at optimum altitudes. The number density of atomic oxygen is

$$[O] \sim I/w \sim 0.1N \tag{19.12}$$

at altitudes where it is formed, where Eq. (19.11) for the atom drift velocity has been used. From this it follows that the concentration of atomic oxygen ($\sim 10\%$) mechanisms for loss of atomic oxygen become weak. Decay of atomic oxygen is determined by the three-body process for recombination of atomic oxygen ($2O + M \rightarrow O_2 + M$, where M = N_2, O, or O_2). The maximum number density of atomic oxygen $[O]_{max}$ is observed at altitudes where a typical time for the three body association process is equal to the time for atomic transport to lower layers. This correspondence gives

$$w[O]_{max}/L \sim K[O]_{max}^2 N.$$

Because the magnitude of K is $K \sim 10^{-33}$ cm^6/s, we obtain $[O]_{max} \sim 10^{13}$ cm^{-3}. Part of the atomic oxygen penetrating to lower layers in the atmosphere is transformed into ozone by processes 40 and 41 of Table 19.1. Thus, the photodissociation process in the upper atmosphere leads to a high ozone concentration (up to 10^{-4}) at altitudes of 40 to 80 km.

19.7 IONS IN THE UPPER ATMOSPHERE

Ions in the upper atmosphere such as N_2^+, O_2^+, O^+, and N^+ are formed by photoionization of the corresponding neutral species. The spectrum of solar radiation in the vacuum-UV range that is responsible for ionization of atmospheric atomic particles is created by the solar corona. Hence the intensity of this radiation can vary over a wide range. The average flux of

photons in the portion of the spectrum at less than 100 nm is about 2.4×10^{10} cm^{-2} s^{-1}. The principal consequence of this part of the spectrum it to cause Lyman-series transitions of atomic hydrogen, including the Rydberg spectrum and the continuum. The contribution in the spectral range of 84 to 103 nm averages about 1.3×10^{10} cm^{-2} s^{-1}. Among the more notable processes are the transition of C III at 99.1 nm (9×10^{8} cm^{-2} s^{-1}), the transition of C III at 97.7 nm (4.4×10^{9} cm^{-2} s^{-1}), the transition of O V at 63 nm (1.3×10^{9} cm^{-2} s^{-1}), the transition of He I at 58.4 nm (1.3×10^{9} m^{-2} s^{-1}), and the Lyman transition of He II at 30.4 nm (7.7×10^{9} cm^{-2} s^{-1}). The maximum rate constant for the generation of electrons as a result of photoionization processes occurs at an altitude of about 160 km and is 4×10^{15} cm^{-3} s^{-1}.

We can make rough estimates of the number density of charged particles at middle altitudes where the photoionization rate constant has a maximum. The photoionization cross section is $\sigma_{\text{ion}} \sim 10^{-18}$–$10^{-17}$ cm^2, so that the number density of molecules is $N_{\text{m}} \sim (\sigma_{\text{ion}} L)^{-1} \sim 10^{11}$–$10^{12}$ cm^{-3} at altitudes where photoionization occurs. The number density N_{i} of molecular ions at these altitudes follows from the balance equation $\alpha N_e N_{\text{i}} \sim I_{\text{ion}}/L$ (where α is the dissociative recombination coefficient of processes 13 to 15 of Table 19.1), and $I_{\text{ion}} \sim 2 \times 10^{10}$ cm^{-2} s^{-1} is the flux of photons whose absorption leads to photoionization. From this it follows that

$$N_{\text{i}} \sim \sqrt{\frac{I_{\text{ion}}}{\alpha L}} \sim 5 \times 10^{5} \text{ cm}^{-3}. \tag{19.13}$$

This corresponds to the maximum number density of ions in the atmosphere. The number density of molecular ions of the lower layers of the atmosphere follows from the balance equation

$$w N_{\text{i}}/L \sim \alpha N_{\text{i}}^2.$$

This gives the number-density relation $N_{\text{i}} N_{\text{m}} \sim 10^{15}$ cm^{-6}, where N_{m} is the number density of molecular nitrogen.

A typical time for establishment of the equilibrium for molecular ions that leads to the estimate (19.13) is $\tau_{\text{rec}} \sim (\alpha N_e)^{-1} \sim 20$ s, whereas a characteristic ion drift time for these altitudes is $\tau_{\text{dr}} \sim 10^4$ s. Therefore, local equilibrium for molecular ions results from the competing ionization and recombination processes. Because of the short time for establishment of this equilibrium, the number density of charged particles for daytime and for nighttime is different. The above estimate refers to the daytime atmosphere. The ion number density of the nighttime atmosphere follows from the relation $\alpha N_{\text{i}} t \sim 1$, where t is the duration of the night. This gives the estimate $N_{\text{i}} \sim 10^2$–10^3 cm^{-3} for the nighttime atmosphere.

Atomic ions formed as a result of the photoionization process participate in ion–molecular reactions listed as processes 27 to 30 of Table 19.1. A

characteristic time for these processes is $\tau \sim (kN)^{-1} \sim 0.01$–$10$ s, and is small compared to a typical recombination time. This explains the fact that ions of the ionosphere are molecular ions. (See Fig. 19.1.) In addition, it shows the origin of molecular ions NO^+. These ions cannot result from photoionization because of the small number density of NO molecules.

Atomic ions found at high altitudes are there because of the short transport time required. We can estimate the maximum number density of oxygen atomic ions by comparing a typical drift time L/w and a characteristic time for ion–molecular reactions listed in Table 19.1, measured by $(k[N_2])^{-1}$. Assuming the basic component of the atmosphere at these altitudes to be atomic oxygen, we find that the maximum number density of atomic ions O^+ occurs at altitudes where $[N_2][O] \sim 3 \times 10^{19}$ cm^{-6}. This corresponds to altitudes of approximately 200 km. The maximum number density N_i of atomic ions follows from the balance equation

$$[O] \int \sigma_{ion}\, dI_{ion} \sim k[N_2]N_i.$$

For photoionization of atomic oxygen, we have $\int \sigma_{ion}\, dI_{ion} = 2 \times 10^{-7}$ s^{-1}, so that the maximum number density is

$$N_i \sim (2 \times 10^5 \text{ cm}^{-3})[O]/[N_2] \sim 10^6 \text{ cm}^{-3}. \tag{19.14}$$

In higher layers of the atmosphere the number density of atomic ions is determined by the barometric formula, because it is proportional to the number density of primary atoms, and declines with increasing altitude.

At altitudes where photoionization occurs, the negative charge of the atmospheric plasma comes from electrons. In the D-layer of the ionosphere, electrons attach to oxygen molecules in accordance with processes 20 to 22 of Table 19.1, and it is negative ions that govern the negative charge of the atmosphere. At the altitudes where this transition takes place, the balance equation $wN_e/L \sim KN_e[O_2]^2$ is appropriate, where $K \sim 10^{-31}$ cm^6/ s is the rate constant of processes 20 and 21 of Table 19.1. From this it follows that formation of negative ions occurs at altitudes where $N[O_2]^2 \sim 3 \times 10^{39}$ cm^{-9}, or $[O_2] \sim 10^{13}$ cm^{-3}. We account for the coefficient of ambipolar diffusion of ions being of the order of the diffusion coefficient of atoms. In the D-layer of the ionosphere, recombination proceeds according to the scheme $A^- + B^+ \rightarrow A + B$, and is characterized by a rate constant of about $\alpha \sim 10^{-9}$ cm^3/ s. This leads to the relation

$$N_i N_m \sim 10^{17} \text{ cm}^{-6} \tag{19.15}$$

for the number density of ions, N_i.

Thus the properties of the middle and upper atmosphere are established by processes in excited and dissociated air involving ions, excited atoms, and excited molecules.

CHAPTER 20

GAS-DISCHARGE PLASMAS

20.1 PROPERTIES OF GAS-DISCHARGE PLASMAS

The passage of an electric current through a gas as the result of an external electric field is called a gas discharge. In the region where the electric current flows, a gas-discharge plasma is formed. Its properties are dependent on both the external electric fields and the geometry of the gas discharge. The most commonly encountered types of gas discharges are glow and arc discharges that take place in a cylindrical tube subjected to a constant electric field. The distinctions between glow and arc discharges arise from the manner in which electrons are generated near the cathode. In a glow discharge, the emission of electrons from the cathode is caused by secondary electrons arising from ion bombardment of the cathode; while in an arc discharge, electrons are formed by thermoemission and auto-electron-emission processes on the cathode.

Figure 20.1 gives, in schematic form, the distribution of electric field strength in a glow discharge established in a cylindrical discharge tube. The main regions of the discharge are a cathode region (or cathode layer), where electrons are generated to compensate their removal on the anode; an anode region, where ions are formed; and the positive column, where a uniform plasma exists. If the length of the discharge tube is altered, the sizes of the cathode and anode regions are preserved, with the length variation confined to the positive column.

The plasma in the positive column has practical applications because of its uniformity. This type of plasma is used in light sources, in gas lasers, and for plasma-generated chemical processes. Properties of a positive-column plasma,

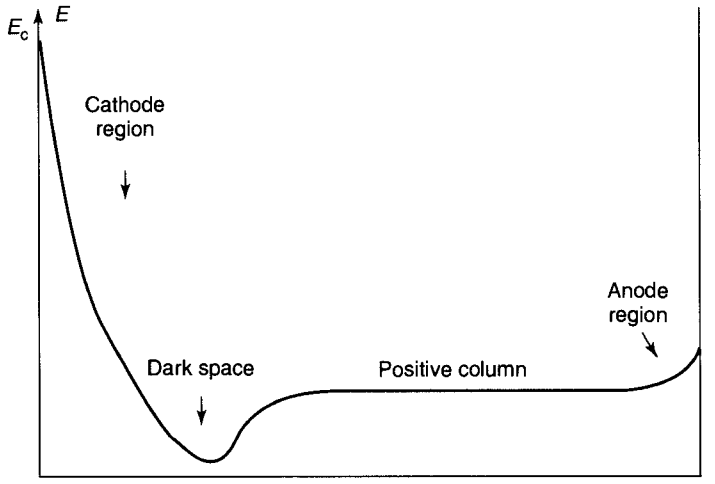

Figure 20.1 The spatial distribution of the electric field strength for a glow discharge in a tube.

including the distribution of charged and excited atomic particles, are determined by processes in which these particles play a central role, and will be considered below.

20.2 ELECTRONS IN THE POSITIVE COLUMN OF A GLOW DISCHARGE

The positive column contains a self-consistent plasma where an equilibrium is established between formation and decay of participating atomic particles. Under the simplest conditions, when the gas temperature is constant over the tube cross section, electron-number equilibrium in the positive column of a cylindrical discharge tube is sustained by the release of electrons formed as a result of electron impact, balanced by their removal through transport to the walls. These conditions are more or less fulfilled in the positive column of glow discharges where the electron number density lies approximately within the limits $N_e \sim 10^9$ to 10^{12} cm^{-3}, corresponding to a Debye-Hückel radius in the range $r_D \sim 1$ to 3 μm. We assume below that the mean free path for both electrons and atoms is small compared to the tube radius r_0. For $r_0 \sim 1$ cm, this requires a gas pressure $p \gg 10^{-5}$ atm at room temperature.

To determine the distribution of the electron number density over the cross section of a cylindrical discharge tube of radius r_0 under the above conditions, we balance the formation of charged particles arising from atomic ionization by electron impact against losses by transport to the walls of the discharge tube in the regime of ambipolar diffusion. The electron number

density satisfies the balance equation

$$D_a \Delta N_e + k_{ion} N_e N_a = 0, \tag{20.1}$$

where D_a is the ambipolar diffusion coefficient, N_a is the atom number density, and k_{ion} is the rate constant for atomic ionization by electron impact. Owing to the cylindrical symmetry, this equation reduces to

$$\frac{D_a}{\rho}\frac{d}{d\rho}\left(\rho\frac{dN_e}{d\rho}\right) + k_{ion} N_e N_a = 0. \tag{20.2}$$

Here ρ is the distance from the axis of the discharge tube. Using the boundary condition $N_e(r_0) = 0$ and taking the parameters D_a and k_{ion} to be independent of ρ, we find the electron number density

$$N_e(\rho) = N_0 J_0\left(\rho\sqrt{\frac{k_{ion} N_a}{D_a}}\right), \tag{20.3}$$

where N_0 is the number density of electrons at the axis and $J_0(x)$ is the Bessel function. The boundary condition $N_e(r_0) = 0$ yields

$$N_a k_{ion} r_0^2 / D_a = 5.78. \tag{20.4}$$

This is essentially the relation between the rate of electron formation ($\sim N_a k_{ion}$) and the rate of electron transport to the walls ($\sim D_a/r_0^2$). This condition allows one to write the expression (20.3) in the form

$$N_e(\rho) = N_0 J_0(2.405\rho/r_0). \tag{20.5}$$

The boundary condition is then automatically satisfied. A simple approximation for the Bessel function, valid to an accuracy of 8% has the form $J_0(2.405\rho/r_0) \approx 1 - (\rho/r_0)^{1.34}$. The regime in which Eq. (20.5) is valid is known as the *Schottky model*. This model corresponds to small discharge currents when the electron number density is relatively small. Then the balance equation (20.1) is linear with respect to N_e, and the gas temperature is constant over the cross section of the discharge tube. This leads to the simple expressions (20.3) and (20.5) for the electron number density.

The average lifetime τ_e of an electron in the plasma is given by

$$\tau_e = \frac{1}{2\pi r_0 j(r_0)} \int_0^{r_0} 2\pi\rho\, d\rho\, N_e(\rho),$$

where the integral is the average number of electrons per unit length of the discharge tube, and the denominator is the number of electrons that reach

the walls per unit time and per unit of tube length, with j the flux of electrons towards the walls. Because

$$j = -D_a \frac{dN_e(r_0)}{d\rho} = \frac{1.25 D_a N_0}{r_0},$$

$$\int_0^{r_0} 2\pi\rho \, d\rho \, N_e(\rho) = 1.36 N_0 r_0^2,$$

we have

$$\tau_e = \frac{1.36 N_0 r_0^2}{2\pi r_0 j} = \frac{0.173 r_0^2}{D_a} = \frac{1}{N_a k_{ion}}. \tag{20.6}$$

To understand the connection between $N_e(\rho)$ and the physical character of the processes in a plasma, we shall consider the case when the formation of electrons passes through a metastable state. Then, instead of the balance equation (20.2), we have the set of equations

$$\begin{aligned} 4D_a \frac{d}{dx}\left(x \frac{dN_e}{dx}\right) + k_{ion} N_e N_m r_0^2 &= 0, \\ 4D_m \frac{d}{dx}\left(x \frac{dN_m}{dx}\right) + k_{ex} N_e N_a r_0^2 &= 0, \end{aligned} \tag{20.7}$$

where $x = \rho^2/r_0^2$, N_m is the number density of metastable atoms, k_{ex} is the rate constant for excitation of the metastable state by electron impact, k_{ion} is the rate constant for ionization of a metastable atom by electron impact, and D_m is the diffusion coefficient of a metastable atom. The equation system (20.7) is accompanied by the boundary conditions $N_e(r_0) = N_m(r_0) = 0$. Let us take the number densities of electrons and metastable atoms in the approximate form

$$N_e = C_1(e^{-ax} - e^{-a}), \qquad N_m = C_2(e^{-bx} - e^{-b}).$$

The parameters of this equation can be found from the balance equations (20.7) for $x = 0$, and from these balance equations integrated over dx. To ascertain the accuracy of this procedure, let us apply it to Eq. (20.2). Then we obtain $a = 0.842$ and

$$\frac{N_a k_{ion} r_0^2}{D_a} = \frac{4a}{1 - e^{-a}} = 5.92.$$

[Compare this with Eq. (20.4).] The above procedure gives

$$\begin{aligned} a &= 1.410, \\ b &= 0.951, \\ N_a k_{ex} r_0^2 / D_m &= 1.550, \\ N_m(0) k_{ion} r_0^2 / D_a &= 1.865. \end{aligned} \tag{20.8}$$

The relations (20.8) reflect the fact that typical times for formation of electrons and metastable atoms are equal to typical times for their transport to the walls. In addition, solution of the equations gives

$$j_m = -D_m \frac{dN_m(r_0)}{d\rho} = \frac{1}{r_0} 1.2 D_m N_m(0),$$

$$j_e = -D_a \frac{dN_e(r_0)}{d\rho} = \frac{1}{r_0} 0.91 D_a N_e(0)$$

for the particle flux at the walls.

20.3 DOUBLE LAYER

We have seen that in a gas-discharge plasma where the mean free path of charged particles is small compared to the dimensions of the discharge, transport of charged particles to the walls in most of the positive column is governed by the ambipolar diffusion process. (See Chapter 11.) This means that an electric field arises in the plasma that decelerates electrons and accelerates ions. Electron and ion fluxes tend to equalize, and the plasma is almost quasineutral. This takes place up to distances from the walls of the order of the mean free path of charged particles.

We now examine the behavior of the plasma near the walls. Introducing the electron and ion temperatures T_e and T_i, the electron and ion fluxes to the walls, j_e and j_i, are

$$j_e = N_e \sqrt{\frac{T_e}{2\pi m_e}}, \qquad j_i = N_i \sqrt{\frac{T_i}{2\pi m_i}}, \tag{20.9}$$

where N_e and N_i are the electron and ion number densities near the wall, and m_e and m_i are the electron and ion masses. Because the fluxes of electrons and ions must be equal at the walls, Eq. (20.9) shows that the plasma can no longer be quasineutral near the walls. An electric field arises that slows the electrons. This phenomenon is known as the *plasma sheath*. The equality of the electron and ion fluxes gives the difference U of the

electric potentials of the plasma and walls [$N_e \sim \exp(-eU/T_e)$] as

$$eU = \frac{T_e}{2} \ln\left(\frac{T_e m_i}{T_i m_e}\right). \tag{20.10}$$

The transition region between the plasma and the walls is called the *double layer*. The appearance of a double layer is a widespread phenomenon observed on the boundary between a plasma and another state of matter.

20.4 THERMAL REGIME OF GAS DISCHARGES

The electric current of a gas discharge causes plasma heating that leads to a temperature increase along the axis of the discharge tube. We shall analyze this process for the positive column of a cylindrical discharge tube where the shape of the temperature distribution over the cross section remains constant along the tube. Assuming the heat transfer to be determined by thermal conductivity leads to the heat balance equation

$$\frac{1}{\rho}\frac{d}{d\rho}\left(\rho\kappa(T)\frac{dT}{d\rho}\right) + p(\rho) = 0 \tag{20.11}$$

in a cylindrical discharge tube, where κ is the thermal conductivity coefficient, E is the electric field strength, and $p(\rho) = iE$ is the specific power of heat release, meaning that i is the current density. Hence, this equation may be represented in the form

$$\frac{1}{\rho}\frac{d}{d\rho}\left(\rho\kappa(T)\frac{dT}{d\rho}\right) + \Sigma E^2 = 0, \tag{20.12}$$

where Σ is the plasma conductivity. Equation (20.12) is known as the *Elenbaas–Heller equation*. A simple solution of this equation that corresponds to the so-called parabolic model has the form $T = T_w + \Sigma E^2(r_0^2 - \rho^2)/(4\kappa)$. It is valid when both the plasma electrical and thermal conductivity are constant over the cross section of the discharge tube.

For a more precise determination of the temperature distribution, it is convenient to introduce the new variable $Z = \int_T^{T_0} \kappa(T)\,dT$, where T_0 is the temperature at the axis. Introducing the variable $x = \rho^2/r_0^2$, we have

$$\frac{d}{dx}\left(x\frac{dZ}{dx}\right) - \frac{pr_0^2}{4} = 0. \tag{20.13}$$

The solution of this equation allows one to determine the temperature difference between the axis and the walls. Taking the specific power of heat release to be proportional to the number density of electrons, we use it in the form $p = p_0(1\text{-}x^{0.67})$ that corresponds to the Schottky regime (20.5) of a low-current positive column. The discharge power per unit tube length is

$$P = -2\pi r_0 \kappa(T_w)\frac{dT(r_0)}{d\rho} = -4\pi\frac{dZ(x=1)}{dx}.$$

Thus, we have $x\,dZ/dx = p_0 r_0^2(x - x^{1.67}/1.67)/4$, and

$$Z = \int_{T_w}^{T_0}\kappa(T)\,dT = 0.13P.$$

This relation gives the difference between the temperatures of the axis and of the walls of the discharge tube for the distribution (20.5).

In a more general case of the electron distribution over the tube cross section, we can approximate the distribution of the specific heat release over the cross section by the expression $p = p_0[1 - (\rho/r_0)^n]$. Then the power of heat release per unit tube length is

$$P = 2\pi r_0\left(-\kappa\frac{dT(r_0)}{d\rho}\right) = 4\pi\frac{dZ(x=1)}{dx} = \pi p_0 r_0^2\frac{n}{n+2}.$$

If we define the function $g(n) = \int_{T_w}^{T_0}\kappa(T)\,dT/P$, then $g(n)$ lies within the limits $g(0) = 0.16$ and $g = 0.13$ for the distribution (20.5). Thus, with an accuracy of about 10%, we have

$$\int_{T_w}^{T_0}\kappa(T)\,dT = \frac{T_0\kappa(T_0) - T_w\kappa(T_w)}{1 + d\ln\kappa/d\ln T} = 0.14P. \qquad (20.14)$$

In particular, if the difference of the temperatures is small ($\Delta T = T_0 - T_w \ll T_0$), this relation yields

$$\Delta T = 0.14P/\kappa. \qquad (20.15)$$

Thus, heating of a gas in a tube with an electric current is not sensitive to the distribution of this current over the tube cross section, and is determined mostly by the total released power inside the tube.

20.5 POSITIVE COLUMN OF A GAS DISCHARGE AT HIGH PRESSURE

We shall now consider a commonly encountered regime of gas discharge in a cylindrical tube in which the gas pressure is of the order of one atmosphere and electric currents are large. Though, according to their definitions, glow

and arc discharges differ only by the nature of electron emission at the cathode, high gas temperatures cause this regime to be that of an arc discharge.

There are two special aspects of the discharge we are treating. First, thermodynamic equilibrium exists at each point in the plasma due to the large number density of electrons and atoms. This allows us to define both the gas temperature T and the electron temperature T_e. Second, thermal processes are of importance because of the high currents. Therefore the analysis of this regime is based on the heat balance equation (20.11) which now has the form

$$\frac{1}{\rho}\frac{d}{d\rho}\left(\rho\kappa(T)\frac{dT}{d\rho}\right)+\frac{1}{\rho}\frac{d}{d\rho}\left(\rho\kappa_e(T_e)\frac{dT_e}{d\rho}\right)+p(\rho)=0, \quad (20.16)$$

where $\kappa(T)$ is the thermal conductivity coefficient of the gas, $\kappa_e(T_e)$ is the electron thermal conductivity coefficient, and $p(\rho)=iE$ is the specific power of heat release. Along with heat transport due to thermal conductivity of the gas, we also account for electron conductivity in this equation.

Because thermodynamic equilibrium exists, the electron number density at each point is given by the Saha relation

$$\frac{N_e^2}{N_a}=\frac{g_e g_i}{g_a}\left(\frac{m_e T_e}{2\pi\hbar^2}\right)^{3/2}\exp\left(-\frac{J}{T_e}\right), \quad (20.17)$$

as in Eq. (2.17). Here g_e, g_i, and g_a are the statistical weights of the electron, ion and atom, respectively, and J is the atomic ionization potential. The difference between electron and gas temperature is given by Eq. (9.44),

$$T_e-T=\frac{M}{3}\left(\frac{eE}{m_e}\right)^2\frac{\langle v^2/\nu\rangle}{\langle v^2\nu\rangle}, \quad (20.18)$$

where T is the gas temperature, M is the mass of the atom, and the averaging indicated by the angle brackets is done on the basis of the Maxwell distribution function for electrons. In particular, in the case when the electron–atom collision frequency does not depend on electron velocities, Eq. (20.18) gives

$$T_e-T=\tfrac{1}{3}Mw^2. \quad (20.19)$$

The electron drift velocity is determined by Eq. (9.43) to be $w=(eE/3T_e)\langle v^2/\nu\rangle$, which in the limiting case $\nu=$ const takes the form $w=eE/(m_e\nu)$. These relations connect plasma parameters, and will be the basis for our analysis.

The validity condition for the regime being analyzed is that local ionization equilibrium exists, and has the form $\tau_{\text{rec}} \ll \tau_{\text{dr}}$, where a typical time for three-body electron–ion recombination is $\tau_{rec} = (KN_e^2)^{-1}$, and a typical time for charged particles to drift to the walls is $\tau_{\text{dr}} = r_0^2/(5.8D_a)$. [See Eq. (20.4).] The three-body electron–ion recombination coefficient is $K = K_0/T_e^{9/2}$ according to Eq. (5.16), K_0 has the value 2.0×10^{-8} cm^6 K$^{9/2}$/s, T_e is the electron temperature, r_0 is the tube radius, and the coefficient of ambipolar diffusion is given by Eq. (11.31) as $D_a = D_i(1 + T_e/T)$, where D_i is the ion diffusion coefficient. Thus the condition for the existence of local ionization equilibrium can be written in the form

$$\tau_{\text{dr}}/\tau_{\text{rec}} = r_0^2 N_a N_e^2 f(T, T_e) \gg 1. \tag{20.20}$$

The function $f(T, T_e)$ in Eq. (20.20) depends on the identity of the gas. This function, when expressed in units of 10^{-46} cm^7, has the value 30 for argon at $T = 2000$ K and $T_e = 6000$ K; it is 7.0 for $T = 3000$ K and $T_e = 8000$ K; and it is 2.3 for $T = 4000$ K and $T_e = 10{,}000$ K. As follows from Eq. (20.18), the regime being considered corresponds to large number densities of electrons and atoms. In addition to the condition in Eq. (20.20), the constraint

$$T_e \ll J. \tag{20.21}$$

must also be satisfied.

Since the electron number density is estimated from the Saha formula as $N_e \sim \exp[-J/(2T_e)]$, it follows from Eq. (20.21) that the plasma is concentrated in a region of the tube where the electron temperature is close to its value on the axis. Then it is convenient to introduce the new variable

$$y = \frac{[T_e(0) - T_e(\rho)]\, J}{2T_e^2(0)}. \tag{20.22}$$

Taking into account the strong dependence of the electron number density on the electron temperature, of the form $N(\rho) = N(0)e^{-y}$, one can neglect the temperature dependence of other parameters of the discharge as, for example, the thermal conductivity coefficient of the gas. Then $p(\rho) = p(0)e^{-y}$, $\kappa_e \sim N_e \sim e^{-y}$, and, introducing a new variable $x = \rho^2/r_0^2$, we have reduced Eq. (20.16) to the form

$$\frac{d}{dx}\left(x(e^{-y} + \zeta)\frac{dy}{dx}\right) - Ae^{-y} = 0. \tag{20.23}$$

The parameters ζ and A introduced in Eq. (20.23), given by

$$\zeta = \frac{T\kappa(T)}{\kappa_e(T_e)}\alpha, \qquad A = \frac{p_0 r_0^2 J}{8T_e^2\kappa_e(T_e)}, \tag{20.24}$$

govern the plasma distribution over the tube cross section; here $\alpha = dT(\rho)/dT_e(\rho)$. In particular, if the velocity dependence for the electron–atom collision frequency goes as $\nu \sim v^\beta$, we obtain

$$\alpha = \frac{1 + \beta - \beta T/T_e}{2T_e/T - 1}.$$

Only values of the parameters at the discharge-tube axis are included in the relations (20.24).

We consider first the case $\zeta \gg 1$, when heat transport is determined by the thermal conductivity of the gas. Then Eq. (20.23) has an analogy with the Fock equation in radio-frequency applications, and we use its solution

$$y = 2\ln\left(1 + \frac{Ax}{2\zeta}\right). \tag{20.25}$$

This solution leads to the distribution of the electron number density over the tube cross section given by

$$N_e(\rho) = N_e(0)e^{-y} = N_e(0)\left(1 + \frac{\rho^2}{\rho_0^2}\right)^{-2}, \qquad \rho_0^2 = \frac{16T_e^2 T\kappa(T)\alpha}{p_0 J}. \tag{20.26}$$

If the parameter ρ_0 that characterizes the size of the plasma region is small compared to the tube radius r_0, then contraction of the discharge current takes place. This deduction confirms that the discharge contraction in this case is determined by thermal processes in the plasma. These relations give the power of an arc discharge as

$$P = IE = \int p_0 e^{-y}\, 2\pi\rho\, d\rho = \frac{16T_e^2 T\kappa(T)\alpha}{J}. \tag{20.27}$$

Equation (20.27) establishes the connection between the discharge power and plasma parameters at the center of a discharge tube.

Consider the other limiting case $\zeta \ll 1$. In a region $y < \ln(1/\zeta)$, where the plasma is mostly concentrated, Eq. (20.16) transforms to

$$\frac{d}{dx}\left(x\frac{dY}{dx}\right) + AY = 0 \tag{20.28}$$

in terms of the new variable $Y = N_e(\rho)/N_e(0) = e^{-y}$. The solution of this equation is

$$Y = J_0(2\sqrt{Ax}). \tag{20.29}$$

From this we obtain

$$P = IE = \int p_0 Y\, 2\pi\rho\, d\rho = 1.36 p_0 \rho_0^2 \tag{20.30}$$

for the total discharge power, where

$$\rho_0^2 = \frac{5.78 r_0^2}{A} = \frac{12 T_e^2 \kappa_e(T_e)}{p_0 J}. \tag{20.31}$$

The total discharge power in this limiting case is thus

$$P = IE = \frac{16 T_e^2 \kappa_e(T_e)}{J}. \tag{20.32}$$

One can combine Eqs. (20.27) and (20.32). This leads to an expression for the discharge power that is valid for both limiting cases in ζ, and hence takes into account both the gas and the electron thermal conductivity:

$$P = IE = \frac{16 T_e^2 \kappa_e(T_e)(1 + 3.2\zeta)}{J}. \tag{20.33a}$$

In the same way, one can introduce the plasma radius in a general case. The plasma radius can be found from the expression

$$\int N_e\, 2\pi\rho\, d\rho = 1.36 N_0 \rho_0^2.$$

This relation corresponds to the discharge-tube radius in the Schottky case of small electric currents in a discharge tube. The discharge-tube radius within

the Schottky model for both limits in ζ gives the plasma radius

$$\rho_0^2 = \frac{12T_e^2\kappa_e(T_e)(1 + 3.2\zeta)}{p_0 J} \tag{20.33b}$$

in general.

Each of the above regimes of heat transport in an arc plasma gives rise to a scaling law for plasma parameters. In the case $\zeta \ll 1$, when the heat transport is determined by the thermal conductivity of the gas, we have

$$\begin{aligned} &\kappa_e \sim N^{-1}, \quad E \sim N, \quad p_0 \sim N^{3/2}, \quad \rho_0 \sim N^{-1}, \\ &P \sim N^{-1/2}, \quad I \sim N^{-3/2}, \quad \eta \approx \text{const}. \end{aligned} \tag{20.34a}$$

In the other limit, $\zeta \gg 1$, when heat transport is determined by the electron thermal conductivity, we obtain the scaling properties

$$\begin{aligned} &E \sim N, \quad p_0 \sim N^{3/2}, \quad \rho_0 \sim N^{-3/4}, \\ &P \approx \text{const}, \quad I \sim N^{-1}, \quad \eta \sim N^{1/2}. \end{aligned} \tag{20.34b}$$

As a consequence of the strong dependence of the electron number density on the electron temperature, we can reduce the problem of the distribution of plasma parameters over the tube cross section to the expression of this distribution in terms of plasma parameters on the axis of the discharge tube. An essential property of the plasma being analyzed is its tendency to contract to the tube center. This phenomenon was considered above (Chapter 18) as an ionization–thermal instability. The explanation for this property comes from the conflict between a weak temperature dependence of the rate of heat removal and a strong temperature dependence of the heat release. To compensate for the strong heat release, the plasma becomes compressed and increases heat removal by an increase of the temperature gradients. We have obtained the analytical expression (20.33b) for the plasma radius in this type of discharge, and also (20.33a) for the discharge power per unit length of a discharge tube. These expressions confirm the above conclusions.

To examine more closely the contraction of the arc discharge, it is convenient to introduce the variable

$$\begin{aligned} Z &= \int^{T_e} \kappa_e(T_e')\, dT_e' + \int^{T} \kappa(T')\, dT' \\ &= \frac{2T_e^2}{J}\kappa_e(T_e) + T\kappa(T)(1 + \gamma), \end{aligned} \tag{20.35a}$$

where T_e and T are the electron and gas temperatures at the axis, $\gamma = d \ln \kappa(T)/dT$, and we assume the electron and gas thermal conductivities at

the tube axis to be greatly in excess of those near the walls. Integrating Eq. (20.16) twice, we get

$$Z = \int_0^{r_0} p(\rho)\rho\, d\rho \ln\frac{r_0}{\rho} \approx \frac{P}{2\pi} \ln\frac{2.3r_0}{\rho_0}. \tag{20.35b}$$

Here P is the total power per unit length of the tube, and ρ_0 is the current radius. If we now use the expression (20.33a) for the specific discharge power and compare it with Eq. (20.35a), we can find the contraction of the positive column plasma. When $\zeta \ll 1$—that is, when the electron thermal conductivity is dominant—Eqs. (20.35a) and (20.32) give

$$Z = \frac{2T_e^2}{J}\kappa_e(T_e) = \frac{P}{8},$$

and the relation (20.35b) can be fulfilled only at $\rho_0 \approx r_0$. That is, there is no contraction of the current in this case. The reason for this is connected with the equivalent behavior of the electric current and the heat transport. In the case $\zeta \gg 1$, contraction of the arc current is possible, and the current radius ρ_0 follows from Eqs. (20.26), (20.27), and (20.35a). The current radius is determined by the equation

$$\left(1 + \frac{\rho_0^2}{r_0^2}\right)\ln\left(1 + \frac{r_0^2}{\rho_0^2}\right) = \frac{JT}{4T_e^2}\frac{\alpha}{1+\gamma}. \tag{20.36}$$

From this it follows that the contraction of the current occurs at small gas temperatures and currents when the gas thermal conductivity is not enough to remove the released heat; and the electron number density is small, so that the electron thermal conductivity is correspondingly small.

The analytical expressions for parameters of the discharge allow us to analyze explicit examples, as in the inert gases Ar, Kr, and Xe. Cross sections for elastic scattering of electrons on atoms of these gases are characterized by a deep minimum at energies of approximately 0.6 to 0.8 eV. This phenomenon is known as the *Ramsauer effect*. The minimum cross section is less than the cross section at zero electron energy by about two orders of magnitude. The Ramsauer effect leads to a specific instability. Equation (20.18) can be written in the form

$$T_e - T = E^2 F(T_e),$$

where E is the electric field strength and $F(T_e)$ has a strong maximum in the temperature region corresponding to the Ramsauer minimum. Hence $E(T_e)$ is a double-valued function; that is, two values of the electron temperature correspond to the same electric field strength. The analysis of this phenomenon is akin to that for thermal explosion (Chapter 14). The lower of the

two electron temperatures corresponds to an unstable state, so that this type of discharge in the inert gases Ar, Kr, and Xe exhibits a minimal electron temperature, with no discharge possible at lower temperatures. Next, because of the temperature dependence (20.33a) of the discharge power, this discharge in the inert gases Ar, Kr, and Xe can exist starting from a specific threshold power. Thus, particulars of the collisions between electrons and atoms establish the specific properties of the discharge.

20.6 POSITIVE COLUMN OF LOW-PRESSURE DISCHARGES

By definition, the plasma of a low-pressure gas discharge satisfies the inequalities

$$r_D \ll L \ll \lambda, \tag{20.37}$$

where L is a characteristic dimension of the discharge, λ is the mean free path for plasma particles, and r_D is the Debye–Hückel radius of the plasma. To show that such a discharge plasma can occur under realistic conditions, we give an example of typical parameters: electron number density $N_e \sim 10^{14}$ cm^{-3}, atom number density $N_a \sim 10^{15}$ cm^{-3}, electron temperature $T_e \sim 1$ eV, and size of the positive column $L = 0.1$ cm. It follows from these parameters that $\lambda \sim 1$ cm, and $r_D \sim 5 \times 10^{-5}$ cm, so that the criteria (20.37) are satisfied for this plasma. These are typical parameters for plasmas in thermoemission converters.

For simplicity, we consider such a plasma located between two infinite plane electrodes. Because of the high number density of charged particles, typical dimensions of the cathode and anode regions are small, and the positive column with its quasineutral plasma occupies almost all of the space between the electrodes. This plasma displays well-defined qualitative characteristics. First, electrons and ions of this plasma travel to the walls, and equilibrium in the positive column is established by ionization of atoms by electron impact. For this reason, the presence of a neutral component in the positive column is of importance. Second, the electron velocity is typically larger by about two orders of magnitude than that of the ions. Hence, a potential well is created in the positive column for conservation of the plasma quasineutrality, and electrons are trapped at least partially in this well. Taking this into account, we can evaluate currents of charged particles that are formed in the positive column and travel to the electrodes. We note that the energy balance of this discharge is determined by phenomena near the electrodes, and we set this matter aside for later consideration.

To examine the quasineutrality of the plasma, we introduce the electric potential $\varphi(x)$ of the plasma, where the x-axis is directed perpendicular to the electrodes, and the origin of the x-coordinate is taken to be centered between the electrodes. Symmetry gives the property $\varphi(x) = \varphi(-x)$, and the

charged-particle currents to both sides from the middle are the same. Hence we will evaluate only the current in the positive direction. Because the electrons are in thermodynamic equilibrium, their number density inside the positive column is

$$N_e = N_0 \exp(e\varphi/T_e).$$

Ions that are generated at a point ξ, reach a point x with a velocity $v_x = \sqrt{2e[\varphi(\xi) - \varphi(x)]/M}$. Introducing $g(\xi)$—the number of ions produced per unit volume at the point ξ—we obtain

$$N_i = \int_0^x \frac{g(\xi)\, d\xi}{\sqrt{2e[\varphi(\xi) - \varphi(x)]/M}}$$

for the ion number density at a point x. Ions collected at a point x are formed at points $0 < \xi < x$, because $x = 0$ corresponds to the top of the potential hump of the self-consistent plasma field for ions. Thus, the condition $N_e = N_i$ for quasineutrality of the plasma gives

$$N_0 \exp\left(\frac{e\varphi(x)}{T_e}\right) = \int_0^x \frac{g(\xi)\, d\xi}{\sqrt{2e[\varphi(x) - \varphi(\xi)]/M}}, \tag{20.38}$$

where N_0 is the electron number density at $x = 0$, and we define the self-consistent-field potential φ so that $\varphi(0) = 0$.

We introduce the reduced variables $\eta(x) = -e\varphi(x)/T_e$ and $j_0 = N_0\sqrt{2T_e/M}$. In terms of these variables, Eq. (20.38) takes the form

$$j_0 e^{-\eta} = \int_0^x \frac{g(\xi)\, d\xi}{\sqrt{\eta(x) - \eta(\xi)}} \tag{20.39}$$

for $\eta > 0$. From this equation, we can evaluate the flux of charged particles from the plasma. Towards this end, we multiply the equation by $(d\eta/dx)[\eta(y) - \eta(x)]^{-1/2}$ and integrate the result over x between ξ and y. Because of the relation

$$\int_0^x \frac{d\eta(x)}{dx}\, dx \frac{1}{\sqrt{[\eta(y) - \eta(x)][\eta(x) - \eta(\xi)]}}$$

$$= \int_{\eta(\xi)}^{\eta(y)} \frac{d\eta}{\sqrt{[\eta(y) - \eta][\eta - \eta(\xi)]}} = \pi,$$

the right-hand side of the equation is

$$\int_0^{\eta(y)} \frac{d\eta(x)}{\sqrt{\eta(y)-\eta(x)}} \int_0^{\eta(x)} \frac{g(\xi)d\eta(\xi)}{\sqrt{\eta(x)-\eta(\xi)}} \frac{d\xi}{d\eta(\xi)}$$

$$= \int_0^{\eta(y)} g(\xi)\, d\eta(\xi) \frac{d\xi}{d\eta(\xi)} \int_{\eta(\xi)}^{\eta(y)} \frac{d\eta(x)}{\sqrt{[\eta(y)-\eta(x)][\eta(x)-\eta(\xi)]}}$$

$$= \pi \int_0^y g(\xi)\, d\xi.$$

Finally, we obtain

$$j(y) = \int_0^y g(\xi)\, d\xi = \frac{j_0}{\pi} \int_0^{\eta(y)} \exp(-\eta) \frac{d\eta}{\sqrt{\eta(y)-\eta}} \tag{20.40}$$

for the ion flux $j(y)$ to the electrode at a given point y.

The flux $j(y)$ of charged particles towards the electrodes increases steadily with increasing distance from the midpoint $x = 0$. As a function of the potential of a self-consistent field, it reaches a maximum at the electrode where the quasineutral property of the plasma is lost. Therefore, the condition $dj/d\eta = 0$ at the electrode corresponds to the condition $d\eta/dx = \infty$, because $dj/d\eta = (dj/dx)/(d\eta/dx)$. Denote $\eta = \eta_0$ at the electrode and find this value. Represent $j(\eta)$ in the form

$$j(\eta) = \frac{j_0}{\pi} \int_0^{\eta} \exp(-\eta') \frac{d\eta'}{\sqrt{\eta-\eta'}}$$

$$= \frac{2j_0}{\pi}\sqrt{\eta} + \frac{2j_0}{\pi} \int_0^{\eta} \exp(-\eta')\sqrt{\eta-\eta'}\, d\eta',$$

so that the condition $dj/d\eta = 0$ at the electrode leads to the equation

$$\sqrt{\eta_0} \int_0^{\eta_0} \exp(-\eta) \frac{d\eta}{\sqrt{\eta_0-\eta}} = 1.$$

The solution of this equation is $\eta_0 = 0.855$. It gives the flux of charged particles towards the electrode as

$$j = \frac{j_0}{\pi\sqrt{\eta_0}} = 0.344 j_0 = 0.344 N_0 \sqrt{\frac{2T_e}{M}}. \tag{20.41}$$

From this one can find the depth of the potential well of the self-consistent field for electrons in the positive column. Taking the Maxwell velocity distribution function for the electrons, we obtain

$$f(v_x) = N_0\sqrt{\frac{m_e}{2\pi T_e}}\,\exp\left(-\frac{m_e v_x^2}{2T_e}\right).$$

The electron flux toward the electrode is

$$j = \int_{v_0}^{\infty} v_x f(v_x)\,dv_x = 0.344 N_0\sqrt{\frac{2T_e}{M}},$$

where $m_e v_0^2/2 = e\,\Delta\varphi$, so that $e\,\Delta\varphi$ is the depth of the potential well. From this we obtain

$$e\,\Delta\varphi = \frac{T_e}{2}\ln\frac{2.7M}{m_e}. \tag{20.42}$$

The above relations follow from the balance of charged particles that are formed in the region of the discharge and subsequently leave this region. This balance equation written in an alternative form allows us to determine the electron temperature. This form is

$$N_0 k_{\text{ion}}(T_e) N_a \int_0^{x_0} e^{-\eta}\,dx = 0.344 N_0\sqrt{\frac{2T_e}{M}}, \tag{20.43}$$

where k_{ion} is the rate constant for atomic ionization by electron impact, and N_a is the number density of atoms. This relation shows that the electron temperature does not depend on the number density of electrons in the trap. Rather, it is determined by the identity of the gas and by the parameter $N_a L$.

We wish to find the domain of validity of the above results. The condition for plasma quasineutrality, as it follows from the Poisson equation, has the form

$$|N_i - N_e| = \left|\frac{1}{4\pi e}\frac{d^2\varphi}{dx^2}\right| \ll N_0, \qquad \text{or} \qquad \frac{d^2\eta}{dx^2} \ll \frac{1}{r_D^2}.$$

Because the value of η varies by about unity in the region of the positive column, Eq. (20.37) shows that the above condition corresponds to $r_D \ll L$. The second condition in Eq. (20.37), $L \ll \lambda$, amounts to the assumption that once an ion has been formed it moves in the discharge region without collisions. The requirement of thermodynamic equilibrium among atoms corresponds to the condition (9.47), and is usually well fulfilled because of

the small number density of atoms in the discharge plasma. The additional requirement of thermodynamic equilibrium among electrons requires that each electron must collide with other electrons many times before leaving the discharge region. That is, the total distance an electron travels in this plasma is far greater than the mean free path λ_e for collisions with other electrons. This leads to the estimate

$$\lambda_e \ll \sqrt{\frac{M}{m_e}}\, L,$$

to be added to the conditions in Eq. (20.37).

Thus the positive column of a low-pressure arc discharge contains a special type of low-density plasma that includes both charged particles (electrons and ions) and neutral atoms. A self-consistent field of this positive column plasma is such that it creates a potential well that nearly traps electrons, while simultaneously being nearly transparent for positive ions. As a result, collisions between trapped electrons establish thermodynamic equilibrium for electrons in the positive column, and ionization collisions of electrons with atoms determine the electron temperature of this plasma.

20.7 IGNITION CONDITIONS FOR LOW-CURRENT DISCHARGES

We shall now investigate the formation and loss of electrons near the cathode of a glow discharge, when electrons are generated at the cathode as a result of positive-ion impact. This occurs in low-current discharges when heating of the cathode by the discharge current is small. Secondary electrons formed on the cathode by ion impact obtain enough energy from the electric field in the cathode region to ionize atoms of a gas. This leads to reproduction of the ions lost in the impact process, and hence the maintenance of the plasma in the cathode region. The balance equation for the electron number density in the cathode region is

$$\frac{dN_e}{dt} = \alpha N_e, \tag{20.44}$$

where $\alpha(E) = N_a\langle v\sigma_{\text{ion}}\rangle / w_e$ is called the *first Townsend coefficient*, N_a is the number density of atoms, σ_{ion} is the cross section for ionization of the atom by electron impact, and w_e is the electron drift velocity. The solution of this equation is $N_e = N_0 \exp(\int \alpha\, dx)$, where N_0 is the electron number density near the cathode, the integral is taken over the cathode region, and the x-axis is perpendicular to the cathode.

The *second Townsend coefficient* γ is now introduced as the probability for generation of an electron as a result of ion impact with the cathode. The

TABLE 20.1. The Second Townsend Coefficient for a Tungsten Cathode

	γ	
Ion	$E_i = 1$ eV	$E_i = 10$ eV
He^+	0.30	0.27
Ne^+	0.21	0.25
Ar^+	0.095	0.11
Kr^+	0.048	0.06
Xe^+	0.019	0.019

value of γ is specific to the identity of the gas and its ion, but also depends weakly on the ion energy. As a demonstration of this, Table 20.1 contains values of the second Townsend coefficient for a tungsten cathode and inert-gas ions at two collision energies.

The condition to have a self-maintained gas discharge in the gap between two plates, where the electric field and hence the first Townsend coefficient α are spatially uniform, can be found readily. If the distance between plates is L, then $e^{\alpha L} - 1$ electrons are formed in the gap from one primary electron. Because each ion colliding with the cathode releases an average of γ electrons, the condition to have a self-maintained gas discharge is $\gamma(e^{\alpha L} - 1) = 1$, or equivalently,

$$\alpha L = \ln(1 + 1/\gamma). \tag{20.45}$$

The functional dependence of the first Townsend coefficient on the electric field strength E and the number density N_a of gas atoms has the form $\alpha = N_a F(eE/N_a)$, where the function $F(x)$ depends on the identity of the gas. Because the atomic ionization potential exceeds the mean electron energy, the ionization rate constant is determined by the tail of the electron distribution function. Hence one can assume that the ionization rate constant is proportional to the electron distribution function at an electron energy close to the atomic ionization potential. Then, according to Eqs. (9.58) and (9.59), the principal dependence on the electric field strength is $F(x) \sim \exp(-C/x)$, where the constant C depends on the type of gas. Thus the first Townsend coefficient can be approximated by the formula

$$\alpha = AN_a \exp(-BN_a/E). \tag{20.46}$$

Table 20.2 gives values of the parameters entering into this formula in a region of reduced electric field strengths.

Using the approximation (20.46) for the first Townsend coefficient and assuming the electric field strength in the gap to be constant, Eq. (20.45) for

TABLE 20.2. Parameters for Ionization in the Cathode Region[a]

Gas	A 10^{-16} cm^2	B Td	Region of E/N_a Td	$(N_aL)_{min}$ 10^{-16} cm^2	U_c V	E_c/N_a Td
He	0.85	96	60–420	5.4	49	140
Ne	1.1	280	280–1100	5.0	130	390
Ar	4.0	510	280–1700	1.8	86	720
Kr	4.8	680	280–2800	2.0	130	980
Xe	7.3	990	280–2300	1.7	160	1400

[a] 1 townsend = 1 Td = 10^{-17} V cm^2.

maintenance of the electric current in the gap gives the expression

$$U_c = \frac{B(N_aL)}{\ln[A/\ln(1 + 1/\gamma)] + \ln(N_aL)} \tag{20.47}$$

for the gap voltage $U_c = EL$. This function has a minimum at

$$(N_aL)_{min} = \frac{e}{A}\ln\left(1 + \frac{1}{\gamma}\right), \tag{20.48}$$

which gives

$$U_{min} = B(N_aL)_{min} = \frac{eB}{A}\ln\left(1 + \frac{1}{\gamma}\right). \tag{20.49}$$

This result affects the electric-field-strength distribution in the cathode region. If the distance between electrodes of a gas discharge is much larger than the size L that corresponds to the minimum of U_c, then the cathode region, where electrons are generated, is separated from the other regions. When this is true, the maximum electric field strength occurs solely in the cathode region. Figure 20.1 shows a schematic distribution of the electric field strength along a cylindrical discharge tube. The region where electrons are formed—the cathode region—is separated from the positive column where the formed plasma is maintained. The cathode region is responsible for formation of electrons. Any variation of the tube length leads to a variation only of the length of the positive column, and the size of the cathode region is unaltered.

20.8 BREAKDOWN OF GASES

An electric potential that can support an electric current in a gas-filled gap and has an analytical form of the type

$$U_c = f(N_aL), \tag{20.50}$$

exemplified by Eq. (20.47), is called a *Paschen's-law* potential. The function in Eq. (20.50) can possess a minimum, and Fig. 20.2 gives an example of this

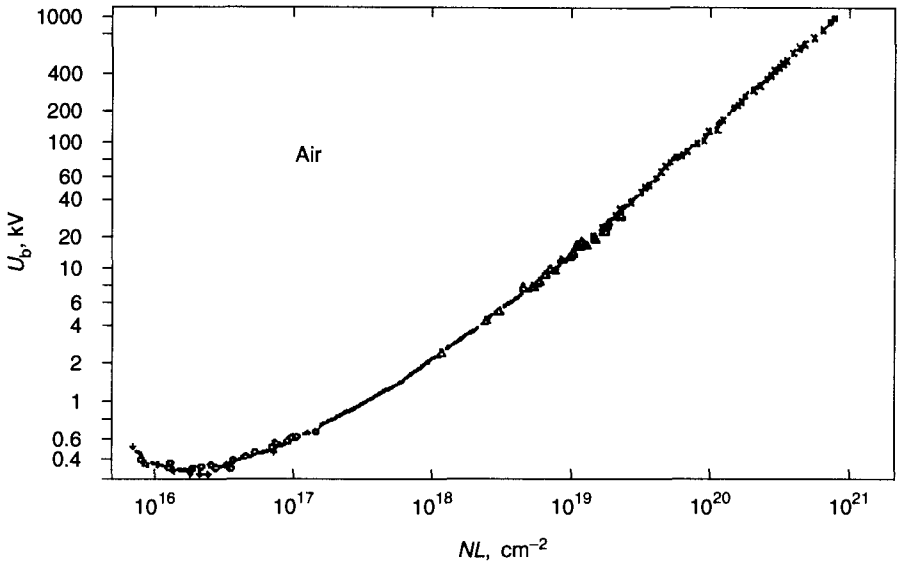

Figure 20.2 The air breakdown electric field in a gap between two parallel electrodes a distance L apart versus NL for air (Paschen's curve), where N is the number density of molecules.

behavior for air. When an electric current is established, the distribution of charged particles in a gap becomes nonuniform. This happens if the number density of electrons and ions is not so small that the Debye–Hückel radius of the plasma is significantly less than the gap size L. Then the cathode layer is separated from other regions of the discharge in the gap, and its size is determined by Eq. (20.48). The remainder of the gap contains the positive column and anode region of the discharge. The electric field in these regions is lower than in the cathode region.

If the electric field is less than that given by Eq. (20.47), then an electric current will not occur in the gap. The potential (20.47) is called the *breakdown potential.* If electron capture to form negative ions takes place, this will change the equation for the breakdown potential. For example, in the case of air, attachment of electrons to the dissociated oxygen molecule ($e + O_2 \rightarrow O^- + O$) occurs, and Eq. (20.45) then takes the form

$$(\alpha - \eta)L = \ln(1 + 1/\gamma). \tag{20.51}$$

Here, η is the rate constant for electron attachment, defined as the average number of electron attachments per unit length of the electron trajectory. In the limit of large values of the product NL (where N is the number density of molecules) this relation takes the form

$$\alpha(E/N) = \eta(E/N), \tag{20.52}$$

which connects the breakdown electric field strength and the number density. For air, this connection is $E/N \approx 90$ Td, corresponding to an electric field of 25 kV/cm at atmospheric pressure.

Gas breakdown starts from an incidental electron that creates new charged particles when accelerated by the electric field. If breakdown occurs in a uniform electric field, a propagating ionization wave in the first stage of breakdown does not disrupt the uniformity of the electric field. A different form of gas breakdown takes place in the case of a needle-shaped electrode that creates a nonuniform electric field. Then the ionization wave propagates in the form of a streamer (see Fig. 20.3). The charge distribution in the streamer strengthens the electric field near its head. Ionization processes are accompanied by excitations of atoms or molecules. Photons generated by radiation from excited particles are absorbed in neighboring regions, and that absorption of photons can lead to ionization and the creation of free electrons. The intensity of this ionization process is weak, but the appearance of free electrons in the region of a heightened electric field leads to their rapid reproduction. In this way, the head of the streamer propagates to a new position following the direction of the electric field. The generation of electron avalanches before the streamer due to photoprocesses and a heightened electric field increases the velocity of this ionization wave, which is of the order of 10^8–10^9 cm/s. The breakdown electric field strength for the streamer mechanism is less than that for a uniform electric field. For example, it is about 5 kV/cm for air at atmospheric pressure, which is about a factor of 5 less than for a uniform electric field. Therefore, if the possibility for streamer formation exists, breakdown proceeds by this mechanism. In particular, lightning in the Earth's atmosphere starts in regions with nonuniform field.

20.9 CATHODE REGION OF A GLOW DISCHARGE

To analyze the spatial distribution of ions and electrons in the cathode region, we start with the Poisson equation

$$\frac{dE}{dx} = 4\pi e(N_i - N_e)$$

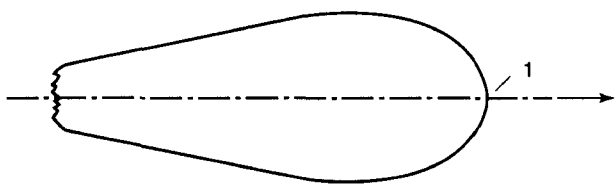

Figure 20.3 A region of space occupied by the plasma in the streamer mechanism for propagation of the ionization wave: 1, the streamer head, where the arrow shows the direction of a streamer motion.

for the electric field strength, where N_i and N_e are the number densities of ions and electrons. Assuming the mean free path of ions and electrons to be small compared to the size L of the cathode region, we use the expressions $i_i = eK_iN_iE$ and $i_e = -eK_eN_eE$ for the current densities of ions and electrons, where K_i and K_e are respective mobilities of the ions and electrons, and for simplicity we assume that the electric field strength is small. Because in the cathode region $i_i \sim i_e$ and $K_e \gg K_i$, then we have $N_e \ll N_i$ in this region. The Poisson equation then becomes $dE/dx = 4\pi eN_i = -4\pi i_i/(K_iE)$. The sign for the electric field is chosen such that the electric field hinders the approach of ions to the cathode.

The total electric current density $i = i_i + i_e$ is conserved in the cathode region, because charge does not accumulate there. The boundary condition at the cathode has the form $i_e(0) = \gamma i_i(0)$, or $i_i(0) = i/(1 + \gamma)$, where γ is the second Townsend coefficient. Since ions are formed outside the cathode region, this relation $i_i = i/(1 + \gamma)$ is valid in the entire cathode region. Then the solution of Poisson's equation is

$$E^2 = E_c^2 - \frac{8\pi i}{K_iE(1 + \gamma)}x, \tag{20.53}$$

where x is the distance from the cathode, and $E_c = E(0)$. Taking the electric field strength to be zero on the boundary of the cathode region (L is small compared to the tube radius), we obtain

$$i = E_c^2K_i(1 + \gamma)/(8\pi L). \tag{20.54}$$

To study the consequences of this result, we observe that the cathode region size L and voltage U_c are both determined by the condition that the cathode voltage should be a minimum. Hence, Eq. (20.54) shows that the current density is constant, so that it does not depend on the total discharge current I. This means that an alteration of the discharge current leads to a change of the cathode area occupied by the current. This area is I/i, and as long as it is smaller than the cathode area πr_0^2 (r_0 is the cathode radius), such a regime can be realized. This regime is known as the *normal* glow discharge. When the discharge electric current exceeds the value $i\pi r_0^2$, the glow discharge becomes *abnormal.* Then the cathode region voltage exceeds that given by Eq. (20.50), and increases with an increase of the discharge current. (See Fig. 20.4.)

We can determine the value of the cathode voltage on the basis of Eq. (20.53) for the electric field strength $E = E_c\sqrt{1 - x/L}$ in the cathode region. The condition $\int \alpha\, dx = \ln(1 + 1/\gamma)$ replaces Eq. (20.45). Using Eq. (20.46) for the first Townsend coefficient, the preceding condition gives

$$Ay\int_0^1 \exp\left(-\frac{b}{z^{1/2}}\right) dz = \ln\left(1 + \frac{1}{\gamma}\right), \tag{20.55}$$

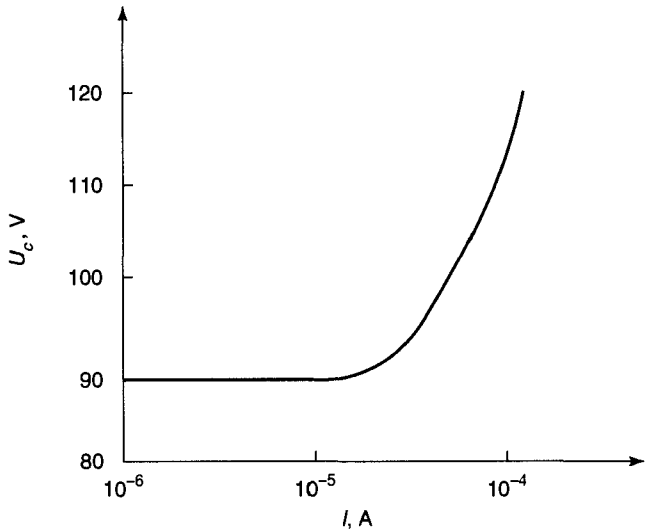

Figure 20.4 The cathode electric voltage as a function of current for argon at the pressure $p = 1$ Torr, where the second Townsend coefficient is $\gamma = 0.1$, and the tube radius is 1 cm.

where $y = N_a L$, $z = \sqrt{1 - x/L}$, and $b = BN_a/E_c$. Because the cathode voltage is $U_c = 2E_c L/3$, we obtain $b = 2BN_a L/(3U_c)$. The condition that the cathode voltage is a minimum is $dU_c/dy = 0$, which gives $db/dy = b/y$. Then from the expression (20.46) for the first Townsend coefficient, the condition for the cathode voltage to be a minimum is

$$J(b) + b\,dJ(b)/db = 0,$$

where $J(b) = \int_0^\infty \exp(-b/z^{1/2})\,dz$. The solution of the above equation yields $b = 0.71$, and we then obtain

$$(N_a L)_{\min} = \frac{3.05}{A} \ln\left(1 + \frac{1}{\gamma}\right), \tag{20.56a}$$

$$U_{\min} = 0.94B(N_a L)_{\min} = 2.87\frac{B}{A} \ln\left(1 + \frac{1}{\gamma}\right). \tag{20.56b}$$

It can be seen that these relations are similar to Eqs. (20.48) and (20.49), which follow from the assumption of a constant electric field strength in the cathode region. Table 20.2 exhibits cathode-region parameters calculated on the basis of Eqs. (20.56). Table 20.3 lists values for the cathode voltage drop for a few gases and cathode materials used in glow discharges.

As the discharge current increases, the cathode voltage drop also increases, until heating of the cathode becomes sufficient for thermoemission

TABLE 20.3. The Normal Cathode Drop U_c of Glow Discharges for Some Gases and Cathode Materials[a]

Gas	U_c (V) for Cathode Material					
	Al	Ag	Cu	Fe	Pt	Zn
He	140	162	177	150	165	143
Ar	100	130	130	165	131	119
H_2	170	216	214	250	276	184
N_2	180	233	208	215	216	216
Air	229	280	370	269	277	277

[a] Cobine (1958).

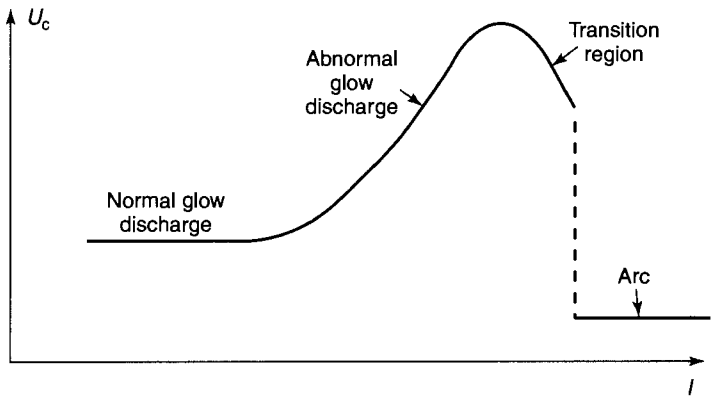

Figure 20.5 A typical form of the dependence of the cathode voltage drop on the discharge electric current I.

of electrons (see Fig. 20.5). Then the cathode voltage drop falls, and the transition from a glow discharge to an arc takes place. The voltage drop of the cathode in an arc is about 20 to 30 V, which is far less than that in glow discharges. The energy that electrons obtain from the field in the cathode layer is sufficient for atomic ionization. The current in the arc cathode layer may be either uniform or in the form of cathode spots.

There is another aspect of this problem. After initiation of a gas discharge, the voltage between the electrodes falls because of plasma formation near the cathode. If there are mechanisms in the system that can quench this plasma, vibrations of the gas discharge may occur. The mechanism for this is that generation of a plasma as a result of ionization of gas atoms causes a drop of the discharge voltage, while the decay of this plasma leads to an increase of the voltage. Such behavior in corona discharges is known as *Trichel pulses*. The leading edge of such a pulse is steep and is determined by times characterizing electron motion, while the trailing edge of the pulse is long, and its time is reflective of times for ion motion. Most commonly, a

time typifying the leading edge of a Trichel pulse is of the order of 1–10 ns at atmospheric pressure, and the total pulse time is greater than this value by several orders of magnitude, depending on the corona geometry and the identity of the gas. Although such vibrations can be observed in a glow discharge, the low stability of a corona discharge causes this vibrational behavior to be encountered frequently.

20.10 CONTRACTION OF THE POSITIVE COLUMN OF A GLOW DISCHARGE

Contraction of a gas discharge means that the electric current occupies only part of the available volume of a discharge tube near its axis. In Chapter 18 and in preceding sections of this chapter, we considered contractions of arc discharges that occur as a result of a strong temperature dependence of the rate of heat release and a weak temperature dependence of heat transport. Now we shall concentrate on mechanisms that lead to contraction of glow discharges.

First we consider the contraction of a glow discharge carrying a small electric current. When analyzing the plasma of a positive column in this case, we assumed the rate constant of atomic ionization in Eq. (20.2) to be constant over the cross section of the discharge tube. This is not actually true in practice. Since the gas is heated by the electric current, the gas temperature near the axis is higher than that near the walls. Equation (20.14) allows one to determine this temperature difference if heat transfer is due to thermal conductivity. Since the gas pressure is constant over the discharge volume, the number density of atoms near the axis is lower than that near the walls. Equation (20.17) predicts a strong dependence of the ionization rate on the atomic number density. Even slight heating of a gas can lead to a situation where ionization takes place near the axis of the discharge tube.

However, this does not lead to contraction of the discharge. Equation (20.2) gives the distribution of the electron number density when electrons occupy the entire cross section of the discharge tube with some functional form $k_{\text{ion}}(\rho)$. Each electron formed at the axis moves to the walls, where it is lost. Therefore, electrons will occupy the entire cross section of the tube.

For contraction of the discharge to occur, production of electrons at the center of the discharge tube must be accompanied by spatial loss of electrons. An example of this behavior occurs when molecular ions are formed in a plasma and pair (dissociative) recombination of electrons and molecular ions occurs. Because of the quasineutrality of the plasma, the balance equation (20.2) takes the form

$$\frac{D_a}{\rho}\frac{d}{d\rho}\left(\rho\frac{dN_e}{d\rho}\right) + k_{\text{ion}}(\rho)N_eN_a - \alpha N_e^2 = 0,$$

where α is the recombination coefficient of electrons and ions. This equation allows us to estimate the size of the region ρ_0 that is occupied by the electric current. Assume that a typical size of the region where the ionization takes place is small compared to ρ_0, and that, in turn, ρ_0 is small compared to the tube radius r_0. Then the radius ρ_0 follows from the relation that the recombination time $\nu_{\text{rec}} \sim 1/(\alpha N_0)$ is of the order of the time for electron transport through a region of size ρ_0, given by $\tau \sim \rho_0^2/D_a$ (where N_0 is a typical electron number density in this region or the number density in the center). This leads to the estimate

$$\rho_0 \sim \sqrt{D/(\alpha N_0)} \ll r_0 \tag{20.57}$$

for the size of a region occupied by the electric current. In a discharge contraction at small currents, a variety of mechanisms exhibiting this phenomenon are possible, especially if the formation of negative ions from electrons is possible in the discharge plasma. Ionization in this case takes place in a narrow region near the tube center, and the loss of electrons occurs inside the plasma.

20.11 PLASMA HARDENING

During the formation of a gas-discharge plasma, the transient processes that occur before equilibrium is attained can have practical applications. One such application is a plasma-chemistry phenomenon—*hardening*—that makes use of nonequilibrium products resulting from plasma cooling. An example of this process is the formation of ozone from rapid cooling of dissociated oxygen. Ozone is a metastable oxygen compound, so that the formation of ozone from oxygen atoms leads to the release of energy. But this process does not occur as a result of collision of two ozone molecules. Therefore, at the final stage of cooling of dissociated oxygen, when oxygen atoms are transformed into molecules of oxygen and ozone, the mixture thus formed is stable.

Ozone can be produced from partially dissociated oxygen or air by the reactions

$$O + 2O_2 \leftrightarrow O_3 + O_2, \tag{20.58a}$$

$$O + O_2 + N_2 \leftrightarrow O_3 + N_2, \tag{20.58b}$$

$$O + O_3 \leftrightarrow 2O_2. \tag{20.58c}$$

We assume the degree of oxygen dissociation in the initial state to be small. This allows us to neglect those recombination processes that require the participation of two oxygen atoms. The cooling rate dT/dt is an important parameter in these reactions.

The hardening phenomenon is associated with a unequilibrium due to rapid cooling. At high temperatures the equilibrium among O, O_2, and O_3 is supported by the processes shown in (20.58), but starting from a typical temperature T_0, the equilibrium between atomic and molecular oxygen is violated. We introduce the equilibrium constants

$$\frac{[O]^2}{[O_2]} = K_1(T) = C_1(T)\exp\left(-\frac{D_1}{T}\right), \tag{20.59a}$$

$$\frac{[O][O_2]}{[O_3]} = K_2(T) = C_2(T)\exp\left(-\frac{D_2}{T}\right), \tag{20.59b}$$

where [X] means the number density of particle X; $K_1(T)$ and $K_2(T)$ are equilibrium constants, so that $C_1(T)$ and $C_2(T)$ are weak functions of T; $D_1 = 5.12$ eV is the dissociation energy of oxygen molecules O_2; and $D_2 = 1.05$ eV is the dissociation energy of ozone molecules O_3. Taking into account the detailed balance principle relating rate constants of the processes, the balance equation for ozone molecules is

$$\frac{d[O_3]}{dt} = -k[O_3][O] + K_a[O_2]^2[O], \tag{20.60}$$

where K_a and k are the rate constants for the processes (20.58a) and (20.58c), respectively. We assume that equilibrium between atomic oxygen and ozone is possible at temperatures of the order of T_0. Then this equation is

$$\frac{d[O_3]}{dt} = -\frac{k[O_3]^2 K_2}{[O_2]} + K_a K_2 [O_2][O_3].$$

At temperatures below T_0, one can neglect the second term on the right-hand side of this equation. Then the ozone number density $[O_3]$ at the end of the process is given by the relation

$$\frac{1}{[O_3]} - \frac{1}{N_0} = \frac{k(T_0)K_2(T_0)}{[O_2]}\frac{T_0^2}{D_2\, dT/dt},$$

where N_0 is the number density of ozone molecules at the temperature T_0, and we assume a weak temperature dependence for $k(T)$. In these estimates we use the magnitude of the cooling rate dT/dt.

From this we find a typical ozone number density at the end of the process to be

$$[O_3] \sim \frac{[O]_{eq}[O_2]_{eq}}{K_2(T_0)} \sim \frac{[O_2]D_2}{k(T_0)K_2(T_0)T_0^2}\frac{dT}{dt}, \tag{20.61}$$

where $[X]_{eq}$ means the equilibrium number density at this temperature. However, typical temperatures T_0 are such that equilibrium does not occur. Then the left-hand side of Eq. (20.60) is of the order of the second term of the right-hand side. This gives the equation

$$k[O]_{eq} \sim \frac{D_2}{T_0^2}\frac{dT}{dt} \tag{20.62}$$

for T_0, where $[O]_{eq} \sim \sqrt{K_1[O_2]}$ is the equilibrium number density of atomic oxygen. Because of Eq. (20.61) for the transition temperature T_0, this temperature is connected with the rate of cooling dT/dt by the relation

$$\frac{dT}{dt} \sim C\exp\left(-\frac{D_1}{2T_0}\right),$$

where C depends weakly on the temperature, and the final ozone number density depends on the cooling rate as

$$[O_3] \sim \left(\frac{dT}{dt}\right)^{1-2D_2/D_1} \approx \left(\frac{dT}{dt}\right)^{0.6}. \tag{20.63}$$

Some useful estimates can be made from the above formulas. From Eq. (20.62) it follows that T_0 lies in the interval 1700–2000 K for a cooling rate 10^4–10^5 K/s. The number density at the end of the process is thus $[O_3] \sim 10^{10}$ cm^{-3}. The first conclusion that can be reached is that the final amount of product is determined by the quantity at temperatures where there is thermodynamic unequilibrium between plasma components. Second, the mechanism considered gives a small contribution compared to ozone formation from electrical phenomena in the Earth's atmosphere. The analog in the atmosphere to the process we are considering is expansion of a lightning channel after passage of an electric current through it. Such a process has low efficiency compared to oxygen dissociation resulting from weak electric currents in the atmosphere. In the latter case, the efficiency of oxygen dissociation is relatively high, and each released oxygen atom combines with an oxygen molecule to create an ozone molecule.

CHAPTER 21

PLASMA INTERACTIONS WITH SURFACES

21.1 CATHODE SPUTTERING AND ITS USES

A positive column containing a uniform ionized gas, such as is found in glow and arc discharges (including gas lasers), can be used as a light source. The excited atoms or molecules in the positive column produce radiation that determines the properties of the light emitted. In other cases the radiation can arise from collisions of plasma particles. For example, photons emitted by arc light sources come from photorecombination collisions between electrons and positive ions. In all these cases, plasma uniformity is of importance to provide optimal conditions for the production of light in as much as possible of the plasma volume. That is, it is advantageous to generate a positive column in a discharge where the plasma is almost uniform, and where the positive column occupies a large proportion of the total discharge volume. Another class of plasma applications uses the fact that collisions of plasma particles with a surface can release surface atoms. This effect is used for etching, cleaning, and depth profiling of surfaces. Also, bombardment of a surface by plasma ions leads to evaporation of surface atoms and ions, which can be used for fabrication of thin films.

We consider first the sputtering process caused by ion bombardment of the discharge cathode. As was seen in Chapter 20, the cathode layer of a glow discharge serves as a source of electrons. Formation of the cathode layer gives the plasma in this region an electric potential that differs from that of the cathode itself, and the plasma ions accelerated by this difference generate the secondary electrons. Ionization of plasma atoms by these electrons leads to reproduction of charged plasma particles in the cathode

TABLE 21.1. Sputtering Yields ξ (the Probability per Ion Collision for Release of a Surface Atom) for Bombardment of Elemental Solid Surfaces by 100 eV Argon Ions

Surface	ξ	Surface	ξ
Ag	0.63	Os	0.057
Al	0.11	Pd	0.42
Au	0.32	Pt	0.20
Be	0.074	Re	0.10
Co	0.15	Rh	0.19
Cr	0.30	Ru	0.14
Cu	0.48	Si	0.07
Fe	0.20	Ta	0.10
Ge	0.22	Th	0.097
Hf	0.16	Ti	0.081
Ir	0.12	U	0.14
Mo	0.13	V	0.11
Nb	0.068	W	0.068
Ni	0.28	Zr	0.12

layer. Sputtering occurs conjointly with the formation of secondary electrons, releasing cathode atoms as both neutral atoms and ions. We now examine this process.

The probability for the release of a surface atom upon the collision of a plasma ion with the cathode surface depends on such parameters as the type of ion, the surface material, and the ion energy. Table 21.1 lists the probabilities for release of a surface atom as a result of bombardment of various elemental surface materials by an argon ion of energy 100 eV. Because this probability is less than unity, sputtering of a single atom may require several ion collisions.

It is clear that the probability for sputtering of atoms increases with an increase of the ion energy. Therefore, for effective sputtering it is necessary to use a type of discharge that is suited to the production of energetic ions to collide with the cathode surface. This can occur in radio-frequency (rf) discharges, in discharges with a hollow cathode, and in magnetron discharges. The geometry and the types of fields in these discharges lead to relatively large energies of ions in the cathode layer, and consequently to effective sputtering from the cathode.

We consider briefly an rf discharge in the context of the sputtering problem. Its cathode layer differs from that of a stationary glow discharge in that the cathode layer of an rf discharge must both create and reproduce the discharge electrons. Therefore, the voltage drop across the cathode layer in an rf discharge is greater than that in a stationary glow discharge. The energy of ions that bombard the cathode in an rf discharge is about 100 eV. To avoid scattering of ions on gas atoms, the gas pressure used for sputtering is small,

usually in the range from 1 to 40 mTorr. There is an optimal frequency for the discharge that corresponds to the maximal ion energy for a given discharge geometry, cathode material, and other parameters of the discharge. The frequency 13.56 MHz is commonly used for rf discharges because it is considered to be a "free frequency" that is not assigned for radio communications. This frequency exceeds that which would be optimal for sputtering.

Sputtering is the first step in the deposition of films. Released atoms and ions form a flow that is directed to a substrate where atoms of the flow attach and form a film. One way to use an atomic flow for this purpose is represented by the so-called *ion-cluster beam* (ICB) method. In this method, a flow of atoms is transformed into a beam of charged clusters by mixing the atomic flow with a stream of cold buffer gas that has passed through a nozzle. Cooling of the atoms as a result of jet expansion leads to their nucleation and consequent formation of clusters. These clusters are electrically charged if the atomic flow from a discharge plasma contains an admixture of ions that can function as condensation nuclei during the formation of clusters, or if additional ionization of beam particles is caused by an intersecting electron beam. At the end of the condensation process, all the evaporated atoms are in the form of clusters.

Films formed from ICB methods are of higher quality than those from an atomic flow. The reason is that transformation of an atomic flow to a film is accompanied by an intense heat release owing to the formation of bonds, with each atom of the atomic beam transforming its binding energy into heat. From Eq. (12.1), the released energy per atom is ε_0 for the atomic beam and $A/n^{1/3}$ for each cluster in a beam. Since $\varepsilon_0 \sim A$, the ratio of specific released energies for the atomic and cluster beams is of the order of $n^{-1/3}$ (where n is the number of atoms in a cluster). In a realistic example, when clusters contain an average of $n \sim 1000$ atoms, this ratio is ~ 0.1. Because the atomic binding energy in the film being formed is much greater than a typical thermal energy of the atoms, film growth from individual atoms can be so nonuniform as to lead to vacancies in the film as it forms. This causes capture of buffer atoms within a film that, along with other side effects, decrease the film quality. When films are formed from beams of clusters, these deleterious effects are much less probable.

The ICB method has other advantages over atomic beams for practical applications. Since clusters have a large mass, the divergence of cluster beams is relatively small, and they can be focused onto small surface areas. Because the beam contains charged clusters, it is convenient to control it by an external electric field. This allows one to select optimal conditions for the application. The ICB method also opens up the possibility of new applications. For example, by accelerating the cluster beam to high velocities with an electric field and directing the beam to a foil, the foil can be perforated with holes of small sizes. This method, suggested by Haberland and collaborators in 1992, makes possible the generation of sieves with a

predetermined orifice diameter. However, because the intensity of cluster fluxes is low, their applications are restricted to small-scale technologies such as microelectronics.

21.2 LASER VAPORIZATION

In addition to the formation of free atoms upon ion bombardment of the cathode, vaporization of atoms in powerful gas discharges can occur when the cathode temperature is high. Cathode vaporization increases with the power of the discharge. Hence this mechanism for generation of atoms can be of critical importance for arc discharges. Cathode phenomena in arc discharges depend upon a diversity of processes, so that the details of these phenomena can be of importance. We shall analyze first the thermal mechanism of surface vaporization in a simple case when the surface is irradiated by a laser beam. When absorbed by the surface, laser radiation heats the material constituting the surface, and makes it possible to reach high local temperatures. In this way, a dense beam of evaporated atoms with an admixture of electrons and ions can be formed.

It is usual to employ pulsed lasers for laser vaporization, and the process occurs subject to the condition

$$t \ll r^2/\chi. \tag{21.1}$$

Here t is the pulse time, r is the radius of the irradiated spot, and χ is the coefficient of thermal diffusivity of the surface material: $\chi = \kappa/(c_p \rho)$, where κ is the thermal conductivity coefficient, c_p is the specific heat capacity, and ρ is the density of the surface material. If condition (21.1) is fulfilled, all of the energy absorbed from the laser radiation is expended on the vaporization of atoms. Then, assuming the laser beam to be uniform and cylindrical with radius r, the energy balance equation is

$$\frac{P}{\pi r^2} = (\varepsilon_0 + 2T) j_{ev}(T), \tag{21.2}$$

where P is the power of absorbed radiation, ε_0 is the binding energy of the released atoms, T is the surface temperature expressed in energy units, and $j_{ev}(T)$ is the flux of evaporated atoms. We use the Maxwell velocity distribution for the atoms, and the mean kinetic energy $2T$ of the released atoms can be taken to be small compared to the atomic binding energy ε_0. The flux of evaporated atoms can be expressed in terms of the pressure p_{sat} of saturated vapor at the given temperature [or the corresponding number density of

atoms, $N_{sat}(T) = p_{sat}(T)/T$], using the principle of detailed balance. According to Eq. (12.39), this flux is

$$j_{ev}(T) = \xi \sqrt{\frac{T}{2\pi m}}\, N_{sat}(T), \tag{21.3}$$

where ξ is the probability for attachment of the atom to the surface upon contact, and m is the atomic mass. The value ξ is of the order of unity. (For example, $\xi = 1$ for tungsten at $T = 3000$–3500 K.) Because of the strong temperature dependence of $N_{sat}(T)$ (see data of Appendix 13 for some metals), one can employ $\xi = 1$ in the above equation.

Equations (21.2) and (21.3) determine the surface temperature and the flux of evaporating atoms at a given power of absorbed laser radiation. The greater the specific power of absorbed radiation, the higher is the temperature of the evaporating atoms, and hence the larger is the number density of electrons and ions in the flux of evaporating atoms. The plasma thus formed absorbs incident laser radiation; the mechanism for the absorption process depends upon recombination collisions of electrons and ions in the flux. There will be some power level at which all the laser radiation will be absorbed by the plasma and none will reach the surface. The absorbed radiation goes principally to electrons, with some atomic ionization also occurring. This leads to an increase in the electron number density that enhances the absorption of laser radiation by the plasma flux. The laser beam does not reach the surface, being absorbed instead by the plasma, which thus leads to laser breakdown. Laser breakdown corresponds to a regime of laser action on the surface other than that we have been discussing, and takes place when the specific powers of absorbed radiation are such that $P > 10^7$ W/cm^2. The mechanisms we have been examining for interaction of laser radiation with the surface correspond to smaller laser intensities. In particular, Table 21.2 gives values of the temperatures and pressures p of evaporating atoms near metallic surfaces if the specific power of absorbed radiation is $P = 3 \times 10^6$ W/cm^2.

TABLE 21.2. The Surface Temperature T and the Vapor Pressure p Near a Surface Evaporated by Laser Irradiation[a]

Metal	T, 10^3 K	p, atm
Au	5.0	160
Co	4.5	80
Cu	4.2	90
Fe	4.4	80
Ni	4.4	80
Pt	6.3	120
Ti	5.0	70
W	9.2	100

[a]The specific power of the absorbed radiation is 3×10^6 W/cm^2.

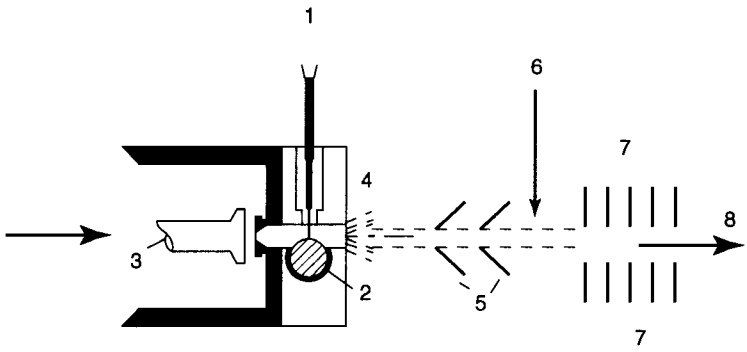

Figure 21.1 A schematic diagram of a laser source of metallic ion clusters: 1, laser beam; 2, target in the form of a metallic rod; 3, buffer gas flow; 4, beam containing buffer gas and clusters emerging from a nozzle; 5, skimmers; 6, intersecting electron beam; 7, ion optics and accelerator; 8, final beam.

Thus laser vaporization can create intense fluxes of evaporating atoms with an admixture of charged particles. Mixing such a flux with a flux of a cool buffer gas (usually He or Ar), and expanding the mixture through a nozzle, one can transform the vapor flux into a flux of clusters. This method is used for generation of cluster beams for scientific research. Figure 21.1 shows a typical arrangement using this method.

We now want to analyze the evolution of the flux of evaporating atoms as it departs from the surface. The atoms initially have a quasi-Maxwellian velocity distribution. At a distance from the surface of the order of a mean free path for the atoms, a directed stream of atoms is formed, and the velocity distribution function changes to that for an atomic flux, with a consequent slight decrease in temperature. Laser vaporization is usually produced in a buffer gas, and the flux parameters depend on the properties of the gas. In particular, if the buffer gas pressure is small compared to the pressure of the evaporating atoms, the evolving flux propagates with the sound velocity $u = (\gamma T_f/m)^{1/2}$ (see formula (15.7)), where T_f is the atomic temperature in the flux, m is the mass of an atom, and $\gamma = c_p/c_V$. (The quantities c_p and c_V are the heat capacities of the vapor per atomic particle at constant pressure and volume, respectively. For an atomic vapor, $\gamma = \frac{5}{3}$.) As the flux moves farther from the surface, it expands so that the angle between its boundary and the normal to the surface ranges from 5° up to 15°. Expansion of the flux leads to a decrease of its temperature and pressure. Mixing of the flux with a buffer gas causes an additional decrease of these values. During mixing, the flux may become subject to disruption.

We turn our attention now to the evolution of charged particles—electrons and ions—in an expanding flux. If atoms of the flux subsequently form clusters, the charged particles are the nuclei of condensation, with the

number density of charged particles being the determining factor in the condensation process. First, thermodynamic equilibrium between electrons, ions, and atoms of the flux is established, so the Saha equation (2.17) can be used to find the number density of charged particles. This equilibrium is sustained by stepwise electron impact ionization of atoms balanced by three-body recombination of electrons and atomic ions as expressed in Eq. (5.15). Because of the strong dependence of the equilibrium number density of charged particles on the temperature, at some stage of the process the recombination rate becomes small compared to the expansion rate. Beyond this stage, the electron concentration becomes "frozen" because the decrease of the electron number density due to the flux expansion is stronger than that due to three-body recombination of electrons and atomic ions.

The transition to the "frozen" electron concentration takes place when the rates of three-body recombination and expansion are equal. That equality can be expressed by the condition

$$KN_e^2 \sim \frac{1}{\tau_{ex}} = \frac{r}{u \tan \alpha}, \tag{21.4}$$

where K is the three-body recombination coefficient of electrons and ions [Eq. (5.16)], τ_{ex} is the expansion time, r is the radius of the flux, u is its velocity, and α is its angle of divergence. Because the Saha formula (2.17) gives a strong temperature dependence for the electron number density [$N_e \sim \exp(-J/T)$], where J is the atomic ionization potential, the criterion (21.4) allows one to determine the transition temperature quite accurately. For typical laser vaporization conditions, transition takes place at an electron number density in the range $N_e \sim 10^{13}$–10^{14} cm^{-3}.

The determining factor in the evolution of the number density of charged particles in an expanding flux is the small rate for three-body recombination of electrons and ions. At low flux temperatures, when molecular ions are formed, an effective channel for electron decrease is opened due to dissociative recombination of electrons and molecular ions as displayed in Eq. (5.27). This can lead to elimination of charged particles from the flux. However, at these temperatures, negative ions can be formed by attachment of electrons to atoms, in addition to the formation of molecular ions and molecules. The transfer of negative plasma charge from electrons to negative ions decreases the recombination rate of charged particles and preserves a portion of the charged particles for the following stage of the process when clustering occurs. Competition of these processes influences the condensation process, and therefore can determine the final state of the expanding flux. From this one can conclude that processes in the expanding flux that occur with the participation of charged particles can be different from other mechanisms described above, and it is a combination of these processes that determines the final state of the flux.

21.3 ETCHING

Etching is a typical example of plasma processing. It is one stage in the fabrication of microelectronics. The process consists of the replication of the desired pattern on an element of an integrated microelectronic scheme. The replicator is a sheet of glass or quartz patterned with a thin film of a metal or metal oxide that absorbs UV radiation. This sheet, or wafer, is a substrate on which several layers of different materials are deposited. The upper layer, with a thickness of the order of 1 μm, is a photoresist—an organic substance that absorbs UV radiation and thus undergoes volatilization at low temperatures. Other deposited materials are exemplified by Si, SiO_2, S_3N_4, and Al, which can play the role of a dielectric, semiconductor, or metal in an integrated manufacturing scheme.

A sequence in the fabrication of patterns is illustrated in Fig. 21.2. The first step of the replication (lithography) process is to establish the replicator pattern on the sample. Then UV radiation is directed to the sample through the replicator. The transmitted radiation evaporates a photoresist and transfers the pattern to the sample in this way (Fig. 21.2b). The following stage is the etching process, in which an underlying film is removed at points where a photoresist has been removed. This may be accomplished with electron beams, ion beams, or X-rays, or by chemical or plasma methods. The etching process must be anisotropic in that material must be removed in a vertical direction only. At the same time, the process must be selective, so that it acts

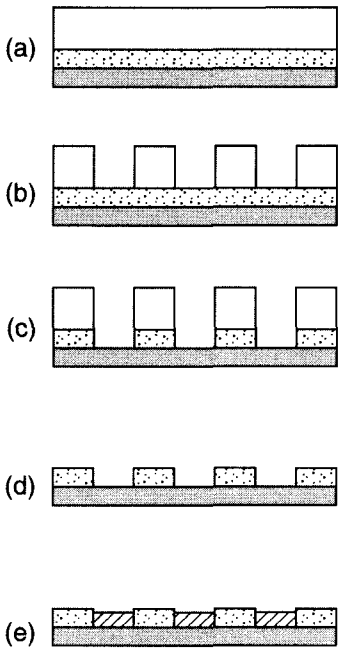

Figure 21.2 Steps of the microfabrication process: (a) the initial view of a sample (the upper layer is a photoresist); (b) irradiation of a sample and removal of a part of the photoresist according to the patterns of a replicator; (c) the etching process; (d) removal of the photoresist; (e) deposition of another material.

only on the material to be removed. These requirements seem to be incompatible. For example, the ion-beam method is anisotropic because ions are directed perpendicular to the surface. But it is not selective, because ions destroy an etching layer and a photoresist to almost equal degrees. Discharge methods that use chemically active particles (O, F, Cl) are selective, as are chemical methods, but they are not anisotropic. Chemically active particles may not act on a photoresist, but they do act on the total surface of a removal layer, and the structure thus formed does not have vertical boundaries. The best result for the etching process comes from a combination of plasma methods that is both selective and anisotropic.

As a demonstration of this possibility, we consider the etching of Al film. This film may be removed by reaction with chlorine atoms or chlorine molecules that are formed in a gas discharge. The product of these reactions is the gas $AlCl_3$, which then departs from the system. Because Cl and Cl_2 do not act on a photoresist, such a process is selective, but it is not anisotropic. Addition of chlorocarbons CCl_4 or $CHCl_3$ to chlorine in the discharge gas leads to the formation of a polymer that covers the sample with a thin film. The film thus formed hampers the penetration of Cl and Cl_2 to the Al, and slows the chemical process. But as a result of ion bombardment, the chlorocarbon protective film is destroyed, and chemical reactions between Cl or Cl_2 and Al proceed at such locations until a chlorocarbon film again forms there. This provides an anisotropy of the etching process due to the vertical direction of the ions. Thus, this process combines selectivity and anisotropy. Using an rf discharge in low-density chlorine with an admixture of chlorocarbons, one can obtain simultaneously an ion beam that is formed on the plasma boundary due to the plasma sheath, chemically active particles Cl and Cl_2, and a material for a polymer film.

Etching is one of the stages of the microfabrication process (Fig. 21.2). In addition, the photoresist must be removed, and structures may be deposited in the etched areas by other materials. Plasma processes may be useful here also. In particular, a simple technique for removal of photoresist is based on its reaction with oxygen atoms, which can be obtained from a gas-discharge plasma.

The explication of the etching process shows the complexity of plasma application methods. Because of the variety of possible plasma systems and methods for any particular applied problem, the choice of an optimal method is not simple.

21.4 EXPLOSIVE EMISSION

There are several mechanisms by which electrons can be emitted from the cathode. In Chapter 20 we considered the Townsend mechanism of electron emission, wherein collisions of ions with the cathode generate secondary electrons. The Richardson–Dushman formula (2.33) describes electron emis-

sion by a hot cathode. The distinction between glow and arc discharges depends upon the manner of electron emission. Electron emission from the cathode in a glow discharge is by the Townsend mechanism, whereas thermoemission takes place in arc discharges. Another mechanism is the field emission that can occur in strong electric fields near surface nonuniformities. In this case, the electric field can be sufficient to transport electrons across the potential barrier at the surface. The existence of surface vaporization leads us to consider one more electron emission mechanism, called the *Mesyats mechanism*, or *explosive emission*.

A schematic representation of the Mesyats type of electron emission is shown in Fig. 21.3. The first stage is field emission near a surface non-

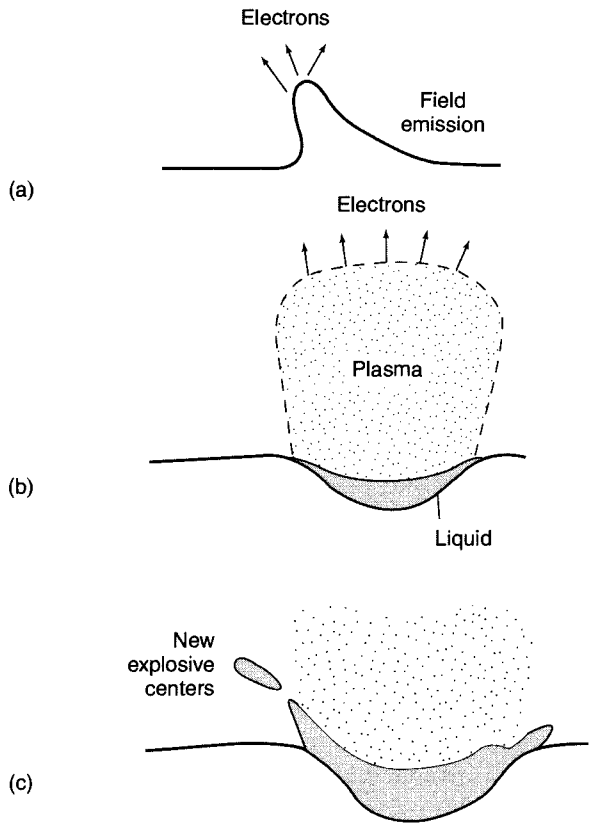

Figure 21.3 Evolution of the Mesyats mechanism or explosive emission. (a) In the first stage of the process, emission of electrons takes place near nonuniformities where an external electric field is intensified by one to two orders of magnitude. (b) In the spark stage of the process, vaporization of the surface under action of the electric current creates an intense atomic flux, which is ionized and transformed into a plasma. (c) An instability destroys this explosive emission center, and a new center arises at another point of the surface.

uniformity. The cause of the field emission is that the emitting element of the surface is heated and atoms evaporate from it. Evaporating atoms form a medium through which an electric current passes. The atoms are ionized by electron impact, and the ions return to the cathode while electrons are removed from it. In the course of this process, the region occupied by the current expands, and the radius of the plasma flux can be estimated to be

$$r \sim (\chi\tau)^{1/2},$$

where χ is the coefficient of thermal diffusivity of the surface material at a given temperature ($\chi \sim 1$ cm^2/s), and τ is the duration of the phenomenon. In time, an instability destroys this structure, but the process can be repeated at other locations on the cathode.

Though the Mesyats mechanism of plasma emission was worked out for a vacuum arc and for high-voltage breakdown in a vacuum, in its general form it can also describe hot spots on the cathode. Hot spots formed on a cathode enable the passage of high currents for a short time. These spots are called explosive emission centers. Their evolution is complicated compared to the above picture. In particular, the velocity of propagation of a plasma governed by the ion velocity is of the order of 10^6 cm/s, while the velocity of evaporating atoms is of the order of 10^5 cm/s. Nevertheless, one can understand distinctive features of the phenomenon. One of these is the ratio of the mass M of evaporated material to the total charge $\int I\,dt$, where I is the current. Evaporated atoms are ionized by electrons so that each evaporating atom gives $2e$ of charge—one electron and one ion, if we assume the ion to be singly ionized. Because formation of one charge pair corresponds to the passage of one charge between electrodes, it follows that

$$\frac{M}{\int I\,dt} = \frac{m}{e}, \tag{21.5}$$

where m is the atomic mass. Since a spray of liquid material can occur concurrently with atomic evaporation, the mass/charge ratio is greater than stated in Eq. (21.5). For copper as an example, Eq. (21.5) gives 0.6 mg/C. Atoms that evaporate from the cathode are ionized and thus ions return to the cathode. In order to have a quasineutral plasma in all of space, it is necessary to generate evaporated material on the anode also. Explosive emission generates observable tracks on electrodes that appear to be duplicated on the cathode. This is evidence of the similarity of the mechanisms for electron emission for the arc cathode and for the electrode at vacuum breakdown. In addition, it confirms that emission takes place in small elements of the surface that become liquefied.

The mechanism described for expansion of the explosive-emission center leads to the energy balance equation

$$C_p\,\Delta T \sim \frac{i^2}{\Sigma}\tau. \tag{21.6}$$

Here $C_p \Delta T \sim 10^6$ J/cm^3 is a typical specific energy that corresponds to heating of metals up to temperatures $T \sim 10^4$ K, and Σ is the plasma conductivity, which [according to the Spitzer formula (11.27)] is estimated to be $\Sigma \sim 100\ \Omega^{-1}$ cm^{-1} at typical electron temperatures $T_e \sim 1$–3 eV. (This temperature leads to a fully ionized plasma under equilibrium conditions.) The above equation leads to the estimate

$$i^2\tau \sim 10^8\ \text{A}^2\ \text{s/cm}^4. \tag{21.7}$$

For a time $\tau \sim 10^{-8}$ s typical for this phenomenon, the above expression gives $i \sim 10^8$ A/cm^2, which corresponds to the flux $j \sim 3 \times 10^{26}$ (cm^2 s)$^{-1}$ of evaporating atoms. The surface temperature can then be found from Eq. (21.3). For example, the result of this procedure for copper is $T = 8500$ K. At this surface temperature, the thermoemission current density according to Eq. (2.33) is 10^7 A/cm^2, an order of magnitude less than that due to the Mesyats mechanism.

To better understand the processes that constitute the Mesyats mechanism for emission, we can estimate other parameters of the phenomenon from the above values. The total number of atoms participating in one event is of the order $jr^2\tau \sim 10^{10}$–10^{11}. The number density of evaporating atoms near the surface is about $j/v \sim 10^{21}$ cm^{-3}, which corresponds to a vapor pressure near the surface of $p \sim 1000$ atm. The number density for atoms that we have just estimated is small compared to the condensed state. Therefore, both the vapor and the plasma formed from it are gaseous systems. Next, the electric field strength in the cathode layer is $E \sim i/\Sigma \sim 10^6$ V/cm, and the thickness of the cathode layer is $l \sim \Delta V/E \sim 10^{-5}$ cm, where $\Delta V \sim 10$ V is the cathode voltage drop. The ion mean free path is $\lambda \sim (N\sigma_{\text{res}})^{-1} \sim 10^{-7}$ cm, where $\sigma_{\text{res}} \sim 10^{-14}$ cm^2 is the cross section of the resonant charge-exchange process. Then the energy that is transferred from the electric field to ions can transit further to atoms of the vapor, but not to the surface. Other types of emission, such as thermoemission, are also of importance for this phenomenon. They create electrons near the surface, and the subsequent ionization of vapor in the cathode layer is caused by these electrons. Thus, the Mesyats mechanism of plasma emission generates an intense emission of charged particles from the electrode surface. As a result of evaporation of the electrode, a medium is created through which high discharge currents can pass.

21.5 SECONDARY ELECTRON EMISSION

We have been discussing above the mechanisms for generation of electrons from the cathode in a gas-discharge plasma. These include the generation of electrons by ion impact (the Townsend mechanism, Chapter 20), by thermoemission (Chapter 2), by autoemission of electrons induced by a strong electric field, and by explosive emission (the Mesyats mechanism). Explosive emission includes a chain of interaction processes between a gas-discharge

TABLE 21.3. Parameters for Secondary Electron Emission

Metal	ε_{max}, eV	δ_{max}	ε_1, eV	ε_2, eV
Ag	800	1.5	200	> 2000
Al	300	1.0	300	300
Au	800	1.4	150	> 2000
Ba	400	0.8	—	—
Bi	550	1.2	—	—
Co	600	1.2	200	—
Cu	600	1.3	200	1500
Fe	400	1.3	120	1400
Mo	375	1.25	150	1200
Nb	375	1.2	150	1050
Ni	550	1.3	150	> 1500
Pt	700	1.8	350	3000
Ta	600	1.3	250	> 2000
Ti	280	0.9	—	—
W	650	1.4	250	> 1500
Zr	350	1.1	—	—

plasma and a metallic surface. Generation of electrons from the anode is a consequence of collisions of plasma electrons with the anode, and is called *secondary electron emission.*

Secondary electron emission resembles ionization of atoms by electron impact. In both cases bound electrons obtain energy from the incident electron, and ionization takes place if the energy gained is sufficient for electron release. Hence, the number of ionization electrons as a function of the energy of the incident electron, $\delta(\varepsilon)$, has a dependence like that of the cross section for atomic ionization by electron impact. The function $\delta(\varepsilon)$ has a maximum δ_{max} at some electron energy ε_{max}. This energy is greater than a typical energy corresponding to the maximum cross section for atom ionization by electron impact, because a slow electron formed inside the anode cannot escape. The value of δ_{max} usually exceeds unity. Table 21.3 lists values of the parameters δ_{max} and ε_{max} for a variety of metals, and also values of the electron energies ε_1 and ε_2 such that $\delta(\varepsilon_1) = \delta(\varepsilon_2) = 1$.

21.6 QUENCHING OF EXCITED PARTICLES ON WALLS

A weakly ionized gas will contain excited atoms or molecules in addition to charged particles. These modes of excitation may include electronically excited atoms and molecules, and vibrationally excited molecules and radicals. The excited particles will influence properties and processes in the gas, which usually is located in a space enclosed by walls (boundaries). Collisions of excited particles with the walls lead to their quenching, the efficiency of this process depending on the identity of the excited particles, the mode of

excitation, and the properties of the walls. The quenching mechanisms are identical to those that are encountered in collisions of atomic particles. In particular, for a gas-discharge plasma enclosed in a cylindrical tube, we assumed the probability of recombination of charged particles on the walls to be unity. For walls made of a dielectric material, charged particles of one sign are captured by the walls into a bound state on the wall surface. Then charged particles of the opposite sign are attracted to the captured surface particles and recombine with them. This process is akin to three-body recombination of charged particles in gases.

The measure of quenching of excited particles on walls is the probability γ of quenching upon contact with the walls. This probability depends strongly on the type of excitation. For highly excited states γ is about one. For example, collisions of metastable atoms $He(2^3S)$, $He(2^1S)$, and $Ne(^3P_2)$ with conducting surfaces like gold or iron exhibit a γ in the range of 0.5–0.7. This process is identical to quenching of these atoms by electron impact in head-on collisions. Quenching of the above atoms by a dielectric surface is identical to the Penning process and proceeds less effectively. In particular, γ lies in the interval 0.1–0.4 for quenching of metastable helium atoms on dielectric walls.

One can take the parameter γ to be of the order of magnitude, or in excess, of the corresponding probability for quenching of a given excitation in atomic and molecular collisions. In particular, the probability of quenching the excited molecule $O_2(^1\Delta_g)$ in thermal collisions with atoms and molecules in a gas is of the order of 10^{-9}–10^{-6}, while the probability of quenching of this molecule on dielectric surfaces lies in the interval 10^{-5} to 4×10^{-5}, depending on the wall material.

Quenching of excited particles on walls alters the spatial distribution of these particles. We shall study this in the following context. We consider an excited gas in a gap between two parallel infinite walls, with excited particles generated at a location centered between the walls. Assuming the distance L between walls to be large compared to the mean free path of the excited particles, we can consider particle motion to be diffusive. The boundary condition that follows from equating the diffusion and kinetic fluxes at the walls is

$$-D\frac{dN_*}{dx} = \gamma\sqrt{\frac{T}{2\pi m}}\,N_*. \tag{21.8}$$

Here the x-axis is directed perpendicular to the walls, N_* is the number density of excited particles, D is the diffusion coefficient for excited particles in the gas, T is the gas temperature, and m is the particle mass. Because excited particles are neither generated nor lost in the bulk of the space, the balance equation for the number density of excited particles in this region is

$$j = -D\frac{dN_*}{dx} = \text{const}.$$

The solution of this equation has the form $N = A - Bx$, where x is the distance from the central plane. Using the boundary condition (21.8), the number density of excited particles in the gas is

$$N_* = N_0\left[1 - \frac{2x}{L}\left(1 + \frac{2D\sqrt{2\pi m}}{L\gamma\sqrt{T}}\right)^{-1}\right]. \tag{21.9}$$

The quenching efficiency γ appears in this expression in the combination $\alpha = \gamma L\bar{v}/D \sim \gamma L/\lambda$, where $\bar{v}$ is the average particle velocity, and λ is the mean free path of excited particles. From this it follows that quenching of excited particles on the walls leads to a decrease of their number density at

TABLE 21.4. The Probability γ of Quenching of Vibrationally Excited Molecules in Thermal Collisions with Walls[a]

Molecule	$\hbar\omega$, cm^{-1}	Wall Material	γ
H_2	4160	Quartz	5×10^{-4}
		Mo glass	6×10^{-4}
		Steel	6×10^{-4}
		Cu	2×10^{-3}
		Ni	1.1×10^{-3}
D_2	2942	Quartz	4×10^{-4}
N_2	2331	Quartz	3×10^{-4}
		Pyrex	5×10^{-4}
		Teflon	1×10^{-3}
		Al_2O_3	1.4×10^{-3}
		Steel	1.7×10^{-3}
		Mo glass	2×10^{-3}
		Cu	2×10^{-3}
CO_2(010)	667	NaCl	0.2
		Pt	0.4
CO_2(001)	2349	Teflon	0.2
		Brass	0.2
		Pyrex	0.25
		Mo glass	0.4
		Quartz	0.4
N_2O(010)	589	NaCl	0.4
		Pt	0.4
N_2O(001)	2224	Mo glass	0.03
		Pyrex	0.2
		Quartz	0.3
CO	2143	Pyrex	0.02
HF	3962	Mo glass	0.01
HCl	2986	Pyrex	0.5

[a] $\hbar\omega$ is the excitation energy of the vibrationally excited state.

distances from walls of the order of λ/γ. Hence, if $L \gg \lambda/\gamma$, quenching can be taken into account by using the boundary condition $N_* = 0$ at the walls. In the other limiting case, $L \ll \lambda/\gamma$, processes at the walls do not influence the spatial distribution of excited particles. Evidently, information about quenching at the walls is of importance only when $L \sim \lambda/\gamma$. Since $L \gg \lambda$, this corresponds to small values of γ. Therefore, the quenching probability is known for processes where γ is small compared to unity. In particular, this applies to quenching of vibrationally excited molecules on walls. A list of quenching probabilities is given in Table 21.4 for a sampling of excited molecules and of materials of a quenching surface. Values of γ vary over a wide range, and depend mostly on molecular excitation.

CHAPTER 22

CONCLUSIONS

We can now summarize the identifying physical features of a weakly ionized gas or plasma. From the foregoing analysis and information, it can be concluded that in most cases, when a plasma satisfies ideality conditions, it resembles a gas in that the interaction between particles is small. However, the presence of charged particles gives rise to some properties unique to a low-density plasma. In the first place, self-consistent electric and electromagnetic fields can be created inside a weakly ionized gas. These fields have important effects on the spatial distribution of particles and processes in the plasma. A weakly ionized gas interacts actively with external fields, which affords a convenient method to govern its state. In the second place, because of the long-range property of the interaction between charged particles, this interaction exists independently of short-range interactions between neutral particles, or between neutral and charged particles. For this reason, collective properties of such plasmas have a universal character. Plasma waves and instabilities resulting from interaction between charged particles can be the determining factor in the behavior of various types of plasmas. In the third place, gases in an ionized state will naturally coexist with excited atoms, molecules, and radicals in a plasma. Thus, a plasma is a chemically active system. It can be a source of characteristic radiation spectra or explicit excited atomic particles.

As for dense plasmas (plasmas with strong coupling), they have some features of condensed systems, and can be so complex as to require individual analysis of each case. As opposed to an ideal plasma, it is impossible to separate interactions between charged and neutral particles in a dense plasma. Therefore, properties of dense plasmas are not universal even though they are due to charged particles. That is, the presence of charged particles does not in itself provide information sufficient to explain the principal properties of these systems.

APPENDICES

APPENDIX 1. PHYSICAL CONSTANTS

Velocity of light	$c = 2.99792 \times 10^{10}$ cm/s
Planck constant	$h = 6.62608 \times 10^{-27}$ erg s
	$\hbar = 1.05457 \times 10^{-27}$ erg s
Electron charge	$e = 4.8032 \times 10^{-10}$ esu
	$e^2 = 2.3071 \times 10^{-19}$ erg cm
Electron mass	$m_e = 9.1094 \times 10^{-28}$ g
Proton mass	$m_p = 1.6726 \times 10^{-24}$ g
Atomic unit of mass	1.6605×10^{-24} g
Avogadro number	6.0221×10^{23} mol^{-1}
Stefan–Boltzmann constant	$\sigma = 5.6705 \times 10^{-12}$ W/(cm^2 K^4)

APPENDIX 2. CONVERSION FACTORS FOR ENERGY UNITS[a]

	erg	eV	cal/mol[b]	cm^{-1}	K
erg	1	6.242×10^{11}	1.4394×10^{16}	5.0346×10^{15}	7.243×10^{15}
eV	1.602×10^{-12}	1	2.3045×10^{4}	8.0660×10^{3}	1.1605×10^{4}
cal/mol[b]	6.952×10^{-17}	4.3393×10^{-5}	1	0.34973	0.50319
cm^{-1}	1.986×10^{-16}	1.2398×10^{-4}	2.8573	1	1.4386
K	1.3806×10^{-16}	8.617×10^{-5}	1.9859	0.69504	1

[a] 1 J = 10^7 erg.
[b] One calorie divided by Avogadro's number.

APPENDIX 3. SOME RELATIONS OF PLASMA PHYSICS EXPRESSED IN CONVENIENT UNITS

No.[a]	Formula[a]	Factor C	Units Used
1	$v = C\sqrt{\varepsilon/m}$	5.931×10^7 cm/s	ε in eV, m in units of m_e[b]
		1.389×10^6 cm/s	ε in eV, m in amu[c]
		5.506×10^5 cm/s	ε in K, m in units of m_e[b]
		1.289×10^4 cm/s	ε in K, m in amu[e]
2	$\omega = C\varepsilon$	1.520×10^{15} s^{-1}	ε in eV
3	$\omega = C/\lambda$	1.885×10^{11} s^{-1}	λ in cm
4	$\omega_p = C\sqrt{N_e}$	5.642×10^4 s^{-1}	N_e in cm^{-3}
5	$r_D = \sqrt{T/N_e}$	525.6 cm	N_e in cm^{-3}, T in eV
		4.879 cm	N_e in cm^{-3}, T in K
6	$\omega_H = CH/m$	1.759×10^7 s^{-1}	H in G, m in units of m_e[b]
		9649 s^{-1}	H in G, m in amu[c]
7	$r_H = C\sqrt{\varepsilon m}\,/H$	3.372 cm	ε in eV, H in G
8	$N = Cp/T$	7.340×10^{21} cm^{-3}	p in atm, T in K
		9.658×10^{18} cm^{-3}	p in Torr, T in K
9	$D = C\sqrt{T/\mu}\,/(N\sigma)$	4.278×10^{19} cm^2/s	T in K, μ in amu[c]
			N in cm^{-3}, σ in Å^2
		1.595 cm^2/s	The same T, μ, σ;
			$N = 2.689 \times 10^{19}$ cm^{-3}
10	$x = CE/(TN\sigma)$	1.160×10^{20}	E in V/cm, T in K,
			σ in Å^2, N in cm^{-3}
11	$f = CT^{3/2}$	7.635×10^{19} cm^{-3}	T in 10^3 K, m in units of m_e[b]
		3.018×10^{21} cm^{-3}	T in eV, m in units of m_e[b]
		1.879×10^{20} cm^{-3}	T in K, m amu[c]

[a]The meaning of the formulas is as follows:

1. The particle velocity $v = \sqrt{2\varepsilon/m}$, where v is the velocity, ε is the energy, and m is the mass of the particle.
2. The photon frequency $\omega = \varepsilon/\hbar$, where ε is the photon energy and ω is the photon frequency.
3. The photon frequency $\omega = 2\pi c/\lambda$, where c is the velocity of light and λ is the wavelength.
4. The frequency of plasma oscillations $\omega_p = \sqrt{4\pi N_e e^2/m_e}$, where N_e is the electron number density and m_e is the electron mass.
5. The Debye–Hückel radius $r_D = \sqrt{T/8\pi N_e e^2}$, where T is the temperature and N_e is the electron number density.

6. The Larmor frequency of a charged particle, $\omega_H = eH/mc$, where H is the magnetic field strength and m is the particle mass.
7. The Larmor radius of the electron, $r_H = v/\omega_H$, where v is the electron velocity and ω_H is the Larmor frequency.
8. The number density of gas particles, $N = p/T$, where p is the gas pressure and T is the temperature.
9. The diffusion coefficient for a particle in a gas according to the Chapman–Enskog approximation, $D = 3\sqrt{2\pi T}/16N\sigma\sqrt{\mu}$, where T is the gas temperature, N is the number density of gas particles, μ is the reduced mass of the test and gas particles, and σ is the mean collision cross section for the test and gas particles.
10. The reduced electric field strength for a charged particle in a gas $x = eE/TN\sigma$, where E is the electric field strength, T is the gas temperature, N is the number density of gas particles, and σ is the collision cross section of the test charged particle with a particle of the gas.
11. The factor of the Saha formula, $f = (mT/2\pi\hbar^2)^{3/2}$, where T is the temperature and m is the particle mass.

[b] $m_e = 9.109 \times 10^{-28}$ g.

[c] 1 amu = 1 atomic mass unit = $m_a = 1.6605 \times 10^{-24}$ g.

APPENDIX 4. THERMAL CAPACITIES OF GASES[a]

	c_p					
Gas	$T = 200$	300	400	600	800	1000 K
H_2	3.28	3.47	3.51	3.53	3.56	3.63
CH_4	4.03	4.31	4.89	6.32	8.00	9.77
CO	3.52	3.51	3.53	3.67	3.84	3.99
N_2	3.51	3.51	3.52	3.62	3.78	3.93
Air	3.51	3.51	3.63	3.67	3.83	3.98
O_2	3.52	3.54	3.67	3.86	4.06	4.20
CO_2	—	4.50	4.99	5.72	6.19	6.51
Kr	2.51	2.51	2.50	2.50	2.50	2.50
Xe	—	2.52	2.51	2.50	2.50	2.50

[a] Per molecule, at 1-atm pressure.

APPENDIX 5. COEFFICIENTS OF SELF-DIFFUSION[a]

Gas	D, cm^2/s	Gas	D, cm^2/s	Gas	D, cm^2/s
He	1.6	H_2	1.3	H_2O	0.28
Ne	0.45	N_2	0.18	CO_2	0.096
Ar	0.16	O_2	0.18	NH_3	0.25
Kr	0.084	CO	0.18	CH_4	0.20
Xe	0.048				

[a] Diffusion coefficients of atoms or molecules in the parent gas are reduced to the number density $N = 2.689 \times 10^{19}$ cm^{-3} corresponding to standard conditions ($T = 273$ K, $p = 1$ atm).

APPENDIX 6. GAS-KINETIC CROSS SECTIONS[a]

Pair	Cross Section, 10^{-15} cm^2									
	He	Ne	Ar	Kr	Xe	H_2	N_2	O_2	CO	CO_2
He	1.5	2.0	2.9	3.3	3.7	2.3	3.0	2.9	3.0	3.6
Ne		2.4	3.4	4.0	4.4	2.7	3.2	3.5	3.6	4.9
Ar			5.0	5.6	6.7	3.7	5.1	5.2	5.3	5.5
Kr				6.5	7.7	4.3	5.8	5.6	5.9	6.1
Xe					9.0	5.0	6.7	6.9	6.8	7.6
H_2						2.7	3.8	3.7	3.9	4.5
N_2							5.0	4.9	5.1	6.3
O_2								4.9	4.9	5.9
CO									5.0	6.3
CO_2										7.8

[a]Values of the gas-kinetic cross sections are obtained from the formula $\sigma_g = T/(\mu v_T ND)$, where D is the diffusion coefficient, T is the room temperature expressed in energy units, N is the number density of atoms or molecules, $v_T = \sqrt{8T/(\pi\mu)}$ is the average particle velocity, and μ is the reduced mass.

APPENDIX 7. THERMAL CONDUCTIVITY COEFFICIENTS OF GASES[a]

Gas	Thermal Conductivity, 10^{-4} W/(cm K)						
	T = 100	200	300	400	600	800	1000 K
H_2	6.7	13.1	18.3	22.6	30.5	37.8	44.8
He	7.2	11.5	15.1	18.4	25.0	30.4	35.4
CH_4	—	2.17	3.41	4.88	8.22	—	—
NH_3	—	1.53	2.47	6.70	6.70	—	—
H_2O	—	—	—	2.63	4.59	7.03	9.74
Ne	2.23	3.67	4.89	6.01	7.97	9.71	11.3
CO	0.84	1.72	2.49	3.16	4.40	5.54	6.61
N_2	0.96	1.83	2.59	3.27	4.46	5.48	6.47
Air	0.95	1.83	2.62	3.28	4.69	5.73	6.67
O_2	0.92	1.83	2.66	3.30	4.73	5.89	7.10
Ar	0.66	1.26	1.77	2.22	3.07	3.74	4.36
CO_2	—	0.94	1.66	2.43	4.07	5.51	6.82
Kr	—	0.65	1.00	1.26	1.75	2.21	2.62
Xe	—	0.39	0.58	0.74	1.05	1.35	1.64

[a]At 1-atm pressure.

APPENDIX 8. VISCOSITY COEFFICIENTS OF GASES[a]

Gas	Viscosity, 10^{-5} g/(cm s)						
	T = 100	200	300	400	600	800	1000 K
H_2	4.21	6.81	8.96	10.8	14.2	17.3	20.1
He	9.77	15.4	19.6	23.8	31.4	38.2	44.5
CH_4	—	7.75	11.1	14.1	19.3	—	—
H_2O	—	—	—	13.2	21.4	29.5	37.6
Ne	14.8	24.1	31.8	38.8	50.6	60.8	70.2
CO	—	12.7	17.7	21.8	28.6	34.3	39.2
N_2	6.88	12.9	17.8	22.0	29.1	34.9	40.0
Air	7.11	13.2	18.5	23.0	30.6	37.0	42.4
O_2	7.64	14.8	20.7	25.8	34.4	41.5	47.7
Ar	8.30	16.0	22.7	28.9	38.9	47.4	55.1
CO_2	—	9.4	14.9	19.4	27.3	33.8	39.5
Kr	—	—	25.6	33.1	45.7	54.7	64.6
Xe	—	—	23.3	30.8	43.6	54.7	64.6

[a]At 1-atm pressure.

APPENDIX 9. CROSS SECTIONS OF RESONANT CHARGE-EXCHANGE PROCESSES[a]

A	σ, 10^{-15} cm^2	A	σ, 10^{-15} cm^2	A	σ, 10^{-15} cm^2	A	σ, 10^{-15} cm^2
H	6.2 (5.0)	S	8.7 (6.7)	Ge	10 (8)	Sb	11 (9.1)
He	3.5 (2.8)	Cl	5.8 (4.6)	As	10 (8.3)	Te	11 (8.6)
Li	26 (22)	Ar	5.5 (4.5)	Se	10 (8.2)	I	7.0 (5.6)
Be	15 (11)	K	41 (35)	Br	5.9 (4.6)	Xe	9.1 (7.5)
B	12 (8.3)	Ca	26 (21)	Kr	7.3 (5.9)	Cs	53 (45)
C	6.2 (5.0)	Ti	22 (19)	Rb	45 (39)	Ba	35 (30)
N	4.9 (2.8)	V	23 (19)	Sr	30 (25)	Ta	19 (16)
O	5.2 (4.3)	Cr	21 (18)	Zr	23 (20)	W	18 (15)
F	3.6 (2.9)	Mn	19 (16)	Nb	22 (19)	Re	21 (17)
Ne	3.2 (2.5)	Fe	21 (18)	Mo	20 (17)	Pt	18 (15)
Na	31 (26)	Co	21 (18)	Pd	22 (19)	Au	17 (14)
Mg	19 (16)	Ni	19 (16)	Ag	20 (17)	Hg	16 (13)
Al	16 (13)	Cu	19 (16)	Cd	17 (14)	Tl	18 (15)
Si	9.8 (7.7)	Zn	16 (13)	In	19 (16)	Pb	17 (14)
P	8.1 (6.5)	Ga	17 (14)	Sn	11 (8.7)	U	26 (22)

[a]Charge-exchange cross sections of ions with parent atoms (A) relate to the collision energies 0.1 and 10 eV (in parentheses) in the laboratory frame. That is, A is at rest during the collision.

APPENDIX 10. IONIZATION POTENTIALS I OF ATOMS IN THE GROUND STATE

Atom	I, eV	Atom	I, eV	Atom	I, eV	Atom	I, eV
H($^2S_{1/2}$)	13.598	K($^2S_{1/2}$)	4.341	Rb($^2S_{1/2}$)	4.177	Cs($^2S_{1/2}$)	3.894
He($^1S_0$)	24.586	Ca($^1S_0$)	6.113	Sr($^1S_0$)	5.695	Ba($^1S_0$)	5.212
Li($^2S_{1/2}$)	5.392	Sc($^2D_{3/2}$)	6.562	Y($^2D_{3/2}$)	6.217	La($^2D_{3/2}$)	5.577
Be($^1S_0$)	9.323	Ti($^3F_2$)	6.82	Zr($^3F_2$)	6.837	Ce($^1G_4$)	5.539
B($^2P_{1/2}$)	8.298	V($^4F_{3/2}$)	6.74	Nb($^6D_{1/2}$)	6.88	Ta($^4F_{3/2}$)	7.89
C($^3P_0$)	11.260	Cr($^7S_3$)	6.766	Mo($^7S_3$)	7.099	W($^5D_0$)	7.98
N($^4S_{3/2}$)	14.534	Mn($^6S_{5/2}$)	7.434	Tc($^6S_{5/2}$)	7.28	Re($^6S_{5/2}$)	7.88
O($^3P_2$)	13.618	Fe($^5D_4$)	7.902	Ru($^5F_5$)	7.366	Os($^5D_4$)	8.73
F($^2P_{3/2}$)	17.423	Co($^4F_{9/2}$)	7.86	*Rh*($^4F_{9/2}$)	7.46	Ir($^4F_{9/2}$)	9.05
Ne($^1S_0$)	21.565	Ni($3F_4$)	7.637	Pd($^1S_0$)	8.336	Pt($^3D_3$)	8.96
Na($^2S_{1/2}$)	5.139	Cu($^2S_{1/2}$)	7.726	Ag($^2S_{1/2}$)	7.576	Au($^2S_{1/2}$)	9.226
Mg($^1S_0$)	7.646	Zn($^1S_0$)	9.394	Cd($^1S_0$)	8.994	Hg($^1S_0$)	10.438
Al($^2P_{1/2}$)	5.986	Ga($^2P_{1/2}$)	5.999	In($^2P_{1/2}$)	5.786	Tl($^2P_{1/2}$)	6.108
Si($^3P_0$)	8.152	Ge($^3P_0$)	7.900	Sn($^3P_0$)	7.344	Pb($^3P_0$)	7.417
P($^4S_{3/2}$)	10.487	As($^4S_{3/2}$)	9.789	Sb($^4S_{3/2}$)	8.609	Bi($^4S_{3/2}$)	7.286
S($^3P_2$)	10.360	Se($^3P_2$)	9.752	Te($^3P_2$)	9.010	Rn($^1S_0$)	10.75
Cl($^2P_{3/2}$)	12.968	Br($^2P_{3/2}$)	11.814	I($^2P_{3/2}$)	10.451	Ra($^1S_0$)	5.278
Ar($^1S_0$)	15.760	Kr($^1S_0$)	14.000	Xe($^1S_0$)	12.130	U($^5L_6$)	6.194

APPENDIX 11. ELECTRON AFFINITIES EA OF ATOMS[a]

Ion	EA, eV	Ion	EA, eV	Ion	EA, eV	Ion	EA, eV
H$^-$(^1S)	0.75416	S$^-$(^2P)	2.0771	Se$^-$(^2P)	2.0207	I$^-$(^1S)	3.0590
He$^-$	Not	Cl$^-$(^1S)	3.6127	Br$^-$(^1S)	3.3636	Xe$^-$	Not
Li$^-$(^1S)	0.618	Ar$^-$	Not	Kr$^-$	Not	Cs$^-$(^1S)	0.4716
Be$^-$	Not	K$^-$(^1S)	0.5015	Rb$^-$(^1S)	0.4859	Ba$^-$	Not
B$^-$(^3P)	0.28	Ca$^-$(^2P)	0.024	Sr$^-$(^2P)	0.026	La$^-$(^3F)	0.5
C$^-$(^4S)	1.262	Sc$^-$(^1D)	0.19	Zr$^-$(^4F)	0.43	Hf$^-$	Not
C$^-$(^2D)	0.035	Ti$^-$(^4F)	0.08	Nb$^-$(^5D)	0.89	Ta$^-$(^5D)	0.32
N$^-$	Not	V$^-$(^5D)	0.53	Mo$^-$(^6S)	0.75	W$^-$(^6S)	0.816
O$^-$(^2P)	1.4611	Cr$^-$(^6S)	0.67	Tc$^-$(^5D)	0.6	Re$^-$(^5D)	0.2
F$^-$(^1S)	3.4012	Mn$^-$	Not	Ru$^-$(^4F)	1.0	Os$^-$(^4F)	1.1
Ne$^-$	Not	Fe$^-$(^4F)	0.151	Rh$^-$(^3F)	1.14	Ir$^-$(^3F)	1.57
Na$^-$(^1S)	0.5479	Co$^-$(^3F)	0.662	Pd$^-$(^2D)	0.56	Pt$^-$(^2D)	2.128
Mg$^-$	Not	Ni$^-$(^2D)	1.15	Ag$^-$(^1S)	1.30	Au$^-$(^1S)	2.3086
Al$^-$(^3P)	0.433	Cu$^-$(^1S)	1.23	Cd$^-$	Not	Hg$^-$	Not
Si$^-$(^4S)	1.385	Zn$^-$	Not	In$^-$(^3P)	0.4	Tl$^-$(^3P)	0.4
Si$^-$(^{2}D)	0.527	Ga$^-$(^2P)	0.43	Sn$^-$(^4S)	1.112	Pb$^-$(^4S)	0.364
Si$^-$(^2P)	0.029	Ge$^-$(^4S)	1.233	Sb$^-$(^3P)	1.05	Bi$^-$(^3P)	0.95
P$^-$(^3P)	0.7465	As$^-$(^3P)	0.80	Te$^-$(^2P)	1.9708	Po$^-$(^2P)	1.9

[a] EA is the electron binding energy of the negative ion in the electron state indicated; "Not" means that the electron affinity of the atom does not have a positive value.

APPENDIX 12. WORK FUNCTIONS W_0 OF ELEMENTS IN A POLYCRYSTALLINE STATE

Element	W_0, eV	Element	W_0, eV	Element	W_0, eV	Element	W_0, eV
Li	2.38	Co	4.41	In	3.8	Hf	3.53
Be	3.92	Ni	4.50	Sn	4.38	Ta	4.12
B	4.5	Cu	4.40	Sb	4.08	W	4.54
C	4.7	Zn	4.24	Te	4.73	Re	5.0
Na	2.35	Ga	3.96	Cs	1.81	Os	4.7
Mg	3.64	Ge	4.76	Ba	2.49	Ir	4.7
Al	4.25	As	5.11	La	3.3	Pt	5.32
Si	4.8	Se	4.72	Ce	2.7	Au	4.30
S	6.0	Rb	2.35	Pr	2.7	Hg	4.52
K	2.22	Y	3.3	Nd	3.2	Tl	3.7
Ca	2.80	Zr	3.9	Sm	2.7	Pb	4.0
Sc	3.3	Nb	3.99	Cd	3.1	Bi	4.4
Ti	3.92	Mo	4.3	Tb	3.15	Th	3.3
V	4.12	Ru	4.6	Dy	3.25	U	3.3
Cr	4.58	Pd	4.8	Ho	3.22		
Mn	3.83	Ag	4.3	Er	3.25		
Fe	4.31	Cd	4.1	Tm	3.10		

APPENDIX 13. PARAMETERS OF SOME LIQUID REFRACTORY METALS AND THEIR CLUSTERS[a]

Metal	T_m, K	T_b, K	ε_0, eV	A, eV	p_0, 10^5 atm	W_0, eV
Be	1560	2744	3.1	1.4	23	3.92
Ti	1941	3560	4.9	3.2	300	3.92
V	2183	3680	5.1	3.7	46	4.12
Fe	1812	3023	3.8	3.0	11	4.31
Co	1768	3200	4.1	3.1	3.5	4.41
Ni	1728	3100	3.2	2.9	41	4.50
Cu	1358	2835	3.4	2.2	15	4.40
Pd	1828	3236	3.7	2.9	6.0	4.8
Ag	1235	2435	2.9	2.0	15	4.3
W	3695	5830	8.6	4.7	22	4.54
Re	3459	5880	7.4	5.3	63	5.0
Os	3100	5300	7.9	4.7	230	4.7
Ir	2819	4700	6.4	4.9	130	4.7
Pt	2041	4100	5.6	3.6	170	5.32
Au	1337	3129	3.6	2.5	12	4.3

[a] In this Table T_m is the melting point of the metal, T_b is its boiling point, W_0 is the work function for the polycrystalline state of the metal, the binding energy of atoms in a liquid cluster consisting of n atoms is given as $E = \varepsilon_0 n - An^{2/3}$, and the saturated vapor pressure for a given metal is $p_{sat}(T) = p_0 \exp(-\varepsilon_0/T)$, where T is the temperature expressed in energy units. Data refer to the liquid state near the melting point. Some differences between T_b and that following from the last formula are due to the inaccuracy of the data and of this approximation.

BIBLIOGRAPHY

[1] A. F. Alexandrov, L. S. Bogdankevich, and A. A. Rukhadze, *Principles of Plasma Electrodynamics*, Springer, Berlin, 1984.

[2] J. A. Bittencourt, *Fundamentals of Plasma Physics*, Pergamon, Oxford, 1982.

[3] H. V. Boenig, *Plasma Science and Technology*, Cornell University Press, Ithaca, 1982.

[4] M. I. Boulos, P. Fauchais, and E. Pfender, *Thermal Plasmas*, Plenum, New York, 1994.

[5] S. C. Brown, *Introduction to Electrical Discharges in Gases*, Wiley, New York, 1966.

[6] R. A. Cairns, *Plasma Physics*, Blackie, Glasgow, 1985.

[7] B. N. Chapman, *Glow Discharge Processes*, Wiley, New York, 1980.

[8] F. F. Chen, *Introduction to Plasma Physics and Controlled Fusion*, Plenum, New York, 1984.

[9] J. D. Cobine, *Gaseous Conductors*, Dover, New York, 1958.

[10] G. Ecker, *Theory of Fully Ionized Plasmas*, New York, Academic, 1972.

[11] V. E. Fortov and I. T. Iakubov, *Physics of Nonideal Plasma*, Hemisphere, New York, 1990.

[12] D. A. Frank-Kamenetskii, *Plasma—the Fourth State of Matter*, Plenum, New York, 1972.

[13] V. E. Golant, A. P. Zhilinsky, and I. E. Sakharov, *Fundamentals of Plasma Physics*, Wiley, New York, 1980.

[14] M. F. Hoyaux, *Arc Physics*, Springer, New York, 1968.

[15] L. G. H. Huxley and R. W. Crompton, *The Diffusion and Drift of Electrons in Gases*, Wiley, New York, 1974.

[16] S. Ishimaru, *Plasma Physics: Introduction to Statistical Physics of Charged Particles*, Benjamin, Menlo Park, 1985.

[17] S. Ishimaru, *Statistical Plasma Physics*, Addison-Wesley, Redwood City, vol. 1, *Basic Principles*, 1992, vol. 2, *Condensed Plasmas*, 1994.

[18] M. A. Kettani and M. F. Hoyaux, *Plasma Engineering*, Wiley, New York, 1973.

[19] A. N. Lagarkov and I. M. Rutkevich, *Ionization Waves in Electrical Breakdown of Gases*, Springer, New York, 1994.

[20] M. A. Lieberman and A. J. Lichtenberg, *Principles of Plasma Discharge and Materials Processing*, Wiley, New York, 1994.

[21] E. M. Lifshits and L. P. Pitaevskii, *Physical Kinetics*, Pergamon, Oxford, 1981.

[22] V. S. Lisitsa, *Atoms in Plasmas*, Springer, Berlin,1994.

[23] F. Llewelyn-Jones, *The Glow Discharge*, Methuen, New York, 1966.

[24] L. B. Loeb, *Basic Processes of Gaseous Electronics*, University of California Press, Berkeley, 1955.

[25] H. S. W. Massey, *Negative Ions*, Cambridge University Press, Cambridge, 1976.

[26] H. S. W. Massey, *Atomic and Molecular Collisions*, Taylor and Francis, London, 1979.

[27] E. W. McDaniel and E. A. Mason, *The Mobility and Diffusion of Ions in Gases*, Wiley, New York, 1973.

[28] E. W. McDaniel, J. B. A. Mitchell, and M. E. Rudd, *Atomic Collisions: Heavy Particle Projectiles*, Wiley, New York, 1993.

[29] G. A. Mesyats and D. I. Proskurovsky, *Pulsed Electrical Discharge in Vacuum*, Springer, Berlin, 1989.

[30] E. Nasser, *Fundamentals of Gaseous Ionization and Plasma Electronics*, Wiley, New York, 1971.

[31] W. Neuman, *The Mechanism of the Thermoemitting Arc Cathode*, Academic-Verlag, Berlin, 1987.

[32] Yu. P. Raizer, *Gas Discharge Physics*, Springer, Berlin 1997.

[33] V. P. Schevel'ko and L. A. Vainshtein, *Atomic Physics for Hot Plasmas*, Institute of Physics, Bristol, 1993.

[34] P. P. J. M. Schram, *Kinetic Theory of Gases and Plasmas*, Kluwer, Dordrecht, 1991.

[35] S. R. Seshardi, *Fundamentals of Plasma Physics*, American Elsevier, New York, 1973.

[36] A. G. Sitenko, *Fluctuations and Nonlinear Wave Interactions in Plasmas*, Pergamon, Oxford, 1982.

[37] A. G. Sitenko and V. Malnev, *Plasma Physics Theory*, Chapman and Hall, London, 1995.

[38] B. M. Smirnov, *Physics of Weakly Ionized Gases*, Mir, Moscow, 1981.

[39] B. M. Smirnov, *Negative Ions*, McGraw-Hill, New York, 1982.

[40] L. Spitzer, *Physics of Fully Ionized Gases*, Wiley, New York, 1962.

[41] T. H. Stix, *Waves in Plasmas*, American Institute of Physics, New York, 1992.

[42] P. A. Sturrock, *Plasma Physics*, Cambridge University Press, Cambridge, 1994.

[43] T. Ohnuma, *Radiation Phenomena in Plasmas*, World Scientific, Singapore, 1994.

[44] A. von Engel, *Electric Plasmas*, Taylor and Francis, London, 1983.

[45] H. S. W. Massey, E. W. McDaniel, and B. Bederson, eds., *Applied Atomic Collision Physics*, vol. 1, *Atmospheric Physics and Chemistry*, Academic, New York, 1982.

[46] A. A. Galeev and R. N. Sudan, eds., *Basic Plasma Physics*, North Holland, Amsterdam, 1983.

[47] J. A. Rees, ed., *Electrical Breakdown in Gases*, Wiley, New York, 1973.

[48] J. M. Meek and J. D. Craggs, *Electrical Breakdown in Gases*, Wiley, New York, 1978.

[49] *Plasma Science: From Fundamental Research to Technological Applications*, National Academy Press, Washington, 1995.

[50] G. A. Kobzev, I. T. Iakubov, and M. M. Popovich, eds., *Transport and Optical Properties of Nonideal Plasma*, Plenum, New York, 1995.

[51] J. M. Lafferty, ed., *Vacuum Arcs*, Wiley, New York, 1980.

INDEX